EMERGING INFECTIOUS DISEASES®

CDC
SAFER • HEALTHIER • PEOPLE™

Zoonotic Infections

December 2016

Jenny Hammond, *The Natural History of Influenza A Viruses* (1990). Stained Glass, 21 in X 56 in/ 53.3 cm X 142.2 cm. Commissioned by Robert and Marjorie Webster, Memphis, TN USA. Digital image courtesy of Robert Webster.

EMERGING INFECTIOUS DISEASES®

Emerging Infectious Diseases is published monthly by the Centers for Disease Control and Prevention, 1600 Clifton Road, Mailstop D61, Atlanta, GA 30329-4027, USA. Telephone 404-639-1960, fax 404-639-1954, email eideditor@cdc.gov.

∞ Emerging Infectious Diseases is printed on acid-free paper that meets the requirements of ANSI/NISO 239.48-1992 (Permanence of Paper)

EMERGING INFECTIOUS DISEASES®

December 2016

On the Cover

Jenny Hammond, *The Natural History of Influenza A Viruses* (1990). Stained Glass, 21 in × 56 in/ 53.3 cm × 142.2 cm. Commissioned by Robert and Marjorie Webster, Memphis, TN USA. Digital image courtesy of Robert Webster.

About the Cover p. 2231

Synopses

Medscape EDUCATION ACTIVITY

Research

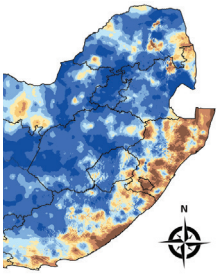

p. 2057

p. 2065

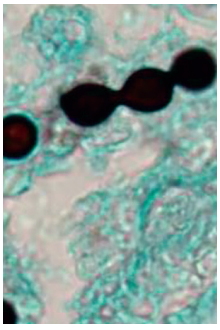

EMERGING INFECTIOUS DISEASES®
December 2016

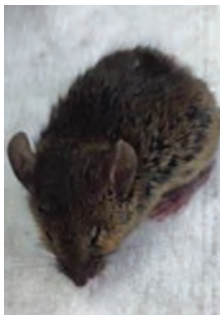

p. 2075

Medscape EDUCATION ACTIVITY

Dispatches

p. 2088

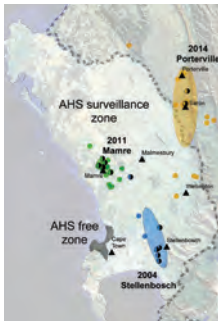

EMERGING INFECTIOUS DISEASES®
December 2016

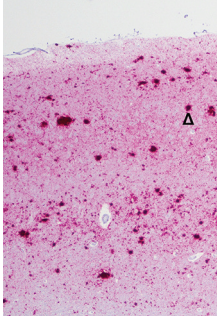

p. 2144

Another Dimension

Letters

p. 2218

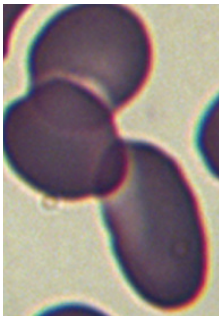

About the Cover

Etymologia

Assessing the Epidemic Potential of RNA and DNA Viruses

Mark E.J. Woolhouse, Liam Brierley, Chris McCaffery, Sam Lycett

Many new and emerging RNA and DNA viruses are zoonotic or have zoonotic origins in an animal reservoir that is usually mammalian and sometimes avian. Not all zoonotic viruses are transmissible (directly or by an arthropod vector) between human hosts. Virus genome sequence data provide the best evidence of transmission. Of human transmissible virus, 37 species have so far been restricted to self-limiting outbreaks. These viruses are priorities for surveillance because relatively minor changes in their epidemiologies can potentially lead to major changes in the threat they pose to public health. On the basis of comparisons across all recognized human viruses, we consider the characteristics of these priority viruses and assess the likelihood that they will further emerge in human populations. We also assess the likelihood that a virus that can infect humans but is not capable of transmission (directly or by a vector) between human hosts can acquire that capability.

A series of recent emerging infectious disease outbreaks, including the 2014 Ebola virus disease (EVD) epidemic in West Africa and the continuing Zika virus disease epidemic in the Americas, have underlined the need for better understanding of which kinds of pathogens are most likely to emerge and cause disease in human populations. Many, although not all, emerging infectious diseases are caused by viruses, and these frequently emerge from nonhuman host reservoirs (*1*–*3*). The enormous diversity (*4*) and high rates of evolution (*5*) of viral pathogens discourage attempts to predict with any precision which ones are most likely to emerge in humans. However, there is some consensus, at least in general terms, regarding the kinds of traits that are most essential in determining the capacity of a virus to infect, cause disease, and spread within human populations (Table 1). We focus on one of these traits, the capacity of a virus to spread from one human to another (by any transmission route other than deliberate laboratory exposure), a key determinant of the epidemic potential of a virus.

A theoretical framework for studying the dynamics of infectious disease outbreaks is well established (*6*). The capacity of an infectious disease to spread in a host population can be quantified in terms of its basic reproduction number, R_0. R_0 is defined as the average number of secondary cases generated by a single primary case in a large, previously unexposed host population, and its value tells us a great deal about the epidemiology of a pathogen. $R_0 = 0$ indicates no spread in that population; this value would apply to zoonotic infections that do not spread between humans. R_0 in the range $0<R_0\leq1$ indicates that chains of transmission are possible but that outbreaks will ultimately be self-limiting. $R_0>1$ indicates that major epidemics can occur or that the disease may become endemic in that host population. A higher value of R_0 also indicates that a greater reduction in transmission rates must be achieved to control an epidemic (*6*). R_0 values have been estimated for >60 common human pathogens (*7*), including human influenza A virus ($R_0\leq2$), measles virus ($R_0\leq18$), and dengue virus ($R_0\leq22$).

R_0 is determined by a combination of pathogen traits, such as its transmission biology, which is itself a complex interplay between the within-host dynamics of the pathogen and the host response to infection, and host traits, such as demography, behavior, genetics, and adaptive immunity. Consequently, for any given infectious disease, R_0 can vary between host species and between host populations. Infectious diseases with R_0 close to 1 are a particular concern because small changes in their epidemiologies can lead to major changes in the threat they pose to public health (*8*).

R_0 is closely related to another conceptual approach to disease emergence, the pathogen pyramid. There are different versions of this scheme (*3*,*9*). We consider a pyramid of 4 levels (Figure 1). Level 1 represents the background chatter of pathogens to which humans are continually or sporadically exposed but most of which are not capable of causing infection. Other levels can be considered in terms of the R_0 of the pathogen in humans: level 2 corresponds to $R_0 = 0$, level 3 to $0<R_0\leq1$, and level 4 to $R_0>1$.

Data and Analysis

Identifying and Characterizing Level 3 and 4 Viruses

We updated our previous systematic literature review (*10*) of the capacity of virus species to transmit between humans (i.e., level 3 and level 4 viruses; online Technical Appendix, http://wwwnc.cdc.gov/EID/article/22/12/16-0123- Techapp1.pdf). Such viruses are

Author affiliation: University of Edinburgh, Edinburgh, UK

DOI: http://dx.doi.org/10.3201/eid2212.160123

Table 1. Virus traits potentially relevant for capacity to emerge and cause disease in human populations*

Trait	Definition
Reservoir host relatedness	Viruses derived from specific host taxa (e.g., other primate species might be of increased concern)
Virus relatedness	Particular virus taxa might be predisposed to infect, cause disease, and transmit among humans
Virus host range	Viruses with a broad or narrow host range might be of greatest concern
Evolvability	Higher substitution rates might make it easier for some viruses to adapt to human hosts
Host restriction factors	Host factors, many still to be identified, are a barrier to viral infection and help determine which viruses can and cannot emerge
Transmission route	Certain transmission routes might predispose viruses to emerge in humans
Virulence	Certain virus or host factors might determine whether a virus causes mild or severe disease in humans
Host–virus coevolution	Lack of a shared evolutionary history might be associated with higher virulence

*Adapted from Morse et al. (*3*).

found in 25 of 29 families containing viruses that infect mammals or birds (discounting 2 reports of family *Nodaviridae* species in mammals/birds). The 4 exceptions comprise 2 families that have no known human-infective viruses (*Arteriviridae* and *Birnaviridae*) and 2 with species that have been reported in humans but only at level 2 (*Asfarviridae* and *Bornaviridae*).

A total of 22 of these families contain level 4 viruses with epidemic potential in humans (sometimes described as human-adapted viruses) (*11*). This finding indicates that this capability is widely distributed among virus taxa. The 3 families with level 3 viruses but no level 4 viruses are the *Arenaviridae*, *Bunyaviridae*, and *Rhabdoviridae*.

A list of 37 presumptive level 3 virus species is provided in Table 2. These species cover a wide taxonomic range and a variety of transmission routes, including vectorborne. Several level 3 viruses have historically been associated with sizeable outbreaks (>100 cases) in human populations: Bwamba, Oropouche, Lake Victoria Marburg, Sudan Ebola, and o'nyong-nyong viruses. For some other viruses, including Guanarito, Junin, lymphocytic choriomeningitis, and Sabia (all arenaviruses); simian virus 40; Titi monkey virus; and influenza A(H5N1) virus, human-to-human transmission is rare or merely suspected. In addition, several viruses are only known or believed to transmit between humans by iatrogenic routes or vertical transmission; this group (Table 2) might be regarded as unlikely epidemic threats.

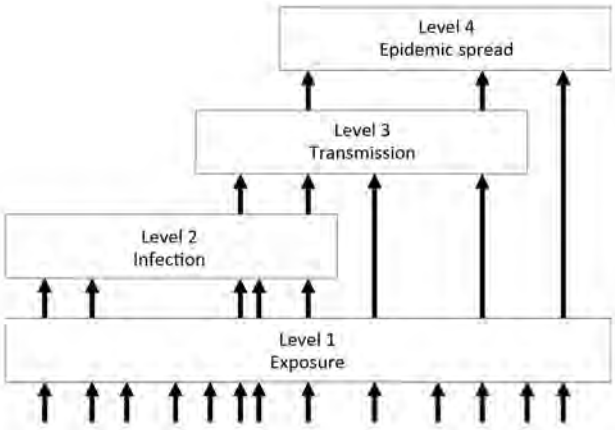

Figure 1. Pathogen pyramid for RNA and DNA viruses. Level 1 indicates viruses to which humans are exposed but which do not infect humans. Level 2 indicates viruses that can infect humans but are not transmitted from humans. Level 3 indicates viruses that can infect and be transmitted from humans but are restricted to self-limiting outbreaks. Level 4 indicates viruses that are capable of epidemic spread in human populations. Transitions between levels (indicated by arrows) correspond to different stages of virus emergence in human populations. Reprinted from Woolhouse et al. (*10*).

When a virus is transmitted by a vector, it can be particularly difficult to confirm or exclude the infectiousness of human cases, as with Semliki forest, Barmah forest, and Rift Valley fever viruses. Similarly, even when human–vector–human transmission is believed to occur, it is often difficult to quantify its contribution to a given outbreak, as with Venezuelan equine encephalitis virus.

Level 2 viruses are those that can infect humans (>100 species) but have never been reported to be transmitted by humans (*10*). In at least some instances, such as influenza A(H5N1) virus (*12*), this finding is attributable to tissue tropisms during human infection that are incompatible with onward transmission.

Shifts in pyramid level equate to shifts in the public health threat posed by a virus. We consider possible shifts in the following sections.

Level 1 to Levels 3 and 4

Virus species of mammalian and, more rarely, avian origin are sometimes observed to be transmissible between humans when first found in humans, which constitutes a jump from level 1 straight to level 3 or 4 (Figure 1), and events of this kind have been reported regularly. Recent examples that appear on the basis of available evidence to fit this model include severe acute respiratory syndrome coronavirus (first reported in humans in 2003), Bundibugyo Ebolavirus (2008), Lujo virus (2009), severe fever with thrombocytopenia syndrome virus (2011), and Middle East respiratory syndrome coronavirus (MERS-CoV) (2012).

We still have incomplete knowledge of the diversity of viruses that infect mammals and birds; the few hundred recognized species (*4*) surely represent only a small fraction of the total (*3*). Moreover, we have few predictors of potential human-to-human transmissibility. One possible indicator

Table 2. Viruses (n = 37) that are known or suspected of being transmissible (directly or indirectly) between humans but to date have been restricted to short transmission chains or self-limiting outbreaks

Genome, virus family	Virus name
Single-stranded RNA (ambisense)	
Arenaviruses	Guanarito, Junin, Lassa, Lujo, Machupo, Sabia, Dandenong,* lymphocytic choriomeningitis*
Bunyaviruses	Andes, Bwamba, Crimean-Congo hemorrhagic fever, Oropouche, Rift Valley, severe fever with thrombocytopenia syndrome
Single-stranded RNA (positive sense)	
Flaviviruses	Japanese encephalitis,* Usutu,* West Nile*
Coronaviruses	Middle East respiratory syndrome
Togaviruses	Barmah Forest, o'nyong-nyong, Ross River, Semliki Forest, Venezuelan equine encephalitis
Single-stranded RNA (negative sense)	
Filoviruses	Bundibugyo Ebola, Lake Victoria Marburg, Sudan Ebola
Paramyxoviruses	Nipah
Rhabdoviruses	Bas-Congo, rabies*
Double-stranded RNA	
Reoviruses	Nelson Bay, Colorado tick fever*
Double-stranded DNA	
Adenoviruses	Titi monkey
Herpesviruses	Macacine herpesvirus 1
Polyomaviruses	Simian virus 40
Poxviruses	Monkeypox, Orf, vaccinia

*Human transmission of these viruses is known only by iatrogenic or vertical routes.

is emergence from nonhuman primates, with suggestions that primate viruses are more likely to be able to, or to acquire the ability to, spread in human populations (*13,14*). However, emergence of human transmissible viruses from bat (e.g., severe acute respiratory syndrome coronavirus) or bird (e.g., influenza) reservoirs indicates that this trait is associated with a wide range of reservoirs.

Level 2 to Levels 3 and 4

The possibility that level 2 viruses might acquire the capacity to be transmitted between humans (i.e., move into level 3 or 4) is a major concern, especially in the context of influenza A(H5N1) virus and other avian influenza virus subtypes. However, there are few examples of this transition throughout the entire recorded history of human viruses going back to 1901. One possible example involves the simian immunodeficiency virus (SIV) and HIV. A SIV_{smm}-derived laboratory strain of SIV has been reported to infect humans, but without onward transmission (*15*). SIV_{smm} is related to HIV-2. SIV_{cpz}, which is related to HIV-1, has not been directly observed in humans. However, different HIV-1 lineages, independently derived from SIV_{cpz}, are variably transmissible in humans, and the pandemic HIV-1 M lineage was the only virus to overcome a key host restriction factor (human tetherin) (*16*). The only other examples of viruses newly transmitted between humans relate to rare instances of iatrogenic transmission (e.g., Colorado tick fever or rabies viruses).

Epidemiologic and phylogenetic considerations routinely inform our assessment of the likelihood of human-to-human transmission being observed in the future. For example, there is markedly less concern about rabies virus than about avian influenza virus, and we suggest 2 reasons for this observation. First, rabies virus has a much longer history of and a much higher incidence of human infection, but human-to-human transmission is extremely rare. Second, there is no evidence that other rhabdoviruses viruses (with the possible exception of Bas-Congo virus, which represents a novel genus) are transmissible in humans (or primates more generally).

Level 3 to Level 4

Level 3 viruses can also become level 4 viruses. We note that virus evolution is not (necessarily) required for R_0 to become >1 in human populations. Differences in host (or vector) behavior, ecology, or demography might be sufficient (*8*).

Instances of shifts from level 3 to level 4 in recent times have been infrequent. Three candidates are Ebolavirus, Zika virus, and chikungunya virus. However, although these viruses have caused epidemics of unprecedented size in humans populations in the past decade, the condition R_0>1 in human populations might had been previously met for all 3 viruses (*17–19*).

For Ebola virus, the epidemic in West Africa in 2014 constituted the first appearance of this virus in high-density, urban populations, which is expected to correspond to a higher value of R_0. The chikungunya virus epidemic in the Indian Ocean region in 2005 was associated with a vector species jump (from *Aedes aegypti* to *Ae. albopictus* mosquitoes) that has been linked to a mutation in the virus envelope 1 protein gene (*18*). The chikungunya virus epidemic in the Caribbean region in 2013 followed the first appearance of chikungunya in the Americas and infected

populations that had no history of exposure to the virus. The current Zika virus epidemic in South America appears to be another example of a transition from a level 3 to a level 4 arbovirus associated with geographic spread into areas with high densities of vectors (*19*). Occasional Zika virus transmission directly from infected humans to other humans are of considerable interest, but probably contribute little to R_0.

Chikungunya, Zika and the other level 4 arboviruses (yellow fever and dengue viruses) illustrate that, for arboviruses, a high potential for spread in human populations is linked to carriage by anthropophilic vector species, particularly mosquitoes of the genus *Aedes*. In contrast, no tick species are regarded as anthropophilic, and there are no level 4 and few level 3 tickborne arboviruses.

Epidemiologic Patterns

The preceding sections illustrate that identifying transitions of viruses between level 2 and level 3 or between level 3 and level 4 is not always straightforward. Standard epidemiologic theory can help clarify our expectations.

As we discussed, pyramid level is related to the basic reproduction number R_0 in human populations. In turn, the value of R_0 is indicative of expected outbreak dynamics. Some key results (Figure 2) are the probability that a single primary case will generate ≥1 secondary cases (for any value of R_0), the expected average size of an outbreak generated (over the range $0 \leq R_0 < 1$), and the probability that an epidemic will spread in the human population (for $R_0 > 1$). These results strictly apply to homogeneous infections in a homogeneous host population, although more general frameworks can accommodate host or pathogen heterogeneity (*20–22*). Nonetheless, the key predictions

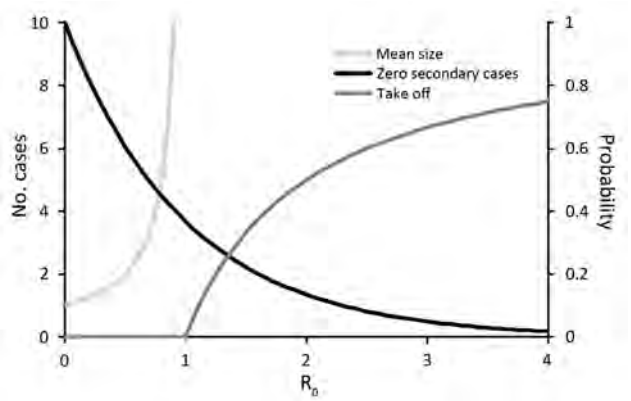

Figure 2. Expected outbreak dynamics for RNA and DNA viruses given a single primary case in a large, previously unexposed host population, as a function of the basic reproduction number R_0. Mean size of outbreak as total number of cases (*N*) is given by $N = 1/(1 - R_0)$ for $R_0 < 1$ (light gray line, left axis). Probability of 0 secondary cases (i.e., outbreak size N = 1) is given by $P_1 = \exp(-R_0)$ (black line, right axis). Probability of a major outbreak is given by $P_{takeoff} = 1 - 1/R_0$ for $R_0 > 1$ (dark gray line, right axis).

that secondary cases do not always occur even if $R_0 > 0$ and that major epidemics do not always occur even if $R_0 > 1$ are robust.

From an epidemiologic perspective, our confidence that a putatively level 2 virus is truly incapable of human-to-human transmission is thus a function of the number of index cases observed. The transition between level 3 and level 4 can be studied in terms of the expected distribution of outbreak sizes (*23*). In the range $0 \leq R_0 < 1$, an overdispersed distribution of outbreak sizes is expected: most outbreaks are small (often just single cases) with a long tail of larger outbreaks. This pattern has been reported for a range of emerging viral diseases (Figure 3). As the critical threshold $R_0 = 1$ is approached, this value is signaled in the outbreak size distribution (Figure 3). This framework has been used successfully to monitor the epidemiology of measles virus in the United Kingdom after a decrease in childhood vaccination rates in the late 1990s and indicated the approach to the critical threshold that corresponded to loss of herd immunity (*23*).

Outbreak size distribution analysis has been applied to human case data for Andes virus (*24*), monkeypox virus (*20*), and MERS-CoV (*25*) (Figure 3). For EVD up to 2013, data are clearly inconsistent with theoretical expectation for $R_0 < 1$ (Figure 3), which suggests that large numbers of small outbreaks have remained undetected or that R_0 was already >1 in at least some settings. Either way, $R_0 \approx 1$ for EVD in humans implies that small differences in the biology or epidemiology of the virus would lead to large changes in scale of outbreaks (*8*), which could make events such as the EVD epidemic in 2014, if not predictable, then much less unexpected.

Evolution

Changes in pyramid level might be mediated by virus evolution or changes in virus ecology (*28*). A major issue is whether the capacity of a virus to spread in human populations arises as a result of adaptation (evolution of transmissibility that occurs during human infection) or preadaptation (genetic variation within nonhuman reservoirs that predisposes a virus not only to infect humans but also transmit between humans, noting that RNA viruses often show high levels of genetic variation such that they are sometimes described as quasi-species [*29*]). These alternatives have been characterized as tailor-made and off-the-shelf, respectively (*28*). The first alternative implies a progression from no or low transmissibility between humans to moderate or high transmissibility. The second alternative implies moderate or high transmissibility at first infection of humans.

We consider that our survey of documented changes of pyramid level is most consistent with the off-the-shelf model of virus emergence. In particular, we can find no

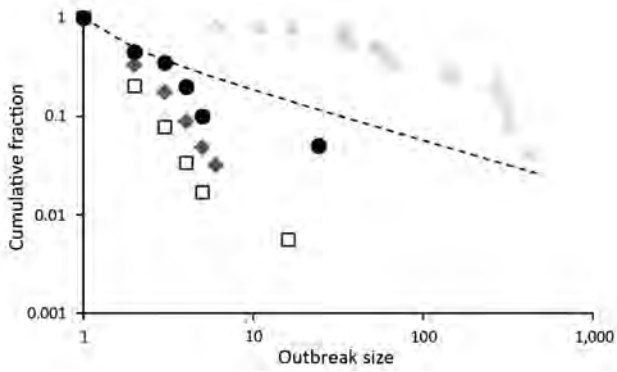

Figure 3. Distribution of outbreak sizes for RNA and DNA viruses as plots of outbreak size *x* (horizontal axis) versus fraction of outbreaks of size ≥*x* (vertical axis), both on logarithmic scales. Data are shown for 4 infectious diseases. Squares indicates Andes virus disease in South America (*24*); diamonds indicate monkeypox in Africa (*26*); circles indicate Middle East respiratory syndrome in the Middle East (*25*); and triangles indicate filovirus (all species) diseases in Africa before 2013 (*27*). For comparison, expected values for the case $R_0 = 1$, obtained from the expression for the probability of an outbreak of size ≥*x*, $P(x) = \Gamma(x - ½)/\sqrt{\pi}\Gamma(x)$, are also shown (dashed line). Data for filoviruses are not consistent with expectation for $R_0<1$.

convincing examples of level 2 viruses becoming level 3 or 4 viruses, which suggests that, if this happens at all, it typically happens sufficiently rapidly (i.e., requires a sufficiently small number of introductions) that we fail to observe the level 2 phase. In contrast, we regularly observe viruses at levels 3 or 4 the first time they are detected in human populations.

Nonetheless, the possibility of virus evolution of transmissibility in a new host has been demonstrated experimentally for influenza A(H5N1) virus in ferrets (*30*). A theoretical study (*31*) suggested that the fact that this virus subtype has been circulating widely in poultry populations, with frequent human exposure and sporadic human infection for almost 20 years, provides little or no reassurance about its future evolutionary trajectory.

HIV lineages show clear evidence of adaptation to humans (*16*), but as discussed earlier, it is not clear whether the SIV lineages that gave rise to HIV-1 or HIV-2 were capable of transmission between human hosts. We speculate that extended infection times make tailor-made emergence more likely for retroviruses.

Transmission

Demonstrating that an infected human has the potential to transmit the infection to another human is not always straightforward. High virus titers in body secretions and excretions, blood, or skin are considered indicative. Case clusters are suggestive, but if persons occupy the same environment (e.g., household), then it might be difficult to rule out common exposure. Case clusters must be epidemiologically plausible (i.e., delimited in space and time in a manner consistent with the known or assumed epidemiology of the virus). Genotyping techniques are useful tools for confirming a cluster but do not resolve the source of infection.

For several of the viruses we studied (e.g., Bas-Congo, Lujo, Nelson Bay, and severe fever with thrombocytopenia syndrome viruses) (Table 2), the evidence for human-to-human transmission is best regarded as tentative, particularly where putative clusters were small. Such assessments can be even more difficult for vectorborne viruses. In many situations, the best evidence for the human-to-human transmission will come from analysis of virus genome sequences.

Phylogenetic Analysis

One approach to resolving the question of human-to-human transmission is analysis of nucleotide sequence data, sometimes referred to as forensic phylogenetics. Nucleotide substitution rates in fast-evolving RNA viruses, such as MERS-CoV and Ebola virus, are $\approx 1–5 \times 10^{-3}$/site/year (*32*,*33*), making it possible to use sequences isolated from different hosts at different times to estimate time-resolved phylogenetic trees. Estimates of the transmission chain from temporal sequence data can be improved by incorporating additional information on the date of onset of individual cases, duration of latent and infectious periods, and overall prevalence (*34*).

We provide some example phylogenetic trees generated from simulated epidemics (Figure 4). In an epidemic in an animal reservoir with occasional transmission to humans (Figure 4, panel A), for each human sequence, the most closely related next sequence is of animal origin. Clusters of closely related human sequences are shown, and the distribution of the expected cluster sizes is a function of R_0 (Figure 4, panels B, C) (*35*).

In an outbreak, it might be difficult to find and sample the putative source animal cases. However, estimating the time to most recent common ancestor (TMRCA) of the human cases will indicate how long the infection has been spreading. For sporadic zoonoses (Figure 4, panel A), most transmission has occurred unobserved in the animal reservoir, and the TMRCA of pairs of human cases will be long because these sequences are not closely related. For outbreaks involving human-to-human transmission (Figure 4, panels B, C), the TMRCA of the cluster of human cases will be closer to the date of the first human infection (whether sampled or not) and provides the estimated date of the zoonotic event.

Use of sequence data to distinguish between multiple instances of human infection from a common animal source and human-to-human transmission in the early stages of an

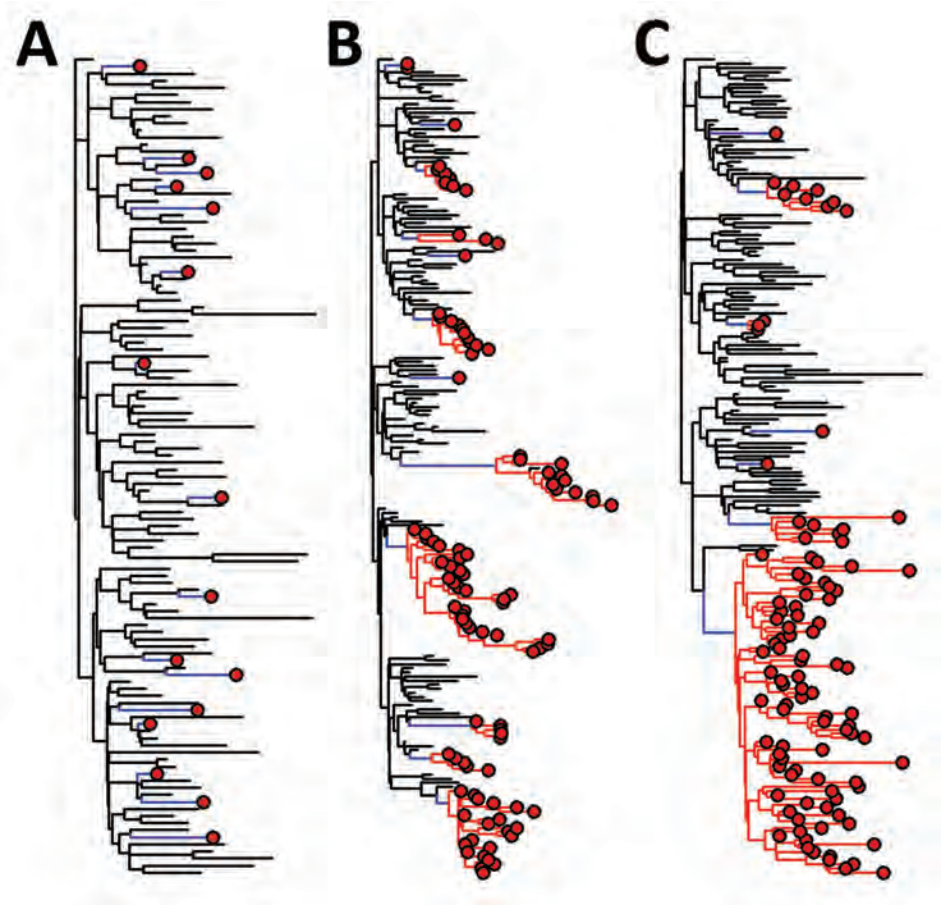

Figure 4. Phylogenetic trees for simulated emerging infectious disease outbreaks caused by RNA and DNA viruses in a mixed population of 1,000 human and 5,000 nonhuman hosts. Trees were constructed by using a standard susceptible–infected–removed model (*6*). For each of 3 infection scenarios in nonhuman hosts (black lines), rare zoonotic transmission events (blue lines), human-to-human transmission (red lines), and human cases (red circles) are indicated. For the nonhuman population $R_0 = 2$ throughout. Transmissibility within the human populations varies from A) spillover: no human–human transmission ($R_0 = 0$); B) limited human–human transmission with $R_0 = 1$; and C) epidemic spread within humans ($R_0 > 1$). A maximum of 100 infections are randomly sampled from each population in each simulated outbreak.

outbreak is extremely challenging because of short timescales, and involvement of few mutations. However, genetic differences and phylogenetic evidence show that at least 2 of the first 3 reported cases of influenza A (H7N9) virus infection in humans were believed to originate from distinct domestic avian sources (*36*).

Further sequencing of avian samples implied that a low-pathogenicity influenza A(H7N9) virus strain had been spreading in domestic birds for ≈1 year before sporadic cases were detected in humans (*37*). Similarly, detection of genetically distant lineages of MERS-CoV, which persisted for only a few months each, suggest multiple introductions from an animal reservoir and only limited human-to-human transmission to date (*32*). In contrast, the influenza A(H1N1) pandemic in 2009 and the EVD epidemic in West Africa in 2014 were believed to be the results of single zoonotic events, followed by sustained human-to-human transmission (*33*), as shown by a single rapidly expanding lineage.

Conclusions

Our survey of the capacity of RNA and DNA virus infections to be transmitted, directly or indirectly, between humans leads to several conclusions and practical suggestions for improving surveillance of emerging infectious diseases and targeting efforts to identify future public health threats. In support of these conclusions, the World Health Organization recently published list of priority emerging infectious diseases and corresponding viruses (*38*) included 6 of the viruses in Table 2.

A major observation is that the taxonomic diversity of viruses that are possible threats to public health is wide, but bounded. Most human infective viruses are closely related to viruses of other mammals and some to viruses of birds. There are no indications that humans acquire new viruses from any other source. However, diversification within human populations occurs and is a prominent feature of some DNA virus taxa (e.g., family *Papillomaviridae*) (*4*).

In general, however, our knowledge of origins of human viruses is still incomplete. Although the origins of HIV-1 have been extensively investigated (*16*), for most other viruses, even level 4 viruses, little or no research has occurred. An origins initiative (*9*) would help establish the routes into human populations that have been used by other viruses.

Transmissibility within human populations is a key determinant of epidemic potential. Many viruses that can infect humans are not capable of being transmitted by humans;

most human transmissible viruses that emerge already have that capability at first human infection or acquire it relatively rapidly. If transmission from humans would require a change in a phylogenetically conserved trait, such as tissue tropism or transmission route (*4*), then such viral paradigm shifts will probably be extremely rare (*39*).

Even when a virus is capable of transmission between humans, the critical threshold R_0>1 is not always achieved. However, because changes in virus traits or host population characteristics can influence R_0, level 3 viruses (Table 2) are of special interest from a public health perspective, and of special concern when, like MERS-CoV, they also cause severe illness. Demonstrating human transmissibility is often difficult, but essential. The best evidence is likely to come from virus genome sequencing studies. These studies should be a public health priority (*40*).

We currently have few clues to help us predict which mammalian or avian viruses might pose a threat to humans and, especially, which might be transmissible between humans. One argument in favor of experimental studies of these traits, including controversial gain of function experiments (*30*), is that they could help guide molecular surveillance for high-risk virus lineages in nonhuman reservoirs.

The first line of defense against emerging viruses is effective surveillance (*40*). A better understanding of which kinds of viruses in which circumstances pose the greatest risk to human health would enable evidence-based targeting of surveillance efforts, which would reduce costs and increase probable effectiveness of this endeavor.

Acknowledgments

We thank David McCulloch, Cristina Moreno, and Matthew Hall for assistance during this study.

This study was supported by the Wellcome Trust Vietnam Initiative on Zoonotic Infections Project grant 093724/B/10/Z to M.E.J.W. and European Union 2020 grant COMPARE #643476. L.B. was supported by a Natural Environment Research Council PhD studentship, and S.L. was supported by a University of Edinburgh Chancellor's Fellowship and the Biotechnology and Biological Sciences Research Council Strategic Programme grant BB/J004227/1.

Dr. Woolhouse is professor of Infectious Disease Epidemiology at the Centre for Immunity, Infection and Evolution at the University of Edinburgh, Edinburgh, UK. His primary research interests are pathogen emergence and antimicrobial drug resistance.

References

1. Taylor LH, Latham SM, Woolhouse ME. Risk factors for human disease emergence. Philos Trans R Soc Lond B Biol Sci. 2001;356:983–9. http://dx.doi.org/10.1098/rstb.2001.0888
2. Jones KE, Patel NG, Levy MA, Storeygard A, Balk D, Gittleman JL, et al. Global trends in emerging infectious diseases. Nature. 2008;451:990–3. http://dx.doi.org/10.1038/nature06536
3. Morse SS, Mazet JA, Woolhouse M, Parrish CR, Carroll D, Karesh WB, et al. Prediction and prevention of the next pandemic zoonosis. Lancet. 2012;380:1956–65. http://dx.doi.org/10.1016/S0140-6736(12)61684-5
4. King AM, Lefkowitz E, Adams MJ, Carstens EB. Virus taxonomy: ninth report of the International Committee on Taxonomy of Viruses. Amsterdam: Elsevier; 2012.
5. Woolhouse ME, Haydon DT, Antia R. Emerging pathogens: the epidemiology and evolution of species jumps. Trends Ecol Evol. 2005;20:238–44. http://dx.doi.org/10.1016/j.tree.2005.02.009
6. Anderson RM, May RM. Infectious diseases of humans: dynamics and control. New York: Oxford University Press; 1991.
7. Hay SI, Battle KE, Pigott DM, Smith DL, Moyes CL, Bhatt S, et al. Global mapping of infectious disease. Philos Trans R Soc Lond B Biol Sci. 2013;368:20120250. http://dx.doi.org/10.1098/rstb.2012.0250
8. Woolhouse ME. Population biology of emerging and re-emerging pathogens. Trends Microbiol. 2002;10(Suppl):S3–7. http://dx.doi.org/10.1016/S0966-842X(02)02428-9
9. Wolfe ND, Dunavan CP, Diamond J. Origins of major human infectious diseases. Nature. 2007;447:279–83. http://dx.doi.org/10.1038/nature05775
10. Woolhouse ME, Adair K, Brierley L. RNA viruses: a case study of the biology of emerging infectious diseases. Microbiol Spectr. 2013;1:OH-0001–2012. http://dx.doi.org/10.1128/microbiolspec.OH-0001-2012
11. Woolhouse ME, Adair K. The diversity of human RNA viruses. Future Virology. 2013;8:159–71 http://dx.doi.org/10.2217/fvl.12.129.
12. Kuiken T, Holmes EC, McCauley J, Rimmelzwaan GF, Williams CS, Grenfell BT. Host species barriers to influenza virus infections. Science. 2006;312:394–7. http://dx.doi.org/10.1126/science.1122818
13. Davies TJ, Pedersen AB. Phylogeny and geography predict pathogen community similarity in wild primates and humans. Proc Biol Sci. 2008;275:1695–701. http://dx.doi.org/10.1098/rspb.2008.0284
14. Cooper N, Nunn CL. 2013 Identifying future zoonotic disease threats. Evol Med Public Health. 2013;1:27–36. http://dx.doi.org/10.1093/emph/eot001
15. Khabbaz RF, Heneine W, George JR, Parekh B, Rowe T, Woods T, et al. Brief report: infection of a laboratory worker with simian immunodeficiency virus. N Engl J Med. 1994;330:172–7. http://dx.doi.org/10.1056/NEJM199401203300304
16. Sharp PM, Hahn BH. Origins of HIV and the AIDS pandemic. Cold Spring Harb Perspect Med. 2011;1:a006841. http://dx.doi.org/10.1101/cshperspect.a006841
17. Chowell G, Hengartner NW, Castillo-Chavez C, Fenimore PW, Hyman JM. The basic reproductive number of Ebola and the effects of public health measures: the cases of Congo and Uganda. J Theor Biol. 2004;229:119–26. http://dx.doi.org/10.1016/j.jtbi.2004.03.006
18. Schwartz O, Albert ML. Biology and pathogenesis of chikungunya virus. Nat Rev Microbiol. 2010;8:491–500. http://dx.doi.org/10.1038/nrmicro2368
19. Fauci AS, Morens DM. Zika virus in the Americas: yet another arbovirus threat. N Engl J Med. 2016;374:601–4. http://dx.doi.org/10.1056/NEJMp1600297
20. Blumberg S, Lloyd-Smith JO. Inference of $R_{(0)}$ and transmission heterogeneity from the size distribution of stuttering chains. PLOS Comput Biol. 2013;9:e1002993. http://dx.doi.org/10.1371/journal.pcbi.1002993
21. Lord CC, Barnard B, Day K, Hargrove JW, McNamara JJ, Paul RE, et al. Aggregation and distribution of strains in

microparasites. Philos Trans R Soc Lond B Biol Sci. 1999; 354:799–807. http://dx.doi.org/10.1098/rstb.1999.0432
22. Yates A, Antia R, Regoes RR. How do pathogen evolution and host heterogeneity interact in disease emergence? Proc Biol Sci. 2006;273:3075–83. http://dx.doi.org/10.1098/rspb.2006.3681
23. Jansen VA, Stollenwerk N, Jensen HJ, Ramsay ME, Edmunds WJ, Rhodes CJ. Measles outbreaks in a population with declining vaccine uptake. Science. 2003;301:804. http://dx.doi.org/10.1126/science.1086726
24. Woolhouse ME, Gaunt E. Ecological origins of novel human pathogens. In: Relman DA, Hamburg MA, Choffnes ER, Mack A, editors. Microbial evolution and co-adaptation, Washington (DC): National Academies Press; 2009. p. 208–29.
25. Breban R, Riou J, Fontanet A. Interhuman transmissibility of Middle East respiratory syndrome coronavirus: estimation of pandemic risk. Lancet. 2013;382:694–9. http://dx.doi.org/10.1016/S0140-6736(13)61492-0
26. Fine PE, Jezek Z, Grab B, Dixon H. The transmission potential of monkeypox virus in human populations. Int J Epidemiol. 1988;17:643–50. http://dx.doi.org/10.1093/ije/17.3.643
27. Centers for Disease Control and Prevention. Outbreaks chronology: Ebola virus disease [cited 2015 Feb 1]. http://www.cdc.gov/vhf/ebola/outbreaks/history/chronology.html#modalIdString_outbreaks
28. Woolhouse M, Antia R. Emergence of new infectious diseases. In: Stearns SC, Koella JK, editors. Evolution in health and disease. 2nd ed. Oxford (UK): Oxford University Press; 2008. p. 215–28.
29. Domingo E, Martínez-Salas E, Sobrino F, de la Torre JC, Portela A, Ortín J, et al. The quasispecies (extremely heterogeneous) nature of viral RNA genome populations: biological relevance: a review. Gene. 1985;40:1–8. http://dx.doi.org/10.1016/0378-1119(85)90017-4
30. Herfst S, Schrauwen EJ, Linster M, Chutinimitkul S, de Wit E, Munster VJ, et al. Airborne transmission of influenza A/H5N1 virus between ferrets. Science. 2012;336:1534–41. http://dx.doi.org/10.1126/science.1213362
31. Arinaminpathy N, McLean AR. Evolution and emergence of novel human infections. Proc Biol Sci. 2009;276:3937–43. http://dx.doi.org/10.1098/rspb.2009.1059
32. Cotten M, Watson SJ, Zumla AI, Makhdoom HQ, Palser AL, Ong SH, et al. Spread, circulation, and evolution of the Middle East respiratory syndrome coronavirus. MBio. 2014;5:e01062–13. http://dx.doi.org/10.1128/mBio.01062-13
33. Gire SK, Goba A, Andersen KG, Sealfon RS, Park DJ, Kanneh L, et al. Genomic surveillance elucidates Ebola virus origin and transmission during the 2014 outbreak. Science. 2014;345:1369–72. http://dx.doi.org/10.1126/science.1259657
34. Jombart T, Cori A, Didelot X, Cauchemez S, Fraser C, Ferguson N. Bayesian reconstruction of disease outbreaks by combining epidemiologic and genomic data. PLOS Comput Biol. 2014;10:e1003457. http://dx.doi.org/10.1371/journal.pcbi.1003457
35. Volz EM, Kosakovsky Pond SL, Ward MJ, Leigh Brown AJ, Frost SD. Phylodynamics of infectious disease epidemics. Genetics. 2009;183:1421–30. http://dx.doi.org/10.1534/genetics.109.106021
36. Gao R, Cao B, Hu Y, Feng Z, Wang D, Hu W, et al. Human infection with a novel avian-origin influenza A (H7N9) virus. N Engl J Med. 2013;368:1888–97. http://dx.doi.org/10.1056/NEJMoa1304459
37. Lam TT, Wang J, Shen Y, Zhou B, Duan L, Cheung CL, et al. The genesis and source of the H7N9 influenza viruses causing human infections in China. Nature. 2013;502:241–4. http://dx.doi.org/10.1038/nature12515
38. World Health Organization. Blueprint for R&D preparedness and response to public health emergencies due to highly infectious pathogens, 2015 [cited 2016 Aug 21]. http://www.who.int/csr/research-and-development/meeting-report-prioritization.pdf?ua=1
39. Belshaw R, Gardner A, Rambaut A, Pybus OG. Pacing a small cage: mutation and RNA viruses. Trends Ecol Evol. 2008;23:188–93. http://dx.doi.org/10.1016/j.tree.2007.11.010
40. Woolhouse ME, Rambaut A, Kellam P. Lessons from Ebola: improving infectious disease surveillance to inform outbreak management. Sci Transl Med. 2015;7:307rv5. http://dx.doi.org/10.1126/scitranslmed.aab0191

Address for correspondence: Mark E.J. Woolhouse, Centre for Immunity, Infection, and Evolution, University of Edinburgh, Ashworth Laboratories, Charlotte Auerbach Rd, Edinburgh EH9 3FL, UK; email: mark.woolhouse@ed.ac.uk

Investigation of and Response to 2 Plague Cases, Yosemite National Park, California, USA, 2015

Mary Danforth, Mark Novak, Jeannine Petersen, Paul Mead, Luke Kingry, Matthew Weinburke, Danielle Buttke, Gregory Hacker, James Tucker, Michael Niemela, Bryan Jackson, Kerry Padgett, Kelly Liebman, Duc Vugia, Vicki Kramer

Medscape EDUCATION ACTIVITY

This activity has been planned and implemented through the joint providership of Medscape, LLC and *Emerging Infectious Diseases.* Medscape, LLC is accredited by the American Nurses Credentialing Center (ANCC), the Accreditation Council for Pharmacy Education (ACPE), and the Accreditation Council for Continuing Medical Education (ACCME), to provide continuing education for the healthcare team.

Medscape, LLC designates this Journal-based CME activity for a maximum of 1.00 ***AMA PRA Category 1 Credit(s)™***. Physicians should claim only the credit commensurate with the extent of their participation in the activity.

All other clinicians completing this activity will be issued a certificate of participation. To participate in this journal CME activity: (1) review the learning objectives and author disclosures; (2) study the education content; (3) take the post-test with a 75% minimum passing score and complete the evaluation at http://www.medscape.org/journal/eid; and (4) view/print certificate. For CME questions, see page 2241.

Release date: November 16, 2016; Expiration date: November 16, 2017

Learning Objectives

Upon completion of this activity, participants will be able to:

- Interpret laboratory and epidemiologic findings regarding 2 human cases of plague in 2015 in patients with recent travel history to Yosemite National Park
- Assess environmental findings regarding 2 human cases of plague in 2015 in patients with recent travel history to Yosemite National Park
- Identify critical risk reduction measures used to help prevent plague transmission to Yosemite visitors and staff.

CME Editor

P. Lynne Stockton Taylor, VMD, MS, ELS(D), Technical Writer/Editor, *Emerging Infectious Diseases. Disclosure: P. Lynne Stockton Taylor, VMD, MS, ELS(D), has disclosed no relevant financial relationships.*

CME Author

Laurie Barclay, MD, freelance writer and reviewer, Medscape, LLC. *Disclosure: Laurie Barclay, MD, has disclosed the following relevant financial relationships: owns stock, stock options, or bonds from Pfizer.*

Authors

Disclosures: ***Mary E. Danforth, PhD; Mark Novak, PhD; Jeannine Petersen, PhD; Paul Mead, PhD, MPH; Luke Kingry, PhD; Matthew Weinburke, MPH; Danielle Buttke, DVM, PhD, MPH; Gregory Hacker, MSc; James R. Tucker, MS; Michael Niemela, MS; Bryan T. Jackson, PhD; Kerry Padgett, PhD; Kelly Liebman, PhD, MPH; Duc Vugia, MD, MPH;*** *and* ***Vicki Kramer, PhD,*** *have disclosed no relevant financial relationships..*

Author affiliations: California Department of Public Health, Sacramento, California, USA (M. Danforth, M. Novak, G. Hacker, J. Tucker, M. Niemela, B. Jackson, K. Padgett, K. Liebman, D. Vugia, V. Kramer); Centers for Disease Control and Prevention, Fort Collins, Colorado, USA (J. Petersen, P. Mead, L. Kingry); National Park Service, El Portal, California, and Fort Collins, Colorado, USA (M. Weinburke, D. Buttke)

DOI: http://dx.doi.org/10.3201/eid2212.160560

In August 2015, plague was diagnosed for 2 persons who had visited Yosemite National Park in California, USA. One case was septicemic and the other bubonic. Subsequent environmental investigation identified probable locations of exposure for each patient and evidence of epizootic plague in other areas of the park. Transmission of *Yersinia pestis* was detected by testing rodent serum, fleas, and rodent carcasses. The environmental investigation and whole-genome multilocus sequence typing of *Y. pestis* isolates from

the patients and environmental samples indicated that the patients had been exposed in different locations and that at least 2 distinct strains of *Y. pestis* were circulating among vector–host populations in the area. Public education efforts and insecticide applications in select areas to control rodent fleas probably reduced the risk for plague transmission to park visitors and staff.

Plague is a zoonotic disease caused by the gram-negative bacterium *Yersinia pestis*; the organism's reservoir is rodents and the vectors are fleas (*1*,*2*). Transmission to humans can occur through bites by infected fleas or through handling *Y. pestis*–infected rodents (*1*,*2*). Epidemics of plague still occur on the continents of Africa, Asia, and North and South America (*3*). Plague was introduced to California in 1900 (*1*,*4*–*6*), where over the next 25 years it caused occasional outbreaks in rats commensally residing with humans in urban areas (*2*,*4*,*6*). Shortly after its introduction, *Y. pestis* moved into wild rodent populations, establishing a sylvatic transmission cycle (*7*,*8*). In subsequent decades, plague spread across California and other western states (*9*) periodically affecting humans (*4*–*6*,*10*–*13*).

The human risk of contracting plague is higher during epizootic transmission when *Y. pestis* is amplified among susceptible rodent hosts (*2*), such as the California ground squirrel (*Otospermophilus beecheyi*), the golden-mantled ground squirrel (*Callospermophilus lateralis*), and certain chipmunk species (*Tamias* spp.) (*2*,*3*,*14*,*15*). Higher mortality rates among these animals lead to the release of infectious fleas into the environment (*2*). The California ground squirrel plays a major role in human exposure in California because its predominant flea species, *Oropsylla montana*, is a competent *Y. pestis* vector (*1*,*2*) that is often abundant on this rodent and in its burrows (*16*) and will readily bite humans (*1*,*11*). Since the 1980s, evidence of *Y. pestis* transmission in rodents in the Sierra Nevada mountains has been generally restricted to locations at elevations >1,200 meters (California Department of Public Health, unpub. data, 1983–2015). Despite ongoing sylvatic transmission, human plague remains rare in the western United States (*17*–*19*), including in California, where no cases have been confirmed since 2006 (*20*,*21*).

During the summer of 2015, the Los Angeles County Department of Public Health (LACDPH) and the Georgia Department of Public Health reported 2 cases of plague in persons who had recently travelled to Yosemite National Park (Yosemite). The California Department of Public Health (CDPH), in collaboration with the US Centers for Disease Control and Prevention (CDC) and the National Park Service (NPS), investigated the increased *Y. pestis* transmission in Yosemite. We summarize the epidemiologic, laboratory, and environmental findings and the public health response.

Methods

Epidemiologic and Laboratory Investigation

We defined a case of plague as clinically compatible illness and isolation of *Y. pestis* from a person with a history of travel to Yosemite during the 7 days before illness onset. Clinically compatible illness included fever, headache, chills, and malaise in conjunction with regional lymphadenitis, septicemia, or pneumonia (*22*). Patients were identified by their county or state health department and reported to CDPH or CDC.

Diagnosis of plague was made after PCR testing of clinical specimens, including blood and bubo aspirates; Laboratory Response Network assays and culture were used. Recovered isolates were confirmed as *Y. pestis* by bacteriophage lysis (*23*). For whole-genome multilocus sequence typing (MLST), DNA extracted from *Y. pestis* isolates was sequenced by using the PacBio RS II platform and sequence reads were assembled by using a hierarchal genome assembly process (Pacific Biosciences, Menlo Park, CA, USA). Allele calls for 3,979 *Y. pestis* open reading frames (ORFs) (4,046,060 bp) and cluster analyses were performed as described (*24*).

Local and state public health officials interviewed patients with confirmed cases and their family members who had traveled with them. Respondents were asked about their illness history, travel, activities, and interactions with rodents in and around the Yosemite area during the week before illness onset.

Environmental Investigation

The environmental investigation was prioritized by patient travel itineraries and historical evidence of *Y. pestis* transmission at these locations or in similar habitats. To assess the scope of *Y. pestis* transmission and the potential exposure risk for visitors and park personnel, the investigation was expanded to include additional locations in Yosemite. At prioritized locations, visual risk assessments were conducted to evaluate the presence and abundance of rodents, the type of human activities in the area, and the potential for human exposure to infective fleas (*25*). In areas with suspected *Y. pestis* transmission, a 30 × 30 cm flannel cloth was used to sample fleas from rodent burrow entrances. Rodents were live-trapped for plague serologic testing and flea collection (*25*). For rodent trapping, Sherman (H.B. Sherman Traps, Tallahassee, FL, USA) and Tomahawk (Tomahawk Live Trap, Hazelhurst, WI, USA) live traps were baited once with a mixture of grains and opened either from overnight through the following midday or from early morning through noon. Relative rodent abundance was estimated by calculating the ratio of captured rodents to the total number of traps set and is referred to as the trap

success rate. Captured rodents were anesthetized with isoflurane, identified to species, brushed to collect fleas, and subjected to collection of ≈0.1 mL of blood for *Y. pestis* antibody testing. Deer mice (*Peromyscus maniculatus*) collected near structures were euthanized; all other rodents were marked with a numbered ear tag (National Band & Tag Company, Newport, KY, USA) and released near the point of capture. Small mammal handling techniques were reviewed and approved by the CDPH Institutional Animal Care and Use Committee, protocol 2015-14. In addition to live rodent trapping, rodent carcasses reported by Yosemite staff or visitors were collected for testing.

Flea and rodent specimens were tested for *Y. pestis* by CDPH, CDC, and NPS. Blood samples from trapped rodents were sent to CDPH for concurrent testing by passive hemagglutination and passive hemagglutination inhibition to detect antibodies against *Y. pestis* F1 antigen (*23*). All positive passive hemagglutination titers ≥1:32, the lowest dilution tested, that were negative by passive hemagglutination inhibition were considered positive (*23*). Fleas collected by burrow swabbing, from live-captured rodents, or from rodent carcasses were sent to CDPH or CDC to be identified to species according to standard taxonomic keys (*26*) and to be tested for *Y. pestis*. Fleas of the same species from the same burrow or rodent host were sorted into pools of up to 10 fleas and then homogenized in brain–heart infusion broth by using glass beads and Mixer Mill MM301 (Retsch, Haan, Germany).

Rodent carcasses were tested at CDPH, CDC, and NPS. Spleen and liver tissues were removed; for direct fluorescent antibody testing, slide touch tissue preparations were incubated with fluorescein isothiocyanate–labeled rabbit anti-F1 antibodies, washed, and then viewed by fluorescence microscopy (*23*). DNA was extracted from flea homogenates and carcass tissues by using the MagNA Pure Compact Nucleic Acid Isolation Kit (Roche Diagnostics, Basel, Switzerland) and amplified by using TaqMan primers and probe targeting the *caf1* gene (*27*). Animal and flea specimens positive by PCR were inoculated onto sheep blood agar plates or onto cefsulodin-irgasan-novobiocin agar plates to enable isolation of *Y. pestis* from contaminated environmental samples (*23*). Isolates were confirmed as *Y. pestis* by bacteriophage lysis and typed by whole-genome MLST (*24*) with the exception that genome sequencing was performed with the MiSeq platform (Nextera XT library preparation, MiSeq Reagent Kit v2, 300 cycle; Illumina, San Diego, CA, USA). Read corrections and assemblies were generated by using SPAdes 3.6 (*28*). All diagnostic tests were performed by using standard negative and positive controls.

Results

Laboratory and Epidemiologic Findings

On August 2, 2015, LACDPH presumptively diagnosed septicemic plague for a 14-year-old male resident of Los Angeles County (patient 1) and reported the suspected case to CDPH and CDC (L. Tovar Padua, David Geffen UCLA School of Medicine, pers. comm., 2016 Jan 7). LACDPH later confirmed the diagnosis. The patient became symptomatic on July 18, after camping at Crane Flat Campground in Yosemite July 12–17 and visiting Yosemite Valley and Rainbow Pool Day Use Area (Stanislaus National

Table 1. *Yersinia pestis* transmission risk assessments in and around Yosemite National Park, California, USA, August–October 2015*

Site	Association	Name	Jurisdiction	Elevation, m	Assessment activity*	*Y. pestis* detection
1	Patient 1 visited	Rainbow Pool Day Use Area	Stanislaus National Forest	850	V, B	None
2	Patient 1 visited	Crane Flat CG	Yosemite National Park	1,890	V, B, T, C	Serology +, flea pool +
3	Patients 1 and 2 visited	Yosemite Valley	Yosemite National Park	1,220	H, V, T, C	None
4	Patient 2 visited	Glacier Point	Yosemite National Park	2,190	V, B, T	Serology +
5	Patient 2 visited	Sentinel Dome	Yosemite National Park	2,470	V, B	None
6	Patient 2 visited	Vernal Falls	Yosemite National Park	1,510	V, B	None
7	Patient 2 visited	Bass Lake	Sierra National Forest	1,040	H	None
8	Patient 2 visited	Lewis Creek	Sierra National Forest	1,280	V, B	None
9	Patient 2 visited	Nelder Grove	Sierra National Forest	1,640	V, B	None
10	Expanded investigation	White Wolf CG	Yosemite National Park	2,400	V	None
11	Expanded investigation	Porcupine Flat CG	Yosemite National Park	2,480	V	None
12	Expanded investigation	Tamarack Flat CG	Yosemite National Park	1,940	V, B, T	Serology +
13	Expanded investigation	Hodgdon Meadows CG	Yosemite National Park	1,450	V	None
14	Expanded investigation	Tuolumne Meadows	Yosemite National Park	2,620	V, B, T, C	Serology +, flea pool +, carcass +
15	Expanded investigation	Crane Flat–NatureBridge Campus	Yosemite National Park	1,890	V	None
16	Expanded investigation	Wawona	Yosemite National Park	1,220	C	None
17	Expanded investigation	Bridalveil Creek CG	Yosemite National Park	2,130	V	None

*B, burrow swabbing; C, carcass collection; CG, campground; H, historical review; T, rodent trapping; V, visual assessment; +, positive for *Y. pestis*.

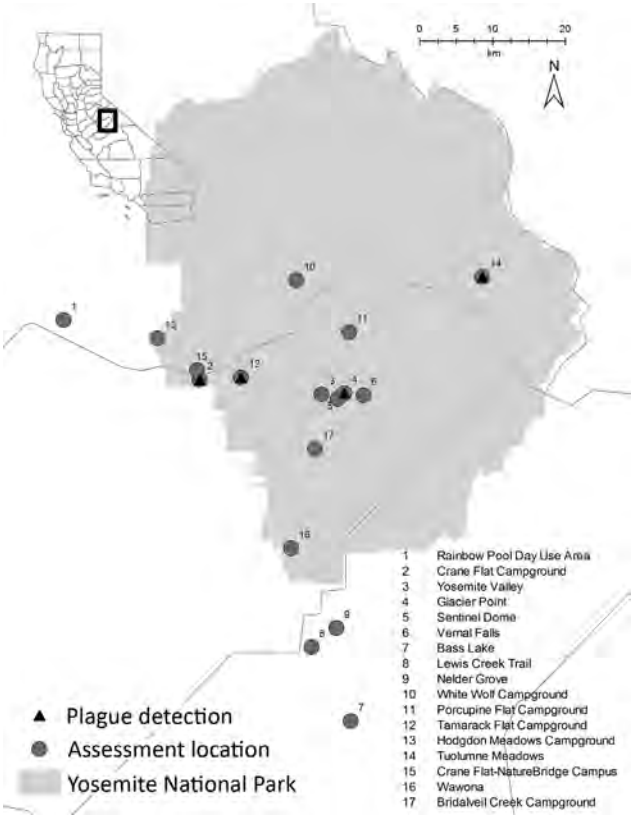

Figure 1. Locations of plague transmission risk assessments in and around Yosemite National Park, California, USA, August–October 2015.

Forest) during this period (Table 1; Figure 1). He reported that he fed squirrels but did not touch them (L. Tovar Padua, pers. comm., 2016 Jan 7).

On August 14, the Georgia Department of Public Health presumptively diagnosed bubonic plague for an 18-year-old female resident of Georgia (patient 2) after she had become symptomatic on August 11. On the same day, CDC was notified of the suspected case and later confirmed the diagnosis. During the prior week, this patient had stayed in a rental home in Oakhurst, California, and visited Yosemite Valley, Vernal Falls, Glacier Point, and Sentinel Dome in Yosemite, as well as Nelder Grove, Lewis Creek, and Bass Lake in the adjacent Sierra National Forest (Table 1; Figure 1). Patient 2 reported having observed numerous squirrels in her vicinity at Vernal Falls and Glacier Point but did not report having had any contact with them.

Neither patient reported seeing dead rodents. Whole-genome MLST showed that the genome sequence of *Y. pestis* isolates from each patient (blood culture from patient 1, bubo aspirate from patient 2) differed at 21 ORFs (Table 2; Figure 2), including 18 single-nucleotide polymorphisms (SNPs). Each patient was accompanied on the trip by family members who did not become ill.

Environmental Findings

Plague risk assessments were conducted for 9 locations in Yosemite and the surrounding national forests visited by the patients (Table 1; Figure 1). Within the park, 8 more sites were also evaluated for *Y. pestis* transmission and potential risk areas for transmission to humans.

Sites Visited by Patient 1

On August 4, the Rainbow Pool Day Use Area (Table 1; Figure 1) was evaluated and deemed to be an area of low risk because of the lack of historical documentation of plague at this habitat and elevation, low abundance of California ground squirrels observed in the day use area, and lack of other diurnal rodent species that are known *Y. pestis* reservoirs in this region. Limited burrow swabbing collected no fleas. A visual evaluation of Yosemite Valley (Table 1; Figure 1) was postponed because it similarly lacked historical documentation of local *Y. pestis* transmission and because no reports of sick or dying rodents from this heavily visited area had been received. The next week, numerous healthy California ground squirrels were noted in Yosemite Valley. At Crane Flat Campground (Table 1; Figure 1), visual assessment and subsequent burrow swabbing suggested recent epizootic activity; California ground squirrel abundance seemed to be very low relative to the number of burrows in the campground, abandoned burrows were noted, and 134 *Y. pestis*–negative fleas were collected from the entrances of 29 (31.5%) of 94 burrows sampled. Carrion flies (*Calliphora latifrons*) were also collected or observed at several burrows. Few chipmunks were observed in the campground, but several Douglas squirrels (*Tamiasciurus douglasii*) were noted. Rodent trapping conducted the following day corroborated the low abundance of rodents (trap success rate 6.9%; Table 3). *Y. pestis* antibodies were detected in 1 (12.5%) of 8 California ground squirrels (Table 4), and a pool of 8 *O. montana* fleas collected from a seronegative California ground squirrel tested positive by PCR for *Y. pestis* (Table 3). Subsequent whole-genome MLST of *Y. pestis* recovered from this flea pool demonstrated 100% sequence identity across all ORFs when compared with the isolate from patient 1 (Figure 2).

Sites Visited by Patient 2

The 7 locations visited by patient 2 were evaluated on August 18 and 19 (Table 1; Figure 1). Bass Lake was not visually assessed because of the historic lack of plague activity in this area. Visual assessments and burrow swabbing at Sentinel Dome, Vernal Falls, Nelder Grove, and Lewis Creek found no obvious indications of *Y. pestis* transmission or increased human risk. Initial evaluation at Glacier Point revealed several abandoned California ground squirrel burrows in close proximity to pathways and picnic areas. From the entrances of the 2 burrows swabbed, 21 fleas

Table 2. MLST alleles in whole-genome sequences of *Yersinia pestis* isolates recovered from humans, animals, and fleas, Yosemite National Park, California, USA, August 2015*†

MLST allele, ORF	*Y. pestis* strain CO92 genome position	Mutation type‡	Group 1 isolates§	Group 2 isolates¶
YPCD1.31	22450	SNP	T	C
YPMT1.46	48841	SNP	T	C
YPO0193	211446	6-bp VNTR	–	Loss
YPO0445	467549	1-bp INDEL	–	Deletion
YPO0776	Multiple	9-bp VNTR	Loss	Gain
YPO0894	980089	15-bp VNTR	–	Gain
YPO0968	1072143	SNP	C	T
YPO0976	1084232	SNP	G	T
YPO1332	1498571	SNP	T	C
YPO1422	1617725	18-bp VNTR	Loss	–
YPO1705	1946021	SNP	C	T
YPO2153	2423508	SNP	C	G
YPO2253	2531428	SNP	T	A
YPO2556	2871852	6-bp VNTR	Gain	–
YPO2840	3170905	SNP	T	A
YPO2842	3172167	SNP	T	G
YPO2859	3196474	SNP	A	T
YPO3032	3385894	SNP	A	G
YPO3339	3725154	SNP	T	C
YPO3409	3807578	SNP	T	C
YPO3419	3821161	SNP	C	T
YPO3481	3886839	SNP	C	T
YPO3490	3898668	SNP	T	C
YPO3828	4296699	8-bp INDEL	–	Insertion
YPO4068	4587603	SNP	G	T

*INDEL, insertion/deletion; MLST, multilocus sequence typing; ORF, open reading frame; SNP, single-nucleotide polymorphism; VNTR, variable number of tandem repeats; –, none.
†PacBio (Pacific Biosciences, Menlo Park, CA, USA) sequencing of patient isolates yielded an average read length of 15,541 bp with 83,608 average filtered subreads and an average quality and coverage of 84.5% and 202×, respectively. Illumina MiSeq sequencing of flea and animal isolates yielded an average ContigN50 of 40,440 for the 6 assemblies and an average read coverage depth of 84.35×.
‡Gain/loss and insertion/deletion are relative to the CO92 reference genome. All identified SNPs, VNTRs, and INDELs demonstrated at least 10× sequence coverage and 100% of the base calls confirming the mutation.
§Group 1; patient 1, flea pool from Crane Flat, animals from Tuolumne Meadows.
¶Group 2; patient 2.

were collected. The rodents observed in the area were habituated to humans, and several were noted coming in close proximity to visitors. On the basis of these assessments, Glacier Point was identified as a potential exposure site for patient 2. Rodents were subsequently trapped and tested (Table 3); 1 (7.1%) of 14 California ground squirrels and 2 (22.2%) of 9 lodgepole chipmunks (*Tamias speciosus*) were seropositive (Table 4). All 118 flea pools obtained from Glacier Point, via burrow swabbing or rodent trapping, were negative for *Y. pestis* by PCR.

Expanded Investigation

On August 10, NPS was notified that 2 dead rodents were found in the Tuolumne Meadows Campground, ≈25 km from the nearest location visited by the patients (Table 1; Figure 1). During the initial assessment, NPS and CDPH staff observed normal rodent diversity and abundance for this location and no fleas were captured by burrow swabbing. Over the following month, 21 rodent carcasses were collected from the campground and adjacent locations, 17 of which were tested for *Y. pestis*; the remaining 4 were too decomposed for testing. The 2 golden-mantled ground squirrel carcasses collected on August 10 and 8 additional rodent carcasses collected in the campground and surrounding area were positive for *Y. pestis* (Table 4). Flea pools from 2 of the rodent carcasses (1 *Megarthroglossus divisus* flea from a Douglas squirrel, 5 *Ceratophyllus ciliatus mononis* fleas from a lodgepole chipmunk) were also

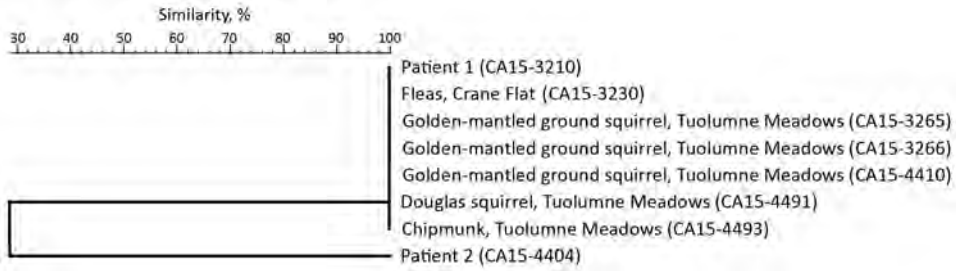

Figure 2. Sequencing results, based on percent similarity, for *Yersinia pestis* isolates from Yosemite National Park, California, USA, August–October 2015.

positive by PCR for *Y. pestis* (Table 4). Of the 18 lodgepole chipmunks trapped in this area (Table 3), 3 (16.7%) were positive for *Y. pestis* antibodies (Table 4). A flea pool (3 *Peromyscopsylla hesperomys adelpha* fleas) from a seronegative deer mouse also tested positive for *Y. pestis* (Table 4). Whole-genome MLST of 5 *Y. pestis* isolates recovered from carcasses from Tuolumne Meadows showed that their genome sequences shared 100% sequence identity across all ORFs, compared with the isolates recovered from patient 1 and the flea pool from Crane Flat Campground (Figure 2).

The expanded environmental investigation found evidence of *Y. pestis* transmission at 1 other location (Table 1; Figure 1). Two visual assessments at Tamarack Flat Campground noted a lower than expected abundance and diversity of rodents and numerous abandoned California ground squirrel burrows. Follow-up trapping (Table 3) led to detection of *Y. pestis* antibodies in 1 (20.0%) of 5 California ground squirrels tested (Table 4). Rodent trapping for testing was also conducted in Yosemite Valley in mid-October. None of 13 California ground squirrels and 15 *Peromyscus* mice tested positive for *Y. pestis* antibodies (Table 3). Six rodent carcasses from developed sites in Yosemite Valley and 3 from the Wawona area also tested negative for *Y. pestis*.

Flea Control

Sites with evidence of recent *Y. pestis* transmission and an increased risk for human exposure were temporarily closed, and rodent burrows were treated with insecticide to reduce flea populations and protect wildlife and human health. The following 5 areas in Yosemite were identified for insecticide treatments: Crane Flat Campground, Glacier Point, Tuolumne Meadows Campground, Tamarack Flat Campground, and the Crane Flat–NatureBridge campus. In total, 16.3 kg of 0.05% deltamethrin was used per label instructions to treat an estimated 3,700 rodent burrows. Although time and logistical constraints precluded pre- and posttreatment flea evaluations at all locations, evidence from limited sampling suggested that the insecticide applications reduced the local flea populations. Before treatment at Crane Flat Campground, 134 fleas had been collected from 94 burrows and the California ground squirrel flea index (total no. fleas on rodents/total no. rodents) was 17.5. After the insecticide application, 58 treated burrows yielded no fleas and the California ground squirrel flea index was 1.0. After insecticide application at Glacier Point, the California ground squirrel flea index declined from 8.1 to 2.7. No pretreatment rodent trapping was conducted at the Tuolumne Meadows Campground to provide comparative flea indices for rodents, but the posttreatment flea index for ground-dwelling rodents was 0.9. Before insecticide application at this site, 80 rodent burrows were marked and sampled, yielding a total of 6 fleas; after treatment, no fleas were found at those same burrows.

Public Outreach

To further reduce the plague risk for Yosemite visitors and staff, NPS and collaborating agencies initiated an aggressive public education campaign. In 2014, ≈4 million persons visited Yosemite (*29*), and, given that plague cases are rare in the United States, it could not be assumed that most visitors were aware of plague risk or prevention measures. The public education campaign included 3 news releases issued August 6–18, media interviews, and website alerts. The park newsletter, The Yosemite Guide, which was given to persons in every entering vehicle, included information about plague. Placards with plague information were posted at park entrances, locations with confirmed *Y. pestis* transmission, all campgrounds, and many day use locations and trailheads. Educational pamphlets were available to visitors at a variety of locations, including affected campgrounds.

Discussion

In August 2015, these 2 cases of plague were linked to exposure in the internationally popular Yosemite National Park. The initial public health investigation and response with broad media coverage of the first case led to the rapid recognition and appropriate treatment of the second case-patient (*30*).

The investigation found little overlap in the travel itineraries of the 2 patients, and isolation of distinct strains of

Table 3. Summary of rodent trapping and seroprevalence of *Yersinia pestis*, by location, Yosemite National Park, August 5–October 22, 2015

Date	Location	Traps set, no.	Rodents caught, no.	Trap success, %	Rodents tested, no.	*Y. pestis*–positive rodents, no.	*Y. pestis* seroprevalence, %
Aug 5	Crane Flat CG	160	11	6.9	11	1	9.1
Aug 25	Glacier Point	100	30	30.0*	27	2	7.4
Aug 25	Crane Flat CG	100	13	13.0*	13	0	0
Aug 25	Tamarack Flat CG	60	11	18.3*	11	1	9.1
Aug 26	Tuolumne Meadows	208	70	33.7*	68	3	4.4
Sep 24	Glacier Point	108	33	30.6	6	1	16.7
Oct 22	Yosemite Valley	175	34	19.4	28	0	0
Total	All	911	202	22.2	164	8	4.9

*Trapping event included overnight hours, which extended the trapping period an additional 12–14 h. CG, campground.

Table 4. Summary of *Yersinia pestis*–positive samples, Yosemite National Park, August 5–October 22, 2015*

Location and date	Species	Sample type (titer or test)	Sequence identification no.
Crane Flat CG			
Aug 5	California ground squirrel	Serum (titer 1:64)	NA
Aug 5	California ground squirrel	Flea pool (DFA, PCR, wgMSLT)	CA15-3230
Tuolumne Meadows			
Aug 10	Golden-mantled ground squirrel	Carcass (DFA, PCR, wgMSLT)	CA15-3265
Aug 10	Golden-mantled ground squirrel	Carcass (DFA, PCR, wgMSLT)	CA15-3266
Aug 11	Chipmunk (species unknown)	Carcass (PCR)	NA
Aug 12	Golden-mantled ground squirrel	Carcass (DFA, wgMSLT)	CA15-4410
Aug 14	Chipmunk (species unknown)	Carcass (DFA, culture)	NA
Aug 17	Lodgepole chipmunk	Carcass (DFA, PCR, culture)	NA
Aug 26	Douglas squirrel	Carcass (DFA, PCR, wgMSLT); flea pool (PCR)	CA15-4491
Aug 26	Lodgepole chipmunk	Carcass (DFA, PCR, wgMLST); flea pool (PCR)	CA15-4493
Aug 26	Lodgepole chipmunk	Serum (1:1,024)	NA
Aug 26	Lodgepole chipmunk	Serum (1:512)	NA
Aug 26	Lodgepole chipmunk	Serum (1:128)	NA
Aug 26	Deer mouse	Flea pool (PCR)	NA
Sep 6	Chipmunk (species unknown)	Carcass (PCR)	NA
Sep 8	Chipmunk (species unknown)	Carcass (PCR)	NA
Glacier Point			NA
Aug 25	California ground squirrel	Serum (1:64)	NA
Aug 25	Lodgepole chipmunk	Serum (1:128)	NA
Sep 24	Lodgepole chipmunk	Serum (1:4,096)	NA
Tamarack Flat CG			
Aug 25	California ground squirrel	Serum (1:128)	NA

*Samples analyzed by wgMLST were cultured first. CG, campground; DFA, direct fluorescence antibody; NA, not applicable because sequencing was not performed; wgMLST, whole-genome multilocus sequence typing.

Y. pestis suggested that at least 2 *Y. pestis* strains were circulating among vector–host populations in the Yosemite area. In the only area visited by both patients, Yosemite Valley, no evidence of *Y. pestis* transmission in rodents was found, and *Y. pestis* has not been detected in the valley's rodent populations in recent decades (CDPH, unpub. data, 1984–2015). We were able to connect the exposure of patient 1 to epizootic transmission at the campground on the basis of the visual observations at Crane Flat Campground, the positive results for rodent serology and the pool of fleas collected there, and whole-genome MLST analysis of *Y. pestis* isolates from patient 1 and the flea pool. The most likely exposure site for patient 2 was Glacier Point, 20 km away, on the opposite side of Yosemite Valley. Although *Y. pestis*–seropositive rodents were found at this location, we did not detect active infection in rodents or fleas and were therefore unable to directly link the patients' exposure to this site by whole-genome MLST. Previous findings indicate that *Y. pestis* whole-genome MLST alleles are not rapidly changing and that most detected changes are caused by the more slowly evolving SNPs than by more rapidly changing variable number tandem repeats (*24*). Our results are consistent with those of a previous SNP-based study, which indicated that widespread plague epizootics are caused by multiple *Y. pestis* clones arising independently in small geographic areas (*31*).

The environmental investigation found evidence of *Y. pestis* transmission in disparate locations of the park, including epizootic activity in the Tuolumne Meadows area, ≈41 and 25 km from Crane Flat and Glacier Point, respectively. Evidence of *Y. pestis* transmission in rodents was found at 4 of the 5 areas trapped. Of the 8 species of rodents live trapped in Yosemite, *Y. pestis* antibodies were detected in only 5 (15.2%) of 33 lodgepole chipmunks and 3 (7.3%) of 41 California ground squirrels (Table 5). However, *Y. pestis* was also isolated from golden-mantled ground squirrel and Douglas squirrel carcasses and a deer mouse flea, indicating broader zoonotic involvement.

Table 5. Summary of *Yersinia pestis* serology results, by species, Yosemite National Park, August 5–October 22, 2015

Animal (taxonomic name)	Tested, no.	*Y. pestis*–positive rodents, no.	*Y. pestis* seroprevalence, %
Deer mouse (*Peromyscus maniculatus*)	59	0	0
California ground squirrel (*Otospermophilus beecheyi*)	41	3	7.3
Lodgepole chipmunk (*Tamias speciosus*)	33	5	15.2
Golden-mantled ground squirrel (*Callospermophilus lateralis*)	18	0	0
Brush mouse (*Peromyscus boylii*)	6	0	0
Douglas squirrel (*Tamiasciurus douglasii*)	5	0	0
Belding's ground squirrel (*Urocitellus beldingi*)	1	0	0
Long-tailed vole (*Microtus longicaudus*)	1	0	0
Total	164	8	4.9

During the environmental investigation, serum samples collected from 2 bears killed in Yosemite earlier in the summer were positive for *Y. pestis* antibodies. One bear, killed in July on Tioga Road ≈18 km from Crane Flat Campground, was a cub, indicating that exposure was probably recent. Bears serve as sentinels for plague distribution (*32*), and in recent decades ≈10% of bear blood samples from the Yosemite area have been positive for *Y. pestis* antibodies (CDPH, unpub. data, 1980–2015).

In addition to Yosemite, in 2015, increased *Y. pestis* transmission was evident in other parts of the Sierra Nevada mountains (*33*). Rodent trapping conducted by CDPH in May and June found elevated *Y. pestis* seroprevalence among rodents in Tulare County. A golden-mantled ground squirrel carcass collected in August from Sequoia-Kings Canyon National Park, also in Tulare County, tested positive. In August, evidence of epizootic activity was also detected in Mono and El Dorado Counties.

The plague activity in Yosemite and other parts of California in 2015 was part of a larger regional trend. Although plague is rare in the United States (median 3 human cases/year during 2001–2012) (*17–19*), in 2015, the rate increased in western states (16 cases reported to CDC) (*19*,*34*). Synchronous increases in *Y. pestis* transmission in the western United States have been documented previously and are potentially driven by large-scale climatic trends (*35*).

The 2015 findings for Yosemite share some striking similarities with those associated with the only human plague case previously associated with Yosemite (*36*). In 1959, a teenage boy became ill after camping along Yosemite Creek trail, ≈5 km from Crane Flat Campground. Subsequent investigation by CDPH and CDC found evidence of a recent epizootic plague event that had decimated the rodent populations near the campsite. During this investigation, *Y. pestis* transmission was also documented in Tuolumne Meadows and at Lake Tenaya.

The rapid interagency investigation and public health response to these cases probably reduced the risk for plague among Yosemite visitors and staff. Critical risk-reduction measures included expanding the investigation to recreational sites beyond those visited by the patients and localized insecticide treatments at sites with *Y. pestis* transmission. Increased educational efforts informing the public about how to reduce their exposure to the cause of this potentially fatal disease contributed to the early diagnosis for patient 2 and to increased reports of finding dead rodents in the park, which led to detection of *Y. pestis* transmission at additional locations.

Acknowledgments

We thank Ben Schwartz, Rachel Civen, Nicole Green, Amanda Kamali, Chelsea Foo, Cherie Drenzek, Amanda Feldpausch, Wendy Smith, and Laura Edison, who identified and interviewed the patients, assisted in the environmental investigation, and conducted the patient diagnostics. We are deeply grateful to Kenneth Gage, Rebecca Eisen, Karen Boegler, John Montenieri, Don Neubacher, Ron Bourne, Linda Mazzu, Caitlin Lee-Roney, Garrett Dickman, Myron Grissom, and David Wong. We also thank Gil Chavez and James Watt for their support of the investigation and response, and we thank the CDPH Vector Borne Disease Section staff for their assistance with the environmental investigation and rodent serology work, particularly Renjie Hu, Joe Burns, Sarah Billeter, Melissa Yoshimizu, Robert Payne, and Robert Dugger. In addition, we extend our appreciation to all the laboratory staff members who tested samples from patients and the environment, including Marty Schriefer, John Young, Ryan Pappert, Chris Sexton, Brook Yockey, Laurel Respicio-Kingry, Fengfeng Xu, Rose Longoria, Yismashoa Gebremichael, Margot Graves, Vishnu Chaturvedi, and Elizabeth Wheeler. We also thank the CDC Genome Sequencing Laboratory for PacBio sequencing. Last, we thank the Delaware North Corporation for their cooperation and assistance with the investigation.

This study was partially supported by contract funding from the NPS to Public Health Foundation Enterprises.

Dr. Danforth is a biologist with Public Health Foundation Enterprises assigned to CDPH. Her research interests focus on public health and the epidemiology of vectorborne diseases.

References

1. Pollitzer R. Plague. Geneva: World Health Organization. 1954.
2. Perry RD, Fetherston JD. *Yersinia pestis*—etiologic agent of plague. Clin Microbiol Rev. 1997;10:35–66.
3. Gage KL, Kosoy MY. Natural history of plague: perspectives from more than a century of research. Annu Rev Entomol. 2005;50:505–28. http://dx.doi.org/10.1146/annurev.ento.50.071803.130337
4. Link VB. A history of plague in United States of America. Public Health Monogr. 1955;26:1–120.
5. Caten JL, Kartman L. Human plague in the United States, 1900–1966. JAMA. 1968;205:333–6. http://dx.doi.org/10.1001/jama.1968.03140320027008
6. Kugeler KJ, Staples JE, Hinckley AF, Gage KL, Mead PS. Epidemiology of human plague in the United States, 1900–2012. Emerg Infect Dis. 2015;21:16–22. http://dx.doi.org/10.3201/eid2101.140564
7. Barnes A. Surveillance and control of bubonic plague in the United States. Symposium of the Zoological Society of London. 1982;50:237–70.
8. Inglesby TV, Dennis DT, Henderson DA, Bartlett JG, Ascher MS, Eitzen E, et al. Plague as a biological weapon: medical and public health management. Working Group on Civilian Biodefense. JAMA. 2000;283:2281–90. http://dx.doi.org/10.1001/jama.283.17.2281
9. Antolin JF, Gober P, Luce B, Biggins DE, van Pelt WE, Seery DB, et al. The influence of sylvatic plague on North American wildlife at the landscape level, with special emphasis on black-footed ferret and prairie dog conservation. In: Transactions of the 67th North American Wildlife and Natural Resources Conference; 2002 Apr 3–7. Washington (DC): Wildlife Management Institute; 2002.

10. Centers for Disease Control and Prevention. Human plague—four states, 2006. MMWR Morb Mortal Wkly Rep. 2006;55:940–3.
11. Craven RB, Maupin GO, Beard ML, Quan TJ, Barnes AM. Reported cases of human plague infections in the United States, 1970–1991. J Med Entomol. 1993;30:758–61. http://dx.doi.org/10.1093/jmedent/30.4.758
12. Wong D, Wild MA, Walburger MA, Higgins CL, Callahan M, Czarnecki LA, et al. Primary pneumonic plague contracted from a mountain lion carcass. Clin Infect Dis. 2009;49:e33–8. http://dx.doi.org/10.1086/600818
13. Lowell JL, Wagner DM, Atshabar B, Antolin MF, Vogler AJ, Keim P, et al. Identifying sources of human exposure to plague. J Clin Microbiol. 2005;43:650–6. http://dx.doi.org/10.1128/JCM.43.2.650-656.2005
14. Smith CR, Tucker JR, Wilson BA, Clover JR. Plague studies in California: a review of long-term disease activity, flea-host relationships and plague ecology in the coniferous forests of the Southern Cascades and northern Sierra Nevada mountains. J Vector Ecol. 2010;35:1–12. http://dx.doi.org/10.1111/j.1948-7134.2010.00051.x
15. Wherry WB. Plague among the ground squirrels of California. J Infect Dis. 1908;5:485–506. http://dx.doi.org/10.1093/infdis/5.5.485
16. Lang JD. Factors affecting the seasonal abundance of ground squirrel and wood rat fleas (Siphonaptera) in San Diego County, California. J Med Entomol. 1996;33:790–804. http://dx.doi.org/10.1093/jmedent/33.5.790
17. Centers for Disease Control and Prevention. Imported plague—New York City, 2002. MMWR Morb Mortal Wkly Rep. 2003;52:725–8.
18. Eisen RJ, Enscore RE, Biggerstaff BJ, Reynolds PJ, Ettestad P, Brown T, et al. Human plague in the southwestern United States, 1957–2004: spatial models of elevated risk of human exposure to *Yersinia pestis.* J Med Entomol. 2007;44:530–7. http://dx.doi.org/10.1603/0022-2585(2007)44[530:HPITSU]2.0.CO;2
19. Kwit N, Nelson C, Kugeler K, Petersen J, Plante L, Yaglom H, et al. Human plague—United States, 2015. MMWR Morb Mortal Wkly Rep. 2015;64:918–9. http://dx.doi.org/10.15585/mmwr.mm6433a6
20. California Department of Public Health. Yearly summaries of selected general communicable diseases in California, 2001–2010. Sacramento (CA): The Department; 2015.
21. California Department of Public Health. Yearly summaries of selected general communicable diseases in California, 2011–2014. Sacramento (CA): The Department; 2015.
22. Centers for Disease Control and Prevention. Nationally notifiable diseases surveillance system: plague (*Yersinia pestis*) 1996 case definition [cited 2015 Dec 9]. http://www.cdc.gov/nndss/conditions/plague/case-definition/1996
23. Chu MC. Laboratory manual of plague diagnostic tests. Washington (DC): US Department of Health and Human Services; 2000.
24. Kingry LC, Rowe LA, Respicio-Kingry LB, Beard CB, Schriefer ME, Petersen JM. Whole genome multilocus sequence typing as an epidemiologic tool for *Yersinia pestis.* Diagn Microbiol Infect Dis. 2016;84:275–80. http://dx.doi.org/10.1016/j.diagmicrobio.2015.12.003
25. California Department of Public Health. California compendium of plague control; plague surveillance risk evaluation form. Sacramento (CA): The Department; 2015.
26. Hubbard CA. Fleas of western North America: their relation to the public health. Ames (IA): Iowa State College Press; 1947.
27. Liu J, Ochieng C, Wiersma S, Ströher U, Towner JS, Whitmer S, et al. Development of a TaqMan array card for acute febrile illness outbreak investigation and surveillance of emerging pathogens including Ebola virus. J Clin Microbiol. 2016;54:49–58. http://dx.doi.org/10.1128/JCM.02257-15
28. Bankevich A, Nurk S, Antipov D, Gurevich AA, Dvorkin M, Kulikov AS, et al. SPAdes: a new genome assembly algorithm and its applications to single-cell sequencing. J Comput Biol. 2012;19:455–77. http://dx.doi.org/10.1089/cmb.2012.0021
29. National Park Service. Yosemite National Park. Park statistics [cited 2015 Dec 9]. http://www.nps.gov/yose/learn/nature/park-statistics.htm
30. Rosales R. Second human case of bubonic plague inside Yosemite National Park. Fox26 KMPH News. August 18, 2015 [cited 2015 Dec 9]. http://kmph-kfre.com/archive/second-human-case-of-bubonic-plaque-inside-yosemite-national-park
31. Lowell JL, Antolin MF, Andersen GL, Hu P, Stokowski RP, Gage KL. Single-nucleotide polymorphisms reveal spatial diversity among clones of *Yersinia pestis* during plague outbreaks in Colorado and the western United States. Vector Borne Zoonotic Dis. 2015;15:291–302. http://dx.doi.org/10.1089/vbz.2014.1714
32. Clover JR, Hofstra TD, Kuluris BG, Schroeder MT, Nelson BC, Barnes AM, et al. Serologic evidence of *Yersinia pestis* infection in small mammals and bears from a temperate rainforest of north coastal California. J Wildl Dis. 1989;25:52–60. http://dx.doi.org/10.7589/0090-3558-25.1.52
33. California Department of Public Health. Vector-Borne Disease Section annual report 2015 [cited 2016 Sep 27]. http://www.cdph.ca.gov/programs/vbds/Documents/VBDSAnnualReport15.pdf
34. Fox M. Oregon girl is the 16th U.S. plague case this year. NBC News. October 30, 2015 [cited 2015 Dec 9]. http://www.nbcnews.com/health/health-news/oregon-girl-16th-u-s-plague-case-year-n454496
35. Ben Ari T, Gershunov A, Gage KL, Snäll T, Ettestad P, Kausrud KL, et al. Human plague in the USA: the importance of regional and local climate. Biol Lett. 2008;4:737–40. http://dx.doi.org/10.1098/rsbl.2008.0363
36. Murray KF, Kartman L. Plague in California during 1959. California Vector Views. 1959;6:66–7.

Address for correspondence: Vicki Kramer, Vector-Borne Disease Section, Infectious Diseases Branch, Division of Communicable Disease Control, California Department of Public Health, 1616 Capitol Ave, MS-7307, PO Box 997377, Sacramento, CA 95899, USA; email: vicki.kramer@cdph.ca.gov

Anomalous High Rainfall and Soil Saturation as Combined Risk Indicator of Rift Valley Fever Outbreaks, South Africa, 2008–2011

Roy Williams, Johan Malherbe, Harold Weepener, Phelix Majiwa, Robert Swanepoel

Rift Valley fever (RVF), a zoonotic vectorborne viral disease, causes loss of life among humans and livestock and an adverse effect on the economy of affected countries. Vaccination is the most effective way to protect livestock; however, during protracted interepidemic periods, farmers discontinue vaccination, which leads to loss of herd immunity and heavy losses of livestock when subsequent outbreaks occur. Retrospective analysis of the 2008–2011 RVF epidemics in South Africa revealed a pattern of continuous and widespread seasonal rainfall causing substantial soil saturation followed by explicit rainfall events that flooded dambos (seasonally flooded depressions), triggering outbreaks of disease. Incorporation of rainfall and soil saturation data into a prediction model for major outbreaks of RVF resulted in the correctly identified risk in nearly 90% of instances at least 1 month before outbreaks occurred; all indications are that irrigation is of major importance in the remaining 10% of outbreaks.

Rift Valley fever (RVF) is an acute viral disease of livestock and humans in Africa, Madagascar, the Comoros Archipelago, and the Arabian Peninsula. Infection is caused by RVF virus (family *Bunyaviridae*, genus *Phlebovirus*), a zoonotic mosquitoborne virus. In animals, RVF causes abortion in pregnant sheep, goats, cattle, and camels, and it can cause death, particularly in newborn animals. Humans become infected through contact with the tissues of infected animals or, less commonly, from the bite of infected mosquitoes; infection usually results in a benign febrile illness, although complications, such as ocular sequelae or fatal encephalitis and hemorrhagic disease, can occur (*1*,*2*). Large epidemics occur at irregular intervals of 5–15 years, or longer, when heavy rainfall facilitates the breeding of the mosquito vectors, and result in substantial economic losses due to livestock deaths and restrictions on animal trade (*3*).

Author affiliations: Agricultural Research Council–Onderstepoort Veterinary Institute, Onderstepoort, South Africa (R. Williams, P. Majiwa); Agricultural Research Council–Institute for Soil, Climate and Water, Pretoria, South Africa (J. Malherbe, H. Weepener); University of Pretoria, Onderstepoort(R. Swanepoel)

DOI: http://dx.doi.org/10.3201/eid2212.151352

RVF was discovered in Kenya in 1930 and was subsequently found in many countries of sub-Saharan Africa (*1*); spread beyond this region into Egypt, Saudi Arabia, and Yemen was noted from 1977 to 2007 (*4*). The disease was first reported in South Africa during 1950–1951, when a large epidemic occurred in the country's central plateau; 2 additional major epidemics affected the same area in 1974–1976 and 2010–2011 and extended into neighboring provinces (*5*,*6*). Limited outbreaks were recorded during the intervening years; these outbreaks initially occurred on the central plateau, but starting in the 1980s, they increasingly occurred in northeastern parts of the country. Outbreaks among animals are defined as the occurrence of ≥1 confirmed cases within an epidemiologic unit, meaning a group of animals that share approximately the same likelihood of exposure to infection (*7*). In the absence of nomadism in South Africa, epidemiologic units in the country essentially coincide with geographic locations of commercial farms or communal grazing areas. Epidemics are not defined, but the term is applied arbitrarily to the occurrence of intense or multiple outbreaks in ≥1 epidemiologic units.

A phylogenetic study of RVF isolates (*8*) indicated that 2 different virus lineages, C and H, were responsible for the 2008–2011epidemics in South Africa. The 2008 and 2009 epidemics in the northeast were associated with lineage C virus and were much less intense than the subsequent epidemic associated with lineage H virus in the central plateau in 2010–2011 (*6*,*8*). However, lineage C virus was associated with major epidemics in Zimbabwe, eastern Africa, Saudi Arabia and Yemen. Furthermore, in 2004, lineage H was associated with only 1 human infection in Namibia in the absence of reported disease in livestock. Thus, differences in epidemic intensity were more likely determined by epidemiologic factors (e.g., climate, topography, vegetation) or vector species than by the virus strains involved.

Distinction is made between 2 types of RVF virus vectors. Floodwater-breeding *Aedes* mosquitoes of the subgenera *Aedimorphus* and *Neomelaniconion* are regarded as endemic or maintenance vectors because they are thought to be responsible for ensuring long-term survival of the virus through transovarial transmission of infection. Their feeding

and egg-laying cycle are completed within 3 weeks of hatching; eggs are laid in mud at the edges of rainwater that temporarily accumulates in pans (shallow depressions), vleis (seasonal wetlands), and the banks of dams and watercourses, collectively known as dambos in Africa. Not all sites flood directly as a result of local precipitation; river banks, large dams, and irrigation schemes may flood weeks to months after heavy rains occur in remote catchment areas (*9*). In contrast to other mosquitoes, the eggs of floodwater-breeding aedines require conditioning by a period of partial desiccation as the water level recedes before they will hatch once they get wet again during the next flood period. Thus, they overwinter as eggs, which can survive for long periods in dried mud, possibly for several seasons if dambos remain dry (*10*). After adequate rainfall floods breeding sites, infected aedines emerge and transmit the RVF virus to available susceptible animals that serve as amplifying hosts for transmission of infection to the principal epidemic vectors, mainly *Culex* species mosquitoes. Other epidemic vectors include other culicines, anophelines, and even biting flies that act as mechanical vectors. Epidemic mosquito vectors breed on standing bodies of water and are able to sustain and spread outbreaks (*11*,*12*).

In RVF virus–endemic areas with warm and moist climates, infected aedines can emerge each year, and even infected culicines can hibernate as adults, resulting in regular exposure of livestock to RVF virus. Thus, most animals are immune by breeding age and are able to transfer maternal immunity to their offspring; hence, disease is seldom seen (*1*). In more arid areas, particularly those with cold winters and prolonged dry spells (e.g., the central plateau of South Africa), intervals between outbreaks may extend to decades. During these long intervals, livestock populations are replaced by animals susceptible to RVF virus, and heavy rains can trigger major epidemics among such animals.

Because it is difficult to convince livestock owners and veterinary authorities to vaccinate livestock during protracted interepidemic periods, attempts have been made to provide early warning of impending outbreaks through remote sensing of climate patterns conducive to large-scale emergence of vectors (*13*,*14*). Measurement of vegetation photosynthetic activity through satellite imaging is used to derive a normalized difference vegetation index (NDVI) as a surrogate for precipitation. NDVI anomalies that exceed the long-term mean (LTM) are interpreted as favorable for the occurrence of outbreaks (*14*), although a lag of 2–8 weeks between heavy rains and the subsequent increase in the NDVI (*15*,*16*) reduces its value for risk mitigation. The ENSO (El Niño and Southern Oscillation) phenomenon is a major determinant of global interannual climate variability, and anomalies, expressed in terms of a derived Southern Oscillation Index (SOI), are used to predict the occurrence of abnormal rainfall with a lead time of 2–5 months; positive SOI (La Niña) events usually precede heavy rains in southern Africa (*17*,*18*). However, such regional forecasts perform poorly for specific geographic locations; thus, SOI can be considered only as a supplementary preseason indicator for the risk of RVF outbreaks. In contrast, soil moisture status is a reliable indicator of potential flash floods on small catchments (*19*) and therefore has potential to indicate when ground is sufficiently saturated for dambos to be flooded after heavy rains. The combined effect of soil saturation and precipitation could therefore serve as a potential risk indicator of optimal ecoclimatic conditions for the upsurge of mosquito vector populations and subsequent outbreaks of RVF. We evaluated the combined aspects of anomalous high rainfall and concurrent soil saturation in a RVF forecast model for South Africa, using accurate temporal and spatial records of the 2008–2011 epidemics to derive risk maps (Directorate of Animal Health, Department of Agriculture, Forestry and Fisheries, pers. comm., 2012 Jul 6).

Data and Methods

RVF Base Map

We constructed an interpolated base map of 1-km spatial resolution, representing the probability of risk for RVF outbreaks throughout South Africa, by using ArcGIS version 10.2.2 (ESRI, Redlands, CA, USA). Interpolation data points included locations of all historic sites of RVF outbreaks from 1950 to 2011 (Directorate of Animal Health, Department of Agriculture, Forestry and Fisheries, pers. comm., 2012 Jul 6) (*6*); additional data points were placed along the perimeters of buffer zones at radii of 30, 50, and 90 km around historic sites. Historic sites were allocated an interpolation value of 1.0, and the values of additional data points were based on the distance from the nearest historic site, decreasing incrementally by a factor of 0.1 for every 10 km; probability values ranged from 1.0 to 0.1. Potential risk areas were empirically grouped into 3 classes based on the distance from historic sites: high risk (≤20 km from historic sites), moderate risk (>20 km to ≤40 km), and low risk (>40 km).

Rainfall and NDVI

The rainfall dataset was produced in near real time (*20*) from a combination of weather station data from the Agricultural Research Council–Institute for Soil, Climate and Water (http://www.arc.agric.za/Pages/Home.aspx) and from the South African Weather Service (http://www.weathersa.co.za/). Weather station data were combined with satellite rainfall estimates available through the Africa Data Dissemination Service for the Famine Early Warning System Network project (http://www.fews.net/). Monthly LTM rainfall was computed in 1-km spatial resolution from monthly rainfall data for 1985–2011 and used to

determine the maximum of monthly LTMs during this period. Anomalies of monthly rainfall during January 2007–May 2012 were computed as the percentage deviation from the maximum LTM: monthly rainfall anomaly = (monthly rainfall – maximum LTM) × 100/maximum LTM.

SPOT NDVI data were downloaded through the VEGETATION Program (http://www.spot-vegetation.com/) and the VGT4AFRICA project (http://postel.obs-mip.fr/?VGT4AFRICA-Project,147), developed by the European Commission and disseminated in Africa through GEONETCast (http://wiki.geonetcast.org/geonetcast/html/index.php/Main_Page). Using the method described for rainfall, we computed anomalies of monthly NDVI for January 2007–May 2012 as the percentage deviation from the maximum LTM.

Soil Saturation Index

The soil saturation index (SSI) represents automated real-time computations of the TOPKAPI hydrologic model, which was adapted to run continuously as a collection of independent 1-km cells at 3-hour intervals (*19*,*21*) beginning in August 2008 (University of KwaZulu-Natal, School of Civil Engineering, Surveying and Construction Management, pers. comm., 2013 Feb 10). Monthly SSI anomalies were computed as the percentage deviation from the LTM (2008–2013) and then computed as 3-month rolling mean SSI anomalies (*14*) for each month from August 2008 through May 2012. For functional compatibility with other model components, SSI anomalies were reclassified as follows: values of 0–3% were reclassified to a value of 0.1, values >3%–6% were reclassified to 0.2, values >6%–9% were reclassified to 0.3, values >9%–12% were reclassified to 0.5, values >12%–15% were reclassified to 0.7, values >15%–18% were reclassified to 0.8, values >18%–20% were reclassified to 0.9, and values >20% were reclassified to 1.0.

Risk Forecast Model

The aim of the forecast model was to map areas at risk for RVF outbreaks based on the combined effect of anomalous high rainfall and soil saturation but regulated by the risk probability as defined by the base map. Risk was computed as follows: risk = monthly rainfall anomaly × 3-month rolling mean SSI anomaly × base map. Risk maps for January–July 2008 were computed without SSI data. Three-month rolling maximum risk maps were used to reflect changing conditions of mosquito habitats (*14*) during January 2007–June 2011. Pixel values were empirically classified as low risk (<0%), moderate risk (0%–50%), and high risk (>50%).

Retrospective Evaluation

The accuracy of the model was evaluated by extracting the risk values of all recorded 2008–2011 outbreaks from their relevant risk maps, and we tabled the results according to the month of outbreak and sorted into 1 of the 3 risk classes. Outbreaks in moderate or high risk areas were considered as correctly identified, and outbreaks in low risk areas were considered as incorrectly identified.

Results

Rift Valley Fever Base Map

All historic sites of RVF outbreaks in South Africa from 1950 through 2011 were mapped (Figure 1, panel A). The base map (Figure 1, panel B) represents the probability of risk for RVF outbreaks; this probability decreases as the distance from outbreak sites increases.

Regions of Outbreaks

Outbreaks during the epidemics of 2008–2011 were grouped by temporal history into 5 geographic regions

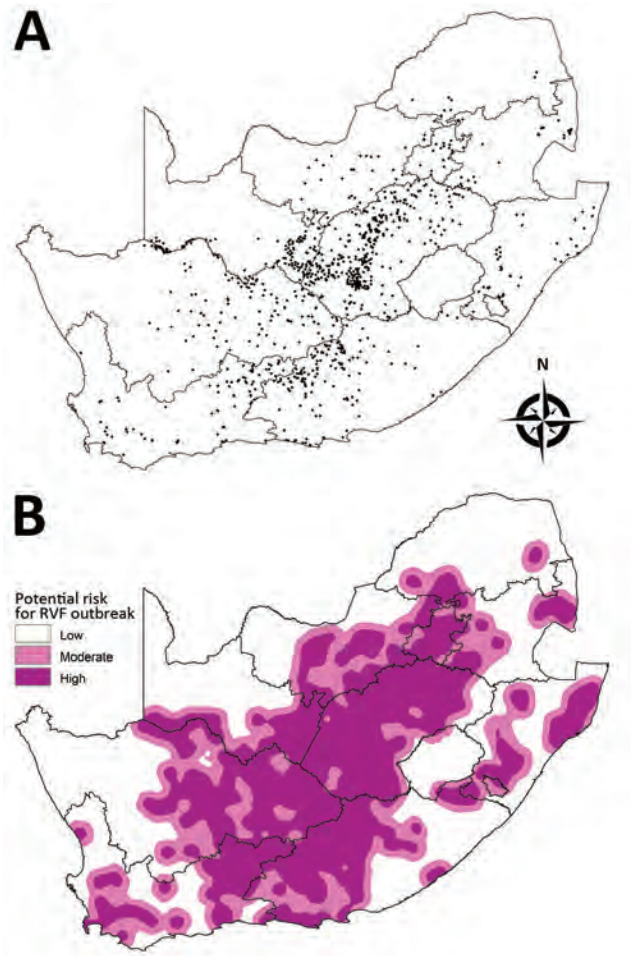

Figure 1. Historic sites of Rift Valley fever (RVF) outbreaks in South Africa from 1950 through 2011 (A) and a base map indicating areas at low, moderate, and high risk for an outbreak (B). Each dot in panel A represents a RVF outbreak. The base map in panel B was created by an interpolation method based on the distance from historic sites: high risk (≤20 km), moderate risk (>20 km to ≤40 km), and low risk (>40 km).

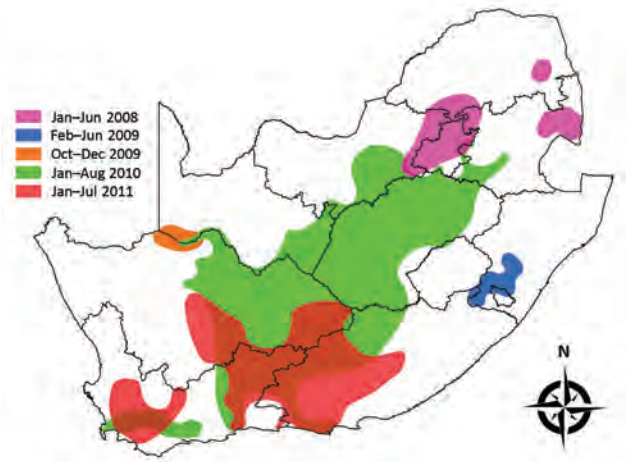

Figure 2. Five regions in South Africa where Rift Valley fever outbreaks occurred during the epidemics of 2008–2011. Regions are grouped, by color, according to their temporal history of outbreaks.

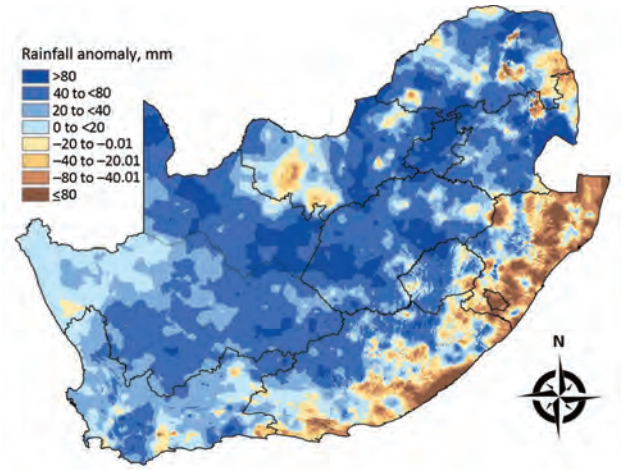

Figure 3. Mean seasonal rainfall anomalies for 4 consecutive seasons (November–March) in South Africa, 2007–2011. The anomalies were computed as deviations from the seasonal long-term mean for 1985–2011.

(Figure 2). The periods and regions were 1) January–June 2008, Mpumalanga Province and adjacent parts of Limpopo, Gauteng, and North West Provinces; 2) February–June 2009, southern KwaZulu-Natal Province; 3) October–November 2009, Orange River region in Northern Cape Province; 4) January–August 2010, central plateau, including Free State Province and adjacent parts of North West and Northern, Eastern, and Western Cape Provinces; and 5) January–July 2011, adjacent parts of the inland region of Northern, Eastern, and Western Cape Provinces.

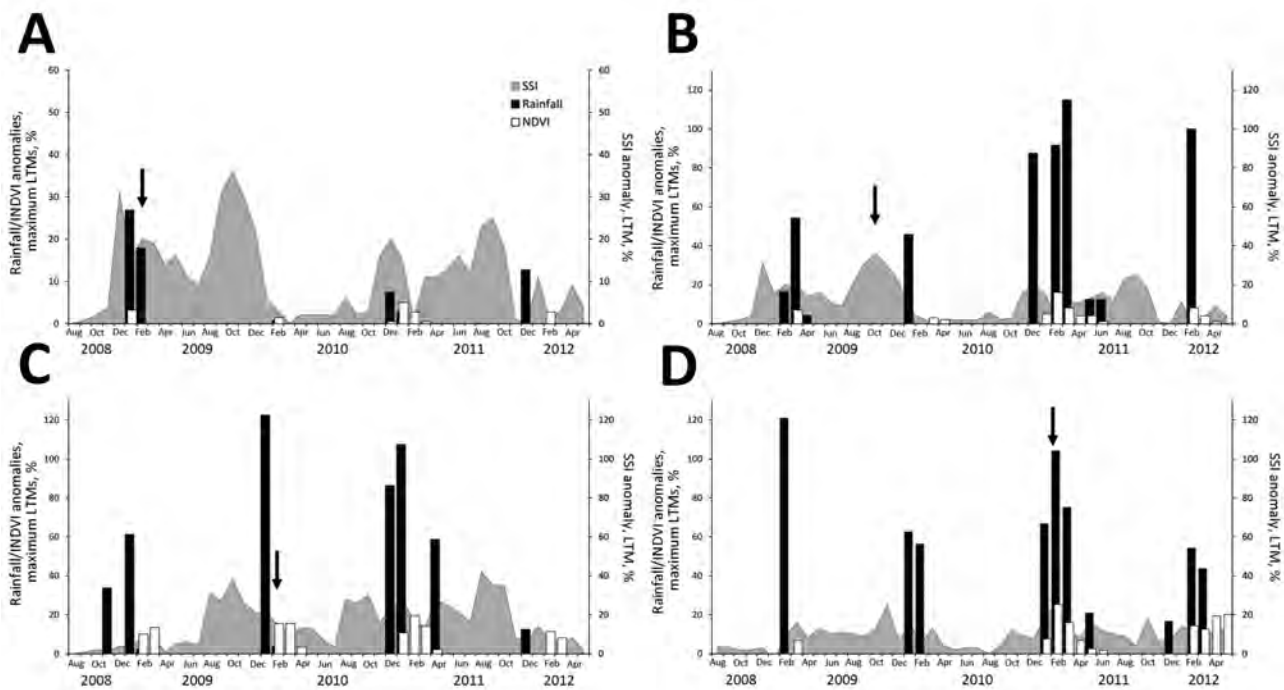

Figure 4. Comparison of monthly rainfall amounts, normalized difference vegetation indices (NDVIs), and soil saturation indices (SSIs) for August 2008–May 2012 for the following 4 areas of South Africa where Rift Valley fever epidemics occurred: A) Southern region of KwaZulu-Natal Province (outbreaks in February–March 2009); B) Orange River region in Northern Cape Province (outbreaks in October–November 2009); C) Bultfontein area of Free State Province (outbreaks in January–February 2010); D) Graaff-Reinet area of Eastern Cape Province (outbreaks in January–February 2011). Rainfall and NDVI anomalies were computed as percentage of the maximum of the long-term means (LTMs); SSI anomalies were computed as percentage of the LTM. Arrows indicate time of first outbreak in the region.

Rainfall, SSI and NDVI

Rainfall data for 2008–2011 indicated a pattern of incessant and widespread seasonal rainfall (Figure 3), resulting in substantial soil saturation, after which explicit rainfall events triggered subsequent outbreaks of RVF in different regions. We also compared rainfall, NDVI, and monthly SSI data from August 2008 through May 2012 for outbreaks that occurred in the first 2 months of each of the following RVF epidemics: 1) southern KwaZulu-Natal Province (February–March 2009), 2) Orange River region in Northern Cape Province (October–November 2009), 3) Bultfontein area of Free State Province (January–February 2010), and 4) Graaff-Reinet area of Eastern Cape Province (January–February 2011) (Figure 4). No SSI data were available for outbreaks that occurred in Mpumalanga Province and adjacent parts of Limpopo, Gauteng, and North West Provinces during January–June 2008.

In the Bultfontein area of Free State Province, where the major inland epidemic of 2010 began (Figure 4, panel C), 2 major rainfall events in November 2008 and January 2009 with concurrent SSI anomalies <5% did not initiate any RVF outbreaks. However, in January 2010, outbreaks started to occur in the region after at least 4 successive months of SSI anomalies above 20% and a major rainfall event in December 2009. Similarly, outbreaks in southern KwaZulu-Natal Province (Figure 4, panel A) and outbreaks that started in the Graaff-Reinet area of Eastern Cape Province (Figure 4, panel D) occurred after rainfall events that were preceded by 1 month of SSI anomalies above 20%. Anomalous rainfall events were regularly followed by elevated NDVI anomalies (Figure 4, panels A, B, and D), usually after a lag of 2–8 weeks. The outbreaks in the Orange River region of Northern Cape Province did not show the same pattern as the previous 3 instances (Figure 4, panel B). Although outbreaks were preceded by 2 months of SSI anomalies >20%, no major rainfall event occurred before the outbreaks, and no elevated NDVI anomalies occurred concurrently with the outbreaks in this region. This finding suggests that irrigation, which is used in vineyards and orchards along the river in this region, could have been responsible for these outbreaks.

Outbreaks of the epidemics of 2010 and 2011 showed a degree of spatial overlap (Figure 2); no outbreaks occurred in Free State Province in 2011, despite highly suitable climatic conditions throughout the season (Figure 4, panel C). A similar pattern was seen for human RVF infections in 2011, when human cases primarily occurred in areas south of the Orange River, away from Free State Province (*22*). The lack of outbreaks in livestock and humans in Free State Province in 2011 was attributed to accumulated herd immunity, which was believed to be the combined result of natural infections in and vaccination of livestock in the province (*22*).

RVF Risk Maps

January–June 2008 Outbreaks

The first outbreaks of the 2008 epidemic in South Africa were recorded in the northeastern part of the country in the region of Kruger National Park; 17 outbreaks were recorded in the area during January–March 2008, and 4 were recorded in June. During March–May 2008, a total of 14 outbreaks were recorded in Gauteng Province and adjacent parts of Limpopo and North West Provinces. The risk map for December 2007 showed moderate risk for the area where outbreaks occurred in January and February 2008 (Figure 5, panel A), and the risk map for January 2008 indicated high to moderate risk in the regions where outbreaks occurred during March–June 2008 (Figure 5, panel B).

February–June 2009 Outbreaks

Outbreaks in the southern region of KwaZulu-Natal Province started in February 2009 with 6 outbreaks, followed by 4 outbreaks in March and another 9 during April–June.

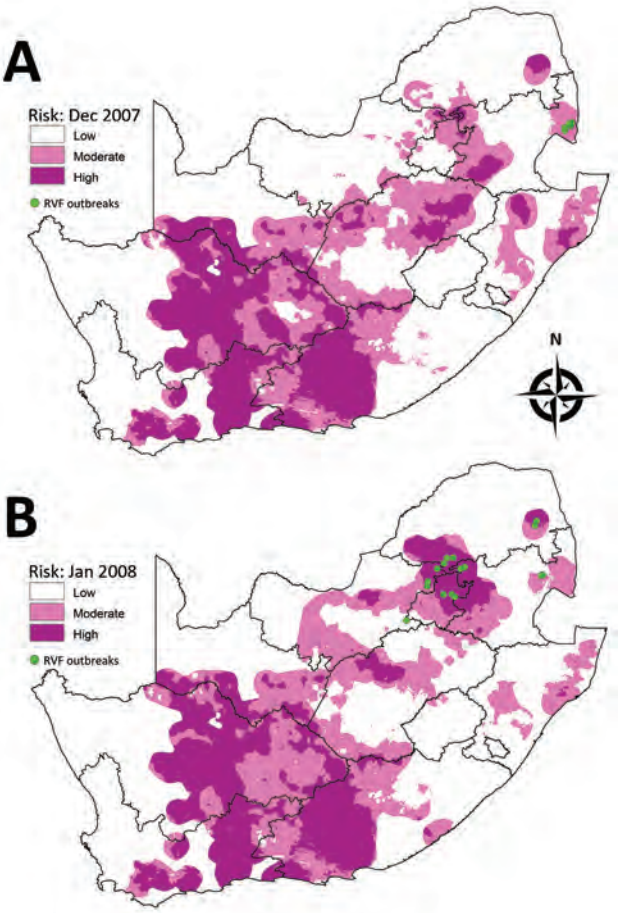

Figure 5. Risk maps for probability of Rift Valley fever (RVF) outbreaks in different areas of South Africa. A) Map for December 2007 showing subsequent outbreaks in January and February 2008. B) Map for January 2008 showing subsequent outbreaks during March–June 2008.

Areas where outbreaks occurred in February and March 2009 were shown as moderate risk in the risk map for January (Figure 6, panel A); likewise, areas where outbreaks occurred during April–June 2009 were shown as moderate risk in the risk map for February (Figure 6, panel B).

October–December 2009 Outbreaks

A total of 38 outbreaks occurred during October–December 2009 in the Orange River area of Northern Cape Province, close to the border with Namibia, although the risk map for September 2009 did not indicate any risk in this region (Figure 7). The outbreaks did, however, coincided with irrigation activity along the river.

January–August 2010 Outbreaks

In January 2010, two outbreaks were recorded in the Bultfontein area of Free State Province, followed by an explosive epidemic of 548 outbreaks during February–August that spread throughout the central plateau of the country to the southern coastal regions of Western Cape Province. The risk map for December 2009 indicated high risk for the area where the first 2 outbreaks occurred in January 2010 (Figure 8, panel A), and the risk map for January 2010 showed moderate to high risk for the whole central plateau, where outbreaks occurred during February 2010 (Figure 8, panel B). The risk map for February 2010 indicated that risk for outbreaks extended even farther south and that outbreaks occurred during March–July 2010 (Figure 8, panel C). No risk for outbreaks was indicated for the southern parts of the Western Cape Province where 8 outbreaks occurred, although irrigation is practiced fairly commonly in the region.

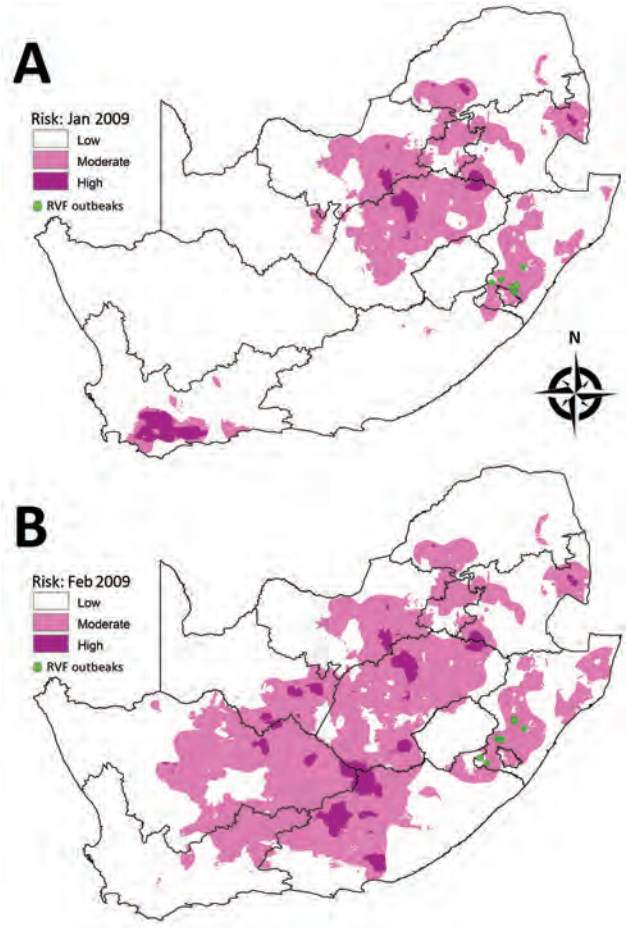

Figure 6. Risk maps for probability of Rift Valley fever (RVF) outbreaks in different areas of South Africa. A) Map for January 2009 showing subsequent outbreaks in February and March 2009. B) Map for February 2009 showing subsequent outbreaks during April–June 2009.

January–July 2011 Outbreaks

A total of 136 outbreaks were recorded during January–July 2011 in the inland part of the country south of the Orange River, including regions of Northern, Eastern, and Western Cape Provinces. In the risk map for December 2010, no risk was shown for a few areas where outbreaks occurred in January 2011 (Figure 9, panel A), but moderate to high risk was indicated in the risk map of January 2011 for areas of outbreaks in February 2011 (Figure 9, panel B). The risk map for February 2011 showed moderate to high risk for areas of outbreaks during March–June 2011 (Figure 9, panel C). Similar to the previous year, a number of outbreaks occurred in the southern parts of the Western Cape Province where no risk was predicted but where irrigation was practiced.

Retrospective Evaluation

A total of 778 outbreaks occurred during the epidemics of 2008–2011; of these, 88 (11.3%) were classified by the model as low risk, 236 (30.3%) as moderate risk, and 454 (58.4%) as high risk, indicating that the model correctly identified 88.7% of outbreaks (Table). For the major inland

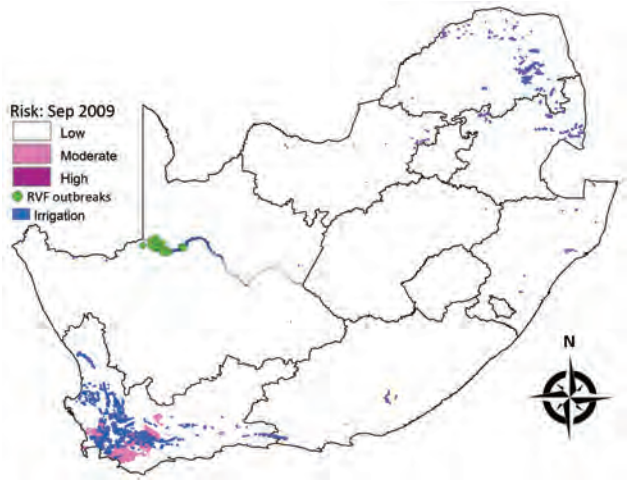

Figure 7. Risk map for probability of Rift Valley fever (RVF) outbreaks in different areas of South Africa. Map for September 2009 indicates irrigation areas and subsequent outbreaks during October–December 2009.

epidemic of January–August 2010, the model correctly identified 95.8% of the outbreaks, compared with 23% of the outbreaks in Northern Cape Province during October–December 2009; this low risk prediction rate for the 2009 outbreaks strengthens the perception that the 2009 epidemic was triggered by irrigation rather than high rainfall (Figure 4, panel B). Irrigation activity was also associated with 8 outbreaks in 2010 (Figure 9, panel C) and 9 outbreaks in

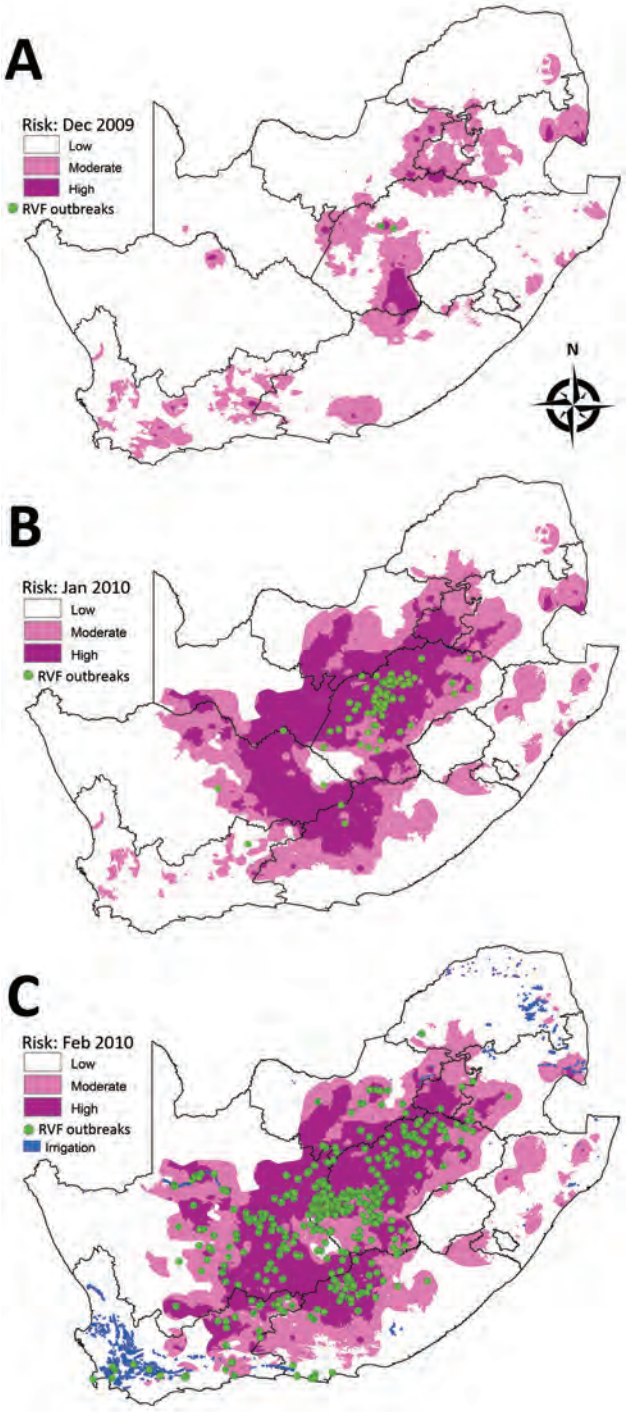

Figure 8. Risk maps for probability of Rift Valley fever (RVF) outbreaks in different areas of South Africa. A) Map for December 2009 showing subsequent outbreaks in January 2010. B) Map for January 2010 showing subsequent outbreaks in February 2010. C) Map for February 2010 indicating irrigation areas and subsequent outbreaks during March–June 2010.

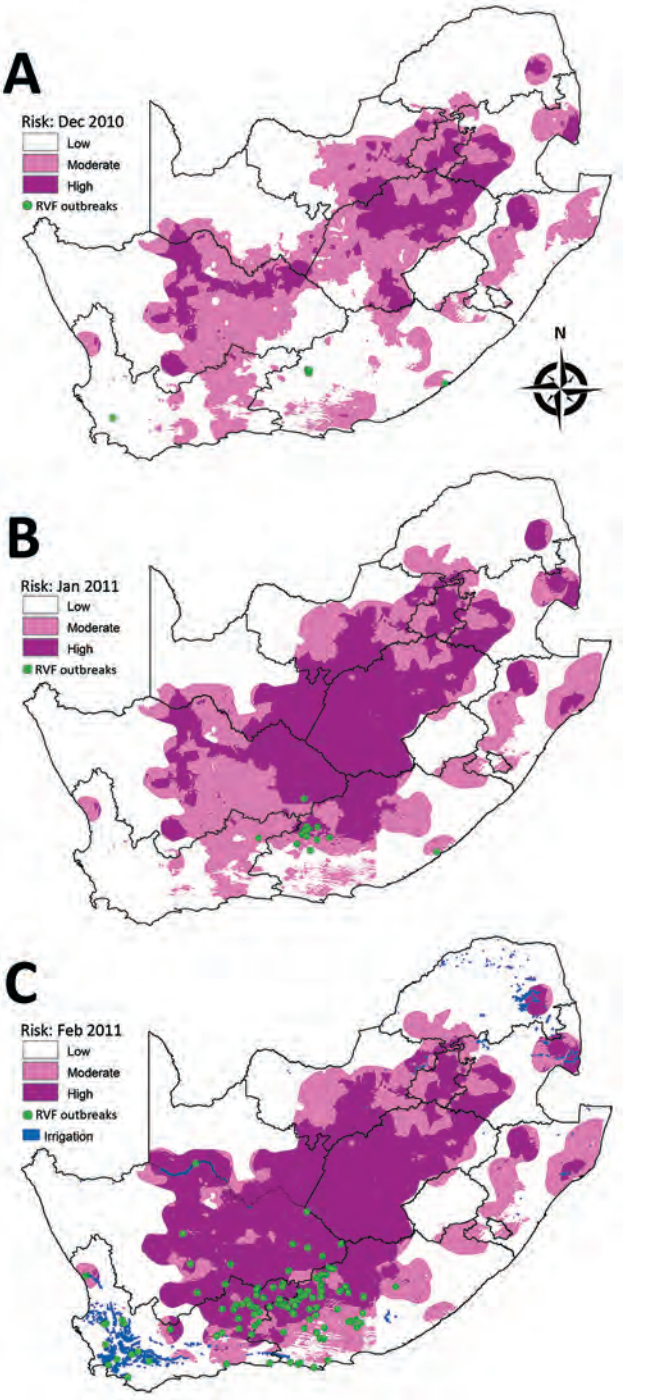

Figure 9. Risk maps for probability of Rift Valley fever (RVF) outbreaks in different areas of South Africa. A) Map for December 2010 showing subsequent outbreaks in January 2011. B) Map for January 2011 showing subsequent outbreaks in February 2011. C) Map for February 2011 indicating irrigation areas and subsequent outbreaks during March–June 2011.

Table. Summary of predicted risk for all Rift Valley fever outbreaks during the epidemics of 2008–2011, South Africa*

Year, month of outbreak	No. outbreaks	3-mo rolling maximum risk map	Risk for outbreak		
			Low	Moderate	High
2008					
Jan	5	2007 Oct–Dec	NA	5	NA
Feb	10	2007 Oct–Dec	NA	10	NA
Mar	5	2008 Nov–Jan	NA	NA	5
Apr	7	2008 Nov–Jan	1	NA	6
May	4	2008 Nov–Jan	NA	NA	4
Jun	4	2008 Nov–Jan	1	3	NA
2009					
Feb	6	2009 Nov–Jan	NA	6	NA
Mar	4	2009 Nov–Jan	NA	4	NA
Apr	7	2009 Dec–Feb	1	6	NA
May	1	2009 Dec–Feb	NA	1	NA
Jun	1	2009 Dec–Feb	NA	1	NA
Oct	22	2009 Jun–Aug	22	4	NA
Nov	16	2009 Jun–Aug	16	5	NA
Dec	1	2009 Jun–Aug	1	NA	NA
2010					
Jan	2	2009 Oct–Dec	NA	1	1
Feb	99	2010 Nov–Jan	2	15	82
Mar	257	2010 Dec–Feb	4	83	170
Apr	140	2010 Dec–Feb	2	39	99
May	38	2010 Dec–Feb	8	16	14
Jun	10	2010 Dec–Feb	5	3	2
Jul	1	2010 Dec–Feb	1	NA	NA
Aug	2	2010 Dec–Feb	1	NA	1
2011					
Jan	6	2010 Oct–Dec	6	NA	NA
Feb	15	2011 Nov–Jan	1	8	6
Mar	51	2011 Dec–Feb	2	19	30
Apr	47	2011 Dec–Feb	5	14	28
May	14	2011 Dec–Feb	8	1	5
Jun	3	2011 Dec–Feb	1	1	1
Total (%)	778		88 (11.3)	236 (30.3)	454 (58.4)

*Values were extracted from relevant 3-mo rolling maximum risk maps. NA, not applicable.

2011 (Figure 5, panel C) in areas of Western Cape Province where the model retrospectively predicted low risk.

Discussion

Although vaccination is the most effective way to protect livestock against RVF outbreaks, it has always been difficult to convince farmers to vaccinate during long interepidemic periods. Vaccine sales have generally been negligible during interepidemic periods, and once epidemics have begun, vaccination has usually been initiated too late and with coverage too limited to avert outbreaks or prevent considerable losses (*1*,*8*). Without a reliable early warning system supported by an effective vaccination strategy, the history of RVF outbreaks in South Africa is bound to repeat itself.

The basis for mapping specific areas with elevated risk for RVF activity during the epidemics of 2008–2011 was the simultaneous occurrence of elevated soil moisture and high rainfall events, which caused flooding of dambos that created suitable habitats for the development of large populations of mosquito vectors and subsequent outbreaks of disease. Our findings show that SSI anomalies that exceed LTMs by an upper threshold of 20%, followed by a sudden high rainfall event, could serve as a reliable risk indicator of imminent RVF outbreaks. Our model correctly identified the risk for an outbreak in nearly 90% of instances ≥1 months before they occurred. During an epidemic, the initial spread of RVF virus by active vector dispersal is followed by other transmission mechanisms of lower intensity and over longer distances, including the movement of infectious animals and passive vector dispersal (e.g., wind) (*23*). The sites of outbreaks caused by these means of transmission would not necessarily be associated with higher than normal rainfall and could probably explain some of the outbreaks that occurred in areas of low risk. In this regard, irrigation is of particular importance in outbreaks in the Orange River region during October–December 2009 and in outbreaks that occurred in low-risk areas of Western Cape Province in 2010 and 2011. Findings from previous studies strongly suggest that irrigation could create suitable breeding habitats for mosquito vectors and lead to subsequent outbreaks of RVF (*9*,*24*).

The well-documented RVF epidemics of 2008–2012 provided a unique opportunity for investigating the multifactorial nature of the disease in South Africa (*18*,*22*,*23*), and it was possible to retrospectively identify the critical link between soil saturation, rainfall, and RVF outbreaks. However, this novel modeling approach enabled limited scope for comparison

with other prediction models, and certain basic assumptions had to be made in the absence of supporting evidence. The model needs prospective validation in future RVF epidemics, including appropriate modification of parameters to enhance performance, and further research is required to identify other possible factors that could improve risk prediction.

Strategic vaccination of susceptible host populations in potential high-risk areas remains the only viable long-term solution to address RVF in South Africa. Essential components of risk management strategy should include regular serologic surveys to evaluate the immune status of livestock populations, an effective immunization protocol backed by adequate strategic stockpiling of vaccine, and a reliable early warning system to identify areas where livestock could be at risk during seasons of high rainfall. The combination of anomalous high soil saturation and rainfall shows promise as a risk indicator for RVF outbreaks, and by incorporating irrigation as an additional element, the accuracy of the prediction model could probably be improved.

Acknowledgments

We thank Grietjie de Klerk, Hannes Pienaar, Sunelle Strydom, and Willie Ungerer (deceased) for providing the electronic RVF data for 2008–2011, which were compiled from the disease reports of provincial veterinary services.

Dr. Williams is a senior veterinary researcher at the Onderstepoort Veterinary Institute. His work involves GIS-related epidemiology of insect-transmitted viral diseases, with a special interest in species distribution modelling of disease vectors.

References

1. Swanepoel R, Coetzer JAW. Rift Valley Fever. In: Coetzer JAW, Tuskin RC, editors. Infectious diseases of livestock with special reference to Southern Africa. Cape Town: Oxford University Press; 2004. p. 1037–70.
2. Davies FG. The historical and recent impact of Rift Valley fever in Africa. Am J Trop Med Hyg. 2010;83:73–4. http://dx.doi.org/10.4269/ajtmh.2010.83s2a02
3. El Mamy ABO, Baba MO, Barry Y, Isselmou K, Dia ML, Hampate B, et al. Unexpected Rift Valley fever outbreak, northern Mauritania. Emerg Infect Dis. 2011;17:1894–6. http://dx.doi.org/10.3201/eid1710.110397
4. Pepin M, Bouloy M, Bird BH, Kemp A, Paweska J. Rift Valley fever virus (*Bunyaviridae: Phlebovirus*): an update on pathogenesis, molecular epidemiology, vectors, diagnostics and prevention. Vet Res. 2010;41:61–100. http://dx.doi.org/10.1051/vetres/2010033
5. Alexander RA. Rift Valley fever in the Union. J S Afr Vet Med Assoc. 1951;22:105–9.
6. Pienaar NJ, Thompson PN. Temporal and spatial history of Rift Valley fever in South Africa: 1950 to 2011. Onderstepoort J Vet Res. 2013;80:384. http://dx.doi.org/10.4102/ojvr.v80i1.384
7. World Organisation for Animal Health. Terrestrial Animal Health Code (2015) [cited 2014 May 25]. http://www.oie.int/international-standard-setting/terrestrial-code/access-online/
8. Grobbelaar AA, Weyer J, Leman PA, Kemp A, Paweska JT, Swanepoel R. Molecular epidemiology of Rift Valley fever. Emerg Infect Dis. 2011;17:2270–6. http://dx.doi.org/10.3201/eid1712.111035
9. Jouan A, Adam F, Coulibaly I, Riou O, Philippe B, Ledru E, et al. Epidemic of Rift Valley fever in the Islamic republic of Mauritania. Geographic and ecological data. Bull Soc Pathol Exot. 1990;83:611–20.
10. Gargan TPI, Jupp PG, Novak RJ. Panveld oviposition sites of floodwater *Aedes* mosquitoes and attempts to detect transovarial transmission of Rift Valley fever virus in South Africa. Med Vet Entomol. 1988;2:231–6. http://dx.doi.org/10.1111/j.1365-2915.1988.tb00189.x
11. McIntosh BM. Rift Valley fever. 1. Vector studies in the field. J S Afr Vet Med Assoc. 1972;43:391–5.
12. McIntosh BM, Jupp PG, Dos Santos I, Rowe AC. Field and laboratory evidence implicating *Culex zombaensis* and *Aedes circumluteolus* as vectors of Rift Valley fever virus in coastal South Africa. S Afr J Sci. 1983;79:61–4.
13. Linthicum KJ, Anyamba A, Tucker CJ, Kelley PW, Myers MF, Peters CJ. Climate and satellite indicators to forecast Rift Valley fever epidemics in Kenya. Science. 1999;285:397–400. http://dx.doi.org/10.1126/science.285.5426.397
14. Anyamba A, Chretien JP, Small J, Tucker CJ, Formenty PB, Richardson JH, et al. Prediction of a Rift Valley Fever outbreak. Proc Natl Acad Sci U S A. 2009;106:955–9. http://dx.doi.org/10.1073/pnas.0806490106
15. Wang J, Rich PM, Price KP. Temporal responses of NDVI to precipitation and temperature in the central Great Plains, USA. Int J Remote Sens. 2003;24:2345–64. http://dx.doi.org/10.1080/01431160210154812
16. Zewdie W, Csaplovics E. Evaluation of rainfall and NDVI anomalies using distributed lag models. Poster presented at: Algorithms and Technologies for Multispectral, Hyperspectral, and Ultraspectral Imagery XXI; 2015 Apr 21–23; Baltimore, MD, USA.
17. Mabaso ML, Kleinschmidt I, Sharp B, Smith T. El Niño Southern Oscillation (ENSO) and annual malaria incidence in southern Africa. Trans R Soc Trop Med Hyg. 2007;101:326–30. http://dx.doi.org/10.1016/j.trstmh.2006.07.009
18. Pienaar NJ. A retrospective analysis of the epidemiology of Rift Valley fever in South Africa [dissertation]. Pretoria (South Africa): University of Pretoria; 2011.
19. Sinclair S, Pegram GGS. A comparison of ASCAT and modelled soil moisture over South Africa, using TOPKAPI in land surface mode. Hydrol Earth Syst Sci. 2010;14:613–26. http://dx.doi.org/10.5194/hess-14-613-2010
20. Malherbe J, Dieppois B, Maluleke M, Van Staden M, Pillay DL. South African droughts and decadal variability. Nat Hazards. 2016;80:657–81. http://dx.doi.org/10.1007/s11069-015-1989-y
21. Sinclair S, Pegram GGS. Modelling soil moisture at national and catchment scale using a spatially distributed hydrological model forced by remote sensing and meteorological products. In: Abstracts of the 16th SANCIAHS National Hydrology Symposium; Pretoria, South Africa; 2012 Oct 1–3. Pretoria: SANCIAHS; 2012.
22. Archer BN, Thomas J, Weyer J, Cengimbo A, Landoh DE, Jacobs C, et al. Epidemiologic investigation into outbreaks of Rift Valley fever in humans, South Africa, 2008–2011. Emerg Infect Dis. 2013;19:1918–24. http://dx.doi.org/10.3201/eid1912.121527
23. Métras R, Porphyre T, Pfeiffer DU, Kemp A, Thompson PN, Collins LM, et al. Exploratory space-time analyses of Rift Valley fever in South Africa in 2008–2011. PLoS Negl Trop Dis. 2012;6:e1808. http://dx.doi.org/10.1371/journal.pntd.0001808
24. Métras R, Jewell C, Porphyre T, Thompson PN, Pfeiffer DU, Collins LM, et al. Risk factors associated with Rift Valley fever epidemics in South Africa in 2008–11. Sci Rep. 2015;5:9492. http://dx.doi.org/10.1038/srep09492

Address for correspondence: Roy Williams, ARC–Onderstepoort Veterinary Institute, Private Bag X05, Onderstepoort 0110, South Africa; email: WilliamsR@arc.agric.za

Cutaneous Granulomas in Dolphins Caused by Novel Uncultivated *Paracoccidioides brasiliensis*

Raquel Vilela, Gregory D. Bossart, Judy A. St. Leger, Leslie M. Dalton, John S. Reif, Adam M. Schaefer, Peter J. McCarthy, Patricia A. Fair, Leonel Mendoza

Cutaneous granulomas in dolphins were believed to be caused by *Lacazia loboi*, which also causes a similar disease in humans. This hypothesis was recently challenged by reports that fungal DNA sequences from dolphins grouped this pathogen with *Paracoccidioides brasiliensis*. We conducted phylogenetic analysis of fungi from 6 bottlenose dolphins (*Tursiops truncatus*) with cutaneous granulomas and chains of yeast cells in infected tissues. *Kex* gene sequences of *P. brasiliensis* from dolphins showed 100% homology with sequences from cultivated *P. brasiliensis*, 73% with those of *L. loboi*, and 93% with those of *P. lutzii.* Parsimony analysis placed DNA sequences from dolphins within a cluster with human *P. brasiliensis* strains. This cluster was the sister taxon to *P. lutzii* and *L. loboi*. Our molecular data support previous findings and suggest that a novel uncultivated strain of *P. brasiliensis* restricted to cutaneous lesions in dolphins is probably the cause of lacaziosis/lobomycosis, herein referred to as paracoccidioidomycosis ceti.

The clinical and phenotypic features of the uncultivated agent of lacaziosis/lobomycosis in dolphins suggested that this pathogen was the same organism as *Lacazia loboi*, which causes skin keloidal-like lesions in humans (*1–6*). Although several studies indicated that *L. loboi* from human resists culture (*4–6*), only 1 well-documented study shows the uncultivated nature of the pathogen causing cutaneous granulomas in dolphins (*7*). Thus, the true ecology, epidemiology, and taxonomy of these 2 uncultivated pathogens of humans and dolphins have been controversial (*4,7*).

Because of their phenotypic resemblance and serologic cross-reactivity with *Paracoccidioides brasiliensis*, at one time these pathogens were believed to be *P. loboi* (*4,8*). This taxonomic controversy was partially resolved in 1999 when Taborda et al. (*9*) proposed the binomial *L. loboi* and concluded that previous terms used to name the etiologic agent of skin keloidal-like lesions in humans and dolphins were invalid. Molecular analysis of internal transcriber spacer (ITS) and chitin synthase 4 (*CHS4*) genes validated their original proposal (*10*). Further phylogenetic analysis of several genomic DNA sequences showed that *L. loboi* was closely related to *Paracoccidioides* spp. (*11*). However, other molecular data showed that *L. loboi* from humans was located in its own genus because of strong bootstrap support (*12*).

The notion that human *L. loboi* was the same organism as those in the skin of dolphins with lacaziosis/lobomycosis was first challenged by Rotstein et al. (*13*), who used molecular analysis. These investigators found that the 28S rDNA amplicon of *L. loboi* in extracted genomic DNA from an infected bottlenose dolphin (*Tursiops truncatus*) in North Carolina, USA, coastal areas had 97% identity with *P. brasiliensis* DNA sequences available in GenBank. However, their DNA sequences are not available. More recently, 3 groups in Japan (*14,15*) and Spain (*16*), who also used molecular methods, reported similar observations for several dolphin species including, *T. truncatus* and *Lagenorhynchus obliquidens*, which had skin granulomas and yeast-like cells in infected tissues. These studies showed that glycoprotein 43 (*gp43*)–like and ITS partial DNA sequences isolated from infected dolphins placed the etiologic agent of skin granulomas among human *P. brasiliensis* strains.

We amplified by using PCR the partial coding DNA sequences of the *Kex* gene in genomic DNA isolated from 6 bottlenose dolphins with cutaneous granulomas. These dolphins were captured in the Indian River Lagoon, Florida, USA, a 156-mile estuary along the eastern coast of the United States. Phylogenetic analysis showed that *Kex* PCR

Author affiliations: Federal University of Minas Gerais, Belo Horizonte, Brazil (R. Vilela); Michigan State University, East Lansing, Michigan, USA (R. Vilela, L. Mendoza); Georgia Aquarium, Atlanta, Georgia, USA (G.D. Bossart); University of Miami Miller School of Medicine, Miami, Florida, USA (G.D. Bossart); SeaWorld, San Diego, California, USA (J.A. St. Leger); SeaWorld, San Antonio, Texas, USA (L.M. Dalton); Colorado State University College of Veterinary Medicine and Biomedical Sciences, Fort Collins, Colorado, USA (J.S. Reif); Florida Atlantic University, Fort Pierce, Florida, USA (A.M. Schaefer, P.J. McCarthy); National Oceanic and Atmospheric Administration, Charleston, South Carolina, USA (P.A. Fair)

DOI: http://dx.doi.org/10.3201/eid2212.160860

amplicons, which contained partial DNA sequences of the Kex protein, clustered among cultivated *P. brasiliensis* strains from humans with systemic paracoccidioidomycosis. Our data suggest that a novel uncultivated *P. brasiliensis* type, different from *L. loboi* from humans, is the probable etiologic agent of cutaneous granulomas in dolphins.

Materials and Methods

Biopsy Specimens from Bottlenose Dolphins

Four formalin-fixed tissues were received from the Harbor Branch Oceanographic Institute (Fort Pierce, FL, USA). Samples were collected in June 2003 from bottlenose dolphins captured in the Indian River Lagoon with cutaneous granulomas displaying chains of yeast cells in the infected tissues (FB 921, FB938, FB946, and FB952). Two additional skin biopsy specimens were obtained from SeaWorld of Texas (San Antonio, TX, USA); 1 specimen (SW070458) was collected during rescue and rehabilitation efforts, and a second 1 specimen (B92-932) was obtained from an animal that came from the Indian River Lagoon and was then kept at SeaWorld of Texas (Table).

Isolation of DNA from Paraffin-Embedded Tissues

Using a sterile microtome, we obtained 10-mm–thick sections from paraffin-embedded tissues. Parts of sections were examined by using histopathologic analysis after staining with Gomori methenamine silver to verify the presence and quantity of yeast-like cells in selected specimens.

Isolation of DNA was performed by using the BioChain FFPET protocol (BioChain Institute, Inc., Newark, CA, USA). In brief, at least three 10-mm–thick sections were placed in a 1.5-mL microcentrifuge tube, and 500 μL of Dewaxil reagent was added. The sample was incubated at 90°C for 1 h, followed by addition of 180 μL of lysis buffer and a brief centrifugation. Two phases were formed; 20 μL of proteinase K was added to the lower phase, and the mixture was incubated at 56°C for 1.5 h. After incubation, the sample was centrifuged for 1 min, and the lower phase was transferred into a new tube. RNase A (2.0 μL, 100 mg/mL) was added, followed by addition of 100 μL of binding buffer and 100 μL of 100% ethanol. The entire mixture was then transferred into a separation column (BioChain Institute, Inc.) and centrifuged at 6,000 × *g* for 1 min. The column was washed twice with the provided buffers. DNA was extracted by adding 50 μL of elution buffer and centrifuging for 1 min at maximum speed. Samples were used immediately or stored at –80°C.

Table. Uncultivated *Paracoccidioides brasiliensis* strains isolated from 6 bottlenose infected dolphins (*Tursiops truncatus*), Indian River Lagoon, Florida, USA

Strain	Dolphin age, y/sex	Year of collection
FB-921	Unknown/F	2003
FB-938	15/M	2003
FB-946	17/M	2003
FB-952	18/M	2003
B92–932	14/F	1992
SW070458	19/F	2007

Amplification and Sequencing of Partial *Kex* Gene Sequences

Because genomic DNA extraction from formalin-fixed tissues usually degrades genome DNA into small pieces, we designed primers targeting fragments <300 bp. To properly verify previous findings, we selected a conserved region of the *Kex* partial DNA sequence to target a DNA epitope other than *gp43* and ITS sequences used by other investigators (*14–16*). We used the protocol of Vilela et al. (*12*) to search for homologous DNA sequences of Kex protein in GenBank, aligned sequences by using ClustalW, version 1.81 (*17*), and inspected them visually.

Conserved regions were selected to construct the set of primers *Kex*-1F 5′-TGCTTYGGTTTGGGGTTG-3′ and *Kex*-2R 5′-CACTGGARCCGTCAGCTA-3′. The set of primers were designed to amplify a 151-bp region of the *Kex* DNA sequence according to the PCR protocol of Vilela et al. (*12*). Amplicons were ligated into the pCR 2.1-TOPO vector (Invitrogen, Carlsbad, CA. USA), purified, and sequenced by using BigDye Terminator Chemistry in an ABI Prim 310 Genetic Analyzer (Applied Biosystems, Foster City, CA. USA).

To further corroborate our results, we used *gp43* DNA sequences reported by Minakawa et al. (GenBank accession no. AB811031) (*14*) and Ueda et al. (GenBank accession no. LC067206) (*15*) and ITS DNA sequences reported by Esperón et al. (GenBank accession no. HQ413323) (*16*) for phylogenetic analysis of several homologous DNA sequences of *P. brasiliensis*, *P. lutzii*, and *L. loboi* in GenBank. We also analyzed 2 unpublished *CHS4* gene sequences (GenBank accession nos. KX267767 [A3] and KX267768 [90A]; A. Schaefer, P, McCarthy, unpub. data) isolated in 2008 from 2 dolphins with lacaziosis/lobomycosis in the Indian River Lagoon.

Phylogenetic Analyses

Homologous DNA sequences of partial *CHS4*, *gp43*, *Kex*, and ITS sequences of *P. brasiliensis*, *P. lutzii*, *L. loboi*, *Ajellomyces capsulatus*, and *A. dermatitidis* were aligned by using default settings in ClustalW, version 1.81 (*17*) inspected visually, and exported for analysis by using maximum-parsimony and neighbor-joining in MEGA6 (http://www.megasoftware.net) (*18*). Aligned sequences were exported for parsimony analysis by using a heuristic search with tree bisection reconnection branch swapping (MEGA6) and distant analysis by neighbor-joining (MEGA6).

We coded large insertions as 1 event by excluding all but 1 nt/insertion. Generated gaps were treated as missing data. Neighbor-joining analyses used either uncorrected distances or maximum-likelihood estimates of distances with a general time reversible model (6ST), empirical base frequencies, and either no rate variation among sites or a gamma distribution (shape parameter 0.5) of variation among sites with 4 rate categories. Support for branches was estimated as the percentage of neighbor-joining trees containing the branch on the basis of neighbor-joining analysis of maximum likelihood distances of 1,000 bootstrapped datasets.

Results

PCR Amplification and Analysis by Using Basic Local Alignment Search Tool

Microscopically, the 6 silver-stained specimens showed branching chains of yeast-like cells connected by small isthmuses, which is typical of this pathogen from infected dolphins with lacaziosis/lobomycosis (Figure 1). PCR amplified the 151-bp DNA sequence from each of the genomic DNAs from the 6 dolphin formalin-fixed tissues. These DNA sequences were deposited into GenBank under accession nos. KX239500 for SW0704, KX239501 for FB946, KX239502 for FB921, KX239503 for FB 952, KX239504 for FB938, and KX239505 for B92-932. Primers targeting other DNA sequences ≥300 bp did not produce amplicons for all 6 DNA specimens.

Alignment of *P. brasiliensis* and *L. loboi* sequences from humans available in GenBank showed that partial *Kex* gene sequences of these fungi from dolphins were similar to those of *P. brasilienis* from humans. The only difference between *P. brasiliensis* sequences from humans and those from dolphins was a gap caused by a missing nucleotide in *P. brasiliensis* sequence from dolphins (Figure 2). *P. lutzii* and *L. loboi* sequences had several nucleotide mismatches and long gaps caused by several missing nucleotides (Figure 2). BLAST (https://blast.ncbi.nlm.nih.gov/Blast.cgi) analysis showed that the 6 partial *Kex* gene sequences had 100% homology with 7 *P. brasiliensis* sequences (GenBank accession nos. EU870193, EF672178, EF672177, EU870183, EU870177, EU870176, and EF672176), 93% homology with 5 *P. lutzii* sequences (GenBank accession nos. EF672176, EU870176, AF486805, EU870183, and EU870177), and 73% homology with 4 *L. loboi* sequences (GenBank accession nos. EU167516, EU167517, EU167518, and EU167519).

Phylogenetic Analysis

Analysis of homologous partial *CHS4*, *Gp43*, *Kex*, and ITS sequences of *P. brasiliensis*, *P. lutzii*, *L. loboi*, *A. capsulatus*, and *A. dermatitidis* (the 2 *Ajellomyces* species sequences were used as outgroups) by parsimony and neighbor-joining showed that dolphin-derived pathogen sequences could be placed among *P. brasiliensis* sequences isolated from humans with paracoccidioidomycosis (Figure 3). *P. lutzii* and *L. loboi* resolved into 2 low-supported clusters. The partial *Kex* gene sequences of *L. loboi* available in GenBank placed this uncultivated pathogen among *Paracoccidioides* species (Figure 3). Placement of dolphin pathogen *Kex* gene sequences within the cluster of *P. brasiliensis* was also phylogenetically corroborated by using *CHS4*, *Gp43*, and ITS sequences available in GenBank (Figure 4). Dolphin-derived pathogen sequences clustered with good bootstrap support among sequences of *P. brasiliensis* isolates from humans.

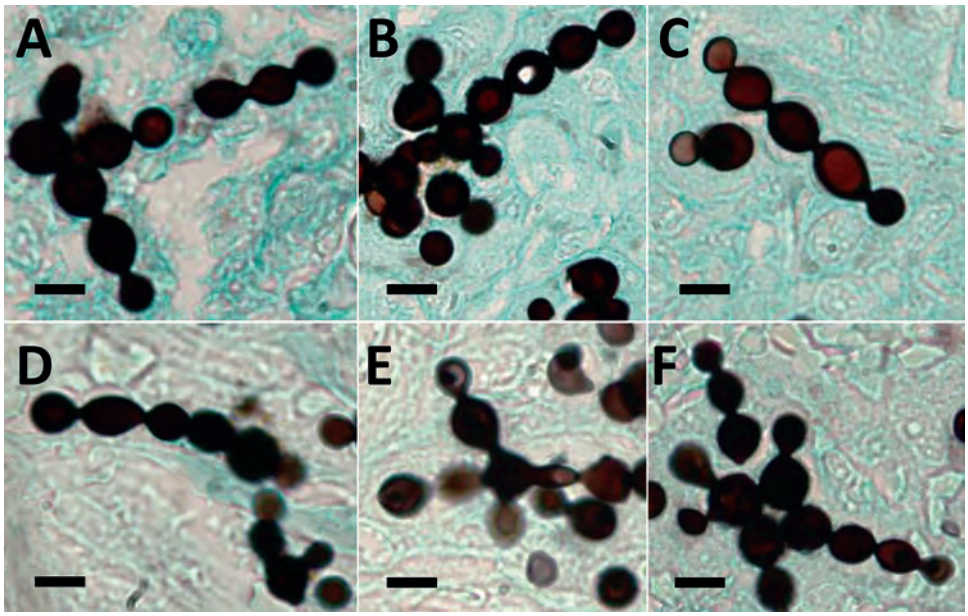

Figure 1. Infected tissues from 6 bottlenose dolphins (*Tursiops truncatus*) with paracoccidioidomycosis ceti, Indian River Lagoon, Florida, USA, showing typical branching chains of yeast-like cells of *Paracoccidioides brasiliensis* connected by small isthmuses. A) Strain FB-921; B) FB-938; C) FB-946; D) FB-952; E) B92-932; F) SW070458. Gomori's methenamine silver stained. Scale bars indicate 10 µm.

```
Pb_Kex_EU870191          85-CTCGTTCATTGGTAAGTGCCAACAAA-GCCCCGCGCCCCCCTTGCTGCTATCCAA-139
Pb_Kex_EF672177          85-CTCGTTCATTGGTAAGTGCCAACAAA-ACCCCGCGCCCCCCTTGCTGCTATCCAA-139
Pb_Kex_Pb18_EF672177     85-CTCGTTCATTGGTAAGTGCCAACAAA-ACCCCGCGCCCCCCTTGCTGCTATCCAA-139
Pb_Kex_Pb73_EF672178     85-CTCGTTCATTGGTAAGTGCCAACAAA-GCCCCGCGCCCCCCTTGCTGCTATCCAA-139
Pb_Kex_Pb2_EU870193      85-CTCGTTCATTGGTAAGTGCCAACAAA-GCCCCGCGCCCCCCTTGCTGCTATCCAA-139
Dolphin_Kex_KX239500     85-CTCGTTCATTGGTAAGTGCCAACAAA-GCCCCGC-CCCCCCTTGCTGCTATCCAA-138
Dolphin_Kex_KX239501     85-CTCGTTCATTGGTAAGTGCCAACAAA-GCCCCGC-CCCCCCTTGCTGCTATCCAA-138
Dolphin_Kex_KX239502     85-CTCGTTCATTGGTAAGTGCCAACAAA-GCCCCGC-CCCCCCTTGCTGCTATCCAA-138
Dolphin_Kex_KX239503     85-CTCGTTCATTGGTAAGTGCCAACAAA-GCCCCGC-CCCCCCTTGCTGCTATCCAA-138
Dolphin_Kex_KX239504     85-CTCGTTCATTGGTAAGTGCCAACAAA-GCCCCGC-CCCCCCTTGCTGCTATCCAA-138
Dolphin_Kex_KX239505     85-CTCGTTCATTGGTAAGTGCCAACAAA-GCCCCGC-CCCCCCTTGCTGCTATCCAA-138
Pl_Kex_Pb01_EF672176     85-CTCGTTCATTGGTAAGTGCCAACAAAAGCCCCCC-----CACTCCTGCTATCCAA-134
Pl_Kex_Pb01_EU870176     85-CTCGTTCATTGGTAAGTGCCAACAAAAGCCCCCC-----CACTCCTGCTATCCAA-134
Pl_kex_AF486805          85-CTCGTTCATTGGTAAGTGCCAACAAAAGCCCCCC-----CACTCCTGCTATCCAA-134
Pl_Kex_EU870183          85-CTCGTTCATTGGTAAGTGCCAACAAAAGCCCCCC-----CACTCCTGCTATCCAA-134
Pl_kex_EU870177          85-CTCGTTCATTGGTAAGTGCCAACAAAAGCCCCCC-----CACTCCTGCTATCCAA-134
Ll_Human_kex_EU167519    85-GTTGTTCACTGGTAAACGCCAACAAA-GCCCC-------------TGCTATCCAA-126
Ll_Human_Kex_EU167516    85-GTTGTTCACTGGTAAACGCCAACAAA-GCCCC-------------TGCTATCCAA-126
Ll_Human_Kes_EU167518    85-GTTGTTCACTGGTAAACGCCAACAAA-GCCCC-------------TGCTATCCAA-126
Ll_Human_kex_EU167517    85-GTTGTTCACTGGTAAACGCCAACAAA-GCCCC-------------TGCTATCCAA-126
```

Figure 2. Nucleotide sequences of partial *Kex* gene exons of *Lacazia loboi* (Ll) and *Paracoccidioides brasiliensis* (Pb), including pathogen DNA sequences isolated from bottlenose dolphins, Indian River Lagoon, Florida, USA, and *P. lutzii* (Pl) containing mismatches (bold) and unique gaps. Red box indicates DNA sequences missing a nucleotide present in *P. brasiliensis* from humans. Numbers before and after sequences indicate nucleotide location of the depicted epitope. –, deletion.

Discussion

We found that fungal DNA sequences isolated from dolphins with skin granulomas containing yeast-like cells had strong homology with sequences of cultivated *P. brasiliesis* from humans (*14–16*). Since cutaneous granulomas containing chains of yeast-like cells in 3 dolphin species (*Sotalia guainensis*, *T. aduncus*, and *T. truncatus*) were initially reported, the etiologic agent of lacaziosis/lobomycosis was believed to be *L. loboi*, which causes similar skin granulomas in humans (*1–7*,*19*). This hypothesis was based on phenotypic characteristics of the pathogen (uniform size yeast-like cells in chains connected by slender isthmuses and resistance to culture) and clinical presentation (keloidal-like granulomas) in humans and dolphins with lacaziosis/lobomycosis (*1*,*4*,*19*). Although some authors had reported minor phenotypic differences, such as smaller size of yeast-like cells in infected dolphins than of yeast-like cells in infected humans (*20*), the true phenotypic differences between the causative agent of keloidal-like skin infections in dolphins and humans are not fully understood (*4*,*20*).

Studies using serum samples from humans and dolphins with lacaziosis/lobomycosis, mice experimentally infected with *L. loboi*, and serum samples from humans with paracocidioidomycosis showed that IgG in serum samples from dolphins and humans infected with *L. loboi* had strong cross-reactivity with the gp43 antigen of *P. brasiliensis* (*4*,*6*,*21*). These findings support the hypothesis that the uncultivated organism causing cutaneous granulomas in humans and dolphins was *L. loboi*. Findings also implied that the gp43 antigen of the etiologic agent of parakeloidal-like granulomas in humans and dolphins was antigenically similar to that of *P. brasiliensis*. On the basis of these serologic studies (*4*,*6*,*21*), current phylogenetic data for *gp43* and *Kex* gene exons, and ITS DNA sequences, placement of *L. loboi* from humans in its own genus is questionable. Efforts to culture the organism from dolphins on classical laboratory media successfully used to isolate *P. brasiliensis* from humans with paracoccidioidomycosis were not successful (*4*,*7*). The physiologic basis of the inability to culture the etiologic agent from dolphins with cutaneous granulomas is not known. Thus, the life cycle features of this agent remain an enigma.

Our phylogenetic (parsimony) analysis of partial *Kex* DNA sequences validated reports suggesting that keloidal-like lesions in dolphins are caused by a novel uncultivated *P. brasiliensis* (*13–16*). We analyzed DNA sequences of pathogens isolated from 6 dolphins with lacaziosis/lobomycosis captured in the Indian River Lagoon. Diverse geographic locations of dolphins in the Atlantic Ocean (*13*,*16*) and the Pacific Ocean (*14*,*15*) and specimens evaluated by molecular methods provide additional support for placement of the etiologic agent of keloidal-like granulomas in dolphins within *P. brasiliensis* (Figure 3). Because these geographic locations, especially for cases from Japan (*14*,*15*), have different ecologic niches than locations for *P. brasiliensis* in South America (*4*), detection of dolphins infected with an uncultivated *P. brasiliensis* type in these ecosystems is a major finding.

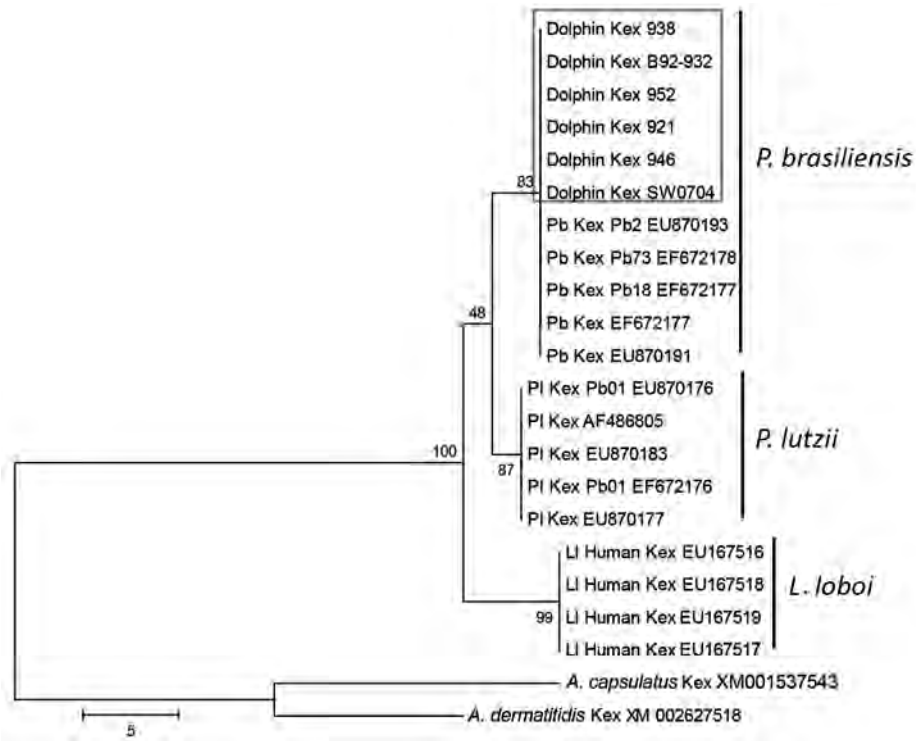

Figure 3. Unrooted maximum-parsimony phylogenetic tree of partial *Kex* gene sequences of *Paracoccidioides brasiliensis* (Pb) from 6 bottlenose dolphins, Indian River Lagoon, Florida, USA, with skin granulomas and homologous sequences of *P. brasiliensis*, *P. lutzii* (Pl), and *Lacazia loboi* (Ll) available in GenBank. *Ajellomyces capsulatus* and *A. dermatitidis* homologous sequences were used as outgroups. Strain names or accession numbers are shown. Numbers along branches are bootstrap values for 1,000 resamplings as obtained by parsimony analysis, which support different clusters. Box indicates uncultivated *P. brasiliensis* from dolphins grouped in the same cluster with cultivated *P. brasiliensis* from humans with paracoccidioidomycosis. Sequences of *P. lutzii* and *L. loboi* were placed with low bootstrap support as the sister group to *P. brasiliensis*. Scale bar indicates nucleotide substitutions per site.

Moreover, our phylogenetic data obtained by using *gp43* gene exons of Minakawa et al. (*14*) and Ueda et al. (*15*), ITS sequences of Esperón et al. (*16*), and 2 CHS4 gene sequences (A. Schaefer, P. McCarthy, unpub. data) strongly support placement of the dolphin pathogen within cultivated *P. brasiliensis* isolates from humans (Figure 4). The distance between ITS sequences from dolphins and *P. brasiliensis* ITS sequences from humans is large (Figure 4, panel A). An evaluation of additional ITS sequences from dolphin uncultivated *P. brasiliensis* strains from dolphins is needed to determine if this variation indicates 2 different populations or rapid substitutions in this DNA region.

Molecular data for dolphins in the Pacific and Atlantic Oceans in previous studies (*13–16*), the 6 pathogen DNA sequences isolated from dolphins (this study), and 2 *CHS4* gene sequences (A. Schaefer, P. McCarthy, unpub. data) place the uncultivated pathogen within cultivated *P. brasiliensis* strains. These studies added support to the notion that a novel uncultivated *P. brasiliensis*, which is different from the cultivated *P. brasiliensis* causing human paracoccidioidomycosis and *L. loboi* causing parakeloidal-like lesions in humans, is the causative agent of lacaziosis/lobomycosis in dolphins. Placement of *L. loboi* in a different cluster from dolphin-derived uncultivated *P. brasiliensis* indicates that, although both pathogens have identical phenotypes and cause similar skin lesions, they have different evolutionary paths.

Disease that shows keloidal-like granulomas in humans and dolphins has been known by several different names, such as Jorge Lobo disease (*4*), Lobo's disease (*3*,*5*,*22*), lobomycosis (*1*,*6*,*13*,*16*,*19*,*23*,*24*), and lacaziosis (*11*,*12*,*14*,*15*). In view of most recent findings, the names used to describe this disease in dolphins are no longer supported. Minakawa et al. (*14*) proposed maintaining the name lacaziosis with the understanding that this name would include *L. loboi* (humans), uncultivated *Paracoccidioides* species, and *P. brasiliensis* (dolphins). However, in our phylogenetic analysis, the *Paracoccidioides* sp. strain (GenBank accession no. AB811031) of Ueda et al. (*15*) from an infected dolphin grouped among human *P. brasiliensis* strains. Thus, this strain is phylogenetically similar to strain LC057206. Furthermore, phylogenetic analysis of ITS sequences from dolphins with lacaziosis/lobomycosis placed *L. loboi* (with strong bootstrap support) in its own genus (Figure 3, panel A). Thus, the proposal by Minakawa et al. (*14*). could add more confusion to the taxonomic status of these 2 uncultivated fungal etiologies. In the interim, we propose paracoccidioidomycosis ceti for the disease caused by uncultivated *P. brasiliensis* in dolphins. This term best describes the current status of infected dolphins with keloidal-like granulomas and yeast-like cells in chains in infected tissues.

Uncultivated *P. brasiliensis* from Japan that causes skin infections in a new species of dolphins (*Lagenorhynchus obliquidens*) suggests that the geographic distribution of this pathogen is expanding and could also infect other species (*14*,*15*). Thus, whales and other cetaceans need to be investigated for this pathogen (*14*). Paniz-Mondolfi et al. (*24*) suggested that distinguishing apparent expansions

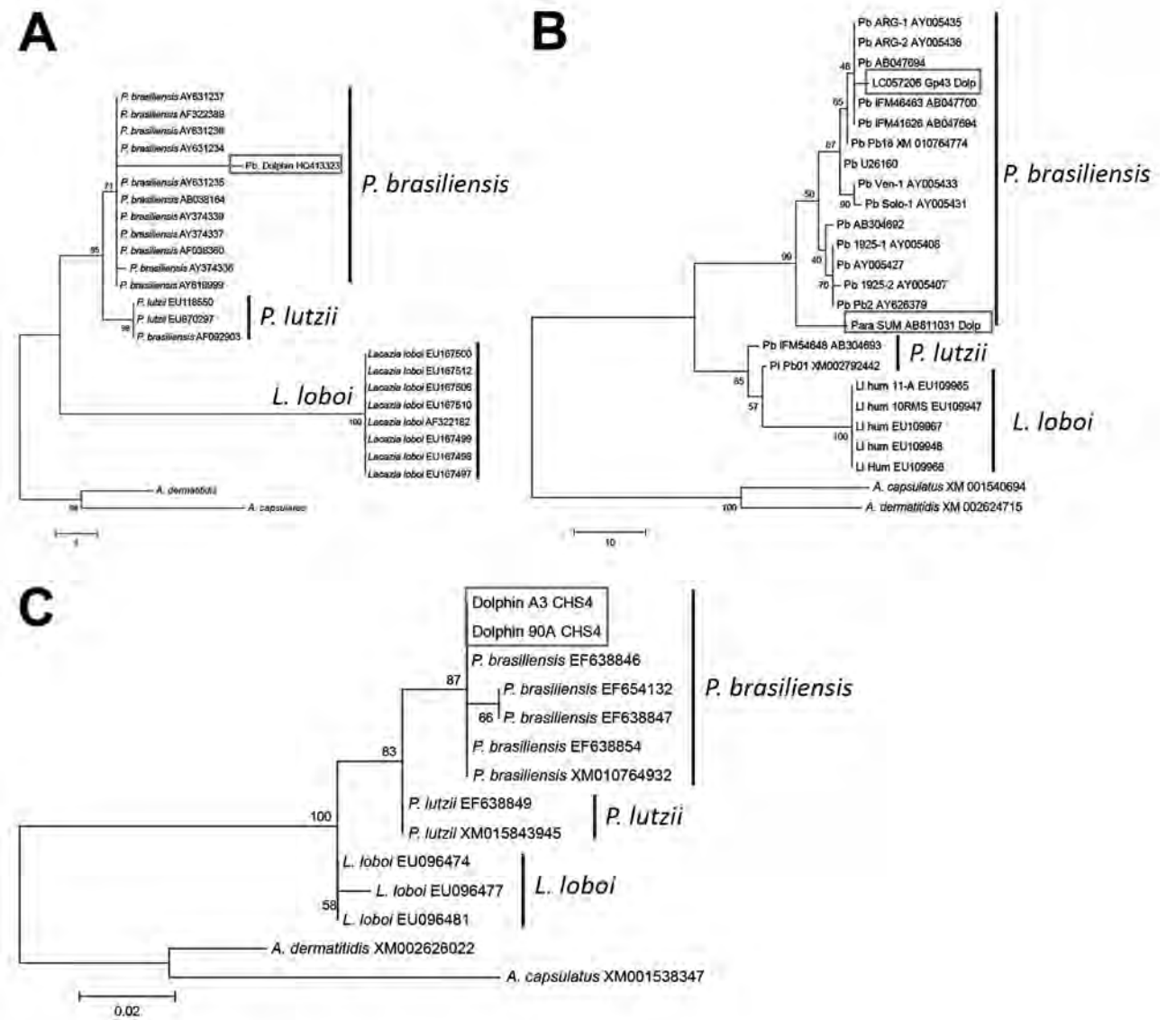

Figure 4. Unrooted maximum-parsimony phylogenetic trees of A) partial internal transcribed spacer (ITS), B) 2 partial glycoprotein 43 (*gp43*) (*12–14*), and C) 2 partial chitin synthase 4 (*CHS4*) (A. Schaefer, P.J. McCarthy, unpub. data) gene sequences of *Paracoccidioides brasiliensis*. Sequences were obtained pathogen-infected bottlenose dolphins, Indian River Lagoon, Florida, USA, and compared with homologous sequences of cultivated *Paracoccidioides brasiliensis* (*Pb*), *P. lutzii* (Pi), and uncultivated *Lacazia loboi* (Ll) available in GenBank. *Ajellomyeces capsulatus* and *A. dermatitidis CHS4*, *gp43*, and ITS homologous sequences were used as outgroups. Strain names or accession numbers are shown. Numbers along branches are bootstrap values for 1,000 resamplings obtained by parsimony analysis, which support different clusters. *P. brasiliensis* ITS sequences from dolphins (*14*) grouped among cultivated *P. brasiliensis* ITS sequences. Distance between uncultivated *P. brasiliensis* from dolphins and cultivated *P. brasiliensis* from humans is unusually large (box in panel A). Placement of 2 *gp43 P. brasiliensis* sequences from dolphins (*12*,*13*) among cultivated *P. brasiliensis* strains (boxes in panel B). *P. brasiliensis* partial *CHS4* gene sequences from 2 dolphins placed these sequences (GenBank accession no. KX267767 [A3] and KX267768 [90A]) within the *P. brasiliensis* cluster (box in panel C). Scale bars indicate nucleotide substitutions per site.

of the ecologic niche caused by increased interest and surveillance by identification programs from a change in distribution would be difficult. The likelihood that this phenomenon is an expansion of its ecologic niche caused by global climate changes or increased surveillance is difficult to prove, but it is an intriguing possibility.

Although the ITS sequences of *L. loboi* from humans still group this pathogen in its own cluster, our molecular data for DNA protein-coding sequences indicate that the 3 species in this study (cultivated and uncultivated *P. brasiliensis*, *P. lutzii* from humans and dolphins, and *L. loboi* from humans) all have the same ancestor. Thus, all 3 species

belong to the same genus (*Paracocidioides*). Comprehensive phylogenetic and genomic analyses of *L. loboi* from humans and uncultivated *P. brasiliensis* from dolphins are needed to corroborate results of these analyses and identify the true evolutionary history of *L. loboi* from humans. Our findings could stimulate new interest in lacaziosis and paracoccidioidomycosis ceti, which has been restricted to humans in South America and dolphins in many oceans.

Acknowledgments

We thank Wayne McFee for performing age analysis on wild dolphins. Free-ranging dolphins were collected under National Marine Fisheries Service Scientific Research permit no. 998-1678 to G.D.B. as part of the Bottlenose Dolphin Health and Risk Assessment Project conducted in the Indian River Lagoon, Florida, and the estuarine waters of Charleston, South Carolina.

This study was supported in part by the Department of Microbiology and Molecular Genetics, Michigan State University.

Dr. Vilela is a physician in the Faculty of Pharmacy, Federal University of Minas Gerais, Belo Horizonte, Brazil. Her research interests include *Lacazia loboi*, *Lagenidium* spp., *Pythium insidiosum*, and *Rhinosporidium seeberi*.

References

1. Bossart GD. Suspected acquired immunodeficiency in an Atlantic bottlenosed dolphin with chronic-active hepatitis and lobomycosis. J Am Vet Med Assoc. 1984;185:1413–4.
2. Bossart GD, Schaefer AM, McCulloch S, Goldstein J, Fair PA, Reif JS. Mucocutaneous lesions in free-ranging Atlantic bottlenose dolphins *Tursiops truncatus* from the southeastern USA. Dis Aquat Organ. 2015;115:175–84. http://dx.doi.org/10.3354/dao02895
3. deVries GA, Laarman JJ. A case of Lobo's disease in the dolphin *Sotalia guianesis.* Journal of Aquatic Mammals. 1973;1:26–33.
4. da Lacaz S, Baruzzi RG, Rosa CB. Lobo's disease [in Portuguese]. São Paulo: Editora da Universidad de IPSIS Gráfica e Editora; 1986.
5. Migaki G, Valerio MG, Irvine B, Garner FM. Lobo's disease in an Atlantic bottle-nosed dolphin. J Am Vet Med Assoc. 1971;159:578–82.
6. Woodard JC. Electron microscopic study of lobomycosis (*Loboa loboi*). Lab Invest. 1972;27:606–12.
7. Schaefer AM, Reif JS, Guzmán EA, Bossart GD, Ottuso P, Snyder J, et al. Toward the identification, characterization and experimental culture of *Lacazia loboi* from Atlantic bottlenose dolphin (*Tursiops truncatus*). Med Mycol. 2016;54:659–65. http://dx.doi.org/10.1093/mmy/myw011
8. Silva ME, Kaplan W, Miranda JL. Antigenic relationships between *Paracoccidioides loboi* and other pathogenic fungi determined by immunofluorescence. Mycopathol Mycol Appl. 1968;36:97–106. http://dx.doi.org/10.1007/BF02049674
9. Taborda PR, Taborda VA, McGinnis MR. *Lacazia loboi* gen. nov., comb. nov., the etiologic agent of lobomycosis. J Clin Microbiol. 1999;37:2031–3.
10. Herr RA, Tarcha EJ, Taborda PR, Taylor JW, Ajello L, Mendoza L. Phylogenetic analysis of *Lacazia loboi* places this previously uncharacterized pathogen within the dimorphic Onygenales. J Clin Microbiol. 2001;39:309–14. http://dx.doi.org/10.1128/JCM.39.1.309-314.2001
11. Vilela R, Mendoza L, Rosa PS, Belone AF, Madeira S, Opromolla DV, et al. Molecular model for studying the uncultivated fungal pathogen *Lacazia loboi.* J Clin Microbiol. 2005;43:3657–61. http://dx.doi.org/10.1128/JCM.43.8.3657-3661.2005
12. Vilela R, Rosa PS, Belone AFF, Taylor JW, Diório SM, Mendoza L. Molecular phylogeny of animal pathogen *Lacazia loboi* inferred from rDNA and DNA coding sequences. Mycol Res. 2009;113:851–7. http://dx.doi.org/10.1016/j.mycres.2009.04.007
13. Rotstein DS, Burdett LG, McLellan W, Schwacke L, Rowles T, Terio KA, et al. Lobomycosis in offshore bottlenose dolphins (*Tursiops truncatus*), North Carolina. Emerg Infect Dis. 2009;15:588–90. http://dx.doi.org/10.3201/eid1504.081358
14. Minakawa T, Ueda K, Tanaka M, Tanaka N, Kuwamura M, Izawa T, et al. Detection of multiple budding yeast cells and a partial sequence of 43-kDa glycoprotein coding gene of *Paracoccidioides brasiliensis* from a case of lacaziosis in a female Pacific white-sided dolphin (*Lagenorhynchus obliquidens*). Mycopathologia. 2016;181:523–9. http://dx.doi.org/10.1007/s11046-016-9988-4
15. Ueda K, Sano A, Yamate J, Nakagawa EI, Kuwamura M, Izawa T, et al. Two cases of lacaziosis in bottlenose dolphins (*Tursiops truncates*) in Japan. Case Reports in Veterinary Medicines. 2013;2013 [cited 2016 Sep 2]. https://www.hindawi.com/journals/crivem/2013/318548/
16. Esperón F, García-Párraga D, Bellière EN, Sánchez-Vizcaíno JM. Molecular diagnosis of lobomycosis-like disease in a bottlenose dolphin in captivity. Med Mycol. 2012;50:106–9. http://dx.doi.org/10.3109/13693786.2011.594100
17. Thompson JD, Higgins DG, Gibson TJ. CLUSTAL W: improving the sensitivity of progressive multiple sequence alignment through sequence weighting, position-specific gap penalties and weight matrix choice. Nucleic Acids Res. 1994;22:4673–80. http://dx.doi.org/10.1093/nar/22.22.4673
18. Tamura K, Peterson D, Peterson N, Stecher G, Nei M, Kumar S. MEGA5: molecular evolutionary genetics analysis using maximum likelihood, evolutionary distance, and maximum parsimony methods. Mol Biol Evol. 2011;28:2731–9. http://dx.doi.org/10.1093/molbev/msr121
19. Reif JS, Mazzoil M, McCulloch SD, Varela RA, Goldstein JD, Fair PA, et al. Lobomycosis in Atlantic bottlenose dolphins (*Tursiops truncatus*) from the Indian River Lagoon, Florida. J Am Vet Med Assoc. 2006;228:104–8. http://dx.doi.org/10.2460/javma.228.1.104
20. Haubold EM, Cooper CR Jr, Wen JW, McGinnis MR, Cowan DF. Comparative morphology of *Lacazia loboi* (syn. *Loboa loboi*) in dolphins and humans. Med Mycol. 2000;38:9–14. http://dx.doi.org/10.1080/714030877
21. Mendoza L, Belone AFF, Vilela R, Rehtanz M, Bossart GD, Reif JS, et al. Use of sera from humans and dolphins with lacaziosis and sera from experimentally infected mice for Western blot analyses of *Lacazia loboi* antigens. Clin Vaccine Immunol. 2008;15:164–7. http://dx.doi.org/10.1128/CVI.00201-07
22. Symmers WS. A possible case of Lôbo's disease acquired in Europe from a bottle-nosed dolphin (*Tursiops truncatus*). Bull Soc Pathol Exot Filiales. 1983;76:777–84.
23. Kiszka J, Van Bressem M-F, Pusineri C. Lobomycosis-like disease and other skin conditions in Indo-Pacific bottlenose dolphins *Tursiops aduncus* from the Indian Ocean. Dis Aquat Organ. 2009;84:151–7. http://dx.doi.org/10.3354/dao02037
24. Paniz-Mondolfi A, Talhari C, Sander Hoffmann L, Connor DL, Talhari S, Bermudez-Villapol L, et al. Lobomycosis: an emerging disease in humans and delphinidae. Mycoses. 2012;55:298–309. http://dx.doi.org/10.1111/j.1439-0507.2012.02184.x

Address for correspondence: Leonel Mendoza, Biomedical Laboratory Diagnostics Program, Department of Microbiology and Molecular Genetics, Michigan State University, North Kedzie Hall, 354 Farm Lane, Rm 324, East Lansing, MI 48824-1031, USA; email: mendoza9@msu.edu

Vertebrate Host Susceptibility to Heartland Virus

Angela M. Bosco-Lauth, Amanda E. Calvert, J. Jeffrey Root, Tom Gidlewski, Brian H. Bird, Richard A. Bowen, Atis Muehlenbachs, Sherif R. Zaki, Aaron C. Brault

Heartland virus (HRTV) is a recently described phlebovirus initially isolated in 2009 from 2 humans who had leukopenia and thrombocytopenia. Serologic assessment of domestic and wild animal populations near the residence of 1 of these persons showed high exposure rates to raccoons, white-tailed deer, and horses. To our knowledge, no laboratory-based assessments of viremic potential of animals infected with HRTV have been performed. We experimentally inoculated several vertebrates (raccoons, goats, chickens, rabbits, hamsters, C57BL/6 mice, and interferon-α/β/γ receptor–deficient [Ag129]) mice with this virus. All animals showed immune responses against HRTV after primary or secondary exposure. However, neutralizing antibody responses were limited. Only Ag129 mice showed detectable viremia and associated illness and death, which were dose dependent. Ag129 mice also showed development of mean peak viral antibody titers >8 $\log_{10}$ PFU/mL, hemorrhagic hepatic lesions, splenomegaly, and large amounts of HRTV antigen in mononuclear cells and hematopoietic cells in the spleen.

Heartland virus (HRTV) is a novel bunyavirus (family *Bunyaviridae*, genus *Phlebovirus*) first identified in the United States in 2 persons with thrombocytopenia/leukopenia in Missouri in 2009 (*1*). The virus has subsequently been isolated from nymphal *Amblyomma americanum* ticks collected at sites adjacent to the residences of the index case-patients (*2*). High seroprevalence rates for HRTV have been reported in northern raccoons (*Procyon lotor*), white-tailed deer (*Odocoileus virginianus*), and horses sampled near the residences of human case-patients (*3*). Additional serosurveillance in wildlife has demonstrated wide-ranging antibody prevalence to HRTV across the geographic host range distribution of *A. americanum* ticks (*4*).

Author affiliations: Centers for Disease Control and Prevention, Fort Collins, Colorado, USA (A.M. Bosco-Lauth, A.E. Calvert, A.C. Brault); Colorado State University, Fort Collins (A.M. Bosco-Lauth, R.A. Bowen); US Department of Agriculture, Fort Collins (J.J. Root, T. Gidlewski); Centers for Disease Control and Prevention, Atlanta, Georgia, USA (B.H. Bird, A. Muehlenbachs, S.R. Zaki)

DOI: http://dx.doi.org/10.3201/eid2212.160472

Genetically, HRTV is most closely related to severe fever with thrombocytopenia syndrome virus (SFTSV) (*1*), a tickborne virus in Asia that causes high fever, thrombocytopenia, leukopenia, gastrointestinal disorders, central nervous system involvement, disseminated intravascular coagulopathy; and multiorgan dysfunction. Infection with this virus shows a case-fatality rate of ≈12% in humans (*5*,*6*). Severe disease progression of patients infected with SFTSV has further been associated with increased cytokine and chemokine responses (*7*) and increased viremias throughout the course of disease (*6*). Infection of rhesus macaques with SFTSV caused mild human disease syndromes similar to those in humans, including thrombocytopenia, leukopenia, and increased levels of hepatic and cardiac enzymes (*8*).

Unlike SFTSV, which has been associated with thousands of cases of symptomatic human disease in China (*5*) and South Korea (*9*), only 8 diagnosed human cases of HRTV infection have been reported in the United States, and 1 death in 2013 (*10*). Of those patients, 7 were from Missouri and 1 from Tennessee (this patient died), which indicated the continued presence of the virus over the course of several years and over a wide geographic range (*11*). Similar to that described for SFTSV, patients infected with HRTV commonly have fever, fatigue, anorexia, thrombocytopenia, leukopenia, and increased levels of hepatic enzymes (*11*).

With the recent discovery of SFTSV, HRTV, and other novel phleboviral agents in recent years (*12*–*14*), it is apparent that tickborne phleboviruses have been largely underrecognized as potential human disease agents. The vertebrate host range associations for SFTSV have been poorly described and have not been addressed for HRTV by experimental animal inoculation studies.

Given the serologic evidence that northern raccoons are commonly exposed to HRTV across the central and eastern United States (*4*) and near the residence of a human index case-patient (*3*), we performed experimental inoculations of raccoons with HRTV. In addition, on the basis of results of goat serosurveillance for SFTSV in China (*15*) and experimental infections (*16*), we performed experimental inoculation of goats with HRTV. We also assessed animal models (chickens, rabbits, hamsters, and mice) for

host competence for HRTV to identify host range restrictions of the virus and establish a potential model for viremic blood feeding for subsequent tick infections.

Materials and Methods

Viruses and Animal Models

We used an isolate of HRTV (Mo4) obtained from serum of an acutely ill human patient in the fall of 2009 for experimental infections and plaque reduction neutralization tests (PRNTs). The isolate was passaged once on Vero E6 cells (African green monkey kidney cell line). Lone Star virus (LSV) strain 2229 was used as a control virus for intraperitoneal and intracranial inoculation of CD-1 mice. All animal models (including strain, age, inoculation route, and dose inoculated) assessed for host competence for HRTV are shown in Table 1. New Zealand white rabbits, chickens, Syrian golden hamsters, C57BL/6 mice, and CD-1 mice were obtained from Charles River Laboratories (Wilmington, MA, USA) and housed at the Centers for Disease Control and Prevention (Fort Collins, CO, USA) in Animal Biosafety Level 3 (ABSL 3) conditions. Ag129 mice (α/β/γ receptor knockout) (*17*) were originally obtained from B & K Universal (Hull, UK) and bred in house. The receptor knockout genotype of the Ag129 mouse breeding line was confirmed by genetic PCR markers generated from tail snip tissues from 10 mice (Transnetyx, Cordova, TN, USA).

Boer goats were obtained from a private vendor and housed in the Colorado State University Animal Disease ABSL 3 Laboratory. Six raccoons were caught in the wild in Larimer County, Colorado, and housed in a US Department of Agriculture facility for several months before being transferred to the Animal Disease ABSL 3 Laboratory at Colorado State University for experimental inoculation. Raccoon serum samples were screened for neutralizing antibodies against HRTV/phlebovirus as described (*3*) and in this report. All animal handling, trapping, and care was in compliance with approved Institutional Animal Care and Use Committee protocols under the oversight of attending veterinarians. At arrival in the laboratory, all animals were housed for a minimum of 3 days for acclimatization before inoculation.

Experimental Inoculations

We inoculated animals with 10^0–10^5 PFU by subcutaneous, intracranial, or intraperitoneal routes (Table 1). Whole blood was collected from individual hamsters, rabbits, chickens and goats daily during 1–7 days postinoculation (dpi), groups of 3 raccoons on alternating days 1–8 dpi, and 3 groups of 5 or 6 C57BL/6 and Ag129 mice every third day 1–9 dpi. Ag129 mice were divided into 5 dosage groups of 15 mice (10^0–10^4 PFU) (Table 1). At 28 dpi, animals from all groups (except raccoons) were bled and then given booster inoculations with 10^4 PFU of HRTV and analyzed through 42 dpi, at which point the animals were bled and euthanized. Terminal blood samples were obtained from mice by cardiac bleed under deep isoflurane anesthesia just before euthanasia. Two Ag129 mice (10^2 PFU dose group) were terminally bled at 4 days postsecondary challenge, and spleens were harvested for production of monoclonal antibodies (MAbs) as described (*18*).

Raccoons were anesthetized with a ketamine:xylazine cocktail (15–20 mg/kg:3–4 mg/kg) (*3*) given by intramuscular inoculation before sampling, and mice and hamsters were anesthetized in an isoflurane chamber before serum sampling. Rabbits, chickens, and goats were manually restrained appropriately for sample collection without use of anesthetics. Whole blood was collected from peripheral saphenous, cheek, or tail veins (mouse and hamster); ear (rabbit); or jugular (chicken and raccoon). Samples were centrifuged, and serum samples were frozen for subsequent virologic or serologic evaluation. Relative neuroinvasive and neurovirulence phenotypes for HRTV were compared with that for LSV strain 2229 by intraperitoneal and intracranial inoculation, respectively. Isoflurane-anesthetized suckling (2 days old) and weanling (17 days old)

Table 1. Experimental inoculation of vertebrate hosts with Heartland virus*

Experimental animal model	Strain	No.	Age, d/sex	Inoculum dose, PFU	Route of inoculation
Mouse	C57BL/6	15	21/ F	10^4	ip
Mouse	Ag129	15	21/M and F	10^4	ip
Mouse	Ag129	15	21/M and F	10^3	ip
Mouse	Ag129	15	21/M and F	10^2	ip
Mouse	Ag129	15	21/M and F	10^1	ip
Mouse	Ag129	15	21/M and F	10^0	ip
Mouse†	CD-1	10	2	10^3	ic
Mouse†	CD-1	10	17	10^3	ip
Chicken	Leghorn	3	Adult/F	10^4	sc
Hamster	Syrian golden	5	21/F	10^4	sc
Goat	Boer	2	Adult/M and F	10^4	sc
Rabbit	New Zealand white	3	Adult/F	10^4	sc
Raccoon	Wild-caught	6	Adult/M and F	10^4	sc

*Ag129, interferon-α/β/γ receptor–deficient; ic, intracranial; ip, intraperitoneal; sc, subcutaneous.
†CD-1 mice were also inoculated similarly with Lone Star virus (same dose and route as for Heartland virus).

CD-1 mice (n = 10) were inoculated with a 20 μL of sterile phosphate-buffered saline (PBS) suspension of 10^3 PFU of either virus. A group inoculated with minimal essential medium was included as an inoculation control for both routes of inoculation.

Serologic Testing

HRTV neutralizing and total immune reactive antibodies were quantified by using a 70% PRNT ($PRNT_{70}$) (*18*) and ELISA, respectively. For PRNTs, serum samples were heat-inactivated at 56°C for 30 min, and 2-fold serially diluted serum samples were mixed with an equal volume of virus suspension. Plaques were enumerated through 10 dpi, and 70% neutralization endpoints were calculated on the basis of comparison with serum negative controls as described (*3*).

ELISAs were performed in 96-well microtiter plates (Immulon 2HB; Thermo Lab Systems, Franklin, MA, USA). Plate wells were coated with purified virus (0.06 μg/well) in buffer (50 mmol/L sodium carbonate, 50 mmol/L sodium bicarbonate, pH 9.6) and incubated at 4°C overnight (*18*). Plates were washed 5 times with a PBS/0.1% Tween wash buffer, and nonspecific binding sites were blocked with Starting Block (Pierce, Dallas, TX, USA) (100 μL/well). Serum samples were added in serial dilutions in PBS (50 μL/well) and incubated at 37°C for 1 h. Plates were washed 5 times before addition of the species-appropriate horseradish peroxidase conjugate (50 μL/well), diluted 1:5,000 in PBS. After an incubation period of 1 h at 37°C, plates were washed and enhanced K-Blue TMB (3,3′,5,5′ tetramethylbenzidine) substrate (Neogen, Lexington, KY, USA) was added to each well (100 μL/well). The plates were incubated in the dark at room temperature for 10 min. Optical density (OD) was read on an automatic plate reader at 450 nm. Endpoints were determined as an OD reading on duplicate samples that was at least twice that of the average OD for control serum samples. Titers were expressed as the geometric mean of the reciprocal of the endpoints.

Immunohistochemical Analysis

HRTV-inoculated Ag129 mice with signs of disease were subjected to necropsy. Spleen, liver, and kidney tissues were removed, fixed in 10% neutral-buffered formalin, and processed by using routine methods (*10*). Immunohistochemical analysis using rabbit polyclonal antisera against HRTV nucleocapsid (N) protein and an immuno-alkaline phosphatase detection system with Fast Red Chromogen (Biocare Medical, Concord, CA, USA) was used as described (*1*).

Results

Viremia, Death, and Clinical Assessment

Serum samples from chickens, raccoons, goats, rabbits, and hamsters obtained during 1–7 dpi did not show detectable HRTV viremia (Table 2). Despite the previous finding that SFTSV replicates to detectable levels in serum and results in pathologic changes in spleens of immunocompetent C57BL/6 mice (*19*), viremia was not detected in any serum samples from this strain of mice inoculated with HRTV. No infection-associated deaths or clinical signs of illness were observed throughout the course of the infection in any of inoculated animals.

In contrast, 100% of CD-1 mice inoculated intracranially with LSV died within 6 dpi. However, illness or death were not observed in mice inoculated with minimal essential medium or HRTV. Similar to intraperitoneally inoculated C57BL/6 mice, intraperitoneally inoculated CD-1 mice showed no signs of illness or death. However, Ag129 mice showed virus dose-dependent death. Deaths were observed in the group inoculated with 10^4 PFU; the first signs of illness appeared on 4 dpi and death occurred on 5 dpi (Figure 1, panel A). Groups inoculated with 10^3, 10^2, 10^1, or 10^0 PFU had mortality rates of 85%, 83%, 80%, and 20%, respectively. Average survival time was inversely proportional to the inoculation dosage. Mean ± SD survival time ranged from 4.1 ± 0.4 d for the 10^4 PFU dose group to 19.4 ± 4.2 d for the 10^1 PFU dose group (Figure 1, panel A).

Table 2. Viremia and antibody responses of animals experimentally inoculated with Heartland virus*

Animal	Inoculum dose, PFU	Mean peak titer†	dpi	Mean ELISA titer‡	ELISA positive, no. (%)	Mean $PRNT_{70}$ titer‡	$PRNT_{70}$ positive, no. (%)
Mouse (C57BL/6)	10^4	<1.5	42§	4.4 (0.6)	15 (94)	0.7 (0.6)	10 (63)
Chicken	**10^4**	**<1.5**	**14**	**NT**	**NA**	**ND**	**0**
Chicken	10^4	NA	42§	3.0 (0.2)	3 (100)	ND	0
Hamster	10^4	<1.5	42§	4.3 (0.5)	4 (100)	1.3 (0.4)	5 (100)
Goat	**10^5**	**<1.5**	**28**	**NT**	**NA**	**1.0**	**2 (100)**
Goat	10^5	NA	42§	3.0	2 (100)	1.3	2 (100)
Rabbit	**10^4**	**<1.5**	**14**	**NT**	**NA**	**ND**	**0**
Rabbit	10^4	NA	42§	4.1	3 (100)	1.2 (0.2)	3 (100)
Raccoon	10^4	<1.5	42	NT	NA	0.4 (0.6)	2 (33)

*Bold indicates initial (not given a booster immunization) sampling of a pair of animals that were later given a booster immunization. dpi, day postinoculation; NA, not assessed; ND, not detected (no titer ≤1:10 for any animal); NT, not tested; $PRNT_{70}$, 70% plaque reduction neutralization test.
†Detection limit was 1.5 log_{10} PFU/mL.
‡log_{10} reciprocal titer (SD).
§Animals were given booster inoculations with 10^4 PFU of Heartland virus at 28 dpi.

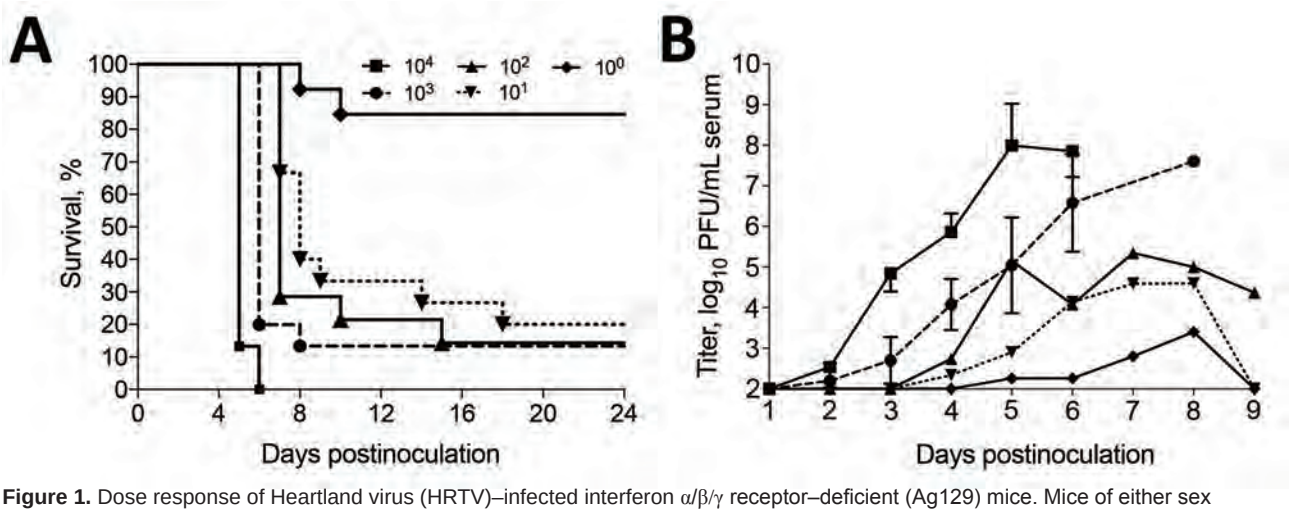

Figure 1. Dose response of Heartland virus (HRTV)–infected interferon α/β/γ receptor–deficient (Ag129) mice. Mice of either sex were inoculated with 10^4–10^0 PFU of HRTV/0.1 mL of inoculum. Mice were observed daily for death through day postinoculation 24. A) Percentage survival. B) Dose-associated HRTV viremias determined by plaque assays on Vero E6 cells. Different groups of 5 mice inoculated with the same dose of HRTV were bled every third day. Thus, a decrease in viremia was observed for the 10^2 PFU dose inoculum group days postinoculation 5 and 6. Error bars indicate SD.

Mean ± SD time of death also showed prolonged survival rates with lower inoculation doses when survivors were omitted from the analyses: 4.1 ± 0.4 d (10^4), 5.1 ± 0.3 d (10^3), 7.7 ± 2.2 d (10^2), 9.1 ± 3.7 d (10^1), and 9 ± 1.4 d (10^0) (Figure 1, panel A). We calculated a 50% lethal dose of 9 PFU by using linear regression analysis of the mortality rate at various viral dilutions (R^2 = 0.84).

Viremia titers were also dose dependent; peak titers were highest in the 10^4 PFU group and lowest in the 10^0 PFU group (Table 3). Onset of viremia in most of the inoculation groups was at 2 dpi or 3 dpi, and the 10^4 PFU inoculation group had the highest initial daily viremia titer at 2 dpi (2.5 ± 0.5 $\log_{10}$ PFU/mL serum) and the highest mean daily peak viremias by 5 dpi (8 $\log_{10}$ PFU/mL serum) (Figure 1, panel B). However, 3 of the mice had viremias at 5 dpi >9 $\log_{10}$ PFU/mL serum. Only 5 of 15 Ag129 mice in the 10^0 inoculation group had detectable viremias; highest detectable titer was 4 $\log_{10}$ PFU/mL serum. Clinical signs in Ag129 mice included hunched back, ruffled fur, mucopurulent ocular discharge, and hematochezia. Mice that had these signs were euthanized and subjected to necropsy for gross and histopathologic analysis of lesions.

Serologic Analysis

All animals except raccoons received booster inoculations at 28 dpi with 10^4 PFU of HRTV. HRTV neutralizing antibodies were not detected in chickens through 42 dpi after booster inoculation, but ELISA titers were evident (3.0 $\log_{10}$) (Table 2). Low, but detectable, $PRNT_{70}$ titers (1 $\log_{10}$–1.3 $\log_{10}$) were observed in rabbits given booster inoculations; ELISA titers were ≤4.1 $\log_{10}$. All hamsters given booster inoculations had neutralizing titers (1 $\log_{10}$–1.9 $\log_{10}$) and ELISA titers (4.3 $\log_{10}$). Despite the high HRTV neutralizing antibody prevalence and magnitude of the immune response identified in the field for raccoons, 0 of 6 experimentally inoculated raccoons had detectable viremia, and only 2 had $PRNT_{70}$ titers (1 $\log_{10}$ and 1.3 $\log_{10}$). ELISA titers for raccoons were not assessed because of a lack of appropriate species-associated conjugate. The 2 goats had low (1.3 $\log_{10}$) neutralizing immune responses after booster inoculation, and ELISA titers of 3.0 $\log_{10}$ were detected. C57BL/6 mice responded to infection with no detectable (0.7 $\log_{10}$) titers detected by PRNT and 4.4 $\log_{10}$ titers detected by ELISA (Table 2).

Serologic Response and Challenge of Surviving Ag129 Mice

Eighteen (24%) of 75 Ag129 mice survived the initial inoculation with HRTV (11 from the 10^0 PFU group, 3 from the 10^1 PFU group, 2 from the 10^2 PFU group, and 2 from the 10^3 PFU group). The 2 surviving Ag129 mice from the 10^3 PFU group were terminally bled for immune responses at 21 dpi. One mouse had an ELISA titer of 1:364,500, and the other mouse had no detectable reactivity (titer <1:500) (Table 3). The 2 Ag129 mice that survived the 10^2 PFU inoculation dose had ELISA titers of 1:121,500 and <1:500 at 28 dpi. These mice were given booster inoculations with 10^4 PFU of HRTV, and spleens harvested 4 days later (32 dpi) for detection of splenocyte fusions and myeloma cells for MAb development as described (*18*). At 32 dpi (4 days post-HRTV booster inoculation/challenge), neutralizing responses were detected in both mice (1.9 $\log_{10}$ and 2.5 $\log_{10}$ reciprocal titers), and no serum viremia or virus was detected in the spleens.

Table 3. Viremia and antibody responses of interferon-α/β/γ receptor–deficient mice experimentally inoculated with Heartland virus*

Inoculum dose, PFU	dpi	Mean peak titer†	Mean ELISA titer	ELISA positive, no. (%)	Mean $PRNT_{70}$ titer‡	$PRNT_{70}$ positive, no. (%)
10^4	**NA**	**8 (1.0)**	**NA**	–	**NA**	–
10^4	NA	–	NA	–	NA	–
10^3	**21**	**6.6 (1.2)**	**4.1 (2.0)**	**1 (50)**	**NT**	–
10^2	**28**	**5.3 (2.3)**	**3.9 (1.7)**	**1 (50)**	**NT**	**NT**
10^2	32	–	NT	–	2.2 (0.4)	2(100)§
10^1	**28**	**4.6 (2.1)**	**3.5 (1.4)**	**1 (33)**	**1.5 (0.6)**	**ND**
10^1	42	–	NT	–	1.3 (0.5)	1 (33)
10^0	**28**	**3.4 (2.2)**	**2.7 (1.4)**	**1 (9)**	**1**	**1 (9)**
10^0	42	–	NT	–	1.5 (0.6)	2 (33)

*Bold indicates initial (not given a booster immunization) sampling of a pair of animals that were later given a booster immunization. dpi, day postinoculation; NA, not applicable because uniform deaths were observed; ND, not detected; NT, not tested; $PRNT_{70}$, 70% plaque reduction neutralization test; –, not assessed for titer.
†Peak titers (log_{10} PFU/mL of serum) (SD). Detection limit was 1.5 log_{10} PFU/mL.
‡log_{10} reciprocal titer (SD).
§Tested at 4 d postchallenge.

Only 1 of the 3 Ag129 mice that survived initial challenge with HRTV at a dose of 10^1 PFU showed immune reactivity to HRTV antigen by ELISA (titer 1:121,500) at 28 dpi. Similarly, 1 of 11 surviving Ag129 mice from the 10^0 PFU dose group showed HRTV immune reactivity (titer 1:1,500) (Table 3) at 28 dpi. An HRTV neutralizing titer of 1:10 was identified in the 28 dpi serum sample from the ELISA-positive surviving mouse from the 10^0 PFU inoculation group. In addition, the surviving mouse with the higher ELISA titer from the 10^1 PFU dose group did not have a detectable $PRNT_{70}$ titer, although neutralizing titers were observed at lower thresholds. These 14 surviving mice were challenged with 10^4 PFU of HRTV at 28 dpi and observed for an additional 14 days through 42 dpi. Eight (57%) of the 14 secondarily challenged Ag129 mice survived through 42 dpi (2/3 in the 10^1 PFU dose group and 6/11 in the 10^0 PFU dose group), which indicated a protective immune response. However, only 3 of the 8 (1 in 10^1 PFU dose group and 2 in 10^0 PFU dose group) surviving mice had detectable neutralizing antibodies against HRTV, and the mean ± $PRNT_{70}$ titers were only 1.9 and 1.5 ± 0.6 for the 2 dose groups, respectively (Table 3).

Pathologic Analysis

At necropsy, hamsters, chickens, rabbits, raccoons, goats, and C57BL/6 mice were in good physical condition and none showed gross pathologic lesions associated with HRTV infection. In contrast, Ag129 mice had clear signs of illness (Figure 2, panel A), including hunched posture, ruffled fur, rectal hemorrhage, weight loss, and conjunctivitis. Euthanized Ag129 mice had grossly enlarged, pale spleens, hepatic hemorrhage, enlarged gall bladders, and excess peritoneal fluid (Figure 2, panel B). Hematoxylin and eosin–stained sections of Ag129 spleen and liver and tissues showed reactive white pulp (Figure 2, panel C), abundant apoptotic debris and hepatic sinusoids (Figure 2, panel D), and increased numbers of mononuclear cells. Immunohistochemical analysis showed abundant HRTV antigen was observed diffusely within splenic mononuclear cells (Figure 2, panel C), hepatic sinusoidal (Kupffer) cells (Figure 2, panel D), and renal interstitial mononuclear cells (Figure 2, panel E).

Discussion

HRTV is a novel bunyavirus known to cause serious disease in a small number of humans. Serologic surveillance and isolation from *A. americanum* tick nymphs suggested that HRTV circulates in an enzootic cycle and spills over into humans when they are exposed to infected ticks (*2*,*3*). However, in the animal models we present in this study, no evidence of replicative infection in any of the wildlife or outbred animals tested was observed, and viremia, illness, and death could only be induced in type I and type II interferon-receptor knockout mice. Likewise, although SFTSV has been found to cause viremia and pathologic manifestations, such as leukopenia and thrombocytopenia in C57BL/6 mice, which is consistent with human pathologic changes, these mice did not show any clinical signs of disease, and evidence of viral replication was limited to the spleen (*19*).

However, all interferon α/β receptor knockout mice (IFNAR –/–) inoculated with SFTSV died within 3–4 dpi and showed marked SFTSV antigen expression and increased viremia profiles than did wild-type mice of the same genetic background (*19*,*20*), which is consistent with our results for Ag129 mice experimentally inoculated with HTRV (*20*). Furthermore, the protective role of the interferon response has also been demonstrated by depleting interferon in age-resistant C57BL/6 mice infected with another phlebovirus (Punta Toro virus) (*21*). These data and the experimental inoculation data in our study indicate that the interferon response is critical for controlling pathologic changes of mice infected with phleboviruses.

Similar to pathologic changes reported for SFTSV infection in C57BL/6 mice (*19*) and IFNAR knockout mice (*20*), viremia and major pathologic changes developed in

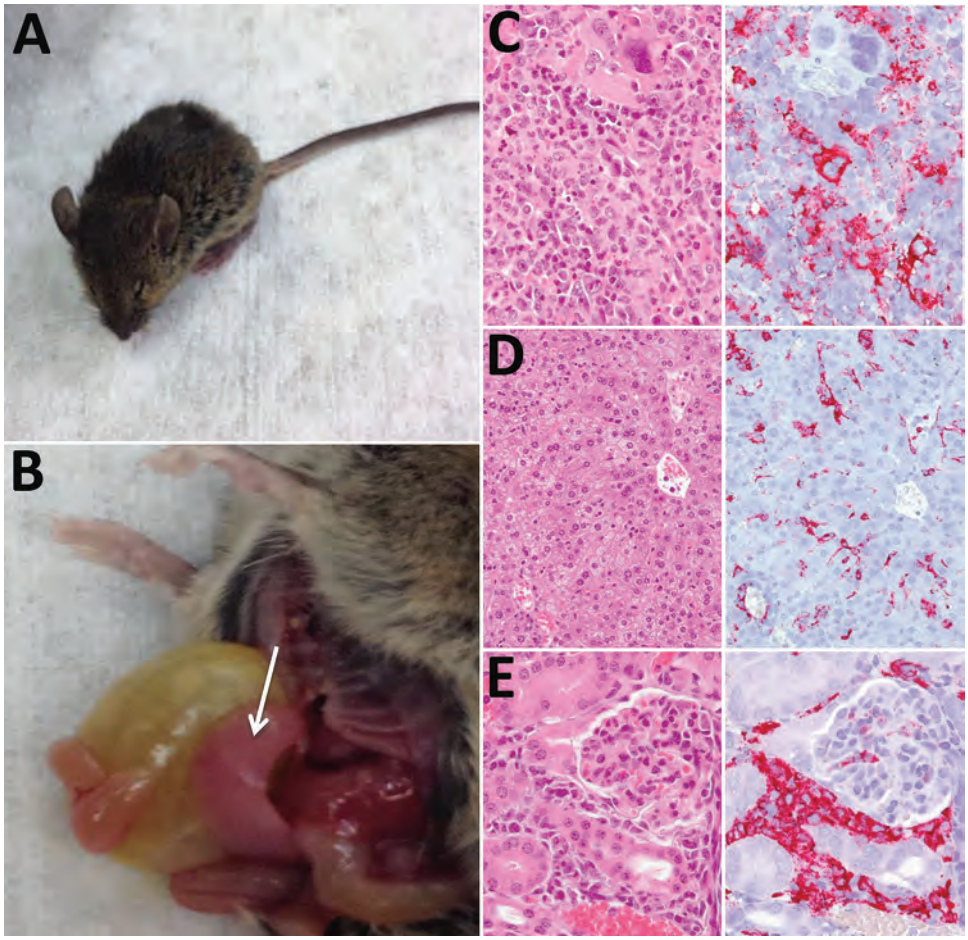

Figure 2. Pathologic changes associated with infection of interferon-α/β/γ receptor–deficient (Ag129) mice with Heartland virus (HRTV). A) Mouse showing typical clinical signs of HRTV infection (ruffled fur, hunched posture, and squinting eyes). B) Dissected mouse showing an enlarged pale spleen (arrow). C–E) Hematoxylin and eosin staining (left panels) and immunohistochemical staining (right panels) for HRTV nucleocapsid protein of spleen (C), liver (D), and kidney (E) of Ag129 mice at 5–7 days postinoculation with 10^4 PFU virus. Original magnifications: C, ×100; D, ×50; E, ×100.

Ag129 mice inoculated with HTRV, which is consistent with platelet depletion and subsequent thrombocytopenia. Histopathologic analysis showed a tropism for mononuclear cells, as shown by detection of HRTV N protein in splenic mononuclear cells, Kupffer cells, and interstitial mononuclear cells within the kidney. Future studies are needed to directly assess the capacity of the Ag129 mouse model to recapitulate leukopenia and thrombocytopenia manifestations observed in human disease progression and the subsequent role of splenic macrophages with platelet depletion (*19*).

Nine hydridomas expressing HRTV MAbs derived from HRTV-inoculated Ag129 splenocyte fusions described in this report have been characterized. All of them were found to be nonneutralizing and reactive to linear epitopes of the HRTV N protein (*18*). These results are not surprising because phlebovirus N protein is the most abundant protein in the virion and in virus-infected cells (*22–24*). Similarly, most MAbs against SFTSV are also specific for N protein and nonneutralizing (*25*,*26*). Because the humoral response to N protein occurs early in infection, this protein is used as a diagnostic antigen (*22*,*27–30*). The presence of N protein-targeted humoral responses, measured by ELISA titers, in C57BL/6 and Ag129 mice with low neutralizing activity supports the hypothesis that the N protein could serve as an immunologic decoy. Poor humoral neutralizing response of infected hosts to another bunyavirus, Crimean-Congo hemorrhagic fever virus (genus *Nairovirus*), has been associated with enhanced strain-specific virulence in humans (*31*). Crimean-Congo hemorrhagic fever virus is rapidly cleared in immunocompetent mice, replicates to high titer, and induces pathologic changes and thrombocytopenia in IFNAR mice, similar to the disparate results obtained in this experiment between C57BL/6 and Ag129 mice (*22*,*27–30*).

The lack of proper receptors, such as dendritic cell–specific intercellular adhesion molecule 3–grabbing nonintegrin (DC-SIGN) on Vero cells, used in neutralization assays could also explain the low neutralization titers we observed. When compared with cells that were modified to express DC-SIGN, Mukherjee et al. found that neutralization titers to dengue virus were found to be increased (*32*). DC-SIGN has been shown to serve as a receptor for attachment and endocytosis in phleboviral infections, including those with SFTSV, Rift Valley fever virus, and Uukuniemi virus (*33*,*34*). The extremely

low level of detected neutralizing antibodies in Ag129 mice that subsequently survived challenge with 1,000 50% lethal doses of HRTV indicates that neutralizing antibody assays are not congruent with humoral protection levels or that cell-mediated immune responses afford considerable protection.

The vertebrate host competence studies reported here also demonstrate the potential host specificity that could have evolved over long periods concomitant with diversification of HRTV from other phleboviruses. Our findings do not exclude the potential role of multiple vertebrate host(s) for maintenance of HRTV; several key animals, such as horses and white-tailed deer, for which there is serologic evidence of field exposures and tick associations, have yet to be assessed for HRTV host competence. Nymphal *A. americanum* ticks, from which HRTV has been isolated (*2*), are known to be catholic feeders, and white-tailed deer may be a major host for the nymphal stage of these ticks (*35*). HRTV could potentially circulate without the need for actual replication in the vertebrate host through direct tick-to-tick transmission while co-feeding nearby on a vertebrate host, as described for the orthomyxovirus, Thogoto virus (*36*).

The role of direct tick transmission of virus to the vertebrate host should be considered because it is related to modulation of the host innate immune response and the potential establishment of a permissive environment for HRTV replication. Previous studies have demonstrated that salivary transmission of Thogoto virus has potentiated the antagonism of interferon-induced Mx1 antiviral activity and resulted in successful transmission of co-feeding ticks on a mouse strain for which parenteral inoculation was unsuccessful (*37*). Salivary transmission by ticks could be a major factor because of immunomodulatory effects of the saliva (*38*,*39*) or differential immune signaling because of specific lectins incorporated onto viral structural proteins, which result from growth in arthropod cells (*40*). This modulation by salivary components could affect initial replication in skin dendritic cells and result in subsequent development of viremias and neutralizing titers in field-collected animals. Repeated exposure of attached ticks salivating virus over prolonged periods could be sufficient for neutralization titers to be manifested in the absence of viral replication.

In conclusion, this study provides an assessment of the relative susceptibility of several vertebrate hosts to parenteral infection with HRTV and a preliminary assessment of a potential model for HRTV-associated disease pathology in humans. Ag129 mice could be used as a source for establishing direct tick infection or as a transmission model for infected *A. americanum* ticks for subsequent assessment of these and alternative natural vertebrate host candidates for HRTV transmission.

Acknowledgments

We thank Jana Ritter and M. Kelly Keating for reviewing veterinary pathologic results, Brigid C. Bollweg for performing immunohistochemical analysis, Jason Velez for providing cell culture support, and the animal care staff in the Division of Vector-Borne Diseases, Centers for Disease Control and Prevention, for breeding Ag129 mice and providing subsequent animal care.

A.M.B.-L. was supported by an American Society for Microbiology postdoctoral fellowship.

Dr. Bosco-Lauth is a veterinary student at Colorado State University, Fort Collins, CO. Her primary research interests are natural transmission cycles and pathogenesis of emerging arboviruses.

References

1. McMullan LK, Folk SM, Kelly AJ, MacNeil A, Goldsmith CS, Metcalfe MG, et al. A new phlebovirus associated with severe febrile illness in Missouri. N Engl J Med. 2012;367:834–41. http://dx.doi.org/10.1056/NEJMoa1203378
2. Savage HM, Godsey MS Jr, Lambert A, Panella NA, Burkhalter KL, Harmon JR, et al. First detection of heartland virus (*Bunyaviridae*: *Phlebovirus*) from field collected arthropods. Am J Trop Med Hyg. 2013;89:445–52. http://dx.doi.org/10.4269/ajtmh.13-0209
3. Bosco-Lauth AM, Panella NA, Root JJ, Gidlewski T, Lash RR, Harmon JR, et al. Serological investigation of heartland virus (*Bunyaviridae*: *Phlebovirus*) exposure in wild and domestic animals adjacent to human case sites in Missouri 2012-2013. Am J Trop Med Hyg. 2015;92:1163–7. http://dx.doi.org/10.4269/ajtmh.14-0702
4. Riemersma KK, Komar N. Heartland virus neutralizing antibodies in vertebrate wildlife, United States, 2009–2014. Emerg Infect Dis. 2015;21:1830–3. http://dx.doi.org/10.3201/eid2110.150380
5. Liu K, Cui N, Fang LQ, Wang BJ, Lu QB, Peng W, et al. Epidemiologic features and environmental risk factors of severe fever with thrombocytopenia syndrome, Xinyang, China. PLoS Negl Trop Dis. 2014;8:e2820. http://dx.doi.org/10.1371/journal.pntd.0002820
6. Gai ZT, Zhang Y, Liang MF, Jin C, Zhang S, Zhu CB, et al. Clinical progress and risk factors for death in severe fever with thrombocytopenia syndrome patients. J Infect Dis. 2012;206:1095–102. http://dx.doi.org/10.1093/infdis/jis472
7. Deng B, Zhang S, Geng Y, Zhang Y, Wang Y, Yao W, et al. Cytokine and chemokine levels in patients with severe fever with thrombocytopenia syndrome virus. PLoS One. 2012;7:e41365. http://dx.doi.org/10.1371/journal.pone.0041365
8. Jin C, Jiang H, Liang M, Han Y, Gu W, Zhang F, et al. SFTS virus infection in nonhuman primates. J Infect Dis. 2015;211:915–25. http://dx.doi.org/10.1093/infdis/jiu564
9. Shin J, Kwon D, Youn SK, Park JH. Characteristics and factors associated with death among patients hospitalized for severe fever with thrombocytopenia syndrome, South Korea, 2013. Emerg Infect Dis. 2015;21:1704–10. http://dx.doi.org/10.3201/eid2110.141928
10. Muehlenbachs A, Fata CR, Lambert AJ, Paddock CD, Velez JO, Blau DM, et al. Heartland virus-associated death in tennessee. Clin Infect Dis. 2014;59:845–50. http://dx.doi.org/10.1093/cid/ciu434
11. Pastula DM, Turabelidze G, Yates KF, Jones TF, Lambert AJ, Panella AJ, et al. Notes from the field: Heartland virus

disease—United States, 2012–2013. MMWR Morb Mortal Wkly Rep. 2014;63:270–1.
12. Gauci PJ, McAllister J, Mitchell IR, St George TD, Cybinski DH, Davis SS, et al. Hunter Island group phlebovirus in ticks, Australia. Emerg Infect Dis. 2015;21:2246–8. http://dx.doi.org/10.3201/eid2112.141303
13. Matsuno K, Weisend C, Kajihara M, Matysiak C, Williamson BN, Simuunza M, et al. Comprehensive molecular detection of tick-borne phleboviruses leads to the retrospective identification of taxonomically unassigned bunyaviruses and the discovery of a novel member of the genus *Phlebovirus.* J Virol. 2015;89:594–604. http://dx.doi.org/10.1128/JVI.02704-14
14. Wang J, Selleck P, Yu M, Ha W, Rootes C, Gales R, et al. Novel phlebovirus with zoonotic potential isolated from ticks, Australia. Emerg Infect Dis. 2014;20:1040–3. http://dx.doi.org/10.3201/eid2006.140003
15. Cui F, Cao HX, Wang L, Zhang SF, Ding SJ, Yu XJ, et al. Clinical and epidemiological study on severe fever with thrombocytopenia syndrome in Yiyuan County, Shandong Province, China. Am J Trop Med Hyg. 2013;88:510–2. http://dx.doi.org/10.4269/ajtmh.11-0760
16. Jiao Y, Qi X, Liu D, Zeng X, Han Y, Guo X, et al. Experimental and natural infections of goats with severe fever with thrombocytopenia syndrome virus: evidence for ticks as viral vector. PLoS Negl Trop Dis. 2015;9:e0004092. http://dx.doi.org/10.1371/journal.pntd.0004092
17. van den Broek MF, Müller U, Huang S, Aguet M, Zinkernagel RM. Antiviral defense in mice lacking both alpha/beta and gamma interferon receptors. J Virol. 1995;69:4792–6.
18. Calvert AE, Brault AC. Development and characterization of monoclonal antibodies directed against the nucleoprotein of Heartland virus. Am J Trop Med Hyg. 2015;93:1338–40. http://dx.doi.org/10.4269/ajtmh.15-0473
19. Jin C, Liang M, Ning J, Gu W, Jiang H, Wu W, et al. Pathogenesis of emerging severe fever with thrombocytopenia syndrome virus in C57/BL6 mouse model. Proc Natl Acad Sci U S A. 2012;109:10053–8. http://dx.doi.org/10.1073/pnas.1120246109
20. Liu Y, Wu B, Paessler S, Walker DH, Tesh RB, Yu XJ. The pathogenesis of severe fever with thrombocytopenia syndrome virus infection in alpha/beta interferon knockout mice: insights into the pathologic mechanisms of a new viral hemorrhagic fever. J Virol. 2014;88:1781–6. http://dx.doi.org/10.1128/JVI.02277-13
21. Pifat DY, Smith JF. Punta Toro virus infection of C57BL/6J mice: a model for phlebovirus-induced disease. Microb Pathog. 1987;3:409–22. http://dx.doi.org/10.1016/0882-4010(87)90011-8
22. Magurano F, Nicoletti L. Humoral response in Toscana virus acute neurologic disease investigated by viral-protein-specific immunoassays. Clin Diagn Lab Immunol. 1999;6:55–60.
23. Schwarz TF, Gilch S, Pauli C, Jäger G. Immunoblot detection of antibodies to Toscana virus. J Med Virol. 1996;49:83–6. http://dx.doi.org/10.1002/(SICI)1096-9071(199606)49:2<83::AID-JMV2>3.0.CO;2-F
24. Swanepoel R, Struthers JK, Erasmus MJ, Shepherd SP, McGillivray GM, Shepherd AJ, et al. Comparative pathogenicity and antigenic cross-reactivity of Rift Valley fever and other African phleboviruses in sheep. J Hyg (Lond). 1986;97:331–46. http://dx.doi.org/10.1017/S0022172400065426
25. Guo X, Zhang L, Zhang W, Chi Y, Zeng X, Li X, et al. Human antibody neutralizes severe fever with thrombocytopenia syndrome virus, an emerging hemorrhagic Fever virus. Clin Vaccine Immunol. 2013;20:1426–32. http://dx.doi.org/10.1128/CVI.00222-13
26. Yu L, Zhang L, Sun L, Lu J, Wu W, Li C, et al. Critical epitopes in the nucleocapsid protein of SFTS virus recognized by a panel of SFTS patients derived human monoclonal antibodies. PLoS One. 2012;7:e38291. http://dx.doi.org/10.1371/journal.pone.0038291
27. Martín-Folgar R, Lorenzo G, Boshra H, Iglesias J, Mateos F, Borrego B, et al. Development and characterization of monoclonal antibodies against Rift Valley fever virus nucleocapsid protein generated by DNA immunization. MAbs. 2010;2:275–84. http://dx.doi.org/10.4161/mabs.2.3.11676
28. Fafetine JM, Tijhaar E, Paweska JT, Neves LC, Hendriks J, Swanepoel R, et al. Cloning and expression of Rift Valley fever virus nucleocapsid (N) protein and evaluation of a N-protein based indirect ELISA for the detection of specific IgG and IgM antibodies in domestic ruminants. Vet Microbiol. 2007;121:29–38. http://dx.doi.org/10.1016/j.vetmic.2006.11.008
29. Paweska JT, Mortimer E, Leman PA, Swanepoel R. An inhibition enzyme-linked immunosorbent assay for the detection of antibody to Rift Valley fever virus in humans, domestic and wild ruminants. J Virol Methods. 2005;127:10–8. http://dx.doi.org/10.1016/j.jviromet.2005.02.008
30. Paweska JT, van Vuren PJ, Kemp A, Buss P, Bengis RG, Gakuya F, et al. Recombinant nucleocapsid-based ELISA for detection of IgG antibody to Rift Valley fever virus in African buffalo. Vet Microbiol. 2008;127:21–8. http://dx.doi.org/10.1016/j.vetmic.2007.07.031
31. Mousavi-Jazi M, Karlberg H, Papa A, Christova I, Mirazimi A. Healthy individuals' immune response to the Bulgarian Crimean-Congo hemorrhagic fever virus vaccine. Vaccine. 2012;30:6225–9. http://dx.doi.org/10.1016/j.vaccine.2012.08.003
32. Mukherjee S, Dowd KA, Manhart CJ, Ledgerwood JE, Durbin AP, Whitehead SS, et al. Mechanism and significance of cell type-dependent neutralization of flaviviruses. J Virol. 2014;88:7210–20. http://dx.doi.org/10.1128/JVI.03690-13
33. Hofmann H, Li X, Zhang X, Liu W, Kühl A, Kaup F, et al. Severe fever with thrombocytopenia virus glycoproteins are targeted by neutralizing antibodies and can use DC-SIGN as a receptor for pH-dependent entry into human and animal cell lines. J Virol. 2013;87:4384–94. http://dx.doi.org/10.1128/JVI.02628-12
34. Lozach PY, Kühbacher A, Meier R, Mancini R, Bitto D, Bouloy M, et al. DC-SIGN as a receptor for phleboviruses. Cell Host Microbe. 2011;10:75–88. http://dx.doi.org/10.1016/j.chom.2011.06.007
35. Allan BF, Goessling LS, Storch GA, Thach RE. Blood meal analysis to identify reservoir hosts for *Amblyomma americanum* ticks. Emerg Infect Dis. 2010;16:433–40. http://dx.doi.org/10.3201/eid1603.090911
36. Jones LD, Davies CR, Steele GM, Nuttall PA. A novel mode of arbovirus transmission involving a nonviremic host. Science. 1987;237:775–7. http://dx.doi.org/10.1126/science.3616608
37. Jones LD, Hodgson E, Nuttall PA. Enhancement of virus transmission by tick salivary glands. J Gen Virol. 1989;70:1895–8. http://dx.doi.org/10.1099/0022-1317-70-7-1895
38. Hermance ME, Thangamani S. Tick saliva enhances Powassan virus transmission to the host, influencing its dissemination and the course of disease. J Virol. 2015;89:7852–60. http://dx.doi.org/10.1128/JVI.01056-15
39. Labuda M, Jones LD, Williams T, Nuttall PA. Enhancement of tick-borne encephalitis virus transmission by tick salivary gland extracts. Med Vet Entomol. 1993;7:193–6. http://dx.doi.org/10.1111/j.1365-2915.1993.tb00674.x
40. Shabman RS, Morrison TE, Moore C, White L, Suthar MS, Hueston L, et al. Differential induction of type I interferon responses in myeloid dendritic cells by mosquito and mammalian-cell-derived alphaviruses. J Virol. 2007;81:237–47. http://dx.doi.org/10.1128/JVI.01590-06

Address for correspondence: Aaron C. Brault, Centers for Disease Control and Prevention, 3156 Rampart Rd, Foothills Campus, Fort Collins, CO 80521, USA; email: abrault@cdc.gov

Whole-Genome Characterization and Strain Comparison of VT2f-Producing *Escherichia coli* Causing Hemolytic Uremic Syndrome

Laura Grande, Valeria Michelacci, Roslen Bondì, Federica Gigliucci, Eelco Franz, Mahdi Askari Badouei, Sabine Schlager, Fabio Minelli, Rosangela Tozzoli, Alfredo Caprioli, Stefano Morabito

Verotoxigenic *Escherichia coli* infections in humans cause disease ranging from uncomplicated intestinal illnesses to bloody diarrhea and systemic sequelae, such as hemolytic uremic syndrome (HUS). Previous research indicated that pigeons may be a reservoir for a population of verotoxigenic *E. coli* producing the VT2f variant. We used whole-genome sequencing to characterize a set of VT2f-producing *E. coli* strains from human patients with diarrhea or HUS and from healthy pigeons. We describe a phage conveying the *vtx2f* genes and provide evidence that the strains causing milder diarrheal disease may be transmitted to humans from pigeons. The strains causing HUS could derive from VT2f phage acquisition by *E. coli* strains with a virulence genes asset resembling that of typical HUS-associated verotoxigenic *E. coli*.

Verotoxigenic *Escherichia coli* (VTEC) infections in humans cause a wide spectrum of clinical manifestations ranging from uncomplicated forms of intestinal illnesses to bloody diarrhea and systemic sequelae, such as hemolytic uremic syndrome (HUS) (*1*). The most severe forms are caused by the damage inflicted by the verocytotoxins (VTs) to the target cells in the intestinal mucosa and the renal blood vessels (*1*). The genes encoding the verocytotoxins (*vtx*) are harbored by lambdoid bacteriophages, which can be transferred to multiple bacterial hosts, generating a great diversity in the bacterial types that produce such toxins (*2*).

The most well-known VTEC serogroup, O157, inhabits the gastrointestinal tract of ruminants, especially cattle. However, this and other VTEC serotypes have been isolated from the feces of several other animal species, including deer, pigs, horses, cats, dogs, and wild birds (*3*).

During a program aimed at the control of the pigeon population in Rome, Italy during 1998, G. Dell'Omo et al. observed that this animal species was a carrier of VTEC (*4*). In that study, VTEC of multiple serogroups were isolated from ≈10% of the animals tested. Of 16 VTEC, 15 carried the *eae* gene encoding the intimin and featured genetic determinants that produced a subtype of verocytotoxin type 2 not described before, later designated VT2f (*4*–*6*). The finding of such a high prevalence of VTEC in pigeons living in Rome led to further research into these bacteria in this and other bird species worldwide. Almost all these studies succeeded in isolating VTEC, with prevalence ranging 3% to >19% in different countries and bird species; most VTEC isolated from pigeon feces and cloacal swab samples harbored the genes encoding the VT2f subtype (*7*–*10*). These findings emphasize the existence of a strict association between VTEC carrying the *vtx2f* genes and pigeons, which represent a reservoir for such strains.

Data on human illness attributable to VT2f-producing *E. coli* has been scarce until recent reports from Germany and the Netherlands described the isolation of such strains from diarrheal stool specimens from humans (*11*,*12*). Furthermore, in the Netherlands, an HUS case was recently reported to be associated with the presence of a VT2f-producing O8:H19 strain (*13*). We aimed to characterize at the whole-genome level 3 *E. coli* strains that produced the VT2f isolated from HUS and to investigate their relationships with VT2f-producing *E. coli* isolated from human diarrheal cases and from the pigeon reservoir.

Materials and Methods

Bacterial Strains

We investigated 22 Vt2f -producing *E. coli* strains. Eight previously described strains were isolated from pigeons in Italy (*4*); eleven strains were isolated in the Netherlands from fecal specimens from humans with diarrhea during

Author affiliations: Istituto Superiore di Sanità, Rome, Italy (L. Grande, V. Michelacci, R. Bondi, F. Gigliucci, F. Minelli, R. Tozzoli, A. Caprioli, S. Morabito); National Institute for Public Health and the Environment, Bilthoven, the Netherlands (E. Franz); Islamic Azad University Faculty of Veterinary Medicine, Garmsar Branch, Garmsar, Iran (M. Askari Badouei); Austrian Agency for Health and Food Safety, Graz, Austria (S. Schlager)

DOI: http://dx.doi.org/10.3201/eid2212.160017

2008–2012 and are part of the collections held at the National Institute for Public Health and the Environment in the Netherlands (RIVM) (*12*). Of the 3 VT2f-producing *E. coli* from HUS patients, 1 was isolated in Austria in 2013 and 2 in Italy during 2013–2014. A total of 23 unrelated VTEC non-O157 strains that produced VT1 and/or VT2 subtypes other than VT2f have been used for the comparison of the profiles of virulence genes with those of the VT2f-producing isolates (Table 1).

Whole-Genome Sequencing of *E. coli* Strains

Sequencing of the strains isolated from fecal samples from humans with diarrhea and from pigeons was outsourced to the Central Veterinary Institute, Wageningen University (Lelystad, the Netherlands). Genome sequences were obtained by using a TruSeq protocol on an Illumina MiSeq PE300 platform (Illumina, San Diego, CA, USA). The genomes of the 3 VT2f-producing isolates from HUS patients were sequenced by using an Ion Torrent PGM (Thermo Fisher Scientific, Waltham, MA, USA) according to 400-bp protocols for library preparation through enzymatic shearing, Ion OneTouch2 emulsion PCR, enrichment, and Hi-Q sequencing kits (Thermo Fisher Scientific).

The whole-genome sequences (WGSs) of the 23 non-O157 VTEC strains are part of the European Molecular Biology Laboratory's European Nucleotide Archive Study (http://www.ebi.ac.uk/ena; accession no. PRJEB11886). The raw reads have been subjected to quality check through FastQC and trimmed with FASTQ positional and quality trimming tool to remove the adaptors and to accept 20 as the lowest Phred value (*14*).

We subjected the sequences obtained with the Ion Torrent apparatus to de novo assembly by using the tool SPADES (*15*) and those from Illumina by using the A5 pipeline (*16*). The genomes have been assembled in several contigs ranging from 42 to 495 (mean 225), with N50 values (the length of the smallest contig among the set of the largest contigs that together cover at least 50% of the assembly) between 40,736 and 347,638 (mean 152,953). All the contigs were uploaded to the EMBL European Nucleotide Archive (accession no. PRJEB12203). We made annotations by using the Prokka tool (*17*). All the bioinformatics tools used are available on the Aries public Galaxy server (https://w3.iss.it/site/aries/).

Virulence Gene Profile Analysis and Serotyping

The presence of *vtx2f* and *eae* genes has been assessed by PCR by using primers and conditions described elsewhere (*5,18*). The activity of VT2f has been evaluated by Vero cell assay (VCA) as previously described (*19*).

We performed detection of the virulence genes *cif*, *efa1*, *espABCFIJP*, *etpD*, *iha*, *iss*, *katP*, *lpfa*, *nleABC*, *tccP*, *tir*, *toxB*, *ehxA*, and *espP* and the serotype determination in silico on the WGSs. We used blastn (available on the Aries public Galaxy server at https://w3.iss.it/site/aries/) to search databases containing the reference sequences of all the known virulence and serotype-associated genes of pathogenic *E. coli* (*20*). To perform the principal component analysis of the virulence gene profiles, we

Table 1. Characteristics of non-O157 verotoxigenic *Escherichia coli* strains used in a comparative analysis of the virulence profile of VT2f-producing strains from humans and the animal reservoir*

Strain	Serogroup	Source†	Year of isolation	Virulence gene profile
ED017	O26	HUS	1989	*eae vtx1*
ED075	O26	Diarrheal feces	1990	*eae vtx1*
ED180	O26	HUS	1994	*eae vtx2*
ED195	O26	HUS	1994	*eae vtx1*
ED392	O26	Diarrheal feces	1998	*eae vtx1*
ED411	O26	HUS	1999	*eae vtx2*
ED423	O26	Diarrheal feces	1999	*eae vtx1*
ED654	O26	HUS	2007	*eae vtx2*
ED669	O26	HUS	2008	*eae vtx1*
ED676	O26	HUS	2008	*eae vtx2*
ED729	O26	Diarrheal feces	2010	*eae vtx1*
ED766	O26	HUS	2010	*eae vtx2*
ED657	O145	HUS	2007	*eae vtx2*
ED603	O121	HUS	2004	*eae vtx2*
ED073	O111	Diarrheal feces	1990	*eae vtx1*
ED082	O111	HUS	1990	*eae vtx1*
ED142	O111	HUS	1992	*eae vtx1 vtx2*
ED178	O111	HUS	1994	*eae vtx1 vtx2*
ED608	O111	HUS	2005	*eae vtx1 vtx2*
ED664	O111	HUS	2007	*eae vtx2*
ED672	O111	HUS	2008	*eae vtx1 vtx2*
ED287	O103	Bovine	1998	*eae vtx1*
ED728	O103	Bloody diarrheal feces	2010	*vtx1*

*All samples are from humans except strain ED287. HUS, hemolytic uremic syndrome.
†HUS samples were isolated from feces.

used SAS/IML studio software version 3.4 (SAS Institute, Inc., Cary, NC, USA).

We investigated plasmid profiles by using PlasmidFinder (*21*; https://cge.cbs.dtu.dk//services/all.php). The intimin subtyping has been performed in silico through a BLAST search (*22*) of the *eae* gene sequences from the WGS against the National Center for Biotechnology Information nucleotide repository. The intimin types of the VT2f-producing strains isolated from pigeons have been published (*6*,*10*).

rpoB Sequencing and Analysis

Amplification and sequencing of the *rpoB* gene were conducted to discriminate between *E. coli* and *E. albertii* species, as previously described (*23*). The amplicons were purified with the SureClean Plus kit (Bioline, London, UK) and sequenced using the BigDye Terminator v1.1 kit on a Genetic Analyzer 3130 (Thermo Fisher Scientific). The obtained sequences were trimmed and aligned to the reference sequences as indicated (*23*), using the Clustal Omega free software (http://www.ebi.ac.uk/Tools/msa/clustalo/).

Typing

We determined *E. coli* phylogenetic groups by using the method of Clermont et al. (*24*). We carried out multilocus sequence typing (MLST) of the VT2f isolates in silico according to the scheme proposed by Wirth et al. (*25*). We analyzed the assembled sequences by using blastn to search the MLST database downloaded from the Internet site of the MLST.UCC Mark Achtman database (http://mlst.warwick.ac.uk/mlst/dbs/Ecoli/).

Single-Nucleotide Polymorphism (SNP) Analysis

We analyzed SNPs by using the tool kSNP3 (*26*) available on the Galaxy project instance Aries (https://w3.iss.it/site/aries/). We set a kmer value of 23.

Results

Characterization of the VT2f-Producing *E. coli* Strains

Serotyping

Of 11 VTEC strains isolated from humans with diarrhea, 5 belonged to the O63:H6 serotype. The remaining 6 isolates contained the $fliC_{H6}$ (3 strains), $fliC_{H7}$ (1 strain), and $fliC_{H34}$ (2 strains) genes (Table 2) and belonged to serogroups O96, O113, O132, O145, and O125. For 1 isolate, the O-antigen–associated genes could not be identified (Table 2) (*12*).

Molecular serotyping of the 8 VT2f-producing strains isolated from pigeons showed that all the isolates had the $fliC_{H2}$ and the O4, O45, O75, and O128 serogroup-associated genes. The O-antigen genes could not be identified for the isolate ED 366 (Table 2). The HUS-associated

Table 2. Characteristics of VT2f-producing *Escherichia coli* investigated in a comparative analysis of the virulence profile of strains isolated from humans with mild and severe disease and from the animal reservoir*

Source and strain	Year isolated	Serotype	Phylotype	MLST	LEE	*adfO*	*efa1*	*cif*	*nleA*	*nleB*	*nleC*	*Hly*	*katP*	*espP*	Intimin type
Human diarrhea															
M856	2008	ONT:H6	B2	ST583	+	+	–	+	–	+	+	–	–	–	α-2
M858	2008	O125:H6	B2	ST583	+	+	–	+	–	+	–	–	–	–	α-2
M859	2009	O113:H6	B2	ST121	+	+	–	+	–	–	–	–	–	–	α-2
M884	2011	O96:H7	B2	ST28	+	+	–	+	+	+	–	–	–	–	β-2
M885	2011	O132:H34	B2	ST582	+	+	–	–	–	+	+	–	–	–	β-2
M900	2012	O145:H34	B2	ST722	+	+	–	–	–	+	–	–	–	–	ι
BCW5711	2012	O63:H6	B2	ST583	+	+	–	+	+	–	+	–	–	–	α-2
BCW5746	2012	O63:H6	B2	ST583	+	+	–	+	–	–	+	–	–	–	α-2
BCW5743	2012	O63:H6	B2	ST583	+	+	–	+	–	–	+	–	–	–	α-2
BCW5739	2012	O63:H6	B2	ST583	+	+	–	+	–	–	+	–	–	–	α-2
BCW5717	2012	O63:H6	B2	ST583	+	+	–	+	–	–	+	–	–	–	α-2
Pigeon															
ED360	1997	O45:H2	B1	ST20	+	+	–	+	+	+	+	–	–	–	β
ED361	1997	O75:H2	B1	ST20	+	+	–	+	+	+	+	–	–	–	β
ED363	1997	O4:H2	B1	UNK	+	+	–	+	+	+	+	–	–	–	β
ED366	1997	ONT:H2	B1	ST2685	+	+	–	+	+	+	+	–	–	–	β
ED369	1997	O45:H2	B1	ST20	+	+	–	+	+	+	+	–	–	–	β
ED377	1997	O4:H2	B1	UNK	+	+	–	+	+	+	+	–	–	–	β
ED430	2000	O45:H2	B1	ST20	+	+	–	+	+	+	+	–	–	–	β
ED444	2000	O128:H2	B1	ST20	+	+	–	+	+	+	+	–	–	–	β
HUS															
EF453	2013	O80:H2	B1	ST301	+	+	+	–	+	+	+	+	–	+	ξ
EF467	2013	O26:H11	B1	ST21	+	+	+	+	+	+	+	+	+	+	β
EF476	2014	O55:H9	B1	ST301	+	+	+	–	+	+	+	+	–	+	ξ

*Human samples were diarrheal or fecal samples from HUS cases and pigeon samples were feces from asymptomatic birds. LEE, locus of enterocyte effacement; MLST, multilocus sequence type; UNK, unknown; +, positive; –, negative.

VT2f-producing *E. coli* strains EF453 and EF476 belonged to serotypes O80:H2 and O55:H9, respectively, while strain EF467 was O26:H11.

Virulence Gene Profiles

The *E. coli* strains carrying the *vtx2f* and isolated from pigeons have been previously reported to produce an active VT2f (*6*). As expected, culture supernatants from VT2f-producing strains isolated from human diarrhea and HUS induced a cytopathic effect on Vero cells morphologically compatible with that caused by verocytoxins.

All the VT2f-producing strains included in the study were positive for the *eae* gene (Table 2) and displayed the presence of the entire locus of enterocyte effacement (LEE) (data not shown). Most of the *E. coli* VT2f-producing strains isolated from diarrheal cases harbored the α-2 intimin type (8/11), followed by the β-2 (2/11) and ι (1/11) types. The VT2f-strains isolated from pigeons had been previously described to have the β-intimin (*6*) in most cases and, more rarely, the α-2 intimin type (*10*). Of 3 HUS-associated VT2f-producing strains, 2 (EF453 and EF476) carried the ξ intimin type and 1 (EF467) had the β intimin (Table 2).

All the pigeon and HUS isolates possessed the complete set of non–LEE-encoded effectors assayed (*nleA*, *nleB* and *nleC*) (*27*), whereas the isolates from human diarrhea cases displayed an unequal presence of these genes (Table 2). The *efa1* gene, hallmark of the OI-122 pathogenicity island (*28*), was not identified in the isolates from pigeons or from human diarrheal specimens; neither were the genes *ehxA*, *espP* and *katP*, usually present on the large virulence plasmid of VTEC O157 and other VTEC associated with severe human disease (Table 2). However, the gene *adfO*, present on the OI-57 (*29*), was detected in all the strains investigated (Table 2).

The HUS strains EF453, EF467, and EF476 had the entire *efa1* gene. Strain EF467 also had the *ehxA*, *espP*, and *katP* genes; the EF453 and EF476 strains had the *ehxA* and *espP* genes only (Table 2). The analysis of the plasmid profiles substantiated the finding that the 3 HUS-associated strains carried the large virulence plasmid of VTEC, revealing the presence of a sequence 100% homologous to the replicon sequence of the pO26-CRL plasmid from a VTEC O26:H- (GenBank accession no. GQ259888.1), which harbors the genes *ehxA*, *espP*, and *katP*.

On the basis of plasmid profiles analysis, 7 of 11 *E. coli* VT2f-producing strains isolated from human diarrheal feces seemed to have the replicon sequence of the plasmid pSFO (GenBank accession no. AF401292) encoding the enterohemolysin and a cluster of *pap*-like genes called *sfp* in a sorbitol-fermenting *E. coli* O157 (*30*). However, the analysis of the WGSs failed to identify the *ehxA* and the *pap*-like sequences, suggesting that the entire pSFO plasmid was not present.

Principal component analysis of the virulence genes profiles showed that the HUS isolates producing VT2f clustered with the set of non-O157 VTEC isolates used for comparison, rather than with the other VT2f-producing strains (Figure 1). Conversely, the VT2f-producing strains from diarrhea and from pigeons grouped together and apart from the HUS strains (Figure 1).

Phylogenetic Analyses

rpoB Analysis

All the VT2f-producing isolates had an *E. coli*-related *rpoB* sequence (*23*). This finding verified that all the strains investigated were *E. coli*.

Typing

All VT2f-producing *E. coli* isolates from pigeons and the strains isolated from HUS belonged to the B1 phylogenetic group. All the strains isolated from human diarrheal feces were of phylotype B2 (Table 2).

By MLST, most of the pigeon strains investigated (5/8) belonged to sequence type (ST) 20; 1 was ST2685, and 2 were of unknown ST (Table 2), mainly because of the absence of a recognizable *adk* gene sequence. The 5 O63:H6, the 1 O125:H6, and the 1 ONT:H6 VTEC strains from diarrheal fecal specimens belonged to ST583; of the remaining 4 strains, 1 each was of sequence types ST28, ST121, ST582, and ST722 (Table 2).

Of 3 HUS-associated VT2f-producing *E. coli*, 2 (EF453 and EF476) belonged to ST301; strain EF467 was of ST21 (Table 2). All of the STs belonged to different clonal complexes or to any clonal complex, indicating that they were not related each other (data not shown).

SNP Analysis

A parsimony tree representing the core-genome SNPs analysis (Figure 2) shows that VT2f-producing strains from pigeons, human diarrheal feces, and HUS cases cluster apart from each other and from other VTEC strains used for comparison. The HUS-associated EF467 strain clusters together with the group of VTEC non-O157 from human disease, in agreement with the principal component analysis (Figures 1, 2).

Identification of a Bacteriophage Containing the *vtx2f* Genes

The contigs containing the *vtx2f* genes in the different strains ranged 2,500–68,480 bp in size. Upon annotation, they showed the presence of phage-associated genes in the proximity of *vtx2f*, including those encoding the

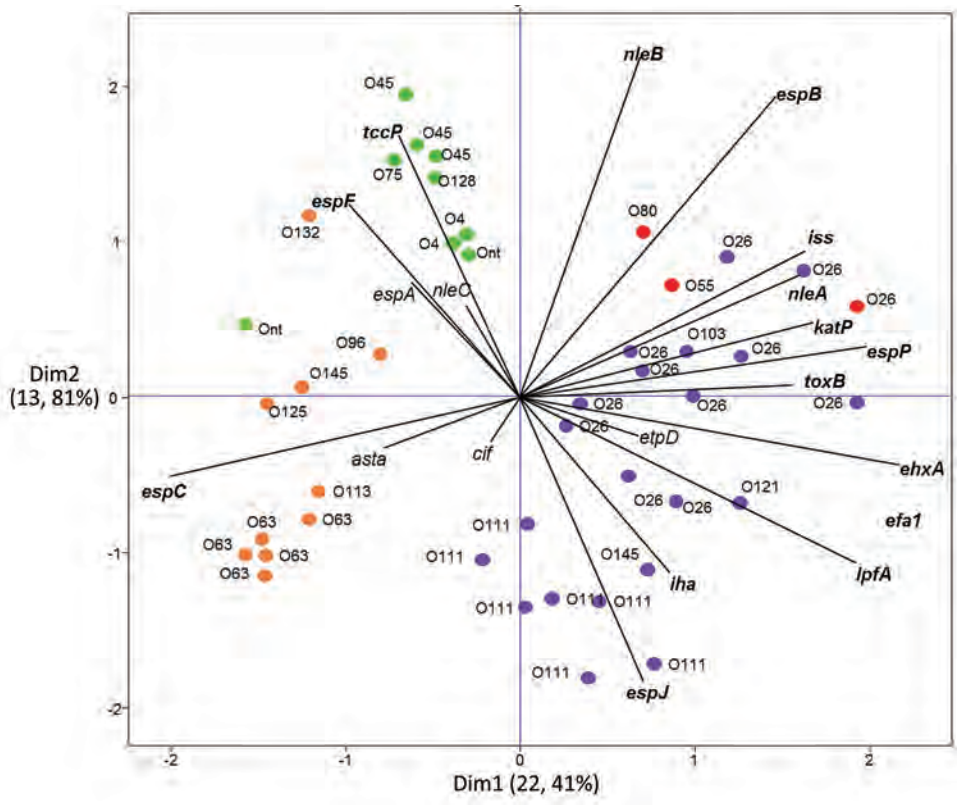

Figure 1. Principal component analysis of the virulence profiles of VT2f-producing verotoxigenic *Escherichia coli* (VTEC) strains isolated from fecal samples from human uncomplicated diarrheal case-patients (orange), human hemolytic uremic syndrome patients (red), and pigeon feces (green). Non-O157 VTEC that do not produce VT2f are indicated in purple. This analysis clusters isolates on the basis of similarities in virulence gene content. Isolates clustering together have similar virulence profiles. Lines represent individual virulence genes. The projected length of the lines on the horizontal and vertical axes indicates the strength of the contribution of a specific virulence marker to the separation of clusters. Dim1 and Dim2 represent the first 2 dimensions of the analysis and indicate the fraction of variation in the dataset that can be explained by the included variables (i.e., virulence genes).

antitermination protein Q, the lysis protein S, a phage terminase, an integrase, and tail-assembly proteins.

We used WGS of HUS strain EF467 to assemble a partial VT2f phage sequence of 38,594 bp (online Technical Appendix, http://wwwnc.cdc.gov/EID/article/22/12/16-0017-Techapp1.pdf). Analysis of the construct highlighted the absence of most of the genes normally involved in the regulation of the switch between the lysogenic state and the lytic cycle of lambdoid phages, such as *cro*, *cI*, *cII*, *cIII*, and N. We confirmed these findings by mapping the raw reads of the WGS of the strain EF467 against the VT2 reference bacteriophage BP933W (GenBank accession no. AF125520) (not shown).

We confirmed the genomic structure of VT2f phage obtained in silico by 4 PCRs performed on the total DNA extracted from strain EF467 by using primer pairs designed on the construct's map and by using a restriction fragment length polymorphism analysis on the obtained PCR fragments (Table 3; online Technical Appendix). The partial VT2f phage sequence was deposited into the EMBL database (accession no. LN997803).

The portion of the VT2f phage spanning the *xerC* gene and the tRNA-Gly and tRNA-Thr loci (online Technical Appendix) was found in the draft genomes of all the VT2f-producing strains. The region downstream to the tRNA loci was also detected, but with different degrees of variation among the WGSs; for example, the presence of an additional DNA stretch of ≈24 kb in the strain BCW5746 (online Technical Appendix).

The presence of a similar phage structure was confirmed by using a long PCR approach in the other 2 VT2f-producing *E. coli* from HUS cases and in 2 strains from pigeons (strains ED377 and ED363). All the strains showed the expected amplicons with PCR 2 and 3 together with the expected product of PCR 1 in 2 pigeon isolates; all the isolates tested did not yield any amplicon with PCR 4 (Figure 3). A comparative analysis of the *xerC* sequences from all the VT2f phage constructs returned a high degree of variation in its sequence, explaining the observed absence of the PCR4-specific amplicon (data not shown). Finally, a BLAST search by using this VT2f phage construct from strain EF467 returned only partial similarity with phages identified in different *Enterobacteriaceae* but did not retrieve similar structures.

Discussion

VTEC producing the VT2f subtype have long been considered a minor public health problem because of their rare association with human infections (*31–34*). Recently, however, an increasing number of reports of human diseases caused by infection with these *E. coli* strains have

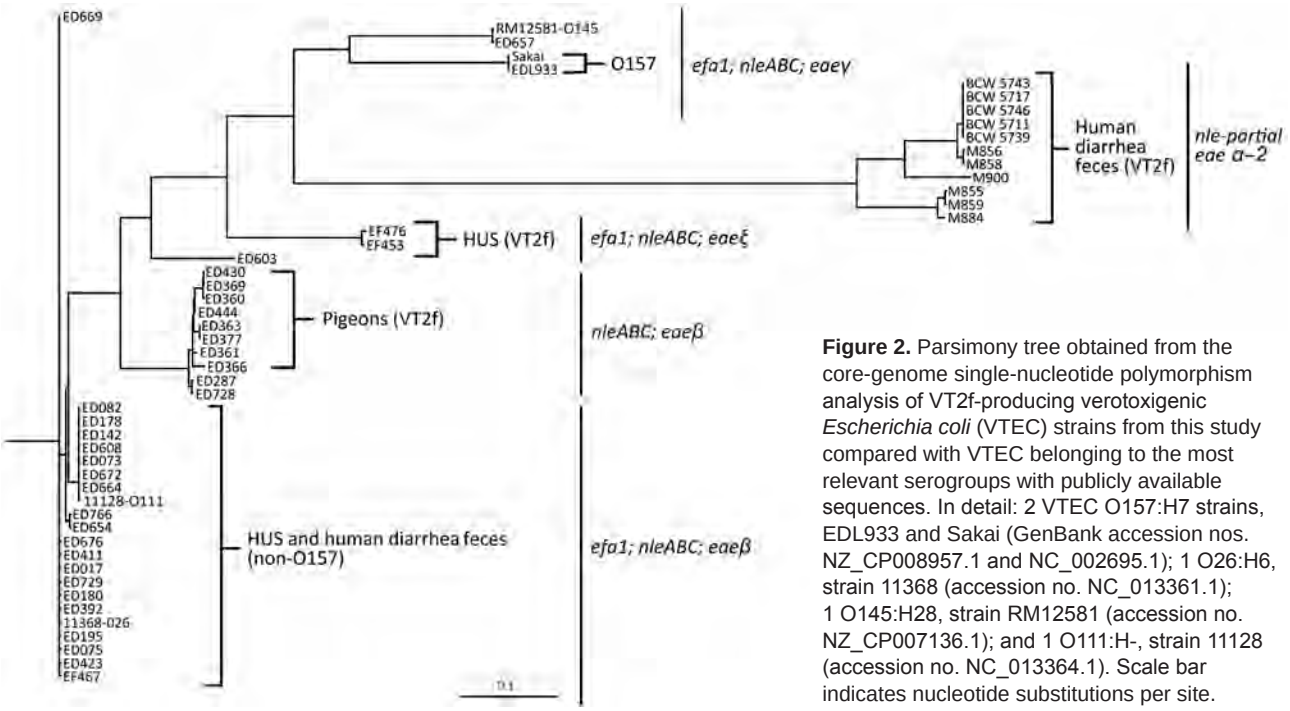

Figure 2. Parsimony tree obtained from the core-genome single-nucleotide polymorphism analysis of VT2f-producing verotoxigenic *Escherichia coli* (VTEC) strains from this study compared with VTEC belonging to the most relevant serogroups with publicly available sequences. In detail: 2 VTEC O157:H7 strains, EDL933 and Sakai (GenBank accession nos. NZ_CP008957.1 and NC_002695.1); 1 O26:H6, strain 11368 (accession no. NC_013361.1); 1 O145:H28, strain RM12581 (accession no. NZ_CP007136.1); and 1 O111:H-, strain 11128 (accession no. NC_013364.1). Scale bar indicates nucleotide substitutions per site.

populated the literature (*11*,*12*,*32*,*35*). The diversity of *vtx2f* gene sequences compared with other *vtx2* subtype genes may have played a role in underestimating the global burden of such infections. PCR primers mostly used for the detection of *vtx2* genes in clinical specimens and the vehicles of infection have been proven to be unable to amplify the *vtx2f* gene (*36*). In addition, the recent description of another *eae*-positive *Escherichia* species often isolated from birds, and sometimes carrying *vtx2f* genes, *E. albertii*, added a further element of confusion. *E. albertii* has been associated both with gastroenteritis in humans and with healthy and diseased birds (*37*,*38*), but this species is difficult to distinguish from *E. coli* when using the usual biochemical or molecular assays.

Most human infections with VTEC producing VT2f have been reported as uncomplicated diarrheal cases (*11*,*12*), which may also have accounted for the underestimation of these infections. Because such cases are not actively surveyed in many countries, these infections may have been overlooked. The recent description of an HUS case associated with a VT2f-producing *E. coli* (*13*) changed the perspective on VT2f-producing *E. coli* and the associated disease, making it necessary to update the current paradigm of HUS-associated VTEC.

Table 3. PCR and restriction fragment length polymorphism analysis conditions used to verify VT2f phage structure in a comparative analysis of the virulence profile of human and zoonotic VT2f-producing *Escherichia coli* strains*

Analysis	Primer name	Sequence, 5′→3′	Position	Thermal profile	Amplicon size, bp	Restriction enzyme (obtained fragments, bp + bp)
PCR1	φ-*vtx2f*_1FW φ -*vtx2f*_1RV	caccatatcccagcaactgc gttggcggttccgactacaa	1,985–2,005 8,315–8,296	95°C for 2 min, 30× (94°C for 30 s, 53°C for 30 s, 70°C for 9 min); 72°C for 10 min	6,331	*Pvu*I (1,773 + 4,558)
PCR2	φ -*vtx2f*_2FW 128–1	gcgcatcaccacttcatctt agattgggcgtcattcactggttg	8,337–8,357 16,502–16,479	95°C for 2 min, 30× (94°C for 30 s, 53°C for 30 s, 70°C for 9 min), 72°C for 10 min	8,166	*Hind*III (1,855 + 6,311)
PCR3	φ -*vtx2f*_3FW φ -*vtx2f*_3RV	ggagtggatattgccgacct gtcttcctgctgaggcgatc	16,808–16,827 20,734–20,715	95°C for 2 min, 30× (94°C for 30 s, 53°C for 30s, 70°C for 9 min), 72°C for 10 min	3,927	*Bgl*II (1,310 + 2,617)
PCR4	φ -*vtx2f*_4FW φ -*vtx2f*_4RV	taatcgcggccgtactcaag tgttcagctccaccttacgg	22,172–22,191 30,979–30,960	95°C for 2 min, 30× (94°C for 30 s, 53°C for 30 s, 70°C for 9 min), 72°C for 10 min	8,808	*Nco*I (5,029 + 3,779)

*Analysis for PCR2, primer 128–1 from (*5*); all other data were compiled for this study. All the long PCR described were performed with the GoTaq Long PCR Master Mix (Promega, Madison, WI, USA) according to manufacturer's instructions. Primer positions refer to the phage sequence deposited into the EMBL database (accession no. LN997803).

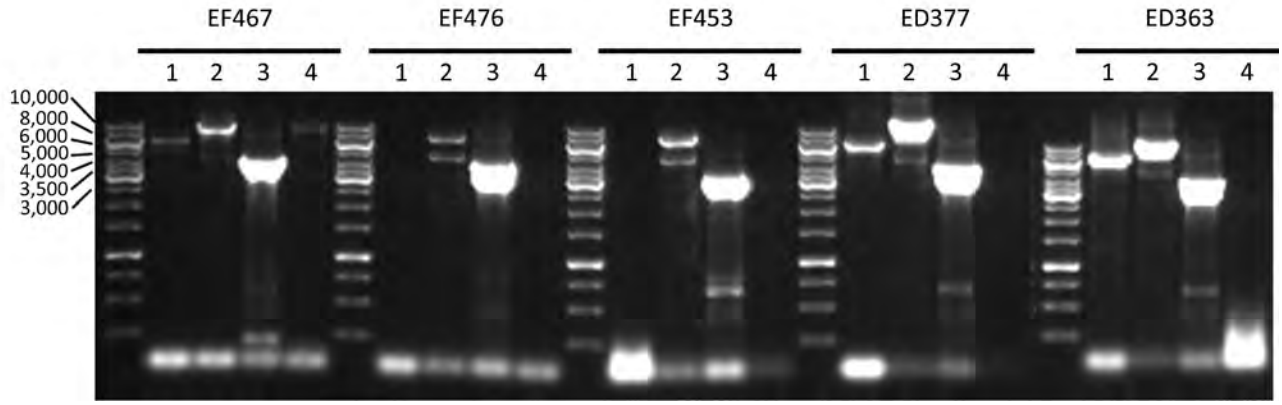

Figure 3. Long PCR analysis of the VT2f phage of verotoxigenic *Escherichia coli* (VTEC) strains isolated from fecal samples from humans with hemolytic uremic syndrome (EF467, EF476, EF453) and from pigeon feces (ED363, ED377). Numbers at left indicate bps; lane numbers indicate PCR 1 to PCR 4. The expected size of the amplicons were 6,331 bp (PCR 1), 8,166 bp (PCR 2), 3,927 bp (PCR 3), and 8,808 bp (PCR 4).

We provide evidence that the VT2f-producing *E. coli* isolated from HUS cases display the complete set of virulence genes described in the typical HUS-associated VTEC (Table 2; Figure 1) (*28*). All VT2f strains from HUS that we examined were positive for pathogenicity island OI-122 (*28*) and the large virulence plasmid first described in VTEC O157 (Table 2) (*39*); the strains from pigeons or from humans with uncomplicated diarrhea did not have these virulence-associated mobile genetic elements (Table 2) (*10–12*,*32*,*40*).

Our study also showed that the LEE was complete in all the genomes investigated, but a complete set of *nleABC* genes was found only in strains from pigeons and from humans with HUS (Table 2), indicating that the VT2f-producing isolates investigated belonged to 3 distinct main virulotypes or subpopulations (Table 2). The intimin subtyping supported this observation. Of 11 diarrheal isolates, 8 had the α-2 gene; all the pigeon isolates had a β intimin coding gene. Finally, 2 of the 3 strains from HUS showed the presence of a gene encoding the ξ intimin (Table 2). Furthermore, the analysis of core genome SNPs confirmed the existence of different subpopulations of VT2f-producing *E. coli* (Figure 2). The analysis of the virulence genes suggests that different populations of VT2f-producing *E. coli* exist and have different potential to cause human disease on the basis of the virulotype to which they belong.

VT2f-producing *E. coli* strains isolated from uncomplicated human cases of diarrhea have been reported in the literature as being ST20 (*11*), which is the same sequence type we identified in most pigeon isolates; this ST was also described in VT2f-producing *E. coli* isolated from pigeons in Japan (*40*). The same study also described an animal isolate of ST722, which was found in 1 strain isolated from human diarrheal feces in our study (Table 2). Similarly, the serotypes in some cases appeared to overlap isolates from pigeons and human cases of diarrhea, such as the serotype O128:H2 that we found in 1 pigeon isolate that was also reported in isolates from human cases of diarrhea in Germany (*11*).

Altogether, these observations indicate that the VT2f-producing *E. coli* causing diarrhea in humans could be a subpopulation of those inhabiting the pigeon reservoir. Alternately, information on the serotypes, ST, and principal component analysis of virulence genes profiles supports the hypothesis that the HUS VT2f-producing strains are more similar to the non-O157 VTEC often isolated from samples from humans with severe disease (Figure 1) than to the other VT2f-producing *E. coli* from humans with diarrhea or from asymptomatic pigeons. This hypothesis suggests that the HUS VT2f-producing strains represent a distinct population of VTEC; whether they are part of the pigeon intestinal flora or arise from an acquisition of the *vtx2*-phage is difficult to ascertain.

The phylogeny of VTEC of different serogroups, investigated by core SNP analysis, showed that the different VT2f-producing *E. coli* cluster into different subpopulations that include strain EF467 grouping together with non-O157 VTEC strains from humans with disease (Figure 2). However, the results from SNP analysis for VTEC of multiple serogroups should be carefully evaluated; the population structure of VTEC belonging to serogroups other than O157 and O26 has not been completely investigated yet.

At the first characterization of the *vtx2f* genes, it was proposed that they were, similar to other VT-coding genes, located on bacteriophages (*5*). Our study confirms this hypothesis and shows that such a phage apparently does not have similar counterparts in the VT-phage genomes reported in the National Center for Biotechnology Information nucleotide repository (http://www.ncbi.nlm.nih.gov/). In addition, we observed that VT2f phage was very similar

in all the VT2f-producing *E. coli* investigated (Figure 3; online Technical Appendix), suggesting that the *vtx2f* genes are present in phages sharing a common ancestor that is different from other phages with the other *vtx1*/*vtx2* subtypes.

In conclusion, we provide evidence that human infections with VT2f-producing *E. coli* are zoonotic diseases transmitted from pigeons. Such an animal reservoir may either directly disseminate VTEC strains causing diarrhea or indirectly release VT2f phages in the environment, which can in turn lysogenize *E. coli* strains that contain accessory virulence determinants and confer them the ability to cause HUS. The isolation of VT2f-producing *E. coli* with a virulence gene profile related to the other HUS-associated VTEC suggests that the severity of the symptoms induced by infection may depend more on the ability to achieve a proficient colonization of the host gut mucosa rather than on the subtype of the produced toxin.

Dr. Grande is a researcher in the field of molecular microbiology. Most of her research activities have been at the European Union Reference Laboratory for *E. coli*, in the unit of Foodborne Zoonoses of the Italian National Institute of Health in Rome, Italy. Her research interests include the investigation and characterization of mobile genetic elements encoding virulence determinants in pathogenic *E. coli*.

References

1. Tozzoli R, Scheutz F. Diarrheagenic *Escherichia coli* infections in umans. In: Morabito S, editor. Pathogenic *Escherichia coli*: molecular and cellular microbiology. Poole (UK): Caister Academic Press; 2014. p. 1–18.
2. Tozzoli R, Grande L, Michelacci V, Ranieri P, Maugliani A, Caprioli A, et al. Shiga toxin–converting phages and the emergence of new pathogenic *Escherichia coli*: a world in motion. Front Cell Infect Microbiol. 2014;4:80. http://dx.doi.org/10.3389/fcimb.2014.00080
3. Caprioli A, Morabito S, Brugere H, Oswald E. Enterohaemorrhagic *Escherichia coli*: emerging issues on virulence and modes of transmission. Vet Res. 2005;36:289–311. http://dx.doi.org/10.1051/vetres:2005002
4. Dell'Omo G, Morabito S, Quondam R, Agrimi U, Ciuchini F, Macrì A, et al. Feral pigeons as a source of verocytotoxin-producing *Escherichia coli*. Vet Rec. 1998;142:309–10. http://dx.doi.org/10.1136/vr.142.12.309
5. Schmidt H, Scheef J, Morabito S, Caprioli A, Wieler LH, Karch H. A new Shiga toxin 2 variant (Stx2f) from *Escherichia coli* isolated from pigeons. Appl Environ Microbiol. 2000;66:1205–8. http://dx.doi.org/10.1128/AEM.66.3.1205-1208.2000
6. Morabito S, Dell'Omo G, Agrimi U, Schmidt H, Karch H, Cheasty T, et al. Detection and characterization of Shiga toxin-producing *Escherichia coli* in feral pigeons. Vet Microbiol. 2001;82:275–83. http://dx.doi.org/10.1016/S0378-1135(01)00393-5
7. Nielsen EM, Skov MN, Madsen JJ, Lodal J, Jespersen JB, Baggesen DL. Verocytotoxin-producing *Escherichia coli* in wild birds and rodents in close proximity to farms. Appl Environ Microbiol. 2004;70:6944–7. http://dx.doi.org/10.1128/AEM.70.11.6944-6947.2004
8. Farooq S, Hussain I, Mir MA, Bhat MA, Wani SA. Isolation of atypical enteropathogenic *Escherichia coli* and Shiga toxin 1 and 2f-producing *Escherichia coli* from avian species in India. Lett Appl Microbiol. 2009;48:692–7.
9. Kobayashi H, Kanazaki M, Hata E, Kubo M. Prevalence and characteristics of *eae*- and *stx*-positive strains of *Escherichia coli* from wild birds in the immediate environment of Tokyo Bay. Appl Environ Microbiol. 2009;75:292–5. http://dx.doi.org/10.1128/AEM.01534-08
10. Askari Badouei M, Zahraei Salehi T, Koochakzadeh A, Kalantari A, Tabatabaei S. Molecular characterization, genetic diversity and antibacterial susceptibility of *Escherichia coli* encoding Shiga toxin 2f in domestic pigeons. Lett Appl Microbiol. 2014;59:370–6. http://dx.doi.org/10.1111/lam.12288
11. Prager R, Fruth A, Siewert U, Strutz U, Tschäpe H. *Escherichia coli* encoding Shiga toxin 2f as an emerging human pathogen. Int J Med Microbiol. 2009;299:343–53. http://dx.doi.org/10.1016/j.ijmm.2008.10.008
12. Friesema I, van der Zwaluw K, Schuurman T, Kooistra-Smid M, Franz E, van Duynhoven Y, et al. Emergence of *Escherichia coli* encoding Shiga toxin 2f in human Shiga toxin-producing *E. coli* (STEC) infections in the Netherlands, January 2008 to December 2011. Euro Surveill. 2014;19:26–32. http://dx.doi.org/10.2807/1560-7917.ES2014.19.17.20787
13. Friesema IH, Keijzer-Veen MG, Koppejan M, Schipper HS, van Griethuysen AJ, Heck ME, et al. Hemolytic uremic syndrome associated with *Escherichia coli* O8:H19 and Shiga toxin 2f gene. Emerg Infect Dis. 2015;21:168–9. http://dx.doi.org/10.3201/eid2101.140515
14. Cuccuru G, Orsini M, Pinna A, Sbardellati A, Soranzo N, Travaglione A, et al. Orione, a web-based framework for NGS analysis in microbiology. Bioinformatics. 2014;30:1928–9. http://dx.doi.org/10.1093/bioinformatics/btu135
15. Bankevich A, Nurk S, Antipov D, Gurevich AA, Dvorkin M, Kulikov AS, et al. SPAdes: a new genome assembly algorithm and its applications to single-cell sequencing. J Comput Biol. 2012;19:455–77. http://dx.doi.org/10.1089/cmb.2012.0021
16. Tritt A, Eisen JA, Facciotti MT, Darling AE. An integrated pipeline for de novo assembly of microbial genomes. PLoS ONE. 2012;7:e42304. http://dx.doi.org/10.1371/journal.pone.0042304
17. Seemann T. Prokka: rapid prokaryotic genome annotation. Bioinformatics. 2014;30:2068–9. http://dx.doi.org/10.1093/bioinformatics/btu153
18. Paton AW, Paton JC. Detection and characterization of Shiga toxigenic *Escherichia coli* by using multiplex PCR assays for stx1, stx2, eaeA, enterohemorrhagic E. coli hlyA, rfbO111, and rfbO157. J Clin Microbiol. 1998;36:598–602.
19. Caprioli A, Nigrelli A, Gatti R, Zavanella M. Isolation of verotoxin-producing *Escherichia coli* from slaughtered pigs. Eur J Clin Microbiol Infect Dis. 1993;12:227–8. http://dx.doi.org/10.1007/BF01967122
20. Joensen KG, Tetzschner AM, Iguchi A, Aarestrup FM, Scheutz F. Rapid and easy in silico serotyping of *Escherichia coli* isolates by use of whole-genome sequencing data. J Clin Microbiol. 2015;53:2410–26. http://dx.doi.org/10.1128/JCM.00008-15
21. Carattoli A, Zankari E, García-Fernández A, Voldby Larsen M, Lund O, Villa L, et al. In silico detection and typing of plasmids using PlasmidFinder and plasmid multilocus sequence typing. Antimicrob Agents Chemother. 2014;58:3895–903. http://dx.doi.org/10.1128/AAC.02412-14
22. Altschul SF, Gish W, Miller W, Myers EW, Lipman DJ. Basic local alignment search tool. J Mol Biol. 1990;215:403–10. http://dx.doi.org/10.1016/S0022-2836(05)80360-2
23. Lindsey RL, Fedorka-Cray PJ, Abley M, Turpin JB, Meinersmann RJ. Evaluating the occurrence of *Escherichia albertii* in chicken carcass rinses by PCR, Vitek analysis, and sequencing of the *rpo*B gene. Appl Environ Microbiol. 2015;81:1727–34. http://dx.doi.org/10.1128/AEM.03681-14

24. Clermont O, Christenson JK, Denamur E, Gordon DM. The Clermont *Escherichia coli* phylo-typing method revisited: improvement of specificity and detection of new phylo-groups. Environ Microbiol Rep. 2013;5:58–65. http://dx.doi.org/10.1111/1758-2229.12019
25. Wirth T, Falush D, Lan R, Colles F, Mensa P, Wieler LH, et al. Sex and virulence in *Escherichia coli*: an evolutionary perspective. Mol Microbiol. 2006;60:1136–51. http://dx.doi.org/10.1111/j.1365-2958.2006.05172.x
26. Gardner SN, Slezak T, Hall BG. kSNP3.0: SNP detection and phylogenetic analysis of genomes without genome alignment or reference genome. Bioinformatics. 2015;31:2877–8. http://dx.doi.org/10.1093/bioinformatics/btv271
27. Dean P, Kenny B. The effector repertoire of enteropathogenic *E. coli*: ganging up on the host cell. Curr Opin Microbiol. 2009;12:101–9. http://dx.doi.org/10.1016/j.mib.2008.11.006
28. Karmali MA, Mascarenhas M, Shen S, Ziebell K, Johnson S, Reid-Smith R, et al. Association of genomic O island 122 of *Escherichia coli* EDL 933 with verocytotoxin-producing *Escherichia coli* seropathotypes that are linked to epidemic and/or serious disease. J Clin Microbiol. 2003;41:4930–40. http://dx.doi.org/10.1128/JCM.41.11.4930-4940.2003
29. Imamovic L, Tozzoli R, Michelacci V, Minelli F, Marziano ML, Caprioli A, et al. OI-57, a genomic island of *Escherichia coli* O157, is present in other seropathotypes of Shiga toxin–producing *E. coli* associated with severe human disease. Infect Immun. 2010;78:4697–704. http://dx.doi.org/10.1128/IAI.00512-10
30. Brunder W, Karch H, Schmidt H. Complete sequence of the large virulence plasmid pSFO157 of the sorbitol-fermenting enterohemorrhagic *Escherichia coli* O157:H- strain 3072/96. Int J Med Microbiol. 2006;296:467–74. http://dx.doi.org/10.1016/j.ijmm.2006.05.005
31. Friedrich AW, Bielaszewska M, Zhang WL, Pulz M, Kuczius T, Ammon A, et al. *Escherichia coli* harboring Shiga toxin 2 gene variants: frequency and association with clinical symptoms. J Infect Dis. 2002;185:74–84. http://dx.doi.org/10.1086/338115
32. Jenkins C, Willshaw GA, Evans J, Cheasty T, Chart H, Shaw DJ, et al. Subtyping of virulence genes in verocytotoxin-producing *Escherichia coli* (VTEC) other than serogroup O157 associated with disease in the United Kingdom. J Med Microbiol. 2003; 52:941–7. http://dx.doi.org/10.1099/jmm.0.05160-0
33. Seto K, Taguchi M, Kobayashi K, Kozaki S. Biochemical and molecular characterization of minor serogroups of Shiga toxin–producing *Escherichia coli* isolated from humans in Osaka prefecture. J Vet Med Sci. 2007;69:1215–22. http://dx.doi.org/10.1292/jvms.69.1215
34. van Duynhoven YT, Friesema IH, Schuurman T, Roovers A, van Zwet AA, Sabbe LJ, et al. Prevalence, characterisation and clinical profiles of Shiga toxin–producing *Escherichia coli* in the Netherlands. Clin Microbiol Infect. 2008;14:437–45. http://dx.doi.org/10.1111/j.1469-0691.2008.01963.x
35. Buvens G, De Rauw K, Roisin S, Vanfraechem G, Denis O, Jacobs F, et al. Verocytotoxin-producing *Escherichia coli* O128ab:H2 bacteremia in a 27-year-old male with hemolytic-uremic syndrome. J Clin Microbiol. 2013;51:1633–5. http://dx.doi.org/10.1128/JCM.03025-12
36. Feng PC, Jinneman K, Scheutz F, Monday SR. Specificity of PCR and serological assays in the detection of *Escherichia coli* Shiga toxin subtypes. Appl Environ Microbiol. 2011;77:6699–702. http://dx.doi.org/10.1128/AEM.00370-11
37. Oh JY, Kang MS, Hwang HT, An BK, Kwon JH, Kwon YK. Epidemiological investigation of *eae*A-positive *Escherichia coli* and *Escherichia albertii* strains isolated from healthy wild birds. J Microbiol. 2011;49:747–52. http://dx.doi.org/10.1007/s12275-011-1133-y
38. Ooka T, Tokuoka E, Furukawa M, Nagamura T, Ogura Y, Arisawa K, et al. Human gastroenteritis outbreak associated with *Escherichia albertii*, Japan. Emerg Infect Dis. 2013;19:144–6. http://dx.doi.org/10.3201/eid1901.120646
39. Karch H, Heesemann J, Laufs R, O'Brien AD, Tacket CO, Levine MM. A plasmid of enterohemorrhagic *Escherichia coli* O157:H7 is required for expression of a new fimbrial antigen and for adhesion to epithelial cells. Infect Immun. 1987;55:455–61.
40. Murakami K, Etoh Y, Ichihara S, Maeda E, Takenaka S, Horikawa K, et al. Isolation and characteristics of Shiga toxin 2f-producing *Escherichia coli* among pigeons in Kyushu, Japan. PLoS ONE. 2014;9:e86076. http://dx.doi.org/10.1371/journal.pone.0086076

Address for correspondence: Laura Grande, European Union Reference Laboratory for *E. coli*, Veterinary Public Health and Food Safety Department, Istituto Superiore di Sanità, Viale Regina Elena 299, 00161 Rome, Italy; email: laur.grande@gmail.com

African Horse Sickness Caused by Genome Reassortment and Reversion to Virulence of Live, Attenuated Vaccine Viruses, South Africa, 2004–2014

Camilla T. Weyer, John D. Grewar, Phillippa Burger, Esthea Rossouw, Carina Lourens, Christopher Joone, Misha le Grange, Peter Coetzee, Estelle Venter, Darren P. Martin, N. James MacLachlan, Alan J. Guthrie

African horse sickness (AHS) is a hemorrhagic viral fever of horses. It is the only equine disease for which the World Organization for Animal Health has introduced specific guidelines for member countries seeking official recognition of disease-free status. Since 1997, South Africa has maintained an AHS controlled area; however, sporadic outbreaks of AHS have occurred in this area. We compared the whole genome sequences of 39 AHS viruses (AHSVs) from field AHS cases to determine the source of 3 such outbreaks. Our analysis confirmed that individual outbreaks were caused by virulent revertants of AHSV type 1 live, attenuated vaccine (LAV) and reassortants with genome segments derived from AHSV types 1, 3, and 4 from a LAV used in South Africa. These findings show that despite effective protection of vaccinated horses, polyvalent LAV may, paradoxically, place susceptible horses at risk for AHS.

African horse sickness (AHS) is a severe, often fatal disease of equids that is caused by AHS virus (AHSV), a member of the genus *Orbivirus*, family *Reoviridae* (*1*). The virus is transmitted to horses by biting midges in the genus *Culicoides* (*2*). Although AHS currently occurs only in sub-Saharan Africa, various species of *Culicoides* midges occur throughout the entire inhabited world, warranting concern that AHSV could spread into areas that are currently free of the virus (*1*,*3*–*5*). Furthermore, the global range of related *Culicoides*-transmitted orbiviruses, such as bluetongue virus, has expanded recently, probably in part as a result of climate change (*6*). In AHS-endemic temperate regions, such as those occurring throughout much of South Africa, the disease is most prevalent in late summer (*7*). Efforts to prevent the catastrophic impact of AHS began soon after the determination of its viral etiology in 1900, at which time it was only the second animal virus ever described (*8*,*9*). Presently, a polyvalent, live, attenuated vaccine (LAV) against AHSV (AHSV-LAV), which is produced by Onderstepoort Biological Products (Pretoria, South Africa) and provides broad protection against all 9 AHSV types (*10*), is used widely in South Africa and adjacent countries. This vaccine is supplied in 2 vials, each containing different combinations of AHSV types: combination 1 is trivalent and contains types 1, 3, and 4, whereas combination 2 is tetravalent and contains types 2, 6, 7, and 8 (*10*). Heterologous immunity is believed to provide protection to the 2 AHSV types, 5 and 9, that are not included in the vaccine.

AHS is the only equine disease for which the World Organisation for Animal Health (OIE) observes official recognition status, such that OIE member countries are required to have legally enforceable AHS control measures in place and are required to immediately notify OIE of any change to their country's AHS status (*11*). The Western Cape Province of South Africa, at the southern tip of the African continent, has historically been free from AHS, and for this reason, a legislatively defined AHS controlled area was created there in 1997 to facilitate movement of horses from South Africa. Within this area are an AHS free zone, consisting of the Cape Town metropolis; an AHS surveillance zone surrounding the free zone; and an outermost AHS protection zone (PZ) (Figure 1) (*12*). Movement of equids into and between these zones is strictly controlled. Vaccination with the polyvalent AHSV-LAV in the surveillance zone and free zone is allowed only with permission

Author affiliations: University of Pretoria, Onderstepoort, South Africa (C.T. Weyer, P. Burger, C. Lourens, C. Joone, M. le Grange, P. Coetzee, E. Venter, N.J. MacLachlan, A.J. Guthrie); Western Cape Department of Agriculture, Elsenburg, South Africa (J.D. Grewar); Wits Health Consortium, Johannesburg, South Africa (E. Rossouw); University of Cape Town, Cape Town, South Africa (D.P. Martin); University of California, Davis, CA, USA (N.J. MacLachlan)

DOI: http://dx.doi.org/10.3201/eid2212.160718

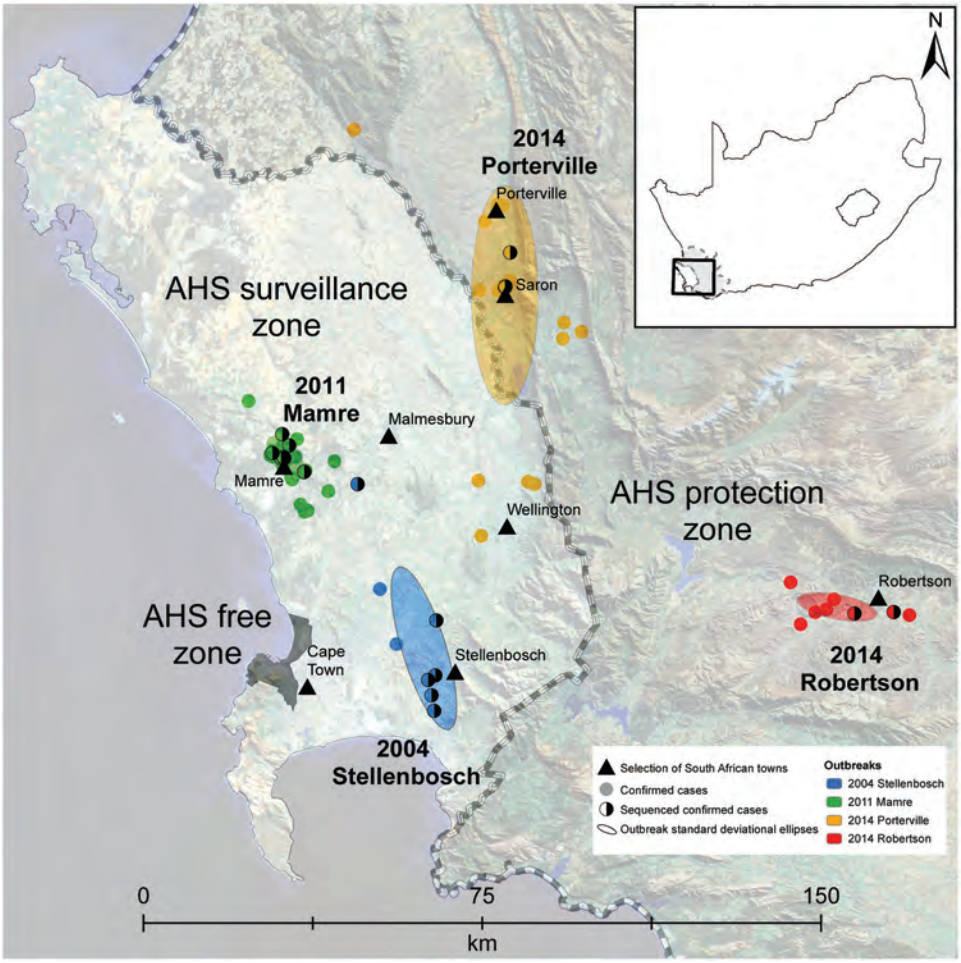

Figure 1. Locations of African horse sickness (AHS) outbreaks in Western Cape Province, South Africa, 2004–2014, including the spatial distribution of each of the AHS virus type 1 outbreaks that have occurred in the AHS controlled area since 1997. The AHS controlled area (shown in inset) is the combination of the AHS free, AHS surveillance, and AHS protection zones (also shown). Individual confirmed cases of AHS are indicated by solid dots. Half-shaded dots indicate confirmed cases for which samples were sent for sequencing (as opposed to confirmed cases that were not sequenced). The directional distribution of each outbreak is indicated by ellipses based on SD.

from the state veterinary service, and since March 2015, only during the period of low vector activity.

Since its creation in 1997, a total of 6 outbreaks of AHS in the AHS controlled area have been reported to OIE, in1999, 2004, 2006, 2011, 2013, and 2014 (*13–17*). Before the 2014 outbreak, these outbreaks were assumed to be caused by illegal movement of viremic animals into the controlled area, although the source was established for only 2 of these outbreaks: a type 7 virus for the 1999 outbreak in the surveillance zone and a type 5 virus for the 2006 outbreak in the PZ (Figure 1) (*18,19*). Because the source of the viruses responsible for the other outbreaks was never established, the goal of our study was to further characterize the epidemiology of AHSV type 1 (AHSV-1) outbreaks in the controlled area by 1) whole-genome sequencing of viruses from individual outbreaks (2004, 2011, and 2014); 2) phylogenetic comparison of these sequences with those of the polyvalent AHSV-LAV and AHSV reference strains; 3) analysis of outbreak viruses for genome segment reassortment; 4) analysis of single-nucleotide variants (SNVs) associated with attenuation of AHSV-LAV to determine whether vaccine-derived viruses have reverted to virulence; 5) correlation of epidemiologic and clinical findings with molecular findings; and 6) confirmation of the source of the virus strains responsible for the 2004, 2011, and 2014 outbreaks of AHS in the controlled area.

Materials and Methods

Virus Isolates

We sequenced complete genomes from 55 AHSV isolates collected during 1961–2014, including 39 field isolates of AHSV-1 from horses during the 2004 Stellenbosch (16 isolates), 2011 Mamre (7 isolates), 2014 Porterville (14 isolates), and 2014 Robertson (2 isolates) outbreaks of AHS in Western Cape Province of South Africa (Figure 1); AHSV LAV strains of types 1, 2, 3, 4, 6, 7, and 8; and Agricultural Research Council–Onderstepoort Veterinary Institute Laboratory reference strains for each of the 9 AHSV types. We included each of these virus isolates in the AHS genome sequencing Bioproject (http://www.ncbi.nlm.nih.gov/bioproject/?term=PRJNA271179) and identified each by a unique virus strain name (online Technical Appendix 1, http://wwwnc.cdc.gov/EID/article/22/12/16-0718-Techapp1.xlsx).

RNA Extraction, Identification, and Typing

We isolated individual viruses of each type included in the polyvalent AHSV-LAV independently, as previously described (*20*,*21*). We extracted genomic double-stranded RNA from all AHSV strains evaluated from virus-infected cells by using TRIzol reagent (Life Technologies, Johannesburg, South Africa). We identified and typed AHSV isolates by using group-specific (GS) real-time reverse transcription PCR (rRT-PCR) assays (*22*) and type-specific (TS) rRT-PCR assays targeting the gene encoding viral protein (VP) 2 (VP2) (*23*).

Genome Sequencing and Assembly

We prepared sequencing templates by using sequence-independent whole-genome RT-PCR amplification (*24*). We sequenced PCR amplicons on an Illumina MiSeq sequencer (Inqaba Biotechnical Industries, Pretoria, South Africa) by using the Nextera XT DNA sample preparation kit and 300-bp paired-end V3 Illumina chemistry. We analyzed Illumina sequence reads by using Geneious version 9 (http://www.geneious.com) (25). We used a combination of de novo assembly followed by mapping to obtain the full-length consensus genome sequences of each virus strain.

Phylogenetic Analysis

We aligned sequences of the concatenated whole virus genomes and individual genome segments by using MAFFT (http://mafft.cbrc.jp/alignment/software) (*26*) implemented within Geneious version 9 (*25*). We then used the Smart Model Selection program included in PhyML version 3 (http://www.atgc-montpellier.fr/phyml) (*27*) to identify the evolutionary models that best fit the individual sequence datasets by applying the corrected Akaike information criterion. We used the parameters from these models to construct maximum-likelihood trees by using PhyML version 3 (*27*) implemented within Geneious version 9 (*25*) with 1,000 bootstrap replicates to estimate branch support.

Genotype Group Analysis

We used RAMI (http://mbio-serv2.mbioekol.lu.se/rami.html) to analyze the concatenated whole genome sequence maximum-likelihood tree to genetically (and not evolutionarily) classify the sequences into genotype groups based on patristic distances (*28*). We ran RAMI with the patristic distance threshold set to 0.000459, enabling us to differentiate between genome sequences that differed from one another by as few as 16 nt variants.

Reassortment Analysis

We used Recombination Detection Program (RDP) version 4.63 (*29*) with default settings, except that we invoked the "scan for reassortment and recombination" setting to identify any reassortment between the gene segments of LAV strains of AHSV types 1, 3, and 4 and the 39 field isolate strains included in this study. We considered reassortment events detected by any of the 8 different recombination detection methods implemented in RDP (RDP, MAXCHI, and GENECONV methods in primary scanning mode and the BURT, Bootscan, CHIMAERA, SisScan, and 3SEQ methods in secondary scanning mode, each with a Bonferroni corrected p value cutoff of 0.05) to represent evidence of reassortment.

Nonsynonymous Single Nucleotide Variants

We aligned consensus concatenated whole virus genomes from 2 AHSV-1 laboratory strains (1/Lab/ZAF/62/OVI-HS29/62 and 1/Lab/ZAF/98/OBP-116) and the 39 field isolate strains by using MAFFT (*26*) and analyzed them by using the find variations/SNPs function in Geneious (*25*) with the find nonsynonymous polymorphisms only option enabled. We then compared the nonsynonymous SNVs in these sequences with the nonsynonymous SNVs previously associated with attenuation of AHSV-1 (*24*).

Results

Phylogenetic and Genotype Group Analysis

We used concatenated genome segments of 55 AHSV genomes to construct a maximum-likelihood phylogenetic tree incorporating best-fit substitution models (online Technical Appendix 2 Table 1, http://wwwnc.cdc.gov/EID/article/22/12/16-0718-Techapp2.pdf) to infer degrees of genetic relatedness (Figure 2). Genotype group analysis of patristic distances inferred from this maximum-likelihood tree by using RAMI (*28*) indicated that the AHSV strains isolated during the 2004, 2011, and 2014 outbreaks of AHS in the controlled area segregate into 3, 1, and 2 unique groups, respectively. Specifically, the groups were 1a, 1b, and 1c for the 2004 outbreak; 2 for the 2011 outbreak; 3a for the 2014 Porterville outbreak; and 3b for the 2014 Robertson outbreak (online Technical Appendix 2 Table 2). For the 2004 outbreak viruses, genotype group 1a includes 4 viruses that group closely with the AHSV-1-LAV strain, 1/Lab/ZAF/98/OBP-116; genotype group 1b includes 11 viruses that are also closely related to 1/Lab/ZAF/98/OBP-116; and genotype group 1c includes a single virus that segregates between 1/Lab/ZAF/98/OBP-116 and 4/Lab/ZAF/98/OBP-116. The Mamre outbreak viruses in genotype group 2 consist of 7 viruses that are all closely related to 1/Lab/ZAF/98/OBP-116. For the 2014 outbreak viruses, genotype group 3a includes 14 viruses that were all isolated from AHSV-infected horses in the Porterville area and genotype group 3b includes 2 viruses that were isolated from AHSV-infected horses in the Robertson area, with both groups of viruses being closely related to 1/Lab/ZAF/98/OBP-116.

Table 1. Attenuation-associated nonsynonymous SNVs of consensus sequences of genome segments of AHSV-1 viruses from 4 AHS outbreaks in the AHS controlled area of Western Cape Province, South Africa, 2004–2014, and reference strains*

Abbreviated strain name	Genome segment and amino acid position							Genotype group
	VP2 357	VP3 232	VP5 422	VP5 434	VP6 81	VP6 169	NS3 201	
1/E.cab-tc/ZAF/62/OVI-HS29/62	N	Y	S	T	A	R	M	
1/Lab/ZAF/98/OBP-116†	K	H	N	I	V	Q	K	
1/E.cab-tc/ZAF/04/Elb-E040019	‡			T§	A	R	E	1a
1/E.cab-tc/ZAF/04/Elb-E040020				T	A	R	E	1a
1/E.cab-tc/ZAF/04/Elb-E040021				T	A	R	E	1a
1/E.cab-tc/ZAF/04/Dkt-E040029				T	A	R	E	1a
1/E.cab-tc/ZAF/04/Tgd-E040031	N			T	A	R	¶	1b
1/E.cab-tc/ZAF/04/Elb-E040034	N			T	A	R	¶	1b
1/E.cab-tc/ZAF/04/Tgd-E040039	N			T	A	R	¶	1b
1/E.cab-tc/ZAF/04/Avt-E040043	N			T	A	R	¶	1b
1/E.cab-tc/ZAF/04/Avt-E040048	N			T	A	R	¶	1b
1/E.cab-tc/ZAF/04/Vdm-E040062	N			T	A	R	¶	1b
1/E.cab-tc/ZAF/04/Tgd-E040064	N			T	A	R	¶	1b
1/E.cab-tc/ZAF/04/Vdm-E040065	N			T	A		¶	1b
1/E.cab-tc/ZAF/04/Avt-E040066	N			T	A	R	¶	1b
1/E.cab-tc/ZAF/04/Avt-E040081	N			T	A	R	¶	1b
1/E.cab-tc/ZAF/04/Kbk-E040086	N			T	A	R	¶	1b
1/E.cab-tc/ZAF/04/Avt-E040061	N		¶	¶	A	R	¶	1c
1/E.cab-tc/ZAF/11/Mre-E110143_1				T	A	R	N	2
1/E.cab-tc/ZAF/11/Mre-E110180_WC44				T	A	R	N	2
1/E.cab-tc/ZAF/11/Mre-E110180_WC61				T	A	R	N	2
1/E.cab-tc/ZAF/11/Mre-E110180_WC165				T	A	R	N	2
1/E.cab-tc/ZAF/11/Mre-E110411_1				T	A	R	N	2
1/E.cab-tc/ZAF/11/Mre-E110418_1				T	A	R	N	2
1/E.cab-tc/ZAF/11/Mre-E110674_3				T	A	R	N	2
1/E.cab-tc/ZAF/14/Ptv-E140485_WC00522				T	A	R	¶	3a
1/E.cab-tc/ZAF/14/Ptv-E140485_WC00528				T	A	R	¶	3a
1/E.cab-tc/ZAF/14/Ptv-E140485_WC00533				T	A	R	¶	3a
1/E.cab-tc/ZAF/14/Ptv-E140485_WC00544				T	A	R	¶	3a
1/E.cab-tc/ZAF/14/Ptv-E140485_WC00555				T	A	R	¶	3a
1/E.cab-tc/ZAF/14/Srn-E140526_WC00481				T	A	R	¶	3a
1/E.cab-tc/ZAF/14/Srn-E140526_WC00482				T	A	R	¶	3a
1/E.cab-tc/ZAF/14/Srn-E140526_WC00488				T	A	R	¶	3a
1/E.cab-tc/ZAF/14/Srn-E140526_WC00491				T	A	R	¶	3a
1/E.cab-tc/ZAF/14/Srn-E140526_WC00493				T	A	R	¶	3a
1/E.cab-tc/ZAF/14/Srn-E140526_WC00502				T	A	R	¶	3a
1/E.cab-tc/ZAF/14/Ptv-E140536_WC00506				T	A	R	¶	3a
1/E.cab-tc/ZAF/14/Ptv-E140536_WC00507				T	A	R	¶	3a
1/E.cab-tc/ZAF/14/Ptv-E140536_WC00508				T	A	R	¶	3a
1/E.cab-tc/ZAF/14/Rbn-E140702_RB00008				T	A	R	¶	3b
1/E.cab-tc/ZAF/14/Rbn-E140816_RB00221				T	A	R	¶	3b

*AHS, African horse sickness; AHSV-1, AHS virus type 1; NS3, nonstructural protein 3; SNV, single-nucleotide variants; VP, viral protein.
†The changes in amino acids are indicated in comparison with the AHSV-1 live, attenuated vaccine-derived strain (1/Lab/ZAF/98/OBP-116) for relevant viral proteins.
‡Sequences that were identical to the consensus sequence of the vaccine-derived strain are indicated by an empty cell.
§Sequences that differed from the consensus sequence of the AHSV-1 live, attenuated vaccine-derived strain are indicated with the letter symbol of the relevant amino acid.
¶Indicates that these segments were not considered due to a recombination event that occurred with another vaccine-derived AHSV type.

Given that reassortment is a major feature of orbivirus evolution (*30*,*31*), we further explored the evolutionary relationships between the 55 AHSV sequences by constructing separate maximum-likelihood trees for each of the VP1, VP2, VP3, VP4, VP5, VP6, VP7, nonstructural (NS) protein 1 (NS1), NS2, and NS3 encoding genome segments (online Technical Appendix 2 Figures 1–10). For the segments encoding VP2, VP3, VP6, NS1, and NS2, viruses included in genotype groups 1a, 1b, 1c, 2, 3a, and 3b all group, with high degrees of associated bootstrap support, together with the AHSV-1-LAV strain, 1/Lab/ZAF/98/OBP-116. For the segments encoding VP1, VP4, and VP7, the viruses included in genotype groups 1a, 2, 3a, and 3b also group with 1/Lab/ZAF/98/OBP-116, whereas those in genotype groups 1b and 1c group with the AHSV-3-LAV strain, 3/Lab/ZAF/98/OBP-116. For the gene encoding VP5, viruses included in all genotype groups except 1c group with 1/Lab/ZAF/98/OBP-116, whereas those in genotype group 1c group with the AHSV-4-LAV strain, 4/Lab/ZAF/98/OBP-116. For genes encoding NS3, viruses included in genotype groups 1a and 2 group with 1/Lab/ZAF/98/OBP-116, whereas those included in the remaining genotype groups group with 4/Lab/ZAF/98/OBP-116. Collectively, these data confirm that all 10 gene segments of

the viruses included in genotype groups 1a and 2 are probably derived from a most recent common ancestor closely resembling 1/Lab/ZAF/98/OBP-116; the viruses included in genotype groups 1b and 1c are probably reassortants derived from parental viruses very closely resembling 1/Lab/ZAF/98/OBP-116, 3/Lab/ZAF/98/OBP-116, and 4/Lab/ZAF/98/OBP-116; and viruses in genotype groups 3a and 3b are probably reassortants derived from parental viruses very closely resembling 1/Lab/ZAF/98/OBP-116 and 4/Lab/ZAF/98/OBP-116 (Figure 3).

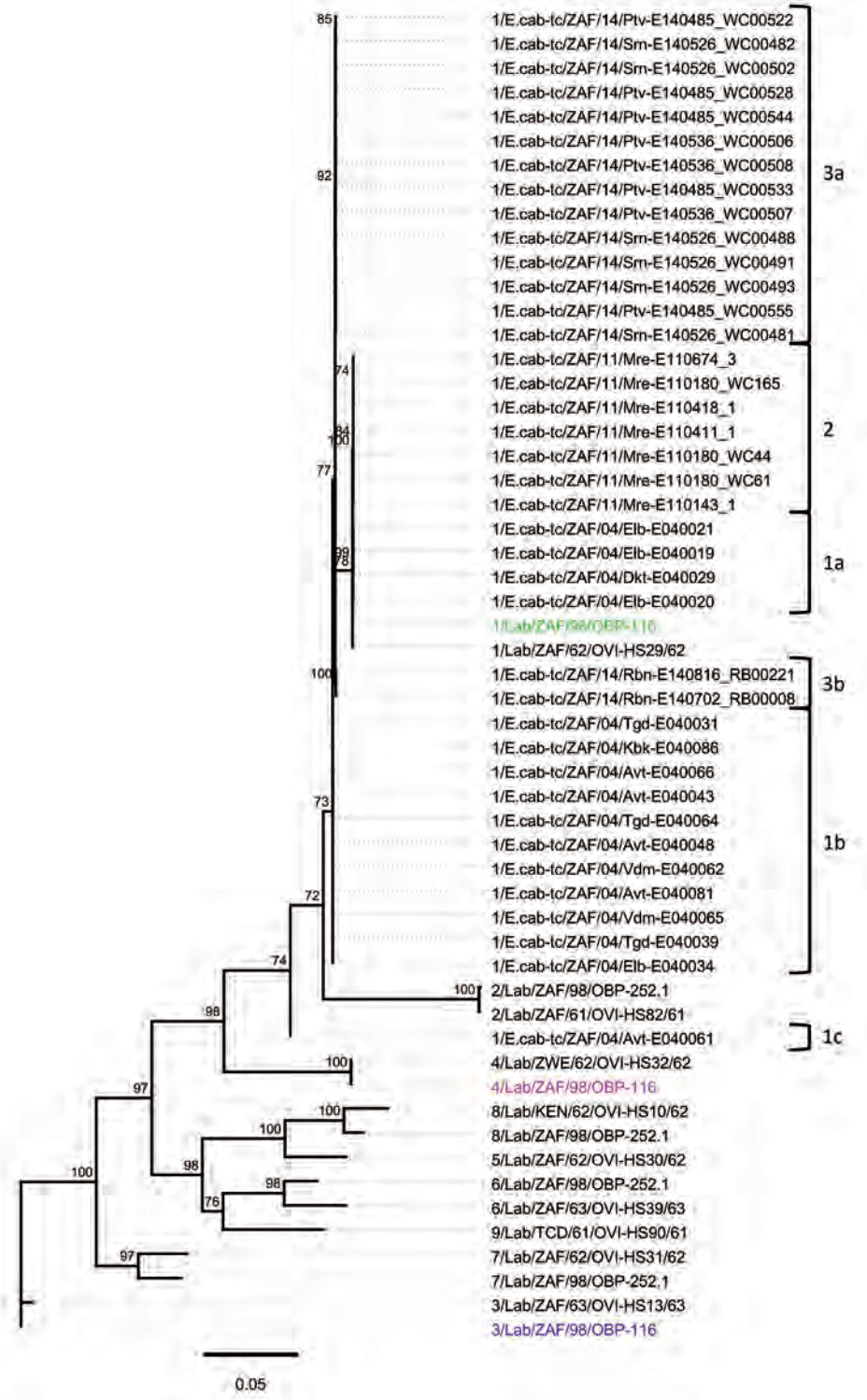

Figure 2. Whole-genome phylogeny of African horse sickness (AHS) viruses identified in AHS outbreaks in Western Cape Province, South Africa, 2004–2014. Maximum-likelihood phylogenetic tree indicating the genetic relationships of concatenated whole genome nucleotide sequences of AHS viruses from affected horses in the 2004, 2011, and 2014 outbreaks in the AHS controlled area in Western Cape Province to the AHS live, attenuated vaccine viruses and reference viruses. Green indicates vaccine-derived 1/Lab/ZAF/98/OBP-116, blue indicates vaccine-derived 3/Lab/ZAF/98/OBP-116, and red indicates vaccine-derived 4/Lab/ZAF/98/OBP-116. Branches are scaled to represent numbers of inferred nucleotide differences per site. Branches supported by full maximum-likelihood bootstrap values >70% are indicated. Genotype groups are indicated at right. Scale bar indicates genetic distance.

Table 2. Epidemiologic parameters for 4 outbreaks involving AHS virus type 1 in the AHS controlled area in Western Cape Province, South Africa, 2004–2014*

Parameter†	2004 Stellenbosch	2011 Mamre	2014 Porterville	2014 Robertson
No. confirmed cases	23 (16)‡	84 (73)§	89	22
No. deaths	18 (16)‡	64 (64)§	13	1
Case-fatality rate, %	78.3 (100)‡	76.2 (87.7)§	14.6	4.5
No. subclinical cases	0	15 (4)†	52	17
% Subclinical	0	17.9 (5.5)§	58.4	77.3
No. vaccinated cases	2/23	2/84	35/89	3/22
% Vaccinated	8.7	2.4	39.3	13.6
No. properties affected	10 (8)‡	47 (45)§	31	8

*AHS, African horse sickness.
†The parameters were calculated by using the current World Organization for Animal Health (OIE) case definition. Parameters calculated by using the case definitions when the outbreaks occurred are in parenthesis for the 2004 and 2011 outbreaks.
‡An additional 5 clinical cases and 2 deaths that met the criteria of the current OIE AHS case definition were not included based on the case definition in place at the time of this outbreak (*13*).
§An additional 11 subclinical cases that met the criteria of the current OIE AHS case definition were not included based on the case definition in place at the time of this outbreak (*15*).

Explicitly testing for intrasegment recombination and reassortment by using RDP4.63 (*29*) yielded no evidence of intracomponent recombination in any virus but strong evidence of reassortment in genotype group 1b, 1c, 3a, and 3b viruses (online Technical Appendix 2 Table 3). Genotype group 1b viruses have 6 genome segments (encoding VP2, VP3, VP5, VP6, NS1, and NS2) derived from a virus resembling 1/Lab/ZAF/98/OBP-116; 2 segments (encoding VP1 and VP7) derived from a virus resembling 3/Lab/ZAF/98/OBP-116 (multiple testing corrected $p = 2.27 \times 10^{-12}$ and 1.13×10^{-31}, respectively); 1 segment (encoding NS3) derived from a virus resembling 4/Lab/ZAF/98/OBP-116 ($p = 9.31 \times 10^{-240}$); and 1 segment (encoding VP4) that could plausibly have been derived from either 3/Lab/ZAF/98/OBP-116 or 1/Lab/ZAF/98/OBP-116 ($p = 7.66 \times 10^{-4}$) (Figure 4). Genotype group 1c viruses display a reassortant pattern resembling that of group 1b viruses except that the segment encoding VP5 is apparently derived from a virus resembling 4/Lab/ZAF/98/OBP-116 ($p = 1.96 \times 10^{-216}$). Genotype groups 3a and 3b viruses have 9 segments derived from a virus resembling 1/Lab/ZAF/98/OBP-116 and a single segment (NS3) derived from a virus resembling 4/Lab/ZAF/98/OBP-116 ($p = 9.31 \times 10^{-240}$) (Figure 4).

Several SNVs relative to the AHSV-LAV–derived viruses 1/Lab/ZAF/98/OBP-116 and 3/Lab/ZAF/98/OBP-116 are present in the NS1-encoding genes of viruses included in genotype groups 3a (2014 Porterville) and 3b (2014 Robertson) (online Technical Appendix 2 Table 4). Only a single nonsynonymous SNV exists between the NS1-encoding genes of 1/Lab/ZAF/98/OBP-116 and 3/Lab/ZAF/98/OBP-116 (NS1 I264T). All viruses included in genotype group 3a (2014 Porterville) have the I amino acid variant that is present in 1/Lab/ZAF/98/OBP-116, whereas viruses in genotype group 3b (2014 Robertson) include the T amino acid variant present in 3/Lab/ZAF/98/OBP-116. Viruses in the 3b genotype group (2014 Robertson) include ≥2 synonymous SNVs and ≥1 nonsynonymous SNV relative to 3/Lab/ZAF/98/OBP-116, which suggests that the NS1 gene of the virus strains in genotype group 3b are most probably derived from 3/Lab/ZAF/98/OBP-116, whereas those in genotype group 3a are more probably derived from 1/Lab/ZAF/98/OBP-116.

Seven nonsynonymous SNVs were identified between the whole genome sequences of the AHSV-1-LAV–derived virus, 1/Lab/ZAF/98/OBP-116, and its parental virus, 1/E.cab-tc/ZAF/62/OVI-HS29/62 (Table 1). SNVs are present at 4 of these 7 sites in the 4 viruses included in genotype group 1a. Intriguingly, 3 of these 4 changes are apparently reversions to the nonsynonymous SNV that is present in the virulent parental virus (I434T in VP5 and V81A and Q169R in VP6) and are therefore potentially reversion-to-virulence mutations. The 1 other SNV in the genotype group 1a viruses is site 201 in NS3, whereas in 1/Lab/ZAF/98/OBP-116 and 1/E.cab-tc/ZAF/62/OVI-HS29/62, a K and an M, respectively, are at this site, and in the group 1a viruses, an E is at this site. In 10 of the 11 field viruses in genotype group 1b, nonsynonymous SNVs were also detected at 4 of the 7 sites that differentiate the attenuated 1/Lab/ZAF/98/OBP-116 virus from its virulent parent, 1/E.cab-tc/ZAF/62/OVI-HS29/62. The remaining field virus in genotype group 1b, 1/E.cab-tc/ZAF/04/Vdm-E040065, includes 3 of these 4 SNVs. The I434T SNV in VP5 and the V81A and Q169R SNVs in VP6 of viruses in genotype group 1a are the same as those found in the genotype group 1b, 2, 3a, and 3b viruses. The K357N SNV in VP2 was detected only among viruses in genotype groups 1b and 1c. All the viruses included in genotype groups 1b, 1c, 3a, and 3b are also reassortants with an NS3-encoding segment derived from a virus resembling 4/Lab/ZAF/98/OBP-116; therefore, SNVs in this component of these viruses were not considered as genuine mutationally derived SNVs.

The 1/E.cab-tc/ZAF/04/Avt-E040061 strain in genotype group 1c has nonsynonymous SNVs at 3 of the 7 loci (K357N in VP2 and V81A and Q169R in VP6) but a

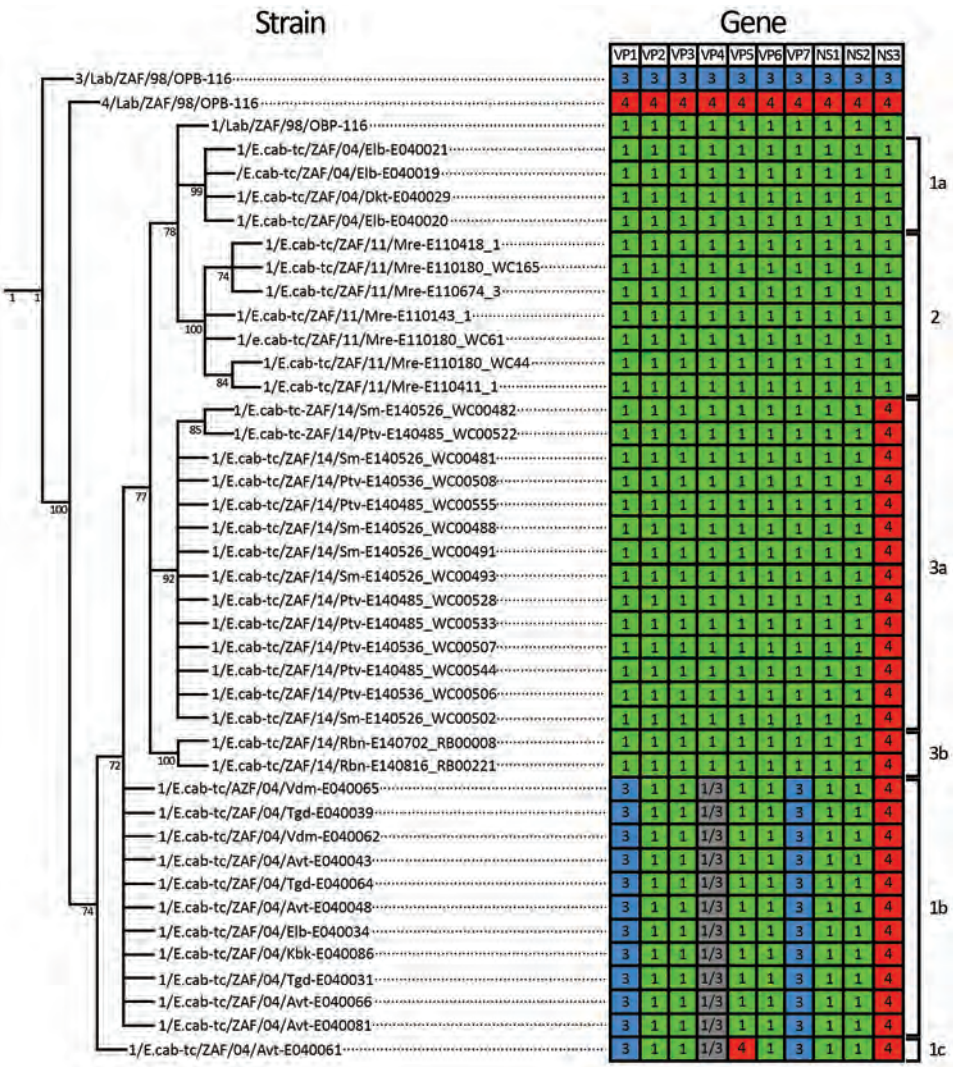

Figure 3. Cladogram and heat map of vaccine-derived African horse sickness (AHS) virus reassortants identified in AHS outbreaks in Western Cape Province, South Africa, 2004–2014. Cladogram indicates genetic relationships of concatenated AHS virus whole-genome nucleotide sequences from affected horses in the 2004, 2011, and 2014 outbreaks in the AHS controlled area in Western Cape Province. Heat map diagram summarizes the origin of the gene segments for each strain with 1/Lab/ZAF/98/OBP-116 (green blocks), 3/Lab/ZAF/98/OBP-116 (blue blocks), and 4/Lab/ZAF/98/OBP-116 (red blocks) vaccine-derived strains. Gray blocks indicate that the segment could be derived from either 1/Lab/ZAF/98/OBP-116 or 3/Lab/ZAF/98/OBP-116. Branches supported by full maximum-likelihood bootstrap values >70% are indicated. Genotype groups are indicated at right.

VP5-encoding gene apparently derived by reassortment from a virus resembling 4/Lab/ZAF/98/OBP-116, such that the SNVs in the VP5 of this strain were also not considered to be mutationally derived.

The 7 viruses included in genotype group 2 and the 16 viruses included in genotype groups 3a and 3b all exhibit potential reversion-to-virulence mutations at 3 of the 7 nonsynonymous SNV sites that differentiate the AHSV-1-LAV virus from its virulent parent (I434T in VP5 and V81A and Q169R in VP6). Additionally, a fourth SNV (K201N in NS3) at 1 of the 7 sites differentiating the AHSV-1 LAV from its parent (which had a K and an M, respectively, at this site) is also present in the genotype group 2 viruses.

Quantification of the Outbreaks

The epidemiologic parameters of the AHS outbreaks in the controlled area in 2004, 2011, and 2014 were inferred by using the current OIE case definition for AHS (*11*) (Table 2). Although the case-fatality rates (CFRs) were very high for the 2004 Stellenbosch (78.3%) and 2011 Mamre (76.2%) outbreaks, they were considerably lower for the 2014 Porterville (14.6%) and Robertson (4.5%) outbreaks. Additionally, the 2011 Mamre and 2004 Stellenbosch outbreaks were associated with the lowest vaccination rates among AHSV-infected horses (2.7% and 8.7%, respectively). Differences in the genetic constitution of the individual outbreak viruses could have been associated with the vastly different CFRs in each outbreak; however, whether these differences in CFRs are a consequence of lower virulence among the outbreak viruses or the result of existing vaccine-induced immunity in the exposed horses is unknown. Similarly, changes in the AHS case definition that only came into effect in 2008 (after the 2004 Stellenbosch outbreak) probably resulted in an underestimation of subclinical AHSV infections during that outbreak. Whereas during the Stellenbosch 2004 outbreak only clinically affected, deceased horses were classified

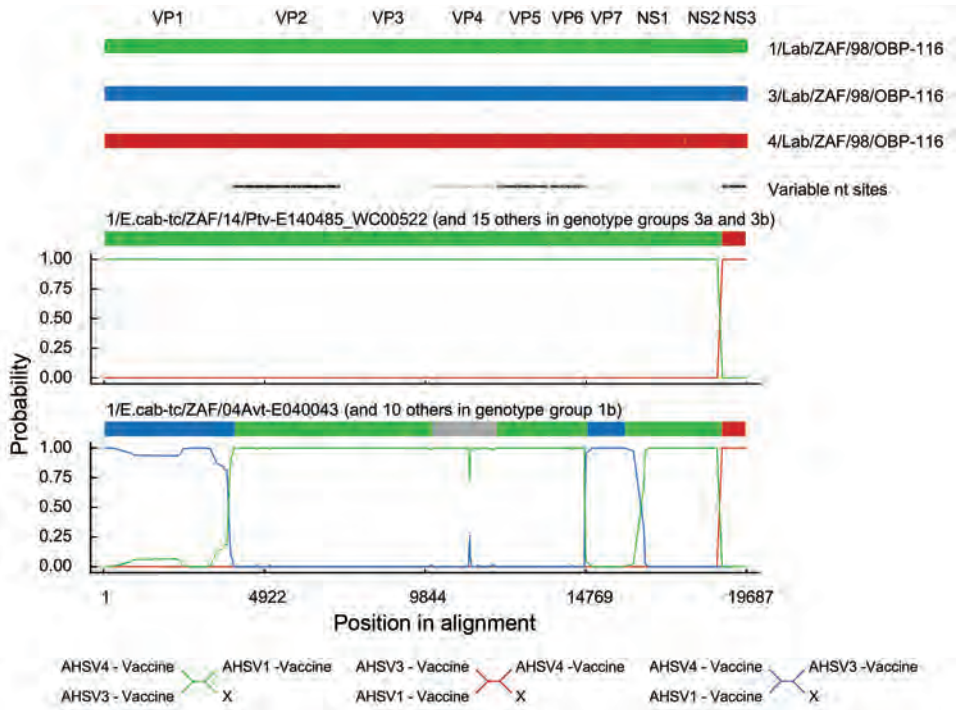

Figure 4. Statistical evidence of reassortment within the genomes of African horse sickness (AHS) virus field isolates identified in outbreaks in the AHS controlled area in Western Cape Province, South Africa, 2004–2014. A hidden Markov model–based approach (BURT-HMM) was used to classify individual nucleotides within each of the 10 segments of individual AHS virus isolates into 3 different categories: 1/Lab/ZAF/98/OBP-116-like (green), 3/Lab/ZAF/98/OBP-116-like (blue), and 4/Lab/ZAF/98/OBP-116-like (red). Probability supports for these classifications yielded by the BURT-HMM with the highest likelihood are plotted along the genome. Positions of segment boundaries are given in the diagram above the plots. The phylogenetic clusterings that are implied by differently colored segments in these plots are indicated below the plots. The segment indicated in gray could not be convincingly classified because it closely resembles both 1/Lab/ZAF/98/OBP-116 and 3/Lab/ZAF/98/OBP-116.

as having confirmed cases (*13*), major advances in AHS diagnostic testing (e.g., rRT-PCR–based methods) have occurred during the past 10 years that likely substantially increased the detection of subclinical infections by the time of the 2014 outbreaks (*15*,*32*).

Discussion

Whole-genome sequences were compared from 55 field, LAV, and laboratory strains of AHSV. The field viruses were obtained from horses during outbreaks of AHS of different clinical severity (CFRs ranging from 4.5% to 78.3%) in the AHS controlled area of South Africa during 2004, 2011, and 2014. Phylogenetic analyses confirmed that genetically distinct viruses were responsible for each outbreak and that these were all closely related to viruses contained in the trivalent AHSV-LAV (combination 1) used in South Africa. Evaluation of nonsynonymous SNVs confirmed some outbreak viruses to be revertants of the vaccine AHSV-1 strain toward the virulent parental type. Furthermore, some outbreak viruses were clearly reassortants with individual genome segments derived from multiple different virus types that are present in the trivalent vaccine preparation.

Potgieter et al. (*24*) hypothesized that changes in VP2 and VP5 can confer virulence or attenuation of individual AHSV strains, based upon comparisons of the consensus sequences of the genome of an attenuated AHSV-1 isolate (GenBank accession nos. FJ183364–FJ183373) and its virulent parent. Potgieter et al. (*24*) also proposed that virulence is related to tissue tropism because the outer capsid proteins are involved in cell entry and trigger apoptosis of host cells. Additionally, other studies have implicated NS3 as a determinant of AHSV virulence (*33*). The results of our study further confirm that changes in multiple VPs can affect the virulence of AHSV. Both reversion (to the virulent parental type) and novel SNVs were present in field-isolated viruses at various residue sites in VP2 (K357N in genotype group 1b viruses), VP5 (I434T in all field viruses evaluated except sample 1/E.cab-tc/ZAF/04/Avt- E040061), and VP6 (V81A in all field viruses and Q169R in all field viruses except sample 1/E.cab-tc/ZAF/04/Vdm-E040065) that differentiate the attenuated AHSV-1-LAV strain from its virulent parental strain. Furthermore, SNVs present at a site in NS3 (K201E in genotype group 1a viruses and K201N in genotype group 2) are potentially associated with reversion to virulence because of the effect of NS3 on virus release, membrane permeability, and viral yield (*34*). However, the determinants of AHSV virulence are probably complex and multigenic (*24*,*34*), which is consistent with the remarkable difference in CFRs between horses in the various outbreaks.

Given the genetic diversity of field strains of AHSV (*14*,*24*,*35*), our analyses overwhelmingly support the

premise that the potential reversion-to-virulence mutants and reassortants that we detected arose from viruses within the polyvalent AHSV-LAV formulation, and predominantly from AHSV-1-LAV. Although these mutants and reassortants most likely arose within vaccinated horses, the reason for the predominance of AHSV-1-LAV components in the emergent outbreak viruses is unknown. The data presented here also indicate that distinct founder events led to the expansion in Stellenbosch (2004) of viruses included in genotype groups 1a and 1b and, similarly, that the outbreaks in 2014 in Porterville (genotype group 3a) and Robertson (genotype group 3b) also probably originated independently from the LAV and were not from the spread of the same outbreak virus.

In summary, results of this study highlight the importance of genetic characterization of circulating strains of AHSV in epidemiologic investigations of AHS outbreaks. Although, the prevailing opinion in South Africa was that illegal movement of viremic equids into the AHS controlled area was responsible for the repeated occurrences of AHS in the controlled area, this is clearly not the only cause. Our data confirm that use of polyvalent AHSV-LAV can result in the emergence and spread of virulent viruses to adjacent susceptible horses, presumably by *Culicoides* midge vectors that are already resident within the AHS controlled area (*36*). Collectively, these findings have major implications for strategies to control AHS, both in AHS-endemic regions and during future incursions into currently AHSV-free areas. However, AHSV-LAV confers critical and effective protection for susceptible horses in AHS-endemic areas and, although potentially safer recombinant AHSV vaccines have proven effective in laboratory studies (*37*,*38*), these are not available commercially and they are yet to be evaluated in the field. Until alternative vaccines become commercially available, control of AHS will remain reliant on the use of AHSV-LAV coupled with the adoption of strategies to minimize the likelihood of natural dissemination of revertant and reassortant vaccine-derived viruses.

Acknowledgments

We thank the private-sector veterinarians, state veterinarians, and horse owners who collected samples and provided data used in this study.

Dr. Weyer is a veterinary research officer employed by the Equine Research Centre, Faculty of Veterinary Science, University of Pretoria, South Africa. She is authorized by the Western Cape provincial veterinary services to assist with equine movement control and disease surveillance within the province. Her areas of interest include African horse sickness epidemiology and other equine diseases, particularly those affecting the movement and trade of equines.

References

1. Zientara S, Weyer CT, Lecollinet S. African horse sickness. Rev Sci Tech. 2015;34:315–27. http://dx.doi.org/10.20506/rst.34.2.2359
2. Du Toit RM. Transmission of blue-tongue and horse-sickness by *Culicoides*. Onderstepoort J Vet Sci Anim Ind. 1944;19:7–16.
3. Maclachlan NJ, Guthrie AJ. Re-emergence of bluetongue, African horse sickness, and other orbivirus diseases. Vet Res. 2010;41:35. http://dx.doi.org/10.1051/vetres/2010007
4. Maclachlan NJ, Mayo CE. Potential strategies for control of bluetongue, a globally emerging, *Culicoides*-transmitted viral disease of ruminant livestock and wildlife. Antiviral Res. 2013;99:79–90. http://dx.doi.org/10.1016/j.antiviral.2013.04.021
5. Guichard S, Guis H, Tran A, Garros C, Balenghien T, Kriticos DJ. Worldwide niche and future potential distribution of *Culicoides imicola*, a major vector of bluetongue and African horse sickness viruses. PLoS One. 2014;9:e112491. http://dx.doi.org/10.1371/journal.pone.0112491
6. Maclachlan NJ, Mayo CE, Daniels PW, Savini G, Zientara S, Gibbs EPJ. Bluetongue. Rev Sci Tech. 2015;34:329–40. http://dx.doi.org/10.20506/rst.34.2.2360
7. Guthrie AJ, Weyer CT. African horse sickness. In: Sprayberry KA, Robinson NE, editors. Robinson's current therapy in equine medicine. 7th ed. Philadelphia: Saunders; 2015. p. 150–1.
8. Theiler A. Die Sudafrikanische Pferdesterbe. Deuts Tierarztl Wschr. 1901;9:201–3, 221–6, 233–7, 241.
9. M'Fadyean J. African horse sickness. J Comp Pathol Ther. 1900;13:1–20. http://dx.doi.org/10.1016/S0368-1742(00)80001-6
10. von Teichman BF, Dungu B, Smit TK. In vivo cross-protection to African horse sickness serotypes 5 and 9 after vaccination with serotypes 8 and 6. Vaccine. 2010;28:6505–17. http://dx.doi.org/10.1016/j.vaccine.2010.06.105
11. World Organization for Animal Health. Infection with African horse sickness virus. Terrestrial Animal Health Code, 2015 [cited 2016 Jul 5]. http://www.oie.int/index.php?id=169&L=0&htmfile=chapitre_ahs.htm
12. Republic of South Africa Department of Agriculture, Forestry, and Fisheries. Animal Diseases Act, 1984 [cited 2016 Jul 5]. http://www.daff.gov.za/daffweb3/Branches/Agricultural-Production-Health-Food-Safety/Animal-Health/importexport/legislation/diseaseact
13. Sinclair M, Bührmann G, Gummow B. An epidemiological investigation of the African horsesickness outbreak in the Western Cape Province of South Africa in 2004 and its relevance to the current equine export protocol. J S Afr Vet Assoc. 2006;77:191–6. http://dx.doi.org/10.4102/jsava.v77i4.376
14. Quan M, van Vuuren M, Howell PG, Groenewald D, Guthrie AJ. Molecular epidemiology of the African horse sickness virus S10 gene. J Gen Virol. 2008;89:1159–68. http://dx.doi.org/10.1099/vir.0.83502-0
15. Grewar JD, Weyer CT, Guthrie AJ, Koen P, Davey S, Quan M, et al. The 2011 outbreak of African horse sickness in the African horse sickness controlled area in South Africa. J S Afr Vet Assoc. 2013;84:1–7. http://dx.doi.org/10.4102/jsava.v84i1.973
16. Grewar JD. Suspected African horse sickness outbreak—Melkbosstrand. Western Cape Government Epidemiology Report, 2013;5(5) [cited 2016 Jul 5]. http://www.elsenburg.com/vetepi/epireport_pdf/May2013.pdf
17. Grewar JD. African horse sickness outbreak resolved. Western Cape Government Epidemiology Report, 2014;6(6) [cited 2016 Jul 5]. http://www.elsenburg.com/vetepi/epireport_pdf/June2014.pdf
18. World Organization for Animal Health. African horse sickness, South Africa [cited 2016 Jul 5]. http://www.oie.int/wahis_2/public/wahid.php/Reviewreport/Review?page_refer=MapFullEventReport&reportid=5493
19. World Organization for Animal Health. African horse sickness, South Africa [cited 2016 Jul 5]. http://www.oie.int/wahis_2/public/

wahid.php/Reviewreport/Review?page_refer=MapEventSummary&reportid=6650
20. Guthrie AJ, Coetzee P, Martin DP, Lourens CW, Venter EH, Weyer CT, et al. Complete genome sequences of the three African horse sickness virus strains from a commercial trivalent live attenuated vaccine. Genome Announc. 2015;3:e00814–5. http://dx.doi.org10.1128/genomeA.00814-15
21. Guthrie AJ, Coetzee P, Martin DP, Lourens CW, Venter EH, Weyer CT, et al. Complete genome sequences of the four African horse sickness virus strains from a commercial tetravalent live attenuated vaccine. Genome Announc. 2015;3:e01375–15. http://dx.doi.org10.1128/genomeA.01375-15
22. Guthrie AJ, Maclachlan NJ, Joone C, Lourens CW, Weyer CT, Quan M, et al. Diagnostic accuracy of a duplex real-time reverse transcription quantitative PCR assay for detection of African horse sickness virus. J Virol Methods. 2013;189:30–5. http://dx.doi.org/10.1016/j.jviromet.2012.12.014
23. Weyer CT, Joone C, Lourens CW, Monyai MS, Koekemoer O, Grewar JD, et al. Development of three triplex real-time reverse transcription PCR assays for the qualitative molecular typing of the nine serotypes of African horse sickness virus. J Virol Methods. 2015;223:69–74. http://dx.doi.org/10.1016/j.jviromet.2015.07.015
24. Potgieter AC, Page NA, Liebenberg J, Wright IM, Landt O, van Dijk AA. Improved strategies for sequence-independent amplification and sequencing of viral double-stranded RNA genomes. J Gen Virol. 2009;90:1423–32. http://dx.doi.org/10.1099/vir.0.009381-0
25. Kearse M, Moir R, Wilson A, Stones-Havas S, Cheung M, Sturrock S, et al. Geneious Basic: an integrated and extendable desktop software platform for the organization and analysis of sequence data. Bioinformatics. 2012;28:1647–9. http://dx.doi.org/10.1093/bioinformatics/bts199
26. Katoh K, Standley DM. MAFFT multiple sequence alignment software version 7: improvements in performance and usability. Mol Biol Evol. 2013;30:772–80. http://dx.doi.org/10.1093/molbev/mst010
27. Guindon S, Dufayard JF, Lefort V, Anisimova M, Hordijk W, Gascuel O. New algorithms and methods to estimate maximum-likelihood phylogenies: assessing the performance of PhyML 3.0. Syst Biol. 2010;59:307–21. http://dx.doi.org/10.1093/sysbio/syq010
28. Pommier T, Canbäck B, Lundberg P, Hagström A, Tunlid A. RAMI: a tool for identification and characterization of phylogenetic clusters in microbial communities. Bioinformatics. 2009;25:736–42. http://dx.doi.org/10.1093/bioinformatics/btp051
29. Martin DP, Murrel B, Golden M, Khoosal A, Muhire B. RDP4: detection and analysis of recombination patterns in virus genomes. Virus Evol. 2015;1:1–5. http://dx.doi.org/10.1093/ve/vev003
30. Sugiyama K, Bishop DHL, Roy P. Analysis of the genomes of bluetongue viruses recovered from different states of the United States and at different times. Am J Epidemiol. 1982;115:332–47.
31. Nomikou K, Hughes J, Wash R, Kellam P, Breard E, Zientara S, et al. Widespread reassortment shapes the evolution and epidemiology of bluetongue virus following European invasion. PLoS Pathog. 2015;11:e1005056. http://dx.doi.org/10.1371/journal.ppat.1005056
32. Weyer CT, Quan M, Joone C, Lourens CW, MacLachlan NJ, Guthrie AJ. African horse sickness in naturally infected, immunised horses. Equine Vet J. 2013;45:117–9. http://dx.doi.org/10.1111/j.2042-3306.2012.00590.x
33. Martin LA, Meyer AJ, O'Hara RS, Fu H, Mellor PS, Knowles NJ, et al. Phylogenetic analysis of African horse sickness virus segment 10: sequence variation, virulence characteristics and cell exit. Arch Virol Suppl. 1998;14:281–93.
34. Huismans H, van Staden V, Fick WC, van Niekerk M, Meiring TL. A comparison of different orbivirus proteins that could affect virulence and pathogenesis. Vet Ital. 2004;40:417–25.
35. Potgieter AC, Wright IM, van Dijk AA. Consensus sequence of 27 African horse sickness virus genomes from viruses collected over a 76-year period (1933 to 2009). Genome Announc. 2015;3:e00921–15. http://dx.doi.org/10.1128/genomeA.00921-15
36. Nevill EM, Venter GJ, Edwardes M, Pajor ITP, Meiswinkel R, van Gas JH. *Culicoides* species associated with livestock in the Stellenbosch area of the Western Cape Province, Republic of South Africa (Diptera: Ceratopogonidae). Onderstepoort J Vet Res. 1988;55:101–6.
37. Guthrie AJ, Quan M, Lourens CW, Audonnet JC, Minke JM, Yao J, et al. Protective immunization of horses with a recombinant canarypox virus vectored vaccine co-expressing genes encoding the outer capsid proteins of African horse sickness virus. Vaccine. 2009;27:4434–8. http://dx.doi.org/10.1016/j.vaccine.2009.05.044
38. Alberca B, Bachanek-Bankowska K, Cabana M, Calvo-Pinilla E, Viaplana E, Frost L, et al. Vaccination of horses with a recombinant modified vaccinia Ankara virus (MVA) expressing African horse sickness (AHS) virus major capsid protein VP2 provides complete clinical protection against challenge. Vaccine. 2014;32:3670–4. http://dx.doi.org/10.1016/j.vaccine.2014.04.036

Address for correspondence: Alan J. Guthrie, University of Pretoria, Equine Research Centre, Faculty of Veterinary Science, Pretoria 0002, South Africa; email: alan.guthrie@up.ac.za

Streptococcus agalactiae Serotype IV in Humans and Cattle, Northern Europe[1]

Ulrike Lyhs,[2] Laura Kulkas, Jørgen Katholm,[3] Karin Persson Waller, Kerttu Saha, Richard J. Tomusk, Ruth N. Zadoks

Streptococcus agalactiae is an emerging pathogen of nonpregnant human adults worldwide and a reemerging pathogen of dairy cattle in parts of Europe. To learn more about interspecies transmission of this bacterium, we compared contemporaneously collected isolates from humans and cattle in Finland and Sweden. Multilocus sequence typing identified 5 sequence types (STs) (ST1, 8, 12, 23, and 196) shared across the 2 host species, suggesting possible interspecies transmission. More than 54% of the isolates belonged to those STs. Molecular serotyping and pilus island typing of those isolates did not differentiate between populations isolated from different host species. Isolates from humans and cattle differed in lactose fermentation, which is encoded on the accessory genome and represents an adaptation to the bovine mammary gland. Serotype IV-ST196 isolates were obtained from multiple dairy herds in both countries. Cattle may constitute a previously unknown reservoir of this strain.

Streptococcus agalactiae (group B *Streptococcus*) is a major cause of neonatal infectious disease in humans in many countries and is carried asymptomatically by a large proportion of adults. It is also recognized as an emerging pathogen in human adults worldwide and as a reemerging mammary pathogen of cattle in northern Europe (*1*–*3*). In adults, *S. agalactiae* is primarily associated with bacteremia, skin and soft tissue infections (SSTI), and urinary tract infections (UTI) and occasionally with necrotizing fasciitis, arthritis, toxic shock syndrome, endocarditis, or meningitis (*4*–*6*). Host and pathogen factors contribute to the emergence of *S. agalactiae* among adults (*3*). Among hosts, at greater risk are elderly patients and persons with chronic underlying conditions such as alcohol abuse, diabetes mellitus, or immunosuppression (*2*,*4*,*6*). Within the pathogen, new strains such as serotype IV may contribute to disease emergence (*7*,*8*). Considering the risk factors for *S. agalactiae* in nonpregnant adults and demographic changes in many countries, the incidence of group B streptococcal disease can be anticipated to increase (*4*).

In the 1950s, *S. agalactiae* was the most common mastitis-causing bacterium among dairy cattle in Europe, severely reducing milk quality and quantity. In the 1960s, development of disease control programs and introduction of legislation resulted in near eradication of *S. agalactiae* from several northern European countries, a situation that continued until the end of the 20th century (*9*). In the 21st century, farm management in northern Europe changed (e.g., fewer herds, increased average herd size, and introduction of automated milking systems). Concomitantly, the prevalence of *S. agalactiae* in bovine milk increased. In Denmark, in the first years of the 21st century, the proportion of *S. agalactiae*–positive herds tripled (*1*,*9*). Similar phenomena have been described for Sweden and Norway (*1*).

The presence of *S. agalactiae* in humans and cattle raises the question of whether interspecies transmission occurs. This question is particularly pertinent in light of the emergence of *S. agalactiae* disease in adult humans and its reemergence in cattle. Several comparisons of *S. agalactiae* in humans and cattle have been published, and most authors conclude that isolates from these species form largely distinct populations with regard to the core genome and the accessory genome (*10*–*12*). Ideally, assessment of the potential for interspecies transmission is based on the analysis of contemporaneous, sympatric isolates. With 1 exception (*13*), however, most comparative studies were not based on isolates from the same geographic region and the same period, or, if they were, they covered a very limited number

Author affiliations: University of Helsinki, Seinäjoki, Finland (U. Lyhs); Valio Ltd., Helsinki, Finland (L. Kulkas); SEGES (formerly Knowledge Centre for Agriculture), Aarhus, Denmark (J. Katholm); National Veterinary Institute, Uppsala, Sweden (K. Persson Waller); Central Hospital, Seinäjoki (K. Saha); University of Glasgow, Glasgow, Scotland, UK (R.J. Tomusk, R.N. Zadoks); Moredun Research Institute, Penicuik, Scotland, UK (R.N. Zadoks)

DOI: http://dx.doi.org/10.3201/eid2212.151447

[1]Preliminary results from this study were presented at the 25th European Congress of Clinical Microbiology and Infectious Diseases; April 24–28, 2015; Copenhagen, Denmark.

[2]Current affiliation: Danish Technical University, Copenhagen, Denmark.

[3]Current affiliation: DNA Diagnostic A/S, Risskov, Denmark.

of *S. agalactiae*–positive farms or animals (*14,15*). Our aim with this study was to provide insight into the hazard of interspecies transmission of *S. agalactiae* by comparing contemporaneous populations of *S. agalactiae* from humans and dairy cattle in Finland and Sweden.

Materials and Methods

Isolates

A total of 81 isolates were collected at the Seinäjoki Central Hospital in the rural South Ostrobothnia district of Finland (2011, 2012) and from epidemiologically unrelated persons by the Department of Clinical Microbiology, University Hospital, Uppsala, in an urban area of Sweden (2012, 2013). Isolates originated from 12 patients with invasive disease (sepsis or meningitis), 37 with UTI, and 15 with SSTI and from 17 healthy carriers who were screened during pregnancy by use of vaginal swab or cervical fluid samples. Isolates represented a convenience sample that covered both sexes and all age classes (online Technical Appendix Figure 1, http://wwwnc.cdc.gov/EID/article/22/12/15-1447-Techapp1.pdf). Data were not collected with regard to farm or animal contact or dietary exposure.

During 2010–2012, a total of 108 isolates from cattle were collected by the laboratory of Valio Ltd, Helsinki, Finland (63 isolates from 29 herds) and by the National Veterinary Institute, Uppsala, Sweden (45 isolates from 45 herds). Isolates were cultured from individual cow or quarter milk samples from animals with suspected intramammary infection with or without clinical signs. In both countries, samples originated from most of the major dairy regions (online Technical Appendix Figure 2). For 9 herds in Finland, isolates from multiple cows were available and 2–14 isolates/herd were used to assess within-herd strain heterogeneity (online Technical Appendix Table 1). For the remaining herds, 1 isolate was used.

Phenotypic identification was based on colony morphology on blood agar, CAMP (Christie, Atkins, Munch-Peterson) reaction, and Lancefield grouping (*15*). Before use, isolates were stored at –80°C in brain–heart infusion broth (Oxoid, Basingstoke, UK) with 15% glycerol. After culture on blood agar, purity was checked and 1 colony was used to confirm species identity by PCR with primers STRA-AgI (5′-AAGGAAACCTGCCATTTG-3′) and 5′-STRA-AgII (TTAACCTAGTTTCTTTAAAACTAGAA-3′). DNA extracts for molecular typing were prepared from overnight cultures in brain–heart infusion broth by using a DNeasy Blood & Tissue Kit (QIAGEN, Manchester, UK). Species confirmation, multilocus sequence typing (MLST), and serotyping were conducted for all isolates. Pilus island (PI) typing and lactose typing were conducted for all isolates from humans and 1 isolate from a bovid per sequence type (ST) per herd.

MLST

MLST was performed by using standard primers and HiMLST or Sanger sequencing of purified PCR amplicons (*16,17)*. Alleles and STs were assigned by using the *S. agalactiae* database (http://pubmlst.org/sagalactiae/) (*18*). New alleles were submitted to the database curator for quality control and allocation of allele numbers and STs. Novel allele combinations were also submitted for ST assignment.

Molecular Serotyping

For detection of molecular serotype (MS) II and MS IV, duplex PCR was used, and for detection of MS V, VI, VII, and VIII, multiplex PCR was used (*19*). PCR reactions for MS Ia, Ib, and III were run individually by using primers for MS Ia and Ib (*19*) and primers IIIcpsHS and IIIcpsHA for MS III (*20*). For all reactions, cycling conditions were 94°C (5 min), followed by 40 cycles of 94°C (60 s), 55°C (60 s), and 72°C (60 s) with final extension at 72°C (5 min). Each isolate was submitted to all molecular serotyping reactions to identify potential cross-reactivity.

PI Typing

Multiplex PCR was used to screen for presence of *sag647* (PI-1), s*ag1406* (PI-2a), and *san1517* (PI-2b); the housekeeping gene *adhP* was used as amplification control (*11*). Isolates that were negative for PI-1 were tested for presence of an intact integration site. Detection of a 684-bp amplicon indicates presence of an intact site, and absence of the amplicon indicates occupation by an alternative, uncharacterized genetic element. Isolates that were positive for PI-2a or PI-2b were further characterized by PI-specific PCR-based restriction fragment length polymorphism analysis to detect allelic variation in the PI-2a adhesin gene (*gbs59*) and the PI-2b backbone protein (*san1519)* (*11*).

Lactose Typing

To detect lactose fermentation, we inoculated a single colony into phenol red broth (neutralized soya peptone with beef extract; Oxoid), supplemented with phenol red and α lactose (L2643; Sigma-Aldrich, Gillingham, UK). Broth was incubated at 37°C without shaking and was checked for change from red to yellow at 24 h, 48 h, and 7 days after inoculation. PCR was used to screen for presence of an ≈2.5-kbp region of *lacEFG*, which is part of the Lac.2 operon that encodes lactose fermentation (*21*).

Data Analysis

Comparisons of categorical variables were conducted in Statistix 10 (Analytical Software, Tallahassee, FL, USA) with use of the Fisher exact or Pearson χ^2 test, as appropriate. Global eBURST analysis was performed by using PHYLOViZ (*22*); double-locus variants were included in eBURST groups.

Results

MLST

All isolates were confirmed as *S. agalactiae* and 33 STs were identified. Isolates from humans belonged to 16 allelic profiles, including 2 new profiles derived from isolates from patients with invasive disease in Sweden. Both profiles were single-locus variants (SLVs) of known STs, with ST751 based on a new combination of known alleles, whereas the second profile was based on a new *atr* allele with an internal deletion (ST not assigned). ST1 was most common, followed by ST19 and ST12 (21, 14, and 10 isolates, respectively). All STs were found in isolates from patients in at least 2 age groups and from 2 clinical sample types (online Technical Appendix Figure 3).

Among 108 isolates from cattle, 22 STs were identified, including 12 new STs (5 from Finland, 7 from Sweden). The proportion of new STs was higher among isolates from cattle than from humans (54.5% vs. 12.5%, respectively; Pearson $\chi^2 = 4.7$, df = 1, p = 0.03). A total of 3 new STs (ST632, ST633, ST726) were detected in multiple herds, whereas the remaining new STs (ST634–636, ST722–725, ST727, ST728) were each obtained from 1 herd. All were SLVs of known STs with 1 new allele. For 9 herds, >1 isolate was available and isolates within a herd belonged to a single ST, with 1 exception in which ST1 and its SLV ST635 were detected (online Technical Appendix Table 1). Both isolates from this herd were included in herd-level analysis and comparison between host species. In herd-level analysis of 74 isolates, ST1 was most common, followed by ST103 and ST196 (20, 10, and 8 herds, respectively; online Technical Appendix Table 2). We found no significant association between ST and country of origin.

Of 33 STs in this study, 5 were detected in both host species (Figure 1). ST1 was the most common shared ST, followed by ST23, ST196, ST12, and ST8 (41, 12, 12, 11, and 7 isolates, respectively). More than half (84) of the 155 isolates (54.2%) belonged to shared STs. Of 5 shared STs, 4 were represented by >10 isolates compared with 2 of 28 host-specific STs (p<0.001 by Fisher exact test). Using global eBURST, we identified 6 clusters, 2 of which were host specific (i.e., ST17 from humans and a cluster around ST103 from cattle). Both host-specific clusters included isolates from both countries (Figure 1).

Molecular Serotyping

Among isolates from humans, MS Ia, Ib, and II–VI were identified. Among isolates from cattle, 2 did not yield conclusive molecular serotyping results. Among the remaining isolates from cattle, MS Ia, Ib, II–V, and VII were identified. We found strong correlation between MS and ST (Table; online Technical Appendix Figure 4). For STs found in both host species, MS did not differ between isolates from humans or cattle, with the exception of ST23: isolates from humans belonged to MS Ia and those from cattle to MS Ia or III (Table).

PI Typing

We identified 5 PI profiles (Figure 2; online Technical Appendix Figure 5). Among PI-1–negative isolates, the integration site was intact in 14 of 19 isolates from humans

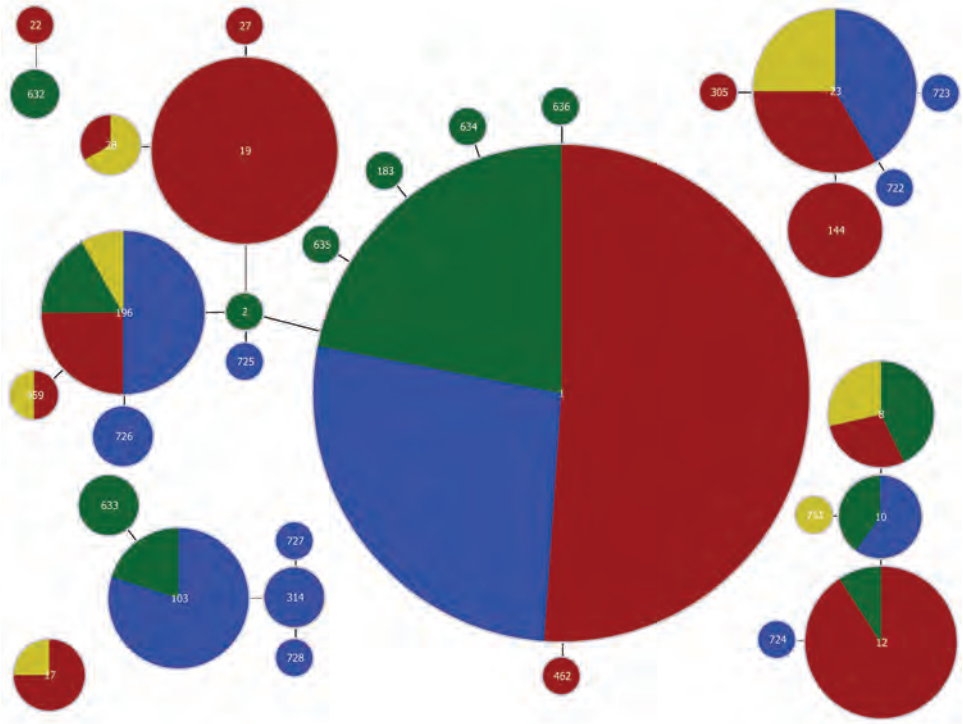

Figure 1. Distribution of host species and countries across clusters of *Streptococcus agalactiae* sequence types (STs), with clusters including single- and double-locus variants. Each circle represents an ST, with size of the circle and its colored segments proportional to the number and origin of isolates, respectively. Red, human in Finland; yellow, human in Sweden; green, bovid in Finland; blue, bovid in Sweden. STs are indicated by numbers in the circles. Single- and double-locus variants are connected by black lines.

Table. *Streptococcus agalactiae* isolates from humans and cattle, Finland and Sweden, 2010–2013*

Molecular serotype	No. isolates from humans/cattle						No. isolates from humans only				No. isolates from cattle only				
	ST1	ST8	ST12	ST23	ST196	Other	ST17	ST19	ST28	ST144	ST10	ST103	ST314	ST633	ST726
Ia	1/0	–	–	7/2	–	1/3	–	–	–	6	–	10	3	3	–
Ib	–	4/3	–	–	–	1/0	–	–	–	–	1	–	–	–	–
II	1/0	–	10/1	–	–	2/1	–	1	3	–	3	–	–	–	–
III	–	–	–	0/2	–	1/4	4	13	–	–	–	–	–	–	–
IV	–	–	–	–	4/8	2/1	–	–	–	–	–	–	–	–	3
V	18/19	–	–	–	–	1/4	–	–	–	–	–	–	–	–	–
Other	1/1	–	–	0/1	–	–	–	–	–	–	1	–	–	–	–

*ST, sequence type; –, no isolates.

and in 8 of 23 isolates from cattle (74% vs. 35%, $\chi^2 = 6.31$, df = 1, p = 0.01). Within host–ST combinations, results for PI-1 and occupation of the integration site were consistent across isolates (online Technical Appendix Table 2). Across both host species, 1 PI-2a allele was identified in ST1, ST8, and ST196, respectively. ST12 included 2 PI-2a alleles among isolates from humans (Figure 2). Within ST23, PI-2a alleles were MS specific. One combination was identified in both host species, and 1 was limited to cattle (Figure 2). PI-2b and PI-1 were present in all ST17 isolates (from humans) and 1 ST724 isolate (from cattle), and PI-2b alone was present in isolates with cattle-specific STs (online Technical Appendix Figure 5). One PI-2b allele was found in ST632, and a second allele was found across the entire bovine-specific eBURST cluster.

Lactose Typing

Of 81 isolates from humans and 73 isolates from cattle, lactose was fermented by 3 (3.7%) and 73 (100%), respectively ($\chi^2 = 142$, df = 1, p<0.001). One isolate from cattle was nonviable and hence not tested. Of 81 isolates from humans, 2 (2.5%) were positive for *lacEFG* compared with 69 (94.5%) of 73 isolates from cattle ($\chi^2 = 131$, df = 1, p<0.0001). Discrepancies between phenotype and genotype were confirmed by repeating culture, DNA extraction, and phenotypic and genotypic testing. Genotypic results that were atypical for the host species were observed only in STs that were found in both host species (i.e., in ST1, ST23, and ST196) (Figure 3).

Discussion

In contrast to results of previous studies (*11*,*12*), our results showed no clear distinction between subpopulations of *S. agalactiae* from humans or cattle according to MLST, molecular serotyping, or PI typing. With few exceptions (*13*,*14*), previous comparative studies were not based on contemporaneous, sympatric isolates across host species. Our study showed that ≈54% of isolates belonged to a population that affects both host species. The convenience sample used may not be fully representative of the distribution of STs across the human population in those countries, and invasive isolates were obtained only from Sweden, but no significant clustering by country or clinical manifestation was observed, suggesting that the observed ST distribution is broadly indicative of the most common types.

The most prevalent shared ST was ST1. Its presence in cattle from several countries has been described, but high prevalence among cattle has been reported in Denmark only (*11*,*12*,*23*). Serotype V and PI type 1/2a were predominant in ST1 from both host species, a finding that agrees with findings from previous studies (*11*,*24*). Surprisingly, ST196 was the second most common shared ST (equally with ST23), and all carried MS IV. Reports of ST196 and serotype IV used to be rare; only 1 of 158 isolates collected in Sweden over a 10-year period (1988–1997) belonged to ST196, but they are now recognized as emerging human pathogens (*7*,*8*,*25*). Furthermore, emergence of new STs with MS IV in humans, such as ST459, has been described (*7*,*8*). We describe the emergence of a new MS IV strain

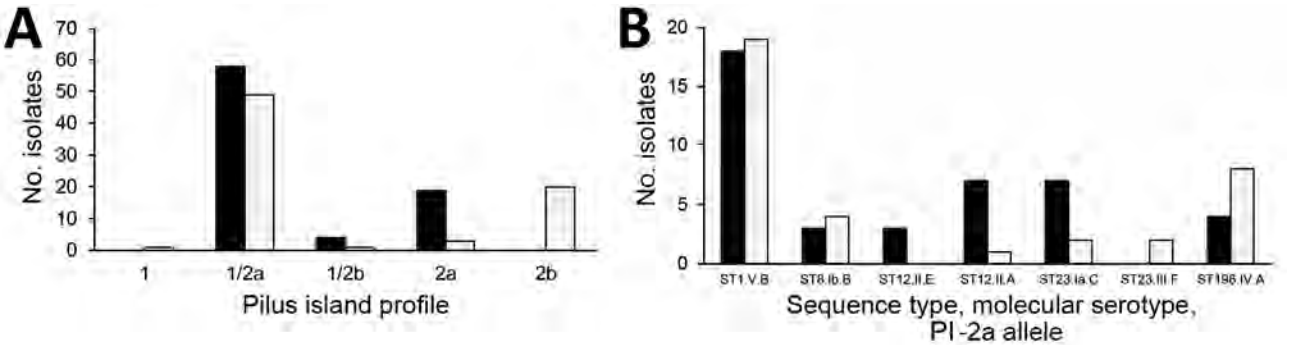

Figure 2. Distribution of pilus island profiles (A) and alleles within pilus island 2a (B) across *Streptococcus agalactiae* isolates from humans (dark bars) and bovids (light bars). Letter and number combinations in B show sequence type (ST), molecular serotype (Roman numeral), and allele for pilus island 2a (capital letter).

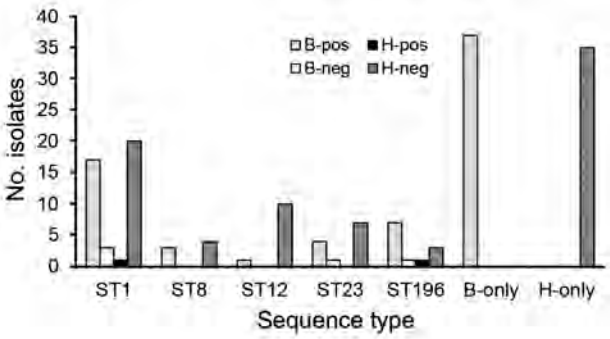

Figure 3. Distribution of *lacEFG* PCR–positive (pos) and –negative (neg) human (H) and bovine (B) *Streptococcus agalactiae* isolates across sequence types (ST). STs found in both host species are shown individually, whereas STs that were found in a single species are grouped by species.

in cattle, ST723, in multiple dairy herds in Sweden. The relatively common occurrence of ST196 and its SLVs in cattle in the Nordic countries (this study; *26*) suggests that cattle may serve as a reservoir for MS IV strains, although our study does not provide evidence for the direction or likelihood of potential transmission between host species.

ST23 affects many host species (*12*,*27*). In humans, it is more commonly associated with carriage than with infection (*16*,*24*), although all ST23 in our study originated from infections. Most ST23 from humans have serotype Ia, and it has been suggested that serotype III originated in cattle, but the association between host and serotype is not absolute (*16*,*23*,*24*). In our collection, ST23 from humans was associated with MS Ia, whereas isolates from cattle were associated with MS Ia or MS III. PI profiles for ST23 matched those described for other countries (*11*). ST8, which was found across countries and species, and ST12, which was limited to Finland but isolated from both host species, have also been associated with carriage and invasive disease in humans, albeit at lower frequency than ST1 or ST23 (*16*,*24*,*25*). ST8 from both hosts had MS 1b and carried PI-1/2a, as previously described for isolates from humans (*11*,*28*). ST12 isolates from our study were associated with MS II, regardless of host species, and mostly carried PI-1/2a. This pattern matches reports of isolates from humans, although ST12 from humans may occasionally have serotype Ib (*11*,*28*).

The shared pathogen population may result from transmission between host species or shared exposure to an external source. Potential routes of transmission from cattle to humans include direct contact, exposure to cattle feces, and consumption of cows' milk. Potential routes of transmission from humans to cattle include direct contact and indirect exposure to excreta from humans. In one prospective study, increased frequency of cattle exposure was associated with human colonization with *S. agalactiae*, although fecal colonization was detected in 1 cow only (*14*). The prevalence of fecal colonization on individual farms can be high (*26*), but gastrointestinal carriage is much more widespread among humans (*16*,*29*), which argues against exposure to cattle feces as a dominant reservoir for human colonization. Case reports and phenotyping of isolates show that raw milk consumption may lead to colonization of the human throat (*30*). This route may be of public health relevance in countries where milk is frequently consumed raw (e.g., Colombia) but not in countries where milk is routinely pasteurized (e.g., Europe and most of North America). In studies conducted in the United States, no significant association has been detected between consumption of milk and colonization of humans (*29*,*31*).

Several lines of evidence suggest that humans may be a source of infection for cattle. Experimental intramammary challenge of cattle with isolates of *S. agalactiae* from humans resulted in mastitis, although the duration of intramammary infection and hence the window of opportunity for transmission was less than that for infection with isolates from cattle (*32*). Similar observations have been made for naturally occurring bovine mastitis, whereby incidental cases in dairy herds were caused by strains that were otherwise predominantly found in humans (*33*). Epidemiologic studies also support the role of *S. agalactiae* sources other than cattle because introduction of the pathogen into dairy herds can often not be attributed to purchase of cattle, implying that alternative sources must exist (*9*). Some on-farm studies suggest that treatment of human oropharyngeal *S. agalactiae* carriers is a crucial step for eliminating *S. agalactiae* from dairy herds (*34*). Considering the frequent colonization of the human throat, gut, and urogenital tract with the shared STs observed in this study and the direct contact between human hands and the bovine mammary gland during milking, with or without use of gloves, a plausible mechanism for human-to-cattle transmission exists. The main difficulty in determining directionality of transmission between host species is establishing the order of events (i.e., which host species was positive first). Furthermore, efforts to detect alternative, potentially shared sources of *S. agalactiae* are limited by the preconceived but mistaken notion that *S. agalactiae* is an obligate intramammary pathogen in dairy cattle. Potentially shared sources include wastewater and surface water, including effluent from sewage treatment plants (*27*,*35*,*36*). Potential routes of within- and between-host species transmission, including horizontal and vertical transmission among humans (*12*,*31*,*37*) and contagious transmission among cattle via milking machines (*12*,*26*), are summarized in online Technical Appendix Figure 6.

Alternatively, the co-occurrence of STs in both host species may not be the result of ongoing interspecies transmission but rather that of incidental spillover, with subsequent adaptation and dissemination within the new host, leading to

parallel circulation of populations that have the same ST but encode host-specific adaptations elsewhere in the genome. This chain of events has been described for *Staphylococcus aureus* (*38*). Among *S. agalactiae* isolates from cattle, >90% are lactose fermenters, whereas the reverse is true among isolates from humans, providing an example of a host adaptation mechanism (*10*,*23*). The genes targeted by our PCR, *lacEFG*, form part of the Lac.2 operon, which is located on an integrative conjugative element and forms part of the *S. agalactiae* mobilome (*10*). Regulation of the *S. agalactiae* mobilome is a relatively new area of study (*39*); little is known about its contribution to host adaptation or interspecies transmission. Atypical combinations (i.e., *lacEFG*-positive isolates from humans and *lacEFG*-negative isolates from cattle) belonged to STs that are shared across host species, potentially indicating recent transmission events.

In our study, 2 STs occurred frequently but in only 1 host species. ST19 was commonly detected in humans but not in cattle. ST19 is generally rare in cattle, although its association with humans is not absolute (*11*,*12*). Conversely, ST103 was commonly found in cattle in our study and in Denmark, Norway, and China (*12*,*26*,*40*) but not in isolates from humans in our study or those mentioned in any of the references cited. ST103 and its SLVs were invariably associated with serotype Ia (*40*) and PI-2b (online Technical Appendix Figure 5). We detected 4 new STs in the eBURST cluster around ST103, indicating ongoing evolution of this cattle-specific subpopulation. Those STs, and all other new STs detected in this study, were SLVs of known STs. The fact that all new STs were limited to 1 country and that they were SLVs of existing STs indicates that we still observe local microevolution but that we are starting to exhaust the variability in the *S. agalactiae* population.

In summary, according to MLST, molecular serotyping, and PI typing of contemporaneous *S. agalactiae* isolates from humans and cattle in Finland and Sweden, we identified 3 subpopulations: 1 from humans, 1 from cattle, and 1 from both hosts. The latter subpopulation accounted for more than half of the isolates, implying that the host species barrier separating *S. agalactiae* from both species may be more porous than previously thought. For STs commonly carried by humans (e.g., ST1 and ST23), the direction of transmission, if any, may be from humans to cattle. ST196/MS IV was relatively common among cattle, which may potentially constitute a reservoir of this recently recognized emerging pathogen of humans. The only characteristic that differentiated most isolates from the 2 species in this study was the ability to ferment lactose, which is encoded in the mobilome. Considering the new evidence for potential interspecies transmission of *S. agalactiae*, its emergence in adult humans and its reemergence in cattle, further studies into the mechanisms and frequency of transmission and host adaptation seem warranted.

Acknowledgments

We thank Charlotta Fasth and Åsa Melhus for providing the bacterial isolates from Sweden, Vince Richards for help with lactose typing, Shannon Manning for help with PI typing, and Ann-Kristin Nyman for production of the map.

This study was financially supported by the Ministry of Agriculture and Forestry, Finland, through project no. 2500/31/2009, "*S. agalactiae*—an increasing risk for dairy herds in loose housing systems."

Ms. Lyhs is head of the Section for Bacteriology and Pathology at the National Veterinary Institute of the Technical University of Denmark. Her research interests include microbiology, food hygiene and safety, the health of production animals, and zoonotic bacterial diseases.

References

1. Katholm J, Bennedsgaard TW, Koskinen MT, Rattenborg E. Quality of bulk tank milk samples from Danish dairy herds based on real-time polymerase chain reaction identification of mastitis pathogens. J Dairy Sci. 2012;95:5702–8. http://dx.doi.org/10.3168/jds.2011-5307
2. Lambertsen L, Ekelund K, Skovsted IC, Liboriussen A, Slotved HC. Characterisation of invasive group B *Streptococci* from adults in Denmark 1999 to 2004. Eur J Clin Microbiol Infect Dis. 2010;29:1071–7. http://dx.doi.org/10.1007/s10096-010-0941-z
3. Skoff TH, Farley MM, Petit S, Craig AS, Schaffner W, Gershman K, et al. Increasing burden of invasive group B streptococcal disease in nonpregnant adults, 1990–2007. Clin Infect Dis. 2009;49:85–92. http://dx.doi.org/10.1086/599369
4. Sendi P, Johansson L, Norrby-Teglund A. Invasive group B streptococcal disease in non-pregnant adults: a review with emphasis on skin and soft-tissue infections. Infection. 2008; 36:100–11. http://dx.doi.org/10.1007/s15010-007-7251-0
5. Sendi P, Christensson B, Uçkay I, Trampuz A, Achermann Y, Boggian K, et al.; GBS PJI Study Group. Group B *Streptococcus* in prosthetic hip and knee joint–associated infections. J Hosp Infect. 2011;79:64–9. http://dx.doi.org/10.1016/j.jhin.2011.04.022
6. Sunkara B, Bheemreddy S, Lorber B, Lephart PR, Hayakawa K, Sobel JD, et al. Group B *Streptococcus* infections in non-pregnant adults: the role of immunosuppression. Int J Infect Dis. 2012; 16:e182–6. http://dx.doi.org/10.1016/j.ijid.2011.11.008
7. Diedrick MJ, Flores AE, Hillier SL, Creti R, Ferrieri P. Clonal analysis of colonizing group B *Streptococcus*, serotype IV, an emerging pathogen in the United States. J Clin Microbiol. 2010;48:3100–4. http://dx.doi.org/10.1128/JCM.00277-10
8. Teatero S, McGeer A, Li A, Gomes J, Seah C, Demczuk W, et al. Population structure and antimicrobial resistance of invasive serotype IV group B *Streptococcus*, Toronto, Ontario, Canada. Emerg Infect Dis. 2015;21:585–91. http://dx.doi.org/10.3201/eid2014.140759
9. Mweu MM, Nielsen SS, Halasa T, Toft N. Annual incidence, prevalence and transmission characteristics of *Streptococcus agalactiae* in Danish dairy herds. Prev Vet Med. 2012;106:244–50. http://dx.doi.org/10.1016/j.prevetmed.2012.04.002
10. Richards VP, Lang P, Bitar PD, Lefébure T, Schukken YH, Zadoks RN, et al. Comparative genomics and the role of lateral gene transfer in the evolution of bovine adapted *Streptococcus agalactiae*. Infect Genet Evol. 2011;11:1263–75. http://dx.doi.org/10.1016/j.meegid.2011.04.019
11. Springman AC, Lacher DW, Waymire EA, Wengert SL, Singh P, Zadoks RN, et al. Pilus distribution among lineages of group B

Streptococcus: an evolutionary and clinical perspective. BMC Microbiol. 2014;14:159. http://dx.doi.org/10.1186/1471-2180-14-159
12. Zadoks RN, Middleton JR, McDougall S, Katholm J, Schukken YH. Molecular epidemiology of mastitis pathogens of dairy cattle and comparative relevance to humans. J Mammary Gland Biol Neoplasia. 2011;16:357–72. http://dx.doi.org/10.1007/s10911-011-9236-y
13. Sukhnanand S, Dogan B, Ayodele MO, Zadoks RN, Craver MP, Dumas NB, et al. Molecular subtyping and characterization of bovine and human *Streptococcus agalactiae* isolates. J Clin Microbiol. 2005;43:1177–86. http://dx.doi.org/10.1128/JCM.43.3.1177-1186.2005
14. Manning SD, Springman AC, Million AD, Milton NR, McNamara SE, Somsel PA, et al. Association of group B *Streptococcus* colonization and bovine exposure: a prospective cross-sectional cohort study. PLoS One. 2010;5:e8795. http://dx.doi.org/10.1371/journal.pone.0008795
15. Oliveira IC, de Mattos MC, Pinto TA, Ferreira-Carvalho BT, Benchetrit LC, Whiting AA, et al. Genetic relatedness between group B streptococci originating from bovine mastitis and a human group B *Streptococcus* type V cluster displaying an identical pulsed-field gel electrophoresis pattern. Clin Microbiol Infect. 2006;12:887–93. http://dx.doi.org/10.1111/j.1469-0691.2006.01508.x
16. Jones N, Bohnsack JF, Takahashi S, Oliver KA, Chan MS, Kunst F, et al. Multilocus sequence typing system for group B *Streptococcus*. J Clin Microbiol. 2003;41:2530–6. http://dx.doi.org/10.1128/JCM.41.6.2530-2536.2003
17. Boers SA, van der Reijden WA, Jansen R. High-throughput multilocus sequence typing: bringing molecular typing to the next level. PLoS One. 2012;7:e39630. http://dx.doi.org/10.1371/journal.pone.0039630
18. Jolley KA, Chan MS, Maiden MC. mlstdbNet—distributed multi-locus sequence typing (MLST) databases. BMC Bioinformatics. 2004;5:86. http://dx.doi.org/10.1186/1471-2105-5-86
19. Poyart C, Tazi A, Réglier-Poupet H, Billoët A, Tavares N, Raymond J, et al. Multiplex PCR assay for rapid and accurate capsular typing of group B streptococci. J Clin Microbiol. 2007;45:1985–8. http://dx.doi.org/10.1128/JCM.00159-07
20. Kong F, Ma L, Gilbert GL. Simultaneous detection and serotype identification of *Streptococcus agalactiae* using multiplex PCR and reverse line blot hybridization. J Med Microbiol. 2005;54:1133–8. http://dx.doi.org/10.1099/jmm.0.46244-0
21. Richards VP, Choi SC, Pavinski Bitar PD, Gurjar AA, Stanhope MJ. Transcriptomic and genomic evidence for *Streptococcus agalactiae* adaptation to the bovine environment. BMC Genomics. 2013;14:920. http://dx.doi.org/10.1186/1471-2164-14-920
22. Francisco AP, Vaz C, Monteiro PT, Melo-Cristino J, Ramirez M, Carriço JA. PHYLOViZ: phylogenetic inference and data visualization for sequence based typing methods. BMC Bioinformatics. 2012;13:87. http://dx.doi.org/10.1186/1471-2105-13-87
23. Sørensen UB, Poulsen K, Ghezzo C, Margarit I, Kilian M. Emergence and global dissemination of host-specific *Streptococcus agalactiae* clones. MBio. 2010;1:e00178–10. http://dx.doi.org/10.1128/mBio.00178-10
24. Manning SD, Springman AC, Lehotzky E, Lewis MA, Whittam TS, Davies HD. Multilocus sequence types associated with neonatal group B streptococcal sepsis and meningitis in Canada. J Clin Microbiol. 2009;47:1143–8. http://dx.doi.org/10.1128/JCM.01424-08
25. Luan SL, Granlund M, Sellin M, Lagergård T, Spratt BG, Norgren M. Multilocus sequence typing of Swedish invasive group B *Streptococcus* isolates indicates a neonatally associated genetic lineage and capsule switching. J Clin Microbiol. 2005;43:3727–33. http://dx.doi.org/10.1128/JCM.43.8.3727-3733.2005
26. Jørgensen HJ, Nordstoga AB, Sviland S, Zadoks RN, Sølverød L, Kvitle B, et al. *Streptococcus agalactiae* in the environment of bovine dairy herds—rewriting the textbooks? Vet Microbiol. 2016;184:64–72. http://dx.doi.org/10.1016/j.vetmic.2015.12.014
27. Delannoy CM, Crumlish M, Fontaine MC, Pollock J, Foster G, Dagleish MP, et al. Human *Streptococcus agalactiae* strains in aquatic mammals and fish. BMC Microbiol. 2013;13:41. http://dx.doi.org/10.1186/1471-2180-13-41
28. Manning SD, Lewis MA, Springman AC, Lehotzky E, Whittam TS, Davies HD. Genotypic diversity and serotype distribution of group B *Streptococcus* isolated from women before and after delivery. Clin Infect Dis. 2008;46:1829–37. http://dx.doi.org/10.1086/588296
29. Bliss SJ, Manning SD, Tallman P, Baker CJ, Pearlman MD, Marrs CF, et al. Group B *Streptococcus* colonization in male and nonpregnant female university students: a cross-sectional prevalence study. Clin Infect Dis. 2002;34:184–90. http://dx.doi.org/10.1086/338258
30. Brglez I. A contribution to the research of infection of cows and humans with *Streptococcus agalactiae*. Zentralbl Bakteriol Mikrobiol Hyg B. 1981;172:434–9.
31. Foxman B, Gillespie BW, Manning SD, Marrs CF. Risk factors for group B streptococcal colonization: potential for different transmission systems by capsular type. Ann Epidemiol. 2007;17:854–62. http://dx.doi.org/10.1016/j.annepidem.2007.05.014
32. Jensen NE. Experimental bovine group-B streptococcal mastitis induced by strains of human and bovine origin. Nord Vet Med. 1982;34:441–50.
33. Dogan B, Schukken YH, Santisteban C, Boor KJ. Distribution of serotypes and antimicrobial resistance genes among *Streptococcus agalactiae* isolates from bovine and human hosts. J Clin Microbiol. 2005;43:5899–906. http://dx.doi.org/10.1128/JCM.43.12.5899-5906.2005
34. Nielsen AL. Group B streptococci in humans as a cause of bovine mastitis [in Danish]. Danish Vet J. 1987;70:154–7.
35. Jensen AN, Berg B. Wastewater and aquatic biotopes are potential reservoirs of group B streptococci. [in Danish]. Danish Veterinary Journal. 1982;65:197–200.
36. Jafar QA, Sameer AZ, Salwa AM, Samee AA, Ahmed AM, Al-Sharifi F. Molecular investigation of *Streptococcus agalactiae* isolates from environmental samples and fish specimens during a massive fish kill in Kuwait Bay. Pak J Biol Sci. 2008;11:2500–4. http://dx.doi.org/10.3923/pjbs.2008.2500.2504
37. Phares CR, Lynfield R, Farley MM, Mohle-Boetani J, Harrison LH, Petit S, et al.; Active Bacterial Core surveillance/Emerging Infections Program Network. Epidemiology of invasive group B streptococcal disease in the United States, 1999–2005. JAMA. 2008;299:2056–65. http://dx.doi.org/10.1001/jama.299.17.2056
38. Spoor LE, McAdam PR, Weinert LA, Rambaut A, Hasman H, Aarestrup FM, et al. Livestock origin for a human pandemic clone of community-associated methicillin-resistant *Staphylococcus aureus*. MBio. 2013;4:e00356-13. http://dx.doi.org/10.1128/mBio.00356-13
39. Lopez-Sanchez MJ, Sauvage E, Da Cunha V, Clermont D, Ratsima Hariniaina E, Gonzalez-Zorn B, et al. The highly dynamic CRISPR1 system of *Streptococcus agalactiae* controls the diversity of its mobilome. Mol Microbiol. 2012;85:1057–71. http://dx.doi.org/10.1111/j.1365-2958.2012.08172.x
40. Yang Y, Liu Y, Ding Y, Yi L, Ma Z, Fan H, et al. Molecular characterization of *Streptococcus agalactiae* isolated from bovine mastitis in eastern China. PLoS One. 2013;8:e67755. http://dx.doi.org/10.1371/journal.pone.0067755

Address for correspondence: Ruth N. Zadoks, Institute for Biodiversity, Animal Health and Comparative Medicine, College of Medical, Veterinary and Life Sciences, Jarrett Building, University of Glasgow, Glasgow G61 1QH, Scotland, UK; email: ruth.zadoks@glasgow.ac.uk

Effect of Live Poultry Market Interventions on Influenza A(H7N9) Virus, Guangdong, China

Jie Wu,[1] Jing Lu,[1] Nuno R. Faria,[1] Xianqiao Zeng, Yingchao Song, Lirong Zou, Lina Yi, Lijun Liang, Hanzhong Ni, Min Kang, Xin Zhang, Guofeng Huang, Haojie Zhong, Thomas A. Bowden, Jayna Raghwani, Jianfeng He, Xiang He, Jinyan Lin, Marion Koopmans, Oliver G. Pybus, Changwen Ke

Since March 2013, three waves of human infection with avian influenza A(H7N9) virus have been detected in China. To investigate virus transmission within and across epidemic waves, we used surveillance data and whole-genome analysis of viruses sampled in Guangdong during 2013–2015. We observed a geographic shift of human A(H7N9) infections from the second to the third waves. Live poultry market interventions were undertaken in epicenter cities; however, spatial phylogenetic analysis indicated that the third-wave outbreaks in central Guangdong most likely resulted from local virus persistence rather than introduction from elsewhere. Although the number of clinical cases in humans declined by 35% from the second to the third waves, the genetic diversity of third-wave viruses in Guangdong increased. Our results highlight the epidemic risk to a region reporting comparatively few A(H7N9) cases. Moreover, our results suggest that live-poultry market interventions cannot completely halt A(H7N9) virus persistence and dissemination.

Since its first notification on March 30, 2013 (*1*), avian influenza A(H7N9) virus caused 3 complete epidemic waves of human infection in China, comprising 670 laboratory-confirmed clinical cases and 274 deaths as of December 28, 2015 (http://www.wpro.who.int/outbreaks_emergencies/H7N9/en/). Despite the accumulating number of human cases, how this virus disseminated and transmitted across the 3 epidemic waves is not yet understood.

Direct or indirect prior exposure to live poultry or poultry-related environments is the major risk for A(H7N9) infection in humans (*2*,*3*). In response to the A(H7N9) outbreak, major efforts were undertaken to temporarily close and sanitize live poultry markets (LPMs) in epicenter cities during epidemics (*4*–*6*). These interventions are thought to temporarily decrease A(H7N9) contamination of LPM environmental samples (*4*,*6*) and to reduce the incidence of clinical infection (*3*,*6*). However, whether these viruses persist locally across epidemic waves despite current interventions has yet to be answered.

Guangdong Province in southern China accounts for ≈10% of China's domestic poultry industry and is thought to be an important epicenter of influenza A virus circulation (*7*). The province reported no clinical cases during the first wave of A(H7N9) infection but represented the epicenter of the second and third epidemic waves. We integrated epidemiologic, spatial, and genetic data to trace the temporal and spatial origins of influenza A(H7N9) in humans during 2013–2015 in Guangdong.

Materials and Methods

Ethics Statement

The institutional ethics committee of the Center for Disease Control and Prevention of Guangdong Province (Guangdong CDC) approved this study. Written consent was signed by patients or their guardian(s) when samples were collected. Patients were informed about the study before providing their written consent, and the data were anonymized for analysis.

Influenza A(H7N9)Surveillance and Sequencing

Since the first A(H7N9) case in late March 2013, an enhanced provincial surveillance program in all 21 prefecture-level cities in Guangdong has been conducted by a total of 871 clinics and 21 local centers for disease control. All specimens from persons with suspected A(H7N9) infections were tested for subtypes H5, H7, and H9 as previously described (*8*,*9*).

In April 2013, Guangdong CDC launched an environmental surveillance program to monitor avian influenza

Author affiliations: Guangdong Provincial Center for Disease Control and Prevention, Guangzhou, China (J. Wu, J. Lu, X. Zeng, Y. Song, L. Zou, L. Yi, L. Liang, H. Ni, M. Kang, X. Zhang, G. Huang, H. Zhong, J. He, X. He, J. Lin, C. Ke); University of Oxford, Oxford, UK (J. Lu, N.R. Faria, T.A. Bowden, J. Raghwani, O.G. Pybus); Erasmus Medical Center, Rotterdam, the Netherlands (M. Koopmans)

DOI: http://dx.doi.org/10.3201/eid2212.160450

[1]These authors contributed equally to this article.

viruses in LPMs (*9*). Environmental samples were collected from LPMs in Guangdong Province during April 15, 2013–May 30, 2015 (*8–10*). Ten to 20 environmental samples per market were collected from selected markets in 21 prefecture-level cities. When A(H7N9) infection was confirmed in a person in a given location and that person had exposure to a specific LPM, at least 20 environmental samples were collected from that market within 24 hours after confirmation of human infection.

Upon reverse transcription PCR testing, H7N9- and H9N2-positive swab materials and sputum samples from patients and LPM environments were blindly passaged for 2–3 generations in 9- to 10-day-old embryonated chicken eggs for virus isolation. All 8 segments of the selected isolates were sequenced by using a next-generation sequencing strategy for influenza A virus with the Ion PGM System and PathAmpFluA Reagents (Life Technologies, Carlsbad, CA, USA). Specific primer sets were used to amplify and fill potential gaps (*8,9*).

Sequence Alignment and Maximum-Likelihood Phylogenetic Analysis

A total of 1,124 nt sequences were generated by this study. These sequences were combined with all publicly available complete gene sequences of influenza A viruses with known sampling dates and locations that belong to subtypes H7N9, H9N2, and other closely related subtypes. Multiple sequence alignment was performed by using ClustalW (*11*), and alignments were minimally edited by using Aliview (*12*). Maximum-likelihood trees were estimated for all 8 gene segments (hemagglutinin [HA], n = 865; neuraminidase [NA], n = 788; nucleoprotein [NP], n = 1,879; basic polymerase proteins 1 and 2 [PB1 and PB2], n = 1,773 and n = 1,826, respectively; polymerase, n = 1,839; matrix, n = 1,841; and nonstructural [NS], n = 838) in RaxML (*13*) by using the generalized time-reversible nucleotide substitution model with gamma -distribution among site rate heterogeneity (*14*). For each gene dataset, we assessed temporal accumulation of genetic divergence from the root-to-tip from maximum-likelihood midpoint-rooted phylogenies using TempEst (formerly Path-O-Gen) (*15*).

Dated Phylogenetic Analysis

To infer dated phylogenetic trees in a reasonable computational time, we reduced the size of our datasets by removing identical sequences collected in the same sampling locations on the same date. We also removed H9N2 sequences that were phylogenetically unrelated to the H7N9 sequences in our study but kept all H7N9 sequences from clinical cases in Guangdong. Bayesian Markov chain Monte Carlo (MCMC) inferences were undertaken by using BEAST, using a SRD06 nucleotide substitution model (*16*), a relaxed molecular clock model with an uncorrelated lognormal rate distribution (*17*), and a Bayesian skygrid coalescent model (*18*). Four independent MCMC runs of 1×10^8 steps were computed and ≈10%–15% burn-in was discarded, resulting in ≈3.5×10^8 total steps for each gene dataset. Parameters and trees were sampled every 35,000th and 70,000th MCMC step, respectively. Convergence of MCMC chains was inspected by using Tracer version 1.6 (http://tree.bio.ed.ac.uk). A subset of 500 trees was drawn randomly from the combined posterior distribution of trees and used as an empirical distribution for subsequent analysis (*19*).

Spatial and Temporal Origins of H7N9

We used a Bayesian discrete phylogeographic approach to investigate spatial dynamics among 9 geographic regions. Specifically, we considered viral movement across eastern China (Shanghai, Zhejiang, Jiangsu, and Shandong provinces); central China (Jiangxi and Hunan provinces); northern China (Beijing, Henan, Hebei, and Xinjiang provinces); southeastern China (Fujian Province); central Guangdong Province (Guangzhou, Huizhou, Foshan, Dongguan, Zhongshan, Shenzhen, Jiangmen, and Zhaoqing Figure 1]); eastern Guangdong Province (Meizhou, Heyuan, Chaozhou, Jieyang, Shantou, and Shanwei); western Guangdong Province (Yangjiang, Maoming, and Yunfu); and other regions (related sequences isolated from other countries before the H7N9 epidemic). To trace the origin of H7N9 infection, we considered sporadic clinical infection cases from Malaysia and Taiwan as a separate discrete location. Hong Kong adjoins central Guangdong, and most imported live poultry in Hong Kong is from central Guangdong (Zhuhai and Shenzhen). Therefore, Hong Kong and central Guangdong were considered as a single spatial unit. To provide a more realistic reconstruction that includes the directionality of virus transmission, we used an asymmetric continuous-time Markov chain model (*20*) to estimate ancestral locations and location posterior probabilities for each node in the dated phylogenies. Finally, we used TreeAnnotator to obtain maximum clade credibility trees for each gene, which were visualized by using FigTree version 1.4.2 (http://tree.bio.ed.ac.uk). Nucleotide sequences generated in this study were submitted to GISAID (Global Initiative on Sharing All Influenza Data, http://www.gisaid.org) under accession nos. EPI655863–EPI656506 and EPI654015–EPI654495.

Results

An Epicenter Shift of A(H7N9) in Humans, Guangdong, 2013–2015

As of October 14, 2015, a total of 182 laboratory-confirmed clinical cases of A(H7N9) infection in humans and

68 deaths were reported in Guangdong (Figure 1; online Technical Appendix Table 1, http://wwwnc.cdc.gov/EID/article/22/12/16-0450-Techapp1.pdf). Guangdong reported no clinical A(H7N9) cases during the first epidemic wave (March 2013–May 2013) but had the highest number of cases during the second (110 cases during June 2013–May 2014) and third (72 cases during June 2014–May 2015) epidemic waves.

Unexpectedly, the geographic distributions of A(H7N9) cases in Guangdong differed during the second and third waves (Figure 1, panels B, C). During the second wave, 110 cases were reported from 14 prefecture-level cities in Guangdong. The epicenter of the outbreak was in central Guangdong in the Pearl River Delta (PRD) region (95 [86%] cases). The highest numbers of human cases were reported from cities in Guangdong that had the most LPMs and the highest population density, such as Guangzhou, Shenzhen, and Foshan (Figure 1, panel A). Citywide LPM closures of 2 weeks' duration were implemented in Guangzhou and Shenzhen cities in February 2014, during the middle of the second wave, and were extended to all prefecture-level cities in central Guangdong in January 2015 during the middle of the third wave (Figure 1, panel B; online Technical Appendix Table 2). All live poultry were removed, and LPM were disinfected once; the markets were cleaned thoroughly with 0.05%–0.1% diluted chlorine solution after poultry removal. Short-term surveillance showed that the A(H7N9) detection rate decreased from 14.83% (112/755) before LPM closure to 1.67% (5/300) on the day when markets reopened, across 31 sampled markets during the second wave (*4*). Another study found that avian influenza virus contamination in LPMs dropped precipitously after cleaning and disinfecting (*21*). Our clinical surveillance data showed that human cases reduced by 55% (online Technical Appendix Table 1) in central Guangdong during the third wave but rose in other regions of Guangdong; eastern Guangdong became a new epicenter of the outbreak. Twenty-eight human cases occurred in eastern Guangdong during the first 2 months of 2015, compared with only 2 during the same period in 2014 (Figure 1). The geographic shift of A(H7N9) infection between the second and third waves became more apparent when incidence per capita was measured (Figure 1, panel C) because eastern Guangdong has a lower average population density than the PRD region.

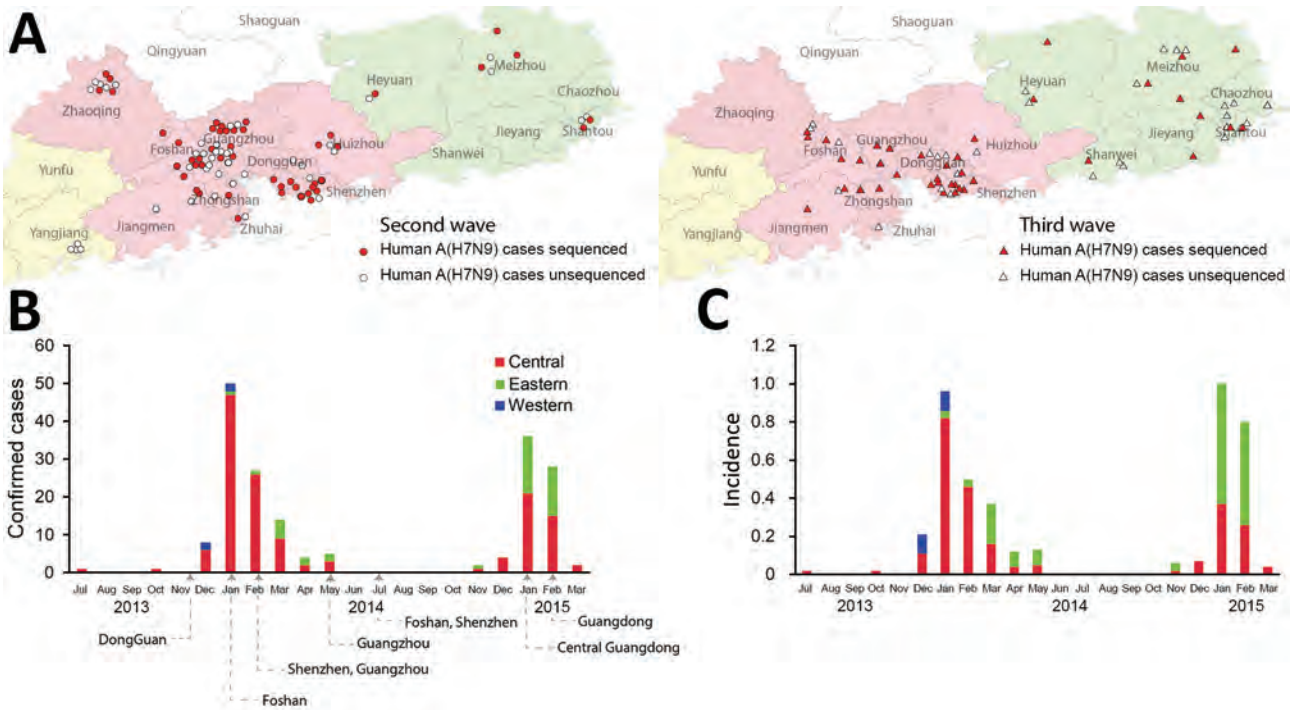

Figure 1. Avian influenza A(H7N9) infection in humans, Guangdong, China, 2013–2015. A) Geographic distribution of H7N9 in humans during the second (June 2013–May 2014) and third (June 2014–May 2015) waves. Confirmed cases in humans identified during the second wave are marked with circles and during the third wave with triangles. H7N9 isolates newly sequenced in this study are highlighted in red. Pink and green shading indicates city prefectures in central and eastern Guangdong Province, respectively. B) Numbers of human H7N9 infections in different regions of Guangdong Province during 2013–2015. Arrows indicate the dates at which live-poultry markets were closed in epicenter cities. No infections were reported during April–October. C) Incidence (human H7N9 infections/1 million population) in each region.

Epidemic Origins of Human A(H7N9) Infections in Guangdong

We undertook a phylogenetic molecular clock analysis to identify the epidemic origins and transmission dynamics of circulating avian influenza A strains during the third wave. The H7N9 sequences included in our analyses represented 55% (60/110) and 49% (35/72) of all diagnosed H7N9 cases in Guangdong during the second and third waves, respectively. H7N9 and H9N2 viruses obtained from poultry and LPM environmental samples during 2013–2015 also were sequenced, resulting in 44 complete and 79 incomplete virus genomes generated using high-throughput sequencing (*8*,*9*).

Phylogeographic analysis of 433 H7 HA genes revealed spatial patterns of A(H7N9) transmission across China (Figure 2, panel A). During the first epidemic wave, A(H7N9) virus spread from eastern China to northern, central, and southeastern China, causing a few human infections (Figure 2, panel A), consistent with previous analyses

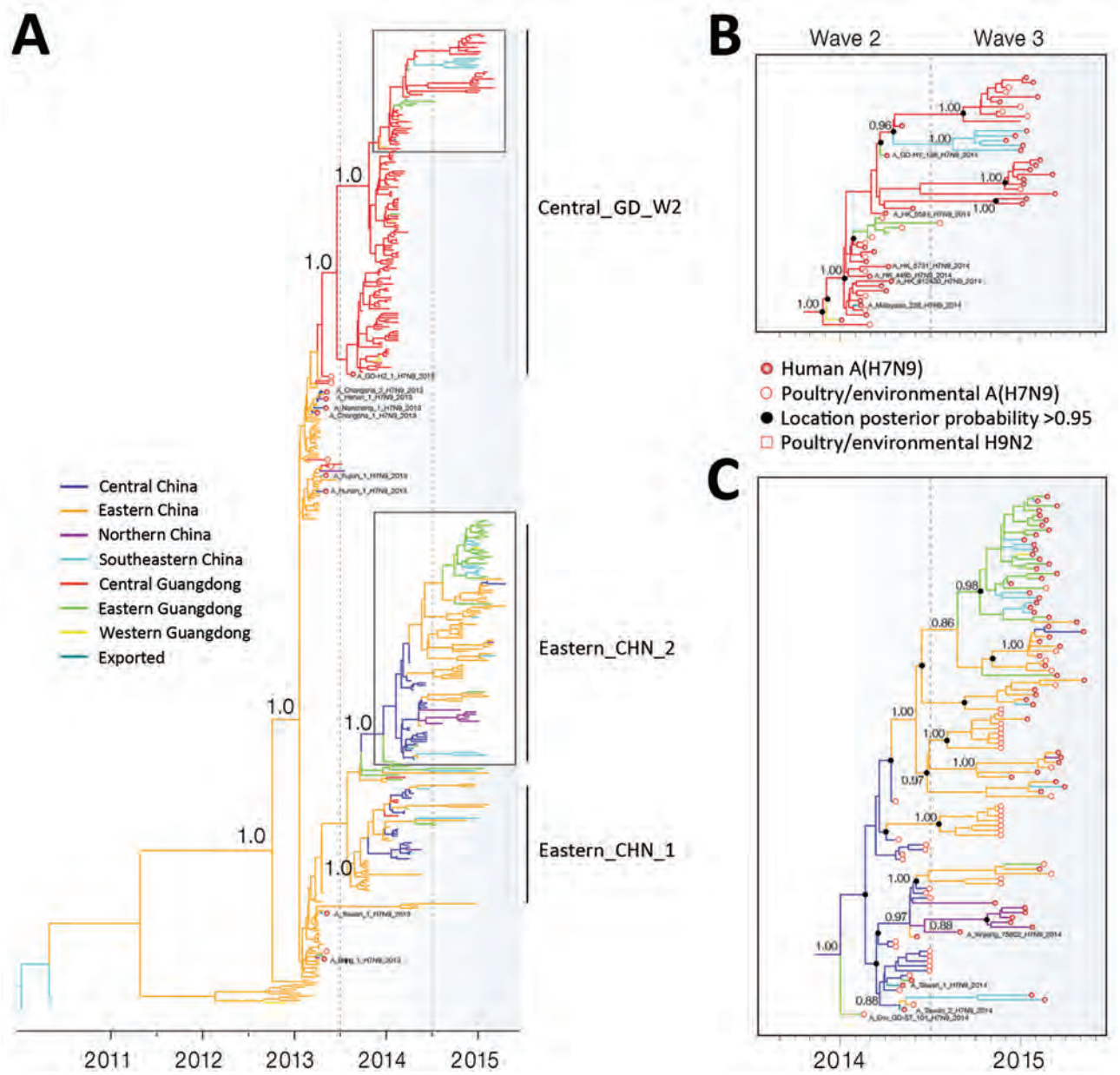

Figure 2. A) Bayesian maximum clade credibility molecular clock tree of influenza virus H7 gene sequences. Branch colors represent the most probable ancestral locations of each branch, inferred from using a spatial phylogenetic model (see Materials and Methods for details). Three major clades of avian influenza A(H7N9) virus were nominated, and phylogenetic posterior probability support is shown for selected clades. B, C) Phylogenies showing hemagglutinin, Guangdong, China, third-wave clades. Phylogenetic posterior probability support is shown for selected clades.

(*22*,*23*). All A(H7N9) viruses identified from chicken and environmental samples in Guangdong during the first wave were derived from viruses circulating in eastern China (Figure 2, panel A). These Guangdong viruses fell into 2 distinct phylogenetic clusters, indicating multiple independent introductions to the region, possibly through different poultry trade routes.

During the second epidemic wave, local transmission and proliferation of A(H7N9) virus was detected in Guangdong, particularly in central Guangdong. The HA phylogeny indicated that 94% of A(H7N9) from clinical cases and 92% of H7 subtypes from LPM environmental samples in Guangdong during the second wave clustered into 1 large clade, designated here as Central_GD_W2 (Figure 2, panel A; Figure 3). The earliest second wave case in this clade was sampled in August 2013 (A_GD-HZ_1_H7N9_2013; Figure 2, panel A). Our analysis suggested that viruses related to A_GD-HZ_1_H7N9_2013 persisted in and disseminated through central Guangdong, giving rise to a large number of A(H7N9) cases in the region during the second wave. Moreover, we found that Central_GD_W2 clade viruses also disseminated from central to eastern and western Guangdong during the second wave and caused human cases (e.g., A_GD-HY_138_2014) (Figure 2, panels A, B). Four isolates from humans in Hong Kong and 1 from a human in Malaysia during the second wave also fell within this clade (Figure 2, panel B). The phylogeny of N9 NA sequences displayed similar virus transmission patterns (online Technical Appendix Figure, panel A). Most (73%) N9 genes from A(H7N9) isolates in Guangdong during the second wave clustered within the Central_GD_W2 clade. In contrast to HA, the NA phylogeny showed that A(H7N9) isolates during the second wave in central Guangdong did not form a single cluster (online Technical Appendix Figure, panel A). However, fewer human cases (27%) were caused by these viruses, and most cases were limited to Shenzhen and Shantou cities, suggesting less transmission of viruses in this clade (online Technical Appendix Figure, panel A).

The incidence of A(H7N9) in humans in central Guangdong decreased by 55% during the third wave (Figure 1, panel B; online Technical Appendix Table 1). However, phylogenetic analysis indicated that the virus persisted in central Guangdong. The H7 phylogeny showed that all A(H7N9) viruses from central Guangdong during the third wave were descended from Central_GD_W2 clade viruses of the second wave (Figure 2, panel B). The outbreaks of A(H7N9) in humans in Fujian Province (southeastern China) during the third wave also were caused by Central_GD_W2 clade viruses, suggesting a possible transmission of A(H7N9) virus from central Guangdong to cities in southeastern China during the second wave.

A major feature during the third epidemic wave was an increase in A(H7N9) cases in humans in eastern Guangdong (Figure 1, panels B, C; online Technical Appendix Table 1). Most (94%) isolates identified in eastern Guangdong during the third wave clustered into a single subclade of Eastern_CHN_W2 clade viruses in both the H7 and N9 phylogenies (Figure 2, panel C; online Technical Appendix Figure, panel A). The Eastern_CHN_W2 clade viruses were mainly found in poultry from central China during the second wave but became predominant (among both poultry and humans) in eastern China and eastern Guangdong during the third wave (Figure 2, panel C). Moreover, these viruses formed location-specific clades during the third wave, suggesting that they have become established and enzootic to the poultry populations in each locality (Figure 2, panel C).

Genetic Diversities of A(H7N9) Virus in Guangdong

During the second wave, sequences from 4 internal genes (NP, NS, PB1, PB2) of A(H7N9) isolates from central Guangdong mostly clustered into a single major clade, together with local A(H9N2) strains; these sequences were distinct from the A(H7N9) sequences from central or eastern China (Figure 4, panel A; online Technical Appendix Figure, panels B, D, F) (*8*,*22*). However, by the third wave, most A(H7N9) viruses from central Guangdong had

Figure 3. Genotypic analysis of influenza A(H7N9) viruses. Proposed genotypes are shown for 68 fully sequenced A(H7N9) viruses isolated from humans in central Guangdong during 2013–2015. Each square represents a gene sequence, and its color indicates the most probable clade to which that sequence belongs, as inferred from the phylogenies in Figures 2 and 4 and online Technical Appendix Figure, panels B–F (http://wwwnc.cdc.gov/EID/article/22/12/16-0450-Techapp1.pdf).

acquired some internal genes from viruses from central or eastern China. In particular, PB1, PB2, NP, and NS sequences obtained from humans with A(H7N9) infection and from H7N9/H9N2 environmental samples in central Guangdong during the third wave were distinct from those from the second wave (Figure 4, panel A; online Technical Appendix Figure, panels B, D, F). For instance, analysis of the PB2 gene revealed that 65 of 69 viruses from clinical samples clustered into the Central_GD_W2 clade during the second wave. However, during the third wave, only 8 of 32 H7N9 viruses from clinical isolates fell into this group. The remaining 24 H7N9 isolates were phylogenetically related to H7N9 or H9N2 isolates from central or eastern China. It therefore appears that >70% of third-wave H7N9 viruses from central Guangdong acquired a PB2 gene through reassortment with strains circulating elsewhere. A similar pattern also was observed for H7N9 and H9N2 isolates from LPM environments (Figure 4). These findings supported the hypothesis that H9N2 viruses previously circulating outside Guangdong were introduced into central Guangdong during the third wave and increased the diversity of internal genes of H7N9 in this place by reassortment.

We further classified all human A(H7N9) isolates from central Guangdong according to the phylogenetic placement of their genome segments. Genome segments of second-wave A(H7N9) from central Guangdong were typically co-inherited (except polymerase) and belonged to the Central_GD_W2 clade (Figure 3; Figure 4, panel A; online Technical Appendix Figure). A total of 12 different

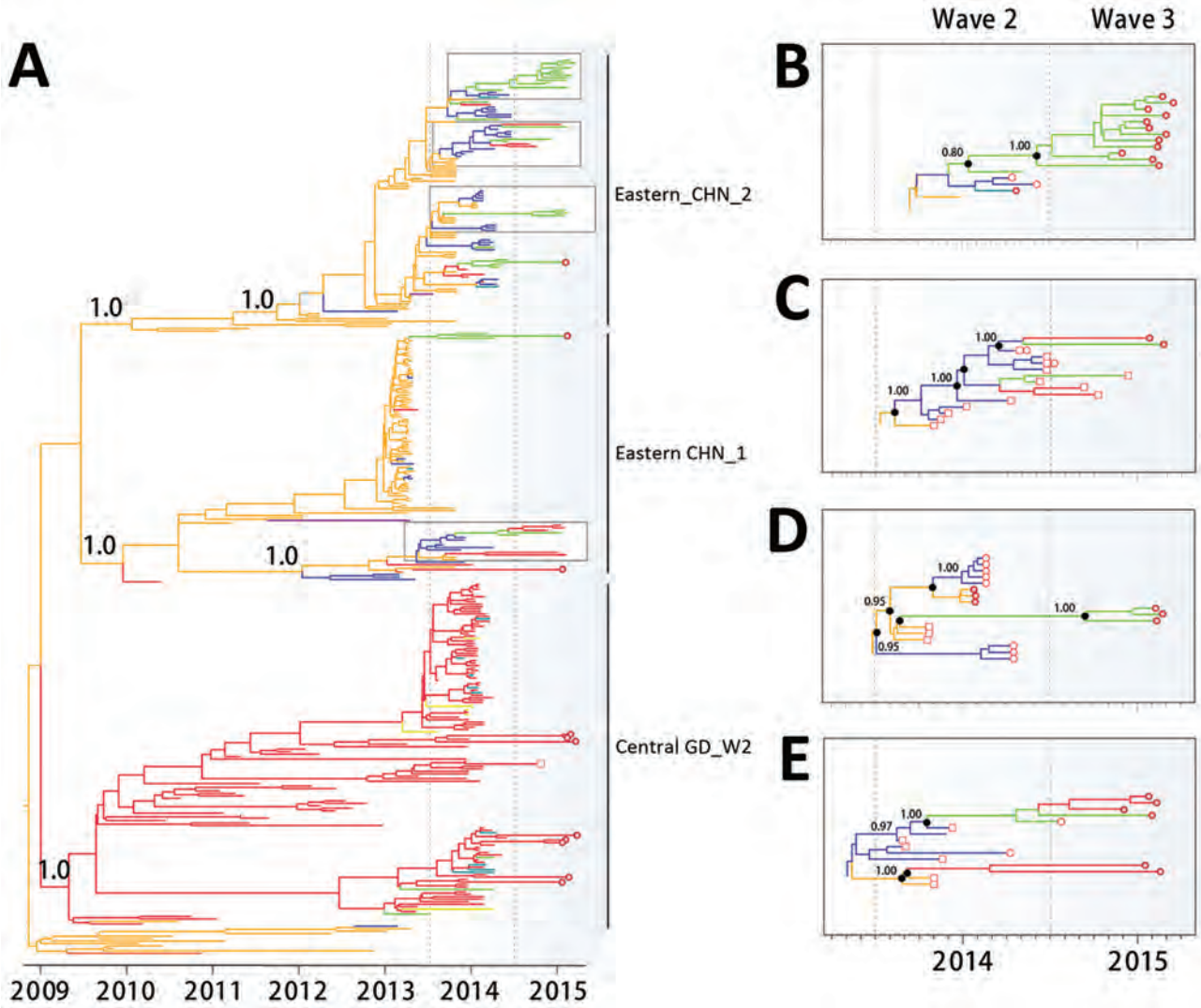

Figure 4. A) Bayesian maximum clade credibility phylogeographic tree of influenza virus polymerase protein 2 gene sequences. Branch colors represent the most probable ancestral locations of each branch, inferred from using a spatial phylogenetic model (see Materials and Methods for details). B–E) Phylogenies showing selected PB2 Guangdong third-wave clades. Empty squares indicate A(H9N2) virus sequences.

lineages were observed in 55 human A(H7N9) viruses isolated during the second wave in central Guangdong. This pattern was absent during the third wave; instead, the genomic structures of human A(H7N9) viruses were highly variable, with the exception of the HA and NA segments, which retained their association with the Central_GD_W2 clade (Figure 3).

In contrast, phylogenetic reconstruction of PB1, PB2, NP, and NS sequences indicated that most third-wave sequences seen in eastern Guangdong were genetically similar (Figure 4, panel B; online Technical Appendix Figure, panels. B–F). These sequences grouped into a single clade, whereas those sampled in central Guangdong were phylogenetically dispersed.

Discussion

We analyzed epidemiologic data pertaining to influenza A(H7N9) virus in humans and virus sequence data from 52% (95/182) of all persons in whom A(H7N9) infection was diagnosed and from LPMs environment samples during 2013–2015 to characterize the origin and transmission of A(H7N9) in humans across epidemic waves in Guangdong. The phylogeographic analyses of HA and NA indicate that the virus strain that caused third-wave outbreaks in central Guangdong descend from second-wave viruses that circulated in the same region. In other words, H7N9 circulating during the second wave probably persisted in targeted cities and/or their neighboring areas until the third epidemic wave.

In contrast, the histories of the H7N9 internal genes, which are affected by frequent reassortment with prevalent H9N2 viruses, most likely mirror the trade routes of live poultry. We found that A(H7N9) viruses from central Guangdong during the second wave possessed 5 (PB2, PB1, matrix, NP, NS) of 6 internal genes mainly from the Central_GD_W2 clade. However, in the third wave, viral internal genes were dispersed in phylogenetic trees; most strains fell into the Eastern_CHN1 or Eastern_CHN2 clades, suggesting another source for the parental viruses of these reassortants (Figure 3). This finding suggests there were changes in nature of A(H9N2) viruses that were cocirculating in central Guangdong (Figure 4, panel C; online Technical Appendix Figures B–F). Our data indicate that the genetic diversity of H7N9 or H9N2 in central Guangdong increased during the third wave, even though the number of human infections was lower in this region.

From a public health standpoint, our results underscore 3 major concerns with current A(H7N9) infections in humans in China. First, the persistence and spread of A(H7N9) have not been completely constrained. A(H7N9) circulating in central Guangdong during the second wave was persistent and caused outbreaks in humans during the third wave. For example, 5 and 3 cases, respectively, were identified in humans in March 2014 in Shenzhen and Guangzhou in Guangdong after the reopening of LPMs in February 2014 (online Technical Appendix Tables 1, 2). This finding suggests that interventions such as the temporary closure and sanitation of LPMs can reduce virus contamination in poultry and environmental samples but apparently cannot eliminate the risk for human infection (*21*). Recent long-term LPM surveillance in Guangzhou suggests that different types of poultry markets were recontaminated by A(H7N9) and other avian influenza A strains; up to 2 days after markets were reopened, detection rates of the viruses in LPM environments were as high as those before market closure (*5*).

Second, a geographic shift of the epicenter of human infections between the second and third waves in Guangdong suggests an epidemic of A(H7N9) infection is difficult to control solely by interfering in the epicenter of an outbreak. Some regions, once contaminated, might act as sources of infection to the wider poultry sector. Current sequence data suggest that the A(H7N9) human infections in eastern, northern, and southeastern China and eastern Guangdong during the third wave were mainly caused by viruses belonging to the Eastern_CHN_W2 clade, which were predominantly isolated from poultry populations in central China at the end of the second wave (Figure 2, panel C). In eastern Guangdong, 94% of A(H7N9) cases in humans during the third wave were caused by Eastern_CHN_W2 clade viruses.

Third, other measures complementary to LPM closures should be considered by government administration. We observed a continued reassortment of Guangdong A(H7N9) lineages with viral strains from central and eastern China since February 2014 (Figures 3, 4), suggesting that live poultry from central and eastern areas might have been introduced into central Guangdong after the local LPMs were closed. Indeed, it is plausible that official closure led to an increase in illicit trading in some markets or neighborhoods (http://gzdaily.dayoo.com/html/2015-03/18/content_2885023.htm; http://shenzhen.sina.com.cn/news/n/2015-04-20/detail-iavxeafs5854802.shtml). In this context, the closure of central LPMs without a strict ban on the live poultry trade could, at least in theory, have detrimental effects. Illicit trading has the potential to change the poultry trade and make officially monitoring and controlling it more difficult. Other less disruptive measures that have been proven to reduce risk can be considered, such as rest days and banning live poultry overnight (*24*).

One limitation of this study is a lack of long-term surveillance of live poultry in Guangdong. Such surveillance is difficult to implement because of a low infection rate and the absence of signs during A(H7N9) infection in poultry. However, most A(H7N9) infection in humans results from direct exposure to live poultry (*25*) (online Technical

Appendix Table 3). Furthermore, we used in our analyses environmental samples from LPMs, which partially reflect the circulation of avian influenza A strains in poultry. In addition, surveillance efforts in different regions might differ and could affect our interpretation on virus origin and transmission. In this study, we have analyzed most publicly available, genetically related A(H7N9) sequences out of Guangdong Province, and the regions of eastern China and central Guangdong that reported most clinical H7N9 cases represent most H7N9-related sequences. However, sampling bias cannot be excluded, especially for environmental and poultry samples. Central China is a major poultry farming area but has a limited number of A(H7N9) sequences from poultry, which could be caused by a lower prevalence of the virus in this region or by a possible limited surveillance effort in poultry population. As a result, sequences data from Eastern_CHN_W2 clade are still limited to illustrate the evolution and transmission route of this clade of A(H7N9) (Figure 2, panel C). Longer-term and larger-scale studies are necessary to provide more robust evidence about the value of interventions for controlling the epidemic at national and regional scales.

During February 5–11, 2016, twenty-eight new A(H7N9)cases were reported in humans. Clearly, the public health risk from A(H7N9) remains. Our results highlight some limitations of the current geographically restricted LPM interventions on the epidemic control of A(H7N9), which might also apply to other avian influenza viruses. To focus only on end-stage epidemic LPM interventions without including the entirety of the LPM transmission chain might, however, be of limited value. Public health organizations might wish to consider the possibility of proactively closing LPMs, and alternative measures as recently suggested (*24*), in areas potentially at-risk, although we recognize that practical, economic, and administrative considerations also contribute to decision-making processes.

Acknowledgment

We thank Tommy Lam for sequence alignments.

C.K., J.W., J. Li, X.H., M. Ko, and J.H. designed the study. J.W., X. Ze, J. Lu, Y.S., L.Z., L.Y., L.L., H.N., M. Ka, X. Zhang, G.H., and H.Z. prepared sample collection and genome sequencing. J. Lu, N.R.F., T.B., J.R., and O.P. analyzed the data. J. Lu, N.R.F., O.P., and C.K. interpreted the data. J. Lu, N.R.F., and C.K. prepared the figures. J. Lu, N.R.F., L.Y., O.P., and C.K. wrote the article.

This work was supported by grants from the Research Project of H7N9 Influenza of Guangdong [2014] (no. 1046), the Scientific, Technological Research of Prevention and Control of H7N9 Subtype Avian Influenza Virus (20140024), and China Scholarship Council (grant no. 201508440009).

Dr. Wu is a virologist in Guangdong CDC. Her primary research interest is the investigation of influenza virus epidemiology, evolution, and transmission.

References

1. Gao R, Cao B, Hu Y, Feng Z, Wang D, Hu W, et al. Human infection with a novel avian-origin influenza A (H7N9) virus. N Engl J Med. 2013;368:1888–97. http://dx.doi.org/10.1056/NEJMoa1304459
2. Li Q, Zhou L, Zhou M, Chen Z, Li F, Wu H, et al. Epidemiology of human infections with avian influenza A(H7N9) virus in China. N Engl J Med. 2014;370:520–32. http://dx.doi.org/10.1056/NEJMoa1304617
3. Yu H, Wu JT, Cowling BJ, Liao Q, Fang VJ, Zhou S, et al. Effect of closure of live poultry markets on poultry-to-person transmission of avian influenza A H7N9 virus: an ecological study. Lancet. 2014;383:541–8. http://dx.doi.org/10.1016/S0140-6736(13)61904-2
4. Kang M, He J, Song T, Rutherford S, Wu J, Lin J, et al. Environmental sampling for avian influenza A(H7N9) in live-poultry markets in Guangdong, China. PLoS One. 2015;10:e0126335. http://dx.doi.org/10.1371/journal.pone.0126335
5. Yuan J, Lau EH, Li K, Leung YH, Yang Z, Xie C, et al. Effect of live poultry market closure on avian influenza A(H7N9) virus activity in Guangzhou, China, 2014. Emerg Infect Dis. 2015;21:1784–93. http://dx.doi.org/10.3201/eid2110.150623
6. Wu P, Jiang H, Wu JT, Chen E, He J, Zhou H, et al. Poultry market closures and human infection with influenza A(H7N9) virus, China, 2013-14. Emerg Infect Dis. 2014;20:1891–4. http://dx.doi.org/10.3201/eid2011.140556
7. Russell CA, Jones TC, Barr IG, Cox NJ, Garten RJ, Gregory V, et al. Influenza vaccine strain selection and recent studies on the global migration of seasonal influenza viruses. Vaccine. 2008;26(Suppl 4):D31–4. http://dx.doi.org/10.1016/j.vaccine.2008.07.078
8. Ke C, Lu J, Wu J, Guan D, Zou L, Song T, et al. Circulation of reassortant influenza A(H7N9) viruses in poultry and humans, Guangdong Province, China, 2013. Emerg Infect Dis. 2014;20:2034–40. http://dx.doi.org/10.3201/eid2012.140765
9. Lu J, Wu J, Zeng X, Guan D, Zou L, Yi L, et al. Continuing reassortment leads to the genetic diversity of influenza virus H7N9 in Guangdong, China. J Virol. 2014;88:8297–306. http://dx.doi.org/10.1128/JVI.00630-14
10. Wu J, Lau EH, Xing Q, Zou L, Zhang H, Yen HL, et al. Seasonality of avian influenza A(H7N9) activity and risk of human A(H7N9) infections from live poultry markets. J Infect. 2015;71:690–3. http://dx.doi.org/10.1016/j.jinf.2015.08.007
11. Larkin MA, Blackshields G, Brown NP, Chenna R, McGettigan PA, McWilliam H, et al. Clustal W and Clustal X version 2.0. Bioinformatics. 2007;23:2947–8. http://dx.doi.org/10.1093/bioinformatics/btm404
12. Larsson A. AliView: a fast and lightweight alignment viewer and editor for large datasets. Bioinformatics. 2014;30:3276–8. http://dx.doi.org/10.1093/bioinformatics/btu531
13. Stamatakis A. RAxML-VI-HPC: maximum likelihood-based phylogenetic analyses with thousands of taxa and mixed models. Bioinformatics. 2006;22:2688–90. http://dx.doi.org/10.1093/bioinformatics/btl446
14. Rodríguez F, Oliver JL, Marín A, Medina JR. The general stochastic model of nucleotide substitution. J Theor Biol. 1990;142:485–501. http://dx.doi.org/10.1016/S0022-5193(05)80104-3
15. Rambaut A, Lam TT, Carvalho LM, Pybus OG. Exploring the temporal structure of heterochronous sequences using TempEst (formerly Path-O-Gen). [Epub 2016 Apr 10].

Virus Evolution. 2016;2:vew007. http://dx.doi.org/10.1093/ve/vew007
16. Shapiro B, Rambaut A, Drummond AJ. Choosing appropriate substitution models for the phylogenetic analysis of protein-coding sequences. Mol Biol Evol. 2006;23:7–9. http://dx.doi.org/10.1093/molbev/msj021
17. Drummond AJ, Ho SY, Phillips MJ, Rambaut A. Relaxed phylogenetics and dating with confidence. PLoS Biol. 2006;4:e88. http://dx.doi.org/10.1371/journal.pbio.0040088
18. Gill MS, Lemey P, Faria NR, Rambaut A, Shapiro B, Suchard MA. Improving Bayesian population dynamics inference: a coalescent-based model for multiple loci. Mol Biol Evol. 2013;30:713–24. http://dx.doi.org/10.1093/molbev/mss265
19. Lemey P, Rambaut A, Bedford T, Faria N, Bielejec F, Baele G, et al. Unifying viral genetics and human transportation data to predict the global transmission dynamics of human influenza H3N2. PLoS Pathog. 2014;10:e1003932. http://dx.doi.org/10.1371/journal.ppat.1003932
20. Edwards CJ, Suchard MA, Lemey P, Welch JJ, Barnes I, Fulton TL, et al. Ancient hybridization and an Irish origin for the modern polar bear matriline. Curr Biol. 2011;21:1251–8. http://dx.doi.org/10.1016/j.cub.2011.05.058
21. Trock SC, Gaeta M, Gonzalez A, Pederson JC, Senne DA. Evaluation of routine depopulation, cleaning, and disinfection procedures in the live bird markets, New York. Avian Dis. 2008;52:160–2. http://dx.doi.org/10.1637/7980-040607-Reg
22. Lam TT, Zhou B, Wang J, Chai Y, Shen Y, Chen X, et al. Dissemination, divergence and establishment of H7N9 influenza viruses in China. Nature. 2015;522:102–5. http://dx.doi.org/10.1038/nature14348
23. Cui L, Liu D, Shi W, Pan J, Qi X, Li X, et al. Dynamic reassortments and genetic heterogeneity of the human-infecting influenza A (H7N9) virus. Nat Commun. 2014;5:3142. http://dx.doi.org/10.1038/ncomms4142
24. Peiris JS, Cowling BJ, Wu JT, Feng L, Guan Y, Yu H, et al. Interventions to reduce zoonotic and pandemic risks from avian influenza in Asia. Lancet Infect Dis. 2016;16:252–8. http://dx.doi.org/10.1016/S1473-3099(15)00502-2
25. Yi L, Guan D, Kang M, Wu J, Zeng X, Lu J, et al. Family clusters of avian influenza A H7N9 virus infection in Guangdong Province, China. J Clin Microbiol. 2015;53:22–8. http://dx.doi.org/10.1128/JCM.02322-14

Address for correspondence: Changwen Ke, Guangdong Provincial Center for Disease Control and Prevention, No.160, Qunxian Rd., Dashi town, Panyu District, Guangzhou City, Guangdong Province, China; email: kecw1965@aliyun.com

Infectious Dose of *Listeria monocytogenes* in Outbreak Linked to Ice Cream, United States, 2015

Régis Pouillot, Karl C. Klontz, Yi Chen, Laurel S. Burall, Dumitru Macarisin, Matthew Doyle, Kären M. Bally, Errol Strain, Atin R. Datta, Thomas S. Hammack, Jane M. Van Doren

The relationship between the number of ingested *Listeria monocytogenes* cells in food and the likelihood of developing listeriosis is not well understood. Data from an outbreak of listeriosis linked to milkshakes made from ice cream produced in 1 factory showed that contaminated products were distributed widely to the public without any reported cases, except for 4 cases of severe illness in persons who were highly susceptible. The ingestion of high doses of *L. monocytogenes* by these patients infected through milkshakes was unlikely if possible additional contamination associated with the preparation of the milkshake is ruled out. This outbreak illustrated that the vast majority of the population did not become ill after ingesting a low level of *L. monocytogenes* but raises the question of listeriosis cases in highly susceptible persons after distribution of low-level contaminated products that did not support the growth of this pathogen.

Understanding the likelihood of developing invasive listeriosis after ingesting a given number of *Listeria monocytogenes* cells (dose-response relationship) is important in managing risks linked to this pathogen in food. Nevertheless, several challenges hamper characterization of this dose-response relationship, including the lack of an appropriate animal model, the relative rarity of outbreaks, long incubation periods that impede the collection of well-preserved implicated food samples, and heterogeneity of the initial contamination level (*1*).

In early 2015, an outbreak of invasive listeriosis linked to ice cream products was identified in the United States (*2*). A total of 10 case-patients with listeriosis related to this outbreak were reported from Arizona and Oklahoma (1 case each); Texas (3 cases); and Kansas (5 cases, all in inpatients of 1 hospital) (*2*). *L. monocytogenes* isolates from 4 of the Kansas case-patients were indistinguishable by pulsed-field gel electrophoresis from isolates recovered from ice cream made in 1 plant of the implicated company (factory 1). The isolate from the fifth Kansas case-patient did not match any isolate recovered in this outbreak investigation. *L. monocytogenes* isolates from patients in other states were linked to ice cream products manufactured in another facility (factory 2) of the same company (*2*). The US Food and Drug Administration (FDA) collected a large volume of ice cream from factory 1 for microbiological testing.

This outbreak provided a unique opportunity to assess exposure levels to *L. monocytogenes* from implicated ice cream products among infected persons and the overall population. Because ice cream has a long shelf life and *L. monocytogenes* does not grow but survives for long periods in frozen products (*3*), the level of *L. monocytogenes* in implicated products manufactured during the outbreak, although collected after the outbreak, was likely to be representative of levels in products eaten by exposed persons. We assessed the outbreak data to gain insight into contamination levels among products from 1 factory implicated in the outbreak, the number of *L. monocytogenes* cells ingested by specific subpopulations during this outbreak, and the dose-response relationship for *L. monocytogenes*.

Materials and Methods

Framework for Dose-Response Derivation

In microbial dose-response frameworks, it is generally assumed that as few as 1 independently acting cell that survives host defense measures can initiate infection (1-hit theory [*4*,*5*]). This minimal infective dose of 1 cell is associated with a probability (r) of infection. Assuming r is low and constant within a subpopulation (online Technical Appendix, http://wwwnc.cdc.gov/EID/article/22/12/16-0165-Techapp1.pdf), r can be estimated by the ratio of the number of invasive listeriosis cases in a

Author affiliations: Food and Drug Administration, College Park, Maryland, USA (R. Pouillot, K.C. Klontz, Y. Chen, D. Macarisin, M. Doyle, E. Strain, T.S. Hammack, J.M. Van Doren); Food and Drug Administration, Laurel, Maryland, USA (L.S. Burall, A.R. Datta); Via Christi Hospitals, Wichita, Kansas, USA (K.M. Bally)

DOI: http://dx.doi.org/10.3201/eid2212.160165

subpopulation (X_p), by the estimated number of *L. monocytogenes* cells ingested by the subpopulation Dp; that is, r = Xp / Dp. In addition to using this classical derivation of r, we estimated in this study r values using the *L. monocytogenes* dose-response model of Pouillot et al. (6) (online Technical Appendix).

Listeriosis Cases

This study considers only the 4 hospitalized Kansas case-patients whose illnesses were confirmed to be linked to ingestion of products manufactured in factory 1. Illness onset dates ranged from January 2014 through January 2015 (Figure). All 4 were >67 years and <84 years of age. Medical records review indicated all 4 had underlying medical conditions that contributed to compromised immune function before exposure to *L. monocytogenes* in milkshakes. Food histories were available for 3 of the Kansas case-patients. All patients with food histories ate product 1 from factory 1 through milkshakes. One patient had 2 milkshakes (1 day at lunch and the following day at dinner); another had 2 milkshakes (1 day at dinner and 6 days later at dinner), and the remaining patient had 3 milkshakes (1 day at dinner and 4 and 9 days later at dinner and lunch, respectively). Two serving units of product 1, each weighing ≈80 g, were used to prepare each milkshake. Strains of *L. monocytogenes* isolated from the 4 patients were indistinguishable by pulsed-field gel electrophoresis to strains recovered from product 1.

Number of *L. monocytogenes* Cells Ingested by the Population

The factory 1 production line linked to the Kansas cases made 8 different types of ice cream products (products 1–8) (*7*). (The website for this reference identifies 10 universal product codes corresponding to 8 different types of ice cream products; 2 products were sold individually and grouped in larger packages). FDA collected and counted *L. monocytogenes* cells in samples of products 1–3 (*8*; L.S. Burall, unpub. data). We characterized the variability of *L. monocytogenes* levels in products 1–3 (online Technical Appendix).

No samples of products 4–8 were collected. In a low-exposure scenario, products that were not tested were assumed to be uncontaminated. In a medium-exposure scenario and in a high- exposure scenario, contamination levels were predicted on the basis of the processes used to produce these products. Specifically, we specified in these scenarios that contamination levels were similar for products 1 and 4 and were similar for products 2 and 5–8 because the process used to produce product 4 was similar to that used for product 1, whereas production processes for products 5–8 were similar to that for product 2.

The number of *L. monocytogenes* cells ingested by the population was then estimated by multiplying the average number of *L. monocytogenes* organisms per serving by the number of servings distributed in the various subpopulations. The number of ice cream servings distributed in the

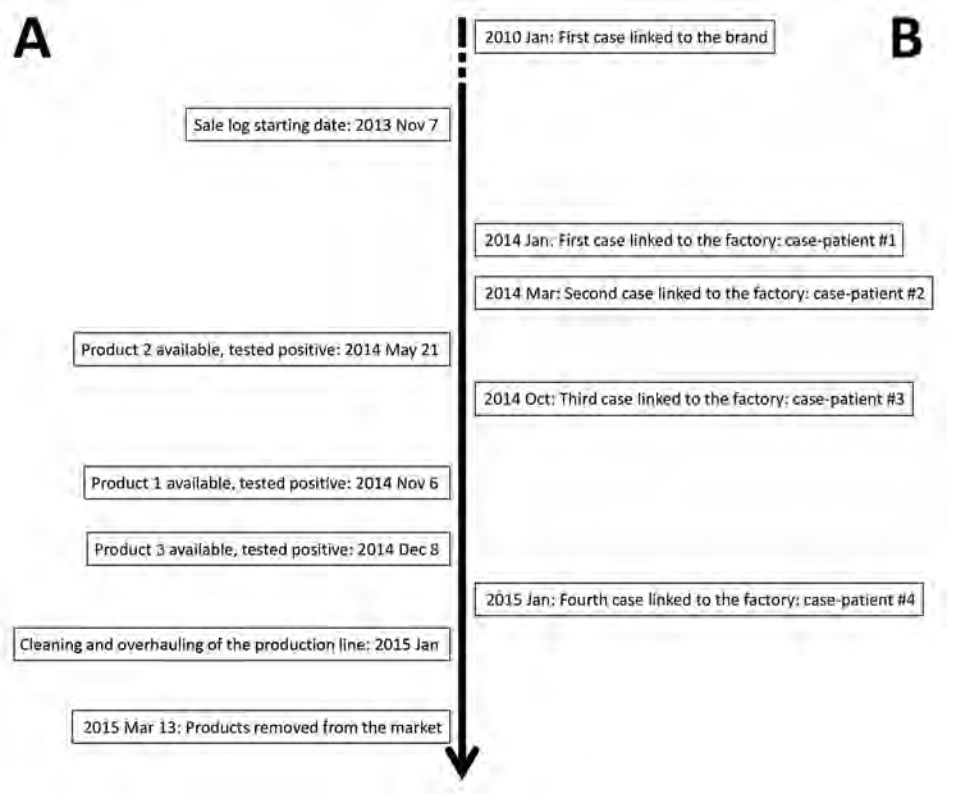

Figure. Timeline of listeriosis outbreak linked to ice cream, United States, 2015. A) Data for products produced in factory 1 (*2*); B) data for outbreak start and 4 case-patients at 1 hospital in Kansas.

various subpopulations was estimated from product distribution records for factory 1.

We do not know when contamination of the production line at factory 1 began. We isolated *L. monocytogenes* from a product manufactured on this line on May 21, 2014, but we had no samples manufactured before this date. Although the first known case associated with the brand of ice cream occurred in January 2010, the first case-patient specifically linked to factory 1 was hospitalized in Kansas on December 24, 2013, and listeriosis was diagnosed in January 2014 (patient 1, Figure). In the low-exposure scenario and medium-exposure scenario, we assumed the date at which contamination began at factory 1 was December 1, 2013, that is, a few weeks before hospitalization of the first case-patient whose illness was linked to ice cream produced at this facility. Contamination could have begun earlier than this date given that 1 listeriosis case-patient whose illness was linked to the same brand, but produced at factory 2, became ill in 2010. In the high-exposure scenario, we assumed contamination began 2.5 years before the outbreak was recognized, that is, midway between 2010 and the date the outbreak was recognized.

To estimate the proportion of servings that reached inpatients deemed to be highly susceptible to listeriosis, we multiplied the proportion of ice cream distributed to hospitals for patient consumption by the overall proportion of intensive care unit (ICU) beds in these hospitals (i.e., 10%) as a surrogate of the proportion of inpatients deemed to be highly susceptible to invasive listeriosis. To estimate the proportion of servings potentially eaten by pregnant women, ≥ 65 y. and ≥ 75 y. persons, we assumed that the implicated brand was eaten by different subpopulations similarly to other brands of ice cream (online Technical Appendix).

To understand why 4 cases of ice cream–associated listeriosis clustered at a single hospital, we created 2 indices for the hospitals that received contaminated product(s) from factory 1 at least 1 time during November 7, 2013–March 16, 2015. The first index ascertained the severity of patient illness at each hospital (illness score) and was calculated by determining the percentage of total beds constituting ICU beds (scale: 0%–4.9%, 1 point; 5%–9.9%, 2 points; 10%–14.9%, 3 points; and ≥15%, 4 points). Hospitals were contacted by telephone and queried about the total number of beds licensed and the number dedicated to treatment of patients in ICU (medical, surgical, pediatric, neonatal, and burn). To quantify the availability of contaminated products at each hospital (supply score), we divided the total number of servings shipped to each facility during the recorded distribution period (16 months) by the total number of hospital beds (scale: <1 serving per bed, 1 point; 1–3.99, 2 points; 4–6.99, 3 points; and >7, 4 points). Using the 2 indices, we summed scores for all hospitals (maximum possible score 8) as an overall measure of patient illness and potential product exposure.

Results

Number of *L. monocytogenes* Cells per Serving

All tested samples of product 1 manufactured before the outbreak was recognized were positive for *L. monocytogenes* (*8*). Assuming the 5 lots of product 1 tested were representative of all lots of contaminated product 1, we estimated the mean number of *L. monocytogenes* cells in each 80-g unit of product 1 at 620 CFU (95% credible interval [CrI] 380–2,100 CFU). From the distribution of contamination level inferred from the model, we estimated that 0.1% of servings of product 1 had a dose >7,400 CFU (95% CrI 4,400–58,000 CFU) (see Table 1 for other statistics). *L. monocytogenes* was recovered from 80% of 294 units of product 2 (unit size 70 g) tested (mean 310 CFU/serving [95% CrI 55–11,000 CFU/serving]). Of the 95 units of product 3 tested, 45% yielded *L. monocytogenes* (mean 0.12 CFU/g).

Table 1. Estimated contamination level of *Listeria monocytogenes* per gram and per serving unit of 3 products in a multistate outbreak of ice cream–associated listeriosis, United States, 2015

	Estimate (95% credible interval)		Quantile (95% credible interval)			
Product/dose	Mean	SD	90%	99%	99.9%	99.99%
Product 1						
Per g	8 (5–26)	10 (6–62)	17 (10–60)	46 (27–270)	92 (55–730)	160 (97–1,500)
Per 80-g serving	620 (380–2,100)	760 (460–4,900)	1,300 (820–4,800)	3,700 (2,200–22,000)	7,400 (4,400–58,000)	13,000 (7,800–120,000)
Product 2						
Per g	5 (1–160)	200 (17–35,000)	2 (1–10)	48 (11–620)	520 (91–12,000)	3,600 (470–140,000)
Per 70-g serving	310 (55–11,000)	14,000 (1,200–2,500,000)	140 (43–710)	3,400 (800–43,000)	37,000 (6,400–840,000)	250,000 (33,000–9,800,000)
Product 3						
Per g	0.12 in 45% of products					
Per 160-g serving	8.64 in 45% of servings					

Number of *L. monocytogenes* Cells Consumed by the Population

Sales data suggested widespread distribution of contaminated products to hospitals and the general population (e.g., schools, grocery stores, restaurants). We estimated that the general population ingested a total of 1.5×10^9 (low-exposure scenario) to 1.4×10^{10} (high-exposure scenario) *L. monocytogenes* cells (Table 2). We estimated that, overall, the highly susceptible population ingested 7.2×10^6 (low-exposure scenario) to 3.3×10^7 (high-exposure scenario) *L. monocytogenes* cells.

Among hospitals that received ≥1 products from the production line of factory 1 known to produce contaminated ice cream, the median percentage of total beds constituting ICU beds (severity of illness score) was 8.7% (range 0%–70.7%; mean 10%). The median number of servings per bed (supply score) over the recorded distribution period (16 months) was 2 (range 0.1–93.7; mean 4.3). The Kansas hospital with the 4 cases of ice cream–associated listeriosis had 62.2 servings of the implicated products per bed (13.5% of beds in the hospital were ICU beds); the servings per bed value for the hospital was exceeded by only 1 other hospital (93.7 servings/bed; 6.5% ICU beds). After combining the severity of illness and supply scores for each hospital, we found the median value was 5 (range 2–7; mean 4.6); a combined score of 7 was achieved by 9% of hospitals, of which 1 was the Kansas hospital with the 4 cases (the hospital with 93.7 servings/bed had a combined score of 6).

Probability of Infection after Ingestion of 1 Cell

Under the low-exposure scenario, we estimated that the probability of infection, *r*, after ingestion of 1 bacterium in the overall population was

$$r = \frac{4}{1.5 \times 10^9} = 2.6 \times 10^{-9}$$

Using this same approach, we determined the value of *r* for the overall population was $r = 6.5 \times 10^{-10}$ under the medium-exposure scenario and $r = 2.9 \times 10^{-10}$ under the high-exposure scenario (Table 2). The integration of the model by Pouillot et al. (*6*), considering a normal distribution of the $\log_{10}$ of the *r* parameter in the population rather than a constant one, led to a distribution with a mean –9.38 and an SD of 0.88 for the overall population under the lower-exposure scenario, a mean of –10.0 for the medium-exposure scenario, and a mean of –10.3 for the high-exposure scenario (Table 2).

We also assessed persons at greatest risk for invasive listeriosis, including pregnant women, highly susceptible persons (e.g., those with compromised immune function), persons ≥65 years of age, and persons ≥75 years of age (Table 2). Because no ice cream–associated cases were reported among pregnant women, we used an estimate of 0.5

Table 2. Probability of invasive listeriosis after ingestion of ice cream products contaminated with *Listeria monocytogenes*, United States, 2015

	Population, no. cases in population				
Exposure scenario/model	All, n = 4	Highly susceptible, n = 4	Pregnant, n = 0*	Age ≥65 y, n = 4	Age ≥75 y, n = 2
Lower†					
r constant					
No. *L. monocytogenes* cells consumed	1.5×10^9	7.2×10^6	2.2×10^7	2.3×10^8	1.2×10^8
Estimated *r* parameter	2.6×10^{-9}	5.5×10^{-7}	$<2.3 \times 10^{-8}$	1.7×10^{-8}	1.7×10^{-8}
Corresponding to 1 case every… servings‡	37,867	181	>4,363	5,756	5,832
$\log_{10}(r)$ normally distributed					
Estimated μ parameter	–9.38	–6.19	<(–7.92)	–8.00	–8.02
Estimated σ parameter	0.88	0.24	0.54	0.54	0.54
Medium§					
r constant					
No. *L. monocytogenes* cells consumed	6.2×10^9	1.5×10^7	8.9×10^7	9.4×10^8	4.8×10^8
Estimated *r* parameter	6.5×10^{-10}	2.7×10^{-7}	$<5.6 \times 10^{-9}$	4.3×10^{-9}	4.2×10^{-9}
Corresponding to 1 case every… servings‡	154,612	375	>17,812	23,501	23,811
$\log_{10}(r)$ normally distributed					
Estimated μ parameter	–10.0	–6.40	<(–8.49)	–8.60	–8.62
Estimated σ parameter	0.88	0.24	0.54	0.54	0.54
High¶					
r constant					
No. *L. monocytogenes* cells consumed	1.4×10^{10}	3.3×10^7	2.0×10^8	2.1×10^9	1.0×10^9
Estimated *r* parameter	2.9×10^{-10}	1.2×10^{-7}	$<2.6 \times 10^{-9}$	1.9×10^{-9}	1.9×10^{-9}
Corresponding to 1 case every… servings‡	339,153	816	>39,071	51,552	52,230
$\log_{10}(r)$ normally distributed					
Estimated μ parameter	–10.3	–6.80	<(–8.83)	–8.97	–8.97
Estimated σ parameter	0.88	0.24	0.54	0.54	0.54

*0.5 used for computation.
†Products 1–3 contaminated beginning 2013 Dec 1; products 4–8 not contaminated.
‡Corresponding to 1 case every… servings, including 10,000 *L. monocytogenes* cells.
§Products 1–8 contaminated beginning 2013 Dec 1.
¶Products 1–8 contaminated beginning 2012 Jun 1.

cases and provided only an upper limit value for *r*. (This value was chosen arbitrarily. A Poisson process with mean 0.5 would have led to 0 cases in 90% of occurrence.)

Discussion

This outbreak investigation provided unique data to characterize the dose-response relationship between *L. monocytogenes* in general and susceptible populations. Multiple factors compelled us to estimate as precisely as possible doses of *L. monocytogenes* ingested by consumers of contaminated products. First, the number of samples microbiologically tested was by far the largest ever reported from an outbreak setting (*8*). Second, because ice cream preserves the viability of *L. monocytogenes* but does not support its growth, levels of contamination were likely to have been accurately measured and have remained relatively constant over the extended shelf lives of the products. Finally, an exceptionally stable level of contamination within product types minimized variability in exposures. Hospital records indicated that patient 4 drank milkshakes made with product 1 on 3 different days during January 11–19, 2015, before sepsis caused by *L. monocytogenes* infection was diagnosed on January 23. This patient could have eaten ice cream from lots we enumerated. Only 4 (0.2%) of 2,320 samples of product 1 yielded a concentration >100 CFU/g, equivalent to a dose of ≥16,000 *L. monocytogenes* cells per milkshake (2 servings of 80 g × 100 CFU/g, assuming the 2 servings were >100 CFU/g). Inferences on the interlot, interbox, and intrabox variability helped us define precisely the distribution of contamination levels from serving to serving and confirmed that a very high concentration of *L. monocytogenes* cells in any given serving unit was not likely. The estimated mean dose per milkshake is 1,240 *L. monocytogenes* cells (95% CrI 760–4,200 *L. monocytogenes* cells). We estimate that 1 of 10,000 milkshakes would have a load >26,000 *L. monocytogenes* cells (95% CrI 15,600–240,000 *L. monocytogenes* cells). Assuming there was no initial contamination of the milkshake machines and no growth of the pathogen in the milkshakes, the mean contamination level of *L. monocytogenes* in the milkshakes (8 cells/g of ice cream) was relatively low compared with contamination levels in some other outbreaks (*9*–*12*). However, in the absence of leftovers from the actual implicated milkshakes, we cannot rule out the possibility that the 4 susceptible patients received some of the highest contaminated products from the factory line, triggering infection. Experimental trials of *L. monocytogenes* growth in milkshakes made from these naturally contaminated ice cream samples held at room temperature showed an absence of growth during 8 hours and an average population level increase after 14 hours limited to 1.14 log CFU/g (*13*). We cannot exclude the possibility that variations in procedures used to clean the milkshake machines might have enabled isolated microbial growth on ≥1 machines. We believe the extremely high prevalence of contamination of product 1 might have inoculated ≥1 machines with repeated preparations over the long period during which contaminated products were distributed; however, no *Listeria* was isolated from samples collected from these machines after the outbreak was recognized (Charles Hunt, Kansas Department of Health and Environment, pers. comm., 2016 Jun 27).

Although the 4 cases of ice cream–associated listeriosis in a single hospital raise the possibility of a systematic problem within the hospital, it is also possible that the combination of severely ill patients, including some with specific risk factors for listeriosis such as hematologic cancers (*14*), in a setting in which a large amount of contaminated ice cream was served contributed to this series of infections. Medical staff at the hospital also might have had a heightened suspicion of listeriosis after diagnosis of the initial case, which might have increased the likelihood of detecting cases. Overall, the Kansas hospital received 55% of all product 1 sold to hospitals. Thus, observing the 4 cases in this specific hospital was not improbable. (The probability to observe 4 successes out of 4 trials is 9% when the independent probability of success is 55%.)

Although precise quantification of exposure to *L. monocytogenes* ingestion through contaminated ice cream is difficult to infer for specific persons, an assessment of exposures among populations is more feasible. Despite the relatively low levels of contamination of ice cream products in this listeriosis outbreak, the exceptionally high prevalence of contaminated products, combined with the protracted duration of contamination of the production line (at least 1 year and possibly longer), contributed to exposure of many persons to *L. monocytogenes*. This finding suggests that widespread distribution of contaminated products with low-dose contamination by *L. monocytogenes* in a product that does not support growth of *L. monocytogenes* might lead to only a limited number of reported infections. We focused our study on 1 cluster of outbreak-related cases, the one for which FDA was able to collect samples of ice cream for microbiological testing. Five other cases of ice cream–associated invasive listeriosis were identified in states other than Kansas; these cases were linked to another production factory operated by the same company, expanding further the quantity of contaminated ice cream sold to the public.

The Food and Agriculture Organization of the World Health Organization (FAO/WHO) (*15*) estimated an *r* parameter of 3.2×10^{-7} in a well-documented listeriosis outbreak involving immunocompromised patients in Finland in 1998–1999 (*16*,*17*); in this outbreak, the median estimated dose ingested was 8.2×10^{3} *L. monocytogenes*. Our estimate of the *r* parameter for the susceptible population is in the same order of magnitude (1.2×10^{-7} to 5.5

$\times 10^{-7}$). In the population of pregnant women, FAO/WHO (*15*) estimated a *r* parameter of 2.6×10^{-11} on the basis of an outbreak of cheese-associated listeriosis involving pregnant Hispanic women in Los Angeles County, California, USA, in 1985 in which the estimated dose was 1.7×10^{7} *L. monocytogenes* (*10*). More recently, Imanishi et al. (*18*) estimated an attack rate of 1 case/10,000 exposed pregnant women in Colorado, USA, during a 2011 multistate outbreak of listeriosis linked to contaminated cantaloupe (*19*); no enumeration data were available in this outbreak. Studies have shown that cut cantaloupe supports the growth of *L. monocytogenes* (*20*,*21*), suggesting that some exposures could have been high during this outbreak. In the ice cream–associated outbreak described here, no cases were reported among pregnant women despite presumably widespread exposures among this subgroup of susceptible persons. Specifically, a large number of contaminated ice cream products were presumably ingested by pregnant women during the long duration of contamination of the production line. From the expected number of *L. monocytogenes* cells ingested by this subpopulation, we estimate, under the various assumptions used in this study, a value of $r < 2.6 \times 10^{-9}$ to $r < 2.3 \times 10^{-8}$. In summary, estimates for *r* derived in the present study are comparable in order of magnitude with estimates derived from previous outbreaks, a finding that is noteworthy in light of the low levels of contamination of ice cream products and the fact that these products did not support growth. Although other outbreaks were linked to higher level of contamination per serving than in the present study, the number of contaminated servings was much lower in those outbreaks than in the present one.

On the other hand, estimates for *r* obtained in the present study are higher than those estimated by using epidemiologic data (*6*,*15*,*17*). Using epidemiologic data, FAO/WHO (*15*) estimated that the probability of infection after consumption of 1 *L. monocytogenes* cell is in the order of $r = 5 \times 10^{-12}$ for susceptible persons (immunocompromised persons, pregnant women, and elderly persons), and 5×10^{-14} for nonsusceptible persons (*15*). These values predict the occurrence of 1 listeriosis case for every 20 million exposures to 10,000 *L. monocytogenes* cells in the susceptible population (10,000, which was chosen arbitrarily, would correspond to the dose after ingestion of 100 g of a product contaminated at 100 CFU/g) and 1 case of listeriosis for every 2 billion exposures to 10,000 *L. monocytogenes* cells in the nonsusceptible population. The estimates obtained in our study were much higher than these values: 1 case expected for every 339,200 servings of 10,000 bacteria per serving, such as for the general population in the high-exposure scenario. Similarly, using the model of Pouillot et al. (*6*), we estimated that values from the ice cream outbreak data are $\approx 2 \log_{10}$ higher than those based on epidemiologic data. A possible explanation for these differences is that a particularly virulent strain of *L. monocytogenes* was present in ice cream. Differences in *r* estimates obtained from outbreak investigations versus epidemiologic data also could result from observation bias, wherein recognition of cases instigates a study, leading to high number of cases for equation input and thus higher estimates for *r*. In contrast, situations where contaminated products are distributed but no cases are recognized are underrepresented in such evaluations.

This outbreak of ice cream–associated listeriosis recognized in 2015 demonstrates that illnesses can occur when products with low-level contamination that do not support growth are distributed widely to the public, even though it is not possible to conclude with certainty whether the cases were linked directly to the products or indirectly after a growth step on a milkshake machine. The outbreak also illustrates that even when the distribution of products contaminated with *L. monocytogenes* is widespread, most consumers of the products will not become ill when contamination levels are low and no growth is facilitated. Finally, this outbreak adds yet further evidence of the risk for listeriosis faced by persons with weakened immune systems and calls for effective risk management to mitigate infections (*22*).

Acknowledgments

We acknowledge the outbreak response partners whose contributions to the listeriosis investigation resulted in identification of the contaminated products, distribution records, and clinical case records vital to this study. We thank the state and local partners from the Alabama Department of Public Health, Kansas Department of Agriculture, Kansas Department of Health and Environment, Oklahoma Department of Agriculture, Food and Forestry, South Carolina Department of Health & Environmental Control, Texas Department of State Health Services, and Tulsa Health Department for their help in the outbreak investigation. We also thank the federal partners at the Centers for Disease Control and Prevention's Division of Foodborne; Waterborne, and Environmental Diseases, National Center for Emerging and Zoonotic Infectious Diseases; FDA's Office of Regulatory Affairs, especially the Dallas, Kansas City, Atlanta, and New Orleans District Offices; FDA's Center for Food Safety and Applied Nutrition; and FDA's Coordinated Outbreak Response and Evaluation Network. We thank Libby Wei and Sara Kreshpanji, each supported by a University of Maryland/Joint Institute for Food Safety and Applied Nutrition student internship, for helping to gather and analyze data. This study used the high-performance computational capabilities of the Scientific Computing Laboratory at the FDA Center for Devices and Radiological Health. We thank Mike Mikailov, Brian Fitzgerald, Stuart Barkley, Luo Fu Jyh, Lohit Valleru, and Stephen Whitney for their invaluable contributions to supercomputing.

Dr. Pouillot is a visiting scientist in the Risk Analysis Branch within the Division of Risk and Decision Analysis, Center for Food Safety and Applied Nutrition, FDA. His research interest is using data analysis and models to understand and evaluate the risk for foodborne illnesses.

References

1. Hoelzer K, Chen Y, Dennis S, Evans P, Pouillot R, Silk BJ, et al. New data, strategies, and insights for *Listeria monocytogenes* dose-response models: summary of an interagency workshop, 2011. Risk Anal. 2013;33:1568–81. http://dx.doi.org/10.1111/risa.12005
2. Centers for Disease Control and Prevention. Multistate outbreak of listeriosis linked to Blue Bell Creameries products (final update). 2015 [cited 2015 Dec 10]. http://www.cdc.gov/listeria/outbreaks/ice-cream-03-15/
3. Palumbo SA, Williams AC. Resistance of *Listeria monocytogenes* to freezing in foods. Food Microbiol. 1991;8:63–8.
4. Haas CN, Rose JB, Gerba CP. Quantitative microbial risk assessment. New York: Wiley; 1999.
5. Teunis PF, Havelaar AH. The Beta Poisson dose-response model is not a single-hit model. Risk Anal. 2000;20:513–20. http://dx.doi.org/10.1111/0272-4332.204048
6. Pouillot R, Hoelzer K, Chen Y, Dennis SB. *Listeria monocytogenes* dose response revisited—incorporating adjustments for variability in strain virulence and host susceptibility. Risk Anal. 2015;35:90–108. http://dx.doi.org/10.1111/risa.12235
7. BlueBell.com. For the first time in 108 years, Blue Bell announces a product recall. 2015 [cited 2016 Jan 7]. http://www.bluebell.com/BB_withdrawal
8. Chen Y, Burall L, Macarisin D, Pouillot R, Strain E, De Jesus A, et al. Prevalence and level of Listeria monocytogenes in ice cream linked to a listeriosis outbreak in the United States. J Food Prot. 2016;79:1828–932.
9. Johnsen BO, Lingaas E, Torfoss D, Strøm EH, Nordøy I. A large outbreak of *Listeria monocytogenes* infection with short incubation period in a tertiary care hospital. J Infect. 2010;61:465–70. http://dx.doi.org/10.1016/j.jinf.2010.08.007
10. Linnan MJ, Mascola L, Lou XD, Goulet V, May S, Salminen C, et al. Epidemic listeriosis associated with Mexican-style cheese. N Engl J Med. 1988;319:823–8. http://dx.doi.org/10.1056/NEJM198809293191303
11. Pérez-Trallero E, Zigorraga C, Artieda J, Alkorta M, Marimón JM. Two outbreaks of *Listeria monocytogenes* infection, northern Spain. Emerg Infect Dis. 2014;20:2155–7. http://dx.doi.org/10.3201/eid2012.140993
12. Heiman KE, Garalde VB, Gronostaj M, Jackson KA, Beam S, Joseph L, et al. Multistate outbreak of listeriosis caused by imported cheese and evidence of cross-contamination of other cheeses, USA, 2012. Epidemiol Infect. 2016;144:2698–708. http://dx.doi.org/10.1017/S095026881500117X
13. Chen Y, Allard E, Wooten A, Hur M, Sheth I, Laasri A, et al. Recovery and growth potential of *Listeria monocytogenes* in temperature abused milkshakes prepared from naturally contaminated ice cream linked to a listeriosis outbreak. Front Microbiol. 2016;7:764. http://dx.doi.org/10.3389/fmicb.2016.00764
14. Goulet V, Hebert M, Hedberg C, Laurent E, Vaillant V, De Valk H, et al. Incidence of listeriosis and related mortality among groups at risk of acquiring listeriosis. Clin Infect Dis. 2012;54:652–60. http://dx.doi.org/10.1093/cid/cir902
15. Food and Agriculture Organization/World Health Organization. Risk assessment of *Listeria monocytogenes* in ready to eat foods. Technical report. Report no.: Microbiological Risk Assessment Series 5. Rome: The Organizations; 2004 [cited 2016 Jan 28]. ftp://ftp.fao.org/docrep/fao/010/y5394e/y5394e.pdf
16. Lyytikäinen O, Autio T, Maijala R, Ruutu P, Honkanen-Buzalski T, Miettinen M, et al. An outbreak of *Listeria monocytogenes* serotype 3a infections from butter in Finland. J Infect Dis. 2000;181:1838–41. http://dx.doi.org/10.1086/315453
17. Food and Drug Administration. Quantitative assessment of relative risk to public health from foodborne *Listeria monocytogenes* among selected categories of ready-to-eat foods [cited 2016 Jan 28]. http://www.fda.gov/downloads/Food/FoodScienceResearch/UCM197330.pdf
18. Imanishi M, Routh JA, Klaber M, Gu W, Vanselow MS, Jackson KA, et al. Estimating the attack rate of pregnancy-associated listeriosis during a large outbreak. Infect Dis Obstet Gynecol. 2015;2015:201479. http://dx.doi.org/10.1155/2015/201479
19. Centers for Disease Control and Prevention. Multistate outbreak of listeriosis associated with Jensen Farms cantaloupe—United States, August–September 2011. MMWR Morb Mortal Wkly Rep. 2011;60:1357–8.
20. Danyluk MD, Friedrich LM, Schaffner DW. Modeling the growth of *Listeria monocytogenes* on cut cantaloupe, honeydew and watermelon. Food Microbiol. 2014;38:52–5. http://dx.doi.org/10.1016/j.fm.2013.08.001
21. Fang T, Liu Y, Huang L. Growth kinetics of *Listeria monocytogenes* and spoilage microorganisms in fresh-cut cantaloupe. Food Microbiol. 2013;34:174–81. http://dx.doi.org/10.1016/j.fm.2012.12.005
22. Silk BJ, Date KA, Jackson KA, Pouillot R, Holt KG, Graves LM, et al. Invasive listeriosis in the Foodborne Diseases Active Surveillance Network (FoodNet), 2004–2009: further targeted prevention needed for higher-risk groups. Clin Infect Dis. 2012;54(Suppl 5):S396–404. http://dx.doi.org/10.1093/cid/cis268

Address for correspondence: Régis Pouillot, US Food and Drug Administration, 5001 Campus Dr, College Park, MD 20740, USA; email: Regis.Pouillot@fda.hhs.gov

Electrolyte and Metabolic Disturbances in Ebola Patients during a Clinical Trial, Guinea, 2015

Johan van Griensven, Elhadj Ibrahima Bah, Nyankoye Haba, Alexandre Delamou, Bienvenu Salim Camara, Kadio Jean-Jacques Olivier, Hilde De Clerck, Helena Nordenstedt, Malcolm G. Semple, Michel Van Herp, Jozefien Buyze, Maaike De Crop, Steven Van Den Broucke, Lutgarde Lynen, Anja De Weggheleire, the Ebola-Tx Consortium

Medscape EDUCATION ACTIVITY

This activity has been planned and implemented through the joint providership of Medscape, LLC and *Emerging Infectious Diseases.* Medscape, LLC is accredited by the American Nurses Credentialing Center (ANCC), the Accreditation Council for Pharmacy Education (ACPE), and the Accreditation Council for Continuing Medical Education (ACCME), to provide continuing education for the healthcare team.

Medscape, LLC designates this Journal-based CME activity for a maximum of 1.00 ***AMA PRA Category 1 Credit(s)™***. Physicians should claim only the credit commensurate with the extent of their participation in the activity.

All other clinicians completing this activity will be issued a certificate of participation. To participate in this journal CME activity: (1) review the learning objectives and author disclosures; (2) study the education content; (3) take the post-test with a 75% minimum passing score and complete the evaluation at http://www.medscape.org/journal/eid; and (4) view/print certificate. For CME questions, see page 2242.

Release date: November 17, 2016; Expiration date: November 17, 2017

Learning Objectives

Upon completion of this activity, participants will be able to:

- Distinguish laboratory abnormalities among patients with Ebola virus disease
- Assess risk factors for mortality among patients with Ebola virus disease
- Determine the risk stratification for mortality outcomes with Ebola virus disease
- Analyze the management of laboratory abnormalities associated with Ebola virus disease

CME Editor

Jude Rutledge, Technical Writer/Editor, *Emerging Infectious Diseases. Disclosure: Jude Rutledge has disclosed no relevant financial relationships.*

CME Author

Charles P. Vega, MD, Clinical Professor of Family Medicine, University of California, Irvine. *Disclosure: Charles P. Vega, MD, has disclosed the following financial relationships: served as an advisor or consultant for Allergan, Inc.; McNeil Consumer Healthcare; served as a speaker or a member of a speakers bureau for Shire Pharmaceuticals.*

Authors

*Disclosures**: Johan van Griensven, PhD; Elhadj Ibrahima Bah, MD; Nyankoye Haba, MSc; Alexandre Delamou, MD; Bienvenu Salim Camara, MD; Kadio Jean-Jacques Olivier, PharmD, MPH; Hilde De Clerck, MD; Malcolm G. Semple, MD, PhD; Michel Van Herp, MD; Jozefien Buyze, PhD; Maaike De Crop, MSc; Steven Van Den Broucke, MD; Lutgarde Lynen, PhD;*** and ***Anja De Weggheleire, MD, MPH,*** have disclosed no relevant financial relationships.* ***Helena Nordenstedt, MD, PhD,*** *has disclosed the following relevant financial relationship: employed by a commercial interest (partner employed): Gilead.*

Author affiliations: Institute of Tropical Medicine, Antwerp, Belgium (J. van Griensven, J. Buyze, M. De Crop, S. Van Den Broucke, L. Lynen, A. De Weggheleire); Donka National Hospital, Conakry, Guinea (E.I. Bah); National Blood Transfusion Center, Conakry (N. Haba, B.S. Camara, K.J.-J. Olivier); National Center for Training and Research in Rural Health of Maferinyah, Forecariah, Guinea (A. Delamou); Médecins Sans Frontières, Brussels, Belgium (H. De Clerck, H. Nordenstedt, M. Van Herp); University of Liverpool, Liverpool, United Kingdom (M.G. Semple)

DOI: http://dx.doi.org/10.3201/eid2212.161136

By using data from a 2015 clinical trial on Ebola convalescent-phase plasma in Guinea, we assessed the prevalence of electrolyte and metabolic abnormalities at admission and their predictive value to stratify patients into risk groups. Patients underwent testing with a point-of-care device. We used logistic regression to construct a prognostic model and summarized the predictive value with the area under the receiver operating curve. Abnormalities were common among patients, particularly hypokalemia, hypocalcemia, hyponatremia, raised creatinine, high anion gap, and anemia. Besides age and PCR cycle threshold value, renal dysfunction, low calcium levels, and low hemoglobin levels were independently associated with increased risk for death. A prognostic model using all 5 factors was highly discriminatory (area under the receiver operating curve 0.95; 95% CI 0.90–0.99) and enabled the definition of risk criteria to guide targeted care. Most patients had a very low (<5%) or very high (>80%) risk for death.

During the 2014–2016 Ebola virus disease (EVD) outbreak in West Africa, a total of 28,646 cases were diagnosed, with a case-fatality rate of 39.4% (*1*). Several research groups have focused on new therapeutic interventions, but none has been found to be very effective (*2–4*). Others have emphasized the importance of good supportive care (*5–11*). Besides indicating appropriate oral and intravenous hydration, a body of research has also made the case for increasing access to point-of-care (POC) devices to detect metabolic and electrolyte abnormalities (*5–8,10–13*) because pronounced abnormalities have been observed in Ebola virus patients treated in the United States and Europe (*14*).

However, the evidence base for this recommendation in busy, resource-limited Ebola treatment units (ETUs) remains limited. If few readily treatable electrolyte disturbances would be detected with these devices, their added value could be questioned because each blood collection puts healthcare workers at risk for infection (*15*). The limited understanding of the prognostic importance of these abnormalities further obscures the evidence base on their clinical value in resource-constrained settings. Moreover, findings might differ within and between countries, and information from various settings is thus required to inform management guidelines. Despite the ≈30,000 EVD cases diagnosed worldwide over the past 40 years, the evidence base on the prevalence and prognostic value of blood abnormalities is limited to a small number of reports on a fraction of all treated Ebola patients (*4,16,17*), many of whom were being treated intensively in high-resource settings (*14,18,19*).

A better understanding of abnormal blood test results could have important clinical consequences. First, more precise information on the prevalence of abnormalities could enable rational decision-making on which testing to prioritize and which abnormalities treatment programs should prepare to appropriately manage. Identified abnormalities could lead to relevant, simple therapeutic interventions (e.g., potassium [K^+] supplementation) that could reduce case-fatality rates. Second, identification of factors independently associated with an increased risk for death could lead to better prognostic classification of patients, identifying those in need of higher levels of care, and improve standardization when analyzing results of future clinical trials. To enable clinical decision-making, estimates of the absolute risk for death would be required for individual patients across the spectrum of independent risk factor values (*20*) and not the mere reporting of group odds or risk ratios, as has been done before (*16,17*). Based on the predicted absolute risk for death, individual risk stratification could be done on admission.

The Ebola-Tx trial evaluated convalescent-phase plasma as an EVD treatment in a Médecins sans Frontières (MSF) ETU in Conakry, Guinea. Trial findings have been published (*2*). MSF introduced a POC device during the trial. We used the opportunity of having access to relatively high-quality data from this clinical trial to 1) describe the prevalence of electrolyte and metabolic disturbances during admission and the association with EVD death and 2) assess the predictive value of these prognostic factors to stratify patients in risk groups.

Methods

Ebola-Tx Trial

The Ebola-Tx trial was conducted at the Conakry ETU supported by MSF. Trial patients were recruited during February 17–July 7, 2015. Patients of all ages, including pregnant women, were eligible, and their outcomes were compared with historical controls treated at the same center before the trial began. As per World Health Organization recommendations, patients received 2 units of 200–250 mL of Ebola convalescent-phase plasma after EVD diagnosis was confirmed by PCR (*2*). For children, a total volume of 10 mL/kg of Ebola convalescent-phase plasma was given. The level of neutralizing antibodies in the donors was unknown at the time of administration. Although the trial was found safe and feasible to organize, the efficacy of convalescent-phase plasma was not proven; the adjusted absolute risk reduction was -3% (95% CI -13% to 8%) (*2*).

Supportive Care at the MSF ETU

Supportive care during the trial was provided by the MSF team as per MSF guidelines. As part of supportive care, MSF staff introduced a POC device (i-STAT; Abbott Point of Care, Princeton, NJ, USA) on February 25, 2015, soon after the trial began. All patients were tested at the time of EVD diagnosis by using CHEM8+ cartridges (Abbott

Point of Care) to determine levels of electrolytes (K^+, sodium [Na^+], chloride [Cl^-], and ionized calcium [iCa^{2+}]), creatinine, and blood urea nitrogen (BUN); the anion gap; the total amount of dissolved carbon dioxide (TCO_2); glucose levels; and hemoglobin/hematocrit values.

The MSF supportive care guidelines recommend empirical systematic prescription of antibiotics and antimalarial drugs. Symptomatic care (e.g., for pain or nausea/vomiting) was given as needed. Fluid replenishment was done with oral rehydration fluids if a patient was alert, not vomiting, and able to participate in their own care. Intravenous fluids were given to patients with insufficient oral intake, severe vomiting or diarrhea, pronounced or persistent hypotension, or clinical signs of severe dehydration (*21*).

Study Population

A total of 102 patients were enrolled in the Ebola-Tx trial, of whom 98 received convalescent-phase plasma. A total of 87 were recruited after the introduction of the POC device.

Data Collection

During the trial, data were entered in an electronic case report form directly from source documents, which, when filled in the high-risk zone, were scanned using mobile phones and transmitted over a secured local wireless network to a central server and automated printer. Data were collected on admission and each day after EVD confirmation, including information on symptoms and clinical signs of EVD, vital signs, and treatment received. For our study, we used all available data on the POC results on admission, cycle threshold (C_t) values of the Ebola diagnostic PCR, baseline patient characteristics, and discharge status.

Definitions

We used definitions based on the POC device normal values and standard definitions for abnormalities: hypokalemia, K^+ <3.5 mmol/L; moderate hypokalemia, K^+ 2.5–3.0 mmol/L; severe hypokalemia, K^+ <2.5 mmol/L; hyperkalemia, K^+ ≥5.0 mmol/L; hyponatremia, Na^+ <135 mmol/L; hypernatremia, Na^+ >146 mmol/L; hypochloremia, Cl^- <98; high anion gap, >20; low TCO_2, <24 mmol/L; low glucose, <70 mg/dL; high glucose >180 mg/dL; creatinine and BUN: mild increase, 1.0–1.5 times the upper limit of normal (ULN); moderate increase, 1.5–3.0 times ULN; severe, >3.0 times ULN; increased BUN/creatinine ratio, >20; and hypocalcemia, iCa^{2+} <1.12 mmol/L. Anemia was defined per World Health Organization guidelines (age/sex adjusted) using hemoglobin values (*22*).

Statistical Analysis

We calculated medians and interquartile ranges (IQRs) for continuous variables and summarized binary/categorical data by using frequencies and percentages. We compared groups by using Fisher exact tests for binary/categorical variables and the Wilcoxon rank-sum test for continuous variables.

The outcome status at the time of discharge from the MSF ETU was classified as alive or dead, excluding patients transferred to another ETU. We performed a risk factor analysis by using multivariate logistic regression modeling to determine independent factors associated with increased risk for death. We selected a restricted number of exposure variables on the basis of theoretical considerations and published studies. We included the following variables in the POC model: K^+, iCa^{2+}, and creatinine levels; anion gap; amount of TCO_2; glucose levels; and hemoglobin levels. The POC+ model included the same POC variables plus age and the C_t of the PCR at EVD diagnosis, given that these 2 additional variables are the most universally accepted prognostic factors (*4*,*23*,*24*). To maximize power, we included the variables as continuous variables and determined the functional form by using the fracpoly command (fractional polynomial regression, which fits fractional polynomials as part of the specific regression model) in Stata version 14 (StataCorp LP, College Station, TX, USA). We reduced the model by using backward stepwise elimination until all variables had a p value <0.05. By using the logistic regression coefficients from the final model, we calculated the predicted risk for death for each patient and plotted the results in a histogram. We summarized the predictive value of the model by calculating the area under the receiver operating curve (AUROC) separately for the POC and the POC+ model.

We tabulated predicted and observed deaths across different predicted risk groups (<5.0%, 5.0%–19.9%, 20.0%–49.9%, 50.0%–79.9%, and ≥80.0%). We formally assessed the goodness-of-fit of the model by using the Hosmer-Lemeshow test, yielding a p value <0.05, which suggests significant discrepancy between the observed and predictive outcomes. We conducted internal validation by using cross-validation (h = 10, k = 10) (*25*). We randomly divided the data into 10 mutually exclusive subsets of the same size. We conducted a 10-fold cross-validation by repeating the analysis 10 times, each time excluding 1 of the independent datasets, and calculating the AUROC. We averaged the summary estimates of the 10 AUROCs to obtain the cross-validation AUROC. We conducted statistical analysis by using Stata version 14.

Results

Of the 87 study patients enrolled in the trial when the POC device was in use, POC results were available for 85 (Table 1). The median age was 30 years (IQR 20–40 years); 48 (56%) patients were female. The median C_t value in the diagnostic PCR was 27 (IQR 18–36).

Hyponatremia (77.6%) was very common, but hypernatremia was only rarely documented (Table 2). Although

Table 1. Baseline characteristics of 85 Ebola patients recruited for the Ebola-Tx trial, Conakry, Guinea, 2015*

Characteristic	Value
Age, median y (IQR)	30 (20–40)
<15	10 (11.8)
Sex	
M	37 (43.5)
F	48 (56.5)
C_t value on diagnostic Ebola PCR, n = 84	
No. cycles, median (range)	26.8 (17.8–35.8)
<25	23 (27.4)
25.0–29.9	40 (47.6)
≥30	21 (25.0)
Duration of symptoms, median d (IQR), n = 74	4 (3–5)
Coexisting chronic medical condition	15 (17.6)
Infectious†	8 (9.4)
Noninfectious‡	7 (8.2)
Selected symptoms on admission	
Nausea and vomiting	43 (50.6)
Diarrhea	29 (34.1)

*Values are no. (%) patients except as indicated. C_t, cycle threshold; IQR, interquartile range.
†For example, tuberculosis, HIV, or malaria.
‡For example, diabetes mellitus, arterial hypertension, chronic cardiac, pulmonary disease, or renal disease.

hypokalemia (33%) was common, severe hypokalemia (K^+ <2.5 mmol/L) and hyperkalemia were rare. Hypocalcemia (64%) was frequently observed. Renal dysfunction (45% with increased creatinine levels), an increased anion gap (28%), and decreased TCO_2 (71%) all were frequently documented. Anemia was observed in 27% of patients.

In the multivariate logistic regression modeling, decreased iCa^+ and hemoglobin levels and increased creatinine levels were associated with increased risk for death (POC model). In the POC+ model, age and the diagnostic PCR C_t value were additionally selected (Table 3). A prediction model based on these 5 factors provided estimates of the risk for death ranging from 0.016% to 99.99%, compared with a baseline (or pretest) risk for death of 34.6% (27/78 patients). The largest risk groups were patients at either very low or very high risk, with 40% of patients having a risk for death <10% and 22% having a risk >80% (Figure 1). This POC+ model had an AUROC of 0.95 (95% CI 0.90–0.99), compared with 0.88 (95% CI 0.78–0.97) for the model that only included creatinine, calcium, and hemoglobin levels (POC model) (Figure 2). AUROC cross-validation values were 0.92 (95% CI 0.85–0.99) for the POC+ model and 0.85 (95% CI 0.75–0.96) for the POC model. The Hosmer-Lemeshow test yielded a p value of 0.98 for the POC+ model and 0.34 for the term POC model. The predicted and observed risk for death was stratified into 5 risk groups (Table 4); most patients were in the <5% or >80% risk group categories.

Discussion

We documented a high prevalence of multiple electrolyte and metabolic abnormalities in Ebola patients at the time of admission during a clinical trial of convalescent-phase plasma in Guinea. Increased creatinine and decreased calcium and hemoglobin levels during admission were independent risk factors for death. The POC model including these factors and the POC+ model additionally including 2 key risk factors (C_t value of the diagnostic Ebola PCR and the age of the patient) both performed well in predicting individual patient outcome. The predicted risk for death ranged from <0.02% to 99.9%, and most patients were found to have either a very low risk (<5%) or a very high risk (>80%) for death.

The frequent observance of electrolyte disturbances is in line with the few available studies from Africa (*17*,*26*). The high prevalence of hypokalemia is of particular interest, although it was rarely severe at the time of admission. Nevertheless, hypokalemia can potentially be fatal and is amenable to relatively simple interventions. A deficiency in iCa^+ was common, a finding also frequently observed in sepsis patients (*27*,*28*). In the case of EVD, renal dysfunction and pancreatitis also could contribute. The high anion gap and low TCO_2 are likely explained by lactic acidosis. Renal failure was also common in our study. The exact cause of renal dysfunction in EVD patients remains undefined, but both prerenal and renal causes probably are involved.

The POC+ model, a 5-measure prognostic tool, enabled the stratification of patients into different risk groups at baseline, with risk for death ranging from <5% to >80%. This tool could enable the refining of clinical care pathways and rational use of scarce human resources. Absolute risks for death could easily be calculated via a spreadsheet or smartphone application. Alternatively, scoring systems could be developed for bedside use (*29*,*30*).

However, several issues need to be addressed before such prognostic tools are taken forward. First, we did not include other potentially relevant measures that can be tested with POC devices, such as liver function tests, coagulation abnormalities, or markers of inflammation. Although our system performed fairly well with only a few markers, evaluation of the full panel of tests could possibly lead to further improvement. Second, the sample size in our study was limited, and all but 2 of the patients received convalescent-phase plasma. Although transfusion of 500 mL of plasma probably will not strongly influence the prognostic associations, larger studies in different study populations are required to assess the generalizability of our findings. Third, corrective measures for some abnormalities (e.g., hypoglycemia or hypokalemia) could have obscured associations with survival. Moreover, because this was an exploratory study, our findings need to be validated in other and larger datasets. Finally, it remains to be seen whether (and if so how much) our prognostic tool would perform substantially better than clinical judgement alone or a prognostic tool relying on clinical signs/symptoms combined

Table 2. Metabolic and electrolyte disturbances in 85 Ebola patients recruited for the Ebola-Tx trial and association with increased risk for death, Conakry, Guinea, 2015*

Analyte	Value			p value
	Total	Deceased	Survived	
Total†	85	27	51	
K^+, mmol/L median (IQR)	3.7 (3.2–4.2)	3.9 (3–2-4.7)	3.7 (3.2–4.0)	0.21
High	4 (4.7)	3 (11.1)	0 (0)	
Normal	53 (62.3)	16 (59.3)	33 (64.7)	
Mild decrease	12 (14.1)	4 (14.8)	7 (13.7)	0.19
Moderate decrease	14 (16.5)	4 (14.8)	9 (17.6)	
Severe decrease	2 (2.3)	0 (0)	2 (3.9)	
Na^+, mmol/L median (range)	135 (132–137)	132 (129–138)	136 (133–137)	0.055
Low	66 (77.6)	20 (74.1)	39 (76.5)	
Normal	18 (21.2)	6 (22.2)	12 (23.5)	0.52
High	1 (1.2)	1 (3.7)	0 (0)	
Cl^-, mmol/L median (IQR)	99 (95–103)	101 (97–105)	99 (96–102)	0.41
Low	34 (40.0)	10 (37.0)	18 (35.3)	1.0
iCa^{2+}, mmol/L median (IQR)	4.3 (4.0–4.6)	3.9 (3.5–4.2)	4.4 (4.2–4.7)	<0.01
Low	54 (63.5)	24 (88.9)	26 (51.0)	<0.01
TCO_2, mmol/L median (IQR	21 (18–24)	17 (16–22)	21 (19–25)	<0.01
Low	60 (70.6)	23 (85.2)	37 (72.5)	0.27
Anion gap, mmol/L median (IQR)	19 (17–21)	19 (18–21)	18 (17–20)	0.26
High	24 (28.4)	11 (40.7)	10 (19.6)	0.061
Creatinine, mmol/L median (IQR), n = 84	106 (75–332)	442 (148–654)	91 (63–116)	<0.01
Normal	47 (55.9)	5 (18.5)	38 (74.5)	
1–3x ULN	16 (19.0)	5 (18.5)	9 (17.6)	<0.01
>3x ULN	21 (25.0)	17 (63.0)	4 (7.8)	
BUN, mmol/L median (IQR), n = 84	16 (9–39)	50 (17–69)	11 (7–21)	<0.01
Normal	53 (63.1)	9 (33.3)	38 (76.0)	
1–3x ULN	26 (30.9)	13 (48.1)	12 (24.0)	<0.01
>3x ULN	5 (6.0)	5 (18.5)	0 (0.0)	
BUN/creatinine ratio, median (IQR), n = 83	10.3 (7.4–13.9)	8.8 (6.8–13.9)	11.2 (7.7–14.0)	0.30
<10	36 (43.4)	15 (55.6)	18 (36.0)	
10–20	39 (47.0)	10 (37.0)	26 (52.0)	0.27
>20	8 (9.6)	2 (7.4)	6 (12.0)	
Glucose, mmol/L median (IQR)	121 (104–148)	112 (88–146)	122 (106–147)	0.24
Low	5 (5.9)	4 (14.8)	1 (2.0)	
Normal	72 (84.7)	19 (70.4)	47 (92.2)	0.022
High	8 (9.4)	4 (14.8)	3 (5.9)	
Hemoglobin, g/dL median (IQR)	14.6 (11.9–16)	13.6 (10.5–17)	14.3 (11.9–15.6)	0.90
Anemia‡	23 (27.1)	9 (33.3)	14 (27.4)	0.61

*Values are no. (%) patients except as indicated. BUN, blood urea nitrogen; C_t, cycle threshold; iCa^{2+}, ionized (free) calcium; IQR, interquartile range; K^+, potassium; Na^+, sodium; Cl^-, chloride; TCO_2, total dissolved carbon dioxide; ULN, upper limit of normal value.
†Denominator for deceased and survived patients combined is 78, excluding 7 patients who were transferred to another Ebola treatment unit, where they received favipiravir.
‡Definition of anemia per World Health Organization guideline (age/sex adjusted; hemoglobin levels used).

with age and the PCR C_t value. Nevertheless, a prognostic clinical tool using laboratory measures will have the advantage of being more objective, less variable between clinicians, and less dependent on specific clinical skills.

In contrast to fixed variables such as age and the PCR C_t value that are only useful as prognostic markers, the detection of hypocalcemia, anemia, and renal dysfunction is amenable to interventions. If these conditions are causally associated with an increased risk for death, their detection could contribute to reducing case-fatality rates. If they are only a proxy for another causal factor, correction of these abnormalities might have minimal effects. For instance, surprisingly limited evidence exists that correction of hypocalcemia in intensive care patients improves survival (*27*), and some evidence suggests that it could even be detrimental (*28*). Similarly, whether blood transfusion in cases of anemia can improve EVD survival (and at what threshold hemoglobin value) requires further study. Anemia has been found to be associated with an increased risk for death in other inflammatory conditions such as sepsis (*31*). However, subsequent studies demonstrated that a liberal blood transfusion strategy could have a negative impact on survival in intensive care patients (*32*).

The association of renal dysfunction with an increased risk for death has been demonstrated before (*4*,*17*,*26*,*33*). However, the added clinical value of being able to diagnose renal dysfunction, beyond its prognostic value, in the typical ETU in countries of Africa remains unclear. It could enable staff to more carefully assess the fluid status and thus avoid over- and under-hydration. However, renal dysfunction could be prerenal (requiring aggressive fluid administration) or renal (requiring more cautious fluid administration) in origin. Carefully assessing fluid status in busy ETUs with

Table 3. Factors associated with increased risk for death among 78 Ebola patients recruited for the Ebola-Tx trial, Conakry, Guinea, 2015*

	POC model		POC+ model‡,
Blood test result†	Crude OR (95% CI)	aOR (95% CI)	aOR (95% CI)
K^+, per unit increase	1.7 (0.9–3.3)	–	–
iCa^{2+}, per 0.1-unit increase)	0.70 (0.59–0.84)	0.78 (0.63–0.96)	0.73 (0.57–0.95)
Glucose, per 50-unit increase)	0.87 (0.50–1.52)	–	–
Creatinine, per 100-unit increase)	2.1 (1.5–3.0)	2.1 (1.3–3.3)	2.3 (1.1–4.6)
TCO_2, per 5-unit increase)	0.38 (0.20–0.74)	–	–
Anion gap, per 5-unit increase)	1.5 (0.6–3.7)	–	–
Hemoglobin, per 1-unit increase)	1.0 (0.9–1.2)	0.79 (0.63–0.99)	0.67 (0.47–0.93)
C_t value, per 1-unit increase)	0.80 (0.70–0.93)		0.73 (0.56–0.94)
Age, per 10-y increase)	1.8 (1.3–2.6)		2.7 (1.2–6.4)

*aOR, adjusted odds ratio; C_t, cycle threshold; iCa^{2+}, ionized (free) calcium; K^+, potassium; OR, odds ratio; POC, point-of-care; TCO_2, total dissolved carbon dioxide.
†No evidence of nonlinearity of the continuous variables except for glucose, which was transformed to the power of –2.
‡POC+ model includes 3 POC measurements (blood creatinine, calcium, and hemoglobin) plus the cycle threshold value of the diagnostic Ebola PCR result and the age of the patient.

brief patient contact remains challenging, and to what extent the ratio of BUN to creatinine is accurate in EVD patients is unclear (*17*). Whether biochemical diagnosis (and management) of kidney dysfunction substantially improves patient outcomes compared with monitoring urine output and clinically assessing fluid status also remains unknown. It would be more useful to monitor for renal dysfunction if compensatory measures such as dialysis could be put in place (*34*). Clinical trials would be required to assess this further, looking at case-fatality rate reduction, risk to healthcare staff, and opportunity costs (*9*). As blood transfusion requires blood group testing and, ideally, bedside cross-matching, risk-benefit assessments for this intervention would also be useful to inform treatment guidelines.

We acknowledge that underestimation of the prevalence of abnormalities is probable because as measurements were not systematically performed during the entire stay in the ETU. Still, our findings show that a POC device is practical to use in the ETU and could be useful in stratifying patients into risk groups at baseline. Information on the extent POC results were used by the clinicians would also have strengthened the study.

In conclusion, in the challenging environment of an ETU, staff wearing full protective equipment were able to use a POC device that frequently detected metabolic and electrolyte abnormalities among EVD patients at admission. Besides age and diagnostic PCR C_t value, renal dysfunction, low calcium levels, and low hemoglobin levels were independently associated with an increased risk for death. A clinical prognostic model using these 5 factors had a high discriminatory potential, with most patients having either very low (<5%) or very high (>80%) risk for death. To what extent interventions aiming at correcting the observed abnormalities can reduce case-fatality rates remains to

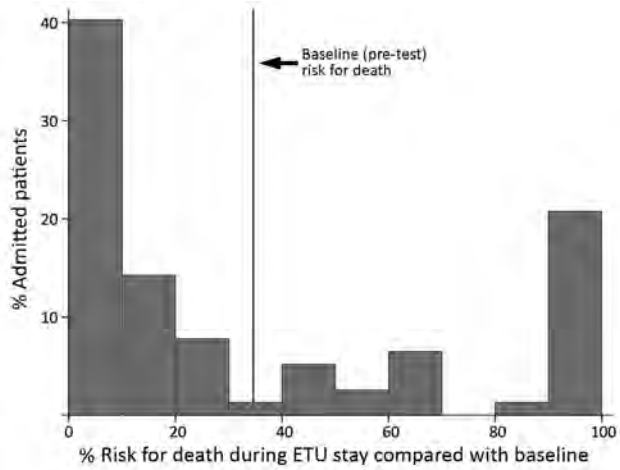

Figure 1. Histogram displaying the distribution of the risk for death for Ebola patients recruited for the Ebola-Tx trial, Conakry, Guinea, 2015, according to a 5-variable point-of-care (POC+) prognostic prediction model. POC+ model includes 3 POC measurements (blood creatinine, calcium, and hemoglobin) plus the cycle threshold value of the diagnostic Ebola PCR result and the age of the patient. ETU, Ebola treatment unit.

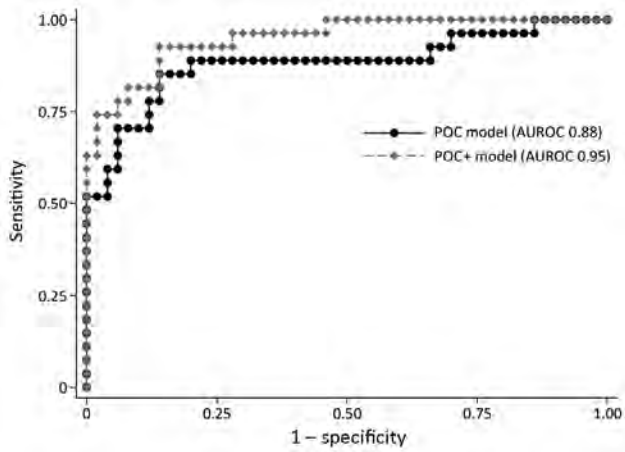

Figure 2. Receiving operating curve summarizing the performance of 3-variable point-of-care (POC) and 5-variable POC+ prognostic prediction models for Ebola patients recruited for the Ebola-Tx trial, Conakry, Guinea, 2015. POC model includes blood creatinine, hemoglobin, and calcium levels. POC+ model includes the same 3 POC measurements plus the cycle threshold value of the diagnostic Ebola PCR result and the age of the patient. AUROC, area under the receiver operating curve; POC, point-of-care.

Table 4. Predicted and observed deaths across risk categories among 77 Ebola patients recruited for the Ebola-Tx trial, according to the POC+ model, Conakry, Guinea, 2015*†

Death risk category (predicted), %	Total no. patients (column %)	No. deaths observed (row %)	No. deaths predicted (row %)
0–4.9	28 (36.4)	1 (3.6)	0.4 (1.5)
5.0–19.9	14 (18.2)	1 (7.1)	1.7 (12.3)
20.0–49.9	11 (14.3)	4 (36.4)	3.7 (34.0)
50.0–79.9	7 (9.1)	4 (57.1)	4.4 (63.5%)
80.0–100	17 (22.1)	17 (100.0)	16.7 (98.1)

*One recruited patient was excluded because of a missing C_t value. C_t, cycle threshold; POC, point-of-care.
†POC+ model includes 3 POC measurements (blood creatinine, calcium, and hemoglobin) plus the cycle threshold value of the diagnostic Ebola PCR result and the age of the patient.

be assessed. Moreover, risk-benefit assessments that consider the risks to healthcare workers are required to inform treatment guidelines.

Acknowledgments

The authors would like to thank the Ebola-Tx consortium and all those who have contributed to the implementation of the Ebola-Tx trial, including public health authorities, National Blood Transfusion Centre staff, Ebola treatment center staff, all Médecins sans Frontières staff, laboratory staff, communities, and Ebola survivors. Our gratitude goes to the Clinical Trials Unit of Institute of Tropical Medicine, which supported the implementation of the trial.

The Ebola-Tx project is funded by the European Union's Horizon 2020 program for research and innovation under grant agreement no. 666094. Additional funding is provided by the Department of Economy, Science, and Innovation of the government of Belgium. The mobile plasma unit used in this trial was provided to Guinea by the Bill and Melinda Gates Foundation. M.G.S. is supported by a grant from the National Institute for Health Research Health Protection Research Unit in the Emerging and Zoonotic Infections Department at the University of Liverpool.

Dr. van Griensven acted as coordinating investigator of the Ebola-Tx trial and is currently leading the unit of HIV and Neglected Tropical Diseases at the Institute of Tropical Medicine in Antwerp, Belgium. His primary research interests include leishmaniasis and emerging infectious disease outbreaks.

References

1. World Health Organization. Ebola situation report—30 March 2016 [cited 2016 Jun 1]. http://apps.who.int/ebola/current-situation/ebola-situation-report-30-march-2016
2. van Griensven J, Edwards T, de Lamballerie X, Semple MG, Gallian P, Baize S, et al. Evaluation of convalescent plasma for Ebola virus disease in Guinea. N Engl J Med. 2016;374:33–42. http://dx.doi.org/10.1056/NEJMoa1511812
3. Dunning J, Sahr F, Rojek A, Gannon F, Carson G, Idriss B, et al. Experimental treatment of Ebola virus disease with TKM-130803: a single-arm phase 2 clinical trial. PLoS Med. 2016;13:e1001997. http://dx.doi.org/10.1371/journal.pmed.1001997
4. Sissoko D, Laouenan C, Folkesson E, M'Lebing AB, Beavogui AH, Baize S, et al. Experimental treatment with favipiravir for Ebola Virus Disease (the JIKI trial): a historically controlled, single-arm proof-of-concept trial in Guinea. PLoS Med. 2016;13:e1001967. http://dx.doi.org/10.1371/journal.pmed.1001967
5. Fletcher TE, Fowler RA, Beeching NJ. Understanding organ dysfunction in Ebola virus disease. Intensive Care Med. 2014;40:1936–9. http://dx.doi.org/10.1007/s00134-014-3515-1
6. Fowler RA, Fletcher T, Fischer WA II, Lamontagne F, Jacob S, Brett-Major D, et al. Caring for critically ill patients with Ebola virus disease. Perspectives from West Africa. Am J Respir Crit Care Med. 2014;190:733–7.
7. Lamontagne F, Clément C, Fletcher T, Jacob ST, Fischer WA II, Fowler RA. Doing today's work superbly well—treating Ebola with current tools. N Engl J Med. 2014;371:1565–6. http://dx.doi.org/10.1056/NEJMp1411310
8. Wong KK, Perdue CL, Malia J, Kenney JL, Peng S, Gwathney JK, et al. Supportive care of the first 2 Ebola virus disease patients at the Monrovia Medical Unit. Clin Infect Dis. 2015;61:e47–51. http://dx.doi.org/10.1093/cid/civ420
9. West TE, von Saint André-von Arnim A. Clinical presentation and management of severe Ebola virus disease. Ann Am Thorac Soc. 2014;11:1341–50. http://dx.doi.org/10.1513/AnnalsATS.201410-481PS
10. Chertow DS, Kleine C, Edwards JK, Scaini R, Giuliani R, Sprecher A. Ebola virus disease in West Africa—clinical manifestations and management. N Engl J Med. 2014;371:2054–7. http://dx.doi.org/10.1056/NEJMp1413084
11. Hunt L, Lee JS. Empiric intravenous fluid and electrolyte therapy in patients with Ebola virus disease. Trop Doct. 2016;46:148–50. http://dx.doi.org/10.1177/0049475516644883
12. Palich R, Gala JL, Petitjean F, Shepherd S, Peyrouset O, Abdoul BM, et al. A 6-year-old child with severe Ebola virus disease: laboratory-guided clinical care in an Ebola treatment center in Guinea. PLoS Negl Trop Dis. 2016;10:e0004393. http://dx.doi.org/10.1371/journal.pntd.0004393
13. Clay KA, Johnston AM, Moore A, O'Shea MK. Targeted electrolyte replacement in patients with Ebola virus disease. Clin Infect Dis. 2015;61:1030–1. http://dx.doi.org/10.1093/cid/civ435
14. Uyeki TM, Mehta AK, Davey RT Jr, Liddell AM, Wolf T, Vetter P, et al. Clinical management of Ebola virus disease in the United States and Europe. N Engl J Med. 2016;374:636–46. http://dx.doi.org/10.1056/NEJMoa1504874
15. Kok J, Sintchenko V, Dwyer DE, Chen SC. Laboratory preparedness for Ebolavirus disease [editorial]. Pathology. 2015;47:397–9. http://dx.doi.org/10.1097/PAT.0000000000000290
16. Hunt L, Knott V. Serious and common sequelae after Ebola virus infection. Lancet Infect Dis. 2016;16:270–1. http://dx.doi.org/10.1016/S1473-3099(15)00546-0
17. Rollin PE, Bausch DG, Sanchez A. Blood chemistry measurements and D-dimer levels associated with fatal and nonfatal outcomes in humans infected with Sudan Ebola virus. J Infect Dis. 2007;196(Suppl 2):S364–71. http://dx.doi.org/10.1086/520613
18. Lyon GM, Mehta AK, Varkey JB, Brantly K, Plyler L, McElroy AK, et al. Clinical care of two patients with Ebola virus disease in the

United States. N Engl J Med. 2014;371:2402–9. http://dx.doi.org/10.1056/NEJMoa1409838
19. Kreuels B, Wichmann D, Emmerich P, Schmidt-Chanasit J, de Heer G, Kluge S, et al. A case of severe Ebola virus infection complicated by gram-negative septicemia. N Engl J Med. 2014;371:2394–401. http://dx.doi.org/10.1056/NEJMoa1411677
20. Steyerberg EW, Moons KG, van der Windt DA, Hayden JA, Perel P, Schroter S, et al. Prognosis Research Strategy (PROGRESS) 3: prognostic model research. PLoS Med. 2013;10:e1001381. http://dx.doi.org/10.1371/journal.pmed.1001381
21. Sterck A. Filovirus haemorrhagic fever guideline [cited 2016 Jun 1]. http://www.medbox.org/ebola-guidelines/filovirus-haemorrhagic-fever-guideline/preview
22. World Health Organization. Haemoglobin concentrations for the diagnosis of anaemia and assessment of severity. Geneva: The Organization; 2011.
23. Bah EI, Lamah MC, Fletcher T, Jacob ST, Brett-Major DM, Sall AA, et al. Clinical presentation of patients with Ebola virus disease in Conakry, Guinea. N Engl J Med. 2015;372:40–7. http://dx.doi.org/10.1056/NEJMoa1411249
24. Faye O, Andronico A, Faye O, Salje H, Boëlle PY, Magassouba N, et al. Use of viremia to evaluate the baseline case fatality ratio of Ebola virus disease and inform treatment studies: a retrospective cohort study. PLoS Med. 2015;12:e1001908. http://dx.doi.org/10.1371/journal.pmed.1001908
25. Harrell FE Jr, Lee KL, Mark DB. Multivariable prognostic models: issues in developing models, evaluating assumptions and adequacy, and measuring and reducing errors. Stat Med. 1996;15:361–87. http://dx.doi.org/10.1002/(SICI)1097-0258(19960229)15:4<361::AID-SIM168>3.0.CO;2-4
26. Hunt L, Gupta-Wright A, Simms V, Tamba F, Knott V, Tamba K, et al. Clinical presentation, biochemical, and haematological parameters and their association with outcome in patients with Ebola virus disease: an observational cohort study. Lancet Infect Dis. 2015;15:1292–9. http://dx.doi.org/10.1016/S1473-3099(15)00144-9
27. Forsythe RM, Wessel CB, Billiar TR, Angus DC, Rosengart MR. Parenteral calcium for intensive care unit patients. Cochrane Database Syst Rev. 2008;4:CD006163. http://dx.doi.org/10.1002/14651858.CD006163.pub2
28. Collage RD, Howell GM, Zhang X, Stripay JL, Lee JS, Angus DC, et al. Calcium supplementation during sepsis exacerbates organ failure and mortality via calcium/calmodulin-dependent protein kinase kinase signaling. Crit Care Med. 2013;41:e352–60. http://dx.doi.org/10.1097/CCM.0b013e31828cf436
29. van Griensven J, Phirum L, Thai S, Buyze J, Lynen L. A clinical prediction score for targeted creatinine testing before initiating tenofovir-based antiretroviral treatment in Cambodia. J Acquir Immune Defic Syndr. 2014;65:e150–2. http://dx.doi.org/10.1097/QAI.0000000000000022
30. van Griensven J, Phan V, Thai S, Koole O, Lynen L. Simplified clinical prediction scores to target viral load testing in adults with suspected first line treatment failure in Phnom Penh, Cambodia. PLoS One. 2014;9:e87879. http://dx.doi.org/10.1371/journal.pone.0087879
31. Hébert PC, Wells G, Tweeddale M, Martin C, Marshall J, Pham B, et al. Does transfusion practice affect mortality in critically ill patients? Transfusion Requirements in Critical Care (TRICC) Investigators and the Canadian Critical Care Trials Group. Am J Respir Crit Care Med. 1997;155:1618–23. http://dx.doi.org/10.1164/ajrccm.155.5.9154866
32. Hébert PC, Wells G, Blajchman MA, Marshall J, Martin C, Pagliarello G, et al. A multicenter, randomized, controlled clinical trial of transfusion requirements in critical care. Transfusion Requirements in Critical Care Investigators, Canadian Critical Care Trials Group. N Engl J Med. 1999;340:409–17. http://dx.doi.org/10.1056/NEJM199902113400601
33. Schieffelin JS, Shaffer JG, Goba A, Gbakie M, Gire SK, Colubri A, et al. Clinical illness and outcomes in patients with Ebola in Sierra Leone. N Engl J Med. 2014;371:2092–100. http://dx.doi.org/10.1056/NEJMoa1411680
34. Faubel S, Franch H, Vijayan A, Barron MA, Heung M, Liu KD, et al. Preparing for renal replacement therapy in patients with the Ebola virus disease. Blood Purif. 2014;38:276–85. http://dx.doi.org/10.1159/000371530

Address for correspondence: Johan van Griensven, Nationalestraat 155, 2000 Antwerp, Belgium; email: jvangriensven@itg.be

Baylisascaris procyonis Roundworm Seroprevalence among Wildlife Rehabilitators, United States and Canada, 2012–2015

Sarah G.H. Sapp, Lisa N. Rascoe, Patricia P. Wilkins, Sukwan Handali, Elizabeth B. Gray, Mark Eberhard, Dana M. Woodhall, Susan P. Montgomery, Karen L. Bailey, Emily W. Lankau,[1] Michael J. Yabsley

Baylisascaris procyonis roundworms can cause potentially fatal neural larva migrans in many species, including humans. However, the clinical spectrum of baylisascariasis is not completely understood. We tested 347 asymptomatic adult wildlife rehabilitators for *B. procyonis* antibodies; 24 were positive, suggesting that subclinical baylisascariasis is occurring among this population.

Baylisascaris procyonis, a roundworm of raccoons (*Procyon lotor*) and rarely dogs, can cause fatal neural larva migrans or ocular larval migrans in numerous bird and mammal species, including humans (*1*). At least 54 human cases have been reported; however, cases may not have been recognized or reported, especially ocular cases, for which parasite identification is rare (*1*–*3*). Most diagnosed cases have been in children and were severe or fatal. Treatment is difficult after onset of neurologic symptoms, and neural larva migrans survivors may have permanent neurologic sequelae (*1*).

The clinical spectrum of baylisascariasis is not fully understood. Limited evidence suggests that subclinical disease may occur (*1*,*2*,*4*,*5*). *Baylisascaris* larvae were an incidental finding in the brain of an Alzheimer disease patient (*4*), and *B. procyonis* antibodies were reported in the parents of a child with baylisascariasis and in 4 of 13 adults in Germany with raccoon contact; assay specificity was not reported (*2*,*5*). The occurrence of subclinical infections with related ascarids (e.g., *Toxocara* species) is well established; up to 14% of persons in the United States are seropositive, although it is unknown how many have clinical manifestations (*6*).

Author affiliations: University of Georgia, Athens, Georgia, USA (S.G.H. Sapp, K.L. Bailey, E.W. Lankau, M.J. Yabsley); Centers for Disease Control and Prevention, Atlanta, Georgia, USA (L.N. Rascoe, P.P. Wilkins, S. Handali, E.B. Gray, M. Eberhard, D.M. Woodhall, S.P. Montgomery); Kentucky Wildlife Center, Lexington, Kentucky, USA (K.L. Bailey)

DOI: http://dx.doi.org/10.3201/eid2212.160467

Wildlife rehabilitators may represent a population at risk for subclinical baylisascariasis due to frequent contact with raccoons and their feces, which may contain infectious larvated *B. procyonis* eggs. We assessed the occurrence of antibodies to *B. procyonis* in a sample of wildlife rehabilitators from the United States and Canada and administered a questionnaire on rehabilitation experience and procedures.

The Study

During 2012–2015, we collected serum samples from and administered questionnaires to wildlife rehabilitators (details in online Technical Appendix, http://wwwnc.cdc.gov/EID/article/22/12/16-0467-Techapp1.pdf). We tested serum samples for *B. procyonis* IgG using a recombinant *B. procyonis* repeat antigen 1 protein Western blot as described (*7*).

Of 347 enrolled persons (Table 1), 315 (91%) reported current involvement in rehabilitation activities. Participants had an average of 10.5 (median 7.0) years of animal rehabilitation experience. Most respondents (92%) reported having contact with raccoons at some point; 64% reported actively rehabilitating raccoons in the past year (Table 2).

Twenty-four (7%; 95% CI 4.7%–10.1%) participants tested positive for *B. procyonis* antibodies; adjusted prevalence, considering assay performance characteristics, was 5.7% (95% CI 2.2%–9.2%) (Figure) (*12*). Of those 24 participants, 22 (92%) were actively rehabilitating wildlife; the other 2 reported occasional wildlife contact, including contact with raccoons, through veterinary clinic activities. All but 2 seropositive persons reported raccoon contact, and 2 practiced rehabilitation in the same household. Nineteen (79%) of the 24 seropositive persons resided in a US state or Canadian province classified as having very high or high *B. procyonis* prevalence among raccoons (Table 2).

Conclusions

We detected antibodies to *B. procyonis* roundworms in 7% of wildlife rehabilitators we tested, suggesting that exposure to this zoonotic parasite may occur without clinical disease. Participants reported various degrees of raccoon contact. Although the transmission source could not be determined (i.e., from rehabilitation of raccoons or from exposure to eggs during other activities), use of gloves and handwashing was generally inconsistent among the

[1]Current affiliation: Ronin Institute, Montclair, New Jersey, USA.

Table 1. Demographic characteristics of participants in a study of *Baylisascaris procyonis* roundworm seroprevalence among wildlife rehabilitators, United States and Canada, 2012–2015

Variable	No. (%) respondents, N = 347	No. (%) seropositive
Sex		
Female	299 (86.2)	21 (7.0)
Male	48 (13.8)	3 (6.3)
Race		
Asian	6 (1.7)	0
American Indian or Alaska Native	1 (0.3)	0
Black or African American	1 (0.3)	0
White	327 (94.2)	23 (7.0)
Other	2 (0.6)	0
Multiracial	10 (2.9)	1 (10.0)
Ethnicity		
Hispanic	5 (1.4)	0
Not Hispanic	315 (90.8)	19 (6.0)
Declined to state	27 (7.8)	5 (18.5)
Geographic region of rehabilitation activities*		
Northeastern	106 (30.5)	4 (3.8)
Midwestern	74 (21.3)	8 (10.8)
Central	23 (6.6)	0
Southern	110 (31.7)	5 (4.5)
Western	34 (9.8)	7 (20.6)

*Geographic regions are defined as follows: Northeastern: Delaware, Maryland, Massachusetts, Maine, New Jersey, New York, Pennsylvania, and Virginia, USA, and Quebec Province, Canada; Midwestern: Illinois, Indiana, Kentucky, Michigan, Minnesota, Missouri, Ohio, and Wisconsin , USA, and Manitoba and Ontario Provinces, Canada; Central: Arizona, Colorado, Kansas, Oklahoma, and Texas, and Alberta, Province, Canada; Southern: Alabama, Florida, Georgia, Louisiana, Mississippi, North Carolina, South Carolina, and Tennessee, USA; and Western: California, Oregon, and Washington, USA, and British Columbia Province, Canada.

seropositive persons in this study (S.G.H. Sapp, data not shown). *B. procyonis* is transmitted by ingestion of larvated eggs; thus, proper use of personal protective equipment (PPE), adherence to cleaning and disinfection protocols, and proper hand hygiene should minimize the risk associated with exposure to feces.

Transmission risk can also occur when handling animals whose fur has been contaminated by infective raccoon eggs, as shown for *Toxocara canis* parasites and dog fur (*13*). More investigations are needed regarding the occurrence of *B. procyonis* eggs on raccoon fur and transmission implications. Lapses in PPE use and hand hygiene may indicate a lack of caution or risk awareness for other pathogens.

Wildlife rehabilitators in areas with a very high prevalence of *B. procyonis* infection among raccoons may be at

Table 2. Rehabilitation work characteristics and experience of wildlife rehabilitators enrolled in a study of *Baylisascaris procyonis* roundworm seroprevalence among wildlife rehabilitators, United States and Canada, 2012–2015

Variable	No. (%) respondents	No. (%) seropositive
Involvement in wildlife rehabilitation, N = 347		
Currently involved	314 (90.5)	22 (7.0)
Formerly involved	19 (5.5)	0 (0)
Other raccoon contact	14 (4.0)	2 (14.3)
Rehabilitation experience, y, N = 322		
<2.0	48 (14.9)	2 (4.2)
2.0–4.9	96 (29.8)	7 (7.3)
5.0–9.9	67 (20.8)	1 (1.5)
10.0–20.0	64 (19.9)	8 (12.5)
>20.0	47 (14.6)	3 (6.4)
Raccoon rehabilitation, N = 347		
Rehabilitated raccoons in past year	222 (64.0)	16 (7.2)
Rehabilitated raccoons (prior to past year)	41 (11.8)	2 (4.9)
Never rehabilitated raccoons	84 (24.2)	6 (7.1)
General raccoon contact, N = 329		
Had contact in past year	266 (80.9)	19 (7.1)
Had contact ever	36 (10.9)	3 (8.3)
Never had contact	27 (8.2)	2 (7.4)
B. procyonis prevalence among raccoons in state or province of residence, N = 347*		
Very high (>50%)	79 (22.8)	14 (21.5)
High (25%–49%)	127 (36.6)	5 (4.6)
Medium (10%–24%)	92 (26.5)	4 (4.3)
Low (<10%), sporadic, or unknown	49 (14.1)	1 (2.1)

*Prevalence levels in the various US states and Canadian Provinces are shown in the Figure.

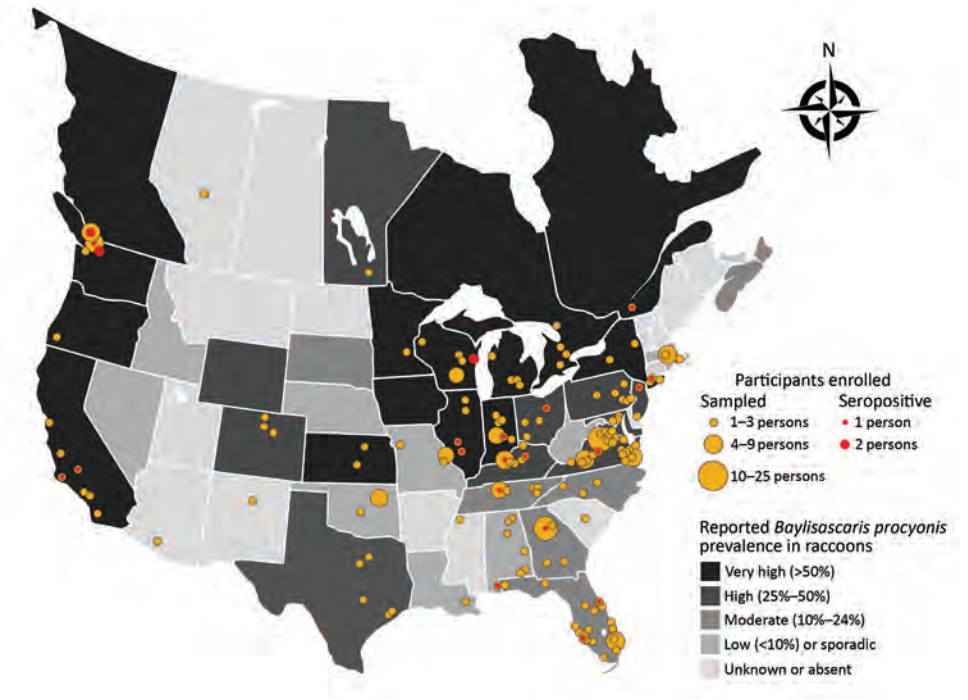

Figure. Locations for participant sampling in a study of *Baylisascaris procyonis* roundworm seroprevalence among wildlife rehabilitators, United States and Canada, 2012–2015. Yellow dots indicate counties (USA) or township/municipality (Canada) in which enrolled persons reported practicing wildlife rehabilitation. Red dots indicate locations of seropositive persons. Shading of states/provinces indicates general state/province level prevalence of *B. procyonis* in raccoons based on published reports (*1*,*8*–*11*).

elevated risk for subclinical infections. Only 1 *B. procyonis*–seropositive wildlife rehabilitator resided in a state with low or sporadic prevalence (Alabama); however, that person lived in an area adjacent to a Florida county where the prevalence of *B. procyonis* infection in raccoons was 9% (M.J. Yabsley, unpub. data) (Figure). Data on *B. procyonis* prevalence in raccoons are outdated or missing for many US states and Canadian provinces. Furthermore, raccoon infections with *B. procyonis* are now being reported in areas where the parasite has historically been absent (e.g., the southeastern United States); thus, awareness of this parasite may be limited in those areas (*8*). More surveillance is needed on the distribution and prevalence of *B. procyonis* infection among raccoons to assess the association with exposure risks among humans.

Rehabilitation facilities housing raccoons can easily be contaminated with *B. procyonis* because high numbers of environmentally hardy eggs are passed by infected raccoons (*1*). Our finding of 2 seropositive raccoon rehabilitators operating out of the same household highlights the importance of infection-control practices. Facility contamination can be prevented by treating raccoons for parasites at intake and at regular intervals thereafter and by sterilizing enclosures using heat-based methods (*14*). Several anthelmintic drugs can kill adult *B. procyonis*, but raccoons with high worm burdens may require retreatment (*15*). Raccoon enclosures and housing should be constructed with materials that are easy to clean and disinfect using heat-based methods.

We tested persons with wildlife (mostly raccoon) contact, so our results describe an exposure risk that likely does not apply to the general public. However, persons in other occupations or activities (e.g., zoo keepers, wildlife biologists) may have similar exposure risks. Domestic dogs, other wildlife species (e.g., skunks, bears), and some exotic pets (e.g., kinkajous) are hosts for *Baylisascaris* spp. parasites and may present exposure risks (*1*). Although the assay we used has a sensitivity of 88% and specificity of 98%, it is time-consuming and not ideal for large-scale epidemiologic studies (*7*). Development of a high-quality ELISA would facilitate larger epidemiologic studies on the risk for baylisascariasis among different demographic groups and help further elucidate specific risk factors.

Our study had several limitations. We used a convenience sampling, so not all regions were well represented, and sample size was relatively small. Our prevalence estimate may be inflated because positive predictive value is reduced in populations in which prevalence is low. The assay we used is the reference standard for clinical diagnosis but has not been used to test asymptomatic persons. Although an association between human *B. procyonis* exposure and seroconversion has not been established, asymptomatic seropositive infections would be expected because clinical disease probably occurs only when larvae cause damage to neural tissue or eyes (*1*). An estimated 95% of migrating larvae enter muscle or visceral organs, where they may stimulate an immune response but not cause clinical disease (*1*). In support of this presumption, the assay we used indicated that experimental infections of *Peromyscus* rodents with low numbers of *B. procyonis* parasites resulted in no

clinical disease with seroconversion (S.G.H. Sapp, unpub. data). Last, participants were primarily licensed rehabilitators who belonged to professional organizations, and many practiced rehabilitation in large, dedicated facilities. Such facilities generally have safety protocols that may encourage more consistent PPE use and awareness of zoonotic diseases, so the risk for infection may be greater in smaller or informal rehabilitation settings.

To prevent infection with *B. procyonis* parasites, proper PPE and hand hygiene practices should be used consistently when handling animals and when contact with animal feces might occur. Education materials and outreach efforts discussing PPE use, infection control, and zoonotic pathogens should be directed to wildlife rehabilitators to increase awareness of potential occupational risks.

Acknowledgments

We thank all study participants for volunteering and members of the National Wildlife Rehabilitators Association, International Wildlife Rehabilitation Council, Florida Wildlife Rehabilitators Association, and Wildlife Center of Virginia for coordinating recruitment events.

Some financial support was provided by the wildlife management agencies of the Southeastern Cooperative Wildlife Disease Study member states through the Federal Aid to Wildlife Restoration Act (50 Stat. 917) and by the US Department of the Interior Cooperative Agreement G11AC20003.

Ms. Sapp is a doctoral student in the Department of Infectious Diseases at the University of Georgia. Her research interests include the epidemiology of parasitic zoonoses and other emerging zoonotic diseases.

References

1. Kazacos KR. *Baylisascaris* larva migrans. Circular series no. 1412. Reston (VA): US Geological Survey; 2016.
2. Cunningham CK, Kazacos KR, McMillan JA, Lucas JA, McAuley JB, Wozniak EJ, et al. Diagnosis and management of *Baylisascaris procyonis* infection in an infant with nonfatal meningoencephalitis. Clin Infect Dis. 1994;18:868–72. http://dx.doi.org/10.1093/clinids/18.6.868
3. Cortez RT, Ramirez G, Collet L, Giuliari GP. Ocular parasitic diseases: a review on toxocariasis and diffuse unilateral subacute neuroretinitis. J Pediatr Ophthalmol Strabismus. 2011;48:204–12. http://dx.doi.org/10.3928/01913913-20100719-02
4. Hung T, Neafie RC, Mackenzie IR. *Baylisascaris procyonis* infection in elderly person, British Columbia, Canada. Emerg Infect Dis. 2012;18:341–2. http://dx.doi.org/10.3201/eid1802.111046
5. Conraths FJ, Bauer C, Cseke J, Laube H. Arbeitsplatzbedingte Infektionen des Menschen mit dem Waschbärspulwurm (*Baylisascaris procyonis*). Arbeitsmed Sozialmed Umweltmed. 1996;31:13–7.
6. Won KY, Kruszon-Moran D, Schantz PM, Jones JL. National seroprevalence and risk factors for zoonotic *Toxocara* spp. infection. Am J Trop Med Hyg. 2008;79:552–7.
7. Rascoe LN, Santamaria C, Handali S, Dangoudoubiyam S, Kazacos KR, Wilkins PP, et al. Interlaboratory optimization and evaluation of a serological assay for diagnosis of human baylisascariasis. Clin Vaccine Immunol. 2013;20:1758–63. http://dx.doi.org/10.1128/CVI.00387-13
8. Blizzard EL, Yabsley MJ, Beck MF, Harsch S. Geographic expansion of *Baylisascaris procyonis* roundworms, Florida, USA. Emerg Infect Dis. 2010;16:1803–4. http://dx.doi.org/10.3201/eid1611.100549
9. Chavez DJ, LeVan IK, Miller MW, Ballweber LR. *Baylisascaris procyonis* in raccoons (*Procyon lotor*) from eastern Colorado, an area of undefined prevalence. Vet Parasitol. 2012;185:330–4. http://dx.doi.org/10.1016/j.vetpar.2011.11.002
10. Cottrell WO, Heagy RL, Johnson JB, Marcantuno R, Nolan TJ. Geographic and temporal prevalence of *Baylisascaris procyonis* in raccoons (*Procyon lotor*) in Pennsylvania, USA. J Wildl Dis. 2014;50:923–7. http://dx.doi.org/10.7589/2014-02-032
11. Pipas MJ, Page LK, Kazacos KR. Surveillance for *Baylisascaris procyonis* in raccoons (*Procyon lotor*) from Wyoming, USA. J Wildl Dis. 2014;50:777–83. http://dx.doi.org/10.7589/2013-10-263
12. Reiczigel J, Földi J, Ozsvári L. Exact confidence limits for prevalence of a disease with an imperfect diagnostic test. Epidemiol Infect. 2010;138:1674–8. http://dx.doi.org/10.1017/S0950268810000385
13. Amaral HLDC, Rassier GL, Pepe MS, Gallina T, Villela MM, Nobre MO, et al. Presence of *Toxocara canis* eggs on the hair of dogs: a risk factor for visceral larva migrans. Vet Parasitol. 2010;174:115–8. http://dx.doi.org/10.1016/j.vetpar.2010.07.016
14. Shafir SC, Sorvillo FJ, Sorvillo T, Eberhard ML. Viability of *Baylisascaris procyonis* eggs. Emerg Infect Dis. 2011;17:1293–5. http://dx.doi.org/10.3201/eid1707.101774
15. Bauer C, Gey A. Efficacy of six anthelmintics against luminal stages of *Baylisascaris procyonis* in naturally infected raccoons (*Procyon lotor*). Vet Parasitol. 1995;60:155–9. http://dx.doi.org/10.1016/0304-4017(94)00774-7

Address for correspondence: Sarah G.H. Sapp, Southeastern Cooperative Wildlife Disease Study, College of Veterinary Medicine; University of Georgia, Wildlife Disease Bldg, Athens, GA 30605, USA; email: sgsapp@uga.edu

Genetically Different Highly Pathogenic Avian Influenza A(H5N1) Viruses in West Africa, 2015

Luca Tassoni, Alice Fusaro, Adelaide Milani, Philippe Lemey, Joseph Adongo Awuni, Victoria Bernice Sedor, Otilia Dogbey, Abraham Nii Okai Commey, Clement Meseko, Tony Joannis, Germaine L. Minoungou, Lassina Ouattara, Abdoul Malick Haido, Diarra Cisse-Aman, Emmanuel Couacy-Hymann, Gwenaelle Dauphin, Giovanni Cattoli, Isabella Monne

To trace the evolution of highly pathogenic influenza A(H5N1) virus in West Africa, we sequenced genomes of 43 viruses collected during 2015 from poultry and wild birds in 5 countries. We found 2 co-circulating genetic groups within clade 2.3.2.1c. Mutations that may increase adaptation to mammals raise concern over possible risk for humans.

In December 2014, a strain of highly pathogenic avian influenza (HPAI) A(H5N1) virus responsible for deaths among poultry was detected in southwestern Nigeria, specifically in a live bird market in Lagos State (*1*). Since then, other outbreaks have occurred in Nigeria, and the HPAI A(H5N1) virus has also been officially reported in Burkina Faso (February 2015) and Niger, Ghana, and Côte d'Ivoire (April 2015), to date causing the death of ≈1.6 million birds (*2*).

Author affiliations: Istituto Zooprofilattico Sperimentale delle Venezie, Legnaro, Italy (L. Tassoni, A. Fusaro, A. Milani, I. Monne); University of Leuven, Leuven, Belgium (P. Lemey); Veterinary Services Directorate of Ministry of Food and Agriculture, Accra, Ghana (J. Adongo Awuni, V.B. Sedor, O. Dogbey, A.N.O. Commey); National Veterinary Research Institute, Vom, Nigeria (C. Meseko, T. Joannis); Laboratoire National d'Elevage, Ouagadougou, Burkina Faso (G. Minoungou); Ministère des Ressources Animales, Ouagadougou (L. Ouattara); Direction de la Santé Animale, Niamey, Niger (A.M. Haido); Ministère des Ressources Animales et Halieutiques, Abidjan, Côte d'Ivoire (D. Cisse-Aman); Laboratoire Central de Pathologie Animale, Bingerville, Côte d'Ivoire (E. Couacy-Hymann); Food and Agriculture Organization of the United Nations, Rome, Italy (G. Dauphin); International Atomic Energy Agency, Seibersdorf, Austria (G. Cattoli)

DOI: http://dx.doi.org/10.3201/eid2212.160578

Previous HPAI A(H5N1) epidemics in West Africa occurred in 2006–2008 and involved exclusively viruses of clade 2.2 (*3*). So far, a full-genome characterization is publicly available for only 1 HPAI A(H5N1) virus, collected in Nigeria in early 2015 (*4*) and classified as clade 2.3.2.1c. To our knowledge, this clade has not been previously detected in Africa. Since 2009, this clade has been widely circulating in domestic and wild birds in several countries in Asia (*5*); in 2010, it was reported in Europe (*6*) and in 2014, in the Middle East (*7*). In 2015, clade 2.3.2.1c was detected in rooks, chickens, and dalmatian pelicans in Russia, Bulgaria, and Romania, respectively (*8*). To trace the evolution of HPAI A(H5N1) virus in West Africa, we examined the genetic characteristics of 43 such viruses collected during January–August 2015 in all affected countries in West Africa.

The Study

From January through October 2015, a total of 248 samples (organ tissue and swab samples) from poultry and wild birds suspected of being infected with HPAI A(H5N1) virus in 6 countries in West Africa were sent for diagnostic confirmation to the World Organisation for Animal Health Reference Laboratory and the Food and Agriculture Organization of the United Nations Reference Center for Animal Influenza at the Istituto Zooprofilattico Sperimentale delle Venezie. Consistent with the laboratory test results provided by the submitting national veterinary laboratories, the presence of HPAI A(H5N1) virus was confirmed for 5 countries: Nigeria, Burkina Faso, Niger, Côte d'Ivoire, and Ghana. All samples positive for influenza A(H5N1) virus were sequenced by using Illumina MiSeq (San Diego, CA, USA) technology; complete coding sequences were obtained for 39 viruses, and the partial genome was obtained for 4 others (Table). To obtain consensus sequences later submitted to public databases (accession numbers in Table), we processed reads as described in Monne et al. (*9*).

We performed phylogenetic analyses for each genome segment by using PhyML 3.0 (*10*), incorporating a general time reversible model of nucleotide substitution with a gamma distribution of among-site rate variation (with 4 rate categories) and a subtree pruning and regrafting branch-swapping search procedure. The topology of the 8 phylogenetic trees shows that viruses collected from West

Table. Epidemiologic information for sequenced samples from poultry and wild birds positive for influenza A(H5N1) virus, West Africa*

Name	Sequenced genome	Collection date	Country, location	DB	Accession nos.
A/chicken/Ghana/15VIR5480-3/2015	Complete	2015 Jul 28	Ghana, Greater Accra	GB	KU971453–60
A/partridge/Ghana/15VIR5480-5/2015	Complete	2015 Jul 27	Ghana; Greater Accra	GB	KU971461–68
A/chicken/Ghana/15VIR5480-7/2015	Complete	2015 Jul 28	Ghana, Greater Accra	GB	KU971469–76
A/chicken/Ghana/15VIR5480-10/2015	Complete	2015 Aug 7	Ghana	GB	KU971397–04
A/chicken/Ghana/15VIR5480-12/2015	Complete	2015 Jul 27	Ghana, Greater Accra	GB	KU971405–12
A/chicken/Ghana/15VIR5480-14/2015	Complete	2015 Aug 7	Ghana, Greater Accra	GB	KU971413–20
A/duck/Ghana/15VIR5480-16/2015	Complete	2015 Jul 27	Ghana, Greater Accra	GS	EPI687323; EPI719449–55
A/chicken/Ghana/15VIR5480-18/2015	Complete	2015 Aug 7	Ghana, Greater Accra	GB	KU971421–28
A/chicken/Ghana/15VIR5480-22/2015	Complete	2015 Aug 7	Ghana, Greater Accra	GS	EPI687324; EPI719911–17
A/duck/Ghana/15VIR5480–24/2015	Complete	2015 Jull 27	Ghana, Greater Accra	GB	KU971429–36
A/chicken/Ghana/15VIR5480-26/2015	Complete	2015 Aug 7	Ghana, Greater Accra	GB	KU971437–44
A/chicken/Ghana/15VIR5480-27/2015	Complete	2015 Aug 7	Ghana, Greater Accra	GB	KU971445–52
A/chicken/Niger/15VIR2060-1/2015	Complete	2015 Apr 2	Niger, Maradi	GB	KU971301–08
A/chicken/Niger/15VIR2060-12/2015	Complete	2015 Apr 2	Niger, Maradi	GB	KU971309–16
A/chicken/Niger/15VIR2060-14/2015	Complete	2015 Apr 2	Niger, Maradi	GB	KU971317–24
A/chicken/Niger/15VIR2060-15/2015	HA	2015 Apr 2	Niger, Maradi	GB	KU971325
A/chicken/Niger/15VIR2060-5/2015	Complete	2015 Apr 2	Niger, Maradi	GB	KU971326–33
A/chicken/Niger/15VIR2060-6/2015	Complete	2015 Apr 2	Niger, Maradi	GB	KU971334–40
A/chicken/Niger/15VIR2060-7/2015	Complete	2015 Apr 2	Niger, Maradi	GB	KU971341–48
A/chicken/Niger/15VIR2060-8/2015	Complete	2015 Apr 2	Niger, Maradi	GB	KU971349–56
A/chicken/Ivory_Coast/15VIR2742-5/2015	Partial	2015 Apr 30	Côte d'Ivoire, Bouaké-Quartier Broukro	GB	KU971578–84
A/turtledove/Ivory_Coast/15VIR2742-7/2015	Complete	2015 Apr 30	Côte d'Ivoire, Bouaké-Quartier Broukro	GB	KU971585–92
A/duck/Ivory_Coast/15VIR2742-2/2015	Complete	2015 Apr 13	Côte d'Ivoire, Bouaké-Quartier Koko	GB	KU971562–69
A/chicken/Ivory_Coast/15VIR2742-3/2015	Complete	2015 Apr 13	Côte d'Ivoire, Bouaké-Quartier Koko	GB	KU971570–77
A/chicken/Burkina_Faso/15VIR1774-1/2015	Partial	2015 Mar 12	Burkina Faso, CPAVI in Ouagadougou	GB	KU971477–83
A/chicken/Burkina_Faso/15VIR1774-2/2015	Complete	2015 Mar 12	Burkina Faso, CPAVI in Ouagadougou	GB	KU971484–91
A/domestic_bird/Burkina_Faso/15VIR1774-22/2015	Complete	2015 Mar 10	Burkina Faso, Sanguiè Province	GB	KU971492–99
A/domestic_bird/Burkina_Faso/15VIR1774-23/2015	Complete	2015 Mar 10	Burkina Faso, Sanguiè Province	GB	KU971500–07
A/domestic_bird/Burkina_Faso/15VIR1774-24/2015	Complete	2015 Mar 10	Burkina Faso, Sanguiè Province	GB	KU971508–15
A/domestic_bird/Burkina_Faso/15VIR1774-25/2015	Complete	2015 Mar 10	Burkina Faso, Sanguiè Province	GB	KU971516–23
A/chicken/Burkina_Faso/15VIR1774-33/2015	Complete	2015 Mar 23	Burkina Faso, Koubri	GB	KU971524–31
A/chicken/Burkina Faso/15VIR1774-35/2015	Complete	2015 Mar 23	Burkina Faso, Koubri	GS	EPI584232; EPI719904–10
A/chicken/Burkina_Faso/15VIR1774-36/2015	Complete	2015 Mar 23	Burkina Faso, Koubri	GB	KU971532–39
A/chicken/Burkina_Faso/15VIR1774-37/2015	Complete	2015 Mar 12	Burkina Faso, CPAVI in Ouagadougou	GB	KU971540–47
A/chicken/Burkina_Faso/15VIR1774-38/2015	Partial	2015 Mar 12	Burkina Faso, CPAVI in Ouagadougou	GB	KU971548–53
A/chicken/Burkina_Faso/15VIR1774-4/2015	Complete	2015 Mar 12	Burkina Faso, CPAVI in Ouagadougou	GB	KU971554–61
A/chicken/Nigeria/15VIR339-1/2015	Complete	2015 Jan 2	Nigeria, Lagos State	GB	KU971593–00
A/chicken/Ghana/15VIR2588-10/2015	Complete	2015 May 8	Ghana, Greater Accra	GB	KU971357–64
A/chicken/Ghana/15VIR2588-11/2015	Complete	2015 May 4	Ghana, Greater Accra	GB	KU971365–72
A/chicken/Ghana/15VIR2588-4/2015	Complete	2015 May	Ghana, Greater Accra	GB	KU971373–80
A/chicken/Ghana/15VIR2588-5/2015	Complete	2015 May	Ghana, Greater Accra	GB	KU971381–88
A/chicken/Ghana/15VIR2588-8/2015	Complete	2015 May 8	Ghana, Greater Accra	GB	KU971389–96
A/chicken/Ghana/15VIR2588-9/2015	Complete	2015 May 4	Ghana, Greater Accra	GS	EPI632942; EPI719456–62

*CPAVI, Centre de Promotion de l'Aviculture Villageoise; DB, database; GB, GenBank; GS, The Global Initiative on Sharing All Influenza Data; HA, hemagglutinin.

Africa in 2015 belong to clade 2.3.2.1c and cluster separately from HPAI A(H5N1) viruses collected from West Africa during the 2006–2008 epidemic (Figure). Specifically, the analyzed viruses grouped with those that have been circulating in Eurasia since 2013 and showed the highest similarity with H5N1 subtype viruses collected in Europe and the Middle East from late 2014 through early 2015. As previously described for influenza A(H5N1) virus (*4*), the viruses from West Africa that we analyzed displayed the same genetic constellation of the A/Alberta/01/2014 virus; the polymerase basic protein 2 segment originated from a reassortment event with subtype H9N2. The hemagglutinin (HA) phylogenetic tree (Figure) shows that the viruses from West Africa constitute 2 main groups, here named WA1 and WA2, supported by high bootstrap values (>73%) and a genetic similarity of 98%–99.1%. WA1 is the most heterogeneous group (identity 98.7%–100%) and contains sequences from all affected countries in West Africa (Nigeria, Niger, Côte d'Ivoire, Burkina Faso, and Ghana). WA2 comprises sequences collected in April 2015

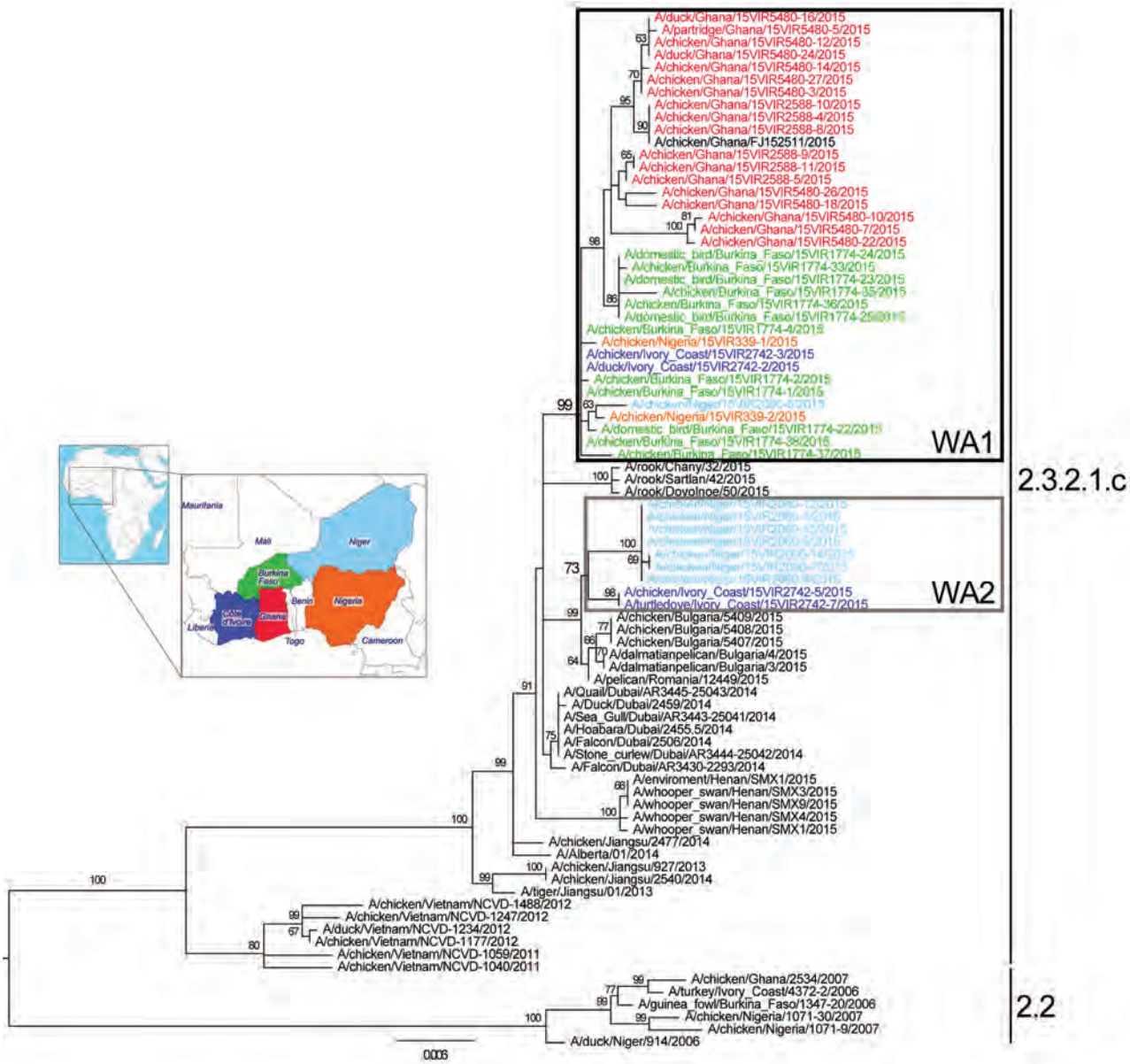

Figure. Maximum-likelihood phylogenetic tree of the hemagglutinin gene segment of highly pathogenic avian influenza (H5N1) viruses from West Africa. Strain colors indicate country of collection (inset). The 2 identified groups (WA1 and WA2) are indicated by boxes (black and gray, respectively). Clades are indicated at right; sequences from the 2006–2008 epidemic (clade 2.2) in West Africa were used as an outgroup. Numbers at the nodes represent bootstrap values >60%, obtained through a nonparametric bootstrap analysis that used 100 replicates. Scale bar indicates nucleotide substitutions per site.

from Niger and Côte d'Ivoire only (identity 99.4%–100%) and clusters together with subtype H5N1 collected during January–March 2015 from wild birds in Europe (Bulgaria and Romania). Of note, viruses in the WA2 group are more closely related to those from Europe (similarity 99.30%–99.65%) than to those in the WA1 group (similarity 97.95%–99.12%), suggesting the occurrence of at least 2 independent introductions of subtype H5N1 in West Africa. Viruses in the WA1 and WA2 groups were isolated in 1 city in Niger and 1 city in Côte d'Ivoire, which suggests their possible co-circulation in the same geographic area.

As with the HA gene, we identified the 2 West Africa groups in all the other phylogenies (supporting bootstrap values >74%), except for the tree of the nonstructural gene segment, in which WA2 does not form a monophyletic group. Unfortunately, only the HA gene segment of the viruses from Europe that clusters with the WA2 group is available in the public database, making the source of the internal genes of the WA2 viruses impossible to trace.

The analysis of molecular markers indicates that all viruses showed mutations D94N (except for A/chicken/Ghana/5480-14/2015), S133A, and S155N (H5 numbering) in the HA protein; these mutations have been shown to increase virus binding to α2,6 sialic acid (*11*). In addition, the analysis of internal proteins identified a mutation associated with enhanced replication efficiency (NP N319K) (*11*) in all WA2 viruses from Niger. Moreover, the alternative reading frame of the polymerase basic protein 1 of the WA2 viruses is truncated (57 aa long), as it is in the Asian and European progenitors. This truncation is common among influenza A viruses of mammals and in HPAI A(H5N1) viruses, and it has been associated with increased virulence in mammals (*12*).

Conclusions

We demonstrated that a reassortant HPAI A(H5N1) clade 2.3.2.1c virus was responsible for infections in 5 West Africa countries. The influenza (H5N1) viruses from West Africa show a close phylogenetic relationship with the HPAI A(H5N1) viruses identified in Europe and the Middle East during late 2014–2015, indicating a Eurasian origin of their progenitors. The route of introduction of this virus is difficult to establish because West Africa offers wintering sites for wild birds coming from the southern Russian regions, Europe, and western Asia (*13*), and it imports live birds from countries in Europe and Asia (*14*).

As with previous epidemics (2006–2008), when distinct introductions and multiple reassortment events were identified (*3*,*15*), we were able to detect the co-circulation of 2 distinct genetic clusters in Côte d'Ivoire and Niger, which suggests that there might have been at least 2 separate introductions into West Africa. However, the limited amount of genetic data available makes it impossible to pinpoint how these viruses entered the continent and spread so widely, and it is not easy to determine the exact number of introductions and where they have occurred in West Africa. Additional virus data from affected countries would help elucidate the epidemiology and the evolution of this virus in this part of the continent.

Of note, all the viruses from West Africa display the same genetic constellation of a strain (A/Alberta/01/2014) isolated from a human, a Canada resident who had returned from China. These viruses contain mutations that have been described as being associated with an enhanced binding affinity for α2,6 sialic acid or with increased virulence in mammals.

As during the 2006–2008 HPAI A(H5N1) epidemics, West Africa countries are again facing devastating economic and social consequences from these infections. It is imperative for regional and international organizations to join forces in generating and making available detailed genetic and epidemiologic information that can be used to better trace the spread and evolution in West Africa of influenza A(H5N1) virus and to provide input for informed decisions on control measures and resource allocation.

Acknowledgments

We thank The World Bank, through the West Africa Agriculture Productivity Project, for financial assistance in the fight to contain HPAI outbreaks in Ghana. We also thank Annalisa Salviato, Alessia Schivo, and Francesca Ellero for their excellent technical assistance. We acknowledge the authors and the originating and submitting laboratories of the sequences from the Global Initiative on Sharing All Influenza Data EpiFlu Database on which this research is based in part (online Technical Appendix, http://wwwnc.cdc.gov/EID/article/22/12/16-0578-Techapp1.pdf).

This study was made possible through technical support provided by the United Nations Food and Agriculture Organization (letter of agreement no. 315535) and partial funding provided by the US Agency for International Development under the OSRO/GLO/407/USA project "Global Health Security in Africa and Asia." The European Union Seventh Framework Programme (FP7/2007-2013) under grant agreement no. 278433-PREDEMICS, also supported part of the sequencing analyses, which generated the study results.

Dr. Tassoni is a biotechnologist at the Istituto Zooprofilattico Sperimentale delle Venezie. His primary research interests include studying the molecular phylogeny and the evolutionary dynamics of viruses.

References

1 World Organization for Animal Health. Highly pathogenic avian influenza in Nigeria—follow-up report no. 27. 15 December 2015 [cited 2016 Jan 11]. http://www.oie.int/wahis_2/temp/reports/en_fup_0000019347_20151215_181155.pdf

2. Food and Agriculture Organization of the United Nations. Worries rise over outbreaks of avian flu in West Africa [cited 2016 Jan 11]. http://www.fao.org/news/story/it/item/297715/icode/
3. Cattoli G, Fusaro A, Monne I, Capua I. H5N1 virus evolution in Europe—an updated overview. Viruses. 2009;1:1351–63. http://dx.doi.org/10.3390/v1031351
4. Monne I, Meseko C, Joannis T, Shittu I, Ahmed M, Tassoni L, et al. Highly pathogenic avian influenza A(H5N1) virus in poultry, Nigeria, 2015. Emerg Infect Dis. 2015;21:1275–7. http://dx.doi.org/10.3201/eid2107.150421
5. World Health Organization/World Organisation for Animal Health/Food and Agriculture Organization (WHO/OIE/FAO) H5N1 Evolution Working Group. Revised and updated nomenclature for highly pathogenic avian influenza A (H5N1) viruses. Influenza Other Respir Viruses. 2014;8:384–8. http://dx.doi.org/10.1111/irv.12230
6. Reid SM, Shell WM, Barboi G, Onita I, Turcitu M, Cioranu R, et al. First reported incursion of highly pathogenic notifiable avian influenza A H5N1 viruses from clade 2.3.2 into European poultry. Transbound Emerg Dis. 2011;58:76–8. http://dx.doi.org/10.1111/j.1865-1682.2010.01175.x
7. Naguib MM, Kinne J, Chen H, Chan KH, Joseph S, Wong PC, et al. Outbreaks of highly pathogenic avian influenza H5N1 clade 2.3.2.1c in hunting falcons and kept wild birds in Dubai implicate intercontinental virus spread. J Gen Virol. 2015;96:3212–22. http://dx.doi.org/10.1099/jgv.0.000274
8. World Organisation for Animal Health. Update on highly pathogenic avian influenza in animals (type H5 and H7) [cited 2016 Jan 11]. http://www.oie.int/en/animal-health-in-the-world/update-on-avian-influenza/2015/
9. Monne I, Fusaro A, Nelson MI, Bonfanti L, Mulatti P, Hughes J, et al. Emergence of a highly pathogenic avian influenza virus from a low-pathogenic progenitor. J Virol. 2014;88:4375–88. http://dx.doi.org/10.1128/JVI.03181-13
10. Guindon S, Dufayard J-F, Lefort V, Anisimova M, Hordijk W, Gascuel O. New algorithms and methods to estimate maximum-likelihood phylogenies: assessing the performance of PhyML 3.0. Syst Biol. 2010;59:307–21. http://dx.doi.org/10.1093/sysbio/syq010
11. Centers for Disease Control and Prevention. H5N1 Genetic Changes Inventory: a tool for international surveillance [cited 2016 Jan 11]. http://www.cdc.gov/flu/avianflu/h5n1-genetic-changes.htm
12. Kamal RP, Kumar A, Davis CT, Tzeng W-P, Nguyen T, Donis RO, et al. Emergence of highly pathogenic avian influenza A(H5N1) virus PB1–F2 variants and their virulence in BALB/c mice. J Virol. 2015;89:5835–46.
13. Olsen B, Munster VJ, Wallensten A, Waldenstrom J, Osterhaus ADME, Fouchier RAM. Global patterns of influenza A virus in wild birds. Science. 2006;312:384–8.
14. Food and Agriculture Organization of the United Nations. H5N1 HPAI spread in Nigeria and increased risk for neighbouring countries in West Africa. Empres Watch. 2015 [cited 2016 Jan 11]. http://www.fao.org/documents/card/en/c/332c88fd-b229-4db7-9a0d-0bd92dfd3374/
15. Fusaro A, Nelson MI, Joannis T, Bertolotti L, Monne I, Salviato A, et al. Evolutionary dynamics of multiple sublineages of H5N1 influenza viruses in Nigeria from 2006 to 2008. J Virol. 2010;84:3239–47. http://dx.doi.org/10.1128/JVI.02385-09

Address for correspondence: Isabella Monne, Istituto Zooprofilattico Sperimentale delle Venezie, Research & Innovation Department, Viale dell'Università 10, 35020, Legnaro, Padova, Italy; email: imonne@izsvenezie.it

Highly Pathogenic Reassortant Avian Influenza A(H5N1) Virus Clade 2.3.2.1a in Poultry, Bhutan

Atanaska Marinova-Petkova,[1,2] John Franks,[1] Sangay Tenzin, Narapati Dahal, Kinzang Dukpa, Jambay Dorjee, Mohammed M. Feeroz, Jerold E. Rehg, Subrata Barman, Scott Krauss, Pamela McKenzie, Richard J. Webby, Robert G. Webster

Highly pathogenic avian influenza A(H5N1), clade 2.3.2.1a, with an H9-like polymerase basic protein 1 gene, isolated in Bhutan in 2012, replicated faster in vitro than its H5N1 parental genotype and was transmitted more efficiently in a chicken model. These properties likely help limit/eradicate outbreaks, combined with strict control measures.

In India and Bangladesh, highly pathogenic avian influenza (HPAI) A(H5N1) viruses of the 2.3.2.1a genetic lineage have circulated in poultry since 2011 (*1*–*3*). Subtype H5N1 endemicity is complicated by co-circulating subtype H9N2, G1_Mideast lineage (*4*,*5*), which derives 5 internal genes from HPAI A(H7N3) virus from Pakistan (*4*). A reassortant H5N1 2.3.2.1a virus, rH5N1, with an H9N2-like polymerase basic protein 1 (PB1) gene (H7N3 origin), was reported in Bangladesh (*2*,*5*,*6*), India, and Nepal (*7*). However, its virulence and transmissibility are undetermined.

In Bhutan, the poultry sector consists of free-range backyard chickens, a rising number of commercial chicken farms, and domestic waterfowl in the south (*8*,*9*). Live-bird markets do not exist, but live birds are imported from India (*8*,*9*).

Bhutan's poultry sector was severely affected by outbreaks of HPAI A(H5N1) clade 2.3.2.1 virus infection during 2012–2013 (*10*). Veterinary authorities enforced strict control measures, including depopulation of poultry in affected regions and burning of related housing and equipment (*11*). Illegal movement of poultry was the major source of outbreaks (*11*). Although the introduction of HPAI A(H5N1) from neighboring H5N1-endemic countries is a constant threat, the subtype is not yet entrenched in poultry in Bhutan.

Author affiliations: St. Jude Children's Research Hospital, Memphis, Tennessee, USA (A. Marinova-Petkova, J. Franks, J.E. Rehg, S. Barman, S. Krauss, P. McKenzie, R.J. Webby, R.G. Webster); National Centre for Animal Health, Ministry of Agriculture and Forests, Thimphu, Bhutan (S. Tenzin, N. Dahal, K. Dukpa, J. Dorjee); Jahangirnagar University, Dhaka, Bangladesh (M.M. Feeroz)

DOI: http://dx.doi.org/10.3201/eid2212.160611

The Study

We isolated HPAI A(H5N1) viruses from samples from 36 chickens and 9 wild birds in Bhutan, all from affected backyard farms adjacent to the highway connecting India with the capital, Thimphu (Figure 1; online Technical Appendix 1 Table 1, http://wwwnc.cdc.gov/EID/article/22/12/16-0611-Techapp1.pdf). Phylogenetic analysis (online Technical Appendix 1) suggested that the 2012–2013 outbreaks in Bhutan were caused by the rH5N1 genotype (2.3.2.1a/H9-like PB1 [H7N3 origin]), reported in Bangladesh and India at that time (online Technical Appendix 1 Figures 1, 2; other data not shown). PB1 phylogeny suggested that this genotype underwent 4 independent reassortment events on the Indian subcontinent (online Technical Appendix 1 Figure 2).

Antigenic analysis of selected H5N1 isolates from Bhutan (online Technical Appendix 1) showed homogeneity and a reactivity pattern similar to that of H5N1 reference viruses from Bangladesh (Table). Amino acid differences were observed between strains A/chicken/Bhutan/346/2012 (Ck/Bh/346) (rH5N1) and A/chicken/Bangladesh/22478/2014 (Ck/BD/22478), representing the parental H5N1 clade 2.3.2.1a genotype (pH5N1) (online Technical Appendix 1 Table 2).

To assess whether the rH5N1-PB1 gene conferred a fitness advantage over the pH5N1 genotype, we examined replication kinetics in vitro (online Technical Appendix 1). The replication patterns of rH5N1 and pH5N1 were similar in Madin-Darby canine kidney (mammalian) cells (Figure 2, panel A). However, in chicken embryo fibroblasts (CEFs), Ck/Bh/346 (rH5N1) titers were significantly higher than those of Dk/BD/21326 (rH5N1) ($p<0.05$) and Ck/BD/22478 (pH5N1) ($p<0.01$) at 12 hours postinoculation (hpi) and those of Ck/BD/22478 (pH5N1) ($p<0.001$), and Dk/BD/19097 (pH5N1) ($p<0.01$) at 24 hpi. Dk/BD/21326 (rH5N1) had significantly higher titers than did Ck/BD/22478 (pH5N1) ($p<0.01$) at 24 hpi

[1]These authors contributed equally to this article.

[2]Current affiliation: Centers for Disease Control and Prevention, Atlanta, Georgia, USA.

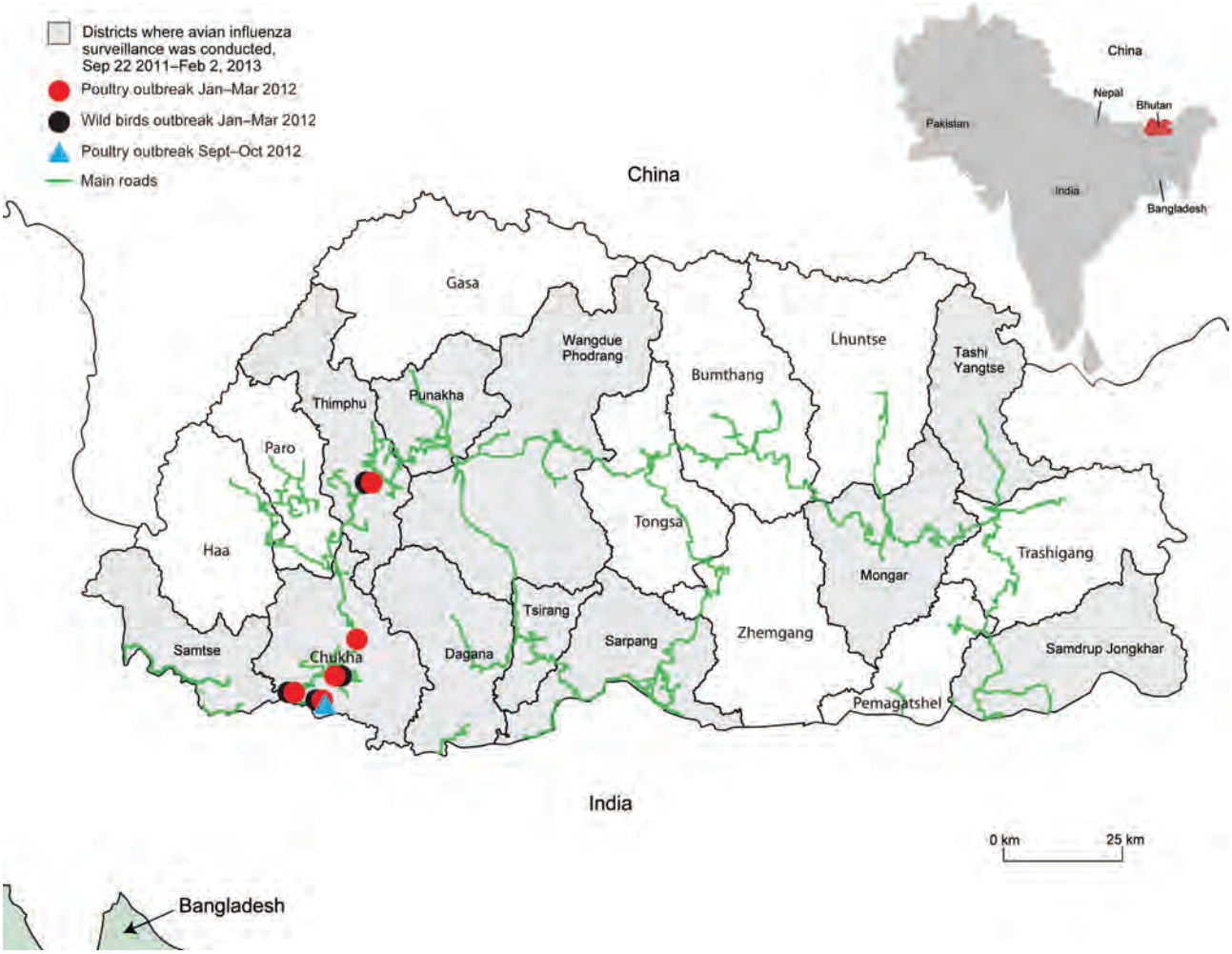

Figure 1. Locations of outbreaks of highly pathogenic avian influenza (H5N1) virus, Bhutan, 2011–2013.

(Figure 2, panel B). These results suggest rH5N1 viruses have a selective growth advantage in avian cells at early time points.

Next, we examined whether this growth advantage reflected higher pathogenicity or transmissibility for Ck/Bh/346 (rH5N1) in chickens than did Ck/BD/22478 (pH5N1) (online Technical Appendix 1). The 50% lethal dose (LD_{50}) for chicken was 16 EID_{50} (50% egg infective dose) for Ck/Bh/346 (rH5N1) and 50 EID_{50} for Ck/BD/22478 (pH5N1). After inoculation with 30 LD_{50} and cohousing with naive contacts, all donors shed virus oropharyngeally and cloacally (Figure 2, panels C, D). All Ck/Bh/346 (rH5N1) donors died within 48 hpi, whereas only 50% of chickens inoculated with Ck/BD/22478 (pH5N1) died. Naive chickens in contact with donors inoculated with Ck/Bh/346 (rH5N1) or Ck/BD/22478 (pH5N1) became infected by day 2 after contact (Figure 2, panel C), started shedding cloacally on day 3 (Figure 2, panel D), and died by day 4. On day 3 after contact, Ck/Bh/346 (rH5N1) contacts had oropharyngeal and cloacal titers >1 $\log_{10}$ EID_{50}/mL higher than those of Ck/BD/22478 (pH5N1) contacts (Figure 2, panels C, D), but the difference was not significant.

We placed Ck/Bh/346 (rH5N1) and Ck/BD/22478 (pH5N1) in direct competition by co-housing chickens inoculated with each virus with naive contacts (online Technical Appendix 1). All donors shed virus oropharyngeally and cloacally, starting at 1 day postinoculation (dpi). By day 3 after contact, real-time reverse transcription PCR to detect PB1 (online Technical Appendix 1) revealed that 7 of 8 naive contacts simultaneously exposed to both viruses were infected with Ck/Bh/346 (rH5N1) alone, none was infected with Ck/BD/22478 (pH5N1) alone, and 1 was co-infected with both viruses. Thus, despite the lower infectious dose used for 30 LD_{50}, Ck/Bh/346 (rH5N1) killed inoculated chickens faster than did Ck/BD/22478 (pH5N1) and was transmitted faster and more efficiently to naive contacts.

Table. Results of hemagglutination inhibition assays of highly pathogenic avian influenza H5N1 viruses isolated in Bhutan, 2012*

Antigens	Genetic clade	Postinfection ferret antisera				
		α-A/BHG/QH/IA clade 2.2	α-A/Hubei/1/2010 clade 2.3.2.1a	α-A/ck/BD/15205 clade 2.3.2.1a	α-A/dk/BD/19097 clade 2.3.2.1a†	α-A/ck/Bhutan/346 clade 2.3.2.1a†
Reference antigens						
A/BHG/QH/IA	2.2	**320**	40	40	80	40
A/Hubei/1/2010	2.3.2.1a	40	**640**	160	1280	80
A/ck/BD/15205	2.3.2.1a	10	80	**80**	320	40
A/dk/BD/19097	2.3.2.1a	-	40	80	**320**	40
A/ck/Bhutan/346	2.3.2.1a	10	40	80	640	**80**
Test antigens						
A/chicken/Bhutan/257/2012	2.3.2.1a	20	40	40	640	40
A/chicken/Bhutan/260/2012	2.3.2.1a	20	40	80	640	80
A/wild bird/Bhutan/357/2012	2.3.2.1a	20	40	80	640	40
A/chicken/Bhutan/1026/2012	2.3.2.1a	40	40	80	1280	80
A/chicken/Bhutan/1030/2012	2.3.2.1a	80	160	320	1280	320
A/chicken/Bhutan/317/2012	2.3.2.1a	10	40	80	640	80
A/wild bird/Bhutan/326/2012	2.3.2.1a	10	80	40	320	20
A/wild bird/Bhutan/328/2012	2.3.2.1a	40	20	40	640	80
A/wild bird/Bhutan/356/2012	2.3.2.1a	40	160	160	640	80
A/chicken/Bhutan/406/2012	2.3.2.1a	20	40	80	320	80
A/chicken/Bhutan/413/2012	2.3.2.1a	20	40	80	640	40
A/chicken/Bhutan/505/2012	2.3.2.1a	80	40	80	640	80
A/chicken/Bhutan/933/2012	2.3.2.1a	40	40	80	640	80
GMT (95% CI)		27.54 (18.36–41.30)	49.51 (34.61–70.83)	80 (56.83–112.6)	640 (502.5–815.1)	68.17 (46.24–100.5)

*Boldface indicates homologous titers. A/BHG/QH/IA, A/bar-headed goose/Qinghai/IA/2005; A/ck/BD/15205, A/chicken/Bangladesh/15205/2012; A/ck/Bhutan/346, A/chicken/Bhutan/346/2012; A/dk/BD/19097, A/duck/Bangladesh/19097/2013; GMT, geometric mean titer.
†The immune response in ferrets was boosted with Freund's incomplete adjuvant (InvivoGen, San Diego, CA, USA) at day 14 postinfection.

We assessed the risk for human infection with rH5N1 by investigating its pathogenicity and transmissibility in ferrets (online Technical Appendix 1). Donors shed 4.5 $\log_{10}$ EID_{50}/mL and 3.4 $\log_{10}$ EID_{50}/mL in nasal wash samples at 2 dpi and 4 dpi, respectively, but cleared the virus by 6 dpi. No direct or aerosol contacts shed virus, suggesting that Ck/Bh/346 (rH5N1) was not transmitted (data not shown). No Ck/Bh/346 (rH5N1)–inoculated ferrets lost >5% of their body weight or showed elevated body temperature (data not shown). Histopathologic analysis showed that 1 donor, who was lethargic at 3–10 dpi, had mild meningoencephalitis at 14 dpi (online Technical Appendix 2, http://wwwnc.cdc.gov/EID/article/22/12/16-0611-Techapp2.pdf). A nucleocapsid protein–positive cell was detected in the brain, suggesting that Ck/Bh/346 (rH5N1) is neurotropic. The other ferrets showed no clinical signs of disease. Virus replication was detected in the lung at 4 dpi ($\log_{10}$ 2.75 EID_{50}/g) (online Technical Appendix 2).

Conclusions

Our study revealed that the viruses that caused the 2012 outbreaks in Bhutan belonged to the rH5N1 genotype (2.3.2.1a/H9-like PB1 [7:1]), whereas neither H9N2 nor the pH5N1 genotype have been detected there. rH5N1 has been isolated sporadically at live-bird markets and from chickens on farms where outbreaks occurred in Bangladesh (*5*,*6*), India (*12*), and Nepal (*7*) in 2011–2013. The lack of data on the effect of the H9-like PB1 gene on the virulence of rH5N1 makes determining its pathogenicity and transmissibility a critical public-health goal for Bhutan and neighboring countries.

Ck/Bh/346 (rH5N1) killed inoculated chickens faster than did Ck/BD/22478 (pH5N1), despite the lower infectious dose used for Ck/Bh/346. In CEFs, Ck/Bh/346replicated with greater efficiency during the first 36 hpi than did Ck/BD/22478, which possibly explains why rH5N1 transmits more efficiently to naive chickens when directly competing with pH5N1. How faster replication contributes to the increased mortality rate of naive chickens might be crucial to eradicating the disease in Bhutan. In a mountainous region with widely separated villages, small-scale poultry farming, and no live-bird markets, the severity and rapid onset of the infection could lead to host-resource exhaustion and self-limitation.

To determine whether the reassortant PB1 gene accounts for the observed phenotypic properties of rH5N1, reverse genetics experiments are required. Despite its enhanced transmissibility, rH5N1 did not supplant pH5N1 in India or Bangladesh after undergoing multiple reassortment events. Possible reasons for this include the involvement of other influenza subtypes, which would complicate the competition/transmission model, especially at live-bird markets, as well as the large duck population, which is prone to inapparent HPAI infection (indicating possible underreporting).

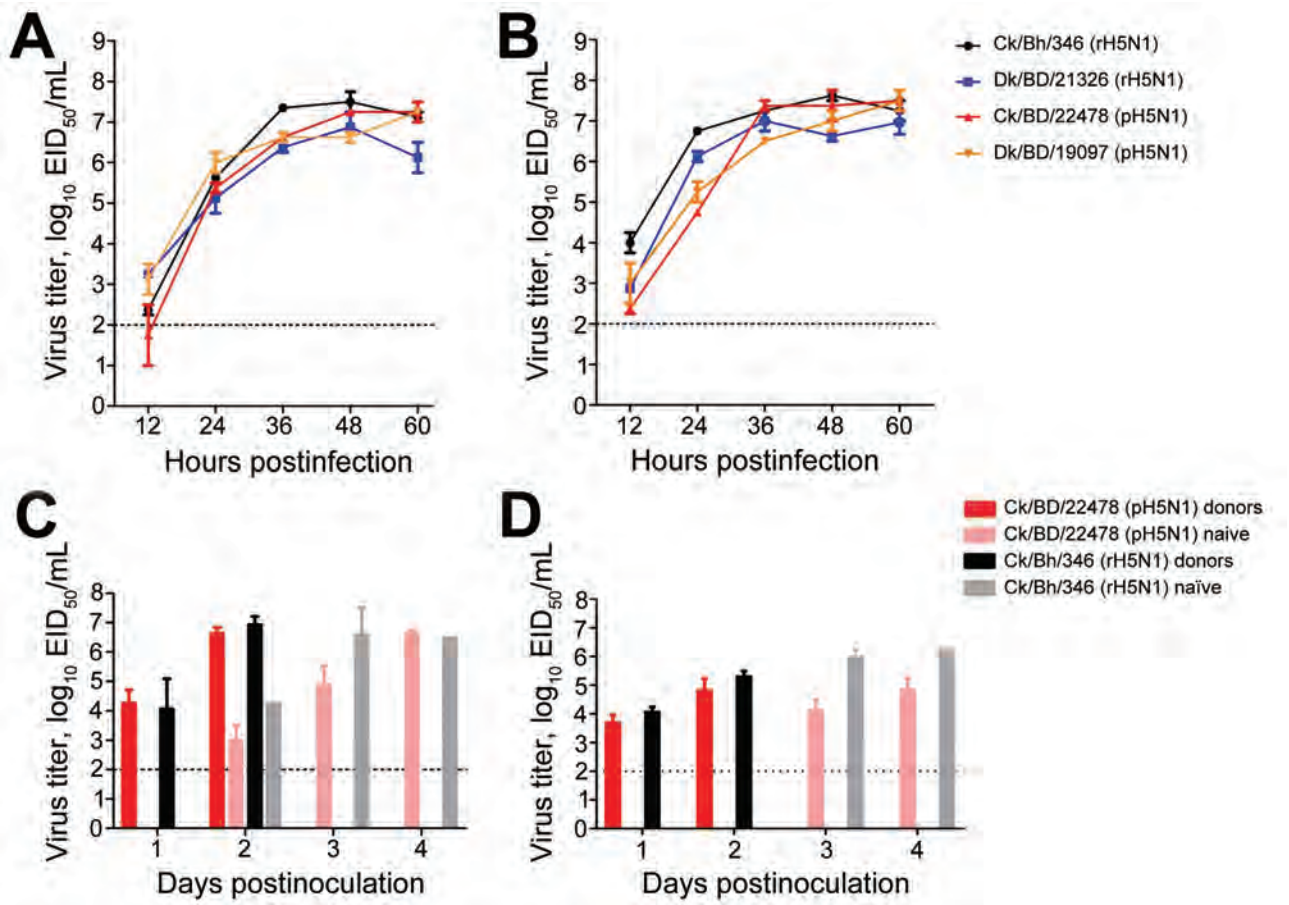

Figure 2. Pathogenesis of influenza virus rH5N1 and pH5N1 2.3.2.1a genotypes in vitro and in vivo. A) Replication kinetics of rH5N1 and pH5N1 in Madin-Darby canine kidney (mammalian) cells. B) Replication kinetics of rH5N1 and pH5N1 in chicken embryonic fibroblast (avian) cells. C) Oropharyngeal shedding and transmissibility of rH5N1 and pH5N1 in a single-virus transmission model in 5-week-old White Leghorn chickens. D) Cloacal shedding and transmissibility of rH5N1 and pH5N1 in a single-virus transmission model in 5-week-old White Leghorn chickens. Naive chickens were co-housed with donors infected with either Ck/22478 (pH5N1) or Ck/Bh/346 (rH5N1) (C and D). The dashed line in each panel represents the limit of virus detection. ANOVA, analysis of variance; Ck/22478, A/chicken/Bangladesh/22478; Ck/Bh/346, A/chicken/Bhutan/346/2012; Dk/BD/23126, A/duck/Bangladesh/23126; Dk/BD/19097/2013, A/duck/Bangladesh/19097; EID, egg infectious dose; dpi, days postinoculation; hpi, hours postinfection; pH5N1, pandemic H1N1; rH5N1, reassortant H5N1.

Our ferret model results suggest that avian-to-human transmission of rH5N1 is possible. However, further adaptation to the host is necessary for rH5N1 to become transmissible among mammals. Similar results have been reported for H5N1 clade 2.3.2.1 (*13*), H5N1 clade 2.3.4 (*14*), and H5Nx clade 2.3.4.4 (*15*). rH5N1 is potentially neurotropic, manifesting clinically as mild meningoencephalitis with no obvious respiratory involvement. This finding has implications on early diagnosis and use of antiviral drugs during the first 48 hours after clinical diagnosis for optimal therapeutic effect.

pH5N1 and H9N2 virus strains will likely continue to co-circulate on the Indian subcontinent, enabling further reassortment events. Our results highlight the need for active surveillance and full-genome sequencing of all H5N1 virus isolates.

Acknowledgments

We thank M. Kamrul Hasan, Sharmin Akhtar, and Jasmine Turner for technical support; Lisa Kercher, Beth Little, and David Carey for help in the enhanced animal Biosafety Level 3 laboratory during animal experiments; James Knowles for administrative support; Elizabeth Stevens for generating Figure 1; Jeremy Jones for critically reviewing the manuscript; and Vani Shanker and Keith A. Laycock for scientific editing.

This work was funded by contracts HHSN266200700005C and HHSN272201400006C from the National Institute of Allergy and Infectious Diseases, the National Institutes of Health, and the Department of Health and Human Services, and by the American Lebanese Syrian Associated Charities.

Dr. Marinova-Petkova was a postdoctoral research associate at St. Jude Children's Research Hospital, Memphis, Tennessee, USA, while this research was conducted. She is now affiliated with the Centers for Disease Control and Prevention, Atlanta, Georgia, USA, where her research interests include emerging influenza viruses at the animal–human interface, the evolution of influenza A viruses, and animal models for studying influenza pathogenesis and transmission.

References

1. Nagarajan S, Tosh C, Smith DK, Peiris JSM, Murugkar HV, Sridevi R, et al. Avian influenza (H5N1) virus of clade 2.3.2 in domestic poultry in India. PLoS ONE. 2012;7:e31844. http://dx.doi.org/10.1371/journal.pone.0031844
2. Gerloff NA, Khan SU, Balish A, Shanta IS, Simpson N, Berman L, et al. Multiple reassortment events among highly pathogenic avian influenza A(H5N1) viruses detected in Bangladesh. Virology. 2014;450–451:297–307. http://dx.doi.org/10.1016/j.virol.2013.12.023
3. Marinova-Petkova A, Feeroz MM, Rabiul Alam SM, Kamrul Hasan M, Akhtar S, Jones-Engel L, et al. Multiple introductions of highly pathogenic avian influenza H5N1 into Bangladesh. Emerg Microbes Infect. 2014;3:e11. http://dx.doi.org/10.1038/emi.2014.11
4. Shanmuganatham K, Feeroz MM, Jones-Engel L, Smith GJD, Fourment M, Walker D, et al. Antigenic and molecular characterization of avian influenza A(H9N2) viruses, Bangladesh. Emerg Infect Dis. 2013;19. Epub 2013 Sep. http://dx.doi.org/10.3201/eid1909.130336
5. Marinova-Petkova A, Shanmuganatham K, Feeroz MM, Jones-Engel L, Hasan MK, Akhtar S, et al. The continuing evolution of H5N1 and H9N2 influenza viruses in Bangladesh between 2013 and 2014. Avian Dis. 2016;60(Suppl):108–17. http://dx.doi.org/10.1637/11136-050815-Reg
6. Monne I, Yamage M, Dauphin G, Claes F, Ahmed G, Giasuddin M, et al. Reassortant avian influenza A(H5N1) viruses with H9N2–PB1 gene in poultry, Bangladesh. Emerg Infect Dis. 2013;19. http://dx.doi.org/10.3201/eid1910.130534
7. Benson DA, Karsch-Mizrachi I, Lipman DJ, Ostell J, Wheeler DL. GenBank. Nucleic Acids Res. 2005;33:D34–8. http://dx.doi.org/10.1093/nar/gki063
8. Nidup K, Tshering P. Status of the family poultry production and HPAI in Bhutan. In: Proceedings of the 8th Asian Pacific Poultry Conference of the World's Poultry Science Association; Bangkok, Thailand; March 2007. p. 78–83 [cited 2016 Mar 8]. http://cms.cnr.edu.bt/cms/files/docs/File/Karma%20Nidup/Poultry/FamilyPoultry&HPAIinBhutan.pdf
9. Ministry of Agriculture and Forests of the Royal Government of Bhutan. Bhutan RNR statistics, 2015 [cited 2016 Mar 8]. http://www.moaf.gov.bt/bhutan-rnr-statistics-2015-online/
10. World Organisation for Animal Health. Update on highly pathogenic avian influenza in animals (type H5 and H7). Immediate notification report, Bhutan. 2012 [cited 2016 Feb 8]. https://web.oie.int/wahis/reports/en_imm_0000011465_20120110_120756.pdf
11. Ministry of Agriculture and Forests of Bhutan. RNR newsletter. 2013; I(3) [cited 2016 Feb 8]. http://www.moaf.gov.bt/rnr-newsletter-september-2013/
12. Bhat S, Bhatia S, Pillai AS, Sood R, Singh VK, Shrivas OP, et al. Genetic and antigenic characterization of H5N1 viruses of clade 2.3.2.1 isolated in India. Microb Pathog. 2015;88:87–93. http://dx.doi.org/10.1016/j.micpath.2015.08.010
13. Xu L, Bao L, Yuan J, Li F, Lv Q, Deng W, et al. Antigenicity and transmissibility of a novel clade 2.3.2.1 avian influenza H5N1 virus. J Gen Virol. 2013;94:2616–26. http://dx.doi.org/10.1099/vir.0.057778-0
14. Sun H, Pu J, Wei YD, Sun Y, Hu J, Liu L, et al. Highly pathogenic avian influenza H5N6 viruses exhibit enhanced affinity for human type sialic acid receptor and in-contact transmission in model ferrets. J Virol. 2016. Epub 2016 Apr 27. http://dx.doi.org/10.1128/JVI.00127-16
15. Pulit-Penaloza JA, Sun X, Creager HM, Zeng H, Belser JA, Maines TR, et al. Pathogenesis and transmission of novel highly pathogenic avian influenza H5N2 and H5N8 viruses in ferrets and mice. J Virol. 2015;89:10286–93. http://dx.doi.org/10.1128/JVI.01438-15

Address for correspondence: Robert G. Webster, Department of Infectious Diseases, MS 330, St. Jude Children's Research Hospital, 262 Danny Thomas Pl, Memphis, TN 38105-3678, USA; email: robert.webster@stjude.org

Horizontal Transmission of Chronic Wasting Disease in Reindeer

S. Jo Moore, Robert Kunkle, M. Heather West Greenlee, Eric Nicholson, Jürgen Richt, Amir Hamir,[1] W. Ray Waters, Justin Greenlee

We challenged reindeer by the intracranial route with the agent of chronic wasting disease sourced from white-tailed deer, mule deer, or elk and tested for horizontal transmission to naive reindeer. Reindeer were susceptible to chronic wasting disease regardless of source species. Horizontal transmission occurred through direct contact or indirectly through the environment.

Reindeer are susceptible to chronic wasting disease (CWD) after experimental oral challenge (*1*), and recently, CWD was identified in a free-ranging reindeer in Norway (*2*,*3*). Horizontal transmission is the primary mode of CWD transmission in deer. Direct horizontal transmission occurs when naive animals are exposed to infectious excreta (i.e., saliva, urine, feces) during close contact with CWD-affected animals (reviewed in *4*). Indirect horizontal transmission occurs through exposure to environments contaminated with infectious material (e.g., excreta or decomposed carcasses) (*5*,*6*).

The Eurasian reindeer (*Rangifer tarandus tarandus*) is closely related to the North American caribou (*R. t. caribou*, *R. t. granti*, *R. t. groenlandicus*). In North America, overlapping geographic ranges of free-ranging populations of potentially CWD-infected white-tailed deer (*Odocoileus virginianus*), mule deer (*O. hemionus*), or elk (*Cervus elaphus nelsoni*) present a risk for horizontal transmission to caribou. Exposure also could occur in farmed populations where contact occurs between reindeer and captive and/or free-ranging CWD-affected cervids. We investigated the transmission of CWD from white-tailed deer, mule deer, or elk to reindeer through the intracranial route and assessed them for direct and indirect horizontal transmission to uninoculated sentinels.

The Study

In 2005, we challenged reindeer fawns from a farm in Alaska, USA, where CWD had never been reported, by intracranial inoculation (*7*) with pooled brain material from CWD-affected elk from South Dakota (CWD^{elk}), CWD-affected mule deer from Wyoming (CWD^{md}), or CWD from white-tailed deer from Wisconsin combined with brain material from experimentally challenged white-tailed deer (CWD^{wtd}) (Table 1; online Technical Appendix, http://wwwnc.cdc.gov/EID/article/22/12/16-0635-Techapp1.pdf). Additional uninoculated fawns served as negative controls, controls for indirect transmission, and controls for direct transmission (Table 1; online Technical Appendix). We determined the prion protein gene (*PRNP*) genotype of each fawn (online Technical Appendix), and we tried to ensure that each *PRNP* genotype was present in each group (Table 2, http://wwwnc.cdc.gov/EID/article/22/12/16-0635-T1.htm). Control reindeer were housed in the same barn as inoculated reindeer but in separate pens that prevented direct physical contact (i.e., nose-to-nose) between control and inoculated animals (online Technical Appendix Figure 1). Indirect and direct contact control groups were formed 25 months after intracranially challenged reindeer were inoculated (online Technical Appendix Figure 1, panel B).

Clinical signs consistent with CWD were first observed 20.9 months after inoculation (Table 2). Common clinical features included found dead without clinical signs noted, loss of body condition, recumbency, and lethargy (Table 2; online Technical Appendix).

At death, a full necropsy was performed on all reindeer. Two sets of tissue samples were collected: 1 set was fixed in 10% buffered formalin, embedded in paraffin wax, sectioned at 5 μm for microscopy examination after hematoxylin and eosin staining or immunohistochemical staining using primary antibody F99/96.7.1 (online Technical Appendix). A second set of tissues was frozen, and selected tissues were used for immunodetection of scrapie prion protein (PrP^{Sc}) by Western blot (brain tissue only) as described previously (*7*) but with some modifications, or an ELISA (brainstem and/or retropharyngeal lymph node) using a commercial kit (IDEXX HerdChek BSE-Scrapie Antigen ELISA; IDEXX, Westbrook, ME, USA) according to the manufacturers' instructions (online Technical Appendix).

In the intracranially inoculated groups, when intercurrent deaths were excluded, reindeer with the NN138 polymorphism (reindeer nos. 2, 6, and 12) had the shortest survival times in each group (Table 2). Different inocula did not produce significantly different survival times (log-rank

Author affiliations: US Department of Agriculture, Ames, Iowa, USA (S.J. Moore, R. Kunkle, E. Nicholson, J. Richt, A. Hamir, W.R. Waters, J. Greenlee): Iowa State University, Ames (M.H. West Greenlee)

DOI: http://dx.doi.org/10.3201/eid2212.160635

[1]Deceased.

Table 1. Animal data for reindeer (*Rangifer tarandus tarandus*) in a study of transmission of CWD*

Group no./animal no.	Genotype codon 002	129	138	169	176	Infectivity source	Exposure route
1							
1	MV	SG	NS	MV	NN	CWD^{wtd}	Intracranial
2	VV	GG	NN	VV	NN	CWD^{wtd}	Intracranial
3	VV	GG	NS	VV	ND	CWD^{wtd}	Intracranial
4	VV	GG	NS	VV	NN	CWD^{wtd}	Intracranial
5	MV	SG	SS	MV	ND	CWD^{wtd}	Intracranial
2							
6	VV	GG	NN	VV	NN	CWD^{elk}	Intracranial
7	MV	SG	NS	MV	NN	CWD^{elk}	Intracranial
8	VV	GG	NS	VV	NN	CWD^{elk}	Intracranial
9	VV	GG	NS	VV	ND	CWD^{elk}	Intracranial
10	NA	SG	SS	MV	NN	CWD^{elk}	Intracranial
3							
11	MV	SG	NS	MV	NN	CWD^{md}	Intracranial
12	VV	GG	NN	VV	NN	CWD^{md}	Intracranial
13	VV	GG	SS	VV	DD	CWD^{md}	Intracranial
14	MV	SG	SS	MV	NN	CWD^{md}	Intracranial
15	VV	GG	NS	VV	ND	CWD^{md}	Intracranial
4 direct							
16	VV	GG	NN	VV	NN	Horizontal (CWD^{wtd})	Cohoused with group 1
17	VV	GG	NN	VV	NN	Horizontal (CWD^{wtd})	Cohoused with group 1
18	VV	GG	NN	VV	NN	Horizontal (CWD^{wtd})	Cohoused with group 1
19	NA	SG	NS	MV	NN	Horizontal (CWD^{wtd})	Cohoused with group 1
4 indirect							
20	MM	SS	SS	MM	NN	Horizontal (CWD^{md})	Housed adjacent to group 3
21	VV	GG	NN	VV	NN	Horizontal (CWD^{md})	Housed adjacent to group 3
4 neg. controls							
22	VV	GG	NS	VV	NN	NA	NA
23	MV	SG	SS	MV	NN	NA	NA

*CWD, chronic wasting disease; D, aspartic acid; G, glycine; horizontal, horizontal transmission; M, methionine; md, mule deer (*Odocoileus hemionus*); N, asparagine; NA, not applicable; neg., negative; S, serine; V, valine; wtd, white-tailed deer (*Odocoileus virginianus*).

test, p = 0.0931), but we observed differences in the amount of vacuolation and PrP^{Sc} in the brain at the clinical stages of disease in CWD^{wtd}- and CWD^{elk}-inoculated reindeer, compared with CWD^{md}-inoculated reindeer (Table 2; online Technical Appendix). In the indirect contact animals, PrP^{Sc} was present in the brain but restricted to the dorsal motor nucleus of the vagus nerve and area postrema.

We observed different patterns of PrP^{Sc} deposition in the brain (Figure 1, panels A–D; online Technical Appendix), the most striking of which was dominated by aggregated deposits of various sizes, including plaque-like deposits (Figure 1, panels A,B). This pattern was seen in reindeer with the NS138 NN176 (no. 8, CWD^{elk}; no. 13, CWD^{md}) or SS138 DD176 (no. 4, CWD^{wtd}) genotypes. With regard to immunoreactivity in the retina (Figure 1, panels E, F; online Technical Appendix), in 2 of 3 reindeer with aggregated deposits in the brain (nos. 8 and 13), aggregated immunoreactivity also was observed in the inner plexiform layer of the retina (Figure 1, panel f).

Reindeer that were negative by immunohistochemical analysis in brain also were negative by Western blot and ELISA. Different Western blot migration patterns were observed in PrP^{Sc}-positive animals (Figure 2), but we found no clear association between migration pattern and challenge group or *PRNP* genotype.

PrP^{Sc} was widespread in lymphoid tissues from most reindeer (Table 2; online Technical Appendix). Reindeer with the NS138 genotype had a significantly lower average percentage of lymphoid follicles positive than did reindeer with NN138 (analysis of variance, p = 0.003) or SS138 (p = 0.003) deer. Excluding intercurrent deaths, PrP^{Sc} was detected in all 4 CWD^{wtd}-challenged reindeer, all 5 CWD^{elk}-challenged reindeer, all 4 CWD^{md}-challenged reindeer, both indirect contact reindeer, and 2 of 4 direct contact reindeer (Table 2).

Conclusions

Potential sources of infectivity for direct contact animals include urine, feces, and saliva from their CWD^{wtd}-challenged pen-mates, as has been shown for CWD-affected white-tailed deer (*6*,*8*,*9*). Pinpointing the source of infectivity in the indirect contact group is more difficult. Infectious prions can travel at least 30 m in airborne particulate (*10*), but because the negative control reindeer in the pen adjacent to the indirect contact reindeer did not become positive, a more direct route of transmission is likely in this case. Penning, feeding, and watering protocols were designed to prevent exposure of negative control and indirect contact reindeer to potential infectivity on feed and water buckets, bedding, or fencing (*6*,*11*). However, reindeer

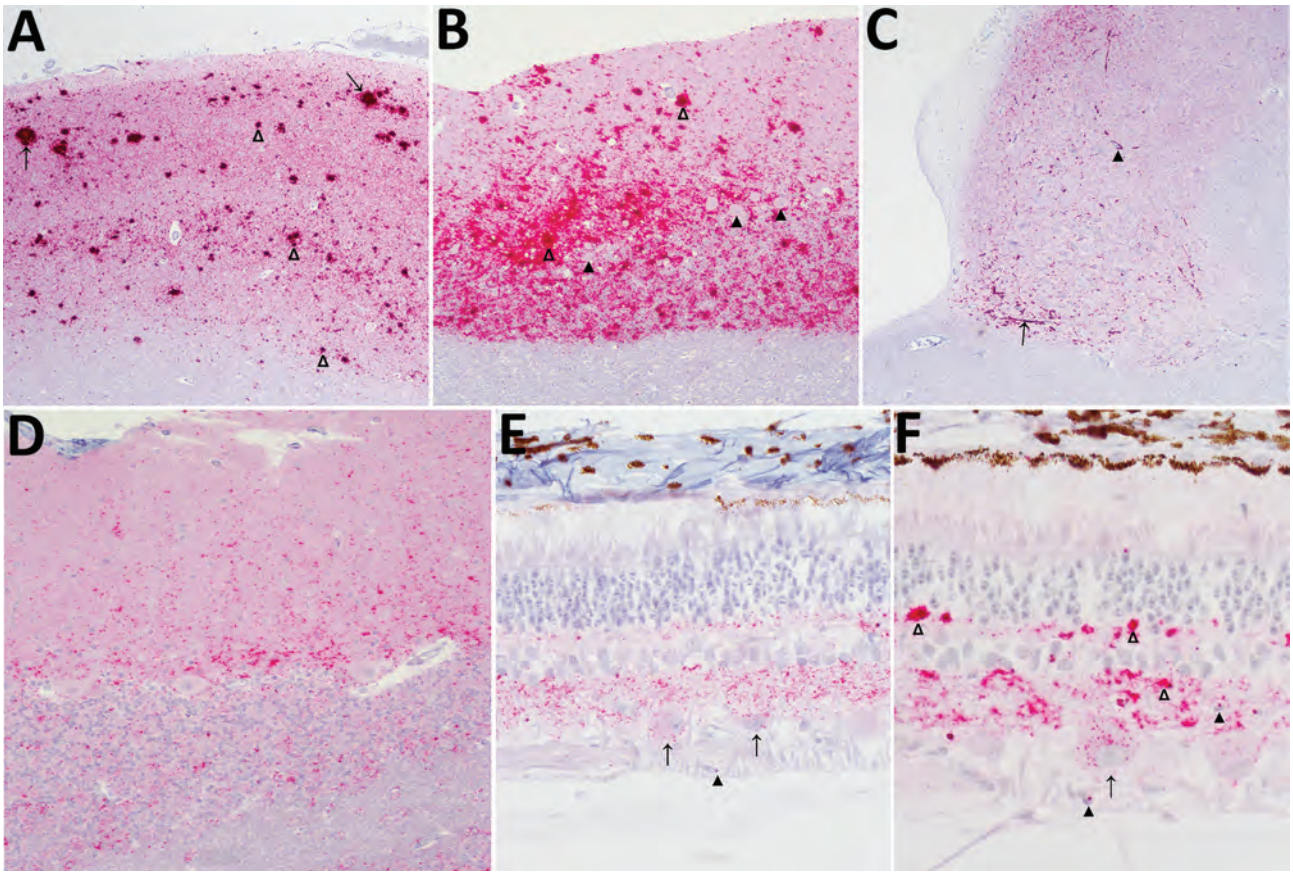

Figure 1. Immunohistochemical analysis for the prion protein showing scrapie prion protein (PrP^{Sc}) deposits in brains (A–D) and retinas (E, F) from reindeer (*Rangifer tarandus tarandus*) with chronic wasting disease. PrP^{Sc} immunodetection using the monoclonal antibody F99/97.6.1. A) Neocortex, showing prominent aggregated (open arrowheads) and plaque-like (arrows) deposits in reindeer no. 4. Original magnification ×5. B) Cerebellum, showing particulate immunoreactivity and aggregated deposits (open arrowheads) in reindeer no. 4. Note absence of intraneuronal immunoreactivity in Purkinje cells (solid arrowheads). Original magnification ×10. C) Brainstem at the level of the obex, showing prominent linear (arrow) and perineuronal (solid arrowhead) immunoreactivity in the dorsal motor nucleus of the vagus nerve in reindeer no. 21. Original magnification ×5. D) Cerebellum, punctate immunoreactivity in the molecular and granular layers and white matter in reindeer no. 12. Original magnification ×5. E) Intraneuronal immunoreactivity in retinal ganglion cells (arrows), punctate deposits in the inner and outer plexiform layers, scattered intramicroglial deposits (solid arrowheads) in reindeer no. 12. Original magnification ×40. F) Particulate to coalescing deposits in the inner and outer plexiform layers (open arrowheads), intraneuronal immunoreactivity in retinal ganglion cells (arrows), and scattered intramicroglial deposits (solid arrowheads) in reindeer no. 13. Original magnification ×40.

might have had access to bedding from adjacent pens that had spread into the central alleyway.

During the 5-year course of this study, reindeer were moved between pens several times to maintain an optimal number of animals per pen (online Technical Appendix Figure 1). Prolonged persistence of prion infectivity in the natural environment has been documented for both CWD (2 years [*5*]) and scrapie (up to 16 years [*12*]). In addition, thorough cleaning and disinfection might not be sufficient to remove all infectivity from the environment, leading to persistence of infectivity under experimental housing conditions (*13*).

In reindeer challenged orally with the agent of CWD, the SS138 genotype (serine/serine at *PRNP* codon 138) has been associated with susceptibility to disease and the NS138 (asparagine/serine) genotype with resistance (*1*). In the study we report, disease developed in reindeer with the NS138 genotype after intracranial inoculation, although the extent of lymphoreticular system involvement was significantly lower than in NN138 and SS138 reindeer. The potential association of the NN138 polymorphism with shorter survival times is interesting. However, as with all potential genotype versus phenotype interactions, care should be taken not to over-interpret these results given the small group sizes and the large number of *PRNP* genotype groups in this study.

Our results demonstrate that reindeer are susceptible to the agent of CWD from white-tailed deer, mule deer, and elk sources after intracranial inoculation. Furthermore, naive reindeer are susceptible to the agent of CWD after

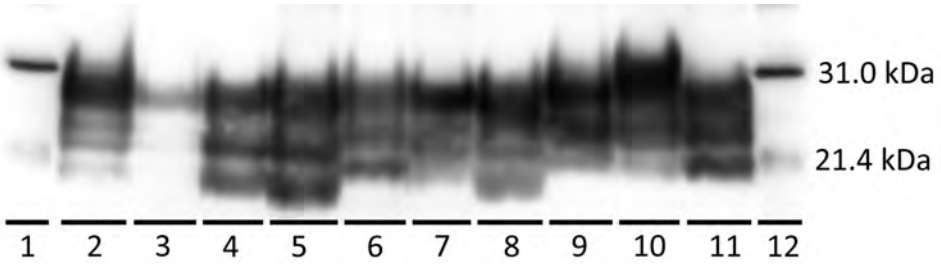

Figure 2. Western blot characterization of the inocula used to inoculate reindeer and brainstem samples from representative reindeer from each experimental group in study of chronic wasting disease transmission. Scrapie prion protein (PrP^{Sc}) immunodetection using the monoclonal antibody 6H4. Positive Western blot results demonstrate a 3-band pattern (diglycosylated, highest; monoglycosylated, middle; and nonglycosylated, lowest) that is characteristic of prion diseases. Lanes: 1, biotinylated protein marker; 2 and 3, indirect contact reindeer (animals no. 20 and 21, respectively); 4 and 5, reindeer inoculated intracranially with CWD^{md} (animals no. 15 and 12 respectively); 6, CWD^{md} inoculum; 7, direct contact reindeer (no. 7, cohoused with CWD^{wtd}-inoculated reindeer); 8, reindeer (no. 5) inoculated intracranially with CWD^{wtd}; 9, CWD^{wtd} inoculum; 10, reindeer (no. 10) inoculated intracranially with CWD^{elk}; 11, CWD^{elk} inoculum; 12, marker. CWD, chronic wasting disease; CWD^{elk}, CWD-affected elk; CWD^{md}, CWD-affected mule deer; CWD^{wtd}, CWD-affected white-tailed deer combined with brain material from experimentally challenged white-tailed deer.

direct and indirect exposure to CWD-infected reindeer, suggesting a high potential for horizontal transmission of CWD within and between farmed and free-ranging reindeer (and caribou) populations.

Acknowledgments

We thank Martha Church, Robyn Kokemuller, Joe Lesan, Virginia Montgomery, Dennis Orcutt, and Trudy Tatum for excellent technical support.

Dr. Moore is a postdoctoral research associate at the National Animal Disease Center, US Department of Agriculture, Ames, Iowa. Her research interests include pathogenesis and pathology of animal diseases with a special interest in neuropathology and prion diseases.

References

1. Mitchell GB, Sigurdson CJ, O'Rourke KI, Algire J, Harrington NP, Walther I, et al. Experimental oral transmission of chronic wasting disease to reindeer (*Rangifer tarandus tarandus*). PLoS One. 2012;7:e39055. http://dx.doi.org/10.1371/journal.pone.0039055
2. Norwegian Veterinary Institute. The first detection of chronic wasting disease (CWD) in Europe. 2016 April 4 [cited 2016 Apr 5]. http://www.vetinst.no/sykdom-og-agens/chronic-wasting-disease/the-first-detection-of-chronic-wasting-disease-cwd-in-europe
3. Becker R. Deadly animal prion disease appears in Europe. 2016 [cited 2016 Jun 16]. http://www.nature.com/news/deadly-animal-prion-disease-appears-in-europe-1.19759
4. Haley NJ, Hoover EA. Chronic wasting disease of cervids: current knowledge and future perspectives. Annu Rev Anim Biosci. 2015;3:305–25. http://dx.doi.org/10.1146/annurev-animal-022114-111001
5. Miller MW, Williams ES, Hobbs NT, Wolfe LL. Environmental sources of prion transmission in mule deer. Emerg Infect Dis. 2004;10:1003–6. http://dx.doi.org/10.3201/eid1006.040010
6. Henderson DM, Denkers ND, Hoover CE, Garbino N, Mathiason CK, Hoover EA. Longitudinal detection of prion shedding in saliva and urine by CWD-infected deer by real-time quaking-induced conversion. J Virol. 2015;89:9338–47. http://dx.doi.org/10.1128/JVI.01118-15
7. Greenlee JJ, Smith JD, Kunkle RA. White-tailed deer are susceptible to the agent of sheep scrapie by intracerebral inoculation. Vet Res. 2011;42:107. http://dx.doi.org/10.1186/1297-9716-42-107
8. Mathiason CK, Hays SA, Powers J, Hayes-Klug J, Langenberg J, Dahmes SJ, et al. Infectious prions in pre-clinical deer and transmission of chronic wasting disease solely by environmental exposure. PLoS One. 2009;4:e5916. http://dx.doi.org/10.1371/journal.pone.0005916
9. Tamgüney G, Richt JA, Hamir AN, Greenlee JJ, Miller MW, Wolfe LL, et al. Salivary prions in sheep and deer. Prion. 2012;6:52–61. http://dx.doi.org/10.4161/pri.6.1.16984
10. Gough KC, Baker CA, Simmons HA, Hawkins SA, Maddison BC. Circulation of prions within dust on a scrapie affected farm. Vet Res. 2015;46:40. http://dx.doi.org/10.1186/s13567-015-0176-1
11. Maddison BC, Baker CA, Terry LA, Bellworthy SJ, Thorne L, Rees HC, et al. Environmental sources of scrapie prions. J Virol. 2010;84:11560–2. http://dx.doi.org/10.1128/JVI.01133-10
12. Georgsson G, Sigurdarson S, Brown P. Infectious agent of sheep scrapie may persist in the environment for at least 16 years. J Gen Virol. 2006;87:3737–40. http://dx.doi.org/10.1099/vir.0.82011-0
13. Hawkins SA, Simmons HA, Gough KC, Maddison BC. Persistence of ovine scrapie infectivity in a farm environment following cleaning and decontamination. Vet Rec. 2015;176:99. http://dx.doi.org/10.1136/vr.102743

Address for correspondence: Justin Greenlee, Virus and Prion Disease Research Unit, National Animal Disease Center, Agricultural Research Service, US Department of Agriculture, 1920 Dayton Ave, Ames, IA 50010, USA; email: justin.greenlee@ars.usda.gov

Highly Divergent Dengue Virus Type 2 in Traveler Returning from Borneo to Australia

Wenjun Liu, Paul Pickering, Sebastián Duchêne, Edward C. Holmes, John G. Aaskov

Dengue virus type 2 was isolated from a tourist who returned from Borneo to Australia. Phylogenetic analysis identified this virus as highly divergent and occupying a basal phylogenetic position relative to all known human and sylvatic dengue virus type 2 strains and the most divergent lineage not assigned to a new serotype.

Outbreaks of dengue have been reported for several centuries in the Old World and the New World. Dengue is a major cause of illness and death globally, and there are high levels of infection in many tropical and subtropical localities populated by *Aedes* mosquito vectors. Despite their role in public health, the origin of the 4 serotypes of dengue virus (DENV-1–DENV-4) that are the causative agents of what now is defined as dengue remains unclear.

In 1967, Rudnick et al. (*1*) combined a fragmentary body of evidence to propose that dengue might have a sylvatic (jungle) cycle similar to that of another flavivirus (yellow fever virus). Isolation of 4 serotypes of DENV from humans in the Asia–Pacific region during 1943–1956 (*2*–*4*) was compatible with the idea that DENV might have originated in this region. Genome sequences of DENV-2 and DENV-4 isolated from sylvatic settings (i.e., from nonhuman primates) occupied basal positions on phylogenetic trees of those serotypes, which suggested that each DENV serotype evolved separately in sylvatic settings before later, independent, cross-species transmission to humans in urban and semiurban settings (*5*,*6*).

DENV-2 and DENV-4 have been isolated from nonhuman primates and occupy divergent phylogenetic positions, which suggests that that they are truly sylvatic. In contrast, no sylvatic strains have been identified as DENV-3, and an early sylvatic strain of DENV-1 probably was a spillback from humans to other primates (*6*). However, a highly divergent sequence of DENV-1, which was isolated from a patient who had vacationed in Brunei, was recently reported (*7*). This virus was basal to all other strains of DENV-1 by phylogenetic analyses, which suggests the presence of another sylvatic virus lineage in Southeast Asia, albeit of unknown animal origin.

Despite the central role of sylvatic viruses in our understanding of evolution and emergence of human dengue (*6*), to our knowledge, there are no reports of continuous transmission of sylvatic strains of DENV in a truly sylvatic setting. Much of the uncertainty over the nature and role of sylvatic DENV arises because of the small number of such isolates available and the lack of studies of DENV ecology outside a human setting. Thus, although phylogenetic divergence alone is insufficient to definitively prove the existence of sylvatic transmission, it at least shows that a greater diversity of viruses exist than are usually assigned as causing dengue in humans. In this report, we describe a highly divergent strain of DENV-2 isolated from an acute-phase serum specimen from a patient (human ethical approval for this study precludes identification of the patient) in whom dengue developed after the patient returned from a vacation in Borneo to Australia in early 2015.

The Study

The study was approved by the Queensland University of Technology (Brisbane, Queensland, Australia) (Human Research Ethics approval no. 1300000333). DENV-2 was isolated from a serum specimen by cultivation in *Aedes albopictus* mosquito C6-36 cells.

The virus was recognized by pan-flavivirus monoclonal antibodies 6B-6C1 (*8*) and 4G2 (*9*) and DENV-2–specific monoclonal antibodies 3H5 (*9*), 5H12, and 6B2 (*10*) in indirect immunofluorescence assays with infected C6-36 cells. However, it was not recognized by monoclonal antibody 6F3.1, which reacts with a serologic epitope ^{9}RNTPFNMLKRE^{19} in the capsid protein of nonsylvatic strains of DENV-2.

The consensus sequence of the viral genome was obtained by using 3′ and 5′ random amplification of cDNA ends (*11*,*12*) and reverse transcription PCR of ≈1-kb overlapping regions of the genome. Sequences of purified cDNA fragments generated by reverse transcription PCR were determined by using the dye di-deoxy chain termination method at the Australian Genome Research Facility (Brisbane).

Phylogenetic analysis of the complete viral genome (10,736 nt) by using maximum-likelihood methods (*13*) unambiguously placed this sequence, denoted QML22/2015 (GenBank accession no. KX274130), as a highly divergent

Author affiliations: Australian Army Malaria Institute, Brisbane, Queensland, Australia (W. Liu, P. Pickering J.G. Aaskov); University of Sydney, Sydney, New South Wales, Australia (S. Duchene, E.C. Holmes); Queensland University of Technology, Brisbane (J.G. Aaskov)

DOI: http://dx.doi.org/10.3210/eid2212.160813

member of DENV-2 with a strikingly basal phylogenetic position relative to all human and sylvatic DENV-2 sequences isolated (Figure 1). This lineage is the most divergent new lineage of DENV identified, even greater than that of DENV-1 Brun2014 (*7*), and is located approximately midway between the genetic divergence seen at the level of serotypes and that of genotypes within serotypes.

Although the nucleotide sequence of the open reading frame of QML22/2015 was strikingly different from those of other strains of DENV-2, sequence and predicted secondary RNA structure of 5′ and 3′ untranslated regions of the QML22/2015 genome were nearly identical with those of other strains of DENV-2, which confirmed the critical role of these elements in virus replication. Sliding-window analysis of genetic distance across the viral genome showed no regions in which QML22/2015 was disproportionately similar to human DENV-2 sequences (Figure 2).

Conclusions

Although it is tempting to estimate the time of origin of this novel DENV-2, as performed for other divergent DENV

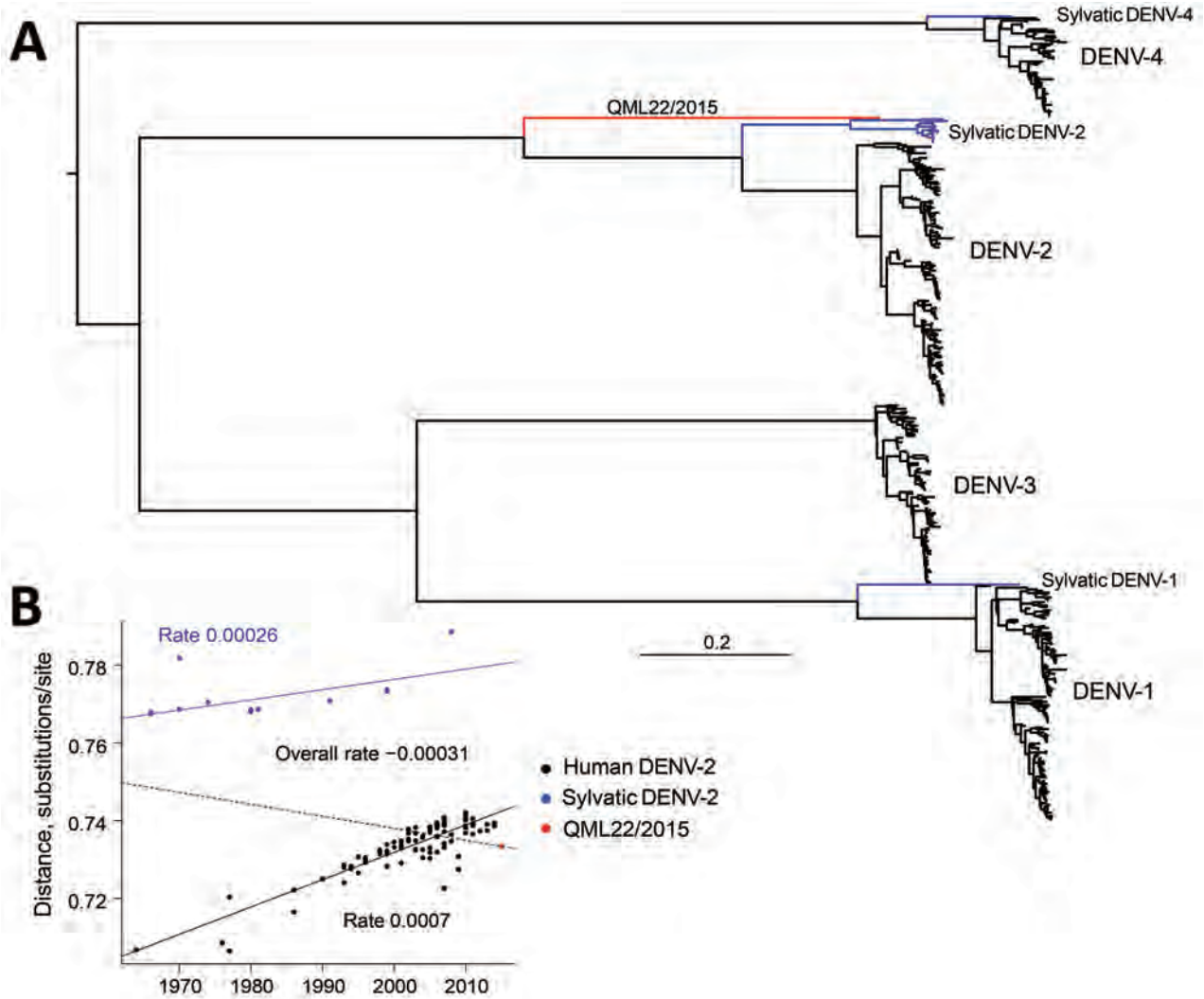

Figure 1. A) Maximum-likelihood phylogenetic tree of 500 complete genome sequences of DENV-1–DENV-4 (alignment length of 10,185 nt), including QML22/2015, estimated by using the generalized time-reversible invariable sites gamma model of nucleotide substitution in PhyML (*13*) and nearest-neighbor interchange plus subtree pruning and regrafting branch-swapping. The tree is midpoint rooted for clarity, and sequences are color coded according to their putative transmission cycle (human, black; sylvatic, blue); red indicates the highly divergent QML22/2015 lineage isolated in this study. B) Regression of root-to-tip genetic distances of 119 representative human and sylvatic complete genome sequences of DENV-2 (alignment length 10,173 nt) against time (year) of sampling. The input phylogenetic tree was estimated by using the same maximum-likelihood procedure. Three regression lines and slopes are shown; slopes indicate an estimate of the virus nucleotide substitution rate (substitutions/site/year). Blue line indicates rate for entire DENV-2 data set; dashed line indicates rate for sylvatic DENV-2 sequences; black line indicates rate for human DENV-2 sequences. There is a marked difference between sylvatic and human rates. DENV, dengue virus.

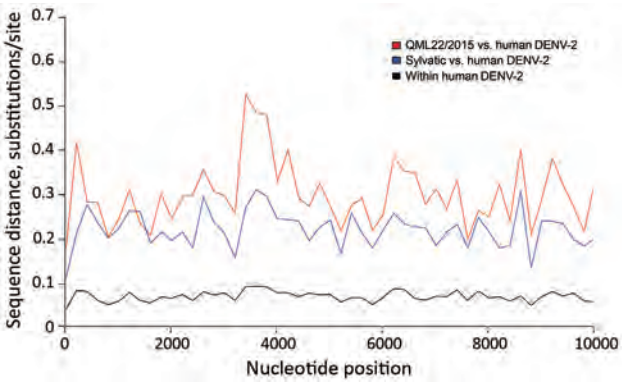

Figure 2. Sliding-window analysis of mean genetic (nucleotide) distance across the dengue virus type 2 (DENV-2) genome. Red line indicates comparison between QML22/2015 and human DENV-2 sequences. Equivalent analyses were performed on sylvatic DENV-2 versus human DENV-2 (blue line) and within the human DENV-2 sequences (black line). This analysis was based on genetic distances calculated by using sliding windows of 200 nt on the DENV-2 data described in Figure 1 and was performed by using the Analysis of Phylogenetics and Evolution Package in R software (*14*).

lineages (*7*), we have not made this estimation because our data provided strong evidence for a marked difference in evolutionary rate between human and sylvatic strains of DENV-2, which will confound all attempts at molecular clock dating. Regression analysis of root-to-tip genetic distances against time (year) of sampling suggests that sylvatic strains of DENV-2 are evolving slower than urban (human) strains, most likely because of differences in selection pressure, replication dynamics, or both, and in contrast to previous observations (*15*).

The QML22/2015 isolate is closer to the human distribution than the sylvatic distribution of root-to-tip genetic distances, which suggests that this lineage might not have had only sylvatic transmission during its evolutionary history. Further studies are needed to determine whether this virus has infected other humans in Indonesia or other localities and identify genotypic changes that might give this virus distinctive phenotypic properties. The discovery of this and other highly divergent strains of DENV further emphasizes the need for biodiversity surveys of this major group of viruses in animals other than humans. It also suggests that gaps in DENV phylogeny might be filled after wider sampling.

Acknowledgment

We thank Queensland Medical Laboratories (Everton Park, Queensland, Australia) for providing anonymous patient specimens for DENV analysis.

This study was supported by grants from the US Global Emerging Infectious Disease Surveillance System, the Cook Foundation, and a National Health and Medical Research Council Australia Fellowship to E.C.H.

Dr. Liu is head of the Department of Arbovirology at the Australian Army Malaria Institute, Brisbane, Australia. His primary research interests are factors that influence emergence and reemergence of arboviral diseases in the Asia–Pacific region.

References

1. Rudnick A, Marchette NJ, Garcia R. Possible jungle dengue: recent studies and hypotheses. Jpn J Med Sci Biol. 1967;20(Suppl):69–74.
2. Kimura R, Hotta S. On the inoculation of dengue virus into mice. Nippon Igaku. 1944;3379:629–33.
3. Sabin AB. Research on dengue during World War II. Am J Trop Med Hyg. 1952;1:30–50.
4. Hammon WM, Rudnick A, Sather GE. Viruses associated with epidemic hemorrhagic fevers of the Philippines and Thailand. Science. 1960;131:1102–3. http://dx.doi.org/10.1126/science.131.3407.1102
5. Wang E, Ni H, Xu R, Barrett AD, Watowich SJ, Gubler DJ, et al. Evolutionary relationships of endemic/epidemic and sylvatic dengue viruses. J Virol. 2000;74:3227–34. http://dx.doi.org/10.1128/JVI.74.7.3227-3234.2000
6. Vasilakis N, Cardosa J, Hanley KA, Holmes EC, Weaver SC. Fever from the forest: prospects for the continued emergence of sylvatic dengue virus and its impact on public health. Nat Rev Microbiol. 2011;9:532–41. http://dx.doi.org/10.1038/nrmicro2595
7. Pyke AT, Moore PR, Taylor CT, Hall-Mendelin S, Cameron JN, Hewitson GR, et al. Highly divergent dengue virus type 1 genotype sets a new distance record. Sci Rep. 2016;6:22356. http://dx.doi.org/10.1038/srep22356
8. Roehrig JT, Mathews JH, Trent DW. Identification of epitopes on the E glycoprotein of Saint Louis encephalitis virus using monoclonal antibodies. Virology. 1983;128:118–26. http://dx.doi.org/10.1016/0042-6822(83)90323-9
9. Henchal EA, Gentry MK, McCown JM, Brandt WE. Dengue virus-specific and flavivirus group determinants identified with monoclonal antibodies by indirect immunofluorescence. Am J Trop Med Hyg. 1982;31:830–6.
10. Jianmin Z, Linn ML, Bulich R, Gentry MK, Aaskov JG. Analysis of functional epitopes on the dengue 2 envelope (E) protein using monoclonal IgM antibodies. Arch Virol. 1995;140:899–913. http://dx.doi.org/10.1007/BF01314966
11. Sambrook J, Rusell DW, editors. Molecular cloning: a laboratory manual. Cold Spring Harbor (NY): Cold Spring Harbor Press; 2001.
12. Biebricher CK, Luce R. Sequence analysis of RNA species synthesized by Q beta replicase without template. Biochemistry. 1993;32:4848–54. http://dx.doi.org/10.1021/bi00069a021
13. Guindon S, Dufayard JF, Lefort V, Anisimova M, Hordijk W, Gascuel O. New algorithms and methods to estimate maximum-likelihood phylogenies: assessing the performance of PhyML 3.0. Syst Biol. 2010;59:307–21. http://dx.doi.org/10.1093/sysbio/syq010
14. Popescu AA, Huber KT, Paradis E. ape 3.0: new tools for distance-based phylogenetics and evolutionary analysis in R. Bioinformatics. 2012;28:1536–7. http://dx.doi.org/10.1093/bioinformatics/bts184
15. Vasilakis N, Cardosa J, Diallo M, Sall AA, Holmes EC, Hanley KA, et al. Sylvatic dengue viruses share the pathogenic potential of urban/endemic dengue viruses. J Virol. 2010;84:3726–7, author reply 3727–8. http://dx.doi.org/10.1128/JVI.02640-09

Address for correspondence: John G. Aaskov, Institute of Health and Biomedical Innovation, Queensland University of Technology, 60 Musk Ave, Kelvin Grove, Brisbane 4059, QLD, Australia; email: j.aaskov@qut.edu.au

Unusual Ebola Virus Chain of Transmission, Conakry, Guinea, 2014–2015

Mory Keita, Sophie Duraffour, Nicholas J. Loman, Andrew Rambaut, Boubacar Diallo, Nfaly Magassouba, Miles W. Carroll, Joshua Quick, Amadou A. Sall, Judith R. Glynn, Pierre Formenty, Lorenzo Subissi,[1] Ousmane Faye[1]

In October 2015, a new case of Ebola virus disease in Guinea was detected. Case investigation, serology, and whole-genome sequencing indicated possible transmission of the virus from an Ebola virus disease survivor to another person and then to the case-patient reported here. This transmission chain over 11 months suggests slow Ebola virus evolution.

As of May 6, 2016, a total of 28,616 Ebola virus disease (EVD) cases, including 11,310 deaths, had been reported since December 2013, mainly from Guinea, Sierra Leone, and Liberia (*1*). Ebola virus often persists in immune-privileged sites of survivors, resulting in detectable virus in semen and other body fluids (*2–5*). Because sperm can shed Ebola virus (EBOV) for ≤10 months after illness onset, exposure to semen of infected survivors can lead to EVD flare-ups (*5–8*). In utero transmission of EBOV from an asymptomatic mother is also possible (*9*).

A powerful tool for following the course of an epidemic of diseases for which human-to-human transmission is prevalent is molecular typing. In Guinea, an in-field sequencing facility was deployed in May 2015, and by September, when the outbreak was fading, EBOV genomes were available for ≈90% of new EVD cases (*10*). We report epidemiologic and molecular evidence of an unusual chain of EBOV transmission. This chain includes an EVD survivor, who recovered in December 2014; possibly his wife (the woman) or a third unknown person; and the woman's brother, who became ill with EVD in October 2015 (the case-patient).

The National Committee of Ethics in Medical Research of Guinea approved use of archived diagnostic samples and corresponding patient data for this study (permit no. 11/CNERS/14). Written consent for publication of confidential data was collected for all patients described here.

The Study

On October 8, 2015, the case-patient in Conakry, Guinea, became ill with fever and appetite loss. His brother-in-law, an EVD survivor and nurse living in the same household, diagnosed malaria, but the case-patient did not respond to malaria treatment; diarrhea, headache, and abdominal pain developed. Four days later, he started bleeding from the nose. On October 13, reverse transmission PCR (RT-PCR) of the case-patient's blood was positive for EBOV (*11*).

From September 2015 until confirmation of EVD for this case-patient, only 7 cases of EVD in Guinea had been reported, all part of the same chain of transmission. Of these cases, virus was not sequenced for 2 because the epidemiologic link was not clearly established. Because the case-patient we report did not have any link with ongoing EVD clusters investigated in Guinea or Sierra Leone, the most likely source of infection was the survivor. Because EBOV is shed in survivors' semen long after recovery (*7*), within-marriage sexual transmission from the survivor to the woman was inferred.

Blood, urine, and buccal swab samples from the couple were collected, together with semen and vaginal swab samples; all were negative for EBOV by RT-PCR. Blood, urine, buccal, and vaginal swab samples were processed as in (*11*) and seminal fluid samples as in (*10*). The woman's serum was positive according to IgG and IgM ELISA testing (both titers ≥1:6,400); the survivor's serum was positive for IgG only (titer ≥1:3,200) (*12*). Serum from the only other household member, the couple's 11-year-old daughter, was negative for IgG and IgM. Although the woman's IgM titer was suggestive of a recent EBOV infection, she reported having had only a mild 2-day clinical episode back in early September, characterized by myalgia, joint pain, and low-back pain (Figure 1). The couple declared that

Author affiliations: World Health Organization, Conakry, Guinea (M. Keita, B. Diallo); Bernhard Nocht Institute for Tropical Medicine, Hamburg, Germany (S. Duraffour); The European Mobile Laboratory Consortium, Hamburg (S. Duraffour, M.W. Carroll); University of Birmingham, Birmingham, UK (N.J. Loman, J. Quick); University of Edinburgh, Edinburgh, Scotland, UK (A. Rambaut); Université Gamal Abdel Nasser de Conakry, Conakry (N. Magassouba); Public Health England, Porton Down, Salisbury, UK (M.W. Carroll); University of Southampton South General Hospital, Southampton, UK (M.W. Carroll); Institut Pasteur, Dakar, Senegal (A.A. Sall, O. Faye); London School of Hygiene and Tropical Medicine, London, UK (J.R. Glynn); World Health Organization, Geneva, Switzerland (P. Formenty); European Centre for Disease Prevention and Control/World Health Organization, Conakry (L. Subissi)

DOI: http://dx.doi.org/10.3201/eid2212.160847

[1]These authors contributed equally to this article.

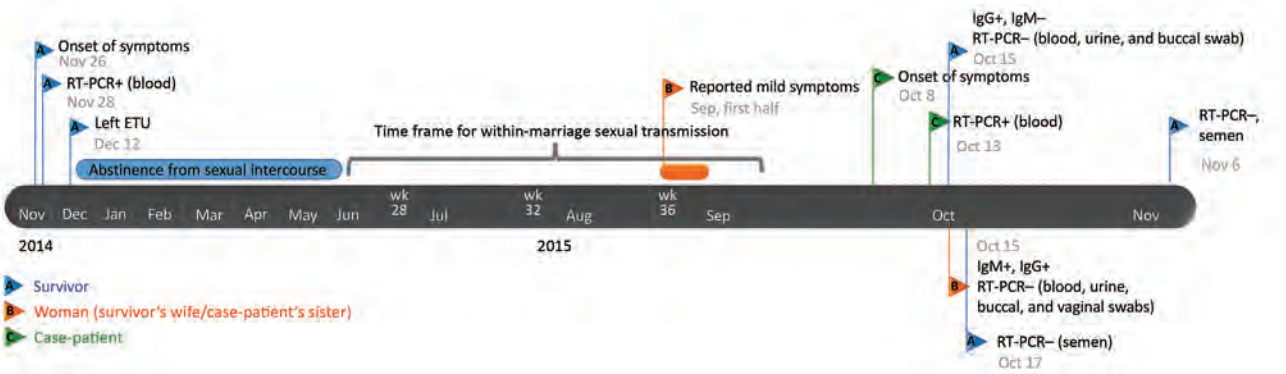

Figure 1. Timeline of the reported chain of transmission of Ebola virus involving 3 persons in Conkary, Guinea, 2014–2015. ETU, Ebola treatment unit; RT-PCR, reverse transcription PCR; –, negative; +, positive.

they had had no sexual intercourse for 6 months after the survivor was discharged from an Ebola treatment unit.

The near full-genome sequence of virus from the case-patient, obtained as previously described (*10*), was available on October 15, 2015. Phylogenetic analysis demonstrated that it belonged to the GN1 lineage rather than the SL3 lineage that was circulating in Conakry during the second half of 2015 (Figure 2, panel A). Thus, the cases were probably not linked to the known ongoing chain of transmission in this area because sequencing of the viruses involved in the Guinea epidemic had been thoroughly performed at this time and no GN1 lineage viruses had been detected in Guinea since the end of June 2015 (*10*). The sequence of the virus isolated from the case-patient, however, could not be closely linked to any known subclusters within GN1. The most closely related viruses were recovered from EVD patients in March 2015, but phylogenetic inference suggests that the new sequence had not evolved from these patients and instead shared a common ancestor from late 2014 (Figure 2, panel B).

Because various samples from the survivor (including semen) and from the woman were negative for EBOV (Figure 1), serum collected during the survivor's acute phase of EVD (November 28, 2014) was retrieved from an archived collection and sequenced, together with a sample from the person who was thought to have transmitted the infection to him (IPD_2163) (Figure 2, panel B). These 2 EBOV sequences were indistinguishable and clustered with virus sequences from the case-patient, differing at 6 nt sites. This difference over an 11-month period is smaller than expected from the estimated EBOV evolutionary rate that would predict 22.5 (95% CI 13–33) mutations (Figure 2, panel C).

Several lines of evidence converge toward an unusual chain of transmission. Most likely, the first patient sexually transmitted EBOV to the woman 9 months after his onset of EVD in 2014, and then either the woman (with a recent history of undetected EBOV infection) or a third unknown person transmitted the virus to the case-patient. After 10.5 months, virus from the case-patient differed from that of the survivor by only 6 nt substitutions. These substitutions were not present in other virus sequences from the GN1 lineage, demonstrating that the isolates are closely related to each other and more distantly related to others.

The number of substitutions between the 2 genomes was 3.7 times lower than would be expected after human-to-human transmission and may indicate virus persistence in 1 person. This hypothesis is in line with reduced evolutionary rates of persistent EBOV reported in Liberia and Sierra Leone (*7*,*8*,*13*).

Serologic data revealed that the woman had recently been infected with EBOV. However, none of her samples (i.e., blood, urine, and vaginal swab) were positive for EBOV by RT-PCR; therefore, no genomic data were available.

The serial interval between the case-patient's onset of symptoms and that of the woman (≈30 days) is longer than the usual EVD maximum incubation period (21 days). Therefore, the woman may have more recently experienced mild or asymptomatic infection.

We have no molecular evidence that the woman was part of this chain of transmission; it is plausible that a third unknown person infected the case-patient. It was impossible to investigate potential direct male-to-male sexual transmission.

Conclusions

A likely explanation of our observations, integrating genomic, serologic, and epidemiologic data, is that within-marriage sexual transmission occurred (inferred from the positive IgM titers of the woman) and then the woman infected her brother through close contact. They all lived in the same small household in poor hygienic conditions; shared toilets, meals, and at times beds; and cared for each other. Alternatively, a third unknown person may have been the link in the transmission from the survivor to the case-patient.

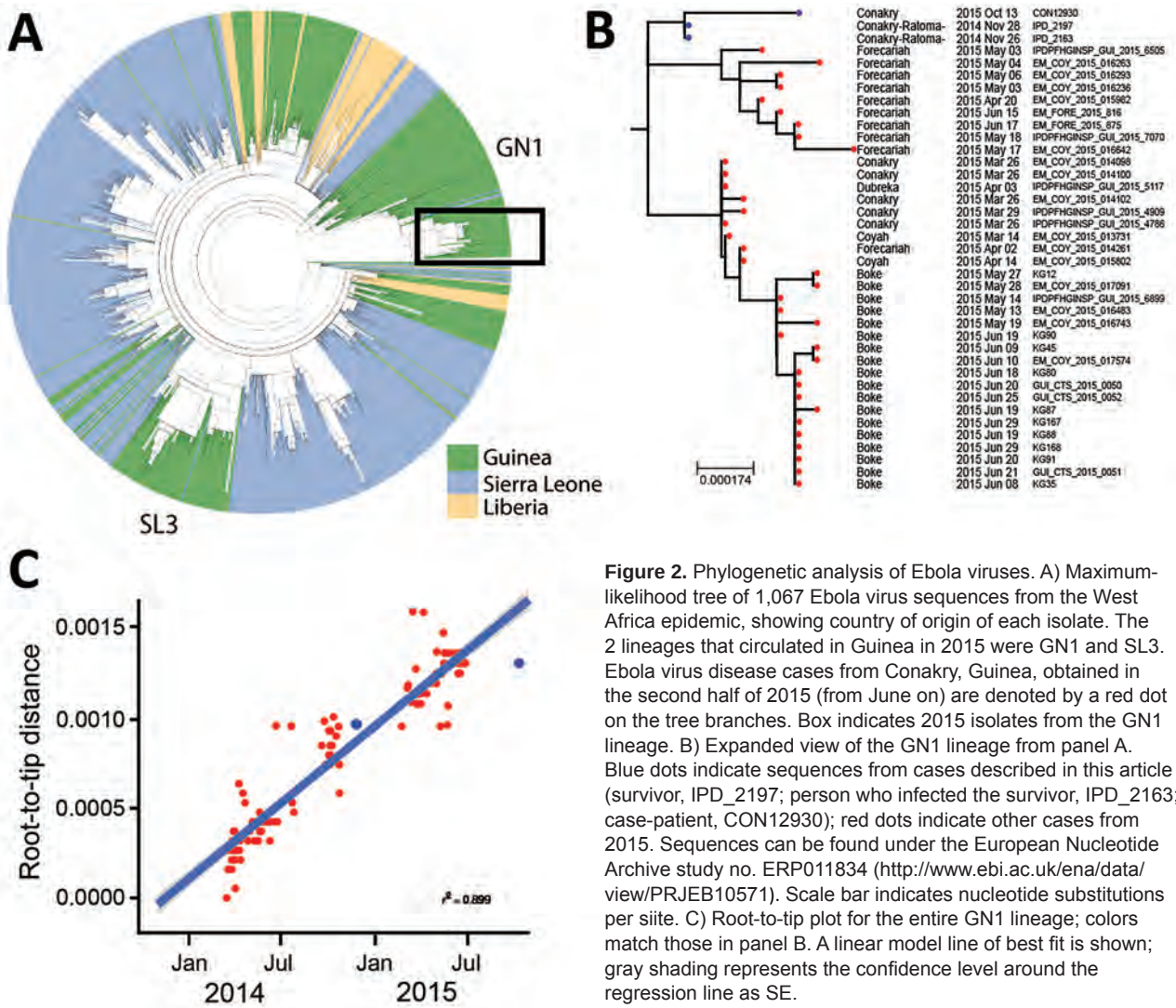

Figure 2. Phylogenetic analysis of Ebola viruses. A) Maximum-likelihood tree of 1,067 Ebola virus sequences from the West Africa epidemic, showing country of origin of each isolate. The 2 lineages that circulated in Guinea in 2015 were GN1 and SL3. Ebola virus disease cases from Conakry, Guinea, obtained in the second half of 2015 (from June on) are denoted by a red dot on the tree branches. Box indicates 2015 isolates from the GN1 lineage. B) Expanded view of the GN1 lineage from panel A. Blue dots indicate sequences from cases described in this article (survivor, IPD_2197; person who infected the survivor, IPD_2163; case-patient, CON12930); red dots indicate other cases from 2015. Sequences can be found under the European Nucleotide Archive study no. ERP011834 (http://www.ebi.ac.uk/ena/data/view/PRJEB10571). Scale bar indicates nucleotide substitutions per siite. C) Root-to-tip plot for the entire GN1 lineage; colors match those in panel B. A linear model line of best fit is shown; gray shading represents the confidence level around the regression line as SE.

Interim advice with regard to sexual transmission of EBOV has been updated recently (*14*). All EVD survivors and their sex partners should receive condoms and counseling to ensure safer sex practices. Safer sex practices should continue until the results of semen testing are negative twice or, if testing is unavailable, for 12 months. The safer sex strategy and testing could be complemented by new medical countermeasures that need to be assessed and include use of antiviral drugs, vaccination of relatives and sex partners of survivors, or both.

Acknowledgments

We thank Josep Jansa for stimulating discussions, and we thank all institutions that are part of the Global Outbreak Alert and Response Network (GOARN) for support to the Ebola outbreak response in Guinea. We also thank the GOARN Operational Support Team at the World Health Organization (WHO) headquarters, which coordinated and supported deployments in West Africa.

The WHO and the Institut Pasteur de Dakar financed this study. The work provided by the EMLab (a technical partner of the WHO Emerging and Dangerous Pathogens Laboratory) and the GOARN was conducted in the context of the projects EVIDENT (Ebola virus disease: correlates of protection, determinants of outcome, and clinical management) and REACTION!, which received funding from the European Union Horizon 2020 research and innovation program under grant agreement nos. 666100 and 666092, respectively, and in the context of service contract IFS/2011/272-372, funded by Directorate-General for International Cooperation and Development.

Dr. Keita is a medical doctor and epidemiologist. During the Ebola outbreak, he worked as a WHO Field Coordinator and

Regional Coordinator. He is interested in communicable diseases epidemiology and health system strengthening.

References

1. World Health Organization. Ebola outbreak 2014–2015 [cited 2016 Jan 20]. http://www.who.int/csr/disease/ebola/en/
2. Varkey JB, Shantha JG, Crozier I, Kraft CS, Lyon GM, Mehta AK, et al. Persistence of Ebola virus in ocular fluid during convalescence. N Engl J Med. 2015;372:2423–7. http://dx.doi.org/10.1056/NEJMoa1500306
3. Rodriguez LL, De Roo A, Guimard Y, Trappier SG, Sanchez A, Bressler D, et al. Persistence and genetic stability of Ebola virus during the outbreak in Kikwit, Democratic Republic of the Congo, 1995. J Infect Dis. 1999;179(Suppl 1):S170–6. http://dx.doi.org/10.1086/514291
4. Jacobs M, Rodger A, Bell DJ, Bhagani S, Cropley I, Filipe A, et al. Late Ebola virus relapse causing meningoencephalitis: a case report. Lancet Lond Engl. 2016; 388:498–503. http://dx.doi.org/10.1016/S0140-6736(16)30386-5
5. Deen GF, Knust B, Broutet N, Sesay FR, Formenty P, Ross C, et al. Ebola RNA persistence in semen of Ebola virus disease survivors—preliminary report. N Engl J Med. 2015 [Epub ahead of print; cited 2015 Nov 25]. http://dx.doi.org/10.1056/NEJMoa1511410
6. Thorson A, Formenty P, Lofthouse C, Broutet N. Systematic review of the literature on viral persistence and sexual transmission from recovered Ebola survivors: evidence and recommendations. BMJ Open. 2016;6:e008859. http://dx.doi.org/10.1136/bmjopen-2015-008859
7. Mate SE, Kugelman JR, Nyenswah TG, Ladner JT, Wiley MR, Cordier-Lassalle T, et al. Molecular evidence of sexual transmission of Ebola virus. N Engl J Med. 2015;373:2448–54. http://dx.doi.org/10.1056/NEJMoa1509773
8. Blackley DJ, Wiley MR, Ladner JT, Fallah M, Lo T, Gilbert ML, et al. Reduced evolutionary rate in reemerged Ebola virus transmission chains. Sci Adv. 2016;2:e1600378. http://dx.doi.org/10.1126/sciadv.1600378
9. Bower H, Grass JE, Veltus E, Brault A, Campbell S, Basile AJ, et al. Delivery of an Ebola virus–positive stillborn infant in a rural community health center, Sierra Leone, 2015. Am J Trop Med Hyg. 2016;94:417–9. http://dx.doi.org/10.4269/ajtmh.15-0619
10. Quick J, Loman NJ, Duraffour S, Simpson JT, Severi E, Cowley L, et al. Real-time, portable genome sequencing for Ebola surveillance. Nature. 2016;530:228–32. http://dx.doi.org/10.1038/nature16996
11. Weidmann M, Mühlberger E, Hufert FT. Rapid detection protocol for filoviruses. J Clin Virol. 2004;30:94–9. http://dx.doi.org/10.1016/j.jcv.2003.09.004
12. Ksiazek TG, West CP, Rollin PE, Jahrling PB, Peters CJ. ELISA for the detection of antibodies to Ebola viruses. J Infect Dis. 1999;179(Suppl 1):S192–8. http://dx.doi.org/10.1086/514313
13. Arias A, Watson SJ, Asogun D, Tobin EA, Lu J, Phan MV, et al. Rapid outbreak sequencing of Ebola virus in Sierra Leone identifies transmission chains linked to sporadic cases. Virus Evol. 2016;2. http://dx.doi.org/10.1093/ve/vew016
14. World Health Organization. Interim advice on the sexual transmission of the Ebola virus disease [cited 2016 Jan 23]. http://www.who.int/reproductivehealth/topics/rtis/ebola-virus-semen/en/

Address for correspondence: Lorenzo Subissi, World Health Organization/European Centre for Disease Prevention and Control, B.P. 611, Papeete, French Polynesia; email: loresubissi@hotmail.com

Human Infection with Novel Spotted Fever Group *Rickettsia* Genotype, China, 2015

Hao Li,[1] Xiao-Ming Cui,[1] Ning Cui, Zhen-Dong Yang, Jian-Gong Hu, Ya-Di Fan, Xue-Juan Fan, Lan Zhang, Pan-He Zhang, Wei Liu, Wu-Chun Cao

Only 4 species of spotted fever group rickettsiae have been detected in humans in China. However, phylogenetic analysis of samples from 5 ill patients in China indicated infection with a novel spotted fever group *Rickettsia*, designated *Rickettsia* sp. XY99. Clinical signs resembled those of severe fever with thrombocytopenia syndrome.

Spotted fever group (SFG) rickettsiae are globally distributed and mostly transmitted by ticks (*1*). Recently, emerging and reemerging SFG rickettsiae, such as *Rickettsia slovaca* (*2*), *R. aeschlimannii* (*3*), *R. massiliae* (*4*), *Candidatus* Rickettsia tarasevichiae (*5*,*6*), and *R. sibirica* subspecies *sibirica* BJ-90 (*7*), previously considered nonpathogenic, were found to infect humans. In addition, *R. parkeri* was confirmed to be pathogenic 65 years after its detection in ticks in 1939 (*8*).

In China, SFG rickettsioses are not listed as reportable diseases, and only 4 species of SFG rickettsiae (*R. heilongjiangensis*, *R. sibirica* subspecies *sibirica* BJ-90, *Candidatus* Rickettsia tarasevichiae, and *R. raoultii*) have been detected in human blood samples (*9*). In contrast, besides these pathogenic species, at least 4 other species of SFG rickettsiae (*R. sibirica* subspecies *mongolotimonae*, *R. monacensis*, *R. slovaca*, *Candidatus* Rickettsia hebeiii) have been detected in ticks, urging a wider search for cases in humans. We report infection of 5 patients with a novel SFG rickettsia in eastern central China.

The Study

From March through November 2015, at the People's Liberation Army 154 Hospital in Xinyang City, Henan Province, China, patients who were acutely symptomatic with fever and had a history of tick bites or animal contact within the past month were screened for SFG rickettsiae infection. At admission, EDTA-anticoagulated samples of peripheral blood were collected. DNA was extracted by using a QIAamp DNA Blood Mini Kit (QIAGEN, Germantown, MD, USA). Nested PCRs selective for outer membrane protein A (*omp*A) and citrate synthase (*glt*A) genes were concurrently performed to detect SFG rickettsial DNA (online Technical Appendix Table 1, http://wwwnc.cdc.gov/EID/article/22/12/16-0962-Techapp1.pdf)). Positive amplicons were purified and then sequenced in both directions. Acute-phase (≤7 days after illness onset) and convalescent-phase (≥14 days after illness onset) serum samples were tested by indirect immunofluorescence assay (IFA) for IgG against *R. rickettsii* by using a commercially available IFA kit (Focus Diagnostics Inc., Cypress, CA, USA).

Positive amplification of *omp*A and *glt*A genes was found for 5 patients, and the obtained sequences for each of the 2 genes from all 5 patients were identical. Nucleotide sequence (350-bp) of *omp*A gene (GenBank accession no. KU853020) from each of the 5 patients showed 10-bp differences from that of *R. massiliae* strain AZT80 (GenBank accession no. CP003319) and 12-bp differences from that of *R. rhipicephali* strain HJ#5 (GenBank accession no. CP013133). Nucleotide sequences (1150-bp) of *glt*A gene (GenBank accession no. KU853022) from each of the 5 patients differed from that of *R. massiliae* strain AZT80 by 4 bp and from that of *R. rhipicephali* strain HJ#5 by 5 bp (online Technical Appendix Table 2). According to phylogenetic analysis, the novel SFG rickettsiae genotype, here designated as *Rickettsia* sp. XY99, seems to represent a distinct lineage and could constitute a new species (Figure 1). For all 5 patients, seroconversion or a 4-fold increase of IgG against *R. rickettsii* was found between the acute- and convalescent-phase samples, and the patients were determined to have acute infection with SFG rickettsiae (online Technical Appendix Table 3). Subsequent testing of the 5 patients for infection with severe fever with thrombocytopenia syndrome virus, *Anaplasma phagocytophilum*, "*A. capra*," and *Babesia microti* by molecular (real-time PCR or nested PCR) and serologic tests (ELISA or IFA) produced no positive results.

All 5 patients were farmers who resided in the villages of Xinyang City. Patient median age was 65 (range 62–80) years, and 3 were male (Table). Two patients had a history of tick exposure, and the other 3 had had contact with livestock. For all 5 patients, illness onset occurred June 20–July 10, 2015. The median time from illness onset to

Author affiliations: State Key Laboratory of Pathogen and Biosecurity, Beijing Institute of Microbiology and Epidemiology, Beijing, China (H. Li, X.-M. Cui, J.-G. Hu, Y.-D. Fan, P.-H. Zhang, W. Liu, W.-C. Cao); The People's Army 154 Hospital, Xinyang, China (N. Cui, Z.-D. Yang, X.-J. Fan, L. Zhang)

DOI: http://dx.doi.org/10.3201/eid2212.160962

[1]These authors contributed equally to this article.

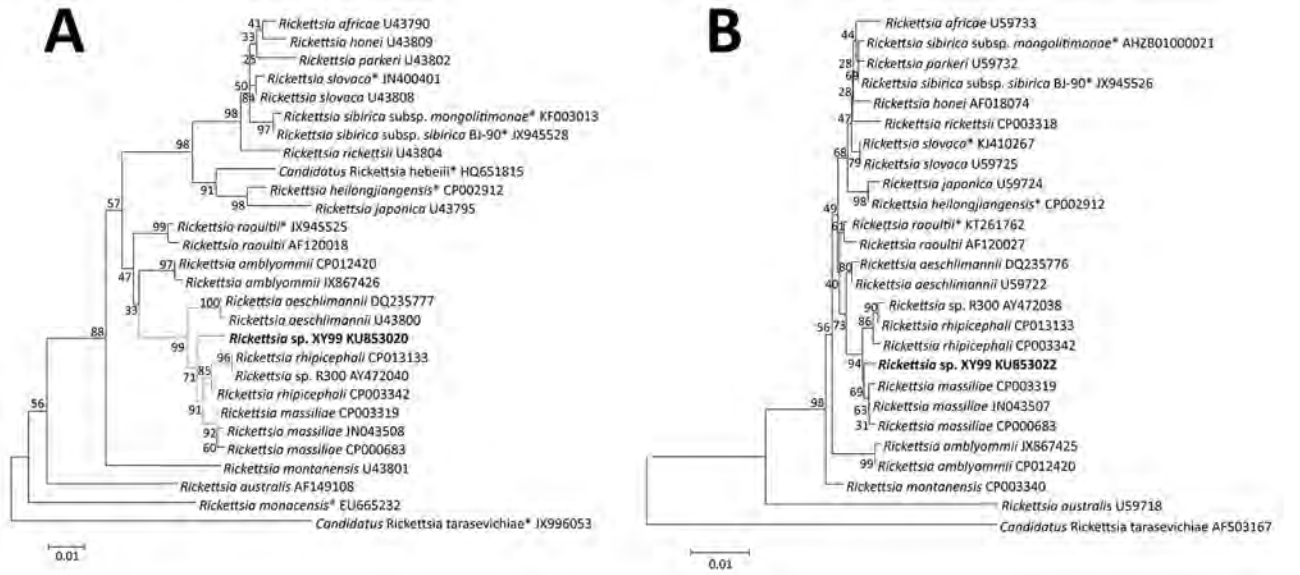

Figure 1. Phylogenetic analyses based on nucleotide sequences of the outer member protein A (307-bp) (A) and citrate synthase (1,150-bp) (B) genes of *Rickettsia*. Boldface indicates the newly discovered *Rickettsia* genotype (*Rickettsia* sp. XY99). Asterisks after taxon names indicate that the sequence of *Rickettsia* species was found in China. Neighbor-joining trees were conducted by using the maximum composite likelihood method by means of MEGA version 5.0 (http://www.megasoftware.net). Bootstrap analysis of 1,000 replicates was applied to assess the reliability of the reconstructed phylogenies. Scale bars indicate estimated evolutionary distance.

admission was 4 (range 3–6) days, and the median duration of hospitalization was 10 (range 8–12) days. All patients experienced fever (highest 38.4°C– 40.0°C), asthenia, anorexia, and nausea; 4 had cough, 3 vomiting, 2 myalgia, 1 headache, and 1 dizziness. Of note, all 5 patients had lymphadenopathy, but none had rash or eschar. At admission, all 5 patients had leukopenia, thrombocytopenia, and elevated hepatic aminotransferase levels; 4 had elevated

Table. Epidemiologic and clinical characteristics of 5 patients with *Rickettsia* sp. XY99 infection, China, 2015*

Characteristic	Patient no. 1	2	3	4	5
Age, y	65	64	66	80	62
Sex	M	F	F	M	M
History of tick bite	No	No	No	Yes	Yes
Time between tick bite and illness onset, d	NA	NA	NA	14	6
Time from onset to admission, d	3	6	5	4	4
Duration of hospitalization, d	12	8	9	12	10
Fever	Yes	Yes	Yes	Yes	Yes
Highest temperature, °C	40.0	39.5	38.7	38.4	39.1
Headache	Yes	No	No	No	No
Dizziness	No	Yes	No	No	No
Asthenia	Yes	Yes	Yes	Yes	Yes
Myalgia	Yes	Yes	No	No	No
Rash	No	No	No	No	No
Eschar	No	No	No	No	No
Lymphadenopathy	Yes	Yes	Yes	Yes	Yes
Anorexia	Yes	Yes	Yes	Yes	Yes
Nausea	Yes	Yes	Yes	Yes	Yes
Vomit	Yes	Yes	Yes	No	No
Cough	Yes	Yes	Yes	No	Yes
Pneumonia	Yes	No	Yes	No	Yes
Hydrothorax	Yes	No	Yes	No	No
Confusion	Yes	No	No	No	No
Meningeal irritation sign	Yes	No	No	No	No
Ecchymosis	Yes	No	No	No	No
Hemoptysis	No	No	No	No	Yes
Hematuria	Yes	Yes	No	No	No

*NA, not applicable.

lactate dehydrogenase levels, and 2 had elevated creatine kinase levels (Figure 2). Treatment included therapy with cefminox and cefoperazone; no doxycycline was used.

Complications included pneumonia (3 patients), hemorrhagic signs (3), hydrothorax (2), and neurologic syndromes (1). For 1 patient, severe complications progressively emerged 6 days after disease onset and included pneumonia and hydrothorax (online Technical Appendix Figure), confusion, meningeal irritation sign, ecchymosis, and hematuria. Laboratory indicators were substantially more out of range 7 days after disease onset, indicative of severe multiorgan dysfunction (Figure 2). Treatment was ineffective, and the patient died 15 days after disease onset. The other 4 patients were discharged after 8–12 days' hospitalization; at that time, all clinical signs and symptoms had resolved, but for certain patients, laboratory values remained out of reference range, suggesting slow recovery of organ dysfunction (Figure 2).

Conclusions

Our detection of *Rickettsia* sp. XY99 DNA in blood samples collected during the acute period of illness (days 3–6 after onset) from 5 patients in the same region of China suggests that this organism was the etiologic agent of the infection. Seroconversion or a 4-fold increase in titers of IgG against *R. rickettsii* provided supportive evidence of SFG *Rickettsia* infection. Phylogenetic analysis indicated that *Rickettsia* sp. XY99 was a novel genotype of SFG rickettsiae.

In contrast to humans with *R. massiliae* infection and many other SFG rickettsioses reported previously (*4*,*10*), none of the 5 patients infected with *Rickettsia* sp. XY99 had rash or eschar, and only 1 had headache. In recent years, the concept of the classic triad of fever, rash, and headache suggesting infection with SFG rickettsiae has been increasingly challenged. Several emerging SFG rickettsiae species, such as *R. slovaca* (*2*), *R. raoultii* (*11*), *R. africae* (*12*), and *R. helvetica* (*13*), can infect humans, but such infections lack these traditional features, which were also lacking in the cases reported here. Therefore, absence of rash and tick-bite history should not exclude suspicion of SFG rickettsiae infection.

Similar to *R. slovaca* and *R. raoultii* infections, which can be associated with tickborne lymphadenopathy and *Dermacentor*-borne necrosis-erythema-lymphadenopathy (*14*), lymphadenopathy was also observed in all 5 patients with *Rickettsia* sp. XY99 infection. Thus, lymphadenopathy might be a typical sign useful for clinical diagnosis of *Rickettsia* sp. XY99 infection. All 5 patients had gastrointestinal syndromes, indicating potential tissue lesions or vascular injury of the gastrointestinal tract. The hydrothorax

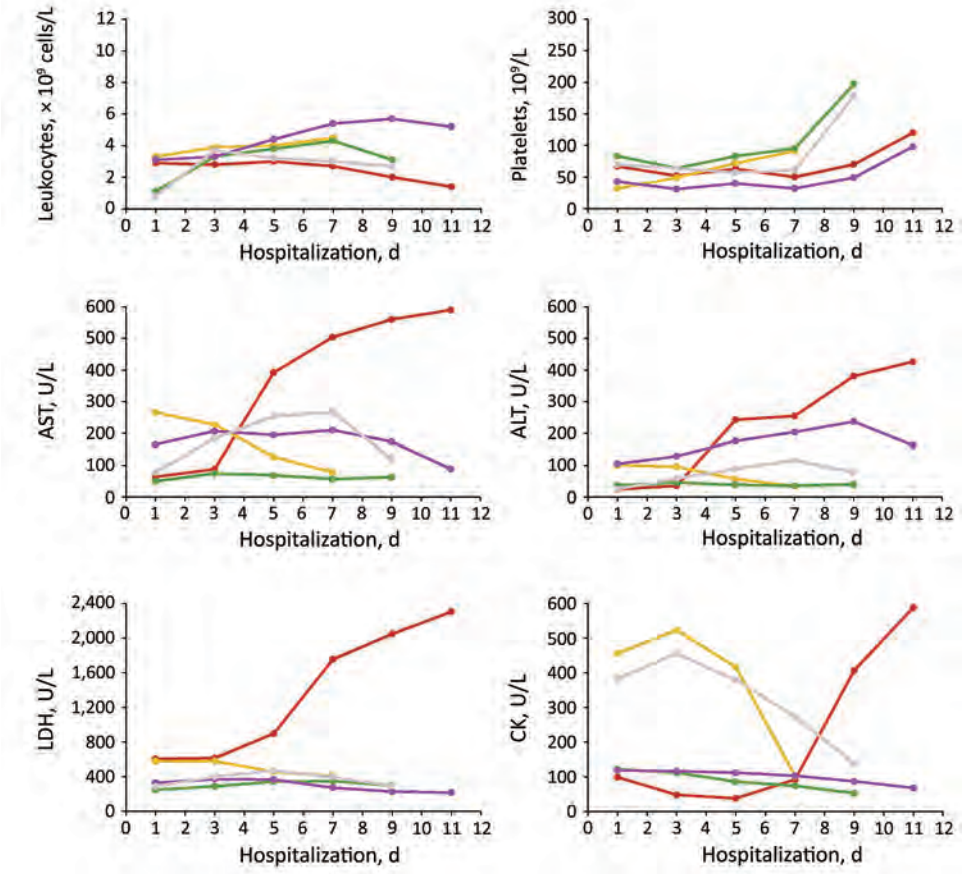

Figure 2. Dynamic changes of 6 laboratory parameters (with 2-day intervals) during hospitalization of 5 patients with *Rickettsia* sp. XY99 infection, China, 2015. Red, patient 1; yellow, patient 2; green, patient 3; purple, patient 4; gray, patient 5. ALT, alanine aminotransferase, reference range 0–40 U/L; AST, aspartate aminotransferase, reference range 0–40 U/L; CK, creatine kinase, reference range 25–200 U/L; LDH, lactate dehydrogenase, reference range 109–245 U/L; platelets, reference range 100–300 × 10^9/L; leukocytes, reference range 4.0–10.5 × 10^9 cells/L.

and multiple hemorrhagic signs in 4 patients is possibly suggestive of vascular invasion or damage caused by this novel *Rickettsia* species.

Confirmation of the novel *Rickettsia* genotype was achieved only by sequencing the *omp*A and *glt*A genes. Although differences based on 2 gene segments support its designation as a novel species, isolation efforts and characterization of all 5 genes (*rrs*, *glt*A, *omp*A, *omp*B, and *gene*D) are warranted, according to the guidelines for classification of a new *Rickettsia* species (*15*).

Physicians in this area of China should be aware of human infections with *Rickettsia* sp. XY99. It should be included in differential diagnoses with severe fever with thrombocytopenia syndrome, which causes similar clinical illness and is also endemic to the same area in eastern central China.

This study was supported by the Natural Science Foundation of China (81222037, 81290344, 81130086, and 81472005).

Dr. Li is a scientist in the State Key Laboratory of Pathogen and Biosecurity, Beijing Institute of Microbiology and Epidemiology. His research interests include microbiology, epidemiology, and ecology of tickborne diseases.

References

1. Parola P, Paddock CD, Socolovschi C, Labruna MB, Mediannikov O, Kernif T, et al. Update on tick-borne rickettsioses around the world: a geographic approach. Clin Microbiol Rev. 2013;26:657–702. http://dx.doi.org/10.1128/CMR.00032-13
2. Raoult D, Berbis P, Roux V, Xu W, Maurin M. A new tick-transmitted disease due to *Rickettsia slovaca.* Lancet. 1997; 350:112–3. http://dx.doi.org/10.1016/S0140-6736(05)61814-4
3. Raoult D, Fournier PE, Abboud P, Caron F. First documented human *Rickettsia aeschlimannii* infection. Emerg Infect Dis. 2002;8:748–9. http://dx.doi.org/10.3201/eid0807.010480
4. Vitale G, Mansuelo S, Rolain JM, Raoult D. *Rickettsia massiliae* human isolation. Emerg Infect Dis. 2006;12:174–5. http://dx.doi.org/10.3201/eid1201.050850
5. Jia N, Zheng YC, Jiang JF, Ma L, Cao WC. Human infection with *Candidatus Rickettsia tarasevichiae.* N Engl J Med. 2013;369:1178–80. http://dx.doi.org/10.1056/NEJMc1303004
6. Liu W, Li H, Lu QB, Cui N, Yang ZD, Hu JG, et al. *Candidatus* Rickettsia tarasevichiae infection in eastern central China: a case series. Ann Intern Med. 2016;164:641–8. http://dx.doi.org/10.7326/M15-2572
7. Jia N, Jiang JF, Huo QB, Jiang BG, Cao WC. *Rickettsia sibirica* subspecies *sibirica* BJ-90 as a cause of human disease. N Engl J Med. 2013;369:1176–8. http://dx.doi.org/10.1056/NEJMc1303625
8. Paddock CD, Sumner JW, Comer JA, Zaki SR, Goldsmith CS, Goddard J, et al. *Rickettsia parkeri*: a newly recognized cause of spotted fever rickettsiosis in the United States. Clin Infect Dis. 2004;38:805–11. http://dx.doi.org/10.1086/381894
9. Fang LQ, Liu K, Li XL, Liang S, Yang Y, Yao HW, et al. Emerging tick-borne infections in mainland China: an increasing public health threat. Lancet Infect Dis. 2015;15:1467–79. http://dx.doi.org/10.1016/S1473-3099(15)00177-2
10. Cascio A, Torina A, Valenzise M, Blanda V, Camarda N, Bombaci S, et al. Scalp eschar and neck lymphadenopathy caused by *Rickettsia massiliae.* Emerg Infect Dis. 2013;19:836–7. http://dx.doi.org/10.3201/eid1905.121169
11. Parola P, Rovery C, Rolain JM, Brouqui P, Davoust B, Raoult D. *Rickettsia slovaca* and *R. raoultii* in tick-borne rickettsioses. Emerg Infect Dis. 2009;15:1105–8. http://dx.doi.org/10.3201/eid1507.081449
12. Raoult D, Fournier PE, Fenollar F, Jensenius M, Prioe T, de Pina JJ, et al. *Rickettsia africae,* a tick-borne pathogen in travelers to sub-Saharan Africa. N Engl J Med. 2001;344:1504–10. http://dx.doi.org/10.1056/NEJM200105173442003
13. Fournier PE, Allombert C, Supputamongkol Y, Caruso G, Brouqui P, Raoult D. Aneruptive fever associated with antibodies to *Rickettsia helvetica* in Europe and Thailand. J Clin Microbiol. 2004;42:816–8. http://dx.doi.org/10.1128/JCM.42.2.816-818.2004
14. Silva-Pinto A, Santos ML, Sarmento A. Tick-borne lymphadenopathy, an emerging disease. Ticks Tick Borne Dis. 2014;5:656–9. http://dx.doi.org/10.1016/j.ttbdis.2014.04.016
15. Fournier PE, Dumler JS, Greub G, Zhang J, Wu Y, Raoult D. Gene sequence-based criteria for identification of new *rickettsia* isolates and description of *Rickettsia heilongjiangensis* sp. nov. J Clin Microbiol. 2003;41:5456–65. http://dx.doi.org/10.1128/JCM.41.12.5456-5465.2003

Address for correspondence**:** Wu-Chun Cao or Wei Liu, State Key Laboratory of Pathogen and Biosecurity, Beijing Institute of Microbiology and Epidemiology, 20 Dong-Da St, Fengtai District, Beijing 100071, China; email: caowc@bmi.ac.cn or lwbime@163.com

Hepatitis E Virus in 3 Types of Laboratory Animals, China, 2012–2015

Lin Wang, Yulin Zhang, Wanyun Gong, William Tianshi Song, Ling Wang

We found seroprevalences for hepatitis E virus (HEV) of 7.5%, 18.5%, and 83.3% in specific pathogen-free (SPF) laboratory rabbits, monkeys, and pigs, respectively, in China. HEV RNA was detected in 4.8% of SPF rabbits, and 11 rabbits had latent infections. Screening for HEV in SPF animals before relevant experiments are conducted is recommended.

Hepatitis E virus (HEV) is a single-stranded, positive-sense RNA virus that belongs to the family *Hepeviridae* and is transmitted by the fecal–oral route (*1*). The lack of an efficient cell culture system for HEV hinders understanding of this pathogen. In most HEV studies, specific pathogen-free (SPF) animals are used (*2*). However, antibodies against HEV have been detected in 5 of 10 SPF rabbits in the United States (*3*). Antibodies against HEV or HEV RNA in laboratory animals will confound experimental results.

In addition, swine HEV is zoonotic to humans, and rabbit HEV-3 has been shown to be infectious to cynomolgus macaques (*4*). A strain of HEV closely related to rabbit HEV has been isolated from a human in France (*5*). These findings suggest that laboratory animals infected with HEV might put laboratory workers at risk for infection. In this study, we investigated the antibodies against HEV and HEV RNA in 3 types of SPF laboratory animals (monkeys, pigs and rabbits) that are commonly used in HEV studies in China.

The Study

This study was approved by the Committee of Laboratory Animal Welfare and Ethics, Peking University Health Science Center. In 2012, we obtained 146 SPF rhesus monkeys (*Macaca mulatta*) and cynomolgus monkeys (*M. fascicularis*) from a commercial institute of biologic resources in Beijing, China. During 2012–2015, we obtained 332 SPF rabbits from 2 qualified vendors in China: supplier A (New Zealand white rabbits) and supplier B (Japanese white rabbits). We also obtained 6 SPF Bama miniature pigs from supplier B (Table 1). Microbes excluded in SPF animals are shown in online Technical Appendix Table 1 (http://wwwnc.cdc.gov/EID/article/22/12/16-0131-Techapp1.pdf).

All animals were bred in China and housed in polycarbonate individual ventilated cages or mini pig stainless steel cages (Suhang, Jiangsu, China). Paired serum and fecal samples were collected weekly from each animal for 4 consecutive weeks. We stopped sampling when we obtained positive results for antibodies against or HEV RNA. Specific procedures of for sample processing were described (*4*).

Serum samples from monkeys were tested by using human anti-HEV IgM and human anti-HEV IgG ELISA kits (Wantai, Beijing, China) (*6*). Serum samples from rabbits and pigs were tested by using an anti-HEV total antibodies ELISA kit (Wantai) and HEV E2 antigen (aa 394–606 of open reading frame 2) (*7*). Signal-to-cutoff values were calculated, and values >1 were considered positive.

Virus RNA was extracted from 100 μL of serum or 50% fecal suspensions by using TRIzol Reagent (Invitrogen, Burlington, Ontario, Canada). All samples were analyzed by using a nested reverse transcription PCR.

HEV-positive samples were sequenced and submitted to GenBank (accession nos. KU217460–KU217473 and KU218407–KU218408). A phylogenetic tree was constructed by using MEGA 6.0 software (*8*). A more detailed description of the complete protocol has been previously published (*4*).

We detected antibodies against HEV in 25 (7.5%) of 332 SPF rabbits and 5 (83.3%) of 6 SPF Bama miniature pigs. The HEV IgM–positive rate was 0% (0/146), and the HEV IgG–positive rate was 18.5% (27/146) for SPF monkeys (Table 2). Among all antibody-positive animals, HEV RNA was not detected in serum or stool samples. The HEV antibody–positive rate for SPF rabbits in China was lower than that for farmed and wild rabbits in other studies (online Technical Appendix Table 2).

HEV RNA was detected in 16 (4.8%) of 332 SPF rabbits. One rabbit (supplier A, sequence no. 16) was viremic and shed virus in feces; the other 15 rabbits (supplier B, sequence nos. 1–15) only shed virus in feces (Table 2). Phylogenetic analysis confirmed that all strains isolated from the SPF rabbits belong to genotype 3 and are in 3 clusters for reported rabbit HEV strains (Figure).

Author affiliations: Peking University Health Science Center, Beijing, China (Lin Wang, Y. Zhang, W. Gong, Ling Wang); Beijing Huijia Private School, Beijing (W.T. Song)

DOI: http://dx.doi.org/10.3201/eid2212.160131

Table 1. Characteristics of laboratory rabbits, monkeys, and pigs tested for hepatitis E virus, China, 2012–2015*

Batch no.	Sampling year	Age	No. animals	Species	No. positive, PCR/antibodies against HEV: Total	First sampling	Subsequent sampling†	Genotype	Acceptability, %‡
1	2012	3 wk	10	NZW	0/0	0/0	0/0	NA	100
2	2012	6 wk	16	NZW	0/0	0/0	0/0	NA	100
3	2012	2.5 y	20	CM	0/18	0/18	0/0	NA	10
3	2012	2.5 y	126	RM	0/9	0/9	0/0	NA	92.9
4	2013	7 wk	21	NZW	0/3	0/3	0/0	NA	85.7
5	2013	7 wk	43	JW	0/0	0/0	0/0	NA	100
6	2013	28 wk	32	JW	0/4	0/4	0/0	NA	87.5
7	2014	12 wk	92	JW	2/10	2/10	0/0	3	87.0
8	2015	4 wk	6	BMP	0/5	0/5	0/0	NA	16.7
9	2015	12 wk	42	NZW	1/2	1/2	0/0	3	92.9
10	2015	12 wk	76	JW	6/13	4/4	2/9	3	75

*BMP, Bama miniature pig (*Sus scrofa domestica*); CM, cynomolgus monkey (*Macaca fascicularis*); HEV, hepatitis E virus; JW, Japanese white rabbit (*Oryctolagus cuniculus*); NA, not applicable; NZW, New Zealand white rabbit (*Oryctolagus cuniculus*); RM, rhesus monkey (*Macaca mulatta*).
†Animals had negative results for PCR or antibodies against HEV at week 1, but results became positive for samples collected in subsequent weeks.
‡An animal was considered acceptable for the HEV study when all test results remained negative for 4 consecutive weeks.

Several cases of latent infection and seroconversion were observed (Table 1). Latency was defined as detection of HEV RNA or antibodies against HEV after negative results were observed during the first week in 4-week observation period. In batch no. 10, we found that 5, 3, and 1 SPF rabbits began excretion of HEV in stool during the second, third, and fourth weeks, respectively. Two rabbits seroconverted to antibodies against HEV during the second and third weeks.

Conclusions

In our survey of 3 types of SPF laboratory animals commonly used for HEV studies in China, we detected previous HEV infection in all 3 types of animals, despite having purchased these animals from qualified vendors. We also detected HEV RNA in SPF rabbits, which suggested ongoing virus circulation in these animals. These findings emphasize the need for HEV screening of laboratory animals, not only for persons studying HEV but also for persons studying other pathogens, because the effects of co-infection are unknown. Before experiments are conducted, laboratory animals should be monitored for ≥2 weeks to ensure that no latent HEV infection is present.

Another concern is risk for zoonotic infection for in research personnel. HEV-3 and HEV-4 infect humans and other animals, and rabbit HEV-3 can infect cynomolgus macaques (*4*) and possibly humans (*5*). Therefore, safety of any research personnel who handle laboratory rabbits or pigs is a primary concern. Personal precautions should be fully implemented in the work environment.

HEV 239 vaccine is available in China, and studies have shown that this vaccine provided sustained protection against hepatitis E for ≤4.5 years (*9*,*10*). Thus, persons in China who have occupational exposure to HEV might benefit from vaccination.

This study has potential limitations. First, our results were determined only for 3 types of laboratory animals. Thus, sampling size should be enlarged to include other types of animals. Second, seroprevalence of antibodies against HEV was not determined for personnel who have close contact with these laboratory animals. Thus, risk for occupational transmission was not assessed. Future studies are warranted to address these issues.

In summary, our findings highlight the need for screening for HEV in laboratory animals. This screening will ensure experimental accuracy and prevent possibly zoonotic transmission of HEV to research personnel.

Table 2. Prevalence of antibodies against hepatitis E virus and virus RNA in laboratory animals, China, 2012–2015*

Animal, species	No. samples	No. (%) positive for antibodies against HEV: IgM	IgG	IgM + IgG	No. (%) positive for HEV RNA: Serum	Stool
Rabbit						
NZW	89	NA	NA	5 (5.6)	1 (1.1)	1 (1.1)
JW	243	NA	NA	20 (8.2)	0 (0)	15 (6.2)
Total	332	NA	NA	25 (7.5)	1 (0.3)	16 (4.8)
Monkey						
RM	126	0 (0)	9 (7.1)	NA	0 (0)	0 (0)
CM	20	0 (0)	18 (90.0)	NA	0 (0)	0 (0)
Total	146	0 (0)	27 (18.5)	NA	0 (0)	0 (0)
Pig						
BMP	6	NA	NA	5 (83.3)	0 (0)	0 (0)

*BMP, Bama miniature pig (*Sus scrofa domestica*); CM, cynomolgus monkey (*Macaca fascicularis*); HEV, hepatitis E virus; JW, Japanese white rabbit (*Oryctolagus cuniculus*); NA, not applicable; NZW, New Zealand white rabbit (*Oryctolagus cuniculus*); RM, rhesus monkey (*Macaca mulatta*).

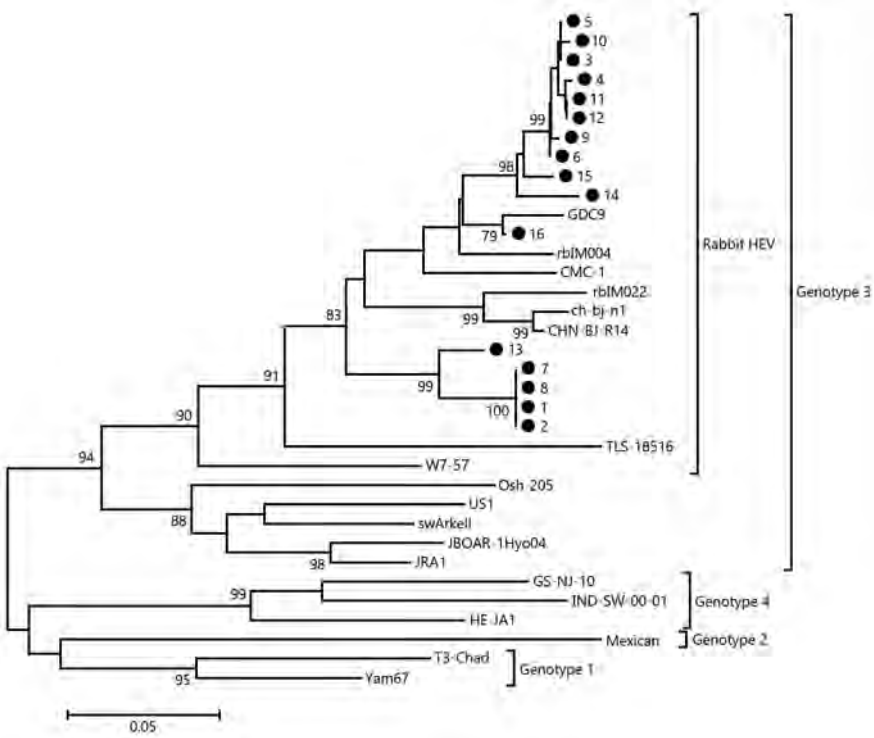

Figure. Phylogenetic analysis of hepatitis E virus (HEV) isolates from specific pathogen-free (SPF) rabbits, China, 2012–2015. The phylogenetic tree was constructed by using the neighbor-joining method, a partial nucleotide sequence of the open reading frame 2 region, and reported HEV sequences in GenBank as references. One thousand resamplings of the data were used to calculate percentages (values along branches) of tree branches obtained. Black circles indicate SPF rabbit isolates obtained during this study. GenBank accession numbers of all reference sequences (in parentheses) are FJ906895 (GDC9), AB740222 (rbIM004), JX565469 (CMC-1), AB740221 (rbIM022), GU937805 (ch-bj-n1), JX121233 (CHN-BJ-R14), JQ013793 (TLS-18516), JQ013792 (W7-57), AF455784 (Osh-205), AF060668 (US1), AY115488 (swArkell), AB189070 (JBOAR-1Hyo04), AP003430 (JRA1), JF309217 (GS-NJ-10), AY723745 (IND-SW-00-01), AB097812 (HE-JA1), M74506 (Mexican), AY204877 (T3-Chad), and AF459438 (Yam67). Scale bar indicates nucleotide substitutions per site.

This study was supported by the National Science Foundation of China (grant no. 81271827) and the Beijing Natural Science Foundation (grant no. 7162103).

Mr. Lin Wang is a doctoral candidate in the Department of Microbiology and Infectious Disease Center, School of Basic Medical Sciences, Peking University Health Science Center, Beijing, China. His primary research interests are the molecular epidemiology and pathogenesis of HEV.

References

1. Kamar N, Bendall R, Legrand-Abravanel F, Xia NS, Ijaz S, Izopet J, et al. Hepatitis E. Lancet. 2012;379:2477–88. http://dx.doi.org/10.1016/S0140-6736(11)61849-7
2. Yugo DM, Cossaboom CM, Meng XJ. Naturally occurring animal models of human hepatitis E virus infection. ILAR J. 2014;55:187–99. http://dx.doi.org/10.1093/ilar/ilu007
3. Birke L, Cormier SA, You D, Stout RW, Clement C, Johnson M, et al. Hepatitis E antibodies in laboratory rabbits from 2 US vendors. Emerg Infect Dis. 2014;20:693–6. http://dx.doi.org/10.3201/eid2004.131229
4. Liu P, Bu QN, Wang L, Han J, Du RJ, Lei YX, et al. Transmission of hepatitis E virus from rabbits to cynomolgus macaques. Emerg Infect Dis. 2013;19:559–65. http://dx.doi.org/10.3201/eid1904.120827
5. Izopet J, Dubois M, Bertagnoli S, Lhomme S, Marchandeau S, Boucher S, et al. Hepatitis E virus strains in rabbits and evidence of a closely related strain in humans, France. Emerg Infect Dis. 2012;18:1274–81.
6. Zhang J, Ge SX, Huang GY, Li SW, He ZQ, Wang YB, et al. Evaluation of antibody-based and nucleic acid-based assays for diagnosis of hepatitis E virus infection in a rhesus monkey model. J Med Virol. 2003;71:518–26. http://dx.doi.org/10.1002/jmv.10523
7. Wang YC, Zhang HY, Xia NS, Peng G, Lan HY, Zhuang H, et al. Prevalence, isolation, and partial sequence analysis of hepatitis E virus from domestic animals in China. J Med Virol. 2002;67:516–21. http://dx.doi.org/10.1002/jmv.10131
8. Tamura K, Stecher G, Peterson D, Filipski A, Kumar S. MEGA6: Molecular Evolutionary Genetics Analysis version 6.0. Mol Biol Evol. 2013;30:2725–9. http://dx.doi.org/10.1093/molbev/mst197
9. Zhu FC, Zhang J, Zhang XF, Zhou C, Wang ZZ, Huang SJ, et al. Efficacy and safety of a recombinant hepatitis E vaccine in healthy adults: a large-scale, randomised, double-blind placebo-controlled, phase 3 trial. Lancet. 2010;376:895–902. http://dx.doi.org/10.1016/S0140-6736(10)61030-6
10. Zhang J, Zhang XF, Huang SJ, Wu T, Hu YM, Wang ZZ, et al. Long-term efficacy of a hepatitis E vaccine. N Engl J Med. 2015;372:914–22. http://dx.doi.org/10.1056/NEJMoa1406011

Address for correspondence: Ling Wang, Department of Microbiology, School of Basic Medical Sciences, Peking University Health Science Center, 38 Xueyuan Rd, Haidian District, Beijing 100191, China; email: lingwang@bjmu.edu.cn

Human Brucellosis in Febrile Patients Seeking Treatment at Remote Hospitals, Northeastern Kenya, 2014–2015

John Njeru, Falk Melzer, Gamal Wareth, Hosny El-Adawy, Klaus Henning, Mathias W. Pletz, Regine Heller, Samuel Kariuki, Eric Fèvre, Heinrich Neubauer

During 2014–2015, patients in northeastern Kenya were assessed for brucellosis and characteristics that might help clinicians identify brucellosis. Among 146 confirmed brucellosis patients, 29 (20%) had negative serologic tests. No clinical feature was a good indicator of infection, which was associated with animal contact and drinking raw milk.

Brucellosis is a zoonotic disease that can cause severe illness in humans and substantial economic losses in livestock production (*1*). The main causative agents of brucellosis in humans are *Brucella abortus*, *B. melitensis*, and *B. suis* (*2*). Infection in humans occurs mainly by ingestion of contaminated animal products, inhalation of contaminated airborne particulates, or direct contact with infected animals or their products (*3*). Clinical signs and symptoms of human brucellosis are nonspecific and highly variable (*4*). Persons who work with animals and their families are considered to be at high risk for infection (*3*,*5*). In animals, brucellosis is asymptomatic but can cause abortions, weak offspring, and sterility (*5*).

In developing countries, serologic assays based on rapid slide agglutination tests are the mainstay for diagnosis of brucellosis, but these assays have poor specificity (*6*). Generally, ELISA is considered to be more specific and sensitive, allowing for a better correlation with the clinical situation. Although PCR assays are highly sensitive and specific tools for rapid diagnosis of human brucellosis and simultaneous differentiation of *Brucella* genotypes, they are often unavailable in many of these countries (*7*).

A review of brucellosis epidemiology in sub-Saharan Africa highlighted the fact that brucellosis is endemic in pastoral production systems where disease surveillance and control programs are poorly implemented (*1*). Within Kenya, seroprevalences of 2% and 7% have been reported among persons at high risk for brucellosis in Nairobi and Nakuru counties, respectively (*8*), and a national seroprevalence of 3% was reported in 2007 (*9*). More recently, Osoro et al. (*10*) showed variation (2.4%–46.5%) in seroprevalence across 3 counties in Kenya.

Diagnosis of febrile illnesses in developing countries is challenging because of the lack of imaging and reliable laboratory support. Clinical management of such illnesses is often done empirically, resulting in inaccurate treatment of patients and routine underreporting of disease (*11*). Data on the prevalence and potential risk factors associated with human brucellosis in Kenya are scant. The prevalent *Brucella* species in Kenya remain largely unknown. The purposes of this study were to assess the proportion of patients with brucellosis at 2 hospitals in northeastern Kenya and to describe patient characteristics that might help clinicians to identify brucellosis cases in areas without laboratory support.

The Study

During 2014–2015, we enrolled patients with acute febrile illness seeking treatment at Garissa and Wajir hospitals in northeastern Kenya (Figure) by using systematic sampling intervals based on previously documented proportions of febrile patients recorded at each hospital. The study protocol was approved by the Scientific and Ethics Review Committee of Kenya Medical Research Institute. We obtained serum samples and tested them for brucellosis by using the modified Rose Bengal Plate Test (RBPT) (VLA Weybridge, United Kingdom) (*12*) and SERION ELISA classic *Brucella* IgM/IgG kits (Virion/Serion, Wurzburg, Germany) according to the manufacturers' instructions. We extracted DNA from serum samples by using the High Pure Template Kit (Roche Diagnostics, Mannheim, Germany). We performed quantitative real-time PCR (qPCR) assays for the detection of brucellosis and speciation of *Brucella* species, as previously described (*13*) (online

Author affiliations: Friedrich-Loeffler-Institut, Jena, Germany (J. Njeru, F. Melzer, G. Wareth, H. El-Adawy, K. Henning, H. Neubauer); Friedrich Schiller University, Jena (J. Njeru, M.W. Pletz, R. Heller); Kenya Medical Research Institute, Nairobi, Kenya (J. Njeru, S. Kariuki); Benha University, Moshtohor, Egypt (G. Wareth); Kafrelsheikh University, Kafr El-Sheikh, Egypt (H. El-Adawy); University of Liverpool, Liverpool, United Kingdom (E. Fèvre); International Livestock Research Institute, Nairobi (E. Fèvre)

DOI: http://dx.doi.org/10.3201/eid2212.160285

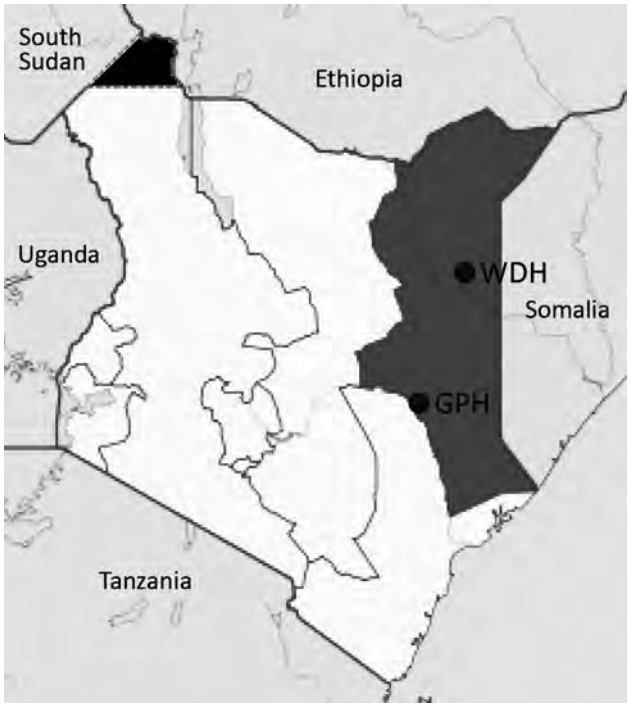

Figure. Locations of the 2 hospitals in the Northeastern Province of Kenya (dark gray shading) where human brucellosis was diagnosed in febrile patients seeking treatment, Kenya, 2014–2015. The solid black area in northwestern Kenya represents disputed territory among Kenya, Ethiopia, and South Sudan. GPH, Garissa Provincial Hospital; WDH, Wajir District Hospital.

Technical Appendix Table 1, http://wwwnc.cdc.gov/EID/article/22/1/15-1200-Techapp1.pdf). We classified patients as having brucellosis if they had positive qPCR results or had positive RBPT results confirmed by positive ELISA results. We fitted multivariate logistic regression models to assess demographic, clinical features, and plausible risk factors associated with brucellosis seropositivity by using a stepwise backward analysis procedure.

Overall, 1,067 patients participated in the study; 580 (54.4%) of participants were female, and 963 (90.3%) were of Somali ethnicity (online Technical Appendix Table 2). Brucellosis was established in 146 patients (13.7%, 95% CI 11.7%–15.9%). Of these, 29 (2.7%) had negative serologic test results for *Brucella* infection. *B. abortus* was the only *Brucella* species found using the *Brucella* species–specific qPCR.

Statistical analyses showed no significant differences in infection by ethnic group, county of residence, education status, or age group. Men had a significantly higher probability (odds ratio [OR] 1.98, p = 0.001) for having brucellosis (Table 1).

Considerable low sensitivity levels were found for clinical diagnosis of brucellosis in both hospitals (online Technical Appendix Table 3). Patients with brucellosis were mainly diagnosed with typhoid fever (63 patients [43.2%]), malaria (30 [20.5%]), pneumonia (12 [8.2%]), and other common tropical fevers or fevers of unknown origin (14 [9.6%]) (Table 1).

In the final combined multivariate analyses, brucellosis was significantly associated ($p<0.05$) with fever lasting >14 days (adjusted OR [aOR] 2.86), contact with cattle (aOR 6.50) or multiple animal species (aOR 2.35), slaughtering of animals (aOR 2.20), and consumption of raw cattle milk (aOR 3.88). Herders were 1.69-fold more likely to be seropositive (Table 2).

Conclusions

This hospital-based study from a predominantly pastoral community in Kenya indicated a high prevalence (13.7%) of brucellosis in febrile patients, highlighting brucellosis as an important cause of acute febrile illnesses in northeastern Kenya. Although brucellosis has previously been described to occur in hospital patients in Kenya (*1*), it was not diagnosed by the treating hospital clinicians in 119/146 (81.5%) cases in our study. Instead, these cases were mainly attributed to other causes of fevers or fevers of unknown origin. In addition, 29 (2.7%) patients who had negative serologic test results for *Brucella* had positive results for *B. abortus* by qPCR.

Our findings strongly suggest that patients with brucellosis were likely to leave the hospital without the specific treatment for brucellosis. This agrees with recent findings that showed that clinicians in Kenya continue to treat febrile patients for presumptive malaria, resulting in missed opportunities to accurately detect and treat other causes of fever (*11*,*14*). The results also highlight the usefulness of qPCR as a complementary assay to a combined ELISA and RBPT diagnostic approach in diagnosis of acute brucellosis and the need to establish national and regional reference laboratories with facilities for performing qPCR assays.

Contact with cattle or multiple animal species and consumption of raw milk from cattle were significantly associated with brucellosis in our study (Table 2). This association can be attributed to occupational and domestic contacts with livestock and social-cultural practices among communities in the study area that increase the risk for *Brucella* transmission, including nomadic movements, taking care of animals during parturition, consumption of raw milk from cattle and camels, and household slaughter of animals during traditional and religious ceremonies (*9*,*15*).

In this study, the only *Brucella* species detected was *B. abortus*, strengthening the assumption that brucellosis might be highly linked to cattle more than other animal species; however, further research is warranted. Additionally, the prevalent *Brucella* genotypes and biovars in Kenya remain to be determined.

Table 1. Selected characteristics of study participants and number of febrile patients with *Brucella*-positive test results, northeastern Kenya, 2014–2015*

Characteristic	No. (%) patients: Positive for brucellosis, n = 146	No. (%) patients: Negative for brucellosis, n = 921	p value	Crude OR (95% CI)
Mean age, y, ± SD	34.8 ± 11.5	33.9 ± 12.6	0.863	NA
Age group, y				
<19	16 (11.0)	127 (13.8)	NA	Referent
20–29	31 (21.2)	206 (22.4)	0.418	1.29 (0.70–2.39)
30–39	48 (32.9)	265 (28.8)	0.063	1.75 (0.97–3.08)
40–49	38 (26.0)	196 (21.3)	0.169	1.52 (0.84–2.76)
>50	13 (8.9)	127 (13.8)	0.764	0.90 (0.43–1.84)
Male sex	86 (58.9)	401 (43.5)	0.001	1.98 (1.30–2.68)
Wajir County resident	81 (55.5)	440 (49.4)	0.201	1.34 (0.97–1.77)
Occupation				
Herder	109 (74.7)	569 (61.8)	0.002	3.81 (2.17–12.38)
Civil servant	16 (11.0)	126 (13.7)	0.199	2.53 (0.71–8.91)
General business	7 (4.8)	67 (7.3)	0.286	1.98 (0.49–7.85)
Student	6 (4.1)	56 (6.1)	0.308	2.08 (0.51–8.48)
Livestock trader	6 (4.1)	53 (5.8)	0.053	3.74 (0.98–14.26)
Other	2 (1.4)	50 (5.4)	NA	Referent
Education level				
None	98 (67.1)	563 (61.1)	NA	Referent
Primary	25 (17.1)	181 (19.7)	0.335	0.79 (0.51–1.27)
Secondary	16 (11.0)	104 (11.3)	0.670	0.88 (0.69–1.56)
Post-secondary	7 (4.8)	73 (7.9	0.146	0.56 (0.25–1.32)
Somali ethnic group member	133 (91.1)	830 (90.1)	0.712	1.12 (0.62–2.63)
Clinical symptoms and signs				
Headache	113 (77.4)	836 (90.8)	0.504	1.45 (0.63–3.12)
Chills	93 (63.7)	482 (52.3)	0.065	1.79 (0.93–2.58)
Arthralgia/myalgia	118 (80.8)	699 (75.9)	0.322	1.48 (0.78–1.85)
Malaise/fatigue	101 (69.2)	646 (70.1)	0.018	2.20 (1.44–4.31)
Anorexia	63 (43.2)	514 (55.8)	0.610	0.91 (0.56–1.93)
Respiratory tract infection	34 (23.3)	263 (28.6)	0.434	1.03 (0.69–1.60)
Constipation	22 (15.1)	171 (18.6)	0.301	1.08 (0.83–3.11)
Night sweats	11 (7.5)	159 (17.3)	0.181	0.90 (0.67–5.90)
Diarrhea	8 (5.5)	106 (11.5)	0.120	0.95 (0.86–2.89)
Weight loss	12 (8.2)	105 (11.4)	0.228	1.24 (0.81- 6.04)
Confusion†	3 (2.3)	42 (5.3)	0.337	0.96 (0.60–2.91)
Rash	3 (2.1)	40 (4.3)	0.172	0.74 (0.22–1.55)
Vomiting	4 (2.7)	28 (3.0)	0.582	0.85 (0.36–1.98)
Abdominal pain	52 (35.6)	215 (23.3)	0.007	1.92 (1.35–5.64)
Hepatomegaly/splenomegaly	33 (22.6)	103 (11.1)	0.011	2.01 (1.63–8.10)
History of fever, >14 d	75 (51.4)	326 (35.3)	<0.001	3.71 (2.75–10.94)
Provisional diagnosis‡				
Typhoid fever	63 (43.2)	371 (45.0)	0.671	NA
Malaria	30 (20.5)	252 (30.5)	0.079	NA
Pneumonia	12 (8.2)	114 (13.8)	0.084	NA
Other§	14 (9.6)	Undefined	NA	NA
Days since fever onset/median	24.5/16	13.0/8	<0.001	NA

*NA, not available; OR, odds ratio.
†Data available for adult and adolescent patients only.
‡includes clinical diagnosis made by attending hospital clinician.
§Data not available for all patients.

Our study failed to better identify reliable clinical predictors for brucellosis. The lack of a clear clinical algorithm predictive of brucellosis supports the need for increasing clinician awareness of the disease and enhancing diagnostic capability for brucellosis in hospital settings.

This study has potential limitations. First, the study used acute-phase serum samples, making it difficult to demonstrate 4-fold titer rise. Follow-up of patients to obtain a convalescent-phase serum sample was not feasible because of ongoing inter-clan conflicts and militia activities in the region. Therefore, the possibility of patients who had previous exposure to *Brucella* but had residual antibodies in circulation cannot be ruled out.

Acknowledgments

We thank the patients for taking part in this study. We acknowledge the staff of Friedrich-Loeffler-Institut and hospital staff for their valuable contributions. We also thank Eric Osoro for his facilitation of the data collection. Finally, we thank the Director

Table 2. Results of univariate and multivariate logistic regression analyses, by demographic, socioeconomic, and dietary risk factors associated with brucellosis, northeastern Kenya, 2014–2015*

Characteristic	No. (%) positive for brucellosis, n = 146	Crude OR (95% CI)	Adjusted OR (95% CI)†	p value
Occupation				
Herder	109 (16.1)	1.82 (1.22–2.71)‡	1.69 (1.25–3.44)	0.023
Other	37 (9.5)	Referent	Referent	NA
History of fever, >14 d				
Yes	75 (18.7)	3.71 (2.75–10.94)‡	2.86 (1.91–6.74)	0.003
No	71 (10.7)	Referent	Referent	NA
Contact with goats§				
Yes	107 (15.5)	1.31 (0.87–2.29)¶	Referent	NA
No	38 (10.1)	Referent	NA	NA
Contact with cattle				
Yes	101 (21.7)	3.15 (2.84–4.87)‡	6.50 (3.48–14.56)	<0.001
No	45 (7.5)	Referent	NA	NA
Contact with multiple animal species				
Yes	78 (19.6)	2.59 (2.16–7.66)‡	2.35 (2.14–8.63)	0.013
No	68 (10.2)	Referent	NA	NA
Frequent slaughtering of animals				
Yes	83 (21.7)	3.86 (3.21–5.69)‡	2.20 (2.07–5.87)	<0.001
No	63 (9.2)	Referent	Referent	NA
Frequent handling of raw milk				
Yes	93 (15.8)	1.41 (0.75–2.15)¶	NA	NA
No	53 (11.1)	Referent	Referent	NA
Frequent consumption of raw cattle milk				
Yes	86 (26.0)	4.07 (2.39–9.55)‡	3.88 (2.16–5.47)	<0.001
No	60 (8.2)	Referent	Referent	NA
Frequent consumption of locally fermented milk products				
Yes	72 (17.6)	1.68 (0.92–3.75)¶	NA	NA
No	74 (11.2)	Referent	Referent	NA
Frequent consumption of raw goat milk				
Yes	33 (17.9)	1.50 (0.98–2.95)¶	NA	NA
No	113 (12.8)	Referent	Referent	NA
Hosmer-Lemeshow goodness-of-fit test	NA	NA	NA	0.228
AUC (ROC)	NA	NA	0.745 (0.680–0.812)	<0.001

*AUC, area under the curve; NA, not available; OR, odds ratio; ROC, receiver operating characteristic.
†Adjusted for age, sex, and site.
‡p<0.05.
§Contact with goats (referent variable in multivariable model).
¶Variables with p<0.20 (Wald test) considered as potential risk and subsequently fitted in the multivariate analysis.

of the Kenya Medical Research Institute for financial support of J.N. and permission to publish this paper.

The study was supported by the German Academic Exchange Service (grant no. A/12/97862), the CGIAR Research Program for Agriculture for Nutrition and Health (led by the International Food Policy Research Institute [grant no. 1100783/1]), and the German Ministry for Science and Education (grant no. 01KI1501).

Dr. Njeru is a research fellow at Friedrich-Loeffler-Institut in Jena, Germany. His primary research interest is the epidemiology of zoonotic diseases.

References

1. McDermott JJ, Arimi SM. Brucellosis in sub-Saharan Africa: epidemiology, control and impact. Vet Microbiol. 2002;90:111–34. http://dx.doi.org/10.1016/S0378-1135(02)00249-3
2. Pappas G. The changing *Brucella* ecology: novel reservoirs, new threats. Int J Antimicrob Agents. 2010;36(Suppl 1):S8–11. http://dx.doi.org/10.1016/j.ijantimicag.2010.06.013
3. Pappas G, Akritidis N, Bosilkovski M, Tsianos E. Brucellosis. N Engl J Med. 2005;352:2325–36. http://dx.doi.org/10.1056/NEJMra050570
4. Buzgan T, Karahocagil MK, Irmak H, Baran AI, Karsen H, Evirgen O, et al. Clinical manifestations and complications in 1028 cases of brucellosis: a retrospective evaluation and review of the literature. Int J Infect Dis. 2010;14:e469–78. http://dx.doi.org/10.1016/j.ijid.2009.06.031
5. Corbel MJ. Brucellosis in humans and animals. Geneva: The Organization; 2006.
6. Al Dahouk S, Tomaso H, Nöckler K, Neubauer H, Frangoulidis D. Laboratory-based diagnosis of brucellosis—a review of the literature. Part II: serological tests for brucellosis. Clin Lab. 2003;49:577–89.
7. Zerva L, Bourantas K, Mitka S, Kansouzidou A, Legakis NJ. Serum is the preferred clinical specimen for diagnosis of human brucellosis by PCR. J Clin Microbiol. 2001;39:1661–4. http://dx.doi.org/10.1128/JCM.39.4.1661-1664.2001
8. Jumba MM, Mirza NB, Mwaura FB. Agglutinins for brucellae antigens in blood sera of an urban and rural population in Kenya. East Afr Med J. 1996;73:204–6.
9. Omballa VO, Musyoka RN, Vittor AY, Wamburu KB, Wachira CM, Waiboci LW, et al. Serologic evidence of the geographic distribution of bacterial zoonotic agents in Kenya, 2007. Am J Trop Med Hyg. 2016;94:43–51. http://dx.doi.org/10.4269/ajtmh.15-0320
10. Osoro EM, Munyua P, Omulo S, Ogola E, Ade F, Mbatha P, et al. Strong association between human and animal *Brucella*

seropositivity in a linked study in Kenya, 2012–2013. Am J Trop Med Hyg. 2015;93:224–31. http://dx.doi.org/10.4269/ajtmh.15-0113
11. Onchiri FM, Pavlinac PB, Singa BO, Naulikha JM, Odundo EA, Farquhar C, et al. Frequency and correlates of malaria overtreatment in areas of differing malaria transmission: a cross-sectional study in rural Western Kenya. Malar J. 2015;14:97. http://dx.doi.org/10.1186/s12936-015-0613-7
12. Díaz R, Casanova A, Ariza J, Moriyón I. The Rose Bengal Test in human brucellosis: a neglected test for the diagnosis of a neglected disease. PLoS Negl Trop Dis. 2011;5:e950. http://dx.doi.org/10.1371/journal.pntd.0000950
13. Gwida MM, El-Gohary AH, Melzer F, Tomaso H, Rösler U, Wernery U, et al. Comparison of diagnostic tests for the detection of *Brucella* spp. in camel sera. BMC Res Notes. 2011;4:525. http://dx.doi.org/10.1186/1756-0500-4-525
14. Juma E, Zurovac D. Changes in health workers' malaria diagnosis and treatment practices in Kenya. Malar J. 2011;10:1. http://dx.doi.org/10.1186/1475-2875-10-1
15. Muga GO, Onyango-Ouma W, Sang R, Affognon H. Sociocultural and economic dimensions of Rift Valley fever. Am J Trop Med Hyg. 2015;92:730–8. http://dx.doi.org/10.4269/ajtmh.14-0363

Address for correspondence: John Njeru, Friedrich-Loeffler-Institut, Institute of Bacterial Infections and Zoonosis, Naumburger str 96a, 07743 Jena, Germany; email: mwanikij@gmail.com

Rift Valley Fever Outbreak in Livestock, Mozambique, 2014

José M. Fafetine, Peter Coetzee, Benjamin Mubemba, Ofélia Nhambirre, Luis Neves, J.A.W. Coetzer, Estelle H. Venter

In early 2014, abortions and death of ruminants were reported on farms in Maputo and Gaza Provinces, Mozambique. Serologic analysis and quantitative and conventional reverse transcription PCR confirmed the presence of Rift Valley fever virus. The viruses belonged to lineage C, which is prevalent among Rift Valley fever viruses in southern Africa.

Rift Valley fever (RVF) virus (family *Bunyaviridae*, genus *Phlebovirus*) is a mosquito-borne virus that affects ruminants and humans. The virion contains 3 single-stranded RNA genome segments, large, medium, and small. In ruminants, RVF virus infection is characterized by high rates of abortion and of death, particularly in newborn animals. In humans, the infection is usually asymptomatic, but in severe cases, hemorrhage, meningoencephalitis, retinopathy, and death can occur (*1*).

Some of the most notable RVF epidemics reported in the past 2 decades occurred in eastern Africa and in southern Africa, where Mozambique is located. In 2006 and 2007, outbreaks of the disease occurred in eastern Africa, including Tanzania (*2*). In 2008 (*3*) and 2010 (*4*), epidemics of the disease were reported in South Africa. However, during the same period, no RVF outbreaks were reported in Mozambique. The few confirmed RVF outbreaks in the country occurred in 1969 in Gaza and Maputo Provinces, resulting in the deaths of 220 and 25 cattle in each province, respectively (*5*). In 1999, cases of abortion in a herd of water buffaloes (*Bubalus bubalis*) in Zambézia Province were attributed to RVF virus, but no virus was detected or isolated (*6*).

In 2010, serosurveys were conducted in the Zambézia and Maputo Provinces of Mozambique. Seroprevalences of 9.2% in sheep and 11.6% in goats was recorded in Zambézia Province (*7*). In Maputo Province, an overall seroprevalence of 36.9% was documented in cattle (*8*). The results indicated the possible circulation of RVF virus during interepidemic periods without the manifestation of typical clinical signs, as has been described elsewhere (*9*).

In this article, we report the detection of specific antibodies against RVF virus and the genetic analysis of RVF virus isolates from outbreaks in Mozambique. We also discuss the possible factors associated with the occurrence of this outbreak.

The Study

In late March 2014, after a period of heavy and persistent rainfall in southern Mozambique, particularly in Maputo and Gaza Provinces, abortions and deaths in ruminant offspring were reported on some farms. The owner of a farm located in the Goba District, Maputo Province (26°3′59.73″S, 32°0′23.36″E), informed the veterinary authorities that 16 of 88 goats aborted their fetuses and 5 newborn kids died. The veterinary authorities also received reports from 2 farms in Xai-Xai (25° 03′24.1S, 33°41′24.7E) and Chibuto (24°42′01.222S, 33°32′24.822E) in Gaza Province, where 26 goats and 8 sheep aborted, respectively, and a total of 7 newborn animals died on both farms. According to the farmers, no animals had been purchased or brought into the herds for >3 years.

Serum samples were collected from farms in Goba (n = 88), Xai-Xai (n = 26), and Chibuto (n = 13). On the Goba farm, liver and spleen tissue samples were also collected from 1 aborted fetus and from 1 dead newborn goat. All the serum samples were tested for the presence of RVF virus IgM by using the IDvet Screen RVF IgM ELISA (IDvet innovative diagnostics kit; IDVet, Montpellier, France). In addition, the serum samples collected in Goba were further tested for RVF virus IgG by using the RVF recN IgG ELISA kit (Biological Diagnostic Supplies Limited, Edinburgh, Scotland, UK).

Viral genomic RNA was extracted from ELISA-positive serum samples and tissue samples by using Trizol (Invitrogen, Manchester, UK) according to the manufacturer's instructions. A quantitative real-time reverse transcription PCR was performed as described (*10*). Positive samples were subsequently subjected to a conventional RT-PCR to amplify a 490-nt region of the medium segment as described (*11*). The amplicons were then purified by using the QIAquick Gel extraction kit (QIAGEN, Manchester, UK) and submitted to Inqaba Biotec (Pretoria, South Africa) for sequencing. The obtained sequences were compared with sequences in GenBank using BLAST (https://blast.ncbi.nlm.nih.gov/Blast.cgi). Sequence data (480 nt) were

Author affiliations: Eduardo Mondlane University, Maputo, Mozambique (J.M. Fafetine, O. Nhambirre); University of Pretoria, Pretoria, South Africa (P. Coetzee, L. Neves, J.A.W. Coetzer, E.H. Venter); Copperbelt University, Kitwe, Zambia (B. Mubemba)

DOI: http://dx.doi.org.10.3201/eid2212.160310

imported into MEGA6 (*12*), in which sequence alignment and evolutionary analyses were carried out. The phylogenetic trees were inferred by using the maximum-likelihood method based on the Kimura 2-parameter model (*13*). The tree with the highest log likelihood (-2055.6526) is shown in the online Technical Appendix Figure (http://wwwnc.cdc.gov/EID/article/22/12/16-0310-Techapp1.pdf). Reference RVF virus isolates used in this study are listed in the online Technical Appendix Table.

Serologic analysis indicated that 31 (24.4%) of 127 (all) sampled animals were positive for RVF virus IgM, and 49 (55.7%) of 88 animals from the Goba Province were positive for RVF virus IgG. Only 25 animals had RVF virus IgG but no RVF virus IgM (Table). The data suggest that the onset of the outbreak on the Goba farm was in early or mid-January 2014 and continued until mid-April because at this time only a few RVF IgM–positive animals (2/26 animals) contained IgM but no IgG against RVF virus, and few abortions were continuing. RVF virus RNA was detected in 16 serum samples and 6 tissue samples analyzed by quantitative real-time RT-PCR, confirming an RVF outbreak in Mozambique. Only PCR products obtained from fetal tissue met the minimum concentration requirement for sequencing. Phylogenetic analysis showed that the Goba-Mozambique isolate belonged to the lineage C group of RVF viruses (online Technical Appendix Figure).

Conclusions

RVF virus IgM and the molecular detection of RVF virus confirmed the cause of abortions and deaths in sheep and goats in Maputo (Goba) and Gaza (Xai-Xai and Chibuto) Provinces of Mozambique in the first quarter of 2014. Outbreaks of RVF in eastern Africa are usually associated with the circulation of a local virus lineages, triggered by abnormal rainfall that favors the multiplication of the mosquito vectors or by the introduction of virus through animal movement. Sequence comparison and phylogenetic analyses indicated that the Maputo RVF viruses belonged to lineage C, which suggested that the outbreaks had close links to the 2007 and 2010 RVF outbreaks in Sudan.

The farms where the outbreaks occurred are noncommercial, small- to middle-scale farming systems with basic management and with no reports of animal importation. Occasionally, animals are bought from other farms, and the animals known to be imported in the southern part of the country come from the neighboring countries (i.e., South Africa and Swaziland). Animal movement is also reported to occur frequently on the border with adjoining countries. Because no new animals were introduced onto the above mentioned farms and no animal importation was indicated either by the farmers or by the veterinary authorities, we hypothesize that the virus might have been introduced in the past. Then, after a 6-fold increase in rainfall in Maputo (31 mm in November 2013 and 208 mm in December 2013; Umbeluzi Weather Station, pers. comm.), the conditions for an increase in the vector population, and therefore in virus circulation, favored the occurrence of the outbreaks. The high level of seroprevalence reported previously in districts close to the study site (*8*) may suggest a continuous low level of virus transmission in the region that is exacerbated by above-average rainfall, resulting in RVF virus infection in naive animals.

With this confirmed genetic evidence of RVF virus in Mozambique, all countries on the eastern coastline of Africa, the Indian Ocean islands of Madagascar and Mayotte, and Yemen and Saudi Arabia have all reported the presence of viruses belonging to lineage C (*11*). The broad geographic distribution pattern of lineage C viruses (in southern and northern Africa) and the related life-cycle dynamics require further investigation to identify the main drivers associated with the circulation and spread of this lineage of viruses.

Acknowledgments

We thank Hermogenes Mucache for help with sample collection.

This study was supported by the Southern African Center for Infectious Disease Surveillance–Wellcome Trust (grant no. WT087546MA), Sida Project at the Eduardo Mondlane University, and the National Research Fund (Fundo Nacional de Investigação–Ministry of Science and Technology Mozambique). This study was carried out at the Centro de Biotecnologia/Faculdade de Veterinaria, Eduardo Mondlane

Table. ELISA and RT-PCR results for sheep and goat serum specimens tested during Rift Valley Fever outbreak, Mozambique, 2014*

Results	Goba District	Xai-Xai District	Chibuto District
Total	88	26	13
No. IgM positive	26	2	3
No. IgG positive	49	NT	NT
No. IgM positive only	2	NA	NA
No. IgG positive only	25	NA	NA
No. RT-PCR positive	12	2	2
No. RT-PCR and IgM positive	1	2	2
No. RT- PCR and IgG positive	0	NA	NA
No. RT-PCR, IgM and IgG positive	11	NA	NA

*RVF, Rift Valley fever; RT-PCR, real-time quantitative reverse transcription PCR; NA, not available; NT, not tested.

University, Mozambique, and at the Department of Veterinary Tropical Diseases, Faculty of Veterinary Sciences, University of Pretoria, South Africa.

Dr. Fafetine is assistant professor of microbiology and immunology at the Veterinary Faculty, Eduardo Mondlane University, Maputo, Mozambique. His primary research interest is the diagnosis and epidemiology of zoonotic and emerging diseases.

References

1. Swanepoel R, Coetzer JAW. Rift Valley fever. In: Coetzer JAW, Thomson GR, Tustin RC, editors. Infectious diseases of livestock, 2nd ed. Oxford (UK): Oxford University Press; 2004. p. 1037–70.
2. World Health Organization. Outbreaks of Rift Valley fever in Kenya, Somalia and United Republic of Tanzania, December 2006–April 2007. Wkly Epidemiol Rec. 2007;82:169–78.
3. Archer BN, Weyer J, Paweska J, Nkosi D, Leman P, Tint KS, et al. Outbreak of Rift Valley fever affecting veterinarians and farmers in South Africa, 2008. S Afr Med J. 2011;101:263–6. http://dx.doi.org/10.7196/SAMJ.4544
4. World Health Organization. Rift Valley fever, South Africa—update 1. Wkly Epidemiol Rec. 2010;21:185–6.
5. Valadão FG. Nota prévia sobre a ocorrência de uma nova doença em Moçambique—a doença do vale do Rift. Veterin Moçamb. 1969;2:13–20.
6. Direcção Nacional de Pecuária. Relatório Anual. Ministério da Agricultura e de Desenvolvimento Rural (Maputo, Mozambique); 2002. p. 5–7.
7. Fafetine J, Neves L, Thompson PN, Paweska JT, Rutten VPMG, Coetzer JAW. Serological evidence of Rift Valley fever virus circulation in sheep and goats in Zambézia Province, Mozambique. PLoS Negl Trop Dis. 2013;7:e2065. http://dx.doi.org/10.1371/journal.pntd.0002065
8. Lagerqvist N, Moiane B, Mapaco L, Fafetine J, Vene S, Falk KI. Antibodies against Rift Valley fever virus in cattle, Mozambique. Emerg Infect Dis. 2013;19:1177–9. http://dx.doi.org/10.3201/eid1907.130332
9. Métras R, Cavalerie L, Dommergues L, Mérot P, Edmunds WJ, Keeling MJ, et al. The epidemiology of Rift Valley fever in Mayotte: insights and perspectives from 11 years of data. PLoS Negl Trop Dis. 2016;10:e0004783. http://dx.doi.org/10.1371/journal.pntd.0004783
10. Bird BH, Bawiec DA, Ksiazek TG, Shoemaker TR, Nichol ST. Highly sensitive and broadly reactive quantitative reverse transcription-PCR assay for high-throughput detection of Rift Valley fever virus. J Clin Microbiol. 2007;45:3506–13. http://dx.doi.org/10.1128/JCM.00936-07
11. Grobbelaar AA, Weyer J, Leman PA, Kemp A, Paweska JT, Swanepoel R. Molecular epidemiology of Rift Valley fever virus. Emerg Infect Dis. 2011;17:2270–6. http://dx.doi.org/10.3201/eid1712.111035
12. Tamura K, Stecher G, Peterson D, Filipski A, Kumar S. MEGA6: molecular evolutionary genetics analysis version 6.0. Mol Biol Evol. 2013;30:2725–9. http://dx.doi.org/10.1093/molbev/mst197
13. Kimura M. A simple method for estimating evolutionary rates of base substitutions through comparative studies of nucleotide sequences. J Mol Evol. 1980;16:111–20. http://dx.doi.org/10.1007/BF01731581

Address for correspondence: José Manuel Fafetine, Eduardo Mondlane University–Universidade Eduardo Mondlane, Faculdade de Veterinária/Centro de Biotecnologia, Av de Moçambique Km 1.5, C. Postal 257, Maputo, Mozambique; email: jfafetine@yahoo.com

Evaluating Healthcare Claims for Neurocysticercosis by Using All-Payer All-Claims Data, Oregon, 2010–2013

Robert H. Flecker, Seth E. O'Neal, John M. Townes

To characterize the frequency of neurocysticercosis, associated diagnostic codes, and place of infection, we searched Oregon's All Payer All-Claims dataset for 2010–2013. Twice as many cases were found by searching inpatient and outpatient data than by inpatient data alone. Studies relying exclusively on inpatient data underestimate frequency and miss less severe disease.

Neurocysticercosis, central nervous system infection caused by the larval form of the pork tapeworm *Taenia solium*, manifests a broad range of neurologic symptoms, including seizure, headache, obstructive hydrocephalus, encephalitis, stroke, and cognitive disorders (*1*). In the United States, neurocysticercosis is increasingly identified in migrants and travelers from nonindustrialized countries, particularly among the Hispanic population (*2*). However, because no reliable surveillance system for neurocysticercosis exists, studies to document the frequency of the disease have relied primarily on hospital discharge data (*3*–*9*). These studies may underestimate the frequency of neurocysticercosis and provide a biased representation of its effects. In this population-based study of neurocysticercosis, we used the newly implemented All-Payer All-Claims (APAC) database in Oregon, which includes healthcare claims from inpatient, outpatient, and emergency care environments.

The Study

We analyzed Oregon's APAC insurance claim data for the 3.5-year period from January 2010 through June 2013. APAC includes claim information collected from most healthcare payers in Oregon and provides a unique person-level identifier allowing analysis at the individual level (*10*). Because no specific code for neurocysticercosis exists, we searched >119 million claim lines for the code for cysticercosis (123.1) from the International Classification of Diseases, Ninth Revision, Clinical Modification (ICD-9-CM), in any of the 13 diagnostic fields at any time during the study period. We extracted all claims from these patients for the entire study period, dropping any claims that were denied to avoid duplication from resubmitted claims. Persons who did not have ≥1 neurocysticercosis-associated diagnostic, procedure, or current procedural terminology code were also excluded, leaving a list of persons whose condition fit our case definition of neurocysticercosis and all of their paid and capitated claims. We required a supporting diagnostic, procedural, or current procedural terminology code in the case definition to reduce the likelihood of including miscoded cases, while accepting that some true-positive cases may have been excluded. We also randomly selected 4 age- and sex-matched controls from all persons in the dataset, extracted data from all of their claims, and compared the proportion of specific diagnostic codes in neurocysticercosis cases versus codes for controls. We calculated odds ratios (ORs) and 95% CIs by using conditional logistic regression. The denominator for prevalence estimates was taken from US Census Bureau estimates of the insured population in Oregon in 2010.

A total of 137 persons were identified with a 123.1 ICD-9-CM code during the 14 quarters of this study. Of these, 12 were excluded because they did not have paid or capitated claims or did not have an associated neurologic diagnostic or procedural code. The remaining 125 persons whose conditions met the case definition of neurocysticercosis yielded a mean 1-year prevalence of 1.1 cases/100,000 insured persons. Age of case-patients ranged from 3 to 84 (median 41) years. Slightly more cases were found among female patients (69/125, 55%). The 125 cases generated a total of 8,224 claims, of which 2,337 contained a neurocysticercosis-associated neurologic diagnosis or procedure code.

Most claims (5,925/8,224, 72%) were made in outpatient settings. Only 10% (818/8,224) were inpatient claims, and <5% (337/8,224) were generated in emergency departments. Of the 125 persons with neurocysticercosis, 70 (56%) had a claim history that included only outpatient claims, 47 (38%) had both outpatient and inpatient claims, and 3 (2%) had inpatient claims only. Paid and capitated claims associated with mental health disorders, headache, seizure/epilepsy, and syncope were made primarily in outpatient settings, whereas claims associated with hydrocephalus, cerebral edema, and cerebrovascular disease were made primarily in inpatient settings (Figure). Private

Author affiliation: Oregon Health & Science University, Portland, Oregon, USA

DOI: http://dx.doi.org/10.3201/eid2212.160370

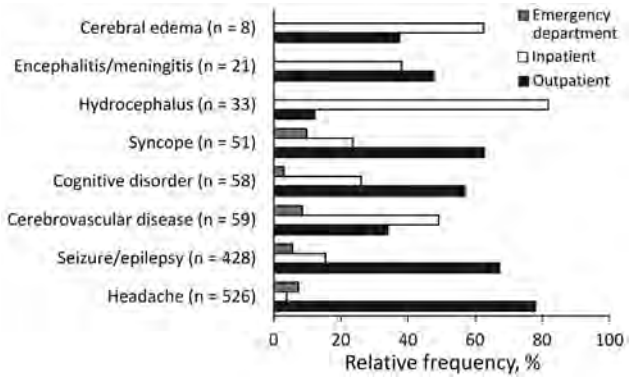

Figure. Frequency of neurocysticercosis claims by associated diagnosis and healthcare setting, Oregon, 2010–2013.

insurance carriers were the primary payers of paid claims, accounting for ≈55% (4,504/8,224) of payments provided. Federally-funded pay sources provided payment for ≈40% of claims.

Headache was the most common diagnostic category coded in claims for persons with neurocysticercosis (63/125, 50.4%), followed by seizures (41/125, 32.8%); both were significantly more common among case-patients than among controls (OR 3.2, 95% CI 2.1–4.8, and OR 13.3, 95% CI 6.8–25.9, respectively). Other diagnostic codes significantly more common in claims for persons with neurocysticercosis include meningitis/encephalitis, stroke, cognitive disorder, syncope, cerebral edema, and hydrocephalus (Table). The median age for those with a diagnostic code for stroke was significantly lower for those with neurocysticercosis (45 years) than for controls (63 years) (p = 0.05 by Kruskal-Wallis test); no significant differences in age were found for the other diagnostic categories evaluated.

Conclusions

Assessing the true prevalence or incidence of neurocysticercosis in the United States is difficult due to the lack of active case reporting from providers to public health entities. Most epidemiologic studies, therefore, use hospital-discharge datasets, which capture inpatient cases only (*3–9*). The results of our study show that twice as many neurocysticercosis cases are found when inpatient and outpatient data are searched than when only inpatient data are searched. Epidemiologic studies that rely solely on inpatient data largely underestimate the number of cases and the frequency and cost of healthcare interactions for neurocysticercosis.

Although our study detected additional cases of neurocysticercosis that were seen exclusively in the outpatient setting, it still falls far short of capturing all neurocysticercosis cases in Oregon because APAC data do not include the uninsured population. Even though only 14.5% of persons in Oregon lack health insurance (*11*), a previous study involving chart review demonstrated that 40% of neurocysticercosis patients in Oregon were uninsured (*5*). This finding suggests that our study may have missed as many as 80 additional neurocysticercosis cases among the uninsured during the study period.

The predominance of outpatient healthcare claims reflects the growing recognition that neurocysticercosis can result in chronic illness and disability even after the infection has been resolved (*12–14*). Patients with neurocysticercosis often require long-term management for disease sequelae such as seizures, hydrocephalus, cerebral edema, and meningoencephalitis, resulting in frequent interaction with specialist providers. This aspect of neurocysticercosis care is not captured in studies based on inpatient data, which tend to highlight acute illness.

We found that cognitive disorders were coded for 1 of 9 neurocysticercosis patients in this study and were 3 times more likely to occur in these patients than in controls; this finding supports results of recent studies showing that cognitive impairment can be a notable sequela of neurocysticercosis (*12*). Cognitive disorders primarily affect learning, memory, perception, and problem solving. A team-based approach to clinical management that includes ancillary support, including social services and rehabilitation, may be beneficial in neurocysticercosis cases, especially when

Table. Diagnostic codes in healthcare claims from persons with neurocysticercosis (cases) versus age- and sex-matched controls, Oregon, 2010–2013

Diagnostic code group	No. (%) cases, n = 125	No. (%) controls, n = 500	Odds ratio (95% CI)
Meningitis/encephalitis	5 (4.0)	1 (0.2)	20.0 (2.3–171.2)
Seizure	41 (32.8)	19 (3.8)	13.3 (6.8–25.9)
Stroke	17 (13.6)	16 (3.2)	5.6 (2.5–12.4)
Headache	63 (50.4)	120 (24.0)	3.2 (2.1–4.8)
Cognitive disorder	11 (8.8)	16 (3.2)	3.1 (1.4–7.1)
Syncope	12 (9.6)	25 (5.0	2.0 (1.0–4.2)
Psychotic disorder	8 (6.4)	21 (4.2)	1.6 (0.7–3.8)
Anxiety disorder	35 (28.0)	124 (24.8)	1.2 (0.8–1.8)
Mood disorder	32 (25.6)	134 (26.8)	0.9 (0.6–1.5)
Hydrocephalus	7 (5.6)	0	*
Cerebral edema	5 (4.0)	0	*

*Hydrocephalus and cerebral edema were significantly more common among cases. However, the odds ratio could not be calculated because these diagnostic codes did not occur in the control group.

long-term adherence to antiepileptic drugs or other therapies are required to maintain quality of life.

Another intriguing finding was that claims coding for stroke were >5 times more likely to appear for patients with neurocysticercosis than for controls and occurred among patients who were significantly younger than controls (data not shown). Although cases of stroke in neurocysticercosis patients have been reported, the effects at the population level have received little attention.

This study has limitations. Although APAC data provided an improved understanding of the neurocysticercosis outpatient population, the data source and quality may introduce bias and limit generalizability. A major limitation of APAC and other healthcare claims datasets is that diagnostic codes associated with a claim may not accurately represent the current clinical context. APAC data are de-identified, which precludes verification of clinical presentation through chart review, a limitation shared by approaches based on other administrative datasets as well. By excluding the uninsured population, this study also underestimates the true prevalence of neurocysticercosis and may present a biased view of diagnostic codes if uninsured cases differ substantially from insured cases. Finally, the composition of neurocysticercosis cases and associated claims in Oregon may not be the same as in other regions of the country.

Acknowledgments

We thank Michael Lasarev for his statistical expertise and the Oregon Health Authority APAC program for their assistance.

This work was partially supported by the N.L. Tartar Trust, School of Medicine, Oregon Health & Sciences University, Portland, Oregon, USA.

Dr. Flecker is currently a Fogarty Fellow in Global Health (Peru), where his research focuses on emerging zoonotic disease.

References

1. Shandera WX, White AC Jr, Chen JC, Diaz P, Armstrong R. Neurocysticercosis in Houston, Texas. A report of 112 cases. Medicine (Baltimore). 1994;73:37–52. http://dx.doi.org/10.1097/00005792-199401000-00004
2. Cantey PT, Coyle CM, Sorvillo FJ, Wilkins PP, Starr MC, Nash TE. Neglected parasitic infections in the United States: cysticercosis. Am J Trop Med Hyg. 2014;90:805–9. http://dx.doi.org/10.4269/ajtmh.13-0724
3. O'Neal SE, Flecker RH. Hospitalization frequency and charges for neurocysticercosis, United States, 2003–2012. Emerg Infect Dis. 2015;21:969–76. http://dx.doi.org/10.3201/eid2106.141324
4. O'Keefe KA, Eberhard ML, Shafir SC, Wilkins P, Ash LR, Sorvillo FJ. Cysticercosis-related hospitalizations in the United States, 1998–2011. Am J Trop Med Hyg. 2015;92:354–9. http://dx.doi.org/10.4269/ajtmh.14-0506
5. Townes JM, Hoffmann CJ, Kohn MA. Neurocysticercosis in Oregon, 1995–2000. Emerg Infect Dis. 2004;10:508–10. http://dx.doi.org/10.3201/eid1003.030542
6. Croker C, Reporter R, Mascola L. Use of statewide hospital discharge data to evaluate the economic burden of neurocysticercosis in Los Angeles County (1991–2008). Am J Trop Med Hyg. 2010;83:106–10. http://dx.doi.org/10.4269/ajtmh.2010.09-0494
7. O'Neal S, Noh J, Wilkins P, Keene W, Lambert W, Anderson J, et al. *Taenia solium* tapeworm infection, Oregon, 2006–2009. Emerg Infect Dis. 2011;17:1030–6. http://dx.doi.org/10.3201/eid/1706.101397
8. Serpa JA, Graviss EA, Kass JS, White AC Jr. Neurocysticercosis in Houston, Texas: an update. Medicine (Baltimore). 2011;90:81–6. http://dx.doi.org/10.1097/MD.0b013e318206d13e
9. Croker C, Redelings M, Reporter R, Sorvillo F, Mascola L, Wilkins P. The impact of neurocysticercosis in California: a review of hospitalized cases. PLoS Negl Trop Dis. 2012;6:e1480. http://dx.doi.org/10.1371/journal.pntd.0001480
10. Oregon Health Authority. Oregon All-Payer All-Claims database. 2013 [cited 2014 Dec 6]. http://www.oregon.gov/oha/OHPR/RSCH/docs/AllCPayer_all_Claims/APAC-Overviewfor-Release-Document.pdf
11. Oregon Health Authority. Oregon health insurance survey. 2013 [cited 2016 Apr 28]. https://www.oregon.gov/oha/OHPR/RSCH/docs/Uninsured/2013_OHIS_Age_FactSheet.pdf
12. Ciampi de Andrade D, Rodrigues CL, Abraham R, Castro LH, Livramento JA, Machado LR, et al. Cognitive impairment and dementia in neurocysticercosis: a cross-sectional controlled study. Neurology. 2010;74:1288–95. http://dx.doi.org/10.1212/WNL.0b013e3181d9eda6
13. Nash TE, Mahanty S, Garcia HH; Cysticercosis Group in Peru. Corticosteroid use in neurocysticercosis. Expert Rev Neurother. 2011;11:1175–83. http://dx.doi.org/10.1586/ern.11.86
14. Kelley R, Duong DH, Locke GE. Characteristics of ventricular shunt malfunctions among patients with neurocysticercosis. Neurosurgery. 2002;50:757–61. http://dx.doi.org/10.1097/00006123-200204000-00014

Address for correspondence: Robert H. Flecker, School of Public Health, Oregon Health & Sciences University and Portland State University, 3181 SW Sam Jackson Park Rd, Portland, OR 97239, USA; email: flecker@ohsu.edu

Time Course of MERS-CoV Infection and Immunity in Dromedary Camels

Benjamin Meyer, Judit Juhasz, Rajib Barua, Aungshuman Das Gupta, Fatima Hakimuddin, Victor M. Corman, Marcel A. Müller, Ulrich Wernery, Christian Drosten, Peter Nagy

Knowledge about immunity to Middle East respiratory syndrome coronavirus (MERS-CoV) in dromedary camels is essential for infection control and vaccination. A longitudinal study of 11 dam–calf pairs showed that calves lose maternal MERS-CoV antibodies 5–6 months postparturition and are left susceptible to infection, indicating a short window of opportunity for vaccination.

In 2012, Middle East respiratory syndrome coronavirus (MERS-CoV) emerged on the Arabian Peninsula (*1*). As of February 2016 the virus has caused 1,638 human infections, including 587 deaths (*2*). Zoonotic transmission of MERS-CoV was suspected early on (*3*). Dromedaries on the Arabian Peninsula and on the African continent have harbored MERS-CoV–specific antibodies for at least 20–30 years (*3*–*7*), long before the first human infections were recognized. Additionally, detection of MERS-CoV nucleotide sequences in throat swab specimens from camels confirmed the presence of the virus in these animals (*8*). The existence of an active animal reservoir receives additional support by epidemiologic investigations that found no sustained human-to-human transmission in MERS-CoV–affected countries such as Saudi Arabia (*9*).

As documented, primary infections in humans have occurred through contact with infected dromedaries, and measures to prevent primary human infections need to focus on the camel-human interface (*8*,*10*). However, it has been unclear how MERS-CoV transmission is maintained in camels and which factors drive virus transmission from camels to humans. Clarifying the infection pattern of MERS-CoV in herds of dromedary camels is key to the design of herd management and vaccination strategies to control the source of human infections. Preliminary information is limited to observations of lower seroprevalences in juvenile compared with adult camels and higher viral load upon MERS-CoV infection in juveniles (*4*,*5*,*11*). Hence, infections in juvenile camels might drive transmission of MERS-CoV to humans.

Author affiliations: University of Bonn Medical Centre, Bonn, Germany (B. Meyer, V.M. Corman, M.A. Müller, C. Drosten); Deutsches Zentrum für Infektionsforschung, Braunschweig, Germany (V.M. Corman, C. Drosten); Emirates Industries for Camel Milk and Products, Dubai, United Arab Emirates (J. Juhasz, R. Barua, A. Das Gupta, P. Nagy); Central Veterinary Research Laboratory, Dubai (F. Hakimuddin, U. Wernery)

DOI: http://dx.doi.org/10.3201/eid2212.160382

The Study

We monitored MERS-CoV–specific antibody levels in 11 pairs of camel dams and their calves at monthly intervals over the course of 1 year postparturition. These animals were born and raised on a closed commercial camel dairy farm in the United Arab Emirates that had a strict animal health and biosecurity program. The total number of camels on the farm was ≈4,500. Animals are kept in open paddocks and are grouped according to the age of their calves and production stage. Despite high standards of hygienic husbandry and biosecurity, the transmission of pathogens within the farm cannot be completely eliminated. Therefore, the entire farm is 1 epidemiologic unit. The 11 dam–calf pairs investigated in this study were kept in different fenced compartments within 100–150 m from each other. However, all these animals were kept together with other dam–calf pairs in the same paddock throughout lactation. All camel calves were born during June 3–15, 2014.

Nasal swab specimens were taken from all 11 mothers and calves, and serum samples were obtained through jugular vein puncture. Blood cells were removed immediately after collection, and samples were stored at -20°C until testing. Serum samples and nasal swabs were taken at the day of parturition, at 1 week and 1 month postparturition, and then at monthly intervals until June 2015. MERS-CoV RNA was detected through amplification of gene targets as described previously (*12*). Virus isolation was performed on Vero cells. MERS-CoV–specific IgG and neutralizing antibodies were determined by ELISA and microneutralization test as described previously (*5*,*10*).

In general, maternal IgG antibodies in camels are not acquired via the transplacental route but through the intake of colostrum during the first 24 hours postparturition (*13*). After 24 hours, antibody levels in the dam's milk decrease rapidly, and IgG levels in calves' serum cease to rise (*13*). This pattern is reflected for MERS-CoV in this study. On the day of parturition, samples were collected from 5 of 11 dam–calf pairs studied. High levels of MERS-CoV–specific antibodies were observed in all dams, whereas no antibodies were detected in calves (Figure, panel A). At day 7 post-

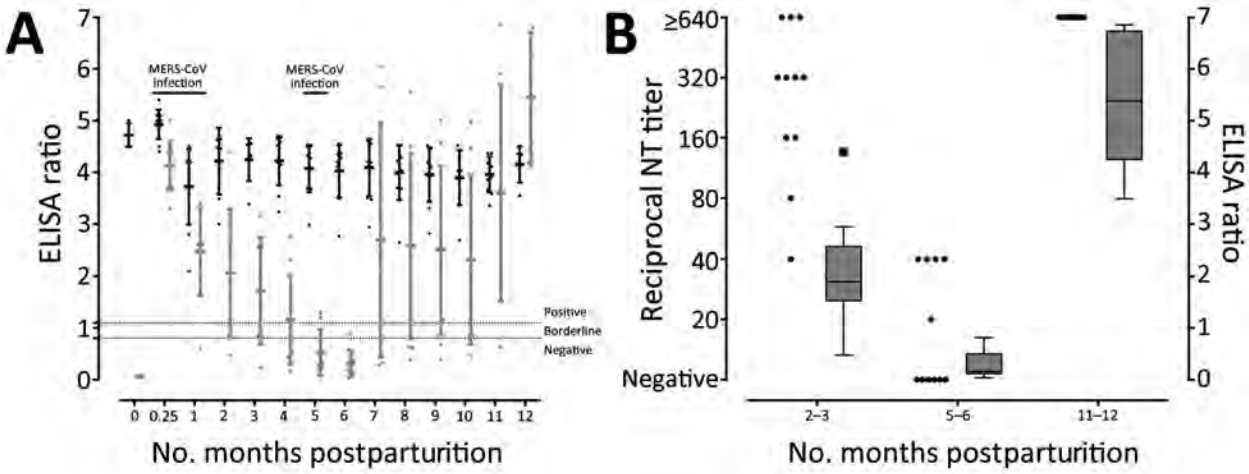

Figure. MERS-CoV–specific IgG antibody levels in dromedary camel dam–calf pairs, United Arab Emirates, 2014–2015. A) MERS-CoV spike protein S1-domain–based ELISA ratios of individual samples (dots) plus mean (horizontal line) and SD (error bars) over the course of 1 year for dams (black dots) and calves (gray dots). Ratios were calculated by dividing the ELISA optical density at 450 nm of each sample by that of a calibrator to minimize interassay variation. Dashed lines indicate cutoff values for positive (ratio 1.1) and borderline (ratio 0.8) samples. MERS-CoV infection indicates time points where MERS-CoV RNA was detected in camels. B) Neutralizing titers of individual samples from camel calves at selected time points determined by microneutralization test (dots). For comparison, ELISA ratios for the selected time points are shown in parallel as a boxplot diagram; box represents 50% of the complete dataset from the first to the third quartile, and whiskers are drawn according to the Tukey method. MERS-CoV, Middle East respiratory syndrome coronavirus; NT, neutralization test.

parturition, however, all 11 camel calves had high MERS-CoV–specific antibody levels. These levels declined during the first 6 months postparturition, whereas IgG in dams remained constantly at high levels. The neutralizing activity of IgG was confirmed by microneutralization tests on serum samples from calves collected 2–3 months, 5–6 months, and 1 year after birth (Figure, panel B). After 5–6 months, serum from 6 of 11 calves had completely lost their neutralizing activity. The remaining 5 calves had low neutralizing titers, ranging from 1:20 to 1:40 (Figure, panel B).

To examine possible correlations between antibodies and MERS-CoV infection, we examined shedding of MERS-CoV in nasal swab specimens. During the first 5 months postparturition, MERS-CoV RNA was detected sporadically on days 7 and 30 (Table). Infectious virus was isolated only from calves but not dams. At 6 months postparturition, when calves showed the lowest antibody titers, MERS-CoV RNA was detected in 2 of 11 calves (Table), indicating active MERS-CoV infection. All calves seroconverted during the following weeks (Figure, panel A); 1 calf had meanwhile been euthanized because of a congenital forelimb deformity. All calves showed high reciprocal neutralizing titers of ≥640 at 11–12 months postparturition.

Conclusions

This longitudinal study of natural MERS-CoV infections in camels confirms assumptions from preliminary cross-sectional studies in camels (*4*,*5*,*11*). MERS-CoV infection appears to predominantly affect young, immunologically naive animals. Serum antibodies might not have been sufficient to mediate protective immunity in the respiratory tract because dams and calves were sporadically infected even as maternal antibodies peaked at day 7 postparturition. These findings are consistent with earlier reports of MERS-CoV reinfection in seropositive camels (*4*,*11*). Nevertheless, our findings of virus isolation from calves but not dams are in line with earlier observations of reduced viral load in seropositive camels on reinfection (*11*,*14*), indicating

Table. MERS-CoV nucleic acid detection in nasal swab specimens from camel dam–calf pairs, United Arab Emirates, 2014–2015*

Months postparturition	No. positive/no. tested (%)	
	Adults†	Calves‡
0	0/5	0/5
0.25	3/11 (27.2)	2/11 (18.2)§
1	2/11 (18.2)	5/11 (45.5)
2	0/11	0/11
3	0/11	0/11
4	0/5	0/5
5	0/11	0/11
6	0/11	2/11 (18.2)¶
7	0/10	0/10
8	0/10	0/10
9	0/10	0/10
10	0/10	0/10
11	0/10	0/10
12	0/10	0/10

*One dam–calf pair was excluded after month 6 because the calf was euthanized for an unrelated condition. MERS-CoV, Middle East respiratory syndrome coronavirus.
†5 MERS-CoV–positive specimens from adult camels were from 4 individual animals.
‡9 MERS-CoV–positive specimens from camel calves were from 6 individual animals.
§Virus was isolated from both infected calves.
¶Virus was isolated from 1 infected calf.

that neutralizing antibodies might not provide sterile immunity but could still reduce the viral replication level. The predominance of infection in young animals is better explained by the absence of immunity than by other factors, such as social group density, because the number of newborn camels in our study was negligible compared with the overall size of the herd at the farm. Moreover, young camels were not kept in a contiguous group but in small compartments, where they had more contact with their mothers than with other young animals. Calves are likely to have been infected through fomites or through adult animals shedding low quantities of virus.

Our findings have important implications for the prevention of human infections through camel herd management and camel vaccination. Camel breeding, even if involving a small number of newborn animals, should be classified as a risk for human acquisition of MERS-CoV. The greatest risk should be assumed for the time after the fourth month of life until the first wave of natural infections, which should occur during the first year of life in camels raised in MERS-CoV–endemic regions. Measures for the prevention of infection, such as personal protective equipment, hand hygiene, and environmental sanitation, as applied on the farm in our study, should be sufficient for protection, given that no human MERS-CoV illnesses occurred among staff and only 2 of 300 workers with regular contact with camels had detectable MERS-CoV–specific IgG antibodies. Because persons with underlying disease and the elderly show the most severe outcomes of MERS-CoV infection, these groups should generally avoid farms where camel calves are being raised.

Our results also suggest that studies dealing with application and efficacy of MERS-CoV vaccines should be modified. A first study involving immunologically naive animals showed a sharp decline in virus secretion after vaccination (*14*). However, future vaccination trials should also investigate the effect of preexisting maternal antibodies on vaccine efficacy (*15*).

Acknowledgments

We thank Monika Eschbach-Bludau, Tobias Bleicker, and Sebastian Brünink for their excellent technical assistance and help with the camel sera.

This work was in part financially supported by the Zoonoses Anticipation and Preparedness Initiative (ZAPI, grant agreement no. 115760) within the Innovative Medicines Initiative (IMI call 11-IMI-JU-11-2013-04) and by the Deutsche Forschungsgemeinschaft (DR772/7-2).

Dr. Meyer is a postdoctoral fellow at the Institute of Virology at the University of Bonn Medical Centre. His research interests include the epidemiology and ecology of MERS-CoV and other zoonotic coronaviruses.

References

1. Zaki AM, van Boheemen S, Bestebroer TM, Osterhaus AD, Fouchier RA. Isolation of a novel coronavirus from a man with pneumonia in Saudi Arabia. N Engl J Med. 2012;367:1814–20. http://dx.doi.org/10.1056/NEJMoa1211721
2. World Health Organization. Middle East respiratory syndrome coronavirus (MERS-CoV)—Saudi Arabia [cited 2016 Feb 25]. http://www.who.int/csr/don/2-february-2016-mers-saudi-arabia/en
3. Reusken CB, Haagmans BL, Müller MA, Gutierrez C, Godeke GJ, Meyer B, et al. Middle East respiratory syndrome coronavirus neutralising serum antibodies in dromedary camels: a comparative serological study. Lancet Infect Dis. 2013;13:859–66. http://dx.doi.org/10.1016/S1473-3099(13)70164-6
4. Alagaili AN, Briese T, Mishra N, Kapoor V, Sameroff SC, Burbelo PD, et al. Middle East respiratory syndrome coronavirus infection in dromedary camels in Saudi Arabia. MBio. 2014;5:e00884–14. http://dx.doi.org/10.1128/mBio.01002-14
5. Meyer B, Müller MA, Corman VM, Reusken CB, Ritz D, Godeke GJ, et al. Antibodies against MERS coronavirus in dromedary camels, United Arab Emirates, 2003 and 2013. Emerg Infect Dis. 2014;20:552–9. http://dx.doi.org/10.3201/eid2004.131746
6. Corman VM, Jores J, Meyer B, Younan M, Liljander A, Said MY, et al. Antibodies against MERS coronavirus in dromedary camels, Kenya, 1992–2013. Emerg Infect Dis. 2014;20:1319–22. http://dx.doi.org/10.3201/eid2008.140596
7. Müller MA, Corman VM, Jores J, Meyer B, Younan M, Liljander A, et al. MERS coronavirus neutralizing antibodies in camels, eastern Africa, 1983–1997. Emerg Infect Dis. 2014;20:2093–5. http://dx.doi.org/10.3201/eid2012.141026
8. Haagmans BL, Al Dhahiry SH, Reusken CB, Raj VS, Galiano M, Myers R, et al. Middle East respiratory syndrome coronavirus in dromedary camels: an outbreak investigation. Lancet Infect Dis. 2014;14:140–5. http://dx.doi.org/10.1016/S1473-3099(13)70690-X
9. Müller MA, Meyer B, Corman VM, Al-Masri M, Turkestani A, Ritz D, et al. Presence of Middle East respiratory syndrome coronavirus antibodies in Saudi Arabia: a nationwide, cross-sectional, serological study. Lancet Infect Dis. 2015;15:559–64. http://dx.doi.org/10.1016/S1473-3099(15)70090-3
10. Memish ZA, Cotten M, Meyer B, Watson SJ, Alsahafi AJ, Al Rabeeah AA, et al. Human infection with MERS coronavirus after exposure to infected camels, Saudi Arabia, 2013. Emerg Infect Dis. 2014;20:1012–5. http://dx.doi.org/10.3201/eid2006.140402
11. Hemida MG, Chu DK, Poon LL, Perera RA, Alhammadi MA, Ng HY, et al. MERS coronavirus in dromedary camel herd, Saudi Arabia. Emerg Infect Dis. 2014;20:1231–4. http://dx.doi.org/10.3201/eid2007.140571
12. Corman VM, Müller MA, Costabel U, Timm J, Binger T, Meyer B, et al. Assays for laboratory confirmation of novel human coronavirus (hCoV-EMC) infections. Euro Surveill. 2012;17:20334.
13. Kamber R, Farah Z, Rusch P, Hassig M. Studies on the supply of immunoglobulin G to newborn camel calves (*Camelus dromedarius*). J Dairy Res. 2001;68:1–7. http://dx.doi.org/10.1017/S0022029900004635
14. Haagmans BL, van den Brand JM, Raj VS, Volz A, Wohlsein P, Smits SL, et al. An orthopoxvirus-based vaccine reduces virus excretion after MERS-CoV infection in dromedary camels. Science. 2016;351:77–81. http://dx.doi.org/10.1126/science.aad1283
15. Niewiesk S. Maternal antibodies: clinical significance, mechanism of interference with immune responses, and possible vaccination strategies. Front Immunol. 2014;5:446. http://dx.doi.org/10.3389/fimmu.2014.00446

Address for correspondence: Christian Drosten, Institute of Virology, University of Bonn, Sigmund Freud Str 25, Bonn 53127, Germany; email: drosten@virology-bonn.de

Detection of Vaccinia Virus in Dairy Cattle Serum Samples from 2009, Uruguay

Ana Paula Moreira Franco-Luiz, Danilo Bretas Oliveira, Alexandre Fagundes Pereira, Mirela Cristina Soares Gasparini, Cláudio Antônio Bonjardim, Paulo César Peregrino Ferreira, Giliane de Souza Trindade, Rodrigo Puentes, Agustin Furtado, Jônatas Santos Abrahão, Erna Geessien Kroon

We detected orthopoxvirus in 28 of 125 serum samples collected during 2009 from cattle in Uruguay. Two samples were PCR-positive for vaccinia virus and had sequences similar to those for vaccinia virus associated with outbreaks in Brazil. Autochthonous circulation of vaccinia virus in Uruguay and other South American countries cannot be ruled out.

Orthopoxviruses (family *Poxviridae*, genus *Orthopoxvirus*) cause several zoonotic diseases worldwide, including diseases caused by monkeypox virus in Africa, cowpox virus mainly in Europe, and vaccinia virus (VACV) in South America and Asia (*1*). During the past few decades, reports about emerging and reemerging zoonotic VACV and buffalopox virus have increased, as have the number of severe cases of disease caused by the viruses (*2*,*3*). VACV has been isolated in Brazil and detected in Argentina (*4*–*6*). During bovine vaccinia outbreaks, VACV affects mainly dairy herds; lesions develop on the animals, especially on the teats and udders, resulting in reduced milk production (*5*,*6*). In humans, most VACV infections occur in persons who milk cattle; infection frequently causes lesions on hands and forearms, but systemic clinical manifestations have been described and represent a challenge to public health services (*5*).

The first notifications of VACV detection in Brazil were in the 1960s and 1970s during a government surveillance campaign that investigated emerging pathogens in wild animals (*5*). However, it was not until 1999 that the first outbreaks of bovine vaccinia were reported in Brazil, when cases occurred in Rio de Janeiro and São Paulo States (*5*). Over the next few years, VACV spread to several more states; since then, all geographic regions of Brazil have been affected by bovine vaccinia, including states bordering other countries in South America, which explains the recent detection of VACV in Argentina (Figure 1) (*4*–*8*). Given these detections, serious concern exists regarding the potential spread of VACV to other countries in South America. Uruguay, a country that borders Brazil, has had no reports of VACV detection. To determine if the virus has spread to Uruguay, we investigated the presence of orthopoxvirus neutralizing antibodies and viral DNA in serum samples from cattle in the country.

The Study

We analyzed serum samples that were collected in May 2009 from 125 dairy cows in Durazno County (33°23′0″S, 56°31′0″W), Durazno State, Uruguay (Figure 2). The cattle herds had no clinical sings of disease at the time of serum collection. To determine the presence of neutralizing antibodies in the serum samples, we used an orthopoxvirus plaque-reduction neutralization test as previously described (*9*). The serum titer was defined as the highest dilution that inhibited >70% of virus plaques compared with negative controls (*4*).

Because previous studies have detected viral DNA in the serum of animals and humans with and without clinical manifestations (*4*,*10*,*11*), we performed a molecular investigation to identify orthopoxvirus. We used quantitative PCR (qPCR) to amplify VACV growth factor gene (C11R) DNA. This qPCR tool has high sensitivity and specificity and, thus, has been routinely used as an orthopoxvirus diagnostic tool by our group (*12*). For molecular characterization, we used the nonconserved orthopoxvirus hemagglutinin gene (A56R) (*13*). We used VACV–Western Reserve as the PCR-positive control for amplification and characterization.

The PCR A56R products obtained from C11R PCR–positive samples were sequenced in both orientations and subjected to capillary electrophoresis (3130 Genetic Analyzer, BigDye Terminator Cycle Sequencing Kit v3.1; Applied Biosystems, Foster City, CA, USA). We used the

Author affiliations: Universidade Federal de Minas Gerais, Belo Horizonte, Brazil (A.P.M. Franco-Luiz, D.B. Oliveira, A. Fagundes Pereira, M.C.S. Gasparini, C.A. Bonjardim, P.C.P. Ferreira, G. de Souza Trindade, J. Santos Abrahão, E.G. Kroon); Universidade Federal dos Vales do Jequitinhonha e Mucuri, Diamantina, Brazil (D.B. Oliveira); Universidad de la Republica Oriental del Uruguay Facultad de Veterinaria, Montevideo, Uruguay (R. Puentes, A. Furtado)

DOI: http://dx.doi.org/10.3201/eid2212.160447

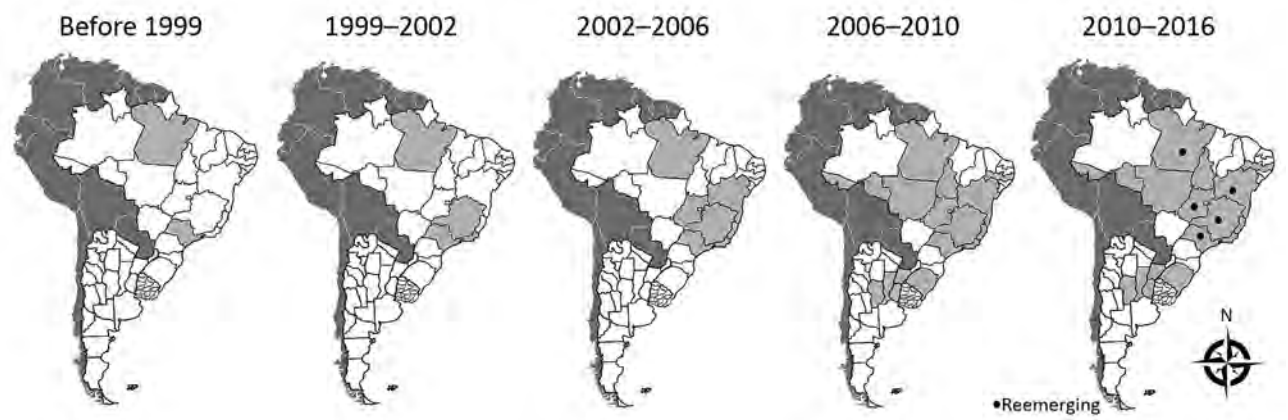

Figure 1. Chronologic representation of vaccinia virus (VACV) emergence and reemergence in South America. Dark gray indicates countries in which VACV outbreaks have not been officially described; light gray indicates states in Brazil, Argentina, and Uruguay where VACV outbreaks were detected by serologic or molecular testing; white indicates states in Brazil and Argentina where VACV has not been detected; black dots indicate areas where VACV is reemerging.

ClustalW (http://www.clustal.org/) method to align sequences with previously published orthopoxvirus sequences from GenBank; alignments were manually checked with MEGA6 (http://www.megasoftware.net/). We constructed phylogenetic trees using the neighbor-joining method with 1,000 bootstrap replicates and the Tamura 3-parameter model in MEGA6. All field and laboratory clinical samples were processed separately to avoid cross-contamination. Serologic and molecular tests were performed in 2 independent experiments and in duplicate.

We detected neutralizing antibodies against orthopoxvirus in 28 (22.4%) of 125 serum samples from cattle in Uruguay; titers were 100 neutralizing units (NU)/mL in 10 (35.7%) samples, 200 NU/mL in 11 (39.3%) samples, 400

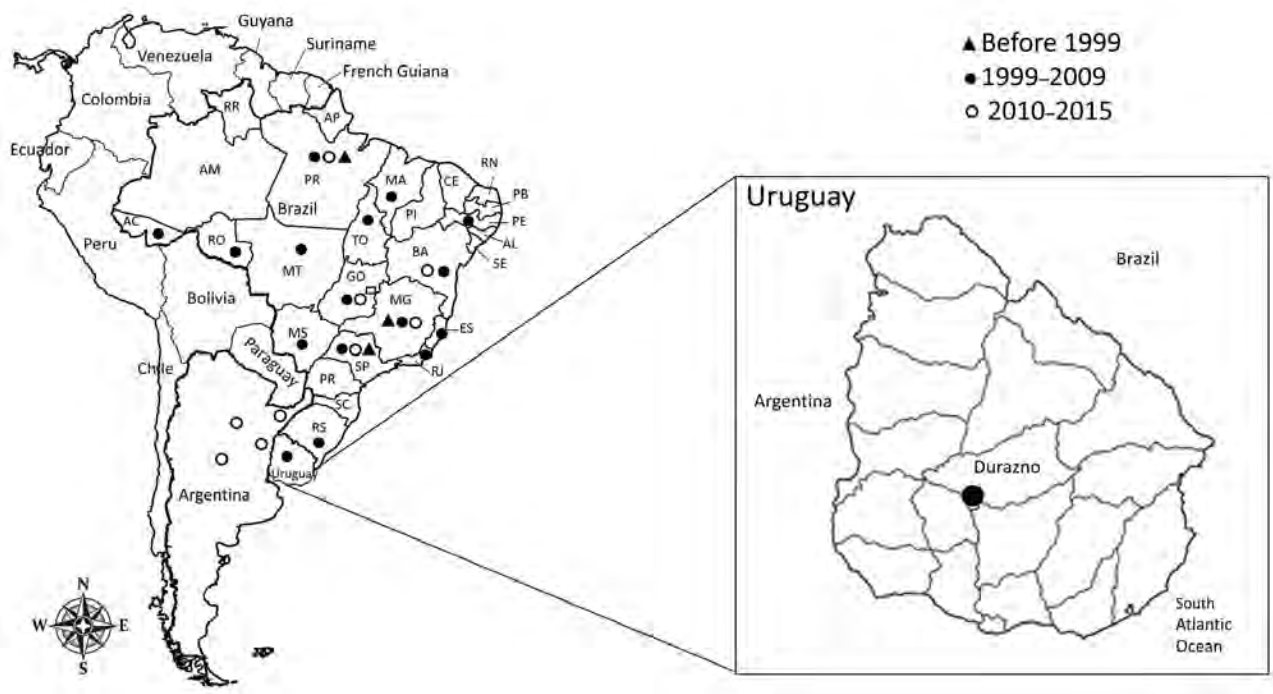

Figure 2. Chronologic detection of vaccinia virus in South America. Zoomed-in map shows location of Durazno County, Uruguay, where serum samples were collected from dairy cattle in 2009 to test for the presence of vaccinia virus. Brazil states: AC, Acre; AM, Amazonas; AL, Alagoas; AP, Amapá; BA, Bahia; CE, Ceará; ES, Espírito Santo; GO, Goiás; MA: Maranhão; MG, Minas Gerais; MS, Mato Grosso do Sul; MT, Mato Grosso; PA, Para; PB, Paraíba; PE, Pernambuco; PI, Piauí; PR, Paraná; RJ, Rio de Janeiro; RN, Rio Grande do Norte; RO, Rondônia; RR, Roraima; RS, Rio Grande do Sul; SC, Santa Catarina; SE, Sergipe; SP, São Paulo; TO, Tocantins.

NU/mL in 5 (17.9%) samples, and 800 NU/mL in 2 (7.1%) samples (online Technical Appendix Figure 1, panel A, http://wwwnc.cdc.gov/EID/article/22/12/16-0447-Techapp1.pdf). To confirm that the orthopoxvirus seropositivity represented seropositivity to VACV, we used the C11R gene to molecularly test DNA in the serum samples; 2 (1.6%) samples were positive by qPCR, and 1 of those was also positive by the plaque-reduction neutralization test.

One of the 2 C11R PCR–positive isolates was also positive for the A56R gene; we sequenced the gene and named the strain VACV Uruguay. Alignment of the A56R nucleotide sequence showed the presence of an 18-nt signature deletion, which is also present in sequences of Brazilian-VACV group I, but not group II, viruses. Unlike sequences for other VACVs, the sequence for VACV Uruguay had an A→T polymorphism (online Technical Appendix Figure 2, panel A). VACV Uruguay exhibited higher identity with group I (98.6% identity) viruses from Brazil and Argentina than to group II (97.3% identity) viruses from Brazil (online Technical Appendix Figure 1, panel B). Furthermore, in the phylogenetic tree based on A56R nucleotide sequences, the VACVs from Uruguay clustered with group I VACVs that had been detected during outbreaks in Brazil and with viruses from Argentina (online Technical Appendix Figure 2, panel B).

Conclusions

Since 1999, VACV has been isolated from symptomatic and asymptomatic cattle, humans, and wildlife from the north to the extreme south of Brazil (*5*,*6*,*8*), and in 2014, VACV was described in bovine serum samples from Argentina (*4*). Although no exanthematous VACV outbreaks have been reported among cattle in Uruguay, we detected orthopoxvirus antibodies and VACV DNA in serum samples from dairy cattle in the country, indicating they have been exposed to VACV. Uruguay shares a border with Brazil, and its western border is shared with Entre Rios Province in Argentina, where VACV DNA has been detected. In addition, Uruguay shares its northern and eastern borders with Rio Grande do Sul State, Brazil, where Pelotas VACV has been isolated from horses (*4*,*5*).

Our finding of orthopoxvirus antibodies and VACV DNA indicates a possible undetected or silent circulation of VACV in Uruguay. Considering the importance of the livestock sector in all countries of South America, concern exists about the possible spread of VACV beyond Brazil, Argentina, and Uruguay (*4*–*6*,*14*). Despite surveillance by veterinarians, efforts to stop the spread of VACV at borders may be hampered by the movement of infected rural workers, the marketing of asymptomatic live animals, and the misdiagnosis of VACV infection. Furthermore, VACV has been shown to circulate in wild environments, and it has been hypothesized that rodents may serve as VACV hosts, as they do for other orthopoxviruses, and facilitate the spread of VACV in border areas (*15*).

Bovine vaccinia outbreaks in South America were first reported in Brazil, but we cannot rule out the possibility of autochthonous circulation of VACV in Uruguay and other countries in South America. Additional studies are needed to elucidate VACV seroprevalence in other countries in South America, and further research is needed to clarify the transmission pathways related to the spread of VACV in South America.

Acknowledgments

We thank colleagues from the Laboratório de Vírus, Universidade Federal de Minas Gerais, for their excellent technical support.

Financial support was provided by the Conselho Nacional de Desenvolvimento Científico e Tecnológico (CNPq); Coordenação de Aperfeiçoamento de Pessoal de Nível Superior (CAPES); Fundação de Amparo à Pesquisa do Estado de Minas Gerais; and Ministério da Agricultura, Pecuária e Abastecimento.

A.P.M.F.L. received fellowships from CAPES. E.G.K., C.A. B., G.S.T., P.C.P. F., and J.S.A. received research fellowships from CNPq.

Dr. Franco-Luiz is a biomedical doctor in the Laboratório de Vírus, Departamento de Microbiologia, Instituto de Ciências Biológicas, Universidade Federal de Minas Gerais. Her research focuses on the monitoring, control, and prevention of vaccinia virus infection.

References

1. Shchelkunov SN. An increasing danger of zoonotic orthopoxvirus infections. PLoS Pathog. 2013;9:e1003756. http://dx.doi.org/10.1371/journal.ppat.1003756
2. Abrahão JS, Campos RK, Trindade GS, Guimarães da Fonseca F, Ferreira PC, Kroon EG. Outbreak of severe zoonotic vaccinia virus infection, Southeastern Brazil. Emerg Infect Dis. 2015;21:695–8. http://dx.doi.org/10.3201/eid2104.140351
3. Goyal T, Varshney A, Bakshi SK, Barua S, Bera BC, Singh RK. Buffalo pox outbreak with atypical features: a word of caution and need for early intervention! Int J Dermatol. 2013;52:1224–30.
4. Franco-Luiz APM, Fagundes-Pereira A, Costa GB, Alves PA, Oliveira DB, Bonjardim CA, et al. Spread of vaccinia virus to cattle herds, Argentina, 2011 [letter]. Emerg Infect Dis. 2014;20:1576–8. http://dx.doi.org/10.3201/eid2009.140154
5. Kroon EG, Mota BE, Abrahão JS, da Fonseca FG, de Souza Trindade G. Zoonotic Brazilian vaccinia virus: from field to therapy. Antiviral Res. 2011;92:150–63. http://dx.doi.org/10.1016/j.antiviral.2011.08.018
6. Medaglia ML, Pessoa LC, Sales ER, Freitas TR, Damaso CR. Spread of cantagalo virus to northern Brazil. Emerg Infect Dis. 2009;15:1142–3. http://dx.doi.org/10.3201/eid1507.081702
7. Damon IK. Poxviruses. In: Knipe DM, Howley PM, editors. Fields virology. 6th ed. Vol II. Philadelphia: Lippincott Williams & Wilkins; 2013. p. 2160–84.
8. de Sant'Ana FJ, Leal FA, Rabelo RE, Vulcani VA, Moreira CA Jr, Cargnelutti JF, et al. Coinfection by *Vaccinia virus* and an *Orf virus*–like parapoxvirus in an outbreak of vesicular disease in dairy

cows in midwestern Brazil. J Vet Diagn Invest. 2013;25:267–72. http://dx.doi.org/10.1177/1040638713475799
9. Silva-Fernandes AT, Travassos CE, Ferreira JM, Abrahão JS, Rocha ES, Viana-Ferreira F, et al. Natural human infections with *Vaccinia virus* during bovine vaccinia outbreaks. J Clin Virol. 2009;44:308–13. http://dx.doi.org/10.1016/j.jcv.2009.01.007
10. Cohen JI, Hohman P, Preuss JC, Li L, Fischer SH, Fedorko DP. Detection of vaccinia virus DNA, but not infectious virus, in the blood of smallpox vaccine recipients. Vaccine. 2007;25:4571–4. http://dx.doi.org/10.1016/j.vaccine.2007.03.044
11. Savona MR, Dela Cruz WP, Jones MS, Thornton JA, Xia D, Hadfield TL, et al. Detection of vaccinia DNA in the blood following smallpox vaccination. JAMA. 2006;295:1898–900. http://dx.doi.org/10.1001/jama.295.16.1898
12. Kroon E, Santos Abrahão J, de Souza Trindade G, Pereira Oliveira G, Moreira Franco Luiz AP, Barbosa Costa G, et al. Natural vaccinia virus infection: diagnosis, isolation, and characterization. Curr Protoc Microbiol. 2016;42:1, 43.
13. de Souza Trindade G, Li Y, Olson VA, Emerson G, Regnery RL, da Fonseca FG, et al. Real-time PCR assay to identify variants of *Vaccinia virus*: implications for the diagnosis of bovine vaccinia in Brazil. J Virol Methods. 2008;152:63–71. http://dx.doi.org/10.1016/j.jviromet.2008.05.028
14. Hutter S, Aviles MM, Matus MCR, Maresca R. Monitoring assessment report of the veterinary services in Uruguay [in Spanish]. Organización Mundial de Sanidad Animal. 2014 [cited 2016 Jan 15]. http://www.oie.int/fileadmin/Home/eng/Support_to_OIE_Members/pdf/PVS-Final-Report-Uruguay-FU.pdf
15. Abrahão JS, Guedes MI, Trindade GS, Fonseca FG, Campos RK, Mota BF, et al. One more piece in the VACV ecological puzzle: could peridomestic rodents be the link between wildlife and bovine vaccinia outbreaks in Brazil? PLoS One. 2009;4:e7428. http://dx.doi.org/10.1371/journal.pone.0007428

Address for correspondence: Erna Geessien Kroon, Laboratório de Vírus, Departamento de Microbiologia, Instituto de Ciências Biológicas, Universidade Federal de Minas Gerais, Av Antônio Carlos, 6627, Caixa Postal 486, CEP 31270-901, Belo Horizonte, Minas Gerais, Brazil; email: ernagkroon@gmail.com

Tuberculosis-Associated Death among Adult Wild Boars, Spain, 2009–2014

Jose A. Barasona, Pelayo Acevedo, Iratxe Diez-Delgado, Joao Queiros, Ricardo Carrasco-García, Christian Gortazar, Joaquín Vicente

We investigated adult Eurasian wild boar (*Sus scrofa*) survival and death in 2 tuberculosis-endemic populations with different harvest pressure in Spain. Overall, tuberculosis accounted for 30% of total deaths. Increased survival in protected areas has direct implications for wild boar management and tuberculosis control.

Eurasian wild boar (*Sus scrofa*) population dynamics and hunting strategies might influence the persistence of disease (*1*). Determining the death rates for wild boar and unfolding the relative contribution of several causes of death and their nature (additive vs. compensatory death) is key to predicting the effects of harvesting, predation, and disease on population dynamics over time and to develop disease control–oriented hunting strategies. In central and northern Europe, the effect of disease-mediated death on wild boars is relatively low, whereas predation, winter starvation, and especially hunting play more important roles (*2*,*3*). In Mediterranean regions, natural death from summer starvation during droughts has been described, but most deaths are attributed to hunting (*4*); no information is available about rates of disease-related death among wild boars.

Animal tuberculosis (TB) caused by the *Mycobacterium tuberculosis* complex (MTC) is a reemerging multihost infectious disease (*5*). In Spain, the Eurasian wild boar is regarded as the key wildlife MTC maintenance host; its infection prevalence rates are >50% in Mediterranean areas that have dense wild boar populations (*6*). Up to one third of wild boar piglets might become infected during their first 6 months of life (*7*). In half of MTC-infected wild boars, generalized lesions develop that affect the lungs, particularly in juveniles (12–24 months of age). In adults (>2 years), the observed proportion of wild boars with generalized TB decreases, suggesting some degree of TB-driven death among juveniles (*6*,*8*). TB is a sporadic cause of death among wild boars (*9*), but no data are available about its actual contribution to mortality.

In the context of growing and expanding wild boar populations and of increasing concern about the effect of wild boar infections (*10*), we hypothesized that TB could be a major component of total wild boar death in Spain and have implications for TB control and wildlife management. We aimed to 1) describe the rates and causes of adult wild boar death and 2) compare the total death and its causes in 2 TB-endemic regions that differ in harvest pressure.

The Study

We compared 2 settings: a mosaic of game estates and a protected area. Montes de Toledo (MT) is a mountain chain in the central Spanish plateau whose large game estates are mainly devoted to recreational hunting. Harvest is conducted by dog-driven hunts; average annual extraction quota is 2.26 wild boar/km^2 and no age or sex are selected (i.e., extraction is random). Doñana National Park (DNP) is a protected area on the Atlantic coast of southern Spain. Harvest is part of population control management because no recreational hunting is allowed within the park; this modality has a minimal extraction capacity (1.11 wild boar/km^2) and targets wild boar seen by park rangers (random and opportunistic). Wild boars, except piglets, have no natural predators (occasionally stray dogs) in the study areas.

During 2009–2014, we captured (*11*) and fitted very high frequency global positioning system–global system for mobile communications (VHF-GPS-GSM) collars (Microsensory, Spain) to 45 free-ranging adult wild boars (24 from MT and 21 from DNP; online Technical Appendix Table, http://wwwnc.cdc.gov/EID/article/22/12/16-0677-Techapp1.pdf) following Animal Experimentation legislation (PR-2015-03-08). We collected serum and tested it for antibodies to MTC by using ELISA (89.6% sensitivity [*12*]). Post-release monitoring was programmed to acquire 1 GPS location per hour. We monitored the animals daily for death (alarm set at 12 h of inactivity) to promptly retrieve carcasses and assess the cause of death. The 18 retrieved carcasses underwent a full postmortem examination, and tissue samples (pooled lymph nodes and lung) were submitted for culture (online Technical Appendix).

Author affiliations: Instituto de Investigación en Recursos Cinegéticos, Ciudad Real, Spain (J.A. Barasona, P. Acevedo, I. Diez-Delgado, J. Queiros, R. Carrasco-Garcia, C. Gortazar, J. Vicente); Universidad Complutense de Madrid, Madrid, Spain (J.A. Barasona, I. Diez-Delgado); Centro de Investigacão em Biodiversidade e Recursos Genéticos, Vairão, Portugal (J. Queiros); Faculdade de Ciências da Universidade do Porto, Porto, Portugal (J. Queiros)

DOI: http://dx.doi.org/10.3201/eid2212.160677

We detected serum antibodies to MTC in 35 (78%) of 45 GPS-collared wild boars. We found no differences in MTC serum antibody prevalence between study sites (p>0.05 by Fisher exact test) and no differences in survival time between antibody-positive and -negative wild boars (p>0.05 by Mann-Whitney U test). MTC infection was confirmed by culture in 13 (72%) of 18 wild boars for which postmortem results were available. The 9 wild boars that died of generalized TB had severe lesions in >1 anatomic region; >70% of lung tissue was affected (online Technical Appendix Figure 1).

We assessed total survival probability and the main causes of death (Figure). The mean annual death rate (45.48% ± 5.6% SE overall) was higher in the regularly hunted MT (56%) than in the protected DNP (34%). Overall, harvest accounted for half (53%) of total annual deaths, whereas TB contributed to 30% of deaths. The remaining 17% of deaths were caused by predation (stray dogs in DNP) and unknown causes (Table). The mean annual death rate for adult wild boars caused by harvest was significantly higher in MT (40%) than in the protected DNP (8%; Fisher exact test, p = 0.011). However, death from TB did not differ between MT (12%) and DNP (14%; p>0.05 by Fisher exact test) (online Technical Appendix Table).

Mean survival time was twice as long in DNP (average 672 ± 96 days) as in MT (297 ± 41 days; Mantel-Cox, χ^2 = 11.42, 1 d.f.; p = 0.001). Kaplan-Meier survival probabilities and causes of death are detailed by study area in online Technical Appendix Figure 2. Two death peaks were found, 1 in summer (July) associated with TB and 1 in autumn (October–January) associated with harvest (online Technical Appendix Figure 3).

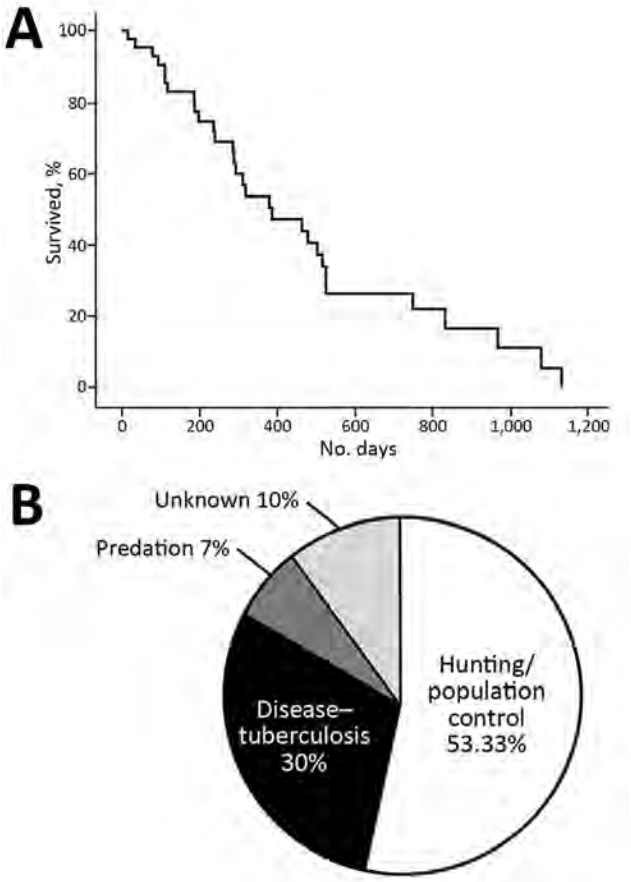

Figure. Total survival probability and the main causes of death among wild boars (*Sus scrofa*), Spain, 2009–2014. A) Kaplan-Meier survival curve representing the proportion of adult wild boars alive over time for all the animals studied. B) Percentage of each cause of death among wild boars (i.e., when considering only all dead animals)

Conclusions

The results confirmed our hypothesis that TB causes a substantial proportion of deaths among adult wild boars in TB-endemic Mediterranean areas of Spain. This information is relevant for TB control at the wildlife–livestock interface and for understanding wild boar and TB dynamics under different harvest pressure.

Severely diseased wild boars, with advanced generalized TB lesions affecting large proportions of the lung, probably are important shedders of MTC (super-shedders [*13*]). The higher survival rate for MTC super-shedders in protected areas, such as DNP, resulting from a low harvest pressure might contribute toward explaining the extremely high spread of TB in sites where risky artificial management, such as feeding, is absent (*5*).

The large proportion of natural death from TB (30% of deaths) contrasts with results obtained in other parts of Europe (total natural death rate 3% [*3*]), although this finding is consistent with differences in TB prevalence within Europe (*14*). Previous findings suggest that TB-induced death is relevant in subadults but decreases in adults (*6*,*8*), hence, deaths of juvenile wild boars deserves special study. However, given the chronic nature of TB and the early reproduction of wild boars, TB is unlikely to substantially contribute to wild boar population regulation. In fact, we observed a mean annual death rate of 45%, which is below the recommended annual harvest or death rate of 65% needed to maintain stable wild boar populations (*3*,*15*).

Two additional aspects about hunting and wild boar TB deserve attention. First, increased hunting might contribute to TB control in wild boars by reducing population size and by reducing survival of super-shedders. Hunting bans should therefore be reconsidered in protected areas in which TB is a concern. Second, TB causes a substantial loss of adult (trophy) wild boars, thus reducing the profitability of the hunting industry. Hunters should therefore actively engage in TB control.

Table. Causes of death of GPS-collared adult wild boars (*Sus scrofa*), Spain, 2009–2014*

Variable	Study site		Total
	Montes de Toledo†	Doñana National Park‡	
No. GPS-collared wild boars	24	21	45
Mean survival time ± SE, d§	297.28 ± 40.91	672.78 ± 96.53	470.43 ± 58.69
Mean annual survival rate ± SE, %¶	44.17 ± 7.55	66.35 ± 7.73	54.52 ± 5.60
Mean annual mortality rate ± SE, %¶	55.83 ± 7.55	33.64 ± 7.73	45.48 ± 5.60
Proportion of deaths, %			
From harvest	72.22	25	53.33
From tuberculosis	22.22	41.67	30.00
From other causes	5.56	33.93	16.67

*GPS, global positioning system.
†High harvest pressure.
‡Low harvest pressure.
§Mantel-Cox log-rank, χ^2 = 11.42, 1 d.f., p = 0.001.
¶Mann-Whitney U test, U = –1.994, p = 0.046.

Acknowledgments

We thank our colleagues from DNP who collaborated in this study, along with the MT managers, Estación Biológica de Doñana monitoring team, and many students for their help with the fieldwork.

This study was supported by the following research grants: Spanish Ministry for Economy and Competitiveness (MINECO; AGL2013-48523), European Union FP7 grant ANTIGONE (278976), and European Union FP7 grant WildTBVac (613779). J.A.B was supported by a Juan de la Cierva contract (FJCI-2015-23643) from MINECO. P.A. was supported by a Ramón y Cajal contract (RYC-2012-11970) from MINECO. I.D.D. holds an Formación de Personal Investigador pre-doctoral scholarship from MINECO.

Dr. Barasona is a disease epidemiologist at the Instituto de Investigación en Recursos Cinegéticos, Ciudad Real, Spain. His main research interests focus on the ecology of infectious pathogen transmission at interfaces of wild and domestic animals.

References

1. Kramer-Schadt S, Fernández N, Thulke HH. Potential ecological and epidemiological factors affecting the persistence of classical swine fever in wild boar *Sus scrofa* populations. Mammal Rev. 2007;37:1–20. http://dx.doi.org/10.1111/j.1365-2907.2007.00097.x
2. Jedrzejewski W, Jedrzejewska B, Okarma H, Ruprecht AL. Wolf predation and snow cover as mortality factors in the ungulate community of the Bialowieza National Park, Poland. Oecologia. 1992;90:27–36. http://dx.doi.org/10.1007/BF00317805
3. Keuling O, Baubet E, Duscher A, Ebert C, Fischer C, Monaco A, et al. Mortality rates of wild boar *Sus scrofa* L. in central Europe. Eur J Wildl Res. 2013;59:805–14. http://dx.doi.org/10.1007/s10344-013-0733-8
4. Massei G, Genov PV, Staines BW, Gorman ML. Mortality of wild boar, *Sus scrofa*, in a Mediterranean area in relation to sex and age. J Zool (Lond). 1997;242:394–400. http://dx.doi.org/10.1111/j.1469-7998.1997.tb05813.x
5. Gortázar C, Torres MJ, Vicente J, Acevedo P, Reglero M, de la Fuente J, et al. Bovine tuberculosis in Doñana Biosphere Reserve: the role of wild ungulates as disease reservoirs in the last Iberian lynx strongholds. PLoS One. 2008;3:e2776. http://dx.doi.org/10.1371/journal.pone.0002776
6. Vicente J, Barasona JA, Acevedo P, Ruiz-Fons JF, Boadella M, Diez-Delgado I, et al. Temporal trend of tuberculosis in wild ungulates from Mediterranean Spain. Transbound Emerg Dis. 2013;60(Suppl 1):92–103. http://dx.doi.org/10.1111/tbed.12167
7. Che' Amat A, González-Barrio D, Ortiz JA, Díez-Delgado I, Boadella M, Barasona JA, et al. Testing Eurasian wild boar piglets for serum antibodies against *Mycobacterium bovis*. Prev Vet Med. 2015;121:93–8. http://dx.doi.org/10.1016/j.prevetmed.2015.05.011
8. Díez-Delgado I, Boadella M, Martín-Hernando M, Barasona JA, Beltrán-Beck B, González-Barrio D, et al. Complex links between natural tuberculosis and porcine circovirus type 2 infection in wild boar. BioMed Res Int. 2014;2014:765715. http://dx.doi.org/10.1155/2014/765715
9. Segalés J, Vicente J, Luján L, Toussaint MJM, Gruys E, Gortázar C. Systemic AA-amyloidosis in a European wild boar (*Sus scrofa*) suffering from generalized tuberculosis. J Vet Med A Physiol Pathol Clin Med. 2005;52:135–7. http://dx.doi.org/10.1111/j.1439-0442.2005.00703.x
10. Ruiz-Fons F. A review of the current status of relevant zoonotic pathogens in wild swine (*Sus scrofa*) populations: changes modulating the risk of transmission to humans. Transbound Emerg Dis. 2015;n/a. http://dx.doi.org/10.1111/tbed.12369
11. Barasona JA, López-Olvera JR, Beltrán-Beck B, Gortázar C, Vicente J. Trap-effectiveness and response to tiletamine-zolazepam and medetomidine anaesthesia in Eurasian wild boar captured with cage and corral traps. BMC Vet Res. 2013;9:107. http://dx.doi.org/10.1186/1746-6148-9-107
12. Boadella M, Lyashchenko K, Greenwald R, Esfandiari J, Jaroso R, Carta T, et al. Serologic tests for detecting antibodies against *Mycobacterium bovis* and *Mycobacterium avium* subspecies paratuberculosis in Eurasian wild boar (*Sus scrofa scrofa*). J Vet Diagn Invest. 2011;23:77–83. http://dx.doi.org/10.1177/104063871102300111
13. Santos N, Santos C, Valente T, Gortázar C, Almeida V, Correia-Neves M. Widespread environmental contamination with *Mycobacterium tuberculosis* complex revealed by a molecular detection protocol. PLoS One. 2015;10:e0142079. http://dx.doi.org/10.1371/journal.pone.0142079
14. Gortazar C, Delahay RJ, Mcdonald RA, Boadella M, Wilson GJ, Gavier-Widen D, et al. The status of tuberculosis in European wild mammals. Mammal Rev. 2012;42:193–206. http://dx.doi.org/10.1111/j.1365-2907.2011.00191.x
15. Genov PW, Massei G, Kostova W. Die nutzung des wildschweins (*Sus scrofa*) in Europa in theorie und praxis. Z Jagdwiss. 1994;40:263–7.

Address for correspondence: Jose A. Barasona, SaBio-IREC (CSIC-UCLM-JCCM), Ronda de Toledo 12, 13005 Ciudad Real, Spain; email: joseangel.barasona@gmail.com

Secondary Shiga Toxin–Producing *Escherichia coli* Infection, Japan, 2010–2012

Tomoko Morita-Ishihara, Sunao Iyoda, Atsushi Iguchi, Makoto Ohnishi

To evaluate the potential public health risk caused by secondary Shiga toxin–producing *Escherichia coli* (STEC) infections in Japan, we investigated the prevalence and characteristics of STEC isolated from healthy adults during 2010–2012. Although prevalence among healthy adults was high, most STEC organisms displayed characteristics rarely found in isolates from symptomatic patients.

Shiga toxin–producing *Escherichia coli* (STEC), which is characterized by production of the Shiga toxin (Stx) or possession of the Stx-encoding genes, is a notable human pathogen that causes diarrhea, hemorrhagic colitis, and hemolytic uremic syndrome (*1*,*2*). In Japan, STEC infection is a notifiable disease, and ≈3,500–4,500 (2.7–3.5/100,000 population) annual cases of STEC infection (including asymptomatic carriers) have been reported since 2006 (*3*–*5*). For ≈50%–60% of these notifiable cases, serotype and Stx type of laboratory-confirmed STEC isolate and clinical manifestations associated with STEC infection are reported (*3*). To date, most STEC isolates from asymptomatic carriers collected in Japan were isolated during laboratory-based investigation of outbreaks or intrafamilial infections, together with those from sporadic patients. Therefore, we believe that the characteristics of such STEC isolates could be similar to those from ill patients. We conducted a large-scale study to investigate the prevalence and characteristics of STEC isolated from healthy adults in Japan to evaluate the potential public health risk of infection due to secondary STEC infection.

The Study

A total of 2,774,824 fecal samples were collected from 472,734 healthy adults throughout Japan during April 2010–March 2012; these samples were examined at Japan Microbiological Laboratory Co., Ltd. (Sendai, Japan) (online Technical Appendix, http://wwwnc.cdc.gov/EID/article/22/12/16-0783-Techapp1.pdf). These healthy persons included food handlers and those who worked in childcare and eldercare facilities; each person was tested ≥1 times over 2 years. When >1 STEC isolate from the same patient had the same serotype and virulence factor type, we used the first detected isolate in this study. Of 472,734 healthy adults examined, 398 (0.08%) were positive for STEC. Therefore, the estimated incidence rate of asymptomatic carriers among healthy adults was 84.2/100,000 population, indicating that asymptomatic STEC infections are highly prevalent among healthy adults.

A total of 399 STEC organisms were isolated from 398 healthy adults. O-serogrouping showed that 339 isolates comprised 61 different O serogroups; 60 isolates were O serogroup untypeable (online Technical Appendix Table). Two isolates obtained from the same person >12 months apart belonged to serogroups O103 (first isolate) and O91 (second isolate). The dominant O serogroup of isolates from healthy adult carriers was O91 (n = 89, 22.3%), followed by O103 (n = 23, 5.8%). Of STEC infection cases associated with patients reported during 2010–2011 in Japan, 97.4% were caused by either STEC O157 (68.8%), O26 (16.9%), O111 (3.9%), O145 (3.1%), O103 (2.8%), or O121 (1.9%) isolates (*4*,*5*). In this study, STEC O157 (n = 13), O26 (n = 6), O145 (n = 2), O103 (n = 23), and O121 (n = 1) isolates were detected, but STEC O111 isolates were not (online Technical Appendix Table). Therefore, the STEC isolates belonging to these 6 O serogroups represented only 11.3% of all isolates from healthy adults. These results show that the prevalence of O serogroups among STEC from healthy adults was clearly different from that among symptomatic patients.

We also determined the *stx* type of STEC isolates and investigated the presence of virulence factors (online Technical Appendix). Of 399 STEC isolates, 201 (50.4%) harbored the *stx1* gene only (*stx1* type), 160 (40.1%) harbored the *stx2* gene only (*stx2* type), and 38 (9.5%) harbored both *stx1* and *stx2* genes (*stx1*/*stx2* type) (Table 1). Adherence factors that contribute to virulence of STEC, *eae*, *saa*, and Eib, were detected in 55 (13.8%), 125 (31.3%), and 102 (25.6%) isolates, respectively (Table 1) (*6*–*8*). No STEC isolate harbored >2 of these adherence genes/factors; *aggR* was not detected in any isolates; and 117 (29.3%) isolates did not contain any adherence genes/factors.

The combination of *stx2* and *eae* genes in STEC is considered a risk factor for high virulence of STEC because these 2 genes are often found together in STEC isolates associated with severe disease such as hemolytic uremic syndrome (*9*). To investigate the prevalence of such risk factors among STEC isolates from healthy adults, we analyzed

Author affiliations: National Institute of Infectious Diseases, Tokyo, Japan (T. Morita-Ishihara, S. Iyoda, M. Ohnishi); University of Miyazaki, Miyazaki, Japan (A. Iguchi)

DOI: http://dx.doi.org/10.3201/eid2212.160783

Table 1. Serogroups, *stx* genes, and virulence genes of Shiga toxin–producing *Escherichia coli* isolates from healthy adults, Japan, 2010–2012

		No. isolates that possessed each gene type					
Serogroup	No. isolates	*stx1*	*stx1/stx2*	*stx2*	*eae*	*saa*	Eib
O91	89	84	5			11	77
O103	23	23			22		
O8	15	1		14		2	
O113	15		2	13		10	
O128	15	4	8	3		8	5
O110	13			13			
O157	13	1	4	8	13		
O146	10	2	4	4		8	1
O174	9		1	8		1	
O100	8			8		1	
O181	8	2		6		7	
O55	7	7				1	
O76	7	7			1	5	
O26	6	6			6		
O74	6			6		6	
O112	5			5		1	2
O115	5	5					
O183	5	4	1			3	
O93	4	3		1		2	
O156	4	4			4		
O163	4	2		2		1	
O186	4	2	2			4	
O38	3		1	2		3	
O78	3	2	1			3	
O159	3			3			
O166	3			3		2	
O168	3			3			
O171	3	1		2		1	
O6	2	1		1		1	
O18	2	1		1			1
O22	2	1		1		1	
O25	2			2			
O28	2			2		2	
O87	2	1		1			
O101	2			2			
O109	2	2				1	
O119	2	2				2	
O130	2			2		2	
O145	2	1	1		2		
O150	2	2				2	
O178	2	1		1		2	
O2	1			1			
O5	1		1				1
O15	1			1			
O53	1			1			
O65	1	1				1	
O75	1		1			1	
O77	1	1					
O82	1	1				1	
O96	1		1			1	
O105	1			1		1	
O108	1	1				1	
O117	1	1					
O121	1			1	1		
O136	1	1					
O137	1	1				1	
O149	1		1			1	
O175	1			1			
O177	1	1			1		
O179	1			1		1	
O185	1			1			
O untypeable	60	21	4	35	5	23	15
Total	399	201	38	160	55	125	102

eae-positive isolates (n = 55). In this study, all STEC isolates belonging to 1 of 6 major O serogroups (O157:H7/H-, O26:H11, O111:H-, O103:H2/H11, O145:H-, O121:H19) frequently found in patient-derived isolates were positive for the *eae* gene, except for an O103:H2 isolate (Table 2; online Technical Appendix). O156:H-/HUT (n = 4), O76:H7 (n = 1), O177:H- (n = 1), and O-untypeable (n = 5) isolates were also positive for the *eae* gene. From analysis of *stx1*, *stx2*, and their subtypes, 16 of 55 *eae*-positive isolates harbored the *stx2* gene; their *stx2* subtypes were *stx2a* (n = 5), *stx2c* (n = 10), and *stx2e* (n = 1) (Table 2; online Technical Appendix Table). *stx2a* and *stx2c* were the *stx2* subtypes most commonly found in patient-derived isolates (*10*,*11*). The STEC isolates harboring both *eae* and *stx2* occupied 4% of all STEC isolates from healthy adults. Therefore, we estimated that the incidence rate of healthy asymptomatic carriers infected with STEC isolates harboring both *eae* and *stx2* was 3.4/100,000 population (16/472,734 isolates). These results highlight the potential risk of serious STEC infection, which may be transmitted by secondary transmission from asymptomatic carriers.

Conclusions

We found that the incidence rate of STEC infection in healthy asymptomatic carriers was 84.2/100,000 population. This finding suggests that the risk of secondary transmission to susceptible persons may be higher than originally thought. However, many STEC isolates from healthy adults belong to O serogroups that are rarely found in STEC isolates from symptomatic patients, and >80% of those isolates did not have the *eae* gene that is frequently detected in STEC isolates from symptomatic patients.

Recently, STEC outbreaks caused by isolates from 6 major O serogroups (O157:H7/H-, O26:H11, O111:H-, O103:H2/H11, O145:H-, O121:H19) have been frequently reported in childcare facilities in Japan (*12*). Person-to-person transmission is considered a major route of infection in such outbreaks, and many adult family members identified in such outbreaks had asymptomatic cases (*12*). In addition, those who work within child- and elder-care facilities are possibly more likely to be exposed to STEC organisms than are the general population because STEC organisms are more likely to be shed in higher numbers in children and elders from such facilities (*13*). We found that STEC O157:H7/H-, O26:H11, O103:H2, O121:H19, and O145:H- were isolated from asymptomatic carriers. These findings suggest that a portion of STEC infection due to these serotypes may be caused by secondary transmission through asymptomatic carriers.

Although the prevalence of STEC O157, O26, and O111 in retail raw foods is monitored by the National Food Surveillance System in Japan, prevalence of STEC belonging to other O serogroups in foods is unknown. In 1 study regarding STEC strains from food-producing animals in Japan during 1999–2001, of the bovine isolates, 30.6% belonged to serotypes frequently implicated in human disease, and 37% harbored the *eae* gene (*14*). Isolates with such serotypes and *eae* were not found among the isolates from swine (*14*). Many STEC isolates from food-producing animals, as with those from healthy adults, displayed characteristics rarely found in patient-derived isolates (*14*). Food handlers may be at a greater risk of STEC transmission through food preparation, because they are more likely to be exposed to organisms from food-producing animals than the general population (*15*).

Our findings provide scientific evidence that can be useful in the management of STEC infection, in particular, in detecting asymptomatic carriers in Japan. Such identification could result in a decrease in asymptomatic carriers and in secondary transmission of STEC organisms.

Acknowledgments

We are grateful to Japan Microbiological Laboratory Co., Ltd., for the generous gift of STEC isolates and their information. We

Table 2. Serotypes and *stx* types of *eae*-positive Shiga toxin–producing *Escherichia coli* isolates from healthy adults, Japan, 2010–2012

Serotype		No. *eae*-positive isolates*	No. *stx*-positive isolates†		
			stx1	*stx1/stx2*	*stx2*
O103:	H2	21	21		
	H11	1	1		
O157:	H7	10		2 (*stx*2a)	8 (*stx*2a [1], *stx*2c [7])
	H-	3	1	2 (*stx*2c)	
O26:	H11	6	6		
O156:	H-	2	2		
	HUT	2	2		
O145:	H-	2	1	1 (*stx*2a)	
O76:	H7	1	1		
O121:	H19	1			1 (*stx*2a)
O177:	H-	1	1		
O	Untypeable	5	3		2 (*stx*2c[1], *stx*2e [1])
Total		55	39	5	11

*The number of *eae*-negative isolates among the same serotype: O103:H2 (1), O76:H19 (5), O76:H- (1).
†The name of the positive subtype is in parentheses; the number subtype-positive isolates are in brackets.

also thank Emiko Furukawa and Toshio Sato for selection of STEC isolates and Nobuko Takai, Hitomi Satou, Yukie Nakajima, Ai Yoshida, Yasunori Saito, and Saomi Ozawa for technical assistance.

This work was supported by Grants-in-Aid for Scientific Research from Japan Society for the Promotion of Science (grant nos. 26870873 to T. M.-I.; 15K08486 to S. I), a grant from the Ministry of Health, Labour and Welfare of Japan (grant H24-Shinko-Ippan-012), and a grant from the Research Program on Emerging and Re-emerging Infectious Diseases from Japan Agency for Medical Research and Development.

Dr. Morita-Ishihara is a senior researcher in the Department of Bacteriology I, National Institute of Infectious Diseases, Tokyo. Her research has focused on the surveillance of pathogenic *E. coli* by molecular epidemiology analysis and the analysis of pathogenicity mechanisms.

References

1. Paton JC, Paton AW. Pathogenesis and diagnosis of Shiga toxin–producing *Escherichia coli* infections. Clin Microbiol Rev. 1998;11:450–79.
2. Nataro JP, Kaper JB. Diarrheagenic *Escherichia coli*. Clin Microbiol Rev. 1998;11:142–201.
3. National Institute of Infectious Diseases, Ministry of Health, Labour and Welfare, Japan. Pathogen surveillance system in Japan and Infectious Agents Surveillance Report (IASR). Infect Agents Surveill Rep. 2010;31:69–70. http://idsc.nih.go.jp/iasr/31/361/tpc361.html
4. National Institute of Infectious Diseases, Ministry of Health, Labour and Welfare, Japan. Enterohemorrhagic *Escherichia coli* infection in Japan as of April 2011. Infect Agents Surveill Rep. 2011;32:125–7.
5. National Institute of Infectious Diseases, Ministry of Health, Labour and Welfare, Japan. Enterohemorrhagic *Escherichia coli* infection in Japan as of April 2012. Infect Agents Surveill Rep. 2012;33:115–7. http://www.niid.go.jp/niid/en/iasr-vol33-e/865-iasr/2134-tpc387.html
6. Jerse AE, Yu J, Tall BD, Kaper JB. A genetic locus of enteropathogenic *Escherichia coli* necessary for the production of attaching and effacing lesions on tissue culture cells. Proc Natl Acad Sci U S A. 1990;87:7839–43. http://dx.doi.org/10.1073/pnas.87.20.7839
7. Lu Y, Iyoda S, Satou H, Satou H, Itoh K, Saitoh T, et al. A new immunoglobulin-binding protein, EibG, is responsible for the chain-like adhesion phenotype of locus of enterocyte effacement-negative, shiga toxin-producing *Escherichia coli*. Infect Immun. 2006;74:5747–55. http://dx.doi.org/10.1128/IAI.00724-06
8. Paton AW, Srimanote P, Woodrow MC, Paton JC. Characterization of Saa, a novel autoagglutinating adhesin produced by locus of enterocyte effacement-negative Shiga-toxigenic *Escherichia coli* strains that are virulent for humans. Infect Immun. 2001;69:6999–7009. http://dx.doi.org/10.1128/IAI.69.11.6999-7009.2001
9. Ethelberg S, Olsen KE, Scheutz F, Jensen C, Schiellerup P, Engberg J, et al. Virulence factors for hemolytic uremic syndrome, Denmark. Emerg Infect Dis. 2004;10:842–7. http://dx.doi.org/10.3201/eid1005.030576
10. Orth D, Grif K, Khan AB, Naim A, Dierich MP, Würzner R. The Shiga toxin genotype rather than the amount of Shiga toxin or the cytotoxicity of Shiga toxin in vitro correlates with the appearance of the hemolytic uremic syndrome. Diagn Microbiol Infect Dis. 2007;59:235–42. http://dx.doi.org/10.1016/j.diagmicrobio.2007.04.013
11. Persson S, Olsen KE, Ethelberg S, Scheutz F. Subtyping method for *Escherichia coli* shiga toxin (verocytotoxin) 2 variants and correlations to clinical manifestations. J Clin Microbiol. 2007;45:2020–4. http://dx.doi.org/10.1128/JCM.02591-06
12. Kanayama A, Yahata Y, Arima Y, Takahashi T, Saitoh T, Kanou K, et al. Enterohemorrhagic *Escherichia coli* outbreaks related to childcare facilities in Japan, 2010-2013. BMC Infect Dis. 2015;15:539–46. http://dx.doi.org/10.1186/s12879-015-1259-3
13. Cornick NA, Jelacic S, Ciol MA, Tarr PI. *Escherichia coli* O157:H7 infections: discordance between filterable fecal shiga toxin and disease outcome. J Infect Dis. 2002;186:57–63. http://dx.doi.org/10.1086/341295
14. Kijima-Tanaka M, Ishihara K, Kojima A, Morioka A, Nagata R, Kawanishi M, et al. A national surveillance of Shiga toxin–producing *Escherichia coli* in food-producing animals in Japan. J Vet Med B Infect Dis Vet Public Health. 2005;52:230–7. http://dx.doi.org/10.1111/j.1439-0450.2005.00852.x
15. Doyle MP. *Escherichia coli* O157:H7 and its significance in foods. Int J Food Microbiol. 1991;12:289–301. http://dx.doi.org/10.1016/0168-1605(91)90143-D

Address for correspondence: Tomoko Morita-Ishihara, National Institute of Infectious Diseases, Department of Bacteriology I, Shinjuku-ku, Tokyo. Japan; email: ishihara@niid.go.jp

Reemergence of St. Louis Encephalitis Virus, California, 2015

Gregory S. White,[1] Kelly Symmes,[1] Pu Sun, Ying Fang, Sandra Garcia, Cody Steiner, Kirk Smith, William K. Reisen, Lark L. Coffey

St. Louis encephalitis virus infection was detected in summer 2015 in southern California after an 11-year absence, concomitant with an Arizona outbreak. Sequence comparisons showed close identity of California and Arizona isolates with 2005 Argentine isolates, suggesting introduction from South America and underscoring the value of continued arbovirus surveillance.

St. Louis encephalitis virus (SLEV; family *Flaviviridae*, genus *Flavivirus*) was recognized in California in 1937 and caused periodic epidemics in humans and equines until 1989, including a 1984 outbreak in Los Angeles (*1*–*3*). Even though US epidemics have not occurred since 1989, SLEV activity was documented continually in California until 2003, the year West Nile virus (WNV) activity was detected in the state. During 2003–2015, no SLEV activity was detected in California despite ongoing SLEV surveillance and a 6-fold statewide increase in mosquito pool testing in response to the invasion of WNV. The absence of SLEV activity suggested its elimination from California (*4*,*5*).

In Arizona, SLEV has been detected less frequently than in California, with low enzootic activity reported most years during 1972–2006 (Arizona State Public Health Laboratory, unpub. data) and a single human case during 2010–2014 (*6*). In Maricopa County, which includes Phoenix, a human SLEV outbreak during July–October 2015 resulted in 23 confirmed cases and 1 death (Arizona State Public Health Laboratory, unpub. data).

Beginning in July 2015, SLEV activity was detected in mosquito pools, and sentinel chicken seroconversions were detected in the Coachella Valley in Riverside County, California. Given the reemergence of SLEV in California and Arizona in summer 2015, the purpose of this study was to describe the temporal and spatial detection of SLEV in California, compare its circulation intensity with that of WNV in California in 2015, and define the genetic relatedness of SLEV from both states to SLEV from elsewhere to infer a possible origin and pattern of spread.

Author affiliations: Coachella Valley Mosquito and Vector Control District, Indio, California, USA (G.S. White); School of Veterinary Medicine, University of California, Davis, California (K. Symmes, P. Sun, Y. Fang, S. Garcia, C. Steiner, W.K. Reisen, L.L. Coffey); Environmental Services Department, Maricopa County, Phoenix, Arizona, USA (K. Smith)

DOI: http://dx.doi.org/10.3201/eid2212.160805

The Study

Mosquito and arbovirus surveillance was conducted in the Coachella Valley in 2015 (Figure 1, panel A). SLEV RNA was first detected in a pool of *Culex tarsalis* mosquitoes by quantitative reverse transcription PCR on July 28, 2015, and subsequently in 37 more pools of the same species through October 6 (*7*). The number of SLEV-positive pools peaked at 23 during the first 2 weeks of August. WNV was detected in mosquitoes during April–November 2015, with a peak in the week of June 21. Although SLEV was detected only in *Cx. tarsalis* pools, WNV RNA was detected in 83 *Cx. quinquefasciatus* pools during April 24–November 5 and in 16 *Cx. tarsalis* pools during May 19–September 29. During the period of co-detection of both viruses (July–November), peak minimum infection rates were higher for WNV than for SLEV.

Vector abundance did not parallel peak infection rates (June for WNV and August for SLEV). Instead, vector abundance in 2015 was lower at most times than the 5-year average, calculated as the geometric mean of female *Cx. tarsalis* and *Cx. quinquefasciatus* mosquitoes collected bimonthly in traps at the same locations during 2010–2014 (*8*). The trend of decreasing mosquito abundance in midsummer in southern California (especially in the Coachella Valley), concurrent with increasing arbovirus activity, has been well documented (*9*). This trend most likely relates to changes in age structure, with progressively more parous female mosquitoes tested as overall vector population numbers decline. Sentinel chicken seroconversion to SLEV, detected by enzyme immunoassay and confirmed by plaque-reduction neutralization test, was detected during August 28–November 9, with a total of 9 seroconversions in 104 chickens (8.7% seropositive) (*10*,*11*). WNV seropositive chicken serum samples were also reported starting on August 28, but with fewer (n = 6 [5.7%] of serum specimens tested) seroconversions to WNV than to SLEV.

Although most mosquito pools contained detectable RNA for only WNV or SLEV, 4 pools tested positive for both viruses. Both viruses were circulating in the summer

[1]These authors contributed equally to this article.

of 2015 at the north and west shores of the Salton Sea in the Coachella Valley (Figure 1, panel B). SLEV activity was more focal than WNV activity and was limited to *Cx. tarsalis* mosquitoes collected in a 20-km radius near wetlands and agricultural habitats by the Salton Sea, whereas WNV activity spanned >80 km and was concentrated in *Cx. quinquefasciatus* mosquitoes collected in more densely populated residential habitats in the central part of the Coachella Valley. Co-circulation of both viruses in ecologically diverse habitats near the Salton Sea at the same time shows that early-season WNV activity did not preclude later SLEV circulation.

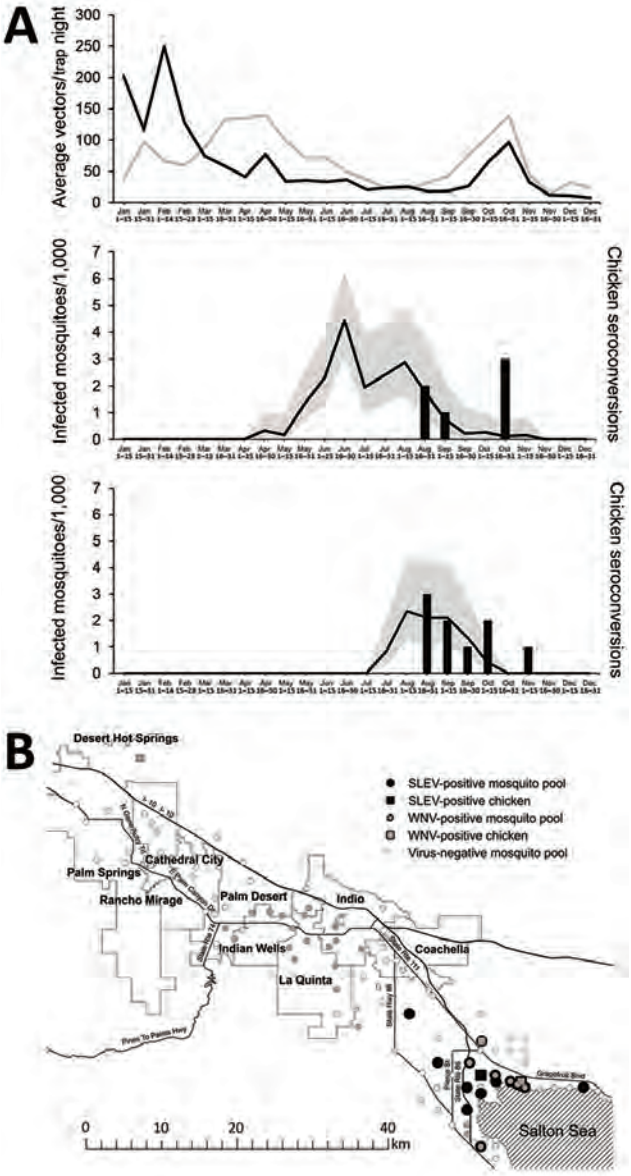

Figure 1. St. Louis encephalitis virus (SLEV) and West Nile virus (WNV) surveillance in mosquitoes and sentinel chickens in Coachella Valley, Riverside County, California, USA, 2015. A) Vector abundance (upper panel) from the same locations in all of Riverside County at bimonthly intervals during 2010–2014 (gray line) and in 2015 (black line), and infection rates for WNV (middle) and SLEV (lower) based on maximum likelihood estimates (black lines) with 95% CI (gray shading) in female *Culex tarsalis* and *Cx. quinquefasciatus* mosquitoes collected in CO_2 and gravid traps and number of sentinel chicken seroconversions (black bars). B) Geographic locations of SLEV (black) and WNV (gray) activity identified by viral RNA detection in mosquito pools (circles) or sentinel chicken seroconversions (squares), July–October 2015.

Unlike California, where continual SLEV testing has been conducted since 1969, the absence of SLEV activity in mosquitoes in Arizona during 2010–2014 may have been due to a lack of recent SLEV testing. Maricopa County began testing mosquito pools for SLEV RNA during the 2015 human epidemic and then retrospectively detected SLEV in an archived WNV-positive mosquito pool from November 2014. We sequenced complete genomes of 1 SLEV isolate from California in 2015 and two isolates from Arizona in 2015, and partial genomes of the 2014 isolate from Arizona and 1 additional 2015 California isolate from reverse transcription PCR amplicons using SLEV primers (Table; GenBank accession nos. KX258460–62 [California], KX965720 [Arizona]). We further determined the phylogenetic relationships of the sequenced isolates with each other and with complete SLEV genomes from GenBank, including another 2015 Arizona isolate (strain 121B, GenBank accession no. KT823415) sequenced by the Centers for Disease Control and Prevention (Figure 2). The 2014 and 2015 California and Arizona SLEV isolates share >99% nucleotide identity with each other and also with their closest published relative, isolated from *Cx. quinquefasciatus* mosquitoes collected in Cordoba, Argentina, in 2005. The 2015 SLEV isolates are genetically distinct from the 2003 Imperial Valley California strain that was isolated before the 11-year absence of SLEV activity in the state. These results suggest that there was likely a single introduction of SLEV into the United States from South America (possibly Argentina) no later than November 2014, the earliest dated sample from which SLEV was isolated in Arizona, and that the virus spread in the summer of 2015 from Arizona to California. Notably, 1,710 mosquito pools representing 65,287 individual mosquitoes from the Coachella Valley were negative for SLEV during 2014.

Because human SLEV viremia levels are low and insufficient to infect mosquitoes, the virus may have been introduced into the United States from South or Central America by a viremic migratory bird or possibly by an infected mosquito exploiting human transportation (*12*). Earlier US SLEV strains from Tennessee and Texas isolated in 1974 and 2001, respectively, are most closely related to 1969 and 1978 Guatemalan strains (Figure 2). A similar ancestral topology of Brazil and Peru strains from the 1970s to the 2003 California isolate also suggests

Table. Primers used to sequence complete genomes of SLEV in study of reemergence of the virus in Arizona and California, USA, 2015*

Name	Sequence, 5′ → 3′	Location of primer binding site at 5′ nucleotide on SLEV 2005 isolate CbAr4005†
2300F	GGATTACACAGGGACTACTTGG	2339
2300R	TCTGTATGCTCTCCCACATTAAG	2672
2700F	CCTGAAGAAGCTGGAAGATGAG	2786
2700R	CGCTTTCAATAACGCCATCAC	3175
5700F	GGTGATTCAGCTAAACAGGAAGA	5753
5700R	GTGATTGCCATGGGTCCATTA	5936
800F	CAATCCTGGATATGCCCTAGTT	852
800R	ACGGTCCACAACATCTCTTT	1241
9000F	CCAAAGTTCTGGGAAATGGTTG	8981
9000R	CATAGGAATTCTCACGGCTCAT	9189
F1	GAGCGGAGAGGAAACAGATTT	17
F10	CGGAGCTGTGACTCTTGATTT	4976
F11	AGGCCGTATTGGGAGAAATC	5981
F12	CACGACGCAGTATGTGAACT	7099
F13	GGAGTGGACGTGTTCCATAA	8069
F15	GAGTGAACACCATGCCAAATC	9099
F16	TGGTAGGAGGAGTGCTGTAA	10393
F2	GGAGAAGTCATGGCTGGTAAA	1584
F3	CCCTGGAGTGAAGGAGAAATAAC	3276
F4	GGGTTCCCAACTACCAAGTTTA	5431
F7	GGTTGAGTGGCTAAGGAAGAA	9635
F8	CATTCTTGGCGGGTTTGTTC	3796
F9	GCAATAGCTGGGCTGATGTA	4315
R1	CGCTGGTCGCTAGAAAGATTAG	2488
R10	CGGAGCTGTGACTCTTGATTT	5418
R12	CAGATAGCCCTGCTTCCTTTAG	9099
R2	AGCACACAAGATGGGAAGAG	3985
R3	GAAGCTGGTGATCCACTCATAC	5651
R4	ACGATTCCGTCTTTCCTGTATG	7761
R5	GCCCACTCCTGTTCTGTTTATC	8417
R6	CATCCTGCTCCTGGTGAAAT	9924
R7	CCTGTCTTTCCAGGTGTCAATA	3185
R8	GGGATTGACCGTAACCAATCT	2023

*SLEV, St. Louis encephalitis virus.
†GenBank accession no. FJ753286.2.

movement from South to North America. The Salton Sea and associated habitats possess diverse avifauna and may serve as a resting point for SLEV-infected migratory birds that traverse the Pacific flyway (*13*). Alternately, SLEV may have come from elsewhere in the United States after being introduced from South or Central America, but sequences from US states reporting SLEV activity in recent years are not publicly available. In the case of east-to-west movement across the United States, postnesting birds may have mediated spread by way of agricultural areas of northern Mexico. However, it is unknown whether SLEV is active in Mexico or the Imperial Valley, which lies between Phoenix and the Coachella Valley, because surveillance is not performed in those regions.

Conclusions

Our findings highlight how mosquitoborne viruses are emerging and reemerging to establish autochthonous transmission, including SLEV in southern California that produced severe and fatal human disease in 2015 in Arizona (*6*). Prospective surveillance can identify viruses circulating in mosquitoes even in the absence of human cases of infection, as in Coachella Valley in 2015, and may provide an early warning of future outbreaks.

A stipend to support K.S. was provided by a Veterinary Medicine Students Training in Advanced Research (STAR) fellowship at the University of California, Davis, School of Veterinary Medicine. The research was supported by start-up funds provided to L.L.C. by the Department of Pathology, Microbiology, and Immunology, at the University of California, Davis, School of Veterinary Medicine.

Dr. White has worked at the Coachella Valley Mosquito and Vector Control District for the past 6 years, studying the transmission of arboviruses and mosquito control methods.

References

1. Murray R, Habel L, Mackey K. Wallace, Peck BA, Mora SJ, et al. Epidemiologic aspects of the 1984 St. Louis encephalitis epidemic in southern California. Proceedings of the California Mosquito and Vector Control Association. 1985;53:5–9.
2. Reisen WK, Meyer RP, Milby MM, Presser SB, Emmons RW, Hardy JL, et al. Ecological observations on the 1989 outbreak of St. Louis encephalitis virus in the southern San Joaquin Valley of California. J Med Entomol. 1992;29:472–82. http://dx.doi.org/10.1093/jmedent/29.3.472

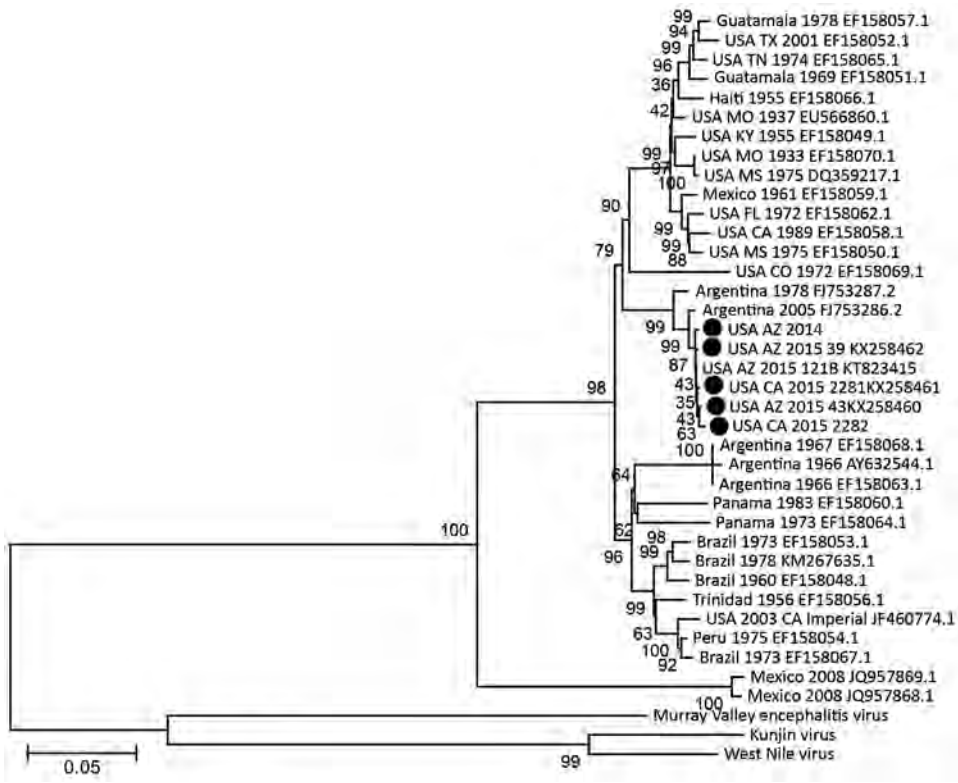

Figure 2. St. Louis encephalitis virus phylogeny with 2015 California (USA CA) and 2014 and 2015 Arizona (USA AZ) genomes (black circles). Complete nucleotide genomes (except for isolate 2282, which included only the E gene) were compared by using a neighbor-joining algorithm and 1,000 bootstrap replicates (support numbers at nodes) by using MEGA 7 (*14*). Isolates are named according to location, year of isolation, strain name for 2014 and 2015 isolates, and GenBank accession number. Scale bar indicates nucleotide substitutions per site.

3. Howitt BF. Viruses of equine and of St. Louis encephalitis in relationship to human infections in California, 1937–1938. Am J Public Health Nations Health. 1939;29:1083–97. http://dx.doi.org/10.2105/AJPH.29.10.1083
4. Reisen WK, Lothrop HD, Wheeler SS, Kennsington M, Gutierrez A, Fang Y, et al. Persistent West Nile virus transmission and the apparent displacement St. Louis encephalitis virus in south-eastern California, 2003-2006. J Med Entomol. 2008;45:494–508.
5. Fang Y, Reisen WK. Previous infection with West Nile or St. Louis encephalitis viruses provides cross protection during reinfection in house finches. Am J Trop Med Hyg. 2006;75:480–5.
6. Venkat H, Krow-Lucal E, Hennessey M, Jones J, Adams L, Fischer M, et al. Concurrent outbreaks of St. Louis encephalitis virus and West Nile virus disease—Arizona, 2015. MMWR Morb Mortal Wkly Rep. 2015;64:1349–50.
7. Brault AC, Fang Y, Reisen WK. Multiplex qRT-PCR for the detection of western equine encephalomyelitis, St. Louis encephalitis, and West Nile viral RNA in mosquito pools (Diptera: Culicidae). J Med Entomol. 2015;52:491–9. http://dx.doi.org/10.1093/jme/tjv021
8. California Department of Public Health, UC Davis Arbovirus Research and Training, Mosquito and Vector Control Association of California. Latest West Nile virus activity in California [cited 2016 Oct 7]. http://www.westnile.ca.gov
9. Zimmer C. Scientists investigate how viruses like Zika cause birth defects. New York Times. 2016 Feb 9. p. D6.
10. Taketa-Graham M, Powell Pereira JL, Baylis E, Cossen C, Oceguera L, Patiris P, et al. High throughput quantitative colorimetric microneutralization assay for the confirmation and differentiation of West Nile virus and St. Louis encephalitis virus. Am J Trop Med Hyg. 2010;82:501–4. http://dx.doi.org/10.4269/ajtmh.2010.09-0297
11. Patiris PJ, Oceguera LF III, Peck GW, Chiles RE, Reisen WK, Hanson CV. Serologic diagnosis of West Nile and St. Louis encephalitis virus infections in domestic chickens. Am J Trop Med Hyg. 2008;78:434–41.
12. Monath TPS. St. Louis encephalitis virus. Washington (DC): American Public Health Association; 1980.
13. Reisen WK, Wheeler SS, Garcia S, Fang Y. Migratory birds and the dispersal of arboviruses in California. Am J Trop Med Hyg. 2010;83:808–15. http://dx.doi.org/10.4269/ajtmh.2010.10-0200
14. Kumar S, Stecher G, Tamura K. MEGA7: Molecular Evolutionary Genetics Analysis version 7.0 for bigger datasets. Mol Biol Evol. 2016;33:1870–4. http://dx.doi.org/10.1093/molbev/msw054

Address for correspondence: Lark L. Coffey, Davis Arbovirus Research and Training, Center for Vectorborne Diseases, Department of Pathology, Microbiology and Immunology, School of Veterinary Medicine, University of California Davis, 1 Shields Ave, 5327 VM3A, Davis, CA 95616, USA; email: lcoffey@ucdavis.edu

Digital PCR for Quantifying Norovirus in Oysters Implicated in Outbreaks, France

David Polo, Julien Schaeffer, Nelly Fournet, Jean-Claude Le Saux, Sylvain Parnaudeau, Catherine McLeod, Françoise S. Le Guyader

Using samples from oysters clearly implicated in human disease, we quantified norovirus levels by using digital PCR. Concentrations varied from 43 to 1,170 RNA copies/oyster. The analysis of frozen samples from the production area showed the presence of norovirus 2 weeks before consumption.

Shellfish have a long history as vectors of human enteric viruses; this relationship is particularly apparent with oysters and norovirus (*1*,*2*). Specific norovirus ligands found in oyster tissues facilitate the persistence of viral particles for several weeks, resistance to depuration, and strain selectivity by the oyster (*1*,*3*). Although advances have been made in virus detection in shellfish, quantification of norovirus in oysters associated with outbreaks still presents a challenge. More accurate quantification is essential for risk analysis and to understand the exact role played by shellfish in norovirus transmission, as this will be important to support the implementation of norovirus regulations.

Norovirus reference materials are essential for quantification by real-time PCR, but they are not widely available for inclusion in standard curves; however, this limitation may be overcome by using digital PCR (dPCR) (*4*). This technology is based on partitioning of the sample into thousands of individual PCRs that contain, in theory, 1 or no copies of the nucleic acid target. After amplification, the total number of target molecules is calculated, with no need for external reference standards (*4*). The partitioning of samples into large numbers of subsamples may also decrease the impact of enzyme inhibitors possibly linked to matrix-type components. This partitioning may be particularly advantageous for the detection of viruses in food and environmental samples, which tend to be complex, with a large variety of inhibitory compounds but relatively low numbers of viruses (*4*,*5*). Norovirus-specific primers and probes targeting the open reading frame 1–2 region used for the real-time reverse transcription PCR were used in a microfluidic-based dPCR to enable norovirus quantification in oyster samples associated with outbreaks.

Author affiliations: Ifremer, Nantes, France (D. Polo, J. Schaeffer, J.-C. Le Saux, S. Parnaudeau, F.S. Le Guyader); Santé Publique France, French National Public Health Agency, Saint-Maurice, France (N. Fournet); Seafood Safety Assessment Ltd., Isle of Skye, Scotland, UK (C. McLeod)

DOI: http://dx.doi.org/10.3201/eid2212.160841

The Study

In France, medical doctors who diagnose norovirus gastroenteritis in ≥2 persons who shared a common meal are required to declare a suspected foodborne illness outbreak. All meal participants then receive a standardized questionnaire that addresses the foods consumed, the symptoms, and the timing of illness, allowing the calculation of the relative risk and its 95% CI. Information on outbreaks to laboratories must be transmitted quickly to enable collection of samples that are directly linked to the clinical cases.

Eight outbreaks were considered for this study on the basis of the following criteria: clinical diagnosis of norovirus in sick consumers; epidemiologic confirmation that oysters were implicated; and rapid notification of responsible oyster production areas. The outbreaks occurred during the winter months in private houses except for 1 that occurred in a nursing home (outbreak 8) (Table). The attack rate varied from 43% to 100%, with median incubation times between 0.5 and 2 days. Fecal samples available for 2 outbreaks (1 for outbreak 6 and 3 for outbreak 8) confirmed the presence of norovirus (National Reference Center for Enteric Viruses, Dijon, France, pers. comm.). Eight shellfish samples were collected from batches that were directly implicated, and 1 sample was taken from leftovers in the nursing home's refrigerator, increasing the likelihood that the samples were representative of consumed oysters. An additional 16 samples were collected from implicated production areas located along different coasts of France, including frozen samples (during the winter and spring months, Ifremer laboratories doing official control monitoring of shellfish for *Escherichia coli* routinely freeze leftover samples). Viruses were eluted from oyster digestive tissues by using the reference method (*6*), and then quantified using the QuantStudio 3D Digital PCR system (Thermo Fisher, Villebon, France) (online Technical Appendix, http://wwwnc.cdc.gov/EID/article/22/12/16-0841-Techapp1.pdf).

No norovirus was detected in 1 oyster sample; norovirus genogroups GI, GII, or both were detected in 9, 11, and 4 samples, respectively (Table). Overall, norovirus concentrations ranged from 43 to 1,170 RNA copies/oyster; the

Table. Characteristics of outbreaks of norovirus infection associated with consumption of oysters, analyzed oyster samples, and virus concentrations obtained by digital PCR*

	Epidemiology information				Samples analyzed		Viral RNA copies/oyster	
Outbreak no.	Date of consumption	No. sick/ no. exposed	Days to illness onset†	Sample no.	Days to sampling‡	Sample location§	Genogroup GI	Genogroup GII
1	2014 Feb 23	7/16	0.5	3486	4	Same batch	ND	1.09×10^2
				3488	7	Prod area	ND	ND
				3489	7	Prod area	ND	2.96×10^2
2	2014 Feb 27	3/4	2	3498	5	Same batch	ND	3.72×10^2
3	2014 Mar 16	4/4	1	3519	2	Prod area	ND	2.02×10^2
				3517	5	Prod area	ND	6.81×10^2
				3518	2	Prod area	3.80×10^2	6.15×10^2
				3531	15	Prod area	1.08×10^3	ND
				3532	15	Prod area	3.88×10^2	ND
4	2014 Dec 12	3/3	No data	3703	6	Same batch	1.18×10^2	ND
				3694	–4	Prod area	ND	1.70×10^2
5	2014 Dec 14	2/2	1.5	3704	3	Same batch	ND	1.21×10^2
				3705	3	Same batch	2.74×10^2	44.1
				3695	–6	Prod area	ND	43.2
				3698	–6	Prod area	1.18×10^2	ND
				3700	–6	Prod area	1.1×10^3	9.50×10^2
6	2014 Dec 27	3/6	0.5	3733	6	Same batch	ND	1.26×10^2
7	2015 Jan 9	3/4	1.5	3740	3	Same batch	9.20×10^2	ND
				3738	–3	Prod area	1.17×10^3	ND
				3739	–3	Prod area	6.38×10^2	53.4
8	2015 Mar 29	16/36	2	3816	3	Consumed	ND	82.1
				3817	3	Same batch	1.85×10^2	ND
				3791	–19	Prod area	ND	1.87×10^2
				3792	–19	Prod area	8.28×10^2	ND
				3822	10	Prod area	1.28×10^2	ND

*ND, not detected; Prod, production.
†Median days to onset of vomiting or diarrhea.
‡Days from date of consumption to sample collection.
§Same batch = samples from batch of oysters consumed.

highest concentrations detected were GI. For outbreak 8, in which a leftover sample from the implicated meal was obtained, norovirus GII was detected at a concentration of 82 RNA copies/oyster, whereas norovirus GI was detected at a concentration of 185 RNA copies/oyster in the same batch collected from the oyster farm.

In a previous dose–response model for norovirus GI and GII based on outbreak investigations, differences were observed between consumers with the secretor phenotype, for which infection and disease probability were high at low doses compared with nonsecretor phenotypes (*7*). Although method sensitivity may need to be improved, the concentrations reported here are consistent with observed illness in dose–response studies to date (*8*). Norovirus GI and GII were detected in oyster samples from the production area and in 4 fecal samples (National Reference Center for Enteric Viruses, pers. comm.).

Because oyster contamination occurs through the filtration of seawater contaminated by human sewage, many contamination events involving both norovirus genogroups and different strains have been described worldwide; this study provides additional evidence of the diversity of contamination (*1*). In contrast to person-to-person transmission in which GII strains dominate, oysters favor the transmission of some specific GI strains, a major consideration for the global epidemiology of norovirus (*1*,*3*). Thus, identifying if oysters implicated in outbreaks are contaminated with norovirus GI or GII is important, because genetic susceptibility means that some consumers do not become infected with certain GI or GII strains; this affects the disease and favors the distribution of some norovirus strains. Such a comprehensive approach will provide information for risk analysis and assist in understanding norovirus infections (*7*,*9*).

Although we obtained some norovirus sequences from 6 implicated batches, confirming the specificity of the dPCR, we believe that the development of technology such as next-generation sequencing will provide more detailed information on the full range of strains present in samples. Obtaining more accurate information on strain diversity and quantification will be valuable for molecular epidemiology studies and management.

In France, oysters are a popular dish, especially during December–April, when they are in the optimal low-fat condition for consumption. They are opened just before consumption and eaten raw; intravalvular seawater is tipped out, thus eliminating food handler contamination. Because this is the highest period for potential contamination by norovirus, samples are kept frozen by laboratories in France for analysis in case of outbreaks. In the current case, this was useful because it demonstrated the presence of norovirus up to 19 days before the shellfish were

marketed. This detection in samples collected 2 weeks before an outbreak suggests that illness could have been prevented. Control shellfish samples from different production areas were analyzed at the same time and were negative for norovirus (data not shown), correlating well with the estimated NoV prevalence of less than 10% in France (*10*).

Conclusions

This study demonstrates that outbreaks could be prevented by performing shellfish analysis at times of the year at which norovirus risk is elevated, such as the winter season, and following microbial alert events such as sewage overflows and heavy rainfall. Application of dPCR to shellfish implicated in outbreaks will provide accurate quantification, which is useful for further risk analysis studies. This application will help to improve regulations and enhance the safety of products on the market, keeping in mind that the sanitary quality of coastal areas is of primary concern.

Acknowledgments

We acknowledge the help of Laboratoire Environnement Ressource and Direction Departementale pour la Protection des Populations colleagues for sampling, and colleagues from the National Reference Center for Enteric Viruses, Dijon, France, for sharing the fecal test results. We are grateful to Mathias Bruyand (French National Public Health Agency) for critical review of the manuscript.

This study was supported by the Food Standards Agency (NovProtOy, FS101068), and by Ifremer (Direction Scientifique) through financial support for DP, by Direction Générale de l'Alimentation (French government DGAL, convention LNR), and by EU-H2020 grant no. 643476 Compare.

Dr. Polo is a postdoctoral researcher at the IFREMER Mmicrobiology laboratory. His interests include the study of shellfish-borne norovirus transmission, surveillance, and the development of new prevention strategies.

References

1. Yu Y, Cai H, Hu L, Lei R, Pan Y, Yan S, et al. Molecular epidemiology of oyster-related human noroviruses and their global genetic diversity and temporal-geographical distribution from 1983 to 2014. Appl Environ Microbiol. 2015;81:7615–24. http://dx.doi.org/10.1128/AEM.01729-15
2. Metcalf TG, Melnick JL, Estes MK. Environmental virology: from detection of virus in sewage and water by isolation to identification by molecular biology—a trip of over 50 years. Annu Rev Microbiol. 1995;49:461–87. http://dx.doi.org/10.1146/annurev.mi.49.100195.002333
3. Le Guyader FS, Atmar RL, Le Pendu J. Transmission of viruses through shellfish: when specific ligands come into play. Curr Opin Virol. 2012;2:103–10. http://dx.doi.org/10.1016/j.coviro.2011.10.029
4. Zhang Y, Jiang H-R. A review on continuous-flow microfluidic PCR in droplets: advances, challenges and future. Anal Chim Acta. 2016;914:7–16. http://dx.doi.org/10.1016/j.aca.2016.02.006
5. Rački N, Morisset D, Gutierrez-Aguirre I, Ravnikar M. One-step RT-droplet digital PCR: a breakthrough in the quantification of waterborne RNA viruses. Anal Bioanal Chem. 2014;406:661–7. http://dx.doi.org/10.1007/s00216-013-7476-y
6. International Organization for Standardization. ISO/TS 15216–1. Microbiology of food and animal feed—horizontal method for determination of hepatitis A virus and norovirus in food using real-time RT-PCR, Part 1: method for quantification. Geneva, Switzerland: The Organization, 2013.
7. Thebault A, Teunis PFM, Le Pendu J, Le Guyader FS, Denis J-B. Infectivity of GI and GII noroviruses established from oyster related outbreaks. Epidemics. 2013;5:98–110. http://dx.doi.org/10.1016/j.epidem.2012.12.004
8. Atmar RL, Opekun AR, Gilger MA, Estes MK, Crawford SE, Neill FH, et al. Determination of the 50% human infectious dose for Norwalk virus. J Infect Dis. 2014;209:1016–22. http://dx.doi.org/10.1093/infdis/jit620
9. Ramani S, Estes MK, Atmar RL. Correlates of protection against norovirus infection and disease—where are we now, where do we go? PLoS Pathog. 2016;12:e1005334. http://dx.doi.org/10.1371/journal.ppat.1005334
10. Schaeffer J, Le Saux J-C, Lora M, Atmar RL, Le Guyader FS. Norovirus contamination on French marketed oysters. Int J Food Microbiol. 2013;166:244–8. http://dx.doi.org/10.1016/j.ijfoodmicro.2013.07.022

Address for correspondence: Françoise S. Le Guyader, IFREMER, Laboratoire de Microbiologie, LSEMSG2M, BP 21105, 44311 Nantes CEDEX 03, France; email: soizick.le.guyader@ifremer.fr

Detection and Genotyping of *Coxiella burnetii* in Pigs, South Korea, 2014–2015

Min-Goo Seo, In-Ohk Ouh, Seung-Hun Lee, Dongmi Kwak

We assessed *Coxiella burnetii* prevalence and genotypes in pigs in South Korea during 2014–2015. Prevalence was low among 1,030 samples tested by ELISA and immunofluorescent assay and 1,124 samples tested by PCR. Despite this finding, possible transmission of *C. burnetii* from pigs to humans cannot be excluded.

Q fever is a zoonotic disease caused by the extremely infectious bacterium *Coxiella burnetii*. Humans can be infected by inhalation of infectious aerosols or contaminated dust from infected ruminants or through contact with infected animal products. Ruminants are known as the primary reservoirs for the bacterium. Wildlife may also serve as reservoirs (*1*). However, epidemiologic data on the occurrence of *C. burnetii* in pigs are limited. Their susceptibility to *C. burnetii* infection has been confirmed by the presence of serum antibodies (*2*), but strong evidence for pigs serving as reservoirs of *C. burnetii* is lacking. In addition, transmission of *C. burnetii* from pigs to humans has not been confirmed.

In the veterinary field, commercial immunologic methods are the easiest to interpret and are used at the herd level to detect *C. burnetii* infection or exposure within a population of animals (*3*). In South Korea, there have been several studies on *C. burnetii* in ruminants (*4*,*5*), but studies evaluating *C. burnetii* in pigs are lacking. As first step toward understanding the epidemiology of *C. burnetii* in pigs, we evaluated the prevalence and genotypes of this bacterium in pigs reared in Gyeongsang Province, South Korea.

The Study

During 2015 in South Korea, a total of 10,332,000 pigs were raised, of which 2,338,521 (22.6%) were raised on 1,134 farms in Gyeongsang Province (*6*). For this study, we collected 1,030 blood and 97 tissue samples from pigs (645 breeding and 479 fattening pigs) reared on 209 pig farms in Gyeongsang Province during 2014–2015. Sample size was determined using a formula with an expected disease prevalence of 50%, accepted absolute error of 5%, and CI of 99% in a simple random sampling design (online Technical Appendix, http://wwwnc.cdc.gov/EID/article/22/12/16-1236-Techapp1.pdf); a minimum of 664 samples were required. Samples were collected by practicing veterinarians during treatment or regular medical checkups; ethical approval was not required. The number of samplings was based on the number of pigs and farms within each of the Province's administrative districts (Figure 1).

Whole blood was used for PCR; the serum was separated for serologic testing. Lung, lymph node, liver, spleen, and kidney samples were collected for differential diagnosis of diseases in pigs that aborted or had a stillbirth, respiratory symptoms, or weakness.

To detect *C. burnetii*–positive samples, we used 2 different assays and nested PCR. We used an indirect multispecies ELISA (ID Screen Q Fever Indirect Multi-species Kit; IDvet, Montpellier, France) according to the manufacturer's instructions to detect *C. burnetii* antibodies in samples; a sample optical density to positive-control optical density value of >50% was considered positive. We also performed an indirect immunofluorescence assay (IFA), using the *Coxiella burnetii* (Q Fever) FA Substrate Slide (VMRD, Pullman, WA, USA), as recommended by the manufacturer; titers $\geq$64 to phase-1 or phase-2 antigens were considered seropositive. We used the DNeasy Blood and Tissue Kit (QIAGEN, Hilden, Germany) according to the manufacturer's instructions to extract DNA from whole blood and tissue samples. The *Coxiella* 16S rRNA gene in extracted DNA was then amplified using nested PCR and sequencing primers (online Technical Appendix). We sequenced amplification products with Macrogen (Seoul, South Korea) and analyzed results using sequence alignment programs and statistical methods (online Technical Appendix).

Of the 1,030 sampled pigs, 70 (6.8%) were positive for *C. burnetii* by ELISA (Table); these pigs were from 32 (15.3%) of the 209 sampled farms. Two of the 32 farms had 8 positive pigs each; the other 30 had 1–3 positive pigs each. Fifty-three (5.2%) sampled pigs had samples identified as phase-1 or phase-2 antigen seropositive by IFA; these samples were also seropositive by ELISA. An additional 17 samples seropositive by ELISA were seronegative by IFA. *C. burnetii* seroprevalence was significantly higher ($p<0.0001$) in breeding than in fattening pigs by ELISA and IFA.

Author Affiliations: Animal and Plant Quarantine Agency, Gimcheon, South Korea (M.-G. Seo, I.-O. Ouh, S.-H. Lee); Kyungpook National University, Daegu, South Korea (M.-G. Seo, S.-H. Lee, D. Kwak); Kyungpook National University Cardiovascular Research Institute, Daegu (D. Kwak)

DOI: http://dx.doi.org/10.3201/eid2212.161236

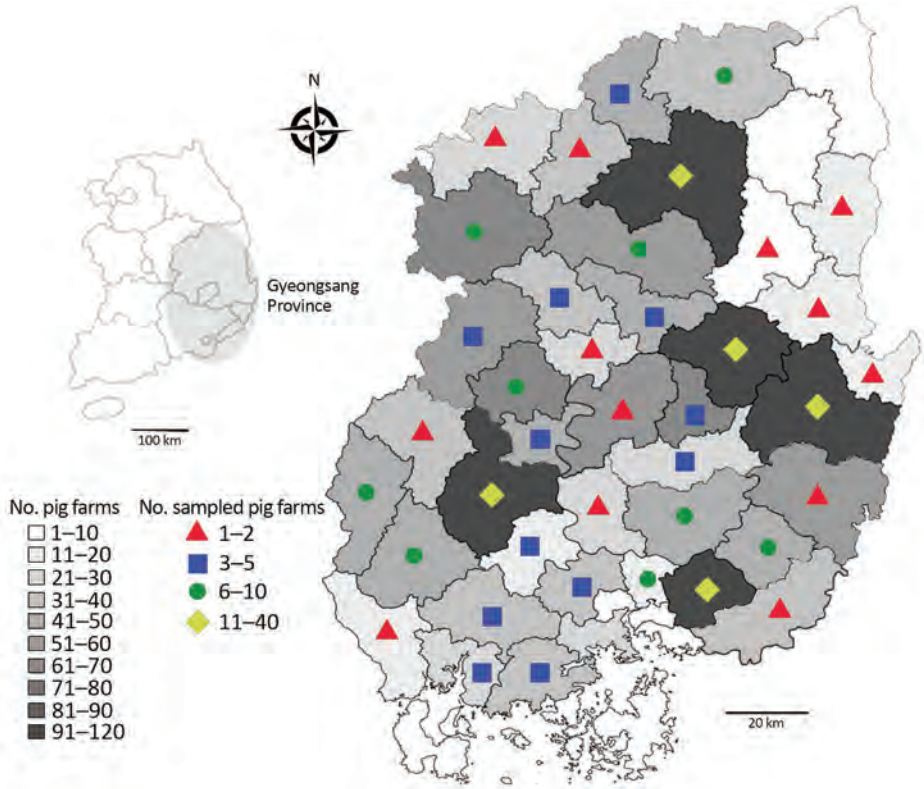

Figure 1. Number of pig farms in the provincial administrative districts and number of farms on which pigs were sampled for the detection and genotyping of *Coxiella burnetii*, Gyeongsang Province, South Korea, 2014–2015. The number of samplings was based on the number of pigs and farms within each of the province's administrative districts.

ELISA and IFA results were in agreement for 1,013 (98.4%) of the 1,030 samples; 53 (5.2%) samples were positive, and 960 (93.2%) were negative. The Cohen κ coefficient was 0.85 (i.e., very good agreement; 95% CI 0.79–0.92).

Three (0.3%) pigs were positive for *C. burnetii* by PCR; all were breeding pigs and seronegative for *C. burnetii*. One positive sample was lung tissue from a pig that appeared to have respiratory signs; other respiratory pathogens were also detected in the sample. Acute *C. burnetii* infection with organ involvement was confirmed by PCR. However, the infection status of seropositive pigs cannot be determined on the basis of a single titer. *C. burnetii*–seronegative pigs can, however, shed the organism and, thus, might serve as a reservoir for transmission of the bacterium to humans. 16S rRNA gene sequences for the 3 *C. burnetii* PCR-positive samples (GenBank accession nos. KT945014–16; Figure 2) showed 100% identity with each other; nucleotide sequences showed high (96.6%–96.9%) identity with those of other *C. burnetii* strains. Phylogenetic analysis showed that the 3 isolates belong to clade A, clustering with previously published *C. burnetii* sequences (Figure 2).

Conclusions

We found that 6.8%, 5.2%, and 0.3% of tested pig samples in Gyeongsang Province were positive for *C. burnetii* by ELISA, IFA, and PCR, respectively. These rates of seropositivity are relatively low compared with the rate found in a study in Uruguay, in which 18.4% (83/479) of the blood samples were seropositive by layer microagglutination (*7*). In that study, the innate susceptibility of pigs to *C. burnetii* was confirmed during a Q fever epidemic. Seropositivity in our study was, however, higher than that reported in blood tested by IFA in Japan (0/396 samples) (*8*) and by complement fixation in Bulgaria (0.05%; 1/1,809 samples) (*9*).

In *C. burnetii*–positive animals, bacterial burden is highest in birth products. We did not test such tissues; however, the positivity rate in our study was similar to that (0/16) in a previous examination of pig placentas by real-time PCR in the Netherlands (*10*). In our study, the PCR-positive pig samples did not test positive by serologic methods.

Similar to results from a previous study (*11*), our results showed that IFA was less sensitive than ELISA at detecting *C. burnetii* in serum. However, serologic diagnosis of coxiellosis in animals is complicated. Animals can maintain seropositivity after acute infection has cleared, and they can seroconvert without shedding (*12*); thus, serologic methods are not useful for determining which animals currently pose a risk for transmission.

In our study, seroprevalence among breeding pigs was significantly high ($p<0.05$). In addition, only breeding pigs were positive for *C. burnetii* by PCR. Because of pregnancy

Table. Assay determinations of *Coxiella burnetii* prevalence among different types of pigs reared in Gyeongsang Province, South Korea, 2014–2015

Assay	No. positive pigs/no. total*	% Pigs positive (95% CI)
ELISA		
Breeding pigs		
Farms	**29/101**	28.7 (19.9–37.5)
Pigs	**66/637**	10.4 (8.0–12.7)
Fattening pigs		
Farms	3/108	2.8 (0–5.9)
Pigs	4/393	1.0 (0.1–2.0)
Subtotal		
Farms	32/209	15.3 (10.4–20.2)
Pigs	70/1,030	6.8 (5.3–8.3)
IFA		
Breeding pigs		
Phase-1 antigens	**46/637**	7.2 (5.2–9.2)
Phase-2 antigens	**48/637**	7.5 (5.5–9.6)
Phase-1 or -2 antigens	**49/637**	7.7 (5.6–9.8)
Fattening pigs		
Phase-1 antigens	4/393	1.0 (0–2.0)
Phase-2 antigens	4/393	1.0 (0–2.0)
Phase-1 or -2 antigens	4/393	1.0 (0.1–2.0)
Subtotal		
Phase-1 antigens	50/1,030	4.9 (3.5–6.2)
Phase-2 antigens	52/1,030	5.0 (3.7–6.4)
Phase-1 or -2 antigens	53/1,030	5.2 (3.8–6.5)
PCR		
Breed type		
Breeding pigs	3/645	0.5 (0–1.0)
Fattening pigs	0/479	0
Sample type		
Blood	2/1,030	0.2 (0–0.5)
Tissue	1/94	1.1 (0–3.1)
Subtotal	3/1,124	0.3 (0–0.6)

*Bold indicates significantly different (p<0.05) compared with fattening pigs.

stress, breeding pigs probably experienced a recrudescent infection, making them more likely to shed the organism. A study on the epidemiology of Q fever suggested that breeding pigs can cause infection in humans (*13*).

The genus *Coxiella* is divided into 4 highly divergent genetic clades (A–D); *C. burnetii* belongs to clade A (*14*). Phylogenetic analysis showed that the 3 *C. burnetii* isolates in our study were closely related to clade A strains from the United States, Japan, and Greenland, indicating a close epidemiologic link.

Although the number of *C. burnetii*–positive pigs was low in our study, a previous study identified contact with pigs as a risk factor for *C. burnetii* seropositivity in humans (*15*). Therefore, pigs may serve as potential reservoirs for *C. burnetii*. However, several questions remain unanswered regarding the epidemiology of *C. burnetii* infection in pigs and possible transmission to humans. Additional investigations of the infection prevalence in other animals are necessary to understand the epidemiology of *C. burnetii*.

This research was supported by a grant from the Basic Science Research Program through the National Research Foundation of Korea (NRF), which is funded by the Ministry of Education (grant no. NRF-2016R1D1A1B02015366).

Dr. Seo works as a research scientist at the Animal and Plant Quarantine Agency, Gimcheon, South Korea. His primary research interests are vectorborne diseases.

References

1. McQuiston JH, Childs JE. Q fever in humans and animals in the United States. Vector Borne Zoonotic Dis. 2002;2:179–91. http://dx.doi.org/10.1089/15303660260613747
2. Marmion BP, Stoker MG. The epidemiology of Q fever in Great Britain; an analysis of the findings and some conclusions. BMJ. 1958;2:809–16. http://dx.doi.org/10.1136/bmj.2.5100.809
3. Guatteo R, Beaudeau F, Joly A, Seegers H. *Coxiella burnetii* shedding by dairy cows. Vet Res. 2007;38:849–60. http://dx.doi.org/10.1051/vetres:2007038
4. Ouh IO, Seo MG, Do JC, Kim IK, Cho MH, Kwak DM. Seroprevalence of *Coxiella burnetii* in bulk-tank milk and dairy cattle in Gyeongbuk Province, Korea. Korean Journal of Veterinary Service. 2013;36:243–8. http://dx.doi.org/10.7853/kjvs.2013.36.4.243
5. Jung BY, Seo MG, Lee SH, Byun JW, Oem JK, Kwak D. Molecular and serologic detection of *Coxiella burnetii* in native Korean goats (*Capra hircus coreanae*). Vet Microbiol. 2014;173:152–5. http://dx.doi.org/10.1016/j.vetmic.2014.06.029
6. Korean Statistical Information Service. Statistics Korea. Number of pig and pig farms by city and province in the third quarter of 2015 [in Korean]. 2015 [cited 2016 Feb 20]. http://kosis.kr/statHtml/statHtml.do?orgId=101&tblId=DT_1EO051&conn_path=I2&language=en/

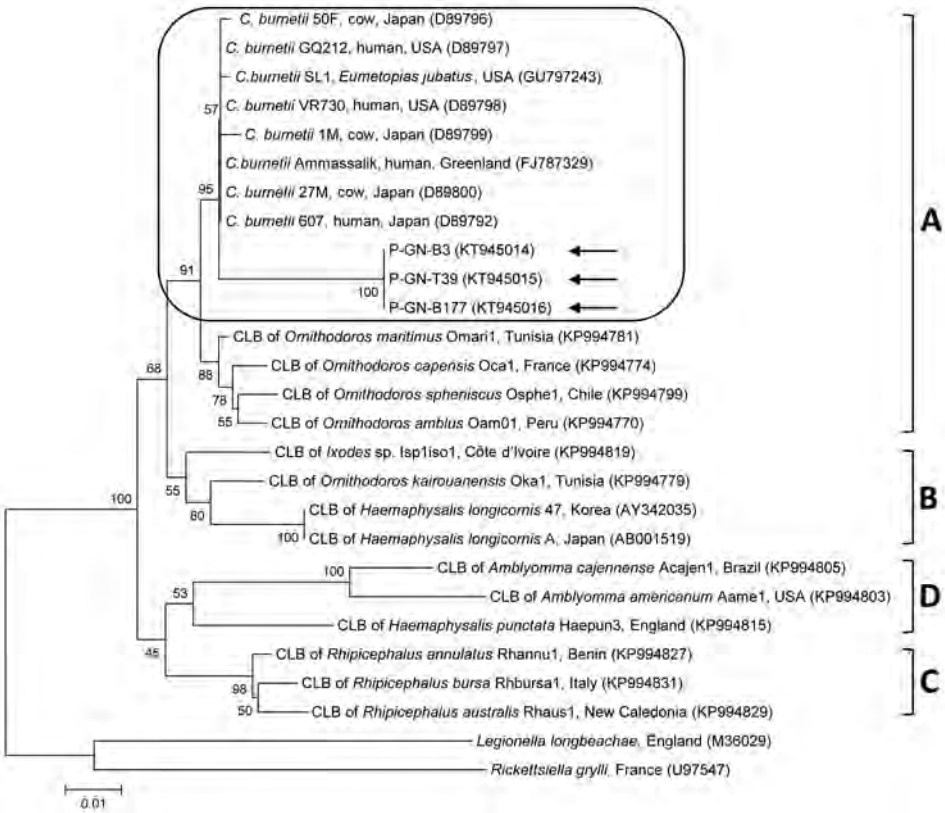

Figure 2. Phylogenetic tree constructed using the maximum-likelihood method from *Coxiella burnetii* 16S rRNA sequences. Arrows indicate *C. burnetii* sequences from study to detect and genotype *C. burnetii* in pigs in Gyeongsang Province, South Korea, 2014–2015. Rounded rectangle indicates *C. burnetii* group. The 4 *Coxiella* clades (A–D) are indicated at right. GenBank accession numbers for other sequences are shown in parentheses. Numbers on branches indicate bootstrap support (1,000 replicates). Scale bar represents the evolutionary distance between sequences. CLB, *Coxiella*-like bacteria.

7. Somma-Moreira RE, Caffarena RM, Somma S, Pérez G, Monteiro M. Analysis of Q fever in Uruguay. Rev Infect Dis. 1987;9:386–7. http://dx.doi.org/10.1093/clinids/9.2.386
8. Htwe KK, Amano K, Sugiyama Y, Yagami K, Minamoto N, Hashimoto A, et al. Seroepidemiology of *Coxiella burnetii* in domestic and companion animals in Japan. Vet Rec. 1992;131:490. http://dx.doi.org/10.1136/vr.131.21.490
9. Martinov SP, Pandarov S, Popov GV. Seroepizootology of Q fever in Bulgaria during the last five years. Eur J Epidemiol. 1989;5:425–7. http://dx.doi.org/10.1007/BF00140133
10. Roest HI, van Solt CB, Tilburg JJ, Klaassen CH, Hovius EK, Roest FT, et al. Search for possible additional reservoirs for human Q fever, The Netherlands. Emerg Infect Dis. 2013;19:834–5. http://dx.doi.org/10.3201/eid1905.121489
11. Péter O, Dupuis G, Burgdorfer W, Peacock M. Evaluation of the complement fixation and indirect immunofluorescence tests in the early diagnosis of primary Q fever. Eur J Clin Microbiol. 1985;4:394–6. http://dx.doi.org/10.1007/BF02148690
12. McQuiston JH, Childs JE, Thompson HA. Q fever. J Am Vet Med Assoc. 2002;221:796–9. http://dx.doi.org/10.2460/javma.2002.221.796
13. Stoker MG, Thompson JF. An explosive outbreak of Q fever. Lancet. 1953;1:137–9. http://dx.doi.org/10.1016/S0140-6736(53)90855-1
14. Duron O, Noël V, McCoy KD, Bonazzi M, Sidi-Boumedine K, Morel O, et al. The recent evolution of a maternally-inherited endosymbiont of ticks led to the emergence of the Q fever pathogen, Coxiella burnetii. PLoS Pathog. 2015;11:e1004892. http://dx.doi.org/10.1371/journal.ppat.1004892
15. Whitney EA, Massung RF, Candee AJ, Ailes EC, Myers LM, Patterson NE, et al. Seroepidemiologic and occupational risk survey for *Coxiella burnetii* antibodies among US veterinarians. Clin Infect Dis. 2009;48:550–7. http://dx.doi.org/10.1086/596705

Address for correspondence: Dongmi Kwak, College of Veterinary Medicine, Kyungpook National University, 80 Daehakro, Bukgu, Daegu 41566, South Korea; email: dmkwak@knu.ac.kr

Flu Days

By Peter Makuck

Shivering, you drag yourself,
as if gun-shot, to the living room,

to the old movie channel,
to a Bogart festival,

your mind fogged over
(like the street on the screen)

edging toward feverish sleep
when Bogey snarls

at Ida Lupino:
"Of all the 14-carat saps…"

Hours later when you wake,
he's smacking Peter Lorre:

"When you're slapped,
you'll take it and like it!"

And as if cuffed, you black out,
head pounding, and come to

upon Ingrid Bergman
and "You must remember this,"

before fading again, then back
to Bogey hacked to death

by Bedoya's machete,
all that gold dust blown away

with the whole bloody day,
everything gone—gone black

as your living room windows—
those previews of The Big Sleep.

Peter Makuck is a writer, essayist, and poet and
Distinguished Professor Emeritus at East Carolina University,
Greenville, North Carolina; email: peter@makuck.com

DOI: http://dx.doi.org/10.3201/eid2212.AD2212

Possible Foodborne Transmission of Hepatitis E Virus from Domestic Pigs and Wild Boars from Corsica

Nicole Pavio, Morgane Laval, Oscar Maestrini, François Casabianca, François Charrier, Ferran Jori

Author affiliations: ANSES (French Agency for Food, Environmental and Occupational Health and Safety), Maisons-Alfort, France (N. Pavio); INRA (National Institute for Agricultural Research), Maisons-Alfort (N. Pavio); University Paris 12, National Veterinary School, Maisons-Alfort (N. Pavio); INRA, Corte, France (M. Laval, O. Maestrini, F. Casabianca, F. Charrier); CIRAD (Agricultural Research for Development), Montpellier, France (F. Jori); Botswana University of Agriculture and Natural Resources, Gaborone, Botswana (F. Jori)

DOI: http://dx.doi.org/10.3201/eid2212.160612

To the Editor: In Western countries, human infection with hepatitis E virus (HEV) is mostly autochthonous and zoonotic through ingestion of contaminated food or direct contact with infected animals and very occasionally is imported from regions to which it is endemic to humans (tropical and subtropical areas) (*1*). Domestic pigs and wild boars are important zoonotic reservoirs of HEV worldwide (*2*).

In continental France, grouped cases of hepatitis E have been described after ingestion of Corsican specialties made with raw pig liver known as ficatelli, traditionally eaten grilled or raw after curing (*3*,*4*). A survey of French food products detected HEV RNA in 30% of ficatelli samples (*5*). A recent nationwide study of blood donors in France showed a high (>60%) HEV seroprevalence in Corsica, suggesting local hyperendemicity (*6*). Estimated prevalences of HEV RNA from wild boars and domestic pigs in Corsica were 2.3% and 8.3%, respectively (F. Jori, unpub. data). We aimed to evaluate, at a molecular level, the role of local wild boars and domestic pigs from Corsica in human infections or food contaminations.

We retrieved partial sequences of HEV open reading frame 2 capsid (*7*) from samples from 8 wild boars hunted during 2009–2013 and from 2 domestic pigs collected at a slaughterhouse in 2013 (F. Jori, unpub. data) and compared them with sequences available in GenBank. This genomic region is used frequently in phylogeny and reflects the diversity of HEV (*8*). After alignment with reference sequences for subtyping (*9*) and their closest sequences, we constructed a phylogenetic tree (Figure). All 10 sequences belonged to HEV genotype 3 and were distributed into 3 distinct clusters.

Cluster 1, subtype 3c, comprised 4 wild boar sequences (FR-HEVWB-1-91, FR-HEVWB-3-07, FR-HEVWB-7-114, FR-HEVWB-8-115) that had 96%–97% nt identity. These sequences were identified during 3 successive hunting seasons (2009, 2010, and 2013) in the same hunting area, suggesting that HEV sequences can be stable, with limited genetic variability, during at least 4 years in a local population of wild boars. These sequences were close to HEV wild boar sequences from Belgium (GenBank accession no. KP296177) and Germany (GenBank accession no. FJ705359; 3c reference sequence). A possible introduction of wild boars from northeast continental France into Corsica during the 1990s could explain such similarity (C. Pietri, pers. comm.). Two human cases reported in southeastern France (GenBank accession nos. GQ426997, KJ742841) in 2008 and 2009 also aggregated within this cluster (94%–95% nt identity), indicating possible zoonotic transmissions from wild boars to humans.

Cluster 2 comprised 2 wild boar sequences (FR-HEVWB-2-101 and FR-HEVWB-6-75) with 99.3% nt similarity, collected in 2009 and 2012 from the same geographic area (Haute Corse, <10 km apart). This cluster is distant from the subtypes assigned by Smith et al. (*9*) and shows <86.5% nt identity with reference sequences (Figure), indicating a possible local and stable evolution in space and time.

Cluster 3, subtype 3f, comprised sequences isolated from wild boars and domestic pigs from Corsica, humans from continental France, and 1 food sample from Corsica. The 2 domestic pig sequences (FR-SHEV-2B-1-182, FR-SHEV-2B-2-190) were 100% identical and shared 97.5% nt identity with a wild boar sequence (FR-HEVWB-4-104), suggesting transmission between domestic and wild pigs. These 2 swine sequences shared 96% nt identity with a sequence amplified in 2011 from a ficatellu sample (FR-HEVFIG-3; GenBank accession no. KJ558438) (*5*) from the same geographic area of Corsica (Haute Corse) and 96% nt identity with an isolate from a patient with acute hepatitis E recorded in France in 2009 (GenBank accession no. JF730424). In addition, the wild boar sequence in this cluster (FR-HEVWB-4-104) shared 96.4% nt identity with the same ficatellu sample and 97.1% nt identity with the same patient in France. This finding suggests that some locally produced ficatelli could be contaminated with HEV from local domestic pigs or wild boars. The human infection also suggests that zoonotic transmission might have occurred through contact with local pig or wild boar reservoirs or through ingestion of contaminated food products. No additional information is available about this human case that might attribute the contamination to 1 of the sources.

Also in cluster 3, another Corsican wild boar sequence (FR-HEVWB-5-117), isolated in 2011, shared 96.2% and 95.7% nt identity with 2 human sequences identified from continental France in 2013 (GenBank accession no. KR027083) and 2009 (GenBank accession no.

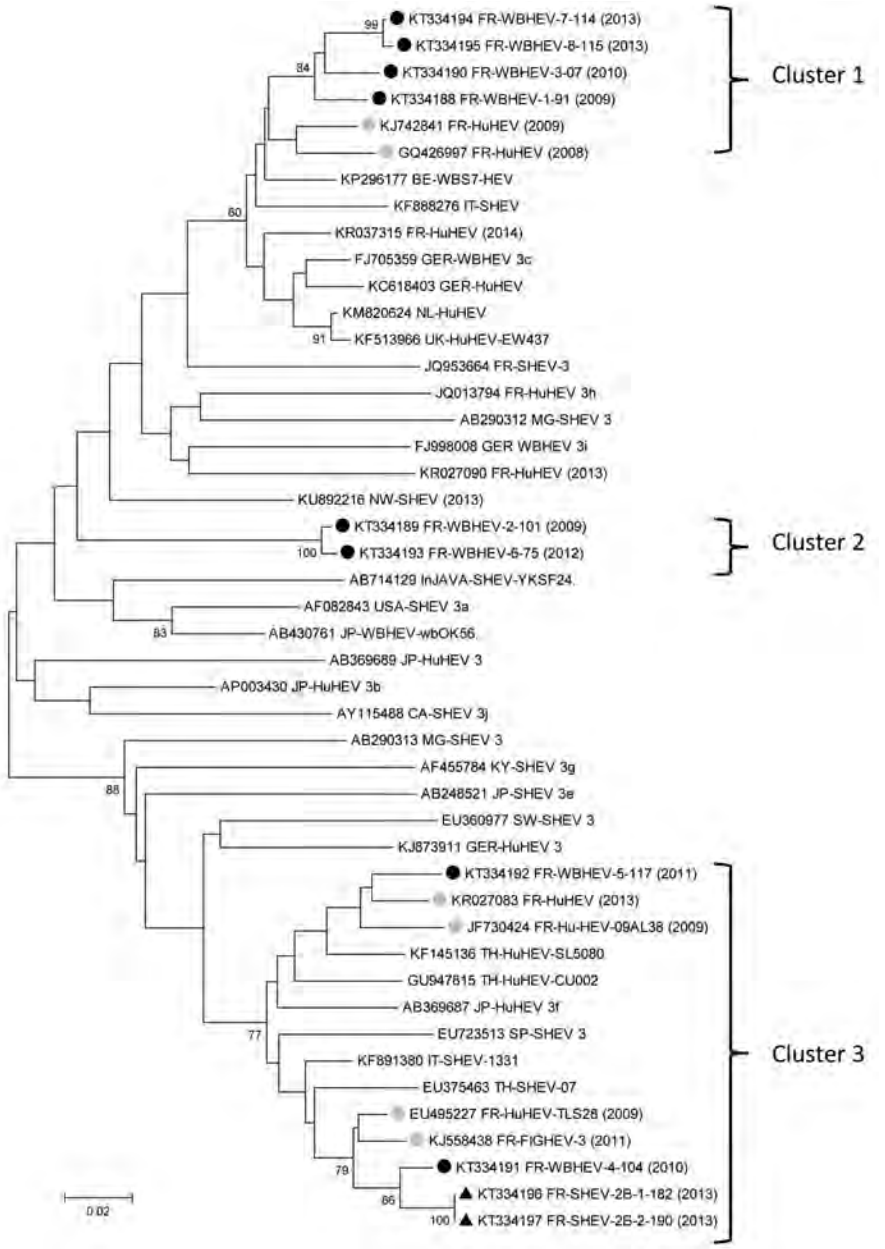

Figure. Phylogenetic tree of hepatitis E virus (HEV) sequences identified in samples from wild boars and pigs from Corsica. All 10 HEV sequences (GenBank accession nos. KT334188–KT334197) corresponding to the open reading frame 2 capsid nucleotides 6044–6334 of the reference sequence AF082843, were obtained by Sanger dideoxy sequencing, from wild boars (WB, black circles) or pigs (S, triangles). Sequences were aligned with Muscle (MEGA6, http://www.megasoftware.net) with the 5 closest sequences (retrieved by using BLAST, http://blast.ncbi.nlm.nih.gov/Blast.cgi) and reference sequences (*9*). The closest HEV sequences from France (gray circles; Hu: human, FIG: figatellu) are identified with their GenBank accession number and year of detection. The tree was constructed by using the neighbor-joining method with a bootstrap of 1,000 replicates. Bootstrap values >70% are indicated on respective branches. Three distinct clusters (1–3) are indicated at right. GenBank reference sequences suggested by Smith et al. for genotype subtyping (*9*): 3a, AF082843; 3b, AP003430; 3c, FJ705359; 3e, AB248521; 3f, AB369687; 3g, AF455784; 3h, JQ013794; 3i, FJ998008; 3j, AY115488; AB290312, JQ953664, AB369689, AB290313, EU360977, KJ873911, EU723513. Countries of origin of the sequences used are as follows: CA, Canada; FR, France; GER, Germany; InJAVA, Indonesia; IT, Italy; JP, Japan; KY, Kyrgyzstan; MG, Mongolia; NL, the Netherlands; NW, Norway; SP, Spain; SW, Sweden; TH, Thailand; UK, United Kingdom; USA, United States. Scale bar represents nucleotide substitutions per site.

JF730424 FR-HuHEV-09AL38). This finding again suggests a zoonotic origin for these human cases. Cluster 3 illustrates well a possible path of transmission between wildlife, domestic pigs, food, and human infection and the potential for dissemination of HEV outside Corsica.

Our results provide evidence suggesting a dynamic exchange of HEV between domestic and wild swine reservoirs and possibly resulting in transmission from those reservoirs to humans through ingestion of infected food products. These animal reservoirs are common and abundant (http://www.oncfs.gouv.fr/IMG/file/mammiferes/ongules/ongules_sauvages/TCD/haute_corse_ongules_sauvages_tableau_departemental.pdf; http://draaf.corse.agriculture.gouv.fr/IMG/pdf/Chiffres_cles_Corse-2015_cle825d93.pdf) and represent a sustainable source of HEV exposure in Corsica.

Acknowledgments

We are grateful to Gaël Stéphant for technical assistance in swine sample analysis. We thank Christian Pietri for sharing his knowledge on the origin of wild boar population in Corsica.

Part of the study including wild boar and domestic pig sample analysis was supported by the European Union Seventh Framework Program (FP7/2007-2013) under grant agreement no. 278433-PREDEMICS and grant agreement no. 311931 (ASFORCE).

References

1. Pavio N, Meng XJ, Renou C. Zoonotic hepatitis E: animal reservoirs and emerging risks. Vet Res. 2010;41:46, http://dx.doi.org/10.1051/vetres/2010018
2. Thiry D, Mauroy A, Pavio N, Purdy MA, Rose N, Thiry E, et al. Hepatitis E virus and related viruses in animals. Transbound Emerg =Dis. 2015;n/a; Epub ahead of print. http://dx.doi.org/10.1111/tbed.12351
3. Colson P, Borentain P, Queyriaux B, Kaba M, Moal V, Gallian P, et al. Pig liver sausage as a source of hepatitis E virus transmission to humans. J Infect Dis. 2010;202:825–34. http://dx.doi.org/10.1086/655898
4. Renou C, Roque-Afonso AM, Pavio N. Foodborne transmission of hepatitis E virus from raw pork liver sausage, France. Emerg Infect Dis. 2014;20:1945–7. Erratum in: Emerg Infect Dis. 2015;21:384. http://dx.doi.org/10.3201/eid2011.140791
5. Pavio N, Merbah T, Thébault A. Frequent hepatitis E virus contamination in food containing raw pork liver, France. Emerg Infect Dis. 2014;20:1925–7. http://dx.doi.org/10.3201/eid2011.140891
6. Mansuy JM, Gallian P, Dimeglio C, Saune K, Arnaud C, Pelletier B, et al. A nationwide survey of hepatitis E viral infection in French blood donors. Hepatology. 2016;63:1145–54. http://dx.doi.org/10.1002/hep.28436
7. Rose N, Lunazzi A, Dorenlor V, Merbah T, Eono F, Eloit M, et al. High prevalence of hepatitis E virus in French domestic pigs. Comp Immunol Microbiol Infect Dis. 2011;34:419–27. http://dx.doi.org/10.1016/j.cimid.2011.07.003
8. Lu L, Li C, Hagedorn CH. Phylogenetic analysis of global hepatitis E virus sequences: genetic diversity, subtypes and zoonosis. Rev Med Virol. 2006;16:5–36. http://dx.doi.org/10.1002/rmv.482
9. Smith DB, Simmonds P, Izopet J, Oliveira-Filho EF, Ulrich RG, Johne R, et al. Proposed reference sequences for hepatitis E virus subtypes. J Gen Virol. 2016;97:537–42. http://dx.doi.org/10.1099/jgv.0.000393

Address for correspondence: Nicole Pavio, ANSES—Animal Health Laboratory, UMR 1161 Virology, 14 rue Pierre et Marie Curie, Maisons-Alfort 94701, France; email: nicole.pavio@anses.fr

Chlamydia-Related Bacteria in Free-Living and Captive Great Apes, Gabon

Anna Klöckner,[1] Michael Nagel,[1] Gilbert Greub, Sébastien Aeby, Karolin Hoffmann, Florian Liégeois, Francois Rouet, Stefania De Benedetti, Nicole Borel, Beate Henrichfreise

Author affiliations: University of Bonn, Bonn, Germany (A. Klöckner, S. De Benedetti, B. Henrichfreise); Kumasi Centre for Collaborative Research in Tropical Medicine, Kumasi, Ghana (M. Nagel); University Hospital Center, Lausanne, Switzerland (G. Greub, S. Aeby); University of Lausanne, Lausanne (G. Greub, S. Aeby); University of Zurich, Zurich, Switzerland (K. Hoffmann, N. Borel); Institut de Recherche pour le Développement, Montpellier, France (F. Liégeois); Université de Montpellier 1, Montpellier (F. Liégeois); International Centre for Medical Research of Franceville, Franceville, Gabon (F. Liégeois, F. Rouet)

DOI: http://dx.doi.org/10.3201/eid2212.150893

To the Editor: Central Africa is the natural habitat for most of the world's gorillas and approximately one third of all chimpanzees. As a result of poaching, diseases, and habitat loss, the western lowland gorilla (*Gorilla gorilla gorilla*) and the central chimpanzee (*Pan troglodytes troglodytes*), both referred to as great apes, have been decreasing in numbers since 1970 and are now red-listed by the International Union for Conservation of Nature (*1*). Infectious diseases are major threats to apes in Africa. In addition to Ebola virus disease, a leading cause of death, the health of great apes is compromised by infections with *Bacillus anthracis*, *Staphylococcus aureus*, and *Plasmodium falciparum* (*1–4*). Chimpanzees and gorillas are closely related to humans and have similar anatomic, physiologic and immunologic features. Transmission of pathogens from humans to wildlife has been considered a major concern of tourism (*1*).

Except 1 report of bacteria of the order Chlamydiales in a fecal sample from a wild-living Congolese *P. troglodytes troglodytes* (*5*), nothing is known about the prevalence of Chlamydiales in great apes. Members of this order are obligate intracellular pathogens that have a unique biphasic life cycle. They infect a wide range of hosts and have major effects on animal and human health worldwide. Until 1993, *Chlamydiaceae* was the only known chlamydial family. However, the discovery of numerous *Chlamydia*-related bacteria species indicated a much broader diversity and host spectrum (*6*). To learn more about the prevalence of Chlamydiales in great apes, we analyzed samples from critically endangered western lowland gorillas and endangered central chimpanzees from Gabon.

We screened 25 samples (8 ocular, 4 vaginal, 7 penile, and 6 rectal swab specimens) obtained noninvasively during routine health checks from 12 apes in captivity. At the time of sampling, the animals were anesthetized and showed no evident signs of disease. All apes were born and reared in captivity at the Primatology Unit of the International Centre for Medical Research of Franceville (Franceville, Gabon) and lived in social groups of ≈10 animals.

We also analyzed feces from wild-living gorillas and chimpanzees, 10 samples from each species, collected in several remote forest areas of Gabon. All samples were collected according to international guidelines used at the

[1]These authors contributed equally to this article.

International Centre for Medical Research of Franceville. For fecal samples obtained immediately after defecation, the outer layer was removed by using a sterile scalpel, and material from the inner part was frozen to avoid degradation and surface contamination.

Extracted DNA from swab specimens and feces was initially screened for *Chlamydiaceae* by using a 23S rRNA real-time PCR and primers Ch23S-F and Ch23S-R (*7*). A internal control amplification was performed with primers EGFP-1-F and EGFP-10-R, and *Chlamydia abortus* DNA was used to prepare a standard curve.

To detect other Chlamydiales, all samples were analyzed by using a broad-range, pan-Chlamydiales 16S rRNA real-time PCR, which had a sensitivity of 94% and showed no cross-amplification with DNA from other bacterial clades (*8*). Plasmid pCR2.1-TOPO (Invitrogen, Basel, Switzerland), which contained a portion of the 16S rRNA gene targeted by the pan-Chlamydiales 16S rRNA real-time PCR, was used to produce a standard curve. Samples with a cycle threshold <35 were sequenced (GATC Biotech AG, Konstanz, Germany), and results were analyzed by using BLAST (http://blast.ncbi.nlm.nih.gov/Blast.cgi). Purification, real-time PCR, sequencing PCR, and electrophoresis were performed in different laboratories to avoid DNA contamination.

The 16S rRNA real-time PCR and sequencing identified Chlamydiales of the non-*Chlamydiaceae* families in captive and free-living chimpanzees and gorillas. However, we did not identify species in the family *Chlamydiaceae* (Table). For captive great apes, BLAST analysis of 1 rectal (gorilla) and 1 penile (chimpanzee) sample showed 100% and 98% sequence identity, respectively, with *Waddlia chondrophila*. Furthermore, *Candidatus* Rhabdochlamydia sp. cvE88 was found in a vaginal swab specimen of 1 chimpanzee (99% sequence identity) and was still detectable in a second sample from the same site 1 month later. Among free-living apes, 3 of 10 chimpanzee samples were positive for Chlamydiales and showed 96%–99% identity with uncultured Chlamydiales CRG97. One fecal sample from a gorilla contained *W. chondrophila* (100% sequence identity). Chlamydiales detected in urogenital samples might have been acquired through smear infections. For omnivorous chimpanzees, Chlamydiales in fecal samples might have originated from ingestion of infected prey.

We detected members of the order Chlamydiales in great apes from Gabon. Our study not only identified a new chlamydial host but could also help to gain deeper insights into the evolution of Chlamydiales. The emerging pathogen *W. chondrophilia* has been implicated in human and bovine miscarriage and reported to be transmitted zoonotically or after exposure to freshwater amebae infected with *Chlamydia*-related bacteria (*9*,*10*). Further studies are required to determine the prevalence of Chlamydiales in primates and their potential for causing disease in great apes in Africa threatened with extinction.

Table. Analysis of 7 captive and free-living apes for *Chlamydia*-related bacteria by using real-time PCR and sequencing, Gabon*

Ape	Source	Species	Mean C_t	DNA copies/μL	Closest BLAST† match for 16S rRNA gene	Sequence identity, %	Fragment size, bp	E-value
Cola‡	Rectal swab	*Gorilla gorilla gorilla*	33.02	10.57	*Waddlia chondrophila* WSU 86–1044, complete sequence	100	230	1×10^{-115}
Cabinda‡	Penile swab	*Pan troglodytes troglodytes*	33.32	8.58	*W. chondrophila* WSU 86–1044, complete sequence	98	241	1×10^{-111}
Djela‡	Vaginal swab§	*P. troglodytes troglodytes*	29.34	122.41	*Candidatus* Rhabdochlamydia sp. cvE88, partial sequence	99	243	8×10^{-118}
1882¶	Feces	*P. troglodytes troglodytes*	34.29	8.24	Uncultured Chlamydiales CRG97, partial sequence	98	201	6×10^{-93}
1883¶	Feces	*P. troglodytes troglodytes*	31.90	43.55	Uncultured Chlamydiales CRG97, partial sequence	99	200	1×10^{-95}
1885¶	Feces	*P. troglodytes troglodytes*	31.16	73.41	Uncultured Chlamydiales CRG97, partial sequence	96	209	1×10^{-90}
Gab2130¶	Feces	*G. gorilla gorilla*	35.30	2.38	*W. chondrophila* WSU 86–1044, complete sequence	100	218	5×10^{-109}

*C_t, cycle threshold.
†http://blast.ncbi.nlm.nih.gov/Blast.cgi
‡Captive ape.
§A second vaginal swab specimen from the same chimpanzee that was collected 1 mo later still showed a positive result by real-time PCR, and sequencing indicated the presence of a *Candidatus* Rhabdochlamydia sp. cvE88.
¶Free-living ape.

References

1. Regional action plan for the conservation of western lowland gorillas and central chimpanzees, 2015–2025 [cited 2016 Aug 2]. http://static1.1.sqspcdn.com/static/f/1200343/25932483/1423326166303/WEA_apes_plan_2014
2. Bermejo M, Rodríguez-Teijeiro JD, Illera G, Barroso A, Vilà C, Walsh PD. Ebola outbreak killed 5,000 gorillas. Science. 2006;314:1564. http://dx.doi.org/10.1126/science.1133105
3. Nagel M, Dischinger J, Türck M, Verrier D, Oedenkoven M, Ngoubangoye B, et al. Human-associated *Staphylococcus aureus* strains within great ape populations in central Africa (Gabon). Clin Microbiol Infect. 2013;19:1072–7. http://dx.doi.org/10.1111/1469-0691.12119
4. Liu W, Li Y, Learn GH, Rudicell RS, Robertson JD, Keele BF, et al. Origin of the human malaria parasite *Plasmodium falciparum* in gorillas. Nature. 2010;467:420–5. http://dx.doi.org/10.1038/nature09442
5. Ochman H, Worobey M, Kuo C-H, Ndjango J-B, Peeters M, Hahn BH, et al. Evolutionary relationships of wild hominids recapitulated by gut microbial communities. PLoS Biol. 2010;8:e1000546. http://dx.doi.org/10.1371/journal.pbio.1000546
6. Subtil A, Collingro A, Horn M. Tracing the primordial Chlamydiae: extinct parasites of plants? Trends Plant Sci. 2014;19:36–43. http://dx.doi.org/10.1016/j.tplants.2013.10.005
7. Ehricht R, Slickers P, Goellner S, Hotzel H, Sachse K. Optimized DNA microarray assay allows detection and genotyping of single PCR-amplifiable target copies. Mol Cell Probes. 2006;20:60–3. http://dx.doi.org/10.1016/j.mcp.2005.09.003
8. Lienard J, Croxatto A, Aeby S, Jaton K, Posfay-Barbe K, Gervaix A, et al. Development of a new Chlamydiales-specific real-time PCR and its application to respiratory clinical samples. J Clin Microbiol. 2011;49:2637–42. http://dx.doi.org/10.1128/JCM.00114-11
9. Baud D, Thomas V, Arafa A, Regan L, Greub G. *Waddlia chondrophila*, a potential agent of human fetal death. Emerg Infect Dis. 2007;13:1239–43. http://dx.doi.org/10.3201/eid1308.070315
10. Baud D, Goy G, Osterheld M-C, Croxatto A, Borel N, Vial Y, et al. Role of *Waddlia chondrophila* placental infection in miscarriage. Emerg Infect Dis. 2014;20:460–4. http://dx.doi.org/10.3201/eid2003.131019

Address for correspondence: Beate Henrichfreise, Institute for Pharmaceutical Microbiology, University of Bonn, Meckenheimer Allee 168, Bonn 53115, Germany, email: bhenrich@uni-bonn.de

Schmallenberg Virus in Zoo Ruminants, France and the Netherlands

Eve Laloy, Cindy Braud, Emmanuel Bréard, Jacques Kaandorp, Aude Bourgeois, Muriel Kohl, Gilles Meyer, Corinne Sailleau, Cyril Viarouge, Stéphan Zientara, Norin Chai

Author affiliations: ANSES, Maisons-Alfort, France (E. Laloy, C. Braud, E. Bréard, C. Sailleau, C. Viarouge, S. Zientara); Safaripark Beekse Bergen, Hilvarenbeek, the Netherlands (J. Kaandorp); Muséum National d'Histoire Naturelle, Paris, France (A. Bourgeois, M. Kohl, N. Chai); École Nationale Vétérinaire de Toulouse, Toulouse, France (G. Meyer)

DOI: http://dx.doi.org/10.3201/eid2212.150983

To the Editor: Schmallenberg virus (SBV), a new orthobunyavirus of the family *Bunyaviridae*, emerged in August 2011 in northwestern Europe (*1*) and spread to most parts of Europe by *Culicoides* vectors (*2*). Most infections are asymptomatic in adult ruminants, yet fever, milk drop, and diarrhea have been reported (*1*). SBV is responsible for congenital malformations in newborn calves, lambs, and goat kids and has also been associated with abortions and early embryonic losses (*3*). The virus affects domestic livestock, but antibodies to SBV have also been found in free-ranging wild ruminants in several European countries (*3–6*) and in wild and exotic ruminants kept in captivity in the United Kingdom and in Austria (*3–5*). We carried out a study to investigate the exposure to SBV of wild and exotic ruminants born in Europe and kept in 1 zoological park in France and 1 in the Netherlands.

We tested 42 serum samples (from 39 animals) collected between 2011 and 2014 in the Safaripark Beekse Bergen (SPBB, Hilvarenbeek, the Netherlands) and 18 serum samples (from 15 animals) collected between 2013 and 2015 in the Ménagerie du Jardin des Plantes, Muséum National d'Histoire Naturelle (MJP, Paris, France). First, we determined the presence of SBV-specific antibodies in the samples by ELISA (ELISA ID Screen SBV Competition; ID Vet, Grabels, France) and by virus neutralization test (VNT) according to a protocol previously described (*7*). The 2 methods gave identical results except for 5 samples found negative by ELISA and positive by VNT. Thirty (55.6%) of 54 animals were found to be seropositive by VNT, which is regarded as the standard for SBV detection (Table). Antibodies to SBV were found in 11 (73.3%) of 15 animals from MJP and 19 (48.7%) of 39 animals from SPBB. Positive results were found in samples collected every year during 2011–2015; the earliest positive result was found in a sample collected in September 2011 (SPBB).

Several seropositive ruminants from MJP were either born in Paris or transferred to Paris from another park in Europe before 2010, which suggests that they were exposed to SBV in Paris. SBV antibodies were found in 3 consecutive samples collected in October 2011, September 2012, and March 2013 from a sable antelope (*Hippotragus niger niger*) in SPBB but also in 3 consecutive samples collected in October 2013, February 2014, and September 2014 in a bharal (*Pseudois nayaur*) from MJP. These data suggest that SBV antibodies can persist for ≥1 year in these 2 species.

We then performed SBV-specific quantitative reverse transcription PCR targeting the small segment (*8*) of the virus on every sample. One sample from an SBV seronegative

Table. Results of virus neutralization testing for Schmallenberg virus among exotic and wild ruminants from 2 zoological parks in France and the Netherlands, 2011–2015*

Common name (species)	No. positive/no. tested	Year(s) of sampling	Animal ages at sampling		Zoological park
			Seropositive	Seronegative	
African buffalo (*Syncerus caffer caffer)*	1/1	2013	3 y		SPBB
Arkal urial sheep (*Ovis aries arkal)*	1/1	2014	5 y		MJP
Axis deer (*Cervus axis)*	0/2	2011–2014		ND, ND	SPBB
Bharal (*Pseudois nayaur)*	2/4	2013, 2014	1 d, 7 y,† 8 y†	10 d, 2 y	MJP
Blackbuck (*Antilope cervicapra*)	0/6	2014		7 mo, 7 y, 15 y, ND, ND, ND	SPBB
Blue wildebeest (*Connochaetes taurinus taurinus)*	3/5	2011	1 y, 6 y, 13 y	1 y, 13 y	SPBB
Common eland (*Taurotragus oryx*)	0/1	2014		1 y	SPBB
Gaur (*Bos gaurus*)	1/1	2015	3 y		MJP
Gemsbok (*Oryx gazella gazella*)	1/1	2011	17 y		SPBB
Markhor *(Capra falconeri*)	2/3	2014	1 y, 10 y	1 y	MJP
Nyala (*Tragelaphus angasii*)	1/2	2012	5 y	ND	SPBB
Père David's deer (*Elaphurus davidianus*)	1/1	2011	15 y		SPBB
Persian fallow deer *(Dama mesopotamica*)	1/1	2013	8 y		SPBB
Pygmy goat (*Capra aegagrus hircus*)	0/1	2014	2 y		MJP
Red forest duiker (*Cephalophus natalensis*)	0/1	2011, 2012		7 y,† 8 y†	SPBB
Rocky mountain goat (*Oreamnus americanus*)	1/1	2014	17 y		MJP
Sable antelope (*Hippotragus niger niger*)	3/3	2011, 2012, 2013	4 y, 5 y,† 6 y,† 7 y,† 10 y		SPBB
Springbok (*Antidorcas marsupialis*)	3/5	2011, 2014	5 y, 14 y, ND	4 y, 5 y	SPBB
Vietnamese sika deer *(Cervus nippon pseudaxis*)	1/1	2014	12 y		SPBB
Vigogna (*Vicugna vicugna)*	1/1	2013	4 y		MJP
Waterbuck (*Kobus ellipsiprymnus ellipsiprymnus*)	1/4	2011, 2014	7 y	6 mo, 4 y, ND	SPBB
Watusi (*Bos taurus taurus watusi*)	0/1	2011		1 y	SPBB
West Caucasian tur (*Capra caucasica caucasica*)	2/2	2014	10 y, 14 y		MJP
Yak (*Bos grunniens grunniens*)	4/5	2012, 2013, 2014	2 y, 3 y, 11 y, ND	1 y	SPBB (4), MJP (1)

*MJP, Ménagerie du Jardin des Plantes (Muséum National d'Histoire Naturelle, Paris, France); ND, not determined; SPBB, Safaripark Beekse Bergen (Hilvarenbeek, the Netherlands).
† Animals sampled more than once.

blue wildebeest (*Connochaetes taurinus taurinus*) collected in September 2011 in SPBB was positive (quantitation cycle value = 30), whereas the other samples were negative. We also performed several in-house conventional reverse transcription PCR targeting the small, large, and medium segments on the positive sample, which enabled us to retrieve a 2,866-bp partial sequence from the medium segment (deposited in GenBank under accession no. KR828816) and a 1,374-bp partial sequence from the L segment (deposited in GenBank under accession no. KR828815). Genetic analyses based on BLAST (http://blast.ncbi.nlm.nih.gov/Blast.cgi) revealed that the large and medium partial sequences had 100% and 99.79% identity, respectively, with SBV sequences from cows (GenBank accession nos. KM047418 and KP731872, respectively).

Subcutaneous inoculation of serum to adult IFNAR$^{-/-}$ mice, which have been reported to be susceptible to SBV infection (*9*,*10*), did not trigger any clinical sign or seroconversion. No genome could be amplified from their blood.

According to the medical records of SPBB, no clinical signs possibly related to an SBV infection were observed in the ruminants during the period studied. Abortions were reported in MJP in 2 bharals in 2011 and 2012 and in 1 West Caucasian tur (*Capra caucasica caucasica*) in 2013, but no correlation could be drawn between these abortions and the SBV serologic results.

This study demonstrates the circulation of SBV in 18 wild and exotic ruminant species kept in captivity in the Netherlands and in France during 2011–2015. Exposure to the virus may occur even in an urban area (such as central Paris). We report evidence of SBV viremia in a blue wildebeest that was seronegative by ELISA and VNT when the serum was collected. SBV RNA has previously been found in an elk (*6*), but the duration of viremia was not determined. Further investigations are required to determine whether zoo ruminants may play a role in dissemination of SBV.

Acknowledgments

We are grateful to Dylan Duby and Claire Réjaud. We thank Manjula Deville and Marc Chodkiewicz for editing the manuscript.

This study was supported and financed by the Muséum National d'Histoire Naturelle (grant identification: ATM—Collections vivantes 2014 and 2015).

References

1. Hoffmann B, Scheuch M, Höper D, Jungblut R, Holsteg M, Schirrmeier H, et al. Novel orthobunyavirus in cattle, Europe, 2011. Emerg Infect Dis. 2012;18:469–72. http://dx.doi.org/10.3201/eid1803.111905
2. Wernike K, Conraths F, Zanella G, Granzow H, Gache K, Schirrmeier H, et al. Schmallenberg virus—two years of experiences. Prev Vet Med. 2014;116:423–34. http://dx.doi.org/10.1016/j.prevetmed.2014.03.021
3. Steinrigl A, Schiefer P, Schleicher C, Peinhopf W, Wodak E, Bagó Z, et al. Rapid spread and association of Schmallenberg virus with ruminant abortions and foetal death in Austria in 2012/2013. Prev Vet Med. 2014;116:350–9. http://dx.doi.org/10.1016/j.prevetmed.2014.03.006
4. EFSA (European Food Safety Authority). Schmallenberg virus: state of the art. EFSA journal. 2014;12(5):3681 [cited 2015 May 17]. http://www.efsa.europa.eu/en/efsajournal/pub/3681.htm
5. Molenaar FM, La Rocca SA, Khatri M, Lopez J, Steinbach F, Dastjerdi A. Exposure of Asian elephants and other exotic ungulates to Schmallenberg virus. PLoS One. 2015;10:e0135532. http://dx.doi.org/10.1371/journal.pone.0135532
6. Larska M, Krzysiak M, Smreczak M, Polak MP, Zmudziński JF. First detection of Schmallenberg virus in elk (*Alces alces*) indicating infection of wildlife in Białowieża National Park in Poland. Vet J. 2013;198:279–81. http://dx.doi.org/10.1016/j.tvjl.2013.08.013
7. Bréard E, Lara E, Comtet L, Viarouge C, Doceul V, Desprat A, et al. Validation of a commercially available indirect ELISA using a nucleocapsid recombinant protein for detection of Schmallenberg virus antibodies. PLoS One. 2013;8:e53446. http://dx.doi.org/10.1371/journal.pone.0053446
8. Bilk S, Schulze C, Fischer M, Beer M, Hlinak A, Hoffmann B. Organ distribution of Schmallenberg virus RNA in malformed newborns. Vet Microbiol. 2012;159:236–8. http://dx.doi.org/10.1016/j.vetmic.2012.03.035
9. Wernike K, Breithaupt A, Keller M, Hoffmann B, Beer M, Eschbaumer M. Schmallenberg virus infection of adult type I interferon receptor knock-out mice. PLoS One. 2012;7:e40380. http://dx.doi.org/10.1371/journal.pone.0040380
10. Ponsart C, Pozzi N, Bréard E, Catinot V, Viard G, Sailleau C, et al. Evidence of excretion of Schmallenberg virus in bull semen. Vet Res. 2014; 45:37.

Address for correspondence: Eve Laloy, UMR Virologie 1161 (ANSES/INRA/ENVA), Laboratoire de Santé animale, ANSES, 14 rue Pierre et Marie Curie, 94700 Maisons-Alfort, France; eve.laloy@vet-alfort.fr

Fatal Case of West Nile Neuroinvasive Disease in Bulgaria

Magdalena Baymakova, Iva Trifonova, Elitsa Panayotova, Severina Dakova, Monia Pacenti, Luisa Barzon, Enrico Lavezzo, Yancho Hristov, Konstantin Ramshev, Kamen Plochev, Giorgio Palu, Iva Christova

Author affiliations: Military Medical Academy, Sofia, Bulgaria (M. Baymakova, S. Dakova, Y. Hristov, K. Ramshev, K. Plochev); National Center of Infectious and Parasitic Diseases, Sofia (I. Trifonova, E. Panayotova, I. Christova); Padova University Hospital, Padova, Italy (M. Pacenti); University of Padova, Padova (L. Barzon, E. Lavezzo, G. Palu)

DOI: http://dx.doi.org/10.3201/eid2212.151968

To the Editor: West Nile virus (WNV) is a mosquitoborne flavivirus. Approximately 80% of human infections are asymptomatic, 10%–20% are characterized by an acute febrile illness, and <1% by involvement of the central nervous system (West Nile neuroinvasive disease) (*1*). Sporadic human cases and small outbreaks of West Nile fever were reported in Europe until the mid-1990s (*2*), when the first large outbreak occurred in Romania in 1996 (*3*).

Since then, and especially in recent years, sporadic human cases and outbreaks have been reported in other countries in Europe and neighboring countries on the Balkan Peninsula (*2*). A large outbreak of WNV lineage 2 infection occurred in Greece in 2010 (*4*). Outbreaks have also been reported in other countries in Europe, which showed spread of WNV lineage 2 (*5*–*8*). Some probable cases of West Nile fever were reported to the Bulgarian Ministry of Health on the basic of serologic test results.

We report a case of fatal West Nile neuroinvasive disease in a man in Bulgaria. This case was confirmed by detection of specific antibodies against WNV and sequencing of the full virus genome.

A 69-year-old man was admitted to the Emergency Center, Military Medical Academy (Sofia, Bulgaria), on August 27, 2015, because of fever, headache, hand tremor, muscle weakness and disability of lower extremities, nausea, and vomiting. These signs and symptoms developed 3 days before hospitalization. The patient reported being bitten by insects through the summer. He also had concomitant cardiovascular disease. In the 24-hour period after hospitalization, a consciousness disorder and deterioration of the extremities' weakness developed, and the patient had a Glasgow come score ≤8.

The patient was transferred to Department of Intensive Care. Neurologic examination showed neck stiffness, positive bilateral symptoms of Kernig and Brudzinski, right facial paralysis, and areflexia of the lower extremities. The patient underwent intubation, and despite complex medical therapy, a cardiopulmonary disorder developed, and he died 14 days after admission.

Laboratory test results at admission were within reference ranges. Lumbar puncture was performed, and cerebrospinal fluid (CSF) testing showed a clear color, leukocytes 39 $\times 10^6$ cells/L (reference range 0–5 $\times 10^6$ cells/L), polymorphonucleocytes 2% (0%–6%), lymphocytes 93%

(40%–80%), monocytes 5% (15%–45%), protein 0.57 g/L (0.2–0.45 g/L), glucose 4.3 mmol/L (2.2–3.9 mmol/L), and chloride 127.9 mmol/L (98–106 mmol/L).

Microbiological investigations of blood, CSF, urine, and throat swab specimens showed no bacterial growth. Immunoserologic test results for neurotropic infectious and parasitologic agents were negative, except for a positive result for IgM against WNV. On the basis of these findings, CSF and urine samples were sent to Bulgarian Reference Laboratory of Vector-Borne Pathogens (Sofia, Bulgaria) for confirmation.

Results of serum and CSF tests (WNV ELISA; EUROIMMUN, Lübeck, Germany) were positive for WNV IgM and negative for WNV IgG. A second serum sample obtained 7 days later showed a marked increase in WNV IgM titer and positive results for WNV IgG. WNV RNA was detected by using real-time reverse transcription PCR (Sacace Biotechnologies, Como, Italy) (cycle threshold 21.9) with a urine sample. Blood samples showed negative results for WNV RNA.

Sequencing of the complete genome of WNV obtained from a urine sample (*9*) was performed (GenBank accession no. KU206781). Phylogenetic analysis showed that the virus belonged to the Central/Southern-European WNV lineage 2 clade and the Greek cluster (*6*). Sequence showed high similarity with Greece Nea Santa 2010 and Hungary/578 strains (99.66% and 99.57% nt identity, respectively), which suggested that the virus probably had a common ancestor with Greek strains.

Accordingly, analysis of the polyprotein identified amino acid substitutions that are typically found in WNV strains from Greece (i.e., NS2B V119I, NS3 H249P, NS4B S14G/T49A/V113M) (*6*) and unique mutations not present in other strains (i.e., E I159M, T436A, NS1 K92N, NS4B N220D, NS5 D141G). These results indicate that the virus might have evolved independently before its emergence in Bulgaria.

European lineage 2 of WNV was detected in Hungary in 2004 (*10*). After its introduction into central Europe, this lineage has spread to neighboring countries (*2*), where it has been responsible for several human outbreaks of neuroinvasive disease associated with a high mortality rate, especially in persons with concurrent illnesses (*8*), such as the patient in this study.

This case of WNV infection provides evidence of WNV lineage 2 circulation in Bulgaria and confirms spread of this lineage in Europe. Sequencing of the complete WNV genome enables us to obtain evidence for the possible origin of the Bulgarian strain from WNV strains circulating in Central Europe, from which the Greek strain has also evolved (*4*,*6*). On the basis of this evidence of WNV circulation in Bulgaria, public health institutions should increase WNV surveillance and control programs in the country. Physicians should also actively search for West Nile fever in patients with acute febrile syndrome during the season of mosquito activity.

M.B. and I.C. designed the study; M.B., I.T., E.P., S.D., M.P., L.B., E.L., Y.H., K.R., and K.P. collected data; M.B., M.P, L.B., G.P., and I.C. interpreted data; M.B., L.B., and I.C. prepared the article; M.B., L.B., and I.C. performed the literature search; and I.T., E.P., M.P., L.B., E.L., G.P., and I.C. conducted laboratory studies. All authors approved the final version of the article.

References

1. Petersen LR, Brault AC, Nasci RS. West Nile virus: review of the literature. JAMA. 2013;310:308–15. http://dx.doi.org/10.1001/jama.2013.8042
2. Rizzoli A, Jimenez-Clavero MA, Barzon L, Cordioli P, Figuerola J, Koraka P, et al. The challenge of West Nile virus in Europe: knowledge gaps and research priorities. Euro Surveill. 2015;20:21135. http://dx.doi.org/10.2807/1560-7917.ES2015.20.20.21135
3. Tsai TF, Popovici F, Cernescu C, Campbell GL, Nedelcu NI. West Nile encephalitis epidemic in southeastern Romania. Lancet. 1998;352:767–71. http://dx.doi.org/10.1016/S0140-6736(98)03538-7
4. Papa A, Bakonyi T, Xanthopoulou K, Vazquez A, Tenorio A, Nowotny N. Genetic characterization of West Nile virus lineage 2, Greece, 2010. Emerg Infect Dis. 2011;17:920–2. http://dx.doi.org/10.3201/eid1705.101759
5. Pem-Novosel I, Vilibic-Cavlek T, Gjenero-Margan I, Pandak N, Peric L, Barbic L, et al. First outbreak of West Nile virus neuroinvasive disease in humans, Croatia, 2012. Vector Borne Zoonotic Dis. 2014;14:82–4. http://dx.doi.org/10.1089/vbz.2012.1295
6. Barzon L, Papa A, Lavezzo E, Franchin E, Pacenti M, Sinigaglia A, et al. Phylogenetic characterization of Central/Southern Europe lineage 2 West Nile virus: analysis of human outbreaks in Italy and Greece, 2013–2014. Clin Microbiol Infect. 2015;21:1122.e1–10.
7. Pervanidou D, Detsis M, Danis K, Mellou K, Papanikolaou E, Terzaki I, et al. West Nile virus outbreak in humans, Greece, 2012: third consecutive year of local transmission. Euro Surveill. 2014;19:20758. http://dx.doi.org/10.2807/1560-7917.ES2014.19.13.20758
8. Popović N, Milosevic B, Urosevic A, Poluga J, Lavadinovic L, Nedelijkovic J, et al. Outbreak of West Nile virus infection among humans in Serbia, August to October 2012. Euro Surveill. 2013;18:20613. http://dx.doi.org/10.2807/1560-7917.ES2013.18.43.20613
9. Barzon L, Pacenti M, Franchin E, Pagni S, Martello T, Cattai M, et al. Excretion of West Nile virus in urine during acute infection. J Infect Dis. 2013;208:1086–92. http://dx.doi.org/10.1093/infdis/jit290
10. Bakonyi T, Ivanics E, Erdelyi K, Ursu K, Ferenczi E, Weissenbock H, et al. Lineage 1 and 2 strains of encephalitis West Nile virus, central Europe. Emerg Infect Dis. 2006; 12:618–23.

Address for correspondence: Magdalena Baymakova, Department of Infectious Diseases, Military Medical Academy, 1606 Sofia, Bulgaria; email: dr.baymakova@gmail.com

Unique Strain of *Borrelia miyamotoi* in *Ixodes pacificus* Ticks, California, USA

Vanessa J. Cook, Natalia Fedorova, Warren P. Macdonald, Robert S. Lane, Alan G. Barbour

Author affiliations: University of California, Irvine, California, USA (V.J. Cook, A.G. Barbour); University of California, Berkeley, California, USA (N. Fedorova, R.S. Lane); San Mateo County Mosquito and Vector Control District, Burlingame, California, USA (W.P. Macdonald)

DOI: http://dx.doi.org/10.3201/eid2212.152046

To the Editor: *Borrelia miyamotoi* causes a recently recognized tickborne zoonosis in Eurasia and North America (*1*). The species has been detected in *Ixodes persulcatus* ticks in Asia and Russia, *I. ricinus* ticks in Europe, and *I. scapularis* and *I. pacificus* ticks in North America. In most of these regions, *B. miyamotoi* is sympatric with Lyme disease agents, such as *B. burgdorferi*, and both pathogens are transmitted locally by the same species of *Ixodes* ticks. *B. miyamotoi* generally is less prevalent than *B. burgdorferi* in nymphs and adults in North America (*2*), except in California, where the prevalences of the 2 species in populations of nymphal and adult *I. pacificus* ticks are similar (*3*–*6*).

Genomes of isolates of *B. miyamotoi* from *I. persulcatus* and *I. scapularis* ticks have been sequenced (*7*). Comparatively less was known about *B. miyamotoi* in *I. pacificus* ticks. Limited sequence data of 16S ribosomal RNA and flagellin genes and the 16S–23S intergenic spacer (IGS) were sufficient to identify the *I. pacificus*–borne spirochete as a sister taxon to *B. miyamotoi* from elsewhere (*3*,*4*). Until *B. miyamotoi* is isolated from *I. pacificus* ticks, determination of additional sequences from *I. pacficus* ticks from California addresses 2 issues of phylogeographic and potential epidemiologic importance: Is the California population of *B. miyamotoi* more akin to the strain across the Pacific Rim or to the strain thousands of kilometers to the east in North America? Will the noted pattern of exclusive association between the genotype of *B. miyamotoi* and the species of *Ixodes* vector continue to hold (*1*)?

We evaluated DNA extracts of *B. miyamotoi*–infected *I. pacificus* ticks collected by and stored at 2 laboratories in the San Francisco Bay area of California. Ticks had been collected while questing either on low vegetation or in leaf litter. To confirm *B. miyamotoi* in candidate extracts and to exclude extracts that also contained *B. burgdorferi* sensu lato, we used a quantitative PCR, which differentiates relapsing fever and Lyme disease group species (*2*). Two extracts that met these criteria were Sonom53 from a nymph in Sonoma County, California (38.328758, –122.625286), and SMA107 from an adult male tick in San Mateo County, California (37.466999, –122.283532). We amplified DNA by PCR for 1,307 bp of the 16S ribosomal RNA gene (*8*) and variable lengths of the IGS (*9*). In addition, we performed PCR amplification and sequencing of partial sequences of 8 chromosomal genes used for multilocus sequence typing (MLST): *clpA*, *clpX*, *nifS*, *pepX*, *pyrG*, *recG*, *rplB*, and *uvrA* (*10*). The primers (and annealing temperatures for 35 cycles) were as given (http://pubmlst.org/borrelia), except for these modifications: *clpA* (53°C); *clpX* forward 5′-CCGTTGCTATTTGTTTTGAATGCTCT-3′ (55°C); *pepX* forward 5′-TTAAAACTTGATGATAAATGGTCATTA-3′ and reverse 5′-TTAAAACTTGATGATAAATGGTCATTA-3′ (52°C); *pyrG* forward 5′-CTTTTAGTAATTGAGATTGGTGGT-3′ and reverse 5′-CAGCATCAAGTATTCCACAAAC-3′ (55°C); *recG* forward 5′-CTAGCATTCCTTTAGTTGAGGC-3′ and reverse 5′-TTSTGTTAAAGGTTCCTTATAAAG-3′ (52°C); *rplB* forward 5′-ATTAAAACTTATAGGCCAAAAAC-3′ and reverse 5′-GGCTGACCCCAAGGAGAT-3′ (55°C); and *uvrA* forward 5′-GCTTAAATTTTTAATTGATGTTGGA-3′ and reverse 5′-CAAGGAACAAAAATRTCAGGC-3′ (52°C). On a Bio-Rad T100 thermal cycler (Hercules, CA, USA) and with Apex Master mix (Genesee Scientific, San Diego, CA, USA), PCR extension at 72°C was 1.5 min for *clpX* and 1.0 min for others; final elongation was for 5 min at 72°C. Products were sequenced over both strands at GENEWIZ (San Diego, CA, USA) by the Sanger method either directly or after cloning into a plasmid vector. Resultant sequences were aligned with homologous sequences (Figure). Alignments and distance neighbor-joining and maximum-likelihood phylograms were generated with Seaview4 (http://doua.prabi.fr/software/seaview). The equal length MLST sequences, as specified (*10*), for each locus were concatenated.

We determined a rooted neighbor-joining phylogram of 16S ribosomal RNA gene sequences of *B. miyamotoi* from different *Ixodes* species and that of *Amblyomma americanum* tickborne *B. lonestari* (Figure, panel A). Other species of the relapsing fever group served as an outgroup. *B. miyamotoi* sequences from *I. pacificus* ticks in 2 San Francisco Bay area counties clustered with sequences from *I. scapularis*–borne organisms rather than with *I. persulcatus*–borne organisms in Asia or an *I. ricinus*–borne isolate in Europe. This analysis confirmed that the organism in *I. pacificus* was *B. miyamotoi*. An unrooted phylogram of 4,776 nt of concatenated MLST sequences originating in *I. pacificus*, *I. scapularis*, *I. persulcatus*, or *I. ricinus* ticks had similar topology and differentiated the different strains (Figure, panel B). The *B. miyamotoi* organisms from 2 counties differed at 1 position, a synonymous transition in *pyrG*, among the MLST loci. IGS

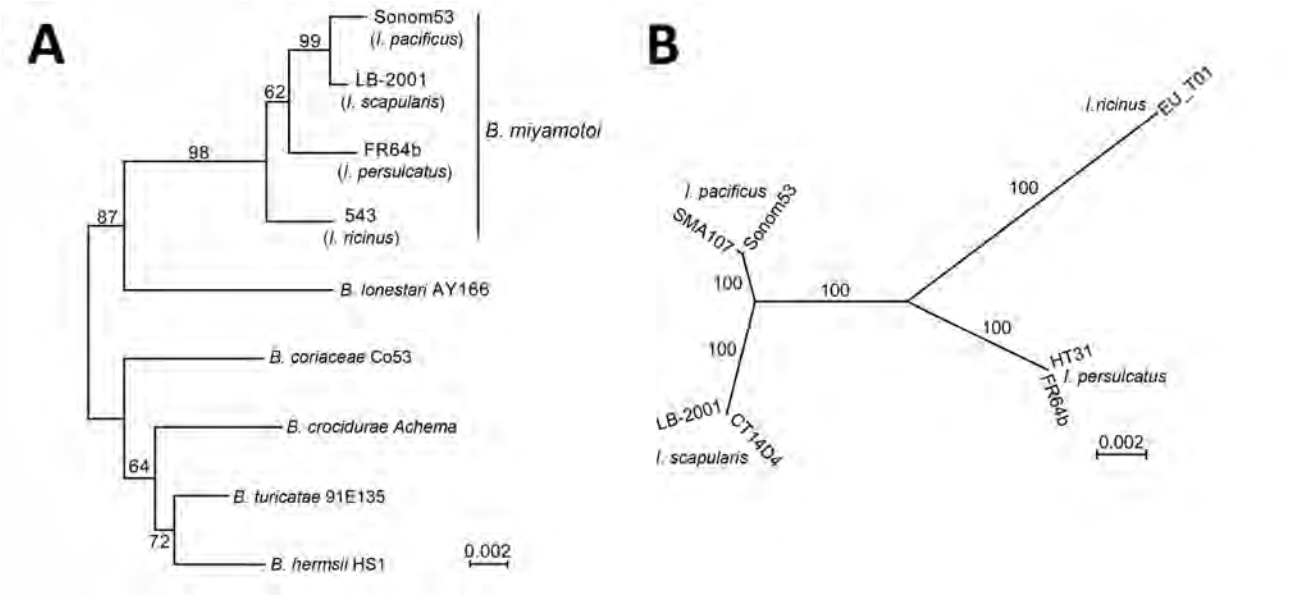

Figure. Phylograms of 16S ribosomal RNA sequences (A) and of multilocus sequence typing (MLST) genes (B) of *Borrelia miyamotoi* strains from *Ixodes* ticks collected in California, USA, and selected other *Borrelia* species. A) Rooted neighbor-joining distance phylogram of observed differences. Percentage support for clades was evaluated by 1,000 bootstrap replications, and values are indicated along branches. The GenBank accession number for the partial 16S ribosomal RNA gene of Sonom53 is KU196080. GenBank accession numbers for 16S ribosomal RNA genes of other *B. miyamotoi* strains are NR_121757 (LB-2001), and KJ847049 (543), and AY604976 (FR64b). GenBank accession numbers for corresponding sequences of designated strains of other species are AY166715 for *B. lonestari* and, for the 4 species constituting the outgroup, AF210134 for *B. coriaceae*, GU350713 for *B. crocidurae*, NR_102958 for *B. turicatae*, and NR_102957 for *B. hermsii*. The tick species sources of the *B. miyamotoi* organisms are indicated. B) Unrooted maximum-likelihood phylogram for 8 concatenated, codon-aligned MLST genes. The model of nucleotide substitution was HKY85 and the empirically estimated γ shape parameter was 0.01. Percentage support for clades was evaluated by 100 bootstrap replications by using full-heuristic search, and values are indicated along branches. GenBank accession numbers for Sonom53 partial sequences of *clpA*, *clpX*, *nifS*, *pepX*, *pyrG*, *recG*, *rplB*, and *uvrA* genes are KU23498–KU234405. The partial sequence of SMA107 *pyrG* is KU307254. The corresponding sequences for FR64b, LB-2001, and CT14D4 were obtained from the complete chromosomes (GenBank accession nos. CP004217, CP006647, and CP010308, respectively). The MLST sequences for strains EU-T01 and HT31 were obtained from the Borrelia MLST Database (http://pubmlst.org/borrelia/), where they have identification numbers of 1279 and 1275, respectively. Scale bar indicates nucleotide substitutions per site.

sequences of the 2 organisms were the same (GenBank accession no. KU184505) and identical to the IGS of other *B. miyamotoi* in *I. pacificus* ticks (e.g., GenBank accession no. KF957669). As observed previously (*4*,*9*), they were distinct from strains associated with other *Ixodes* species.

In conclusion, we identified differences in several genetic loci between *B. miyamotoi* in *I. pacificus* ticks and organism strains associated with other *Ixodes* species. However, we found a close phylogenetic relationship between organisms from the far-western and the northeastern United States.

Acknowledgments

We thank Parth Sitlani for technical assistance.

This research was supported in part by grant R21 AI100236 from the National Institute of Allergy and Infectious Diseases, National Institutes of Health, to A.G.B. and by a generous gift from Tom Eames and Geneva Anderson to R.S.L.

References

1. Krause PJ, Fish D, Narasimhan S, Barbour AG. *Borrelia miyamotoi* infection in nature and in humans. Clin Microbiol Infect. 2015;21:631–9. http://dx.doi.org/10.1016/j.cmi.2015.02.006
2. Barbour AG, Bunikis J, Travinsky B, Hoen AG, Diuk-Wasser MA, Fish D, et al. Niche partitioning of *Borrelia burgdorferi* and *Borrelia miyamotoi* in the same tick vector and mammalian reservoir species. Am J Trop Med Hyg. 2009;81:1120–31. http://dx.doi.org/10.4269/ajtmh.2009.09-0208
3. Mun J, Eisen RJ, Eisen L, Lane RS. Detection of a *Borrelia miyamotoi* sensu lato relapsing-fever group spirochete from *Ixodes pacificus* in California. J Med Entomol. 2006;43:120–3. http://dx.doi.org/10.1603/0022-2585(2006)043[0120:DOABMS]2.0.CO;2
4. Fedorova N, Kleinjan JE, James D, Hui LT, Peeters H, Lane RS. Remarkable diversity of tick or mammalian-associated borreliae in the metropolitan San Francisco Bay area, California. Ticks Tick Borne Dis. 2014;5:951–61. http://dx.doi.org/10.1016/j.ttbdis.2014.07.015
5. Padgett K, Bonilla D, Kjemtrup A, Vilcins IM, Yoshimizu MH, Hui L, et al. Large scale spatial risk and comparative prevalence of *Borrelia miyamotoi* and *Borrelia burgdorferi* sensu lato in *Ixodes pacificus*. PLoS ONE. 2014;9:e110853. http://dx.doi.org/10.1371/journal.pone.0110853

6. Salkeld DJ, Nieto NC, Carbajales-Dale P, Carbajales-Dale M, Cinkovich SS, Lambin EF. Disease risk and landscape attributes of tick-borne *Borrelia* pathogens in the San Francisco Bay area, California. PLoS ONE. 2015;10:e0134812. http://dx.doi.org/10.1371/journal.pone.0134812
7. Barbour AG. Phylogeny of a relapsing fever *Borrelia* species transmitted by the hard tick *Ixodes scapularis*. Infect Genet Evol. 2014;27:551–8. http://dx.doi.org/10.1016/j.meegid.2014.04.022
8. Barbour AG, Maupin GO, Teltow GJ, Carter CJ, Piesman J. Identification of an uncultivable *Borrelia* species in the hard tick *Amblyomma americanum*: possible agent of a Lyme disease–like illness. J Infect Dis. 1996;173:403–9. http://dx.doi.org/10.1093/infdis/173.2.403
9. Bunikis J, Tsao J, Garpmo U, Berglund J, Fish D, Barbour AG. Typing of *Borrelia* relapsing fever group strains. Emerg Infect Dis. 2004;10:1661–4. http://dx.doi.org/10.3201/eid1009.040236
10. Margos G, Gatewood AG, Aanensen DM, Hanincova K, Terekhova D, Vollmer SA, et al. MLST of housekeeping genes captures geographic population structure and suggests a European origin of *Borrelia burgdorferi*. Proc Natl Acad Sci U S A. 2008;105:8730–5. http://dx.doi.org/10.1073/pnas.0800323105

Address for correspondence: Alan G. Barbour, Department of Microbiology and Molecular Genetics, University of California Irvine, 843 Health Sciences Rd., Irvine, CA 92697-4028, USA; email: abarbour@uci.edu

Xenopsylla brasiliensis Fleas in Plague Focus Areas, Madagascar

Adélaïde Miarinjara, Christophe Rogier, Mireille Harimalala, Tojo R. Ramihangihajason, Sébastien Boyer

Author affiliations: Université d'Antananarivo, Antananarivo, Madagascar (A. Miarinjara); Institut Pasteur, Antananarivo (A. Miarinjara, C. Rogier, M. Harimalala, T.R. Ramihangihajason, S. Boyer);

DOI: http://dx.doi.org/10.3201/eid2212.160318

To the Editor: Plague is a life-threatening infectious disease caused by the gram-negative bacterium *Yersinia pestis* (*1*). *Y. pestis* primarily infects rodents but can also cause outbreaks of plague in humans. The infection is usually transmitted within murine populations and then to humans by bites from infected fleas. The oriental rat flea, *Xenopsylla cheopis*, is considered the most efficient plague vector (*1*). Plague remains a major public health threat, causing annual epidemics, especially in Madagascar.

From November 2013 through January 2014, Madagascar reported 427 suspected cases and 45 confirmed cases of plague (both bubonic and pneumonic) in 4 districts. We report here on the flea species associated with rodents and those collected from human dwellings in the Mandritsara District where plague occurred (online Technical Appendix Figure, http://wwwnc.cdc.gov/EID/article/22/10/16-0318-Techapp1.pdf). Four villages in the district were investigated 1 month after the end of the human plague epidemic and after an insecticide-based vector control intervention had taken place. Fleas were collected, either from rats or by using candle traps set inside houses, and preserved in 70% ethanol (online Technical Appendix Table). Rats were trapped alive inside houses and in the cultivated lands.

During the survey, 180 rodents were trapped; they belonged to species *Rattus rattus* (93.3%, n = 168), *Mus musculus* (5.6%, n = 10), and *Suncus murinus* (1.1%, n = 2). A total of 50 fleas were collected from these rodents. The fleas belonged to 4 species: *Sinopsyllus fonquerniei* (n = 26), *Xenopsylla brasiliensis* (n = 14), *X. cheopis* (n = 9), and *Echidnophaga gallinacea* (n = 1) (Table). The first 3 are known to be *Y. pestis* vectors. Of fleas caught in candle traps placed inside houses, ≈98% were the human flea *Pulex irritans*, whose role in plague outbreaks is unknown (*2*,*3*).

Although *X. cheopis* and *S. fonquerniei* fleas are common *Y. pestis* vectors in Madagascar (*1*), the major finding of this study was the discovery of *X. brasiliensis* fleas, which may be involved in plague transmission in Madagascar. Fleas were identified to the species under binocular magnification by using systematic keys (*4*,*5*). Each flea specimen was identified independently by 2 different technicians. The morphologic identification of *X. brasiliensis* (Baker, 1904) was also confirmed by Jean-Claude Beaucournu (*6*). Specimens of *X. brasiliensis* fleas identified in this study exhibit the morphologic characteristics of the species, which distinguish it from *X. cheopis* fleas, as follows: antepygidial bristle of male is marginal, inserted on the long pedestal, process 1 of the clasper with 8 or 9 bristles (which are stout, straight, spiniform, and 1 angled) and the process 2 of the clasper with the tip turned up (*5*). Compared with females of other *Xenopsylla* spp., *X. brasiliensis* females have a distinct spermathecal shape with a very swollen bulga, which is larger than the base of the hilla (*4*). Moreover, DNA of *X. brasiliensis*, *P. irritans*, and *X. cheopis* fleas collected during this study was extracted and amplified by using primers targeting the D3 segment of the 28S ribosomal RNA-encoding gene (*7*) and sequenced. *X. brasiliensis* sequences isolated showed 100% nucleotide similarity with those from Mauritius (*4*) and were different from *X. cheopis* and *P. irritans* sequences. All sequences are available in GenBank (accession nos. KU759935–KU759954).

Table. Number of fleas collected from rodents and by candle traps per species and per study site, Madagascar, 2013–2014

Source	Flea species	Beranimbo	Ambiamamy	Sahakondro	Antsiatsiaka*
Rattus rattus rat	*Synopsyllus fonquerniei*	21	1	4	0
	Xenopsylla cheopis	1	0	0	8
	Xenopsylla brasiliensis	0	0	7	7
	Echidnophaga gallinacea	0	1	0	0
Candle trap	*Tunga penetrans*	2	0	3	1
	Pulex irritans	0	0	0	138
	Synopsyllus fonquerniei	0	0	0	1

*Control village where no plague cases and no insecticide treatment occurred.

Given the vital maritime exchange between Madagascar, the countries of East Africa, and the islands of the Indian Ocean, the presence of *X. brasiliensis* fleas in Madagascar was almost predictable. *X. brasiliensis* fleas originated in sub-Saharan Africa and have spread to other parts of the world, notably Brazil and India (*8*). This species is among the most common flea species found on rodents in southern and eastern Africa, where it is considered a key *Y. pestis* vector, especially in rural environments (*9*). This species has been described on the Comoros archipelago and Mauritius since the early 20th century (*5*) and, more recently, on Reunion Island (*10*). However, to our knowledge, *X. brasiliensis* fleas had not previously been found in Madagascar, although >40 species of fleas have been identified in this country since the 1930s. In this study, we found that *X. brasiliensis* fleas were parasitizing *R. rattus* rats caught inside human dwellings. *R. rattus* rats are considered the main plague reservoir in Madagascar (*1*).

This study's key finding is the discovery of a third vector species that may be involved in *Y. pestis* transmission in Madagascar. Further genetic studies are necessary to clarify when *X. brasiliensis* fleas arrived in Madagascar and where they originated. Additional studies are also needed to determine the distribution of *X. brasiliensis* fleas on the island and their role in plague transmission.

Acknowledgments

We are grateful to the field team that included agents of the Plague Unit (Institut Pasteur de Madagascar), the Laboratoire Centrale de la Peste (Ministry of Health), and agents of the Unité d'Entomologie Médicale (Institut Pasteur de Madagascar). We also wish to highlight the work of Jean-Claude Beaucournu in the identification and confirmation of *X. brasiliensis* fleas. In addition, we thank Catherine Bourgouin for reading the manuscript.

References

1. Duplantier J-M, Duchemin J-B, Chanteau S, Carniel E. From the recent lessons of the Malagasy foci towards a global understanding of the factors involved in plague reemergence. Vet Res. 2005;36:437–53. http://dx.doi.org/10.1051/vetres:2005007
2. Leulmi H, Socolovschi C, Laudisoit A, Houemenou G, Davoust B, Bitam I, et al. Detection of *Rickettsia felis, Rickettsia typhi, Bartonella* species and *Yersinia pestis* in fleas (Siphonaptera) from Africa. PLoS Negl Trop Dis. 2014;8:e3152. http://dx.doi.org/10.1371/journal.pntd.0003152
3. Ratovonjato J, Rajerison M, Rahelinirina S, Boyer S. *Yersinia pestis* in *Pulex irritans* fleas during plague outbreak, Madagascar. Emerg Infect Dis. 2014;20:1414–5.
4. Duchemin JB. Biogeography of fleas from Madagascar [in French] [doctoral thesis]. Créteil (France): Université de Paris XII Val de Marne; 2003. http://doxa.u-pec.fr/theses/th0212881.pdf
5. Hopkins G, Rothschild M. An illustrated catalogue of the Rothschild collection of fleas (Siphonaptera) in the British Miseums. Cambridge: Cambridge University Press; 1953.
6. Beaucournu JC, Fontenille F. Contribution to a catalogue of fleas from Madagascar (Insecta, Siphonaptera) [in French]. Arch Inst Pasteur Madagascar. 1993; special edition.
7. Koekemoer LL, Lochouarn L, Hunt RH, Coetzee M. Single-strand conformation polymorphism analysis for identification of four members of the *Anopheles funestus* (Diptera: Culicidae) Group. J Med Entomol. 1999;36:125–30. http://dx.doi.org/10.1093/jmedent/36.2.125
8. Amatre G, Babi N, Enscore RE, Ogen-Odoi A, Atiku LA, Akol A, et al. Flea diversity and infestation prevalence on rodents in a plague-endemic region of Uganda. Am J Trop Med Hyg. 2009;81:718–24. http://dx.doi.org/10.4269/ajtmh.2009.09-0104
9. Gratz NG. Rodent reservoirs and flea vectors of natural foci of plague. In: Plague manual: epidemiology, distribution, surveillance and control; 1999. Geneva: World Health Organization; 1999. http://www.who.int/csr/resources/publications/plague/WHO_CDS_CSR_EDC_99_2_EN/en/
10. Guernier V, Lagadec E, LeMinter G, Licciardi S, Balleydier E, Pagès F, et al. Fleas of small mammals on Reunion Island: diversity, distribution and epidemiological consequences. PLoS Negl Trop Dis. 2014;8:e3129. http://dx.doi.org/10.1371/journal.pntd.0003129

Address for correspondence: Adélaïde Miarinjara, Institut pasteur de Madagascar, Unité d'Entomologie Médicale, Institut Pasteur de Madagascar-BP 1274-Antananarivo 101, Madagascar; email: amiarinjara@pasteur.mg

Highly Pathogenic Avian Influenza A(H5N1) Virus among Poultry, Ghana, 2015

Ivy Asantewaa Asante, Stephanie Bertram, Joseph Awuni, Abraham Nii Okai Commey, Ben Aniwa, William Kwabena Ampofo, Gülsah Gabriel

Author affiliations: Heinrich Pette Institute, Leibniz Institute for Experimental Virology, Hamburg, Germany (I.A. Asante, S. Bertram, G. Gabriel); Noguchi Memorial Institute for Medical Research, University of Ghana, Accra, Ghana (I.A. Asante, W.K. Ampofo); Center for Structural and Cellular Biology in Medicine at the University of Lübeck, Lübeck, Germany (S. Bertram, G. Gabriel); Veterinary Services Directorate, Accra (J. Awuni, A.N.O. Commey, B. Aniwa)

DOI: http://dx.doi.org/10.3201/eid2212.160639

To the Editor: Outbreaks of highly pathogenic avian influenza (HPAI) A(H5N1) virus among poultry were first reported in Africa in 2006, with initial reports from Nigeria (*1*). The virus then spread to several countries (e.g., Egypt, Côte d'Ivoire, Burkina Faso, Niger) in Africa, leading to large economic losses (*1*,*2*). In 2007, Ghana reported the first HPAI H5N1 cases among poultry in 3 regions: Greater Accra, Volta, and Brong Ahafo (*3*,*4*). The outbreak was contained by measures such as destruction of all birds on affected farms, disinfection of affected farms, and restricted movement of poultry and poultry products. Soon after containment, active influenza surveillance was initiated among birds, domestic poultry, and the human population throughout the country (*5*). Until 2015, no influenza-positive samples among birds had been detected in Ghana since the 2006–2007 outbreak. In January 2015, Nigeria resumed reporting HPAI H5N1–positive samples among poultry (*6*). One month later, HPAI H5N1–positive samples among chickens were confirmed in Burkina Faso (*7*). Then, in April 2015, chicken farmers in the Greater Accra region in Ghana reported a large number of deaths among domestic chicken flocks. Tracheal swabs collected from dead chickens and tested at the laboratories of the Veterinary Services Directorate in Accra, Ghana, confirmed the presence of HPAI H5N1 virus infection. By June 2015, the poultry populations in 5 of Ghana's 10 regions were affected, leading to the death or culling of ≈100,000 poultry (*7*). Affected farms in Ghana (in the Greater Accra, Volta, and Ashanti regions) included medium-scale commercial farms with ≈30,000 chickens (broilers and layers) ranging from day-old chicks to layers >21 weeks of age; small-scale commercial bird farms with 200–1,000 chickens; and free-range local poultry of mixed species raised with low levels of biosafety. The death rate for chickens during the period of sample collection (April 13–June 11, 2015) was 17.6% (6,919 of 39,281 poultry died) (*7*). No direct links among farms were evident at this time. However, further spread in the Greater Accra region has been attributed to movement of live poultry. Outbreaks have been documented in live bird markets and backyard poultry, leading to a ban on movement of live poultry, feed, and equipment from affected regions. These counter-measures resulted in reduced incidence among poultry. For a lower-middle–income country like Ghana, such outbreaks are a major threat to food security and human health. We describe the outbreak strain found in Ghana during 2015 and its zoonotic potential.

We obtained and analyzed sequences for the major viral genes involved in viral pathogenicity, such as the hemagglutinin (HA), polymerase basic protein 2 (PB2), nucleoprotein, and neuraminidase (NA) genes (online Technical Appendix, http://wwwnc.cdc.gov/EID/article/22/12/16-0639-Techapp1.pdf). Sequence analysis of HA revealed that the 2015 Ghana outbreak strain possessed a multibasic cleavage site (RERRRKR/GLF), which is common for the HPAI H5N1 virus (*8*). Substitutions (D94N, S133A, S155N, T156A [H5 numbering]) associated with increased virus binding to human-type α2-6-linked sialic acids were detected. Phylogenetic analysis confirmed that the Ghana outbreak strain belonged to clade 2.3.2.1c (Figure, panel A), as reported by the World Organisation for Animal Health in May 2015 (*7*). The strain clustered with contemporary viruses from Europe, Asia, the Middle East, and other West Africa countries (i.e., Burkina Faso, Côte d'Ivoire, Niger, and Nigeria). HA sequences of viruses isolated from 3 regions (Greater Accra, Volta, Ashanti) in Ghana were highly homologous, comparable to other Ghana viruses isolated in 2015 deposited in the Global Initiative on Sharing Avian Influenza Data (http://platform.gisaid.org) and GenBank databases (Figure, panel A). In total, 9 aa substitutions were detected in the Ghana strains as compared with the HPAI H5N1 virus that caused the 2015 outbreak in Nigeria (online Technical Appendix Table). Genetic analysis of PB2 showed that the Ghana viruses lacked the known human adaptive signatures E627K or D701N, which enable increased replication and virulence in the human host (*9*,*10*). Phylogenetic analysis revealed that PB2 of this virus clustered with H9N2 viruses isolated in Asia during 2007–2013 (Figure, panel B). Nucleoprotein sequences of the Ghana 2015 outbreak strain show 99% homology with the Nigeria 2015 outbreak strain. NA mutations known to reduce susceptibility to oseltamivir in NA H254Y were not observed.

Our phylogenetic analysis suggests that the Ghana HPAI H5N1 strains belong to clade 2.3.2.1c, as was reported for the 2015 Nigeria outbreak. Because of the high homology (>90%) between the Ghana and Nigeria strains, the HPAI H5N1 Ghana outbreak strain likely originated in Nigeria (Figure, panel A). Migratory bird

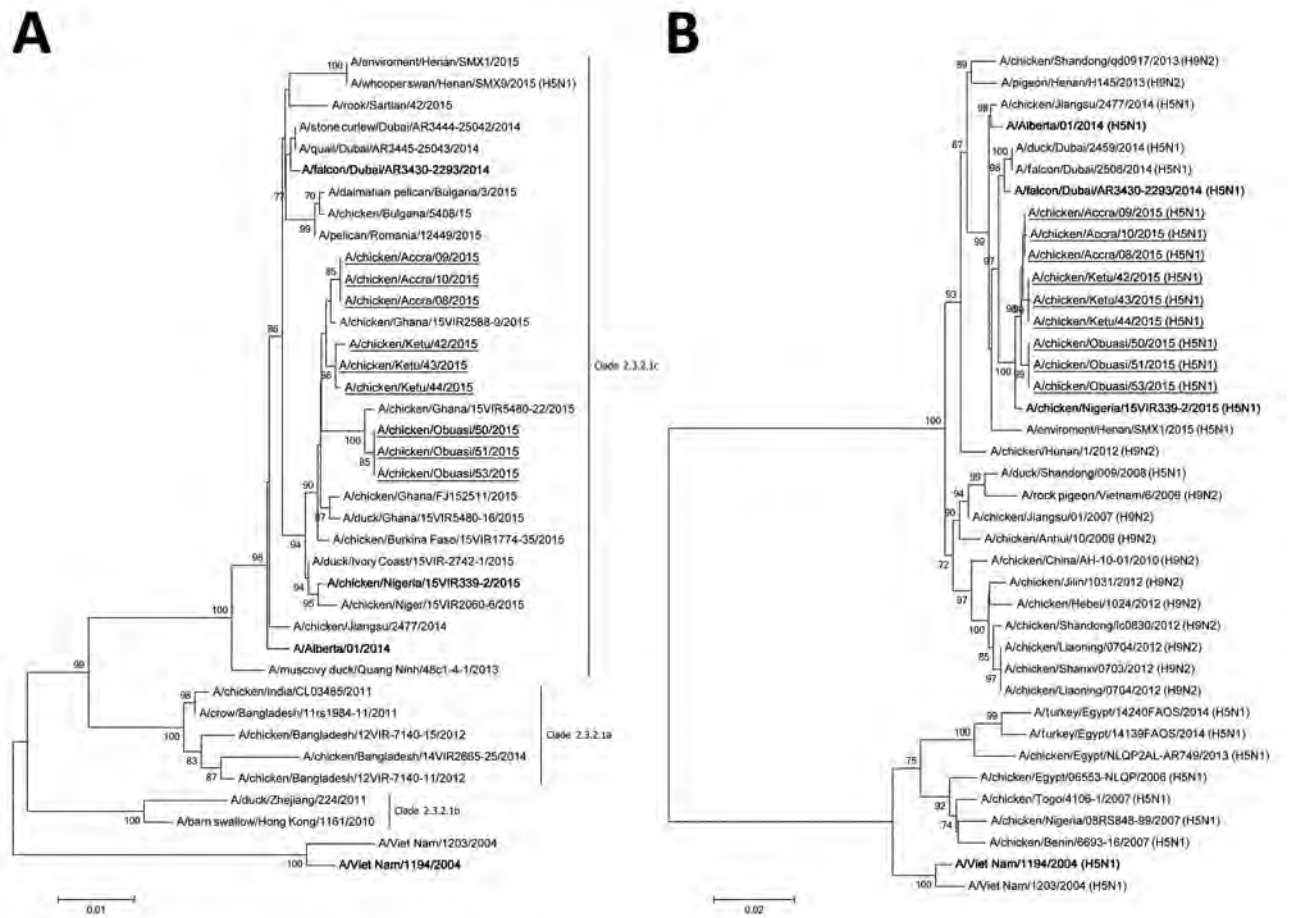

Figure. Phylogenetic analysis of highly pathogenic avian influenza A(H5N1) viruses isolated from poultry in Ghana in 2015: A) hemagglutinin; B) polymerase basic protein 2. Viruses sequenced for this study are underlined and reference viruses are in bold; other sequences were downloaded from the Global Initiative on Sharing Avian Influenza Data (http://platform.gisaid.org) and GenBank databases. Evolutionary analyses were conducted with MEGA6 (http://www.megasoftware.net/). Bootstrap values >70% of 500 replicates are shown at the nodes. Scale bars indicate number of nucleotide substitutions per site.

movements and human activities have been implicated in the virus's introduction to the Africa continent. However, intercountry borders in West Africa are known to be porous because of frequent trading activities, possibly accounting for the spread of the virus in the subregion of West Africa.

Because the HPAI H5N1 virus of clade 2.3.2.1c has previously caused deaths in humans, the potential risk for transmission from infected poultry to humans is a major concern. Increased vigilance and rapid implementation of countermeasures are required to mitigate further virus adaptation and potential outbreaks among humans.

Acknowledgments

We thank the director and head of the laboratory of the Veterinary Services Directorate in Accra, Ghana, for their support. We thank Carola Dreier, Géraldine Engels, and Swantje Thiele at the Heinrich Pette Institute for constructive discussions about methods and sequence analysis. We are also grateful to the director and staff of the Virology Department at the Noguchi Memorial Institute for Medical Research, University of Ghana, for support with sample collection and shipment of samples.

References

1. Cattoli G, Monne I, Fusaro A, Joannis TM, Lombin LH, Aly MM, et al. Highly pathogenic avian influenza virus subtype H5N1 in Africa: a comprehensive phylogenetic analysis and molecular characterization of isolates. PLoS ONE. 2009;4:e4842. http://dx.doi.org/10.1371/journal.pone.0004842
2. Peiris JSM, de Jong MD, Guan Y. Avian influenza virus (H5N1): a threat to human health. Clin Microbiol Rev. 2007;20:243–67. http://dx.doi.org/10.1128/CMR.00037-06
3. Danso EF, Ampofo W, Afari E, Wurapa F, Aryee M, Koney E, et al. Avian influenza surveillance in domestic poultry and wild bird—Tema Metropolis, Ghana, 2010. Journal of Commonwealth Veterinary Association. 2011;27:155–64.
4. Odoom JK, Bel-Nono S, Rodgers D, Agbenohevi PG, Dafeamekpor CK, Sowa RML, et al. Troop education and avian

influenza surveillance in military barracks in Ghana, 2011. BMC Public Health. 2012;12:957. http://dx.doi.org/10.1186/1471-2458-12-957
5. Agbenohevi PG, Odoom JK, Bel-Nono S, Nyarko EO, Alhassan M, Rodgers D, et al. Biosecurity measures to reduce influenza infections in military barracks in Ghana. BMC Res Notes. 2015;8:14. http://dx.doi.org/10.1186/s13104-014-0956-0
6. Monne I, Meseko C, Joannis T, Shittu I, Ahmed M, Tassoni L, et al. Highly pathogenic avian influenza A (H5N1) virus in poultry, Nigeria, 2015. Emerg Infect Dis. 2015;21:1275–7. http://dx.doi.org/10.3201/eid2107.150421
7. World Organisation for Animal Health. Update on highly pathogenic avian influenza in animals (type H5 and H7). Last updated Aug 8 [cited 2016 Feb 5]. http://www.oie.int/animal-health-in-the-world/update-on-avian-influenza/2016/
8. Horimoto T, Kawaoka Y. Reverse genetics provides direct evidence for a correlation of hemagglutinin cleavability and virulence of an avian influenza A virus. J Virol. 1994;68:3120–8.
9. Subbarao EK, London W, Murphy BR. A single amino acid in the PB2 gene of influenza A virus is a determinant of host range. J Virol. 1993;67:1761–4.
10. Gabriel G, Dauber B, Wolff T, Planz O, Klenk H-D, Stech J. The viral polymerase mediates adaptation of an avian influenza virus to a mammalian host. Proc Natl Acad Sci U S A. 2005;102:18590–5. http://dx.doi.org/10.1073/pnas.0507415102

Address for correspondence: Gülsah Gabriel, Heinrich-Pette-Institute, Leibniz Institute for Experimental Virology, Martinistr 52, Hamburg 20251 Germany; email: guelsah.gabriel@hpi.uni-hamburg.de

Hepatitis E Virus in Yellow Cattle, Shandong, Eastern China

Bingyu Yan,[1] Li Zhang,[1] Lianfeng Gong, Jingjing Lv, Yi Feng, Jiaye Liu, Lizhi Song, Qing Xu, Mei Jiang,[1] Aiqiang Xu

Author affiliations: Shandong University, Jinan, China (B. Yan, L. Zhang, J. Lv, Y. Feng, J. Liu, L. Song, Q. Xu, A. Xu); Shandong Center for Disease Control and Prevention, Jinan (B. Yan, L. Zhang, J. Lv, Y. Feng, J. Liu, L. Song, Q. Xu, A. Xu); Yantai Center for Disease Control and Prevention, Yantai, China (L. Gong, M. Jiang)

DOI: http://dx.doi.org/10.3201/eid2212.160641

To the Editor: Hepatitis E, caused by hepatitis E virus (HEV), is recognized as a zoonosis (*1*). HEV has been identified in a wide range of animals, and swine is the primary reservoir (*2*). In cattle, HEV strains have been recently described in yak (*3*), Holstein cows and their milk (*4*), and dairy cows in Xinjiang Province, China (*5*), but not in other cattle. Yellow cattle (*Bos taurus*), the predominant breed (≈80%) in China (*6*), widely distributed over the country, and commonly used for meat and milk production or as a draft animal, could act as a potential HEV reservoir. The objective of this study was to determine whether HEV strains are circulating among yellow cattle in Shandong Province of eastern China.

During April–November 2011, a total of 842 blood samples from yellow cattle of local breeds were collected monthly as part of a severe fever with thrombocytopenia syndrome virus study. These samples were obtained from Laizhou and Penglai Counties (≈100 km apart) of Yantai Prefecture in Shandong Province.

Because the prevalent seasons for human HEV in this region were winter and spring, 254 samples (Laizhou = 131; Penglai = 123) collected only in April and November were selected for detection of HEV. All 254 cattle appeared to be healthy. Sixteen were <1 year of age, 108 were 1–3 years of age, and 130 were >3 years of age. The cattle came from 20 villages (10 villages per county) and were raised by the local peasants, who owned an average of 2 cattle (range 1–8). The animals were bred mainly to produce meat and seldom to produce milk.

Additional serum samples from domestic sheep, dogs, and chickens were also collected in this region simultaneously (online Technical Appendix Table 1, http://wwwnc.cdc.gov/EID/article/22/12/16-0641-Techapp1.pdf). All blood samples were centrifuged, and the separated serum was stored at -70°C until use. The protocol for animal sampling was approved by the Animal Care Committee of the Chinese Center for Disease Control and Prevention.

We tested serum samples for total antibodies against HEV by using a double-antigen sandwich ELISA kit (Wantai Biological, Beijing, China) that uses a recombinant peptide of HEV open reading frame 2 (aa 394–606) from the virus as the antigen (*7*). Overall, the proportion seropositive for antibodies against HEV in yellow cattle was 47% (120/254; 95% CI 41%–54%), in line with the 28.2% positivity ratio previously reported in cattle from 26 provinces of China (*8*), suggesting that a high proportion of yellow cattle were exposed to HEV in this region. The proportions seropositive among sheep, dogs, and chickens were 32% (70/222), 41% (80/194), and 8% (41/484), respectively (online Technical Appendix Table 1).

We used nested reverse transcription PCR to amplify 644 nt within HEV open reading frame 2 region, as described previously (*9*). We detected HEV RNA in 8 of 254 cattle samples; the overall proportion seropositive was 3%. Positive yellow cattle included one <1 year of age, three 1–3 years of age, and four >3 years of age. The 8 sequences obtained in this study (GenBank accession nos. KU904271, KU904273, KU904274, KU904278–KU904282) were subjected to phylogenetic analysis along with reference sequences for subtyping (*10*).

[1]These authors contributed equally to this article.

Using MEGA 7.0 software (http://www.megasoftware.net) with the maximum-likelihood algorithm and a bootstrap of 1,000 replicates, we constructed a phylogenetic tree (online Technical Appendix Figure). All 8 sequences clustered within subtype 4d of HEV. The sequences were similar to each other (95.5%–99.8% similarity in nucleotide sequence) and similar to sequences reported for other cattle (83.3%–85.3%; online Technical Appendix Figure). Moreover, these sequences shared 96.1%–96.6% similarity with a human HEV strain (GenBank accession no. KC163335) from the Yantai Prefecture in 2012 and 95.7%–97.9% similarity with a swine strain (GenBank accession no. KF176351) isolated in Shandong Province the same year.

Our data strongly indicate that HEV infection occurs in yellow cattle and that they could also play a role as a reservoir of HEV. Because these animals serve mainly as a source of food, consumption of undercooked meat from yellow cattle, similar to pork, might also contribute to the transmission of HEV to humans. Additionally, we also detected HEV RNA in 8 of 70 sheep (online Technical Appendix Table 2). Eight sequences from yellow cattle had 95.1%–99.8% nt homology with 8 sheep-derived HEV strains, possibly because mixed raising of domestic livestock is popular in this region. Our finding of high sequence similarity between yellow cattle, sheep, swine, and human populations suggests a complicated interspecies transmission of HEV occurred in this province. Further studies are required to evaluate the contribution of the yellow cattle reservoir to human HEV infection.

Acknowledgments

We thank our colleagues at the China CDC at the prefectural and county level for sample collection in this study.

This study was supported by a grant from Taishan Scholar Program of Shandong Province (No. ts201511105) and a grant from the Shandong Medical Health Science and Technology Development Program (2015ws0042).

References

1. Kamar N, Bendall R, Legrand-Abravanel F, Xia NS, Ijaz S, Izopet J, et al. Hepatitis E. Lancet. 2012;379:2477–88. http://dx.doi.org/10.1016/S0140-6736(11)61849-7
2. Pérez-Gracia MT, García M, Suay B, Mateos-Lindemann ML. Current knowledge on hepatitis E. J Clin Transl Hepatol. 2015;3:117–26. http://dx.doi.org/10.14218/JCTH.2015.00009
3. Xu F, Pan Y, Baloch AR, Tian L, Wang M, Na W, et al. Hepatitis E virus genotype 4 in yak, northwestern China. Emerg Infect Dis. 2014;20:2182–4. http://dx.doi.org/10.3201/eid2012.131599
4. Huang F, Li Y, Yu W, Jing S, Wang J, Long F, et al. Excretion of infectious hepatitis E virus into milk in cows imposes high risks of zoonosis. Hepatology. 2016;64:350–9. http://dx.doi.org/10.1002/hep.28668
5. Hu GD, Ma X. Detection and sequences analysis of bovine hepatitis E virus RNA in Xinjiang autonomous region [in Chinese]. Bing Du Xue Bao. 2010;26:27–32.
6. Li K, Zhang Y, Mao Y, Cornforth D, Dong P, Wang R, et al. Effect of very fast chilling and aging time on ultra-structure and meat quality characteristics of Chinese yellow cattle *M. longissimus lumborum*. Meat Sci. 2012;92:795–804. http://dx.doi.org/10.1016/j.meatsci.2012.07.003
7. Wang YC, Zhang HY, Xia NS, Peng G, Lan HY, Zhuang H, et al. Prevalence, isolation, and partial sequence analysis of hepatitis E virus from domestic animals in China. J Med Virol. 2002;67:516–21. http://dx.doi.org/10.1002/jmv.10131
8. Geng Y, Wang C, Zhao C, Yu X, Harrison TJ, Tian K, et al. Serological prevalence of hepatitis E virus in domestic animals and diversity of genotype 4 hepatitis E virus in China. Vector Borne Zoonotic Dis. 2010;10:765–70. http://dx.doi.org/10.1089/vbz.2009.0168
9. Li F, Meng JH, Dong C, Dai X, Yang YG, Zhou ZX. Design and application of a set of universal PCR primers for genotyping of hepatitis E virus [in Chinese]. Bing Du Xue Bao. 2009;25:9–16.
10. Smith DB, Simmonds P, Izopet J, Oliveira-Filho EF, Ulrich RG, Johne R, et al. Proposed reference sequences for hepatitis E virus subtypes. J Gen Virol. 2016;97:537–42. http://dx.doi.org/10.1099/jgv.0.000393

Address for correspondence: Aiqiang Xu, Shandong Center for Disease Control and Prevention, 16992, Jingshi Road, Jinan, 250014, China; email: aqxuepi@163.com

Introgressed Animal Schistosomes *Schistosoma curassoni* and *S. bovis* Naturally Infecting Humans

Elsa Léger, Amadou Garba, Amina A. Hamidou, Bonnie L. Webster, Tom Pennance, David Rollinson, Joanne P. Webster

Author affiliations: Royal Veterinary College, University of London, London, UK (E. Léger, T. Pennance, J.P. Webster); RISEAL Niger, Niamey, Niger (A. Garba, A.A. Hamidou); Natural History Museum, London (B.L. Webster, D. Rollinson)

DOI: http://dx.doi.org/10.3201/eid2212.160644

To the Editor: Schistosomiasis, a disease caused by infection with parasitic worms (schistosomes), is a neglected tropical disease across many parts of the world. Numbers of infected livestock are unknown, but >250 million persons are infected; the greatest number of cases are in sub-Saharan Africa (*1*). Schistosome eggs are excreted through urine or feces, depending on the species, and hatch into miracidia upon contact with freshwater. Larvae are transmitted to the mammalian host indirectly through a molluscan intermediate host. Goals to eliminate schistosomiasis by 2020 in select countries in Africa have

been proposed by the World Health Organization (http://www.who.int/neglected_diseases/NTD_RoadMap_2012_Fullversion.pdf) and a coalition of partners combating neglected tropical diseases (*2*).

Selective pressures imposed by natural phenomena and human activities affect the dynamics and distribution of schistosomiasis. For example, ongoing changes in agricultural practices in some regions are creating new water bodies shared by humans and domestic livestock. These anthropogenic changes increase opportunities for mixing of and subsequent exposure to different *Schistosoma* species, especially those that infect humans and livestock. Such mixing could increase the potential for novel zoonotic hybrid parasites to emerge and become established (*3*,*4*).

Since the 1940s, researchers have suspected that natural hybridization within and between human and animal schistosome species occurs in definitive and intermediate hosts. In western Africa, hybrids, predominantly between *S. haematobium* (human schistosome) and *S. bovis* or *S. curassoni* (livestock schistosomes), have been isolated from children and snails (*5*,*6*). Hybrids between these livestock-only *Schistosoma* species have also been reported in cattle and sheep but not in other hosts (*7*). As demonstrated in the field and under experimental laboratory conditions, neither *S. bovis* nor *S. curassoni*, as single species, can fully develop in humans or nonhuman primates (*8*,*9*).

We report evidence of a child in Niger who was infected by livestock-specific schistosomes through the hybridization and introgression of *S. bovis* with *S. curassoni*. Samples were collected from a 10-year-old girl in Kokourou, Tillaberi region, Niger (14°20′61.50″N, 0°91′94.0″E), as part of longitudinal monitoring and evaluation of national disease control interventions in the area. Tillaberi has an ongoing high prevalence and infection intensity of schistosomiasis, despite more than a decade of high-coverage mass treatment with praziquantel.

Schistosoma eggs were recovered from the child's urine. Miracidia that hatched from the eggs were stored on a Whatman FTA card (Sigma-Aldrich, St. Louis, MO, USA), providing the opportunity to perform noninvasive molecular characterization on schistosome larvae without any necessity for laboratory passage. Multilocus analyses of mitochondrial and nuclear DNA regions (*6*) on all 42 larvae collected from the child identified 2 individual miracidia with a livestock *S. bovis* × *S. curassoni* hybrid profile with no genetic signal from human-specific *S. haematobium*. Although no species-specific markers exist for determining parental lineages, internal transcribed spacer (ITS), a powerful marker for detecting introgression, has been used successfully to detect hybridization events across the *Schistosoma* genus. A partial mitochondrial *cox*1 sequence for miracidia was identical to that for *S. bovis*, and the nuclear ITS and partial 18S rDNA sequences were identified as *S. curassoni*.

One miracidium from the child had a pure *S. haematobium* profile, 13 had *S. bovis* (*cox*1) × *S. haematobium* (ITS) profiles, and 5 had *S. bovis* (*cox*1) × *S. haematobium* × *S. curassoni* (ITS) profiles, suggesting the potential for repeated interactions and cross-pairings among these 3 species. No *S. curassoni* mitochondrial DNA was found in miracidia. The molecular data suggest that these hybrids were not first generation, but a result of parental and/or hybrid backcrosses. The data confirm the occurrence of bidirectional introgression between *Schistosoma* species that infect livestock and those that infect humans in Niger. Our data also show that hybrid livestock:livestock schistosomes can directly infect humans without combining with a *Schistosoma* species that infects humans.

Hybridization of parasites is an emerging public health concern at the interface of infectious disease biology and evolution (*3*). Our results raise several critical questions regarding the evolution, epidemiology, health effects, and ultimate control of schistosomiasis. Hybrid schistosomes, and, in particular, hybridized livestock:livestock schistosomes infecting humans, could potentially extend intermediate and definitive host ranges; confer altered infectivity, virulence, and drug efficacy; or even potentially replace existing single species (*3*,*4*). Hybrid vigor has been observed experimentally for schistosomes, and similar evidence is gathering from experiments with other parasites. Our results strongly indicate that hybrid livestock:livestock schistosomes can infect a human definitive host, even when neither of its single parental livestock species appears compatible. Such novel livestock schistosome hybrids infecting humans could be predicted to spread to wherever suitable intermediate snail hosts are endemic, as has recently been reported for zoonotic *Schistosoma* hybrids in Corsica (*10*).

It is imperative to identify and understand the transmission dynamics of introgressed *Schistosoma* species combinations. The detection of multiple introgressed hybrids with mixed ancestry in a single child suggests that *Schistosoma* species may be adapting to recent anthropogenic changes. If novel zoonotic hybrid species are playing a role in maintaining and exacerbating schistosome transmission, illness caused by infection, or both, treatments for humans and livestock may have to be adjusted accordingly within a One Health framework (*4*).

Acknowledgments

We thank Aidan Emery, Fiona Allan, and Muriel Rabone for accessing our parasite samples archived within the Schistosome Collections at the Natural History Museum, London, UK.

This research was funded by a combined Biotechnology and Biological Sciences Research Council, Medical Research Council, Economic and Social Research Council, Natural Environment Research Council, Defence Science and Technology Laboratory, and Department for International Development

Zoonoses and Emerging Livestock Systems (ZELS) research grant, no. BB/L018985/1.

The data used in this study were collected as part of the monitoring and evaluation processes of the Schistosomiasis Control Initiative programs taking place in Niger. Sequences were obtained using the DNA sequencing facilities in the Natural History Museum. Ethical approval for this research was granted by the Niger Ministry of Health Ethical Review Board and by the Imperial College Research Ethics Committee (ICREC_8_2_2, EC no. 03.36, R&D no. 241 03/SB/003E) in combination with ongoing Schistosomiasis Control Initiative activities. All infected children in the study were provided treatment with 40 mg/kg praziquantel.

References

1. Steinmann P, Keiser J, Bos R, Tanner M, Utzinger J. Schistosomiasis and water resources development: systematic review, meta-analysis, and estimates of people at risk. Lancet Infect Dis. 2006;6:411–25 http://dx.doi.org/10.1016/S1473-3099(06)70521-7
2. Uniting to Combat Neglected Tropical Diseases. London declaration on neglected tropical diseases [cited 2016 Jan 22]. http://unitingtocombatntds.org/resource/london-declaration
3. King KC, Stelkens RB, Webster JP, Smith DF, Brockhurst MA. Hybridization in parasites: consequences for adaptive evolution, pathogenesis, and public health in a changing world. PLoS Pathog. 2015;11:e1005098 http://dx.doi.org/10.1371/journal.ppat.1005098
4. Webster JP, Gower CM, Knowles SC, Molyneux DH, Fenton A. One Health—an ecological and evolutionary framework for tackling neglected zoonotic diseases. Evol Appl. 2016;9:313–33 http://dx.doi.org/10.1111/eva.12341
5. Huyse T, Webster BL, Geldof S, Stothard JR, Diaw OT, Polman K, et al. Bidirectional introgressive hybridization between a cattle and human schistosome species. PLoS Pathog. 2009;5:e1000571 http://dx.doi.org/10.1371/journal.ppat.1000571
6. Webster BL, Diaw OT, Seye MM, Webster JP, Rollinson D. Introgressive hybridization of *Schistosoma haematobium* group species in Senegal: species barrier break down between ruminant and human schistosomes. PLoS Negl Trop Dis. 2013;7:e2110. http://dx.doi.org/10.1371/journal.pntd.0002110
7. Rollinson D, Southgate VR, Vercruysse J, Moore PJ. Observations on natural and experimental interactions between *Schistosoma bovis* and *S. curassoni* from West Africa. Acta Trop. 1990;47: 101–14 http://dx.doi.org/10.1016/0001-706X(90)90072-8
8. Taylor MG, Nelson GS, Smith M, Andrews BJ. Comparison of the infectivity and pathogenicity of six species of African schistosomes and their hybrids. 2. Baboons. J Helminthol. 1973;47:455–85 http://dx.doi.org/10.1017/S0022149X00027462
9. Vercruysse J, Southgate VR, Rollinson D. *Schistosoma curassoni* Brumpt, 1931 in sheep and goats in Senegal. Journal of Natural History. 1984;18:969–76 http://dx.doi.org/10.1080/00222938400770851
10. Moné H, Holtfreter MC, Allienne JF, Mintsa-Nguéma R, Ibikounlé M, Boissier J, et al. Introgressive hybridizations of *Schistosoma haematobium* by *Schistosoma bovis* at the origin of the first case report of schistosomiasis in Corsica (France, Europe). Parasitol Res. 2015;114:4127–33 http://dx.doi.org/10.1007/s00436-015-4643-4

Address for correspondence: Elsa Léger, Department of Pathology and Pathogen Biology, Centre for Emerging, Endemic and Exotic Diseases, Royal Veterinary College, University of London, London AL9 7TA, UK; email: eleger@rvc.ac.uk

Rickettsia raoultii in *Dermacentor reticulatus* Ticks, Chernobyl Exclusion Zone, Ukraine, 2010

Grzegorz Karbowiak, Kateryna Slivinska, Tomasz Chmielewski, Kamila Barszcz, Stanisława Tylewska-Wierzbanowska, Joanna Werszko, Tomasz Szewczyk, Piotr Wróblewski

Author affiliations: W. Stefański Institute of Parasitology, Polish Academy of Sciences, Warsaw, Poland (G. Karbowiak, J. Werszko, T. Szewczyk, P. Wróblewski); I.I. Schmalhausen Institute of Zoology, National Academy of Sciences of Ukraine, Kiev, Ukraine (K. Slivinska); National Institute of Public Health–National Institute of Hygiene, Warsaw (T. Chmielewski, K. Barszcz, S. Tylewska-Wierzbanowska)

DOI: http://dx.doi.org/10.3201/eid2212.160678

To the Editor: The Chernobyl Exclusion Zone (CEZ) surrounds the center of the 1986 Chernobyl nuclear power plant disaster. Preliminary study shows predominance of *Dermacentor reticulatus* ticks in the CEZ; ticks of other species, such as *Ixodes ricinus*, are surprisingly rare, even in habitats where they should be relatively common (*1*). A few reports document presence of *Ix. triangulicep*s ticks (*2*,*3*). Prevalence of pathogens (*Anaplasma phagocytophilum*, *Borrelia burgdorferi* s.l., *Babesia* spp.) in these ticks is higher in the CEZ than in other regions (*3*,*4*). One pathogen transmitted by *Dermacentor* spp. ticks is *Rickettsia raoultii*, which has been isolated from species of *Dermacentor* ticks found in Asia (*5*,*6*) and since 1999 has also been detected in Europe.

In our study, *D. reticulatus* ticks were collected by use of the flagging method (*1*) in the CEZ in September 2010. Ticks were collected from areas where they were known to occur, around the former villages of Korohod (51°16′02″N; 30°01′04″E) and Cherevach (51°12′44″N; 30°07′45″E) and around Chernobyl city (51°17′04″N; 30°13′25″E). The habitats investigated included open areas and the remnants of farmlands. A total of 201 *D. reticulatus* ticks, 87 males and 114 females, were collected and investigated (Table).

DNA was extracted by use of the ammonium hydroxide method (*7*). Isolated DNA was examined for the presence of the *Rickettsia* sp. citrate synthase gene (*gltA*) by use of PCR with *Rp*CS.409d and *Rp*CS.1258n primers (*8*). Positive amplicons were sequenced, and sequences were edited by using AutoAssembler software (Applied Biosystems, Foster City, CA, USA) and compared with GenBank entries by using blastn version 2.2.13 (http://www.ncbi.nlm.nih.gov/blast/download.shtml). All obtained sequences were submitted to GenBank (accession nos. KX056493 and KX056494).

Table. Prevalence of *Rickettsia raoultii* infection among *Dermacentor reticulatus* ticks, Chernobyl Exclusion Zone, Ukraine, 2010

Area of tick collection	No. ticks infected/no. ticks examined (prevalence, %)		
	Male	Female	Total
Korohod	40/48 (83.33)	40/60 (66.66)	80/108 (74.07)
Cherevach	21/28 (75.00)	32/46 (69.56)	53/74 (71.62)
Chernobyl	9/11 (81.82)	4/8 (50.00)	13/19 (68.42)
All 3 areas	70/87 (80.46)	76/114 (66.66)	146/201 (72.64)

Infection with *Rickettsia* spp. was detected in 72.64% of ticks (Table). A higher proportion of males (80.46%) than females (66.66%) were infected. Sequence analysis showed 100% identity with *R. raoultii* isolated from *D. marginatus* ticks from China (GenBank accession nos. KU171018.1 and KT261764.1) and *D. reticulatus* ticks from Poland (KT277489) and Hungary (LC060714.1). In the CEZ, the predominant tick species is *D. reticulatus*; no *D. marginatus* ticks have been found in the CEZ (*1*). Thus, in this area, the *R. raoultii* vector is *D. reticulatus* ticks.

The prevalence of *R. raoultii* infection among *D. reticulatus* ticks (68.42%–74.07%) is significantly higher in the CEZ than in other regions. A previous study found prevalence of *A. phagocytophilum* infection in the CEZ to be high, mainly associated with *Ixodes* ticks (*9*) and rarely associated with *D. reticulatus* ticks. The prevalence of *Babesia canis* infection, also vectored by this tick, was within the usual range (*4*). The reason for prevalence of at least 2 vectored pathogens being higher in *D. reticulatus* ticks in the CEZ than in other region is not known and needs more study. The prevalence of these pathogens among mammals that inhabit the CEZ is also not known; the influence of radiation on pathogen level has not been studied. The nucleotide sequences of *R. raoultii* detected in ticks in the CEZ are identical to sequences originating from other regions and deposited in GenBank; the sequences of *A. phagocytophilum* and *B. canis* from the CEZ were also similar to those described elsewhere (*4*). If the reason for the higher *R. raoultii* infection prevalence is radiation, then radiation also influences the ticks—some morphologic abnormalities have been noted on *D. reticulatus* ticks collected from the CEZ (*10*).

This study confirms presence of *R. raoultii* in *D. reticulatus* ticks in the CEZ. The structure of zoonotic foci in the CEZ seems to differ from that in other regions. Confirmation of this hypothesis needs follow-up study of tick-borne pathogens in wild mammals that might serve as a source of infection for ticks in the CEZ.

Acknowledgments

We thank Alexander Borovsky for his help during the study.

The study was supported by a Polish–Ukrainian joint research project for the years 2012–2014, from grant NCN 2011/01/B/NZ7/03574, and partially from National Institute of Public Health–National Institute of Hygiene funds (12/EM/2016).

References

1. Karbowiak G, Slivinska K, Werszko J, Didyk J. 2013. The occurrence of hard ticks in Chernobyl Exclusion Zone. In: The 15th International Symposium Parasitic and Allergic Arthropods—Medical and Sanitary Significance; 2013 Jun 3–5; Kazimierz Dolny, Poland. p. 48–9.
2. Akimov IA, Nebogatkin IV. Ixodid ticks (Acarina, Ixodidae, Acarina) and Lyme disease in Ukraine. Vestnik Zoologii. 1995;1:76–8.
3. Movila A, Deriabina T, Morozov A, Sitnicova N, Toderas I, Uspenskaia I, et al. Abundance of adult ticks (Acari: Ixodidae) in the Chernobyl nuclear power plant exclusion zone. J Parasitol. 2012;98:883–4. http://dx.doi.org/10.1645/GE-3131.1
4. Karbowiak G, Víchová B, Slivinska K, Werszko J, Didyk J, Peťko B, et al. The infection of questing *Dermacentor reticulatus* ticks with *Babesia canis* and *Anaplasma phagocytophilum* in the Chernobyl Exclusion Zone. Vet Parasitol. 2014;204:372–5. http://dx.doi.org/10.1016/j.vetpar.2014.05.030
5. Rydkina E, Roux V, Rudakov N, Gafarova M, Tarasevich I, Raoult D. New rickettsiae in ticks collected in territories of the former Soviet Union. Emerg Infect Dis. 1999;5:811–42. http://dx.doi.org/10.3201/eid0506.99061
6. Mediannikov O, Matsumoto K, Samoylenko I, Drancourt M, Roux V, Rydkina E, et al. *Rickettsia raoultii* sp. nov., a spotted fever group rickettsia associated with *Dermacentor* ticks in Europe and Russia. Int J Syst Evol Microbiol. 2008;58:1635–9. http://dx.doi.org/10.1099/ijs.0.64952-0
7. Rijpkema S, Golubić D, Molkenboer M, Verbeek-De Kruif N, Schellekens J. Identification of four genomic groups of *Borrelia burgdorferi* sensu lato in *Ixodes ricinus* ticks collected in a Lyme borreliosis endemic region of northern Croatia. Exp Appl Acarol. 1996;20:23–30.
8. Roux V, Rydkina E, Eremeeva M, Raoult D. Citrate synthase gene comparison, a new tool for phylogenetic analysis, and its application for the rickettsiae. Int J Syst Bacteriol. 1997;47:252–61. http://dx.doi.org/10.1099/00207713-47-2-252
9. Welc-Falęciak R, Kowalec M, Karbowiak G, Bajer A, Behnke MJ, Siński E. Rickettsiaceae and Anaplasmataceae infections in *Ixodes ricinus* ticks from urban and natural forested areas of Poland. Parasites & Vectors 2014;7:121. http://dx.doi.org/10.1186/1756-3305-7-121
10. Karbowiak G, Slivinska K, Didyk J, Akimov I, Wita I. The morphological abnormalities of *Dermacentor reticulatus* ticks in Chernobyl Exclusion Zone. In; The 13th International Symposium Parasitic and Allergic Arthropods—Medical and Sanitary Significance; 2011 Jun 6–8; Kazimierz Dolny, Poland; 2011. p. 29–30.

Address for correspondence: Grzegorz Karbowiak, W. Stefanski Institute of Parasitology of Polish Academy of Sciences, Twarda 51/55, Warsaw 00-818, Poland; email: grzgrz@twarda.pan.pl

Locally Acquired Eastern Equine Encephalitis Virus Disease, Arkansas, USA

Jeremy Garlick, T. Jacob Lee, Patrick Shepherd, W. Matthew Linam, Daniel M. Pastula, Susan Weinstein, Stephen M. Schexnayder

Author affiliations: University of Arkansas for Medical Sciences, Little Rock, Arkansas, USA (J. Garlick, T.J. Lee, P. Shepherd, W.M. Linam, S.M. Schexnayder); Centers for Disease Control and Prevention, Fort Collins, Colorado, USA (D.M. Pastula); University of Colorado School of Medicine, Aurora, Colorado, USA (D.M. Pastula); Arkansas Department of Health, Little Rock (S. Weinstein)

DOI: http://dx.doi.org/10.3201/eid2212.160844

To the Editor: Eastern equine encephalitis virus (EEEV) is an arbovirus (family *Togaviridae*, genus *Alphavirus*) transmitted to humans primarily from *Aedes*, *Coquillettidia*, and *Culex* mosquitoes. EEEV is maintained in a transmission cycle between *Culiseta melanura* mosquitoes and birds in freshwater hardwood swamps (*1*). Affected humans and horses are considered to be dead-end hosts; that is, they usually do not develop sufficient levels of viremia to infect mosquitoes. Although human EEEV disease is rare, it has a case-fatality rate of >30% and >50% of survivors may have permanent neurologic sequelae (*2*–*5*). Cases occur sporadically each year, primarily along the eastern and Gulf coasts of North America, but no cases have been previously reported in Arkansas (*1*). We report a locally acquired case of human EEEV disease in Arkansas.

In October 2013, a male teenager from southwestern Arkansas sought care at a local hospital after 3 days of headache and 3 new-onset focal seizures. He had a history of recent multiple mosquito bites and no history of recent travel. Initial laboratory studies on postsymptom onset day (PSOD) 3 showed normal peripheral leukocyte count, electrolytes, and liver function tests. Cerebrospinal fluid (CSF) exam showed 5 leukocytes/mm^3 (reference 0–5), 7 erythrocytes/mm^3 (reference 0), 55 mg/dL glucose (reference 45–80), and 36 mg/dL protein (reference 15–40). Noncontrast computed tomography (CT) of the head was normal. He was transferred to a regional academic pediatric hospital on PSOD 3.

On PSOD 4, the patient became increasingly lethargic, febrile (39.2°C), tachycardic, and hypotensive. He received intravenous fluids and broad-spectrum antimicrobial drugs (e.g., vancomycin, ceftriaxone, acyclovir, and doxycycline). Magnetic resonance imaging of the brain on PSOD 4 revealed left frontal lobe edema and multiple T2 signal abnormalities in the basal ganglia and midbrain. Repeat CSF examination on PSOD 4 showed 1,170 leukocytes/mm^3 (74% neutrophils), 137 erythrocytes/mm^3, 204 mg/dL protein, 66 mg/dL glucose, and a negative Gram stain. CSF bacterial cultures, CSF herpes simplex virus PCR, and CSF enterovirus reverse transcription PCR tests were negative.

Repeat CT scan of the brain on PSOD 6 showed frontal and temporal lobe edema. Physicians initiated measures to monitor and control elevated intracranial pressure, including placement of an external ventricular drain, hyperosmolar therapy with mannitol and 3% sodium chloride, cooling to 34°C, chemical paralysis, and a pentobarbital-induced coma. Pressors were subsequently added to maintain cerebral perfusion pressures >60 mm Hg (i.e., minimum for adequate brain perfusion). Despite these measures, elevated intracranial pressure (from low 20s mm Hg to mid-30s mm Hg) continued for 2 weeks. On PSOD 19, the patient's intracranial pressure increased to 71 mm Hg. A repeat CT scan of the brain showed widespread cerebral edema, uncal herniation, intraparenchymal hemorrhages, and obstructive hydrocephalus. Given clinical worsening, the family elected to withdraw care and the patient died.

Serologic testing from PSOD day 4 for immunoglobulin (Ig) M and G antibodies against St. Louis encephalitis, West Nile, and California serogroup viruses was negative. A commercial EEEV IgM antibody immunofluorescence assay (IFA) performed on CSF collected on PSOD 4 was positive (titer 8). Confirmatory testing was performed at the Centers for Disease Control and Prevention's Arboviral Diseases Branch (Fort Collins, CO, USA). Serum collected on PSOD 12 tested positive for EEEV IgM antibodies by microsphere immunoassay and for EEEV neutralizing antibodies by plaque reduction neutralization testing (titer >20,480) (*6*). Additional CSF collected on PSOD 12 also tested positive for EEEV IgM antibodies by microsphere immunoassay and for EEEV neutralizing antibodies by plaque reduction neutralization testing (titer 32).

Although human EEEV disease cases had been reported in neighboring Louisiana, Mississippi, and Texas, no cases had previously been reported in Arkansas (*1*). However, EEEV was identified in horses in Arkansas before 2013 and in the patient's county of residence in 2013, indicating that the virus was already present in the area (*7*). Several freshwater swamps, which are known to be important ecologic environments in the EEEV transmission cycle, were within a 6-mile radius of the patient's residence (*8*). This case shows that human EEEV disease can occur in areas where EEEV is circulating in the environment, highlighting the need for continued surveillance for EEEV and other arboviruses. Furthermore, the lack of a specific antiviral therapy for EEEV disease indicates the importance of mosquito-bite prevention strategies (e.g., using insect repellent and wearing long-sleeved shirts and pants outdoors).

For those who develop EEEV disease, supportive care is currently the only treatment option. Elevated intracranial pressure should be watched for, monitored, and aggressively managed. Hyperosmolar therapy, external ventricular drain placement, cooling, sedation, and paralysis have been used in the management of elevated intracranial pressure for other conditions and have been used with varying degrees of success in treating EEEV disease (*9*,*10*). Further research regarding the management of EEEV disease is needed.

Acknowledgments

We thank Marc Fischer and the Arbovirus Diagnostics Laboratory of the CDC, Charles Glasier, and other Arkansas clinicians and public health officials who were involved in the care of this patient and in investigation of this case.

The findings and conclusions in this report are those of the authors and do not necessarily represent the official position of the Centers for Disease Control and Prevention or the Arkansas Department of Health.

References

1. US Centers for Disease Control and Prevention. Eastern equine encephalitis. Updated 2016 Apr 5 [cited 2016 May 22]. http://www.cdc.gov/EasternEquineEncephalitis.
2. Feemster RF. Equine encephalitis in Massachusetts. N Engl J Med. 1957;257:701–4 http://dx.doi.org/10.1056/NEJM195710102571504
3. Przelomski MM, O'Rourke E, Grady GF, Berardi VP, Markley HG. Eastern equine encephalitis in Massachusetts: a report of 16 cases, 1970–1984. Neurology. 1988;38:736–9. http://dx.doi.org/10.1212/WNL.38.5.736
4. Letson GW, Bailey RE, Pearson J, Tsai TF. Eastern equine encephalitis (EEE): a description of the 1989 outbreak, recent epidemiologic trends, and the association of rainfall with EEE occurrence. Am J Trop Med Hyg. 1993;49:677–85.
5. Reimann CA, Hayes EB, DiGuiseppi C, Hoffman R, Lehman JA, Lindsey NP, et al. Epidemiology of neuroinvasive arboviral disease in the United States, 1999–2007. Am J Trop Med Hyg. 2008;79:974–9.
6. Basile AJ, Horiuchi K, Panella AJ, Laven J, Kosoy O, Lanciotti RS, et al. Multiplex microsphere immunoassays for the detection of IgM and IgG to arboviral diseases. PLoS One. 2013;8:e75670. http://dx.doi.org/10.1371/journal.pone.0075670
7. US Department of Agriculture. 2013 Summary of eastern equine encephalitis cases in the United States—January 1, 2013–December 31, 2013. 2014 May [cited 2016 May 22]. https://www.aphis.usda.gov/animal_health/downloads/animal_diseases/2013_EEE_FINAL.pdf
8. Komar N, Spielman A. Emergence of eastern encephalitis in Massachusetts. Ann N Y Acad Sci. 1994;740:157–68. http://dx.doi.org/10.1111/j.1749-6632.1994.tb19866.x
9. Wendell LC, Potter NS, Roth JL, Salloway SP, Thompson BB. Successful management of severe neuroinvasive eastern equine encephalitis. Neurocrit Care. 2013;19:111–5. http://dx.doi.org/10.1007/s12028-013-9822-5
10. Nakagawa K, Chang CW, Koenig MA, Yu M, Tokumaru S. Treatment of refractory intracranial hypertension with 23.4% saline in children with severe traumatic brain injury. J Clin Anesth. 2012;24:318–23. http://dx.doi.org/10.1016/j.jclinane.2011.10.011

Address for correspondence: Stephen M. Schexnayder, University of Arkansas for Medical Sciences, College of Medicine, Section of Critical Care Medicine, Arkansas Children's Hospital, 1 Children's Way, S-4415, Little Rock, AR 72202, USA; email: SchexnayderSM@uams.edu

Tick-Borne Relapsing Fever, Southern Spain, 2004–2015

Luis Castilla-Guerra,[1] Jorge Marín-Martín,[1] Miguel Angel Colmenero-Camacho

Author affiliations: Hospital Universitario Virgen Macarena, Seville, Spain (L. Castilla-Guerra, M.A. Colmenero-Camacho); Universidad de Sevilla, Seville (L. Castilla-Guerra, M.A. Colmenero-Camacho); Hospital de la Merced, Seville (J. Marín-Martín)

DOI: http://dx.doi.org/10.3201/eid2212.160870

To the Editor: Surveillance data indicate that tick-borne diseases are substantial and increasing global public health problems (*1*). Various pathogens, including viruses, bacteria, protozoa, and helminthes, are transmitted from ticks to vertebrates (*2*). Tick-borne relapsing fever (TBRF) is a zoonosis that is enzootic in many countries (*3*). This illness is caused by ≥10 *Borrelia* species and is transmitted to humans through the bite of soft ticks of the genus *Ornithodoros* (*3*).

Currently, TBRF is endemic in various foci around the world. However, few TBRF cases are reported in the United States, and in most western European countries, such as Spain, TBRF occurs sporadically, usually after opportunistic infections in persons exposed to ticks (*3*,*4*). Many authors consider TBRF to be underrecognized and underreported (*5*). Although molecular tools such as PCR can dramatically improve diagnosis of this illness, methods used to diagnose TBRF have changed little since the discovery of the spirochete.

To evaluate the prevalence and clinical features of TBRF in a rural area of southern Spain, we retrospectively reviewed clinical data for all patients ≥14 years of age who sought care for TBRF during January 2004–December 2015 at Hospital de la Merced, a county hospital in Seville, Spain. We defined a case of TBRF as detection of spirochetes on thin- or thick-blood smears or in cerebrospinal fluid (CSF) samples by using conventional microscopy after Giemsa or Wright staining (Figure).

Of 75 patients, 42 (56%) were male and 33 (44%) were female. Mean age was 33 (range 14–72) years. Nine (12%)

[1]These authors contributed equally to this article.

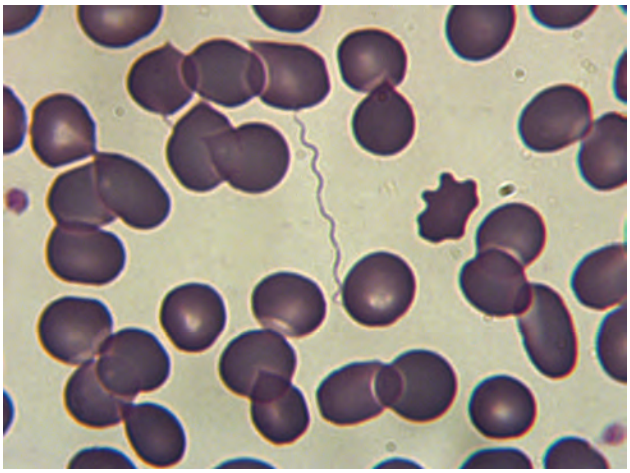

Figure. Spirochetes on a thick peripheral blood smear from a patient with tick-borne relapsing fever, southern Spain, 2004–2015. Original magnification ×1,000.

patients reported tick bites. The most common symptoms were fever (64 [85.3%] patients), headache (41 [54.6%]), vomiting (26 [34.6%]), muscle ache (22 [29.3%]), and abdominal pain (21 [28%]). At the time of the hospital visit, 9 (12%) patients had signs and symptoms suggesting meningeal involvement; 3 (4%) others had clear meningeal signs. These 12 patients underwent lumbar puncture, and CSF abnormalities were found in the 3 (4%) patients with meningismus. Spirochetes were found in the CSF sample of 1 patient. Of the total 75 patients, this patient was the only 1 with spirochetes, and no patient had facial palsy or other neurologic manifestation. The main laboratory findings were elevated C-reactive protein, found in 74 (98.6%) patients; thrombocytopenia, found in 67 (89.3%); and anemia, found in 37 (49.3%).

Preferred treatment was oral doxycycline, which was used for a mean duration of 10 (range 7.3–14) days in 55 patients (73.3%). Among 3 TBRF patients with neurologic involvement, 1 was treated with penicillin G (3 million units/4 h), and 2 were treated with ceftriaxone (2 g/d for 4 d). Jarisch-Herxheimer reaction occurred in 7 (9.3%) patients, none of whom had meningitis. All patients recovered completely.

Currently, TBRF is widely distributed in various foci around the world. In much of sub-Saharan Africa, TBRF is associated with a high number of illnesses and deaths. Indeed, it is reportedly the most common bacterial infection from Senegal and is listed among the 10 leading causes of death in children <5 years of age in Tanzania (*6*). Elsewhere in the world, this infection is regarded as rare. Although TBRF borreliosis occurs infrequently in developed countries, our study highlights TBRF endemicity in an area of southern Spain.

Reports on TBRF in Spain are scarce. The only previous study involving numerous cases of TBRF in Spain (*7*) described 230 cases and was published in the early 20th century. That research showed that, although disease caused by *B. hispanica* is less severe than that of other TBRFs, ≈5% of patients had neurologic complications. In our study, 3 (4%) patients had meningitis caused by TBRF borreliosis, a finding that accords with the previous report.

A recent study conducted among children in southern Spain (*8*) identified 9 cases of TBRF during a 10-year period. Two children, 3 and 5 years of age, had meningeal involvement but no other neurologic complication. Similar to observations in our study, Jarisch-Herxheimer reaction was infrequent, occurring in only 1 of the 9 children.

Neurologic complications are well known features of infection with 2 spirochetes, *B. burgdorferi* and *Treponema pallidum* (*9*). Nevertheless, little is published and known about the predilection of TBRF borreliosis to infect the nervous system. One of the few studies reviewing neurologic involvement of TBRF borreliosis reported that *B. turicatae* and *B. duttonii*, the agents of TBRF in southwestern North America and sub-Saharan Africa, respectively, cause neurologic involvement as often as *B. burgdorferi* causes Lyme disease (*10*).

Our study confirms that TBRF is an endemic, underreported disease in many countries and is common in southern Spain. Although the disease caused by *B. hispanica* is among the less severe illnesses caused by the relapsing fever group, serious neurologic complications can occur. With increasing globalization, physicians will likely see increased numbers of travel-related infections and will face imported and emerging TBRF cases.

References

1. Hook SA, Nelson CA, Mead PSUS. U.S. public's experience with ticks and tick-borne diseases: results from national HealthStyles surveys. Ticks Tick Borne Dis. 2015;6:483–8. http://dx.doi.org/10.1016/j.ttbdis.2015.03.017
2. Baneth G. Tick-borne infections of animals and humans: a common ground. Int J Parasitol. 2014;44:591–6. http://dx.doi.org/10.1016/j.ijpara.2014.03.011
3. Dworkin MS, Schwan TG, Anderson DE Jr, Borchardt SM. Tick-borne relapsing fever. Infect Dis Clin North Am. 2008; 22:449–68. http://dx.doi.org/10.1016/j.idc.2008.03.006
4. Rebaudet S, Parola P. Epidemiology of relapsing fever borreliosis in Europe. FEMS Immunol Med Microbiol. 2006;48:11–5. http://dx.doi.org/10.1111/j.1574-695X.2006.00104.x
5. Dworkin MS, Shoemaker PC, Fritz CL, Dowell ME, Anderson DE Jr. The epidemiology of tick-borne relapsing fever in the United States. Am J Trop Med Hyg. 2002;66:753–8.
6. Cutler SJ. Relapsing fever—a forgotten disease revealed. J Appl Microbiol. 2010;108:1115–22. http://dx.doi.org/10.1111/j.1365-2672.2009.04598.x
7. Mas de Ayala I. Estudio clınico de la fiebre recurrente española (230. observaciones). Medicina Paıses Cálidos. 1931;4:369–89.
8. Croche Santander B, Sánchez Carrión A, Campos E, Toro C, Marcos L, Vargas JC, et al. Tick-borne relapsing fever in a rural area of southern Spain. An Pediatr (Barc). 2015;82:e73–7. http://dx.doi.org/10.1016/j.anpedi.2013.10.052

9. Halperin JJ. A tale of two spirochetes: Lyme disease and syphilis. Neurol Clin. 2010;28:277–91. http://dx.doi.org/10.1016/j.ncl.2009.09.009
10. Cadavid D, Barbour AG. Neuroborreliosis during relapsing fever: review of the clinical manifestations, pathology, and treatment of infections in humans and experimental animals. Clin Infect Dis. 1998;26:151–64. http://dx.doi.org/10.1086/516276

Address for correspondence: Luis Castilla-Guerra, Servicio de Medicina Interna, Hospital Universitario Virgen Macarena, 41009, Seville, Spain; email: castillafernandez@hotmail.com

New Hepatitis E Virus Genotype in Bactrian Camels, Xinjiang, China, 2013

Patrick C.Y. Woo,[1] Susanna K.P. Lau,[1] Jade L.L. Teng,[1] Kai-Yuan Cao, Ulrich Wernery, Tony Schountz, Tsz Ho Chiu, Alan K.L. Tsang, Po-Chun Wong, Emily Y.M. Wong, Kwok-Yung Yuen

Author affiliations: The University of Hong Kong, Hong Kong, China (P.C.Y. Woo, S.K.P. Lau, J.L.L. Teng, T.H. Chiu, A.K.L. Tsang, P.-C. Wong, E.Y.M Wong, K.-Y. Yuen); Sun Yat-sen University, Guangzhou, China (K.-Y. Cao); Central Veterinary Research Laboratory, Dubai, United Arab Emirates (U. Wernery); Colorado State University, Fort Collins, Colorado, USA (T. Schountz)

DOI: http://dx.doi.org/10.3201/eid2212.160979

To the Editor: Hepatitis E virus (HEV) is a member of the family *Hepeviridae*, genus *Orthohepevirus*, which comprises 4 species, *Orthohepevirus A–D*. *Orthohepevirus A* contains 7 genotypes (HEV1–7) (*1*,*2*). HEV1 and HEV2 infect humans only; HEV3, HEV4, and HEV7 can infect humans and other mammals; and HEV5 and HEV6 have been detected in animals only.

Worldwide, HEV is the most common cause of acute viral hepatitis in humans. The disease is generally self-limiting, but high death rates have been observed among HEV-infected pregnant women. Chronic HEV infection is a problem in immunocompromised patients, such as solid organ transplant recipients (*3*). Human HEV3 and HEV4 infections have been associated with consumption of undercooked pork or game meat *(4)*.

In 2014, we described the discovery of a novel genotype of HEV in dromedaries (*Camelus dromedarius* or 1-humped camels), suggesting another possible source of human HEV infection (*5*). This dromedary HEV was subsequently classified as a novel *Orthohepevirus A* genotype, HEV7 (*1*,*2*). Recently, this HEV7 genotype was also isolated from a liver transplant recipient from the Middle East with chronic HEV infection (*6*). The patient regularly consumed dromedary camel meat and milk, implying camel-to-human transmission of the virus (*6*).

Like the dromedary, the Bactrian camel (*Camelus bactrianus* or 2-humped camels) is an Old World camelid species. Thus, we hypothesize that Bactrian camels may also be reservoirs of HEV. To test this hypothesis and increase our understanding of the epidemiology of HEV in camels, we performed a molecular epidemiology study using feces samples from camels in China.

During November 2012–May 2013, we collected and tested 1 feces sample each from 205 Bactrian camels on a farm in Xinjiang, China. We performed RNA extraction and reverse transcription PCR (RT-PCR) as previously described (*7*). We screened for HEV by PCR amplification of a 251-bp fragment of open-reading frame (ORF) 2, using primers 5′-GTTGTCTCAGCCAATGGCGA-3′ and 5′-GTAGTTTGGTCATACTCAGCAGC-3′. PCR was performed, using previously described conditions (*7*), with the annealing temperature set at 50°C. DNA sequencing and quantitative real-time RT-PCR were performed as previously described (*7*). Three samples were positive for HEV; we performed complete genome sequencing of these samples as described (online Technical Appendix, http://wwwnc.cdc.gov/EID/article/22/12/16-0979-Techapp1.pdf) (*5*,*7*). We also performed comparative genomic analysis as previously described (*1*,*2*,*8*). We constructed a phylogenetic tree using the maximum-likelihood method and MEGA7 (*9*); bootstrap values were calculated from 1,000 trees. The optimal substitution model for each ORF was selected by MEGA7 (Figure).

RT-PCR for a 251-bp fragment in ORF2 of HEV was positive for 3 (1.5%) of the 205 fecal samples; virus loads were 1.6×10^3, 2.1×10^3, and 1.8×10^4 copies/mg, respectively. Whole-genome sequencing of the 3 Bactrian camel HEV (BcHEV) strains (GenBank accession nos. KX387865–7) showed genome sizes of 7,212–7,223 bp and a G + C content of 52.7%–53.1%. Overall, nucleotides in the BcHEV genome differed by >20% compared with those in all other HEVs. Genomes of the 3 BcHEV isolates contained 3 major ORFs; genome organization was typical of and characteristics were similar to those of HEVs from other *Orthohepevirus A* species. Phylogenetic trees constructed using ORF1, ORF2, ORF3, and concatenated ORF1/ORF2, excluding the hypervariable region, showed that these 3 BcHEV isolates clustered with the 2 dromedary camel HEV7 strains and the HEV7 strain from the liver-transplant recipient with chronic hepatitis (Figure; online Technical Appendix Figure 1)

[1]These authors contributed equally to this article.

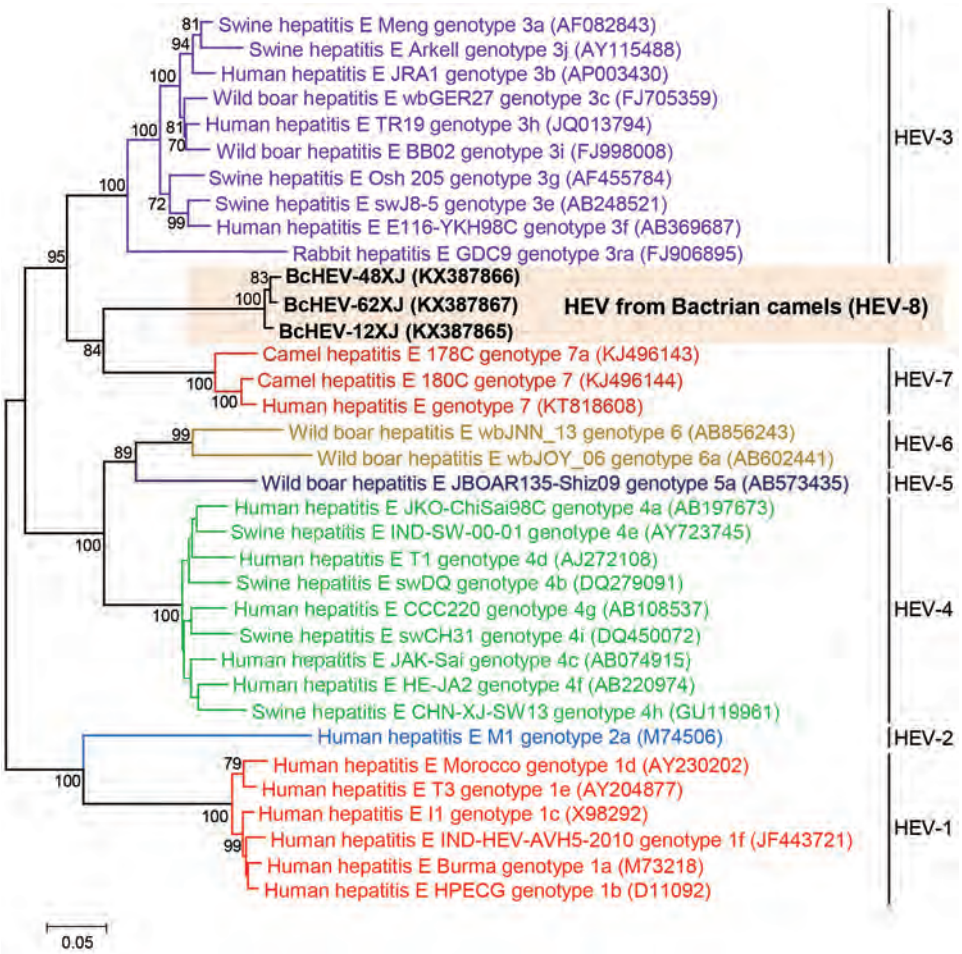

Figure. Phylogenetic analyses of the proteins of concatenated ORF1/ORF2, excluding the hypervariable region, of Bactrian camel hepatitis E virus (HEV) and other HEV genotypes (HEV1–HEV7) within the species *Orthohepevirus A* (family *Hepeviridae*). The tree was constructed using the maximum-likelihood method using the Jones–Taylor–Thornton substitution model with invariant sites and gamma distributed rate variation. The analysis included 2,282 amino acid positions (aa residues 1–706 and 789–2409, numbered with reference to GenBank sequence M73218). Bold indicates the 3 strains of BcHEV with complete genomes sequenced in this study. GenBank accession numbers are shown in parentheses. Scale bar indicates the estimated number of substitutions per 20 aa. ORF, open-reading frame.

(*5*,*6*). However, amino acid distances based on the concatenated ORF1/ORF2, excluding the hypervariable region of the 3 BcHEV isolates and the existing genotypes, ranged from 0.095 to 0.148, which was greater than the threshold (p-distance = 0.088) to demarcate intergenotype distance (*1*,*2*). Using this criterion, we propose that the 3 BcHEV isolates should constitute a new HEV genotype, HEV8.

A recent study in Dubai, United Arab Emirates, showed that HEV accounted for 40% of acute hepatitis cases (*10*). Even though HEV is an emerging pathogen in the Middle East, limited sequence data exist regarding the virus on the Arabian Peninsula. Recently, we discovered the HEV7 genotype in 1.5% of 203 feces samples from dromedaries in Dubai (*5*). In the current study, we detected a new HEV genotype in 1.5% of 205 Bactrian camels on a farm in Xinjiang. Comparative genomic and phylogenetic analyses showed that BcHEV represents a previously unrecognized HEV genotype. It has been shown that HEV7 from dromedaries can be transmitted to humans; thus, meat and milk from Bactrian camels might pose a similar risk to humans. The increasing discoveries of camel viruses and of their transmission to humans highlight the need for caution when handling these mammals and processing food products derived from them.

This work was partly supported by the Theme-based Research Scheme (project no. T11/707/15), Research Grant Council Grant, University Grant Committee; the Hong Kong Special Administrative Region Health and Medical Research Fund; and the Strategic Research Theme Fund, The University of Hong Kong.

References

1. Smith DB, Simmonds P, Izopet J, Oliveira-Filho EF, Ulrich RG, Johne R, et al. Proposed reference sequences for hepatitis E virus subtypes. J Gen Virol. 2016;97:537–42. http://dx.doi.org/10.1099/jgv.0.000393
2. Smith DB, Simmonds P, Jameel S, Emerson SU, Harrison TJ, Meng XJ, et al.; International Committee on Taxonomy of Viruses Hepeviridae Study Group. Consensus proposals for classification of the family Hepeviridae. J Gen Virol. 2014;95:2223–32. http://dx.doi.org/10.1099/vir.0.068429-0
3. Kamar N, Selves J, Mansuy JM, Ouezzani L, Péron JM, Guitard J, et al. Hepatitis E virus and chronic hepatitis in organ-transplant

recipients. N Engl J Med. 2008;358:811–7. http://dx.doi.org/10.1056/NEJMoa0706992
4. Debing Y, Moradpour D, Neyts J, Gouttenoire J. Update on hepatitis E virology: implications for clinical practice. J Hepatol. 2016;65:200–12. http://dx.doi.org/10.1016/j.jhep.2016.02.045
5. Woo PC, Lau SK, Teng JL, Tsang AK, Joseph M, Wong EY, et al. New hepatitis E virus genotype in camels, the Middle East. Emerg Infect Dis. 2014;20:1044–8. http://dx.doi.org/10.3201/eid2006.140140
6. Lee GH, Tan BH, Teo EC, Lim SG, Dan YY, Wee A, et al. Chronic infection with camelid hepatitis E virus in a liver transplant recipient who regularly consumes camel meat and milk. Gastroenterology. 2016;150:355–7.e3. http://dx.doi.org/10.1053/j.gastro.2015.10.048
7. Woo PC, Lau SK, Lam CS, Tsang AK, Hui SW, Fan RY, et al. Discovery of a novel bottlenose dolphin coronavirus reveals a distinct species of marine mammal coronavirus in *Gammacoronavirus*. J Virol. 2014;88:1318–31. http://dx.doi.org/10.1128/JVI.02351-13
8. Smith DB, Purdy MA, Simmonds P. Genetic variability and the classification of hepatitis E virus. J Virol. 2013;87:4161–9. http://dx.doi.org/10.1128/JVI.02762-12
9. Kumar S, Stecher G, Tamura K. MEGA7: Molecular Evolutionary Genetics Analysis version 7.0 for bigger datasets. Mol Biol Evol. 2016;33:1870–4. http://dx.doi.org/10.1093/molbev/msw054
10. Abro AH, Abdou AM, Saleh AA, Ustadi AM, Hussaini HS. Hepatitis E: a common cause of acute viral hepatitis. J Pak Med Assoc. 2009;59:92–4.

Address for correspondence: Patrick C.Y. Woo, State Key Laboratory of Emerging Infectious Diseases, Department of Microbiology, The University of Hong Kong, University Pathology Building, Queen Mary Hospital, Hong Kong; email: pcywoo@hku.hk; Kwok-Yung Yuen, State Key Laboratory of Emerging Infectious Diseases, Department of Microbiology, The University of Hong Kong, University Pathology Bldg., Queen Mary Hospital, Hong Kong; email: kyyuen@hku.hk

Avian Influenza Virus H5 Strain with North American and Eurasian Lineage Genes in an Antarctic Penguin

Gonzalo P. Barriga, Dusan Boric-Bargetto, Marcelo Cortez-San Martin, Víctor Neira, Harm van Bakel, Michele Thompsom, Rodrigo Tapia, Daniela Toro-Ascuy, Lucila Moreno, Yesseny Vasquez, Michel Sallaberry, Fernando Torres-Pérez, Daniel González-Acuña, Rafael A. Medina

Author affiliations: Pontificia Universidad Católica de Chile, Santiago, Chile (G.P. Barriga, R.A. Medina); Pontificia Universidad Católica de Valparaíso, Valparaíso, Chile (D. Boric-Bargetto, F. Torres-Pérez); Universidad de Santiago, Santiago (M. Cortez-San Martin, D. Toro-Ascuy, Y. Vasquez); Universidad de Chile, Santiago (V. Neira, R. Tapia, M. Sallaberry); Icahn School of Medicine at Mount Sinai, New York, New York, USA (H. van Bakel, R.A. Medina); Universidad de Concepción, Concepción, Chile (M. Thompsom, L. Moreno, D. González-Acuña); Millennium Institute on Immunology and Immunotherapy, Santiago (R.A. Medina)

DOI: http://dx.doi.org/10.3201/eid2212.161076

To the Editor: Previous studies have reported avian influenza virus (AIV)–positive serum samples obtained from Adélie (*Pygoscelis adeliae*), chinstrap (*Pygoscelis antarcticus*), and gentoo (*Pygoscelis papua*) penguins (*1–4*). Only recently was an H11N2 subtype virus isolated from Adélie penguins in Antarctica (5). We performed AIV surveillance in the Antarctic Peninsula to identify the strains currently circulating in different penguins species in this area.

During 2015–2016, we sampled penguin colonies from 9 locations on the Antarctic Peninsula. We collected 138 blood samples from Adélie penguins at Ardley Island (62°13′S, 58°56′W), Arctowski Base (62°9′S, 58°28′W), and Bernardo O'Higgins Base (63°19′S, 57°53′W) and identified 5 serum samples positive for influenza. We also collected 513 cloacal swabs from Adélie, chinstrap (online Technical Appendix Figure 1, panel A; http://wwwnc.cdc.gov/EID/article/22/12/16-1076-Techapp1.pdf), and gentoo penguins from Mikkelsen Harbor (63°54′S, 60°47′W), Dorian Bay and Port Lockroy (64°48′S, 63°30′W), Pleneau Island (65°06′S, 64°04′W), Brown Base (64°53′S, 62°52′W), Orne Harbor (64°37′S, 62°32′W), and Aitcho Island (62°23′S, 59°46′W) during January–March of 2 consecutive seasons (2015 and 2016; online Technical Appendix Figure 1, panel B; http://wwwnc.cdc.gov/EID/article/22/12/16-1076-Techapp1.pdf). Quantitative reverse transcription PCR (RT-PCR) analysis of the matrix segment (*6*) identified 21 positive AIV samples from penguins (8 chinstrap, 13 gentoo) on Aitcho Island, demonstrating the presence of AIV in 2 additional penguin species in a new location in Antarctica.

Using multisegment RT-PCR performed with influenza-specific universal primers, we amplified all 8 virus segments from a chinstrap penguin specimen, which yielded cDNA products suitable for next-generation sequencing with a HiSeq 2500 System (Illumina, San Diego, CA, USA). This virus was subtyped as an H5N5 and named A/chinstrap_penguin/Antarctica/B04/2015 (H5N5). Analysis of its cleavage site confirmed this was a typical low pathogenicity AIV (LPAIV) containing cleavage motif PQRETRGLF (*7*).

To trace the origin of this H5N5 virus, we performed phylogenetic analyses of its hemagglutinin and neuraminidase genes (Figure, panels A, B; online Technical Appendix Figures 2, 3, http://wwwnc.cdc.gov/EID/article/22/12/16-1076-Techapp1.pdf). The hemagglutinin gene was placed

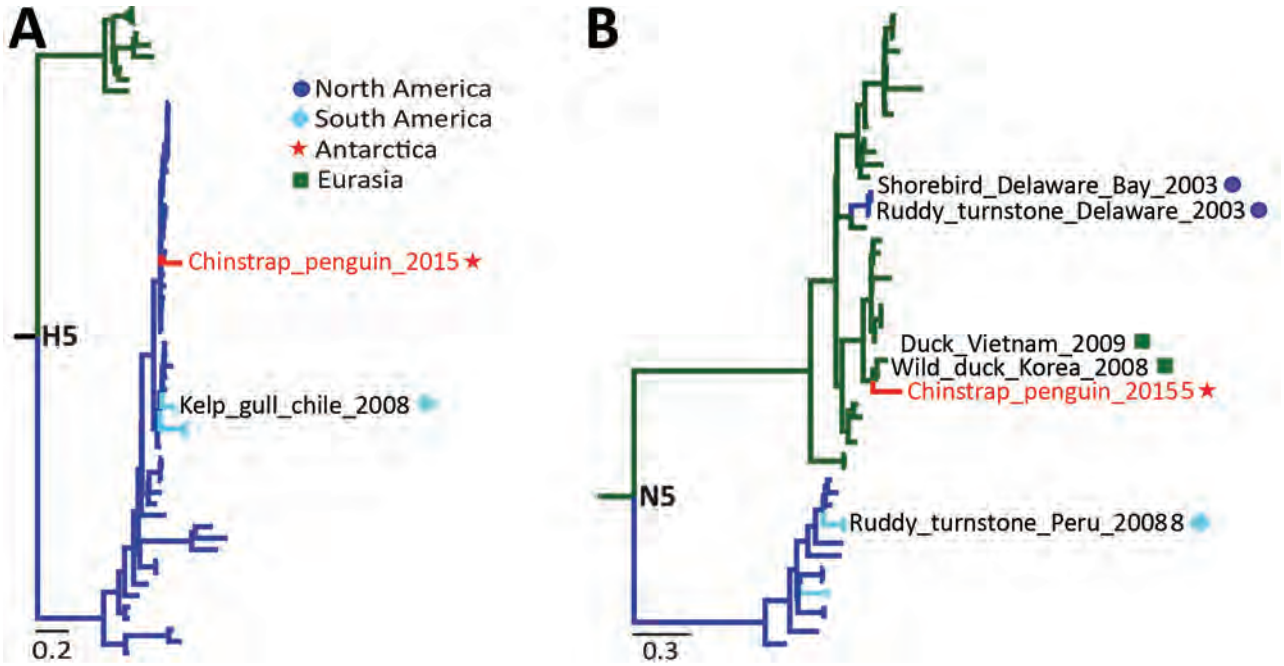

Figure. Low pathogenicity avian influenza virus (AIV) (H5N5) found in Antarctic penguin. A) Phylogenetic analysis of the HA gene showing its relationship to H5 low pathogenicity North American lineage viruses. B) Phylogenic analysis of the NA gene showing its relationship to N5 viruses from Eurasia. Antarctic strains: red lines, stars; Eurasian strains: green lines, squares; North American strains: dark blue lines, circles; South American strains: light blue lines, diamonds. Sequences were selected from public databases to cover a wide diversity of AIV strains from different years and geographic locations and aligned with MUSCLE (http://www.drive5.com/muscle/). The maximum-likelihood trees of 325 HA and 319 NA nucleotide sequences were constructed with MEGA6 (http://www.megasoftware.net) and IQ-TREE on the IQ-TREE web server (http://www.cibiv.at/software/iqtree/) by using the maximum-likelihood method with 1,000 ultrafast bootstrap replicates. Summarized trees are shown for the H5 and N5 clusters. Further details are provided in online Technical Appendix Figures 2, 3 (http://wwwnc.cdc.gov/EID/article/22/12/16-1076-Techapp1.pdf)**.** The best-fit model of substitution was found by using the auto function on the IQ-TREE web server and Akaike information criterion. Scale bars indicate nucleotide substitutions per site. AIV, avian influenza virus; HA, hemagglutinin; NA, neuraminidase.

into a clade within the H5 American LPAIV lineage, clustering with AIVs isolated from ducks in the United States during 2007–2014 and blue-winged teals from Guatemala in 2010 (online Technical Appendix Figure 2). This finding suggests a possible introduction of this H5 AIV into Antarctica via the Pacific or the Mississippi–American flyways, although we cannot rule out that this H5 strain is endemic to other South America locations.

The timing of arrival of migratory birds that breed in Antarctica (e.g., skua, shags, petrel, and gulls) overlaps with that of the penguins as they return to colonies for breeding and nesting during the summer in the Southern Hemisphere. These birds share a habitat, enabling close contact (*5*,*8*) and introducing the possibility of AIV spillover from flying birds to penguins. The chinstrap penguin H5 strain also clustered near the H5 strain isolated in 2008 from a kelp gull (*Larus dominicanus*) in Chile (*9*), indicating a potential route of transmission and introduction of AIV into Antarctic penguins (Figure, panel A). Kelp gull colonies are found in the Antarctic, the sub-Antarctic territory, and along the coastline of Chile and Argentina. Hence, gulls and other intermediate vector hosts, such as the south polar skua (*Stercorarius maccormicki*), might represent natural reservoirs that play a role in the introduction and maintenance of AIVs into Antarctica.

The chinstrap penguin neuraminidase segment clustered within a Eurasian N5 clade that includes sequences from 2001–2010 (Figure, panel B; online Technical Appendix Figure 3). The closest sequences were isolated from wild ducks from South Korea in 2008 (GenBank accession no. JX679163) and Vietnam in 2009 (GenBank accession no. AB593481). Eurasian N5s have sporadically been found in ruddy turnstones (*Arenaria interpres*) and an unidentified shore bird at Delaware Bay (GenBank accession nos. CY144466.1, CY144458.1, and CY102738.1). This finding suggests a plausible entryway of this gene into Antarctica from South America through the Atlantic or Pacific-American flyway, which are common routes used by shore birds, such as the ruddy turnstone, white-rumped sandpiper (*Calidris fuscicollis*), and red knot (*Calidris canutus*) (*10*).

As previously suggested for H11N2 viruses from Antarctica, our data supports the idea that these AIVs are

evolutionarily distinct from other AIVs (*5*). This H5N5 strain is a contemporary reassortant virus related to North American and Eurasian strains.

The positive animals we identified originated from a single location on the Antarctic Peninsula, which suggests recent introduction of this AIV H5N5 in the colonies sampled. Antarctica is refuge for most penguin colonies, including the near-threatened emperor penguins. Previous reports suggested that AIV could have caused Adélie penguin chick death (*3*). Four positive samples (including the sequenced virus) were obtained from juvenile chinstrap penguins that were weak, depressed, and possibly ill (i.e., they had ruffled feathers, lethargy, and impaired movement). Thus, additional studies are warranted to assess the health and conservation status of resident bird species and potential pathologic effects of AIV.

These data provide novel insights on the ecology of AIV in Antarctica. Our findings also highlight the need for increased surveillance to understand virus diversity on this continent and its potential contribution to the genetic constellation of AIV in the Americas.

Acknowledgments

We are grateful to K. Tapia, who was an excellent and invaluable technical assistance during the course of this study. We also thank the Instituto Antartico Chileno (INACH) staff for all their support during the expeditions to Antarctica.

This study was partly funded by the Center for Research in Influenza Pathogenesis (CRIP), a National Institute of Allergy and Infectious Diseases–funded Center of Excellence in Influenza Research and Surveillance (CEIRS), contract number HHSN272201400008C to R.A.M., and by the Programa de Investigación Asociativa from the Comisión Nacional de Investigación Científica y Tecnológica, project CONICYT-PIA Anillo1408 to R.A.M., F.T.P., and V.N. D.G.-A. is supported by grant RT_12-13, and M.C.-S.M. is supported by the grant RT_08-13, both awarded from INACH. G.P.B is supported by the Fondo Nacional de Desarrollo Científica y Techológica (FONDECYT) de Postdoctorado 3150564 from CONICYT, and D. B.-B. is supported by Vicerrectoría de Investigación y Estudios Avanzados-Pontificia Universidad Católica de Valparaíso.

References

1. Austin FJ, Webster RG. Evidence of ortho- and paramyxoviruses in fauna from Antarctica. J Wildl Dis. 1993;29:568–71. http://dx.doi.org/10.7589/0090-3558-29.4.568
2. Baumeister E, Leotta G, Pontoriero A, Campos A, Montalti D, Vigo G, et al. Serological evidences of influenza A virus infection in Antarctica migratory birds. Int Congr Ser. 2004;1263:737–40. http://dx.doi.org/10.1016/j.ics.2004.02.099
3. Morgan IR, Westbury HA. Virological studies of Adelie penguins (*Pygoscelis adeliae*) in Antarctica. Avian Dis. 1981;25:1019–26. http://dx.doi.org/10.2307/1590077
4. Wallensten A, Munster VJ, Osterhaus AD, Waldenstr J, Bonnedahl J, Broman T, et al. Mounting evidence for the presence of influenza A virus in the avifauna of the Antarctic region. Antarct Sci. 2006;18:353–6. http://dx.doi.org/10.1017/S095410200600040X
5. Hurt AC, Vijaykrishna D, Butler J, Baas C, Maurer-Stroh S, Silva-de-la-Fuente MC, et al. Detection of evolutionarily distinct avian influenza A viruses in Antarctica. MBio. 2014;5:e01098-14. http://dx.doi.org/10.1128/mBio.01098-14
6. Spackman E, Senne DA, Myers TJ, Bulaga LL, Garber LP, Perdue ML, et al. Development of a real-time reverse transcriptase PCR assay for type A influenza virus and the avian H5 and H7 hemagglutinin subtypes. J Clin Microbiol. 2002;40:3256–60. http://dx.doi.org/10.1128/JCM.40.9.3256-3260.2002
7. Senne DA, Panigrahy B, Kawaoka Y, Pearson JE, Süss J, Lipkind M, et al. Survey of the hemagglutinin (HA) cleavage site sequence of H5 and H7 avian influenza viruses: amino acid sequence at the HA cleavage site as a marker of pathogenicity potential. Avian Dis. 1996;40:425–37. http://dx.doi.org/10.2307/1592241
8. Fretwell PT, Trathan PN. Penguins from space: faecal stains reveal the location of emperor penguin colonies. Global Ecology and Biogeography. 2009 [cited 2016 Sep 8]. http://onlinelibrary.wiley.com/doi/10.1111/j.1466-8238.2009.00467.x/abstract
9. Mathieu C, Moreno V, Pedersen J, Jeria J, Agredo M, Gutiérrez C, et al. Avian influenza in wild birds from Chile, 2007─2009. Virus Res. 2015;199:42–5. http://dx.doi.org/10.1016/j.virusres.2015.01.008
10. Krauss S, Stallknecht DE, Negovetich NJ, Niles LJ, Webby RJ, Webster RG. Coincident ruddy turnstone migration and horseshoe crab spawning creates an ecological 'hot spot' for influenza viruses. Proc Biol Sci. 2010;277:3373–9. http://dx.doi.org/10.1098/rspb.2010.1090

Address for correspondence: Rafael A. Medina, Department of Pediatric Infectious Diseases and Immunology, Escuela de Medicina, Pontificia Universidad Católica de Chile, Marcoleta 391, Santiago, Chile; email: rmedinas@med.puc.cl

Pathogenic Lineage of *mcr*-Negative Colistin-Resistant *Escherichia coli*, Japan, 2008–2015

Toyotaka Sato, Akira Fukuda, Yuuki Suzuki, Tsukasa Shiraishi, Hiroyuki Honda, Masaaki Shinagawa, Soh Yamamoto, Noriko Ogasawara, Masaru Usui, Hiroki Takahashi, Satoshi Takahashi, Yutaka Tamura, Shin-ichi Yokota

Author affiliations: Sapporo Medical University School of Medicine, Sapporo, Japan (T. Sato, Y. Suzuki, T. Shiraishi, H. Honda, S. Yamamoto, N. Ogasawara, H. Takahashi, S. Takahashi, S. Yokota); Rakuno Gakuen University, Ebetsu, Japan (A. Fukuda, M. Usui, Y. Tamura); Sapporo Medical University Hospital, Sapporo (M. Shinagawa)

DOI: http://dx.doi.org/10.3201/eid2212.161117

To the Editor: Colistin is a last-line drug for treatment of multidrug-resistant, gram-negative bacterial infections, including those caused by *Escherichia coli*. We report colistin-resistant *E. coli* isolates from Japan, including a global-spreading pathogenic lineage, serotype O25b:H4, sequence type (ST) 131, and subclone *H*30-R (O25b:H4-ST131-*H*30R).

We tested 514 *E. coli* isolates obtained from clinical specimens taken at Sapporo Clinical Laboratory Inc. (Sapporo, Japan) and Sapporo Medical University Hospital in Japan during 2008–2009 (*1*) and 2015, respectively. Samples were processed according to Clinical and Laboratory Standards Institute guidelines (*2*). Identification of O25b:H4-ST131, O25b, H4, and ST131 were determined as described previously (*1*). For identification of the *H*30Rx subclone of O25b:H4-ST131, *H*30 was determined by PCR using a specific primer set (*3*), R was determined according to ciprofloxacin MIC, and x was determined by detecting 2 single-nucleotide polymorphisms, as previously described (*4*).

Four *E. coli* isolates exceeded the colistin resistance breakpoint (>2 mg/mL) (Table). None of the patients from whom the *E. coli* isolates were derived had a history of colistin treatment. Three of the 4 colistin-resistant isolates belonged to a pandemic lineage, O25b:H4-ST131-*H*30R, which has been isolated from urinary tract and bloodstream infections (*3*,*4*). The frequency of colistin-resistant ST131 *E. coli* isolates among O25b:H4-ST131 was 2.2%. This lineage is fluoroquinolone resistant and is frequently resistant to β-lactams because it possesses CTX-M–type extended-spectrum β-lactamase genes (*1*,*3*,*4*).

The colistin-resistant isolates reported were resistant to fluoroquinolones, and 1 (SME296) was resistant to cephalosporins (due to expression of $bla_{\text{CTX-M-14}}$). Another colistin-resistant *E. coli* isolate (SME222) belonged to O18-ST416, which is also known as an extraintestinal pathogenic *E. coli* (*5*), although this lineage has not previously been reported to exhibit colistin resistance.

The colistin-resistant *E. coli* isolates we identified were sensitive to carbapenems and aminoglycosides, including amikacin, whereas previously it was reported that some *E. coli* ST131 isolates exhibited resistance to carbapenems by possessing carbapenemases, such as NDM-1 and KPC-2; the NDM-1–possessing ST131 isolate also exhibited resistance to amikacin (*6*,*7*). Thus, these findings may affect future antimicrobial choices because of the clonal dominance, multidrug resistance, and pathogenicity of the isolates.

Recent studies reported a plasmid-mediated colistin resistance gene, *mcr-1*, in various countries (*8*). In addition, a novel plasmid-mediated colistin resistance gene, *mcr-2* (76.7% nucleotide identity to *mcr-1*), was found in *E. coli* isolates in Belgium (*9*). These genes encode a phosphoethanolamine transferase family protein, which modifies the lipid A component of lipopolysaccharide (*8*,*9*). The colistin-resistant *E. coli* isolates we identified did not possess *mcr-1*or *mcr-2*, although the MICs for colistin were the same as or higher than that of the transconjugant of a *mcr-1*–harboring plasmid in an *E. coli* ST131 isolate (4 mg/L) reported by Liu et al. (*8*). Thus, these colistin-resistant isolates may have other colistin resistance mechanisms. For example, modification of lipid A with 4-amino-4-deoxy-L-arabinose or phosphoethanolamine, caused by chromosomal mutations in *mgrB*, *phoPQ*, and *pmrAB* genes, might occur and could be responsible for the resistance. This polymyxin-resistance mechanism is seen in *Enterobacteriaceae*; however, other novel mechanisms are also conceivable.

In conclusion, we report colistin resistance in a major global-spreading extraintestinal pathogenic *E. coli* strain, O25b:H4-ST131-*H*30R, in Japan. This strain acquired colistin resistance without carrying a plasmid bearing the *mcr* gene. Clarifying the colistin-resistance mechanisms in these isolates is necessary if we are to forestall the emergence of multidrug (including

Table. Characterization of colistin-resistant *Escherichia coli* isolates, Japan, 2008–2105*

Strain	Specimen type	Patient age, y/sex	Year	Serotype	ST	MIC, mg/L†									
						PIP	CAZ	CPD	FEP	IPM	GEN	AMK	CIP	CST	PMB
SRE34	Urine catheter	UNK/F	2008	O25b:H4	131-H30Rx	128 (R)	1 (S)	1 (S)	0.06 (S)	0.12 5 (S)	0.5 (S)	2 (S)	32 (R)	16 (R), 16 (R)‡	8, 8‡
SRE44	Urine catheter	UNK/M	2008	O25b:H4	131-H30Rx	64 (R)	2 (S)	1 (S)	0.13 (S)	0.25 (S)	0.5 (S)	1 (S)	64 (R)	16 (R), 16 (R)‡	16, 8‡
SME222	Indwelling pericardial drain	76/M	2015	O18	416	2 (S)	0.5 (S)	0.5 (S)	<0.0 3 (S)	0.13 (S)	0.5 (S)	2 (S)	0.03 (S)	4 (R), 4 (R)‡	8, 4‡
SME296	Urine	67/M	2015	O25b:H4	131-H30R	>128 (R)	32 (R)	>128 (R)	16 (R)	0.13 (S)	0.5 (S)	2 (S)	64 (R)	4 (R), 8 (R)‡	1, 4‡

*All isolates were phylogentic group B2. AMK, amikacin; CAZ, ceftazidime; CIP, ciprofloxacin; CPD, cefpodoxime; FEP, cefepime; CST, colistin; GEN, gentamicin; IPM, imipenem; PIP, piperacillin; PMB, polymyxin B; R, resistant; S, susceptible; ST, sequence type; UNK, unknown.
†EUCAST (http://www.eucast.org/) breakpoints were used for resistance determination because the colistin breakpoint for *E. coli* was undetermined by the Clinical and Laboratory Standards Institute. MICs were determined by the agar dilution method unless otherwise stated. Breakpoints: PIP, >16; CAZ, >16; CPD, >1; FEP, >4; IPM, >8; GEN, >4; AMK, >16; CIP, >1; CST, >2.
‡Broth microdilution method.

colistin)–resistant O25b:H4-ST131-*H*30R. The worst-case scenario is the global spread of this isolate, which has acquired resistance to the last-line antimicrobial drug, colistin.

Acknowledgments

We thank Osamu Kuwahara for providing some of the *E. coli* clinical isolates.

This study was partly supported by grants from JSPS KAKENHI (grant nos. 15H06521 and 25861574) and the Yuasa Memorial Foundation.

References

1. Yokota S, Sato T, Okubo T, Ohkoshi Y, Okabayashi T, Kuwahara O, et al. Prevalence of fluoroquinolone-resistant *Escherichia coli* O25:H4-ST131 (CTX-M-15-nonproducing) strains isolated in Japan. Chemotherapy. 2012;58:52–9. http://dx.doi.org/10.1159/000336129
2. Clinical and Laboratory Standards Institute. Performance standards for antimicrobial susceptibility testing (M100-S25). Wayne (PA): The Institute; 2015.
3. Colpan A, Johnston B, Porter S, Clabots C, Anway R, Thao L, et al.; VICTORY (Veterans Influence of Clonal Types on Resistance: Year 2011) Investigators. *Escherichia coli* sequence type 131 (ST131) subclone *H*30 as an emergent multidrug-resistant pathogen among US veterans. Clin Infect Dis. 2013;57:1256–65. http://dx.doi.org/10.1093/cid/cit503
4. Price LB, Johnson JR, Aziz M, Clabots C, Johnston B, Tchesnokova V, et al. The epidemic of extended-spectrum-β-lactamase-producing *Escherichia coli* ST131 is driven by a single highly pathogenic subclone, *H*30-Rx. mBio. 2013;4: e00377–13. http://dx.doi.org/10.1128/mBio.00377-13
5. Lau SH, Reddy S, Cheesbrough J, Bolton FJ, Willshaw G, Cheasty T, et al. Major uropathogenic *Escherichia coli* strain isolated in the northwest of England identified by multilocus sequence typing. J Clin Microbiol. 2008;46:1076–80. http://dx.doi.org/10.1128/JCM.02065-07
6. Peirano G, Schreckenberger PC, Pitout JD. Characteristics of NDM-1-producing *Escherichia coli* isolates that belong to the successful and virulent clone ST131. Antimicrob Agents Chemother. 2011;55:2986–8. http://dx.doi.org/10.1128/AAC.01763-10
7. Morris D, Boyle F, Ludden C, Condon I, Hale J, O'Connell N, et al. Production of KPC-2 carbapenemase by an *Escherichia coli* clinical isolate belonging to the international ST131 clone. Antimicrob Agents Chemother. 2011;55:4935–6. http://dx.doi.org/10.1128/AAC.05127-11
8. Liu YY, Wang Y, Walsh TR, Yi LX, Zhang R, Spencer J, et al. Emergence of plasmid-mediated colistin resistance mechanism MCR-1 in animals and human beings in China: a microbiological and molecular biological study. Lancet Infect Dis. 2016;16:161–8. http://dx.doi.org/10.1016/S1473-3099(15)00424-7
9. Xavier BB, Lammens C, Ruhal R, Kumar-Singh S, Butaye P, Goossens H, et al. Identification of a novel plasmid-mediated colistin-resistance gene, *mcr-2*, in *Escherichia coli*, Belgium, 2016. Euro Surveill. 2016;21. http://dx.doi.org/10.2807/1560-7917.ES.2016.21.2730280

Address for correspondence: Toyotaka Sato, Department of Microbiology, Sapporo Medical University School of Medicine, S1 W17, Chuo-ku, Sapporo, 060–8556, Japan; email: sato.t@sapmed.ac.jp

Dual Emergence of Usutu Virus in Common Blackbirds, Eastern France, 2015

Sylvie Lecollinet, Yannick Blanchard, Christine Manson, Steeve Lowenski, Eve Laloy, Hélène Quenault, Fabrice Touzain, Pierrick Lucas, Cyril Eraud, Céline Bahuon, Stéphan Zientara, Cécile Beck, Anouk Decors

Author affiliations: ANSES Animal Health Laboratory of Maisons-Alfort, Maisons-Alfort, France (S. Lecollinet, S. Lowenski, C. Bahuon, S. Zientara, C. Beck); ANSES Ploufragan, Ploufragan, France (Y. Blanchard, H. Quenault, F. Touzain, P. Lucas); Departmental Veterinary Laboratory of Haut-Rhin (LVD68), Colmar, France (C. Manson); ENVA, Maisons-Alfort (E. Laloy); ONCFS, Paris, France (C. Eraud, A. Decors)

DOI: http://dx.doi.org/10.3201/eid2212.161272

To the Editor: Usutu virus (USUV) is a mosquito-borne flavivirus amplified in an enzootic cycle involving passeriform and strigiform birds as reservoir hosts and *Culex* mosquitos as vectors (*1*). Although originating from Africa, USUV has been introduced at least twice into central and western Europe, leading to substantial bird fatalities in central Europe (particularly in Austria, Hungary, Italy, Germany, and Switzerland) since 1996 (*2*). Its zoonotic potential has been recently highlighted in Italy in immunosuppressed patients who sought treatment for encephalitis (*3*).

Even though every country bordering France, apart from Luxembourg, has reported USUV in mosquitoes or wild birds recently, USUV outbreaks had not been reported in France, and only indirect evidence indicated circulation of USUV-like viruses in Eurasian magpies (*Pica pica*) in southeastern France (*4*). In 2015, the French event-based surveillance network SAGIR (*5*) reported increased fatalities of common blackbirds (*Turdus merula*) in 2 departments in eastern France, Haut-Rhin near the German border and Rhône (Figure). Five birds, 2 in Haut-Rhin and 3 in Rhône, were subjected to molecular detection for flaviviruses. During necropsy, their brains, hearts, livers, and kidneys (from 2 birds only) were sampled for RNA extraction and virus isolation. Tissues were homogenized in DMEM with ceramic beads (Qbiogen) and FastPrep ribolyzer (ThermoSavant). Total RNA was extracted with RNeasy kit (Qiagen) and flavivirus genomic RNA was amplified by conventional reverse transcription PCR with all of the tissues from 2 birds in Haut-Rhin that were found dead on August 5–10, 2015, and from 1 bird sampled on September 23 in Rhône (*6*). USUV was systematically identified in blackbird tissues

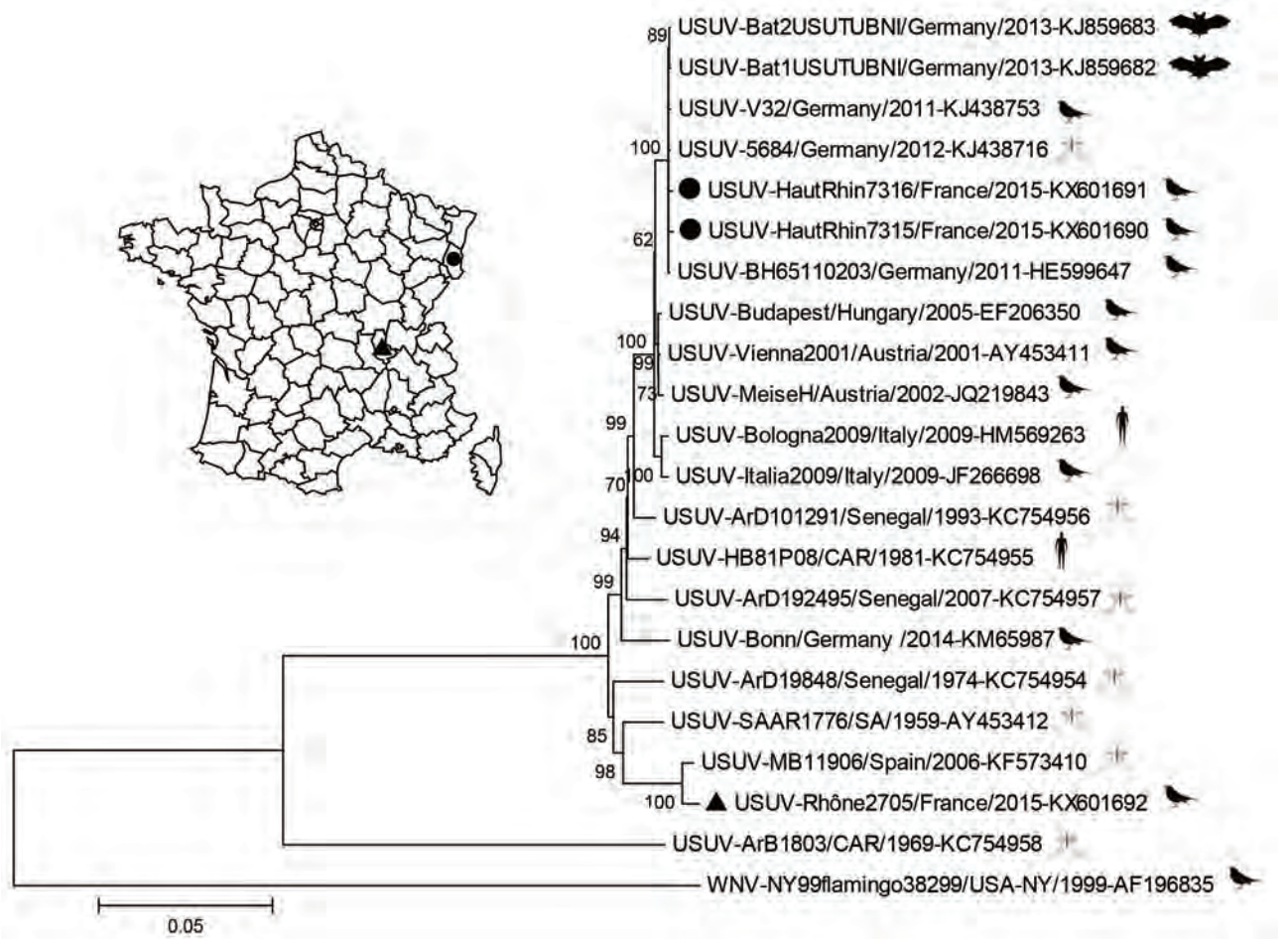

Figure. Phylogeny of Usutu virus (USUV) Haut-Rhin strains (black circles) and Rhône strain (black triangle), isolated in 2015 in eastern France compared with reference strains. Inset map shows locations where isolates were obtained. The strains from France are genetically distinct, with a homology of 95.7% at the nucleotide level and 98.8% (3,392–3 aa/3,434 aa) at the amino acid level. The evolutionary history was inferred by using the neighbor-joining method. The optimal tree with the sum of branch length 0.60224968 is shown. The percentage of replicate trees in which the associated taxa clustered together in the bootstrap test (1,000 replicates) are shown at the nodes. Evolutionary analyses were conducted in MEGA6 (http://www.megasoftware.net), and the evolutionary distances were computed by using the Jukes-Cantor method. The resulting tree is drawn to scale, with branch lengths in the units of number of base substitutions per site. The analysis involved 22 strains, including West Nile virus (WNV) as the root; GenBank accession numbers are indicated. All positions containing gaps and missing data were not included; 10,684 positions were included in the final dataset. An outline of the organism from which the virus was isolated (bat, bird, mosquito, or human) is placed next to the strain name. Scale bar indicates substitutions per site.

by Sanger sequencing of the 1085-nt PCR fragment and BLAST analysis (https://blast.ncbi.nlm.nih.gov). Three USUV isolates were obtained after 2–3 passages in Vero cells, and whole-genome sequencing of every isolate was performed as previously described (*7*). Postmortem examination revealed hepatomegaly and splenomegaly in a USUV-infected blackbird and marked emaciation and kidney hemorrhages in another infected animal. A subset of samples was submitted for histologic analysis, but no microscopic lesions were found in any of the 3 USUV-positive blackbirds, suggesting that infection was hyperacute.

Phylogenetic analysis of the whole genome for the 3 USUV isolates demonstrated close genetic relatedness between USUV isolates from Haut-Rhin, France, and Germany (99.8% nucleotide identity with USUV-5684/Germany/2011, GenBank accession no. KJ438716) and between strains from Rhône, France, and Spain (99.2% identity with USUV-MB11906/Spain/2006, GenBank accession no. KF573410). Results showed that French USUV strains from Haut-Rhin and Rhône departments were clearly distinct from each other (95.7% nucleotide identity) and arose from ≥2 independent introduction events. In total, 41–42 nonsynonymous mutations were identified along

the 3,434-aa long polyprotein, with capsid, nonstructural protein 2A, and nonstructural protein 4B having the highest nonsynonymous substitution rates of 96.0% (121/126), 97.4% (221/227), and 97.8% (311/318), respectively.

Symptomatic USUV infections were discovered in wild birds in France, indicating the emergence of USUV in counties in eastern France. Unusual and grouped bird fatalities observed in August and September 2015 in common blackbirds in Haut-Rhin and Rhône did not seem to alter blackbird population dynamics (data not shown). The viral strain recovered in Haut-Rhin, which borders Germany, is genetically similar to USUV strains isolated in central Europe, in particular in southwestern Germany in 2011. Such a finding further exemplifies the continuing and gradual diffusion of the Vienna USUV strain since 2001 (Austria in 2001, Hungary in 2005, Italy and Switzerland in 2006, Germany and Czech Republic in 2011, and Belgium in 2012) (*1*). The USUV strain isolated from the 1 blackbird in Rhône shared the highest genetic homology with USUV strains identified on 2 occasions in Spain: once in 2006 in Catalonia from *C. pipiens* mosquitoes and once in 2009 in Andalusia from *C. perexiguus* mosquitoes (*8*).

Our findings indicate that the USUV/Spain strain can be pathogenic in birds. Symptomatic USUV infections in wild avifauna are difficult to quantify (because of low reporting rates and quick removal of dead birds by scavengers), and dynamic modeling of USUV in Austria indicated that a low proportion (0.2%) of USUV-killed birds had been effectively detected by USUV-specific surveillance programs (*9*). Mutations between USUV-Rhône2705/France/2015 and USUV-MB11906/Spain could also account for differential virulence in birds. These 2 strains differed by 14 nonsynonymous mutations (online Technical Appendix Table, http://wwwnc.cdc.gov/EID/article/22/12/16-1272-Techapp1.pdf). Although little is known about molecular determinants of USUV virulence, one can try to infer the importance of these mutations from data gained from studies on a closely related flavivirus, West Nile virus. In this respect, none of the 14 mutations observed have been found to be critical in flavivirus virulence.

Concomitantly with USUV emergence in France, another *Culex*-borne flavivirus, West Nile virus, has reemerged in southeastern France (*10*). Climatic and environmental conditions during the summer of 2015 seem to have promoted the spread of *Culex*-borne pathogens. However, risk factors for flavivirus emergence in France in 2015 have not been comprehensively analyzed.

Acknowledgments

We are grateful to Eliette Gretillat and the whole team at the veterinary laboratory of Haut-Rhin department for processing bird samples. We are grateful to the technicians of the Hunting Federation and of the National Hunting and Wildlife Agency for their contribution to wildlife surveillance.

This work was partially supported by the European Union Horizon 2020 Framework Program for Research and Innovation under grant agreement no. 643476 (COMPARE).

References

1. Ashraf U, Ye J, Ruan X, Wan S, Zhu B, Cao S. Usutu virus: an emerging flavivirus in Europe. Viruses. 2015;7:219–38. http://dx.doi.org/10.3390/v7010219
2. Weissenböck H, Bakonyi T, Rossi G, Mani P, Nowotny N. Usutu virus, Italy, 1996. Emerg Infect Dis. 2013;19:274–7. http://dx.doi.org/10.3201/eid1902.121191
3. Vazquez A, Jimenez-Clavero M, Franco L, Donoso-Mantke O, Sambri V, Niedrig M, et al. Usutu virus: potential risk of human disease in Europe. Euro Surveill. 2011;16:19935.
4. Vittecoq M, Lecollinet S, Jourdain E, Thomas F, Blanchon T, Arnal A, et al. Recent circulation of West Nile virus and potentially other closely related flaviviruses in southern France. Vector Borne Zoonotic Dis. 2013;13:610–3. http://dx.doi.org/10.1089/vbz.2012.1166
5. Decors A, Hars J, Faure E, Quintaine T, Chollet J, Rossi S. Le réseau Sagir: un outil de vigilance vis-à-vis des agents pathogènes exotiques [in French]. Bulletin épidémiologique santé animale-alimentation. 2014;66:35–9. [cited 2016 Sep 28]. http://bulletinepidemiologique.mag.anses.fr/sites/default/files/BEP-mg-BE66-art10_0.pdf
6. Weissenböck H, Kolodziejek J, Url A, Lussy H, Rebel-Bauder B, Nowotny N. Emergence of Usutu virus, an African mosquito-borne flavivirus of the Japanese encephalitis virus group, central Europe. Emerg Infect Dis. 2002;8:652–6. http://dx.doi.org/10.3201/eid0807.020094
7. Grasland B, Bigault L, Bernard C, Quenault H, Toulouse O, Fablet C, et al. Complete genome sequence of a porcine epidemic diarrhea S gene indel strain isolated in France in December 2014. Genome Announc. 2015;3:e00535-15. http://dx.doi.org/10.1128/genomeA.00535-15
8. Bakonyi T, Busquets N, Nowotny N. Comparison of complete genome sequences of Usutu virus strains detected in Spain, central Europe, and Africa. Vector Borne Zoonotic Dis. 2014;14:324–9. http://dx.doi.org/10.1089/vbz.2013.1510
9. Rubel F, Brugger K, Hantel M, Chvala-Mannsberger S, Bakonyi T, Weissenböck H, et al. Explaining Usutu virus dynamics in Austria: model development and calibration. Prev Vet Med. 2008;85:166–86. http://dx.doi.org/10.1016/j.prevetmed.2008.01.006
10. Bahuon C, Marcillaud-Pitel C, Bournez L, Leblond A, Beck C, Hars J, et al. West Nile virus epizootics in Camargue, France, in 2015, and reinforcement of West Nile virus surveillance and control networks. Paris: World Organisation for Animal Health; 2016 [cited 2016 Sep 28]. http://www.oie.int/fileadmin/Home/eng/Publications_%26_Documentation/docs/pdf/bulletin/Bull_2016-1-ENG.pdf

Address for correspondence: Sylvie Lecollinet, ANSES Laboratoire de santé animale de Maisons-Alfort, 14 rue Pierre et Marie Curie, Maisons-Alfort 94701, France; email: sylvie.lecollinet@anses.fr

Zika Virus Infection in the Central Nervous System and Female Genital Tract

Emanuele Nicastri, Concetta Castilletti, Pietro Balestra, Simonetta Galgani, Giuseppe Ippolito

Author affiliations: National Institute for Infectious Diseases Lazzaro Spallanzani, Rome, Italy (E. Nicastri, C. Castilletti, P. Balestra, G. Ippolito); Azienda Ospedaliera San Camillo-Forlanini, Rome (S. Galgani)

DOI: http://dx.doi.org/10.3201/eid2212.161280

To the Editor: On April 9, 2016, a 32-year-old woman from Italy traveled to Santo Domingo in the Dominican Republic. She worked as a volunteer nurse in the outpatient clinic of a primary school of a nongovernmental organization based in Italy. She returned to Italy on April 17. She did not have sexual intercourse during her stay abroad.

On April 26, she was referred to the travel clinic of the National Institute for Infectious Diseases Lazzaro Spallanzani in Rome for a febrile syndrome with rash, generalized headache, and weakness, which started on April 21. Approximately 24 hours later, she was admitted to the institute's medical facility for a suspected neurologic involvement. At admission, she had abnormal gait, strong asthenia, and a disseminated pruritic rash on her face, abdomen, chest, and arms, but she did not have a fever.

During physical examination, the patient was alert and fully oriented. Temperature was 36.9°C, pulse rate 90 beats/min, blood pressure 100/60 mm Hg, and respiratory rate 20 breaths/min. She had a diffuse erythematous macular rash and bilateral nonpurulent conjunctival hyperemia without meningeal signs. Findings of a neurologic examination of the upper limbs were within reference ranges.. Muscular strength was reduced in both legs (left > right), whereas tendon reflexes and all sensory modalities were within reference ranges. Results of a contrast-enhanced magnetic resonance imaging of the brain and spinal cord (on day 7), nerve conduction studies

etymologia

Usutu [*oo-soo'too*] virus

Usutu virus, named for the Usutu River in Swaziland, is a mosquito-borne flavivirus closely related to Japanese encephalitis virus, West Nile virus, Murray Valley encephalitis virus, and St. Louis encephalitis virus. Usutu virus was first isolated in 1959 from *Culex neavei* mosquitoes in South Africa. The first recognized infection in a human was in an African man with fever and rash in 1959 but was not reported until 1981.

In 2001, Usutu virus emerged in Europe, when it was identified as the etiologic agent of bird—mainly blackbird—mortality. Retrospective analysis of archived tissue samples from wild bird deaths in the Tuscany region of Italy in 1996, however, revealed an earlier introduction of the virus to Europe. It was not thought to be associated with severe or fatal disease in humans until a neuroinvasive infection was reported to have occurred in an Italian woman in 2009.

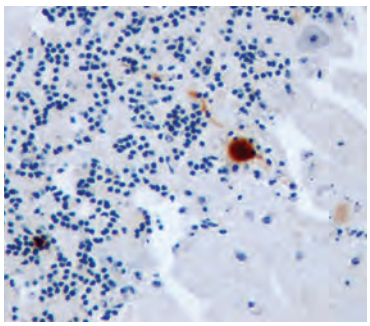

Immunohistochemical staining for Usutu virus antigen in a Purkinje cell of the cerebellum of a song thrush that died of encephalitis. Original magnification ×400.

Sources

1. Ashraf U, Ye J, Ruan X, Wan S, Zhu B, Cao S. Usutu virus: an emerging flavivirus in Europe. Viruses. 2015;7:219–38. http://dx.doi.org/10.3390/v7010219
2. Pecorari M, Longo G, Gennari W, Grottola A, Sabbatini A, Tagliazucchi S, et al. First human case of Usutu virus neuroinvasive infection, Italy, August–September 2009. Euro Surveill. 2009;14:19446.
3. Weissenböck H, Bakonyi T, Rossi G, Mani P, Nowotny N. Usutu virus, Italy, 1996. Emerg Infect Dis. 2013;19:274–7. http://dx.doi.org/10.3201/eid1902.121191
4. Weissenböck H, Kolodziejek J, Url A, Lussy H, Rebel-Bauder B, Nowotny N. Emergence of Usutu virus, an African mosquito-borne flavivirus of the Japanese encephalitis virus group, central Europe. Emerg Infect Dis. 2002;8:652–6. http://dx.doi.org/10.3201/eid0807.020094

Address for correspondence: Ronnie Henry, Centers for Disease Control and Prevention, 1600 Clifton Rd NE, Mailstop E03, Atlanta, GA 30329-4027, USA; email: boq3@cdc.gov

DOI: http://dx.doi.org/10.3201/eid2212.ET2212

and electromyography (on day 8), and an electroencephalogram (on day 16) were within reference ranges. A lumbar puncture (on day 7) showed normal cell counts (<10 cells/mL), a normal glycorrachia/glycemia ratio (>0.5), and a slight increase in protein concentration (0.48 g/L [reference range 0.32–0.80 g/L]) in cerebrospinal fluid. Complete neuropsychologic examinations (on days 9 and 10) showed mild deficits in attention and mental processing speed and mental flexibility and moderate deficits in verbal and nonverbal memory tasks (online Technical Appendix, http://wwwnc.cdc.gov/EID/article/22/12/16-1280- Techapp1.pdf).

Real-time reverse transcription PCR (rRT-PCR) results for dengue viruses 1–4 and chikungunya virus were negative in serum and cerebrospinal fluid (CSF), whereas Zika virus RNA was detected in serum (day 6), urine (up to day 27), CSF (day 7), saliva (up to day 13), and vaginal swab (up to day 13) (online Technical Appendix). Specific dengue and chikungunya IgG and IgM were not detected in serum and CSF. Zika virus IgM was detected in serum starting on day 6. Zika virus–specific antibodies in serum were confirmed by microneutralization assay (Table).

Starting on day 7, intravenous polyvalent immunoglobulins were administered (0.4 g/kg/day for 5 days); no adverse events were observed. A second neuropsychologic examination was performed on day 16 and indicated persistent impairment in memory performances and an improvement in mental concentration and flexibility tasks (online Technical Appendix).

A second lumbar puncture (on day 17) showed an increased cell count (70 cells/mL, mostly lymphocytes), and CSF was negative for Zika virus RNA by rRT-PCR. The patient was discharged on day 20; she showed a progressive neurologic recovery starting on day 16. At 60-days follow-up visit, no neurologic deficits were reported.

During the 2013–2014 outbreak of Zika virus in French Polynesia and in the context of the 2015–2016 Zika virus circulation (*1*), an apparent increase in Guillain-Barré syndrome incidence was reported. Few anecdotal cases of encephalopathy in patients with Zika virus infection have been recently described in affected countries: 1 case in a man on a 4-week cruise through an area in the South Pacific that included New Caledonia, Vanuatu, the Solomon Islands, and New Zealand in 2015 (*2*); and 2 cases in Martinique (*3*) in February 2016. Recently, Zika virus has been detected in the genital tract of a virus-infected woman after Zika virus had disappeared from blood and urine (*4*), and a suspected case of Zika virus by sexual transmission from a woman to a man has been reported in New York City (*5*).

In our patient, Zika virus RNA was found in different systems, including the central nervous system and the genital tract. Recently, a mouse model of Zika virus infection by vaginal exposure demonstrated that Zika virus replicated within the genital mucosa, persisted postinfection, and was detected in the fetal brain of the mice (*6*). In our case, the patient reported early neurologic symptoms and moderate memory impairment in neuropsychologic examinations, all

Table. Virologic test results during Zika virus infection in a 32-year-old woman after she returned from the Dominican Republic to Italy, April–June 2016*

Test/specimen type	1st sample, day 6†	2nd sample, day 7†	3rd sample, day 10†	4th sample, day 13†	5th sample, day 17†	6th sample, day 28†
Zika virus						
rRT-PCR‡ serum	Positive (32.9)	Negative	Negative	Negative	Negative	Negative
rRT-PCR‡ urine	Positive (34.2)	Positive (31.8)	Positive (32.4)	Positive (29.8)	Positive (32.1)	Positive (32.2)
rRT-PCR‡ saliva	ND	Positive (29.9)	Positive (33.5)	Positive (34.1)	Negative	Negative
rRT-PCR‡ CSF	ND	Positive (37.0)	ND	ND	Negative	ND
rRT-PCR‡ cervical swab sample	ND	Positive (31.1)	Negative	Positive (34.3)	Negative	Negative
IFA§ IgM titer	<1:20	1:40	1:160	1:80	1:320	1:1,280
IFA§ IgG titer	<1:20	<1:20	1:40	1:320	1:320	1:320
MNT¶ Ab titer	ND	ND	1:40	ND	1:160	≥1:640
Dengue virus IFA§ IgM titer	<1:20	<1:20	<1:20	<1:20	<1:20	<1:20
Dengue virus IFA§ IgG titer	<1:20	<1:20	<1:20	<1:20	<1:20	<1:20
Chikungunya virus IFA§ IgM titer	<1:20	<1:20	<1:20	<1:20	<1:20	<1:20
Chikungunya virus IFA§ IgG titer	<1:20	<1:20	<1:20	<1:20	<1:20	<1:20

*Ab, antibody; CSF, cerebrospinal fluid; IFA, immunofluorescence assay; MNT, microneutralization test; ND, not done; rRT-PCR, real-time reverse transcription PCR.
†Days from symptom onset.
‡Zika virus–specific rRT-PCR (RealStar Zika Virus RT-PCR Kit 1.0; Altona Diagnostics GmbH; Hamburg, Germany). Numbers in parentheses indicate cycle threshold values (online Technical Appendix, http://wwwnc.cdc.gov/EID/article/22/12/16-1280-Techapp1.pdf).
§IgG and IgM IFA (Arbovirus Mosaic 2; Euroimmun AG; Luebeck, Germany). Reference values (titer) serum: <1:20 = negative; ≥1:20 = positive (online Technical Appendix).
¶MNT titers <1:20 were considered negative (online Technical Appendix).

features consistent with the diagnosis of Zika virus–related encephalitis, which represents a rare atypical presentation, particularly in areas to which Zika virus infection is not endemic. A recent article shows that Zika virus can infect adult murine neural stem cells, leading to cell death and reduced proliferation (*7*). It raises the possibility that Zika is not simply a transient infection in adult humans and that exposure in the adult brain could have an effect on long-term memory or the risk for depression (*7*).

Our case highlights the potential for Zika virus neurotropism and the need for early identification of Zika virus–related neurologic symptoms. Moreover, the presence of Zika virus in the genital tract supports the recommendation of safe sex practice for women returning home from areas with ongoing Zika virus transmission.

The study was funded by Ricerca Corrente of the Italian Ministry of Health.

References

1. European Centre for Disease Prevention and Control. Rapid risk assessment. Zika virus disease epidemic. Sixth update, 20 May 2016. Stockholm: The Centre; 2016 [cited 2016 Aug 1]. http://ecdc.europa.eu/en/publications/Publications/zika%20virus%20rapid%20risk%20assessment%2010-05-2016.pdf
2. Carteaux G, Maquart M, Bedet A, Contou D, Brugières P, Fourati S, et al. Zika virus associated with meningoencephalitis. N Engl J Med. 2016;374:1595–6. http://dx.doi.org/10.1056/NEJMc1602964
3. Rozé B, Najioullah F, Signate A, Apetse K, Brouste Y, Gourgoudou S, et al. Zika virus detection in cerebrospinal fluid from two patients with encephalopathy, Martinique, February 2016. Euro Surveill. 2016;21:30205. http://dx.doi.org/10.2807/1560-7917.ES.2016.21.16.30205
4. Prisant N, Bujan L, Benichou H, Hayot P-H, Pavili L, Lurel S, et al. Zika virus in the female genital tract. Lancet Infect Dis. 2016;pii: S1473-3099(16)30193-1. http://dx.doi.org/10.1016/S1473-3099(16)30193-1
5. Davidson A, Slavinski S, Komoto K, Rakeman J, Weiss D. Suspected female-to-male sexual transmission of Zika virus—New York City, 2016. MMWR Morb Mortal Wkly Rep. 2016;65):716–7. http://dx.doi.org/10.15585/mmwr.mm6528e2
6. Yockey LJ, Varela L, Rakib T, Khoury-Hanold W, Fink SL, Stutz B, et al. Vaginal exposure to Zika virus during pregnancy leads to fetal brain infection. Cell. 2016;166:1247–1256.e4. http://dx.doi.org/10.1016/j.cell.2016.08.004
7. Li H, Saucedo-Cuevas L, Regla-Nava JA, Chai G, Sheets N, Tang W, et al. Zika virus infects neural progenitors in the adult mouse brain and alters proliferation. Cell Stem Cell. 2016;pii:1934-5909(16)30252-1. http://dx.doi.org/10.1016/j.stem.2016.08.005

Address for correspondence: Concetta Castilletti, National Institute for Infectious Diseases INMI-IRCCS, Via Portuense 292, 00149 Rome, Italy; e-mail: concetta.castilletti@inmi.it

Jenny Hammond, The Natural History of Influenza A Viruses (1990). Stained Glass, 21 in × 56 in / 53.3 cm × 142.2 cm. Commissioned by Robert and Marjorie Webster, Memphis, TN, USA. Digital image courtesy of Robert Webster.

Illustrating the Natural History of Influenza A Viruses through Art

Robert G. Webster

On a rainy and misty day in late 1989, my wife (Marjorie) and I were walking the path along the remnants of Hadrian's Wall, a UNESCO world heritage site near the border between England and Scotland. The Romans began building this wall—which extends from the banks of the river Tyne on the west coast to Solvay Firth on the east coast of England—ostensibly to keep the "barbarian" Scots from plundering their English territory.

Author affiliation: St. Jude Children's Research Hospital, Memphis, Tennessee, USA

DOI: http://dx.doi.org/10.3201/eid2212.AC2212

During lunch in a local pub, we discovered in a local publication a picture of a wonderful stained glass window depicting a dragon. We arranged to visit the artist, Jenny Hammond, at her nearby farm in Highgreenley-cleugh, Northumberland, England, where we viewed her stained glass works firsthand and commissioned her to create a unique stained glass window that would detail the natural history of influenza. After we returned to our home in Memphis, Tennessee, we sent Hammond several review articles and electron micrographs to provide her some background on influenza A viruses. Hammond, in turn, shared her ideas through penciled sketches and over

the next year completed the version that appears on this month's EID journal cover.[1]

After its transport by air, Marjorie and I installed the stained glass window into the premeasured window frame near the front door of our home. Visiting students and colleagues from around the world invariably ask to photograph the window. This stained glass window offers viewers a concise introduction to influenza in a One Health system in which viruses emerge from wild bird reservoirs and periodically cause pandemic diseases (such as influenza) in humans.

Although the term "One Health" was recently coined, it describes an ancient concept recognized by Hippocrates in his text "On Airs, Waters, and Places." Scientists have noted the similarity in disease processes between animals and humans since the 1800s. Rudolf Virchow, a 19th century German pathologist and anthropologist, devised the term "zoonosis" to indicate web of the infectious diseases links between animals and humans, saying that "... between animal and human medicine there are no dividing lines—nor should there be." In the 20th century, the One Health concept coalesced and gained momentum in the public health and animal health communities. The work of art depicted on this month's cover depicts that interrelationship of human, animal, and environmental health.

The dark blue glass prominently positioned in the upper right signifies the global problem of influenza A viruses, which are associated with yearly epidemics and intermittent pandemics. The came strips, which provide structure for the window, also depict the spread of virus, which has a large reservoir and vast gene pool in wild migratory aquatic birds—including ducks and gulls represented in the window as well as shorebirds, geese, and terns. The influenza viruses can spread to pigs, considered the intermediate host, and to humans. The red background depicts the high fever in pigs and humans infected with the influenza virus.

Hammond also incorporated microscopic details essential to natural history of influenza A. Her depiction of the influenza virus particles show the spiky surface made up of the hemagglutinin that attaches the virus to the respiratory tract of the host and the neuraminidase that releases the virus from infected cells so that the virus can spread. She has depicted the RNA genome of 8 segments as separate threads. The particles with multiple threads illustrate how reassortment between influenza viruses gives rise to new pandemic strains.

Stained-glass windows have been appreciated for their utility and splendor for more than 1,000 years, and this engaging work of art reminds us that influenza A viruses—which can be easily spread between animals and human, use various host species, and exist in many different environments—remain an enduring and global health concern.

[1]A different perspective of this stained glass window has also appeared on the cover of the book *Microbial Threats to Health: Emergence, Detection, and Response* (2003), by the Committee on Emerging Microbial Threats to Health in the 21st Century, Board on Global Health, Institute of Medicine, National Academies Press; another appears on the cover of a series of workshop summaries also published by the Institute of Medicine, National Academies Press.

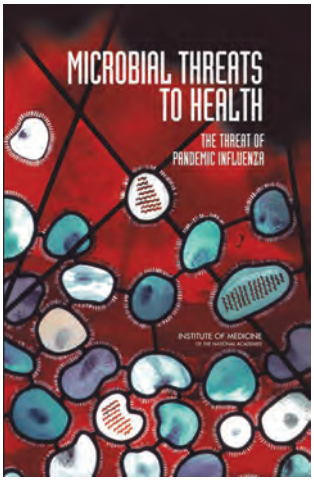

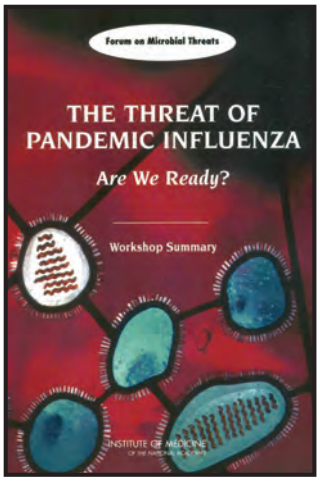

Bibliography

1. Centers for Disease Control and Prevention. Influenza type A viruses [cited 2016 Aug 12]. http://www.cdc.gov/flu/avianflu/influenza-a-virus-subtypes.htm
2. Centers for Disease Control and Prevention. One Health [cited 2016 Aug 23]. https://www.cdc.gov/onehealth/index.html
3. English Heritage. History of Hadrian's Wall [cited 2016 Aug 12]. http://www.english-heritage.org.uk/visit/places/hadrians-wall/history/
4. Schultz M. Photo quiz: Rudolf Virchow. Emerg Infect Dis. 2008;14:1480–1. http://dx.doi.org/10.3201/eid1409.086672
5. Sonnberg S, Webby RJ, Webster RG. Natural history of highly pathogenic avian influenza H5N1. Virus Res. 2013;178:63–77. http://dx.doi.org/10.1016/j.virusres.2013.05.009

Address for correspondence: Robert G. Webster, Department of Infectious Diseases, St. Jude Children's Research Hospital, 262 Danny Thomas Pl, Memphis, TN 38105-3678, USA; email: robert.webster@stjude.org

EMERGING INFECTIOUS DISEASES®

Upcoming Issue

- Epidemiology of Hospitalizations for Invasive Candidiasis, United States, 2002–2012
- Epidemiology of Human Anthrax in China, 1955–2014
- Oral Cholera Vaccine Coverage during an Outbreak and Humanitarian Crisis, Iraq, 2015
- Cost-effectiveness of Increasing Access to Contraception during the Zika Virus Outbreak, Puerto Rico, 2016
- Reconstruction of Zika Virus Introduction in Brazil
- Upsurge of Enterovirus D68, the Netherlands, 2016
- *Haemophilus influenzae* Type B Invasive Disease in Amish Children, Missouri, USA, 2014
- Prolonged Detection of Zika Virus in Vaginal Secretions and Whole Blood
- Acute Respiratory Disease in US Army Trainees 3 Years after Reintroduction of Adenovirus Vaccine
- Persistent Zika Virus Detection in Semen in a Traveler Returning to the United Kingdom from Brazil, 2016
- Increased Invasive Pneumococcal Disease, North East England, 2015–2016
- Travel-Related Tick-Borne Encephalitis, Israel, 2006–2014
- Guillain-Barré Syndrome and Healthcare Needs during Zika Virus Transmission, Puerto Rico, 2016
- Streptococcal Toxic Shock Syndrome Caused by Group G *Streptococcus*, United Kingdom
- Multidrug-Resistant Pathogens in Hospitalized Syrian Children
- Puumala Virus in Bank Voles (*Myodes glareolus*), Lithuania
- Chikungunya Fever in Traveler from Angola to Japan, 2016
- Loiasis in US Traveler Returning from Bioko Island, Equatorial Guinea, 2016
- Human Tick-Borne Encephalitis, the Netherlands

Complete list of articles in the January issue at http://www.cdc.gov/eid/upcoming.htm

Upcoming Infectious Disease Activities

December 3–8, 2016
ASLM
African Society for Laboratory Medicine
Cape Town, South Africa
http://aslm2016.org/

March 29–31, 2017
SHEA
Society for Healthcare Epidiemiology of America
St Louis, MO, USA
http://www.shea-online.org/

April 22–27, 2017
ECCMID
European Congress of Clinical Microbiology and Infectious Diseases
Vienna, Austria
http://www.eccmid.org/

February 13–16, 2017
CROI
Conference on Retroviruses and Opportunistic Infections
Seattle, WA, USA
http://www.croiconference.org/

June 1–5, 2017
ASM
American Society for Microbiology
New Orleans, LA, USA
http://www.showsbee.com/fairs/25161-ASM-Microbe-2017.html

Announcements

To submit an announcement, send an email message to EIDEditor (eideditor@cdc.gov). Include the date of the event, the location, the sponsoring organization(s), and a website that readers may visit or a telephone number or email address that readers may contact for more information.

Announcements may be posted on the journal Web page only, depending on the event date.

REVIEWER APPRECIATION

EMERGING INFECTIOUS DISEASES™
A Peer-Reviewed Journal Tracking and Analyzing Disease Trends

Emerging Infectious Diseases thanks the following reviewers for their support through thoughtful, thorough, and timely reviews in 2016. We apologize for any inadvertent omissions.

Raquel Abad
Kaja Abbas
Jônatas Abrahão
Joana Abrantes
Andrew Abutu
Bishwa Adhikari
Jennifer Adjemian
Cornelia Adlhoch
Danielle Adney
Martin Adokiya
Toïdi Adékambi
Rakesh Aggarwal
Maria Aguero-Rosenfeld
Clas Ahlm
Yukihiro Akeda
Waleed Al Salem
Jaffar Al-Tawfiq
Munirul Alam
Heidi Albert
Jared Aldstadt
Heather Alexander
Ibne Ali
Ijaz Ali
Sheikh Taslim Ali
Tobias Allander
David Allen
Franz Allerberger
Robert Allison
Alzira Almeida
Harvey Alter
Daniel Altmann
Brian Amman
Valerianna Amorosa
Abhijeet Anand
Alicia Anderson
Danielle Anderson
John Anderson
Kathryn Anderson
Larry Anderson
David Andes
Theodore Andreadis
Claire Andrejak
Antoine Andremont
Olivier Andreoletti
Emmanouil Angelakis
Denise Antona
Charles Apperson
Yaseen Arabi
Vidya Arankalle
Prema Arasu
Carmen Ardanuy
Matthew Arduino
Nimalan Arinaminpathy
Koya Ariyoshi
Philip Armstrong
Lawrence Ash
Kingsley Asiedu
Abdullah Assiri
Barry Atkinson
Robert Atmar
Stephen Attwood
Kari Auranen
John Austin
Tatjana Avsic
Koku Awoonor-Williams
Abdu Azad
Andrew Azman
Roseric Azondékon
Eduardo Azziz-Baumgartner
Thierry Baron
Sylvie Benestad
Idir Bitam
Carmen Buchrieser
Thomas Butler
Tadasha Baba
Eran Bacharach
Kay Backues
Justin Bahl
Jean-Luc Bailly
Carol Baker
Craig Baker-Austin
Tamas Bakonyi
Nandhakumar Balakrishnan
Amanda Balish
Sapna Bamrah
Gad Baneth
Krisztian Banyai
Chang-jun Bao
J.J. Bara
Veronique Barban
Aristides Barbosa
Lisa Barco
Stephen Barenkamp
Christopher Barker
John Barnwell
Lyric Bartholomay
Karen Bartlett
Alessandro Bartoloni
Casey Barton Behravesh
Jason Bartz
Luisa Barzon
Corey Basch
Leonardo Basco
Armanda Bastos
Michael Batz
David Baud
Daniel Bausch
Bernard Beall
David Beasley
Maria Serena Beato
Christiane Bebear
Melinda Beck
Emily Beeler
Martin Beer
Irmgard Behlau
Bill Bellini
Jessica Belser
Graham Belsham
Yanis Ben Amor
Kaitlin Benedict
Laura Benitez
Allan Bennett
Sarah Bennett
Kimberley Benschop
Jean-Michel Berenger
Elizabeth Berkow
Stuart Berman
Kathryn Bernard
Kristen Bernard
Xavier Bertrand
Marianne Besnard
Darlene Bhavnani
Zulfiqar Bhutta
Dominique Bicout
Martina Bielaszewska
Brad Biggerstaff
Matthew Biggerstaff
Brian Bird
Leslie Birke
Werner Bischoff
Carina Blackmore
Stuart Blacksell
Radu Blaga
Carol Blair
Isobel Blake
José Ramón Blanco
David Blaney
Lucas Blanton
Bradley Blitvich
Evan Bloch
Sandra Blome
Sharon Bloom
Johannes Blum
Michael Boeckh
Pierre Bogaerts
Christian Bogdan
Andrea Boggild
John Bohnsack
Guy Boivin
James Bono
Robert Bonomo
Marc Bonten
Severine Bontron
Nicole Borel
Maria José Borrego
María Laura Boschiroli
Ana Botelho
German Bou
Donald Bouyer
Anna Bowen
Richard Bowen
Andrew Bowman
Dwight Bowman
Richard Bradbury
Oliver Brady
Anna Bramley
Mary Brandt
Patricia Brasil
Aaron Brault
Aodhan Breathnach
Byron Breedlove
Justin Breown
Elizabeth Briere
Benjamin Bristow
Seth Britch
William Brogdon
John Brooks
Richard Brooks
Richard Brostom
Philippe Brouqui
Corrie Brown
Kevin Brown
John Brownstein
Karen Brudney
Babette Brumback
Udo Buchholz
Christopher Buck
Christine Budke
James Buehler
Pierre Buffet
Lorraine Buis
Marc Bulterys
Peter Burbelo

Howard Burkom
Carey-Ann Burnham
Anne Buschmann
Karen Bush
Jeff Butler
Thomas Butler
Cécile Bébéar
Jingxian Cai
Charles Calisher
Amanda Calvert
Angela Campbell
Gerald Campbell
Helen Campbell
Paul Cantey
Rafael Cantón
Van-Mai Cao-Lormeau
Eric Cardinale
Mary Cardosa
Cristina Casalone
Kenneth Castro
Vincent Cattoir
Mike Catton
Simon Cauchemez
Joseph Cavanaugh
Peter Cegielski
José Cerbino Neto
Serafeim Chaintoutis
Trinad Chakraborty
Victoria Chalker
Christina Chambers
Martin C.W. Chan
Emmanuel Chanda
Chulhun Chang
Gwong-Jen Chang
Sui-Yuan Chang
Dennis Chao
David Chapman
Louisa Chapman
Nora Chapman
Rémi Charrel
Tanittha Chatsuwan
Sandra Chaves
Bob Chen
Lin Chen
Shaohong Chen
James Cherry
Harrell Chesson
Lauren Childs
Tom Chiller
Charles Chiu
Young June Choe
Mary Choi
Bruno Chomel
Christina Chommanard
Teo Chong-Gee
Terence Chorba
Anuradha Chowdhary
Gerardo Chowell
Bryan Christensen
Daniel Chu
Hee Kyoung Chun
Massimo Ciccozzi
Carol Ciesielski
Paul Cieslak
Isa Ciglenecki
Hannah Clapham
Kerry Clark
Jean-Michel Claverie
Jan Clement
Barnett Cline
Axel Cloeckaert
Frank Cobelens
Nicole Cohen
Ted Cohen
Amanda Cohn
Randall Cohrs
James Colborn
Matthew Coldiron
Robert Colebunders
Dan Colley
Nikail Collins
Tonya Colpitts
Philippe Colson
Nicholas Conger
Matteo Convertino
Laura Cooley
Jennifer Cope
Teresa M Coque
Victor Corman
Martin Cormican
Anton Cornel
Marti Cortey
Sara Louise Cosby
Caitlin Cossaboom
Yaya Coulibaly
Ben Cowling
Nancy Cox
Carolyn Coyne
Keith Crandall
Curtis Croker
Robert Cross
Natasha Crowcroft
John Crump
Zulma Cucunuba Perez
Jing Cui
Kevin Cummings
Matthew Cummings
Bart Currie
Pascal Delaunay
Juliana Da Silva
Cristina Da Silva Carias
Ron Dagan
Harry R. Dalton
Inger Damon
David Dance
Aparup Das
Gregory Dasch
Michael David
Bionca Davis
Charles Davis
Jeffrey Davis
Larry Davis
Meghan Davis
Michael Day
Gustavo Dayan
Anindya De
Erwin De Bruin
Astrid De Greeff
Niall De Lappe
Camila de Oliveira
Henry de Vries
Charla (Chas) DeBolt
Kevin DeCock
Malini DeSilva
Tom Decroo
Takashi Deguchi
Jorge Del Pozo
F. Deleo
Eric Delwart
Zygmunt Dembek
Abraham Deng
Catherine Dentinger
Don Des Jarlais
Jean-Claude Desenclos
Jagadish Deshpande
Gregor Devine
Muthuchelvan Dhanavelu
Mamadou Diallo
Luis Diaz
Linda Dixon
Gerhard Dobler
Yohei Doi
Mariano Domingo
Samuel Dominguez
Lu Dong
Rodney Donlan
Christl Donnelly
Nargesalsadat Dorratoltaj
Jeffrey Doty
John Douglas
Walter Dowdle
David Dowdy
Scott Dowell
Michel Drancourt
Steven Drews
Jan Felix Drexler
Amanda Driscoll
Jan Drobeniuc
Francis Drobniewski
Barbara Drolet
Christian Drosten
Betânia Drumond
Edward Dubovi
Mariette Ducatez
Vivien Dugan
Priya Duggal
Roger Dumke
John Dumler
Angela Dunn
John Dunn
Myrielle Dupont-Rouzeyrol
W. Paul Duprex
Alan Dupuis
Christopher Dye
José Alberto Díaz-Quiñonez
Andrew Easton
Gregory Ebel
Mark Eberhard
Hideki Ebihara
Laura Eckard
Isabella Eckerle
Paul Edelstein
Tom Edrington
James Edwards
Morven Edwards
Paul Effler
Joseph Egger
Lars Eisen
Laila El Attar
Maged El-Ashker
Miriam Elfstrom
Barbara Ellis
Joanna Ellis
Miriam Elman
Ginny Emerson
Andrea Endimiani
Tim Endy
Luis Enjuanes
Jonathan Epstein
Dean Erdman
Onder Ergonul
Bobbie Erickson
Kacey Ernst
Julia Ershova
Mathew Esona
Susanna Esposito
Paul Ettestad
Jim Evermann
Anna-Bella Failloux
Shamsudeen Fagbo
Rick Fairhurst
Jessica Fairley
Joseph Falkinham
Dennis Falzon
Jeremy Farrar
Alicia Feagins
Beth Feingold
Heinz Feldmann
Kevin Fennelly
Andrew Ferguson
Laura Ferrando

David Fidler
Patricia Fields
Antonietta Filia
Stacy Finkbeiner
Andrew Firth
Marc Fischer
Robert Fischer
Dale Fisher
Matthew Fisher
Robert Fisher
Nahuel Fittipaldi
Collette Fitzgerald
Tom Fletcher
Anthony Fok
Onikepe Folarin
Jason Folster
Emanuela Foni
Kevin Fonseca
Antônio Fonseca Júnior
Arnaud Fontanet
Anthony Fooks
Ivo Foppa
Ken Forbes
Naomi Forrester
Brett Forshey
Stephen Forsythe
Ron Fouchier
Pierre-Edouard Fournier
Vance Fowler
Betsy Foxman
Brian Foy
Fabio Francesconi
Carlos Franco-Paredes
Richard Franka
Laura Franzin
Carl Frasch
David Fredricks
David Freedman
Täger Frey
Scott Fridkin
AM Fry
Kai Frölich
King-Wa Fu
Isaac Chun-Hai Fung
Jennifer Furin
Luis Furuya-Kanamori
Alice Fusaro
Eric Garnotel
Beatrice Grasland
Kenneth Gage
Manjusha Gaglani
Amandine Gagneux-Brunon
Gale Galland
Mark Gallivan
Manoj Gambhir
Qian Gao
Dario Garcia de Viedma
Chris Gardiner
Trenton Garner
Christiane Gaudreau
Philippe Gautret
Joel Gaydos
Robert Gaynes
Aiah Gbakima
David Geiser
Kathleen Gensheimer
Christine George
Sue Gerber
Dale Gerding
Peter Gerner-Smidt
Corine Geurts van Kessel
Marc Ghany
Michael Giladi
Suzanne Gilboa
Joseph Gillespie
John Gimnig
Victoria Girard
Carol Glaser
John Glasser
Daniel Glikman
Judith Glynn
Gauri Godbole
Sylvain Godreuil
Marvin Godsey
Heidi Goethert
G. Goff
Tony Goldberg
Gabriel Gonzalez
Stevan Gonzalez
David González-Barrio
Christin Goodman
Jim Goodson
Abraham Goorhuis
Aubree Gordon
Stephen Gordon
E. Gormley
Magnus Gottfredsson
Marcelo Gottschalk
Fred Gould
L. Hannah Gould
Prabhu Gounder
Nelesh Govender
John Grabenstein
Christopher Graber
Yonatan Grad
Christine Graham
Julia Granerod
Kathie Grant
Steve Gray
Kim Green
Rachel Greenberg
Bradford Greening
Patricia Griffin
Jonathan Gubbay
Duane Gubler
Jeanine Guidry
Nicole Guiso
Jonathan Guito
Frances Gulland
Amita Gupta
Kalpana Gupta
Ankur Gupta-Wright
Emily Gurley
Brian Gushulak
Philippe Guérin
Teresa Gárate
Patrick Gérardin
Beatriz Gómez
Bart Haagmans
Andrew Haddow
Stephen Hadler
Aron Hall
Ian Hall
Eric Halsey
Scott Halstead
Davidson Hamer
Keith Hamilton
Alan Hampson
Grant Hansman
Stephan Harbarth
Jennifer Harcourt
Timm Harder
Heli Harvala
Eric Harvill
Mohammad Reza Hasanjani Roushan
Masahiro Hashizume
Todd Hatchette
Thomas Haupt
Ben Hause
Arie Havelaar
Fiona Havers
Hal Hawkins
Murray Hazlett
Craig Hedberg
James Heffelfinger
Mark Heise
Stephane Helleringer
Marieke Hemels
Olga Henao
D.A. Henderson
David Henderson
Rene Hendriksen
Emily Henkle
Morgan Hennessy
Ronnie Henry
Heikki Henttonen
David Heymann
Andrew Hill
Julia Hilliard
Itai Himelboim
Joe Hinnebusch
Kenji Hirayama
Jason Hodgson
Robert Hoekstra
Karin Hoelzer
Thomas Hoenen
Maria Hoffmann
Alex Hoffmaster
Mike Holbrook
Steven Holland
Patricia Holman
Scott Holmberg
Edward Holmes
Mark Holmes
Natasha Holmes
Lori Holtz
Stacy Holzbauer
Michael Hombach
Margaret Honein
Jay Hoofnagle
Thomas Hooton
Edward Hoover
Petter Hopp
Peter Horby
Taisuke Horimoto
Paul Horwood
Paul Hoskisson
Peter Hotez
Joppe Hovius
Rosalind Howes
Yana Emmy Hoy-Schulz
Christopher Hsu
Rong-Hong Hua
Michael Huffman
Martin Hugh-Jones
Holly Hughes
James Hughes
Ralph Huits
Olav Hungnes
A.C. Hurt
Christoph Härtel
Kazuo Imai
Allison Imrie
Tawin Inpankaew
Hon Ip
Patrick Ip
Seth Irish
Michael Ison
Danielle Iuliano
Jacques Izopet
Hidemasa Izumiya
Brendan Jackson
Mary Anne Jackson
Michael Jackson
Nitin Jain
Denise Jamieson
J. Michael Janda
Ernesto Jaramillo
Sophie Jarraud
Aurelie Jayol

Stephen Jenkins
Sanne Jespersen
Dirk Jochman
Michael Johansson
Reimar Johne
Barbara W. Johnson
Judith Johnson
Jeffrey Jones
Jeremy Jones
Morris Jones
Nicola Jones
Jaume Jorba
Hannah Jorgensen
Kwonil Jung
Antarpreet Jutla
S. Kachur
Tamilarasu Kadhiravan
Rebekah Kading
Barbara Kahl
Emily Kahn
Adriana Kajon
Alexander Kallen
Nassim Kamar
Mary Kamb
Hajime Kanamori
Mark Kane
Bryan Kapella
Amit Kapoor
Erik Karlsson
Mohamed Karmali
Sandor Karpathy
Stephanie Karst
Matt Karwowski
Sophia Kathariou
Midori Kato-Maeda
Carol A. Kauffman
Daniel R. Kaul
Ghazi Kayali
Keith Kaye
Crystal Kelehear
Colleen Kelly
Daryl Kelly
Sarah Kemble
Alan Kemp
Eben Kenah
Brian Kendall
Emily Kendall
Joan Kenney
Thomas Kerkering
Olen Kew
Hunter Keys
Jay Keystone
Ali Khan
Sahil Khanna
Ameneh Khatami
Alena Khromova
Yury Khudyakov
Sarah Kidd
Tom Kiedrzynski
Nicolas Kieffer
Mariana Kikuti
Peter Kilmarx
Sung-Han Kim
Karin Kirchgatter
Martyn Kirk
Robert Kirkcaldy
Hannah Kirking
Peter Kirkland
Carl Kirkwood
Uriel Kitron
Paul Kitsutani
Jeffrey Klausner
Terry Klein
Steven Kleinman
Gregory Kline
Marjolein Knoester
Mirjam Knol
Barbara Knust
Miwako Kobayashi
Gary Kobinger
Gavin Koh
Naomi Komadina
Nicholas Komar
Essi Marjaana Korhonen
Mark Kortepeter
Michael Kosoy
Camille Kotton
Antonis Kousoulis
Barbara Kowalcyk
Natalia Kozak-Muiznieks
Moritz Kraemer
Colleen Kraft
Laura Kramer
Florian Krammer
Peter Krause
Scott Krauss
Rosina Krecek
Pavla Krizova
Jesper Krog
Elisabeth Krow-Lucal
Adam Kucharski
Roman Kuchta
Matthew Kuehnert
Kiersten Kugeler
Jeffrey Kugelman
Thijs Kuiken
Mark Kuniholm
Shu-Chen Kuo
Ekaterina Kurbatova
Ivan Kuzmin
Gaurav Kwatra
Giuseppina La Rosa
Bernard La Scola
Desiree LaBeaud
Shannon LaDeau
Norma Labarthe
Niklaus Labhardt
Marcelo Labruna
Theresa Lamagni
Amy Lambert
Lauren Lambert
Claudio Lanata
Robert Lanciotti
J. Michael Lane
Robert Lane
Adam Langer
Marion Lanteri
Brent Lasker
Paul Latkany
Eric Lau
Max Siu Yin Lau
Susanna K.P. Lau
Anne Laudisoit
A Laulajainen-Hongisto
James Lawler
Ramanan Laxminarayan
Helen Lazear
Kirsty Le Doare
Francoise Le Guyader
Jacques Le Pendu
James LeDuc
Phillip Lederer
John Lednicky
Dong-Hun Lee
Min-Shi Lee
Vernon Lee
Youn-Jeong Lee
Florence Legrand-Abravanel
David Leiby
Katrin Leitmeyer
Eva Leitner
Isabelle Leparc-Goffart
Agnes Lepoutre
Eyal Leshem
Tomasz Leski
Fernanda Lessa
Justin Lessler
Eric Levenson
Min Levine
Paul Lewis
Sheri Lewis
Sheng Li
Yiming Li
Valdirene Lima
Brandi Limbago
Michael Lin
Yeou-Liang Lin
Yusen Lin
Kimberly Lindblade
John Linder
William Lindsley
Kitty C.F.M. Linssen
Virginia Lipke
W. Ian Lipkin
Susan Lippold
Susan Lipsett
Marc Lipsitch
Anastasia Litvintseva
Huili Liu
Jinhua Liu
Leo Liu
Ming-Tsan Liu
Shelan Liu
Yi-Chun Lo
Shawn Lockhart
Ira Longini
Anna Lena Lopez
Benjamin Lopman
Maria Loroño-Pino
Anice Lowen
Juan Lubroth
Naomi Lucchi
Daniel Lucey
Yaniv Lustig
Ruth Lynfield
Marshall Lyon
Simon Lévesque
Daniel Lévy-Bruh
Fatima M'zali
Jean Michel Mansuy
Max Maurin
Leonard Mayer
Derek MacFadden
Jessica MacNeil
Kevin Macaluso
Alexandre Macedo de Oliveira
Lisa Macera
Ian Mackay
John Mackenzie
Ken Maeda
Roger Maes
Matthew Magee
Shelley Magill
Brian Mahy
Alexandra Mailles
Taronna Maines
Maimuna Majumder
Antonio Maldonado-Barragán
Denis Malvy
Caterina Mammina
Anna Mandalakas
Brian Mann
L.L. Maragakis
Ben Marais
Nina Marano
Olivier Marcy
Tony Marfin
Gabriele Margos
Atanaska Marinova-Petkova

Wanda Markotter
Florian Marks
Suzanne Marks
John Marr
Theodore Marras
Jeanne Marrazzo
Tom Marrie
Glenn Marsh
Laurent Marsollier
Vito Martella
Douglas Marthaler
C. Martin
Emily Martin
Irene Martin
Stacey Martin
Valeria Martinez
Jaime Martinez-Urtaza
Joel Maslow
Robert Massung
Almea Matanock
Gregory Mayr
William McBride
Emma McBryde
Andrea McCollum
Orion McCotter
Nicky McCreesh
Anita McElroy
Peter McElroy
Lesley McGee
John E. McGowan, Jr.
Peter McIntyre
Donald McManus
Jennifer McQuiston
Jodie McVernon
Oleg Mediannikov
Jane Megid
Aneesh Mehta
Jacques Meis
Martin Meltzer
Martin Mengel
Stefano Merler
Marco Mesa Frias
Kevin Messacar
David Metzgar
Dik Mevius
Uta Meyding-Lamade
Hermann Meyer
Sarah A. Meyer
Wieland Meyer
Susan Mikota
Benjamin Miller
Loren Miller
Michele Miller
Mathieu Million
Harriet Mills
James Mills
Anna Minta
A. Mirand
Mary Elizabeth Miranda
Nischay Mishra
Rajal Mody
Chris Mok
Igor Mokrousov
Andrew Monaghan
Fernando Monteiro
Susan Montgomery
Hélène Moné
Patrick Moonan
Cynthia Moore
David Moore
Hector Mora-Montes
Stefano Morabito
Jose Moraes
Jacob Moran-Gilad
David Morens
Daniel Morgan
Jess Morgan
Oliver Morgan
Shigeru Morikawa
Kozo Morimoto
J. Glenn Morris
Kathleen Moser
Eric Mossel
Elke Muhlberger
Rami Mukbel
Claude Muller
Mark Mulligan
Michael Mulvey
U.G. Munderloh
Jose F. Munoz
Vincent Munster
Edward L. Murphy
Frederick Murphy
Trudy Murphy
Joseph Murray
Kristy Murray
Michael Murtaugh
Didier Musso
Jean-Paul Mutebi
Jorge Muñoz-Jordán
Khin Saw Myint
Marcel Müller
Pierre Nabeth
Osamu Nakagomi
Allyn Nakashima
Masa Narita
Roger Nasci
Avindra Nath
Pontus Naucler
Maria Negron
David Neitzel
Gary Nelson
Kenrad Nelson
Lisa Nelson
Martha Nelson
Noele Nelson
Jason Newland
Fei Fan Ng
Lisa Ng
Oon Tek Ng
Duc Nguyen
John Nicholls
Ainsley Nicholson
William Nicholson
David P. Nicolau
Lindsay Nicolle
Matthias Niedrig
Karin Nielsen
Hubert Niesters
Nathan Nieto
Eric Nilles
Allan Nix
Harold Noel
Carl Erik Nord
Patrice Nordmann
Hans Nothdurft
Shannon Novosad
Norbert Nowotny
Marcio Nunes
Gerard Nuovo
Thomas Nutman
Luke Nyakarahuka
Sarah O'Brien
Kerry O'Donnell
Seth O'Neal
Steve Oberste
Sophie Octavia
John Oeltmann
Myoung-don Oh
Makoto Ohnishi
Nobuhiko Okabe
Iruka Okeke
Francisco Olea-Popelka
Kevin Olival
James Oliver
Russ Olmsted
Sonja Olsen
Samuel Opoku
Tanja Opriessnig
Eyal Oren
Walter Orenstein
Justin Ortiz
Anthony Orvedahl
Michael Osterholm
José A. Oteo
Michele Ottmann
Osman Ozaltin
Christopher Paddock
Kristen Page
Hélène Pailhories
Subhamoy Pal
Gustavo Palacios
Mark Pallansch
Xiuzhen Pan
Anna Papa
Igor Paploski
John Papp
Marguerite Pappaioanou
Umesh Parashar
Dimitrios Paraskevis
Satya Parida
Daniel Paris
Benjamin Park
Sarah Park
Philippe Parola
Gabriel Parra
Colin Parrish
Michele Parsons
Sally Partridge
Frank Pasmans
Daniel Pastula
Anita Patel
Jean Patel
Payal Patel
Christophe Paupy
Andrew Pavia
Nicole Pavio
Janusz Paweska
Daniel Payne
Elspeth Payne
Samuel Peasah
Richard Pebody
Karl Pedersen
Malik Peiris
L. Peixe
Patricia Penilla
Mary-Louise Penrith
Maurice Pensaert
Pasi Penttinen
Daniel Perez
Stanley Perlman
Carmem Pessoa da Silva
Jurriaan Peters
Philip Peters
Brett Petersen
Lyle Petersen
A. Townsend Peterson
Nicola Petrosillo
Eric Pevzner
Lorenzo Pezzoli
Michael Pfaller
Varun Phadke
Renaud Piarroux
Ted Pierson
David Pigott
Benjamin Pinsky
James Pipas
Johann Pitout
Mateusz Plucinski
Patrick Plésiat
Laura Podewils
Laurent Poirel

Marjorie Pollack
Art Poon
Leo Poon
Yong Poovorawan
Vsevolod Popov
Kyle Popovich
Sam Posner
Tonia Poteat
Morris Potter
James Poupard
S.J. Pravinkumar
Ian Pray
Joseph Prescott
Andrew Preston
Marthi Pretorius
Lance Price
Bobbi Pritt
Celine Pulcini
Joanna Pulit-Penaloza
Michael Purdy
Chaturong Putaporntip
Oliver Pybus
Ana Pérez de Ayala
Liu Quan
Isabelle Quatresous
Krista Queen
Patricia Quinlisk
Ingrid Rabe
Vincent Racaniello
Sheryl Racelis
Gabriel Rainisch
Nipunie Rajapakse
T. Ramamurthy
Andrew Ramey
Pilar Ramon-Pardo
Angela Rankine-Mullings
Stéphane Ranque
Sari Rantala
Didier Raoult
Brian Raphael
James Rasheed
Lasse Rasmussen
Ruwan Ratnayake
Mario Raviglione
Jonathan Rayner
Jennifer Read
Susan Reef
Jennita Reefhuis
Joanna Regan
Hugh Reid
Arthur Reingold
William Reisen
Michael Reiskind
Chantal Reusken
Gabor Reuter
Ludovic Reveiz
Mary Reynolds
Florence Ribadeau Dumas
Guilherme Ribeiro
Steven Riley
Mario Rizzetto
Suelee Robbe-Austerman
Emmanuel Robesyn
Guy Robinson
Trisha Robinson
Juan Rodríguez
Luis Rodríguez
Jesús Rodríguez-Baño
Pablo Rojo
Pierre Rollin
Lars Rombo
Thomas Romig
Anne-Marie Roque-Afonso
Patricia Rosa
Jason Rosch
Nancy Rose
Jennifer Rosen
Ronald Rosenberg
Joshua Ross
Gian Maria Rossolini
Paul Rota
Virginie Rougeron
Dominique Rousset
Alexander Rowe
David Rowlands
Matthew Rubach
Charles Rupprecht
Thomas Russo
Victor Rutten
Mark Rweyemamu
Isabelle Régner
Nicole Rübsamen
Florent Sebbane
Alex Soriano
Claude Sabeta
David Sack
David Safronetz
Linda Saif
Yoshihiro Sakoda
Oscar Salomon
Vittorio Sambri
Aaron Samuels
Orjan Samuelsen
Jose Sanchez
Marianne Sandberg
Carlos Santos
R. Tedjo Sasmono
M.J. Satlin
Sarah Satola
Elaine Scallan
Gaia Scavia
Joanna Schaenman
Sean Schafer
William Schaffner
Braydon Schaible
Franco Schiavon
Robert Schlaberg
William Schluter
Axel Schmidt
John Paul Schmidt
Jonas Schmidt-Chanasit
Anthony Schmitt
Elizabeth Schnaubelt
Eileen Schneider
Randal Schoepp
Karen-Beth Scholthof
Stephanie Schrag
Anne Schuchat
Audrey Schuetz
Amy Schuh
Stacey Schultz-Cherry
Eli Schwartz
Stefan Schwarz
Martin Schwemmle
Jessica Schwind
Glen Scoles
Dorothy Scott
Janet Scott
Katherine Scott
Anna Seale
Cynthia Sears
William Secor
Isaac See
Mauricio Seguel
Mariela Segura
James Sejvar
Tara Sell
Sarah Sengstake
Varadan Sevilimedu
Sean Shadomy
Andi Shane
Nong Shang
Manjunath Shankar
Aditya Sharma
Colin Sharp
Tyler Sharp
Jeanne Sheffield
Chau-Chyun Sheu
Patricia Shewmaker
Wun-Ju Shieh
Miriam Shiferaw
Nahoko Shindo
Kayoko Shioda
Stanford Shulman
Eva Sierra
Kimberley Simmonds
Peter Simmonds
O. Simon
R.J. Simonds
Lone Simonsen
Amy Sims
Edina Sinanovic
Julie Sinclair
Andreas Sing
Ros Singelton
Bhoj Singh
Tarja Sironen
Daouda Sissoko
L. Kristopher Siu
Maria Sjölund-Karlsson
Jacek Skarbinski
Tami Skoff
Pierre Smeesters
David Smith
Donald Smith
Duncan Smith
Graham Smith
Noel Smith
Rachel Smith
Tara Smith
Saskia Smits
David Sniadack
Georges Snounou
Jeremy Sobel
Olusegun Soge
Robert Sogomonian
Marylou Solbrig
Uffe Skov Sorensen
Frank Sorvillo
Mark Sotir
Erica Spackman
Craig Spencer
David Spiro
Armand Sprecher
David Stallknecht
Gerold Stanek
J. Staples
Jeffrey Starke
Molly Steele
Robert Steffen
Laura Steinhardt
Roger Stephan
Dennis Stevens
James Stevens
Lori Stevens
Paul Stickings
Paula Stigler Granados
Timothy Stinear
Charles Stoecker
Gregory Storch
Masja Straetemans
Susan Stramer
Lynne Strasfeld
Marc Strassburg
Thomas Strecker
Luke Strnad
Nancy Strockbine
Ellen Stromdahl
James Strong
Ute Ströher
James Stuart
John Su

David Suarez
Kanta Subbarao
Jonathan Sugimoto
Amy Sullivan
Kelly Sullivan
Rebecca Sunenshine
Philip Supply
Leonardo Susta
Roland Sutter
Deanna Sutton
Jeannette Sutton
Shunji Suzuki
Larry Svenson
Geeta Swamy
Robert Swanepoel
David Swayne
Marie Sweeney
Sabrina Swenson
William Switzer
Matias Szabo
Danielle Tack
Daisuke Takamatsu
Ben Tall
Eldin Talundzic
Clarence Tam
Azaibi Tamin
Ming Tan
Robert Tanz
Caroline Tapparel
Dennis Tappe
Cheryl Tarr
Phillip Tarr
Jeffery Taubenberger
Robert Tauxe
John Taylor
William Taylor
Thomas Taylor, Jr.
Asmaa Tazi
Richard Tedder
Joseph Telfair
Sam Telford
Bernd-Alois Tenhagen
Chong-Gee Teo
Eyasu Teshale
Larissa Thackray
Elitza Theel
Dana Thomas
Jason Thomas
Kimberly Thomas
Stephen Thomas
George Thompson
William Thompson
Nicholas Thomson
Kwai Lin Thong
Sharmi Thor
John Threlfall
Peter Tijssen
Peter Timoney
Tejpratap Tiwari
Ewen Todd
Suxiang Tong
Mia Torchetti
Enrico Tortoli
Joseph Tota
Jonathan Towner
Cuc Tran
Dat Tran
Donato Traversa
Rita Traxler
David Trees
Eija Trees
William Trick
Giliane Trindade
Suvang Trivedi
Susan Trock
Adriana Troyo
Carine Truyens
Kun-Hsien Tsai
Ying-ying Tsai
Raymond Tsang
Zion Tsz Ho Tse
Costas Tsiamis
Sotirios Tsiodras
Terrence Tumpey
Mike Turell
Claire Turner
Paul Turner
John Turnidge
Kenneth Tyler
Georgina Tzanakaki
Venkatachalam Udhayakumar
Anne-Catrin Uhlemann
David Ussery
Timothy Uyeki
George Varghese
Ronald Valdiserri
Peter Valentin-Weigand
Snigdha Vallabhaneni
Florent Valour
Chris Van Beneden
Marie Francoise Van Bressem
Barbara Van Der Pol
H. Rogier van Doorn
Neeltje van Doremalen
James Van Etten
Marjolein van Gent
Michel van Herp
Willem Van Panhuis
Annelies van Rie
Rafael Van den Bergh
Lia van der Hoek
Marianne van der Sande
Sabine van der Sanden
Edouard Vannier
Olli Vapalahti
Nikos Vasilakis
Muriel Vayssier-Taussat
Everardo Vega
Ana Isabel Vela
John Mark Velasco
Ramesh Vemulapalli
Vito Vetrugno
Pauline Vetter
Cecile Viboud
Marco Vigilato
Nicolas Vignier
Dhanasekaran Vijaykrishna
Jordi Vila
Amy Vincent
Joseph Vinetz
Jan Vinjé
Veronika von Messling
C. Fordham von Reyn
Neil Vora
Setu Vora
Wilna Vosloo
Jaap Wagenaar
Jesse Waggoner
David Wagner
Henry Walke
David Walker
Sandra Walser
Xiu-Feng Wan
Lin-Fa Wang
Ling Wang
Quanyi Wang
Wei Wang
Xin Wang
David Wareham
David Warnock
Sean Wasserman
Stephen Waterman
Ray Waters
John Watson
Simon Watson
Scott Weaver
Hattie Webb
Richard Webby
J. Todd Weber
Robert Webster
Scott Weese
Robert Weinstein
Don Weiss
Louis Weiss
Bruce Weniger
Christine Wennerås
David Wentworth
Guilherme Werneck
Joel Wertheim
Laura Wesolowski
Stephen Wharton
Joseph L. Wheat
Jean Whichard
Jennifer White
Peter White
Cynthia Whitney
Steven Wiersma
John Williams
Tom Wingfield
Kevin Winthrop
Matthew Wise
Alan Wolfe
Frank Wong
Patrick C.Y. Woo
John Wood
Kimberly Workowski
Gary Wormser
Jonathan Wortham
Grzegorz Woźniakowski
Anita Wright
Henry Wu
Joseph Wu
Mireille Wulf
Nico Wulffraat
William Wunner
Ning-Shao Xia
Cuiling Xu
Laith Yakob
Hiroshi Yamasaki
Dan Yamin
Bingyu Yan
Jing-Jou Yan
X. Frank Yang
Chaoqun Yao
Steven Yeh
Hui-Ling Yen
Jae-Joon Yim
Jingjing Yin
Jonathan Yoder
InKyu Yoon
Hongjie Yu
Xuejie Yu
Thomas Yuill
Mark Zabel
Jean Ralph Zahar
Sherif Zaki
Maria Zambon
Hassan Zaraket
Aleksandra Zasada
Jean-Pierre Zellweger
John Zelner
Marcus Zervos
Jian Zhang
Sean Zhang
Wenqing Zhang
Fangjun Zhou
Steven Zink
Jakob Zinsstag
Kate Zinszer
Hosam Zowawi

Earning CME Credit

To obtain credit, you should first read the journal article. After reading the article, you should be able to answer the following, related, multiple-choice questions. To complete the questions (with a minimum 75% passing score) and earn continuing medical education (CME) credit, please go to http://www.medscape.org/journal/eid. Credit cannot be obtained for tests completed on paper, although you may use the worksheet below to keep a record of your answers. You must be a registered user on Medscape.org. If you are not registered on Medscape.org, please click on the "Register" link on the right hand side of the website to register. Only one answer is correct for each question. Once you successfully answer all post-test questions you will be able to view and/or print your certificate. For questions regarding the content of this activity, contact the accredited provider, CME@medscape.net. For technical assistance, contact CME@webmd.net. American Medical Association's Physician's Recognition Award (AMA PRA) credits are accepted in the US as evidence of participation in CME activities. For further information on this award, please refer to http://www.ama-assn.org/ama/pub/about-ama/awards/ama-physicians-recognition-award.page. The AMA has determined that physicians not licensed in the US who participate in this CME activity are eligible for AMA PRA Category 1 Credits™. Through agreements that the AMA has made with agencies in some countries, AMA PRA credit may be acceptable as evidence of participation in CME activities. If you are not licensed in the US, please complete the questions online, print the certificate and present it to your national medical association for review.

Article Title

Investigation of and Response to 2 Plague Cases, Yosemite National Park, California, USA, 2015

CME Questions

1. You are advising the National Parks Service about detection and prevention of plague. According to the public health report by Danforth and colleagues, which of the following statements about the laboratory and epidemiologic findings regarding 2 human cases of patients with plague in 2015 with recent travel history to Yosemite National Park is correct?

A. Both patients had bubonic plague
B. Both patients had similar travel itineraries and were diagnosed at the same time
C. Distinct *Yersinia pestis* strains were isolated from the patients, with different whole-genome multilocus sequence typing (wgMLST)
D. Both patients had fed squirrels and had seen dead rodents

2. According to the public health report by Danforth and colleagues, which of the following statements about the environmental findings regarding 2 human cases of patients with plague in 2015 with recent travel history to Yosemite is correct?

A. Environmental samples indicated that the patients were exposed in the same location
B. Isolates from rodent serum, fleas, and rodent carcasses showed at least 2 distinct *Y. pestis* strains circulating among vector-host populations in the area
C. Plague antibodies were detected in all 8 rodent species live-trapped in Yosemite
D. The findings contrast with a previous single-nucleotide polymorphism (SNP)–based study showing widespread plague epizootics caused by multiple *Y. pestis* clones arising independently at small geographic scales

3. According to the public health report by Danforth and colleagues, which of the following statements about critical risk reduction measures used to help prevent plague transmission to Yosemite visitors and staff is correct?

A. Rapid interagency investigation and public health response to these patients lowered the risk for plague transmission to Yosemite visitors and staff
B. The investigation was limited to recreational sites visited by the patients
C. Insecticides were widely dispersed throughout the park
D. Educational efforts targeted only Yosemite staff

Activity Evaluation

1. The activity supported the learning objectives.				
Strongly Disagree				Strongly Agree
1	2	3	4	5
2. The material was organized clearly for learning to occur.				
Strongly Disagree				Strongly Agree
1	2	3	4	5
3. The content learned from this activity will impact my practice.				
Strongly Disagree				Strongly Agree
1	2	3	4	5
4. The activity was presented objectively and free of commercial bias.				
Strongly Disagree				Strongly Agree
1	2	3	4	5

Earning CME Credit

To obtain credit, you should first read the journal article. After reading the article, you should be able to answer the following, related, multiple-choice questions. To complete the questions (with a minimum 75% passing score) and earn continuing medical education (CME) credit, please go to http://www.medscape.org/journal/eid. Credit cannot be obtained for tests completed on paper, although you may use the worksheet below to keep a record of your answers. You must be a registered user on Medscape.org. If you are not registered on Medscape.org, please click on the "Register" link on the right hand side of the website to register. Only one answer is correct for each question. Once you successfully answer all post-test questions you will be able to view and/or print your certificate. For questions regarding the content of this activity, contact the accredited provider, CME@medscape.net. For technical assistance, contact CME@webmd.net. American Medical Association's Physician's Recognition Award (AMA PRA) credits are accepted in the US as evidence of participation in CME activities. For further information on this award, please refer to http://www.ama-assn.org/ama/pub/about-ama/awards/ama-physicians-recognition-award.page. The AMA has determined that physicians not licensed in the US who participate in this CME activity are eligible for AMA PRA Category 1 Credits™. Through agreements that the AMA has made with agencies in some countries, AMA PRA credit may be acceptable as evidence of participation in CME activities. If you are not licensed in the US, please complete the questions online, print the certificate and present it to your national medical association for review.

Article Title

Electrolyte and Metabolic Disturbances in Ebola Patients during a Clinical Trial, Guinea, 2015

CME Questions

1. You are evaluating a febrile, tachycardic 26-year-old woman who was living with 2 family members who were recently diagnosed with Ebola virus disease. She is quickly ushered into an isolation unit and undergoes an initial laboratory evaluation. In the current study by van Griensven and colleagues, what was the most common laboratory abnormality associated with Ebola virus disease?

A. Hypokalemia
B. Hyperkalemia
C. Hyponatremia
D. High anion gap

2. Which electrolyte was included in the current study's algorithm to determine the risk for mortality associated with Ebola virus disease?

A. Sodium
B. Potassium
C. Calcium
D. Magnesium

3. What else regarding the risk algorithm for mortality in the current study is most accurate?

A. It included the patient's pulse level
B. It included the patient's blood pressure level
C. Most patients fell in the low- or high-risk groups for mortality
D. Adding age and baseline polymerase chain reaction (PCR) cycle threshold value made the algorithm less precise

4. According to the results of the current study, what is the best advice regarding treatment of this patient?

A. Aggressive correction of hypocalcemia
B. Aggressive treatment of anemia
C. Aggressive fluid replacement
D. Careful supportive care

Activity Evaluation

1. The activity supported the learning objectives.				
Strongly Disagree				Strongly Agree
1	2	3	4	5
2. The material was organized clearly for learning to occur.				
Strongly Disagree				Strongly Agree
1	2	3	4	5
3. The content learned from this activity will impact my practice.				
Strongly Disagree				Strongly Agree
1	2	3	4	5
4. The activity was presented objectively and free of commercial bias.				
Strongly Disagree				Strongly Agree
1	2	3	4	5

CDC PROVIDES INFORMATION ABOUT MRSA SKIN INFECTIONS.

Visit www.cdc.gov/MRSA or call 1-800-CDC-INFO (800-232-4636) TTY: (888) 232-6348 to order provider materials including:

- Clinician guidelines
- Evaluation & treatment recommendations
- Patient education materials
- Posters
- Fact sheets
- Flyers

cdcinfo@cdc.gov

Developed with support from the CDC Foundation through an educational grant from Pfizer Inc.

Emerging Infectious Diseases is a peer-reviewed journal established expressly to promote the recognition of new and reemerging infectious diseases around the world and improve the understanding of factors involved in disease emergence, prevention, and elimination.

The journal is intended for professionals in infectious diseases and related sciences. We welcome contributions from infectious disease specialists in academia, industry, clinical practice, and public health, as well as from specialists in economics, social sciences, and other disciplines. Manuscripts in all categories should explain the contents in public health terms. For information on manuscript categories and suitability of proposed articles, see below and visit http://wwwnc.cdc.gov/eid/pages/author-resource-center.htm.

Summary of Authors' Instructions

Author's Instructions. For a complete list of EID's manuscript guidelines, see the author resource page: http://wwwnc.cdc.gov/eid/page/author-resource-center.

Manuscript Submission. To submit a manuscript, access Manuscript Central from the Emerging Infectious Diseases web page (www.cdc.gov/eid). Include a cover letter indicating the proposed category of the article (e.g., Research, Dispatch), verifying the word and reference counts, and confirming that the final manuscript has been seen and approved by all authors. Complete provided Authors Checklist.

Manuscript Preparation. For word processing, use MS Word. Set the document to show continuous line numbers. List the following information in this order: title page, article summary line, keywords, abstract, text, acknowledgments, biographical sketch, references, tables, and figure legends. Appendix materials and figures should be in separate files.

Title Page. Give complete information about each author (i.e., full name, graduate degree(s), affiliation, and the name of the institution in which the work was done). Clearly identify the corresponding author and provide that author's mailing address (include phone number, fax number, and email address). Include separate word counts for abstract and text.

Keywords. Use terms as listed in the National Library of Medicine Medical Subject Headings index (www.ncbi.nlm.nih.gov/mesh).

Text. Double-space everything, including the title page, abstract, references, tables, and figure legends. Indent paragraphs; leave no extra space between paragraphs. After a period, leave only one space before beginning the next sentence. Use 12-point Times New Roman font and format with ragged right margins (left align). Italicize (rather than underline) scientific names when needed.

Biographical Sketch. Include a short biographical sketch of the first author—both authors if only two. Include affiliations and the author's primary research interests.

References. Follow Uniform Requirements (www.icmje.org/index.html). Do not use endnotes for references. Place reference numbers in parentheses, not superscripts. Number citations in order of appearance (including in text, figures, and tables). Cite personal communications, unpublished data, and manuscripts in preparation or submitted for publication in parentheses in text. Consult List of Journals Indexed in Index Medicus for accepted journal abbreviations; if a journal is not listed, spell out the journal title. List the first six authors followed by "et al." Do not cite references in the abstract.

Tables. Provide tables within the manuscript file, not as separate files. Use the MS Word table tool, no columns, tabs, spaces, or other programs. Footnote any use of boldface. Tables should be no wider than 17 cm. Condense or divide larger tables. Extensive tables may be made available online only.

Figures. Submit editable figures as separate files (e.g., Microsoft Excel, PowerPoint). Photographs should be submitted as high-resolution (600 dpi) .tif or .jpeg files. Do not embed figures in the manuscript file. Use Arial 10 pt. or 12 pt. font for lettering so that figures, symbols, lettering, and numbering can remain legible when reduced to print size. Place figure keys within the figure. Figure legends should be placed at the end of the manuscript file.

Videos. Submit as AVI, MOV, MPG, MPEG, or WMV. Videos should not exceed 5 minutes and should include an audio description and complete captioning. If audio is not available, provide a description of the action in the video as a separate Word file. Published or copyrighted material (e.g., music) is discouraged and must be accompanied by written release. If video is part of a manuscript, files must be uploaded with manuscript submission. When uploading, choose "Video" file. Include a brief video legend in the manuscript file.

Types of Articles

Perspectives. Articles should not exceed 3,500 words and 50 references. Use of subheadings in the main body of the text is recommended. Photographs and illustrations are encouraged. Provide a short abstract (150 words), 1-sentence summary, and biographical sketch. Articles should provide insightful analysis and commentary about new and reemerging infectious diseases and related issues. Perspectives may address factors known to influence the emergence of diseases, including microbial adaptation and change, human demographics and behavior, technology and industry, economic development and land use, international travel and commerce, and the breakdown of public health measures.

Synopses. Articles should not exceed 3,500 words in the main body of the text or include more than 50 references. Use of subheadings in the main body of the text is recommended. Photographs and illustrations are encouraged. Provide a short abstract (not to exceed 150 words), a 1-line summary of the conclusions, and a brief biographical sketch of first author or of both authors if only 2 authors. This section comprises case series papers and concise reviews of infectious diseases or closely related topics. Preference is given to reviews of new and emerging diseases; however, timely updates of other diseases or topics are also welcome. If detailed methods are included, a separate section on experimental procedures should immediately follow the body of the text.

Research. Articles should not exceed 3,500 words and 50 references. Use of subheadings in the main body of the text is recommended. Photographs and illustrations are encouraged. Provide a short abstract (150 words), 1-sentence summary, and biographical sketch. Report laboratory and epidemiologic results within a public health perspective. Explain the value of the research in public health terms and place the findings in a larger perspective (i.e., "Here is what we found, and here is what the findings mean").

Policy and Historical Reviews. Articles should not exceed 3,500 words and 50 references. Use of subheadings in the main body of the text is recommended. Photographs and illustrations are encouraged. Provide a short abstract (150 words), 1-sentence summary, and biographical sketch. Articles in this section include public health policy or historical reports that are based on research and analysis of emerging disease issues.

Dispatches. Articles should be no more than 1,200 words and need not be divided into sections. If subheadings are used, they should be general, e.g., "The Study" and "Conclusions." Provide a brief abstract (50 words); references (not to exceed 15); figures or illustrations (not to exceed 2); tables (not to exceed 2); and biographical sketch. Dispatches are updates on infectious disease trends and research that include descriptions of new methods for detecting, characterizing, or subtyping new or reemerging pathogens. Developments in antimicrobial drugs, vaccines, or infectious disease prevention or elimination programs are appropriate. Case reports are also welcome.

Another Dimension. Thoughtful essays, short stories, or poems on philosophical issues related to science, medical practice, and human health. Topics may include science and the human condition, the unanticipated side of epidemic investigations, or how people perceive and cope with infection and illness. This section is intended to evoke compassion for human suffering and to expand the science reader's literary scope. Manuscripts are selected for publication as much for their content (the experiences they describe) as for their literary merit. Include biographical sketch.

Research Letters Reporting Cases, Outbreaks, or Original Research. EID publishes letters that report cases, outbreaks, or original research as Research Letters. Authors should provide a short abstract (50-word maximum), references (not to exceed 10), and a short biographical sketch. These letters should contain no more than 850 words (including the abstract) and may include either 1 figure or 1 table. Do not divide Research Letters into sections.

Letters Commenting on Articles. Letters commenting on articles should contain a maximum of 300 words and 5 references; they are more likely to be published if submitted within 4 weeks of the original article's publication.

Commentaries. Thoughtful discussions (500–1,000 words) of current topics. Commentaries may contain references (not to exceed 15) but no abstract, figures, or tables. Include biographical sketch.

Books, Other Media. Reviews (250–500 words) of new books or other media on emerging disease issues are welcome. Title, author(s), publisher, number of pages, and other pertinent details should be included.

Conference Summaries. Summaries of emerging infectious disease conference activities (500–1,000 words) are published online only. They should be submitted no later than 6 months after the conference and focus on content rather than process. Provide illustrations, references, and links to full reports of conference activities.

Online Reports. Reports on consensus group meetings, workshops, and other activities in which suggestions for diagnostic, treatment, or reporting methods related to infectious disease topics are formulated may be published online only. These should not exceed 3,500 words and should be authored by the group. We do not publish official guidelines or policy recommendations.

Photo Quiz. The photo quiz (1,200 words) highlights a person who made notable contributions to public health and medicine. Provide a photo of the subject, a brief clue to the person's identity, and five possible answers, followed by an essay describing the person's life and his or her significance to public health, science, and infectious disease.

Etymologia. Etymologia (100 words, 5 references). We welcome thoroughly researched derivations of emerging disease terms. Historical and other context could be included.

Announcements. We welcome brief announcements of timely events of interest to our readers. Announcements may be posted online only, depending on the event date. Email to eideditor@cdc.gov.

In This Issue

Synopsis

Research

Dispatches

Vol 22, No 12, December 2016

EMERGING INFECTIOUS DISEASES

Pages 2037–2244

DEPARTMENT OF HEALTH & HUMAN SERVICES
Public Health Service
Centers for Disease Control and Prevention (CDC)
Mailstop D61, Atlanta, GA 30329-4027

Official Business
Penalty for Private Use $300
Return Service Requested

MEDIA MAIL
POSTAGE & FEES PAID
PHS/CDC
Permit No. G 284

ISSN 1080-6040